Palladium-Catalysed Directed C(sp^3)–H Functionalisation of Saturated N-Heterocycles at Unactivated C4 Positions

A Thesis submitted by

Daniele Antermite

In partial fulfilment of the requirements for the degree of

DOCTOR OF PHILOSOPHY

Department of Chemistry

Imperial College London

Molecular Sciences Research Hub

White City Campus

London W12 0BZ

United Kingdom

2020

Declaration

I confirm that the work presented within this document is my own. Clear acknowledgement has been made when referring to the work of others, or where help has been received.

The copyright of this thesis rests with the author and is made available under a Creative Commons Attribution - Non Commercial - No Derivatives 4.0 International Licence (CC BY-NC-ND). Researchers are free to copy, distribute or transmit the thesis on the condition that they attribute it, that they do not use it for commercial purposes and that they do not alter, transform or build upon it. For any reuse or redistribution, researchers must make clear to others the licence terms of this work.

Acknowledgments

First, I would like to thank Dr James Bull for giving me the opportunity to join his group. His guidance throughout my PhD has been invaluable. During the last four years, he has been a constant source of advice and support, and for this I am very grateful. His help and encouragement have been of extreme importance, allowing me to make the most out of the opportunities I had during my PhD.

I would like to thank all present and past members of the Bull group, who have made my time at Imperial very enjoyable. Special thanks to Dom for helping me to get started in the lab and to Sahra for making me feel at home when I first arrived in London. Thanks to Maryne and Alex for sharing the lab with me since the beginning, and to everyone who joined along the way. You have been a great company over the years, and I have learned so much from all of you. Many thanks to Sofia and Joe for being fantastic new entries in the C–H activation team, and for all your suggestions and ideas. Thanks to Joe, Sinth-Di, Ahmed, Thomas and Luka for making me a better teacher. I would especially like to thank Maryne for the huge effort of proof-reading this thesis.

I am thankful to everyone who contributed to this work in any ways. In particular, I would like to thank Prof Luis Casarrubios for incredibly extensive computational studies, and for being always available to discuss new ideas. Thanks to Eric Gouaux and Jonathan Coleman for believing in the potential of our synthetic route and for being great collaborators.

Many thanks to Andrew White for an amazing crystal structure, and to Pete Haycock and Corey Fulop for their crucial help with a vast number of NMR samples they have run for me. I am also grateful to Lisa Haigh for her support with mass spec analysis.

Grazie ai miei genitori e a Salvatore for essere sempre al mio fianco, nei momenti felici e in quelli più difficili. Non ci sono parole per ringraziarvi dell'amore che mi trasmettete ogni giorno. Grazie per sostenermi sempre, anche quando le mie decisioni mi portano lontano. Spero di rendervi sempre orgogliosi. Questa tesi è dedicata a voi.

Finally, thank you Maryne for everything. Thank you for the long weekends in the lab, the countless pizzas, the hiking around the world, the French lessons and for the habit of having breakfast in the morning. But most importantly, thank you for always being there for me, sharing happy moments and helping me getting through difficult ones. Thank you for inspiring me to improve and for always believing in me more than I do. None of this would have been possible without you.

Abstract

Saturated N-heterocycles are prevalent motifs in bioactive compounds and represent important structures for pharmaceutical screening. As such, synthetic methods that can readily access these derivatives with high regio- and stereocontrol would be of significant value for the discovery of new therapeutics.

Catalytic C–H functionalisation offers high potential for the iterative and divergent synthesis of substituted N-heterocycles from simple cyclic precursors. The research in this thesis describes the selective synthesis of *cis*-3,4-disubstituted pyrrolidines and piperidines by Pd-catalysed C(sp^3)–H functionalisation with aryl iodides.

As described in chapter 3, high regio- and stereoselectivity is achieved using an aminoquinoline amide directing group at C(3), with C(4)-functionalisation always preferred over competing C(2). Divergent directing group removal delivers various biologically relevant building blocks, containing amide, carboxylic acid and alcohol functionalities.

The synthetic utility of this protocol for drug discovery applications is described in chapter 4. C(4)–H arylation followed by directing group removal enables the stereocontrolled formal synthesis of antidepressant (–)-paroxetine and the total synthesis of enantiopure Br- and I-paroxetine analogues. Furthermore, the synthesis of a library of arylated pyrrolidine and piperidine fragments for pharmaceutical screening is demonstrated.

Mechanistic investigations into the observed regio- and stereoselectivity are discussed in chapter 5. Deuteration studies, kinetic analysis and DFT calculations suggest reversible C–H activation to occur at different positions on the ring. Subsequent stereodetermining oxidative addition of Pd^{II} to Pd^{IV} and turnover-limiting reductive elimination deliver the C(4)-arylated products as *cis*-diastereomers. During this study, evidence for a fast catalyst deactivation process is observed.

Attempts to overcome this limitation are finally discussed in chapter 6. This ultimately results in the development of an improved 4-dimethylamino-8-quinolinyl amide directing group. This novel removable auxiliary provides a faster reaction rate, higher yields and a broader substrate scope, and enables the late-stage functionalisation of complex biorelevant compounds.

Table of Contents

Declaration **2**

Acknowledgments **3**

Abstract **4**

i **List of Acronyms & Abbreviations** **9**

ii **Stereochemical Notation** **14**

1. Introduction **15**

1.1 The Drug Discovery Process **15**

1.2.1 Desirable Properties for Potential Therapeutics 16

1.2.2 Importance of Organic Synthesis within Drug Discovery 20

1.2 Saturated N-Heterocycles in Medicinal Chemistry **21**

1.3 Synthetic Approaches towards Functionalised Pyrrolidines and Piperidines **22**

1.3.1 Direct Functionalisation on the Intact Ring 22

1.3.2 C–H Bonds as Attractive Sites for Functionalisation 24

1.4 Transition Metal-Catalysed C–H Functionalisation **30**

1.4.1 C(sp^3)–H Functionalisation Using Removable Directing Groups 32

1.4.2 Directed C(sp^3)–H Arylation of Saturated N-Heterocycles 36

2. Project Aims **45**

3. C–H Arylation of Pyrrolidines and Piperidines using C(3)-Directing Groups **47**

3.1 4-Aryl Pyrrolidines and Piperidines in Bioactive Compounds **47**

3.2 Development of Regio- and Stereoselective C(4)–H Arylation **48**

3.2.1 Initial Screenings and Products Identification 49

3.2.2 Optimisation of Regio- and Stereoselective C(4)–H Arylation 51

3.3 Scope of Pyrrolidine C(4)–H Arylation **58**

3.3.1 Variation of *N*-Protecting Groups 58

3.3.2 Variation of Aryl Iodide Coupling Partners 60

3.4 Base-Mediated Epimerisation for the Formation of *trans*-Isomers 62

3.4.1 Synthesis of *trans*-3,4-Disubstituted Pyrrolidines.....62

3.4.2 Boc Deprotection and Stereochemical Assignments 64

3.5 Piperidine C(4)–H Arylation.....66

3.5.1 Scope of *N*-Protecting Groups and Aryl Iodides.....66

3.5.2 Stereochemical Assignment.....68

3.5.3 Studies into Epimerisation and Stereochemical Outcome 69

3.6 Towards Medicinal Chemistry Applications: Divergent Removal of the Directing Group.....73

3.6.1 Carboxylic Acid Derivatives 73

3.6.2 Alcohol, Methyl Ester and Secondary Amide Derivatives 76

3.6.3 Primary Amide Derivatives.....80

3.7 Conclusions 81

4. Applications of C(4)–H Arylation in Drug Discovery 83

4.1 Stereocontrolled Synthesis of (–)-Paroxetine 83

4.1.1 Antidepressant (–)-Paroxetine: An Overview 83

4.1.2 Recent Advances in the Synthesis of (–)-Paroxetine.....84

4.1.3 Retrosynthetic Analysis and Proposed Strategy 86

4.1.4 Stereocontrolled Formal Synthesis of (+)- and (–)-Paroxetine 87

4.2 Total Synthesis of Br- and I-Analogues of (–)-Paroxetine.....89

4.2.1 C(4)–H Arylation Step 90

4.2.2 Synthesis of Key Alcohols Intermediates 91

4.2.3 Final Steps.....93

4.3 Preparation of a Library of Pyrrolidine and Piperidine Fragments by C–H Arylation 94

4.3.1 Fragment-Based Drug Discovery.....94

4.3.2 Design of Pyrroline and Piperidine Fragments.....97

4.3.3 Synthesis of Target Fragments.....98

4.3.4 Physicochemical Properties Analysis....110
4.4 Conclusions....115
5. Mechanism and Selectivity of Pd-Catalysed C(4)–H Arylation....117
5.1 Mechanism of C(sp^3)–H Functionalisation *via* Pd^{II}/Pd^{IV} Catalytic Cycle....117
5.2 Investigations into the C–H Activation Step....119
5.2.1 Deuterium Labelling Experiments on Pyrrolidine-3-AQ Amide....119
5.2.2 Synthesis and Reactivity of 5,5-*cis*-Palladacycle Complexes....122
5.3 Kinetic Analysis to Determine the Turnover-Limiting Step....125
5.3.1 Evaluation of Kinetic Isotope Effect....125
5.3.2 Kinetic Order in Reaction Components....130
5.3.3 Electronic Effect of the Aryl Iodides on the Reaction Rate....136
5.4 Computational Modelling of Reaction Mechanism....140
5.4.1 DFT Study on the C–H Activation Step....141
5.4.2 Stereodetermining Oxidative Addition....144
5.4.3 The Case of Piperidine-3-Carboxamide....147
5.5 Investigations into Product Inhibition and Catalyst Deactivation....149
5.5.1 Deuteration Studies on 4-Arylated Pyrrolidine Product....149
5.5.2 Reaction Progress Kinetic Analysis (RPKA)....154
5.5.3 Estimation of Catalyst Deactivation Profile....157
5.7 Conclusions: Proposed Catalytic Cycle....161
6. Discovery of Dimethylaminoquinolinyl (DMAQ) Amide as an Improved Directing Group....163
6.1 Initial Attempts to Overcome Catalyst Deactivation....163
6.1.1 Spiking Experiments....163
6.1.2 Ligand Screening....164
6.1.3 Alternative Reaction Conditions....167

6.2 Evaluation of Steric and Electronic Effects on the Directing Group 168

6.2.1 Synthesis of Pyrrolidine Substrates 169

6.2.2 Directing Group Effect on Reaction Outcome 171

6.3 Scope of Pyrrolidine C(4)–H Arylation with DMAQ Directing Group 175

6.4 Piperidine C(4)–H Arylation with DMAQ Directing Group 178

6.5 Mechanistic Rationale for the Improvement in Reactivity.....180

6.5.1 Estimation of Catalyst Deactivation with DMAQ Directing Group.....180

6.5.2 Kinetic Effect of 4-Substituents on the Directing Group 181

6.6 Removal of DMAQ Directing Group 185

6.7 Medicinal Chemistry Applications: Late-Stage Functionalisation of Acid-Containing Drugs.....187

6.8 Conclusions 190

7. Conclusions and Future Work 191

8. Experimental 195

8.1 General Experimental Considerations 195

8.2 Experimental Details and Characterisation Data 197

8.2.1 Compounds for Chapter 3.....197

8.2.2 Compounds for Chapter 4: Synthesis of (–)-Paroxetine, Br-(–)-Paroxetine and I-(–)-Paroxetine 263

8.2.3 Compounds for Chapter 4: Fragment Library Synthesis 280

8.2.4 Compounds for Chapter 5.....316

8.2.5 Compounds for Chapter 6.....321

8.2.6 General Procedures and Raw Data for Mechanistic and Kinetic Experiments 370

9. References 387

10. Appendices.....403

i List of Acronyms & Abbreviations

5-HT	5-Hydroxytryptamine
Ac	Acetyl
Ad	1-Adamantanyl
ADMET	Absorption, Distribution, Metabolism, Excretion, Toxicity
aq	Aqueous
AQ	8-Aminoquinoline
APCI	Atmospheric pressure chemical ionisation
Ar	Aryl
BDE	Bond dissociation energy
Bn	Benzyl
Boc	*tert*-Butyloxycarbonyl
BQ	Benzoquinone
Bu	Butyl
CAN	Ceric(IV) ammonium nitrate
Cbz	Benzyloxycarbonyl
CMD	Concerted metalation deprotonation
COD	Cyclooctadiene
*m*CPBA	*m*-Chloroperbenzoic acid
Cy	Cyclohexyl
CYP450	Cytochrome P450
dba	Dibenzylideneacetone
DBU	1,8-Diazabicyclo[5.4.0]undec-7-ene
DCE	Dichloroethane
DCB	Dichlorobenzene
DFT	Density-functional theory

DG	Directing group
DIAD	Diisopropyl azodicarboxylate
DIPEA	*N*,*N*-Diisopropylethylamine
DMAP	4-(Dimethylamino)pyridine
DMAQ	4-(Dimethylamino)-8-aminoquinoline
DME	Dimethoxyethane
DMF	*N*,*N*-Dimethylformamide
DMS	Dimethylsulfide
DMSO	Dimethyl sulfoxide
dr	Diastereomeric ratio
EDC	1-Ethyl-3-(3-dimethylaminopropyl)carbodiimide
EDG	Electron donating group
ee	Enantiomeric excess
EM	Electron microscopy
EWG	Electron withdrawing group
ESI	Electrospray ionisation
FDA	Food and Drug Administration
Fsp^3	Fraction of saturated carbon sp^3
FBDD	Fragment-based drug discovery
FT-IR	Fourier-transform infrared spectroscopy
Gly	Glycine
GSK	GlaxoSmithKline
HAT	Hydrogen atom transfer
HATU	Hexafluorophosphate azabenzotriazole tetramethyl uronium
HBA	Hydrogen bond acceptor
HBD	Hydrogen bond donor

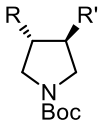
hERG	Human ether-a-go-go-related gene
HFIP	Hexafluoroisopropanol
HOAt	*N*[1]-Hydroxy-7-azabenzotriazole
HOBt	1-Hydroxybenzotriazole
HPLC	High performance liquid chromatography
HRMS	High resolution mass spectroscopy
HTS	High throughput screening
IBX	2-Iodoxybenzoic acid
KIE	Kinetic isotope effect
cLogP	Calculated partition coefficient
Me	Methyl
Mes	Mesityl (2,4,6-trimethylphenyl)
mp	Melting point
M_W	Molecular weight
NHC	N-Heterocyclic carbene
NHPI	*N*-Hydroxyphthalimide
NMP	*N*-Methyl-pyrrolidone
NMR	Nuclear magnetic resonance spectroscopy
NOE	Nuclear Overhauser effect
NROT	Number of rotatable bonds
OA	Oxidative additon
ORTEP	Oak ridge thermal ellipsoid plot
PA	Picolinamide
PBF	Plane of best fit
PG	Protecting group
pK_a	Negative logarithm of the acid dissociation constant K_a

Ph	Phenyl
Phth	Phthalimide
PMI	Principle moment of inertia
pNSI	Pneumatically assisted nanospray ionisation
PPI	Protein-protein interaction
ppm	Parts per million
Pr	Propyl
PSA	Polar surface area
Piv	Pivaloyl
Q	Quinolin-8-yl
R&D	Research and development
RE	Reductive elimination
RPKA	Reaction progress kinetic analysis
rpm	Revolutions per minute
RSM	Recovered starting material
rt	Room temperature
SAR	Structure-activity relationship
sat	Saturated
SET	Single electron transfer
SERT	Serotonin transporter
S_NAr	Nucleophlic aromatic substitution
S_EAr	Electrophilic aromatic substitution
SSRI	Selective serotonin reuptake inhibitor
STE	Structural *trans*-effect
TBAI	Tetrabutylammonium iodide
TFA	Trifluoroacetic acid/acetate

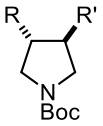
TFAA	Trifluoroacetic anhydride
THF	Tetrahydrofuran
THIQ	Tetrahydroisoquinoline
TMB	Trimethoxybenzene
TMEDA	*N,N,N',N'*-Tetramethylethylenediamine
Ts	Tosyl
VTNA	Variable time normalisation analysis

ii Stereochemical Notation

Throughout this thesis, stereochemistry will be represented according to Maehr's convention.[1] Solid and broken wedges denote absolute configuration, while solid and broken bold lines are used to represent relative configuration (*e.g. cis* and *trans*). When absolute configuration is shown, a compound is enantioenriched or has been prepared as a single enantiomer. On the other hand, when relative configuration is depicted, the compound has been prepared as a racemate.



Absolute Configuration



Relative Configuration

1. Introduction

1.1 The Drug Discovery Process

Over the last century, the development of ground-breaking medicines has revolutionised the treatment of life-threatening diseases and improved the health of patients worldwide. The discovery of new drugs remains of fundamental importance to address unmet or more challenging medical needs. A typical drug discovery project starts with the identification and validation of a biological target involved in a specific disease (Figure 1.1).[2,3] Large libraries of compounds are then screened against the selected target in order to identify any "hit" with detectable activity. This is followed by a long process of synthesis and screening of analogues to improve potency, selectivity and physiochemical profiles. If a suitable candidate is identified during these stages of "lead identification" and "lead optimisation", it can proceed to pre-clinical and clinical trials and eventually reach the market.



Figure 1.1 Schematic representation of the drug discovery and development process.

This is an extremely long and expensive process, facing increasingly complex challenges. The launch of a new drug on the market generally requires 10–14 years from project inception, and the R&D investment cost for single commercialised therapeutic has been estimated to range between $1.0 and $2.6 billion.[4] Although recent years have seen a positive trend in the number of new drug approvals,[5] late-stage failure of candidates remains one of the biggest challenges in the pharmaceutical industry.[6,7] The average success rate of a candidate entering Phase I of clinical trials is currently lower than 10%, ranging from 16% to 3% based on the therapeutic area.[7] This contrast between high levels of R&D investment and low pipeline productivity could ultimately result in an unsustainable business model. Understanding the causes of late-stage attrition and how these could be addressed in earlier stages of the process is therefore of crucial importance.

Following an ongoing trend visible from early 2000s, 79% of clinical failures in the period 2016–2018 was attributed to lack of efficacy or safety.[7,8] Several strategies have been proposed to tackle this formidable challenge, mainly highlighting the need for better target selection and lead generation processes. In addition, increasing the quality of compounds screened at early

stages, both in terms of higher diversity and improved physicochemical properties, has been proposed as a critical strategy to reduce late-stage attrition.[9]

1.2.1 Desirable Properties for Potential Therapeutics

A complex combination of factors needs to be considered in order to design and select clinical candidates. Potency and target selectivity are crucial to produce the desired therapeutic effect. However, these pharmacologic parameters alone are not enough to provide a successful drug. Pharmacokinetic and toxicological profiles are also essential to determine whether a bioactive compound can achieve commercialisation.[8b,10] For example, in order to exercise its biological activity, an oral drug needs to be absorbed from the gastrointestinal tract, while being resistant to the wide pH range of stomach and intestine. The absorption depends on the aqueous solubility of the compound, as well as on its capability to permeate through lipophilic membranes.[11] Once absorbed into the bloodstream, it needs to be distributed to the target tissues in a concentration sufficient to modulate the biological target, while avoiding toxic interactions. The therapeutic efficacy is also strongly affected by the rate at which the compound is converted into inactive metabolites and/or excreted from the body, with too rapid clearance resulting in low bioavailability. Careful optimisation of the ADMET parameters (Absorption, Distribution, Metabolism, Excretion and Toxicity) is therefore of fundamental importance to develop successful medicines.

The ADMET profile of a drug compound is intrinsically dependent on its chemical structure and physicochemical properties.[10] In fact, control over these simple, easily measurable and predictable properties offers high potential to improve ADMET parameters and increase the success rate within drug discovery.

1.2.1.1 Lipophilicity and Molecular Weight (M_W)

Lipophilicity and M_W are arguably the properties that most deeply influence and determine the ADMET profile of a compound.[12,13,14] These parameters generally increase at the same time during lead optimisation, due to the drive to maximise potency which can often be achieved by increasing hydrophobic interactions within the target's binding site.[15] However, lipophilicity and M_W can have independent effects on several ADMET parameters.[12]

Lipophilicity refers to the compound's affinity for lipids and non-polar media. This is typically expressed as the logarithm of the octanol/water partition (logP) and/or distribution (logD) coefficients, and several *in silico* models are available to allow its prediction (*e.g.* clogP).[16] Lipophilicity is directly linked to both the aqueous solubility of the compound and its permeability through biological membranes, ultimately resulting in a strong influence on drug absorption. Although solubility is also affected by the ionisation features (pK_a) of the molecule,

highly lipophilic compounds are typically affected by poor intrinsic solubility.[10] For example, it has been estimated that logP < 3.25 is necessary to achieve optimal solubility (> 100 μM).[13,17] Upon analysis of 44,584 GSK compounds, Gleeson showed that higher solubility is observed for clogP < 3, and that below this value the solubility becomes less dependent on ionisability.[12] In the same study, a negative correlation was also shown between solubility and M_W, with optimal values observed for M_W < 400.[12]

The interaction between molecular size and lipophilicity is more complex with regards to the effect on permeability.[18] For polar compounds, permeability typically increases with lipophilicity. However, this trend is inverted at high logD values, as highly lipophilic molecules tend to remain in the membrane instead of moving into the surrounding aqueous media. On the other hand, lower permeability is observed for higher M_W values, as this is generally associated to higher number of heteroatoms, rotatable bonds, hydrogen bond donor/acceptors and polar surface area (*vide infra*), all of which have a negative influence on permeability.[19] In a specific example, Waring suggested that high permeability (> 100 nm/s) can be achieved for compounds with M_W = 350–400 and logD > 1.7, while bigger compounds (M_W > 500) require much higher distribution coefficients (logD > 4.5).[14]

High lipophilicity has also been associated with increased metabolic clearance.[13,20] This derives from the activity of metabolising enzymes that convert lipophilic substrates into more polar compounds to facilitate their excretion. This has been illustrated by Johnson showing that logD < 3 resulted in higher metabolic stability for a Pfizer dataset of 47,018 compounds.[18] At the opposite end of the spectrum however, very polar compounds (logD ≤ 0) are affected by elevated renal clearance, highlighting the importance of a subtle balance in lipophilicity to achieve optimal bioavailability.[11,13]

Finally, high lipophilicity has a major impact on toxicity risks, as it generally leads to an increase in non-specific binding to undesired targets.[13] Leeson and Springthrope identified a clear link between lipophilicity and off-target promiscuity, which increased significantly for compounds with clogP > 3.[9c] Similarly, compounds with clogP < 3 are less likely to act as inhibitors of CYP450 enzymes or hERG cardiac potassium channel.[12,21]

1.2.1.2 Shape and Complexity

The molecular architecture of drug candidates has also been recognised as a crucial determinant of their ADMET properties and success rates.

For instance, the number of hydrogen-bond donors (HBD) and acceptors (HBA) is linked to the potential of a compound to develop specific interactions with the target. However, high H-bond count has been associated to reduced membrane permeability and bioavilability.[19,22] H-

Bonds donors and acceptors are also directly linked to the polar surface area (PSA) of a molecule, *i.e.* the total surface (Å^2) occupied by polar atoms (typically -O and -N).[23] Important correlations have been identified between PSA and several ADMET parameters, including solubility, permeability and *in vivo* toxicity.[19,24] For example, Hughes showed that compounds with clogP < 3 and PSA > 75 Å^2 are associated to lower toxicological risks in pre-clinical trials.[24]

The number of rotatable bonds (NROT), defined as single, non-cyclic and non-amide (C–N) bonds, linked to a non-terminal heavy atom, was also found to have a negative impact on permeability.[19] This is likely due to the entropic costs associated with the conformational changes necessary for an optimal interaction with the hydrophobic membranes. Accordingly, Veber suggested that more rigid compounds (NROT ≤ 10) with PSA ≤ 140 Å^2 (or total H-bond count ≤ 12) are more likely to have optimal oral bioavailability.[19]

In 2009, a seminal report by Lovering highlighted the importance of complexity and saturation as fundamental molecular descriptors for drug design.[25] Architecturally complex, three-dimensional molecules are more similar in structure to bioactive natural products. Therefore, these are more likely to develop better binding interactions with complex or more challenging biological targets.[26] Increasing saturation would allow access to more complex and 3-dimensional molecules, and enable more efficient exploration of chemical space,[27] without a significant increase in M_W. Complexity and saturation can be quantified using the fraction of sp^3 hybridised carbon atoms (Fsp^3 = number of sp^3 carbons / total carbon count) and the number of chiral centres. A positive correlation was identified between these parameters and the successful progression of candidates through the discovery process.[25] Furthermore, higher Fsp^3 and chiral count were linked to higher solubility[25] and lower risk of promiscuity-derived toxicity.[28]

At a similar time, Richie and Macdonald showed that an excessive number of aromatic rings (> 3) is associated to lower aqueous solubility and increased risk of candidate failure.[29] This detrimental effect is mainly determined by the presence of carboaromatic rings (*e.g.* benzene), while heteroaromatic rings (*e.g.* pyridine) had only a smaller negative effect on compounds developability.[30] On the other hand, the incorporation of saturated heterocycles (*e.g.* piperidine) typically resulted in improved ADMET profiles.[30]

The identification of these close relations between physicochemical properties and ADMET behaviour have driven the construction of several guidelines to aid the design of new potential drugs.

1.2.1.3 Guidelines for Desirable Physicochemical Properties

In 1997, Lipinski first reported an extremely influential set of guidelines, known as "rule of 5", to predict the oral bioavailability of drug compounds.[22] Molecules with M_W < 500, clogP < 5, HBD < 5 and HBA < 10, were anticipated to offer better solubility and permeability, and therefore have higher chances to become successful drugs. More recently, several modifications of the Lipinski rules have been proposed to increase chances of success, mainly involving a reduction in the upper limits for logP and M_W, as well as recognising PSA and molecular rigidity as additional key descriptors.[12,19,24] Rules such as GSK "4/400" (clogP/M_W)[12] and Pfizer "3/75" (clogP/PSA)[24] are suggested to provide more general delimitations of "drug-like" space, as accounting also for toxicological risks.

The average physicochemical properties tend to evolve as compounds progress through the different stages of pre-clinical development. Extensive lead optimisation is generally required to maximise potency and selectivity, and to improve pharmacokinetic and safety profiles. This is usually accompanied by an increase in size and lipophilicity compared to the original hit or lead compounds (Figure 1.2).[31] The choice of suitable starting points for optimisation is therefore essential to obtain clinical candidates that fit in optimal drug-like space. Churcher suggested that "lead-like" compounds, defined as smaller, more polar molecules (M_W = 200–350 and clogP = 0–3), with higher 3-dimensional character (aromatic ring count < 3), offer higher chances to provide optimal drug candidates upon elaboration.[31]

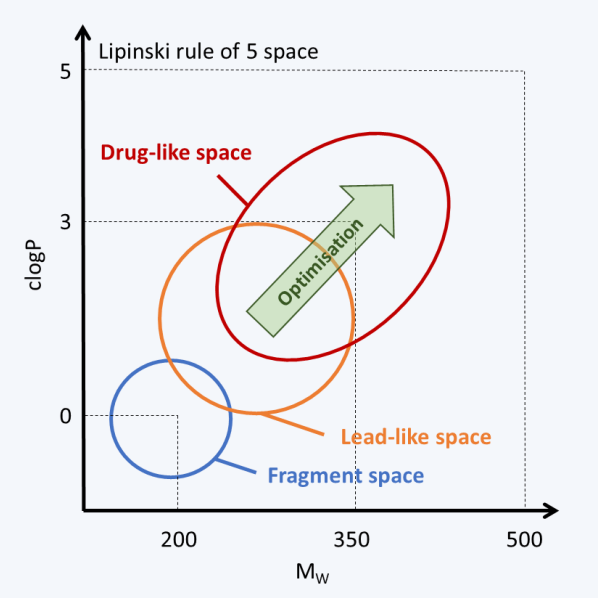


Figure 1.2 Churcher's representation of the typical hit-to-drug progression during pre-clinical discovery. Figure adapted from ref. 31.

This concept is further extended in the field of Fragment-Based Drug Discovery (FBDD), where much smaller "fragment" molecules are used as starting points for hit identification and

optimisation (for a more detailed discussion, see section 4.3.1).[32] Desirable criteria for fragment-like compounds were first summarised by scientists at Astex with the "rule of 3", specifying clogP < 3, M_W < 300, HBA ≤ 3 and HBD ≤ 3.[33] Reducing NROT (≤ 3) and PSA (≤ 60 Å^2) was also proposed to be beneficial for the construction of suitable fragment libraries.[33] Klebe subsequently suggested that increasing the upper limit for H-bond acceptors (≤ 6) could be advantageous to increase binding interactions and synthetic developability of the fragments.[34] More recently, Rees revised the original Astex guidelines, suggesting that smaller (M_W = 140–230), more polar (clogP = 0–2) fragments, with higher three-dimensional shape, are more likely to reach the lead stage.[35]

Since Lipinski's seminal work, the importance of physicochemical and structural properties for the success of drug candidates is much better understood. The resulting guidelines have provided invaluable tools to design molecules with higher potential to become new medicines. The development of new synthetic methodologies that can provide practical access to such compounds is therefore of tremendous importance.[31,35,36,37]

1.2.2 Importance of Organic Synthesis within Drug Discovery

Synthetic organic chemistry plays an essential role in many different stages of pharmaceutical research, offering great opportunities to promote success and innovation.[36] However, it also faces significant challenges, limiting the molecules that can be designed and tested, or produced on large scale for market distribution.[37] In the initial stages of development, thousands of molecules, preferentially fitting fragment- or lead-like criteria, need to be synthesised and submitted to biological screenings. When one or more hits are identified, significant time-consuming synthetic effort is required to produce analogues with better potency and/or beneficial ADMET profiles. Even when only few candidates are finally selected for clinical trials, their synthesis needs to be scaled-up, and robust and safe synthetic processes need to be optimised.

Due to the elevated time and financial pressure, the pharmaceutical industry has relied mainly on well-established and robust synthetic methods, amenable to the high-throughput synthesis of a huge number of analogues, especially in early development. These methods for example include amide-bond formation, S_NAr and sp^2-sp^2 cross-coupling reactions.[38] Despite the utility and success of such strategies, this trend has unintentionally reduced the diversity of screening libraries and limited the production of molecules with more desirable properties, resulting in detrimental effects on drug discovery.[25,31,38] For example, compounds with high 3-dimensional character remain under-represented in pharmaceutical research.[39] Therefore, the development of robust reactions that can reliably access diverse 3-dimensional scaffolds would be of high value for the discovery of new therapeutics.[40]

Such methods should be highly tolerant to polar functionalities, such as amines and nitrogen-containing heterocycles, that are prevalent in drug molecules.[37] In addition, new reactions that can enable the stereoselective synthesis of highly desirable but often challenging scaffolds, such as heteroaliphatic rings, would be of significant importance.[37]

1.2 Saturated N-Heterocycles in Medicinal Chemistry

Saturated nitrogen-containing heterocycles are highly attractive structures in drug discovery. In particular, five- and six-membered pyrrolidines and piperidines are central structural motifs in bioactive molecules, ranging from very simple proteinogenic aminoacid L-proline, to complex natural products and therapeutic agents (Figure 1.3).[41,42]

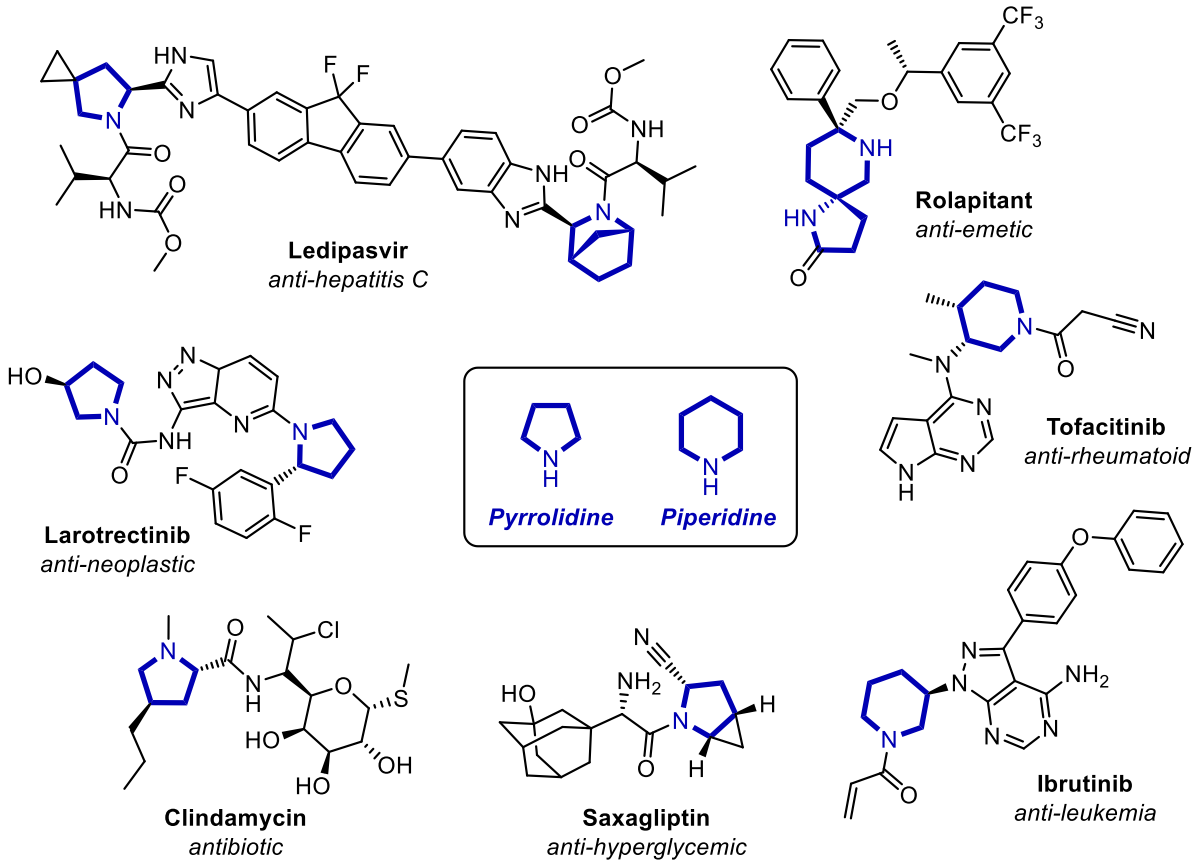


Figure 1.3 Selected examples of approved medicines containing pyrrolidine and piperidine scaffolds.[43]

The prevalence of saturated N-heterocycles in medicinal chemistry is well documented.[42,44] For instance, piperidine and piperazine were respectively the 3rd and 4th most common rings in drugs approved before 2013, just after benzene and pyridine, while the pyrrolidine moiety followed in 8th position.[42a] A similar trend was also independently reported by Njardarson, who found that 59% of all FDA-approved small-molecule pharmaceuticals up to 2012 contains a nitrogen heterocycle.[42c] Three of the five most commonly-utilised N-heterocycles were

saturated, with piperidine being the most prevalent N-ring system overall, followed by pyridine, piperazine, bicyclic cephem and pyrrolidine.[42c]

In addition, saturated N-heterocycles are low-M_W, 3-dimensional, polar scaffolds. Thus, these offer high potential as fragments for screening and building blocks for the preparation of lead compounds that satisfy the desirable properties outlined in section 1.2.1. The rigid, sp^3-rich framework of these rings allows for installation of out-of-plane substituents at different positions relative to the heteroatom. Probing the full 3D space around the ring can be advantageous to improve complementarity with complex biological targets, and to develop potency and selectivity profiles. Furthermore, the presence of aromatic substituents on the ring would be of particular interest to develop binding interactions without determining a detrimental increase in molecular flexibility. As such, methods that can provide regio- and stereocontrolled access to arylated N-heteroaliphatic rings, would be highly beneficial in drug discovery projects.

1.3 Synthetic Approaches towards Functionalised Pyrrolidines and Piperidines

The most common strategy for the synthesis of saturated N-heterocycles arguably relies on the ring-closure of pre-functionalised acyclic precursors, proceeding *via* C–N or C–C bond formation.[45,46] This is an extremely broad area, involving many different mechanistic scenarios from nucleophilic substitution to metal-catalysed and radical cyclisation processes, and will not be discussed in detail here.[47] A common feature among all these strategies is the requirement for reactive functionalities on the acyclic substrate to trigger the cyclisation event (*e.g.* (pseudo)halides, alkenes, carbonyl groups, etc.), although metal-catalysed and radical protocols for the intramolecular amination of simple C–H bonds have also been developed.[48]

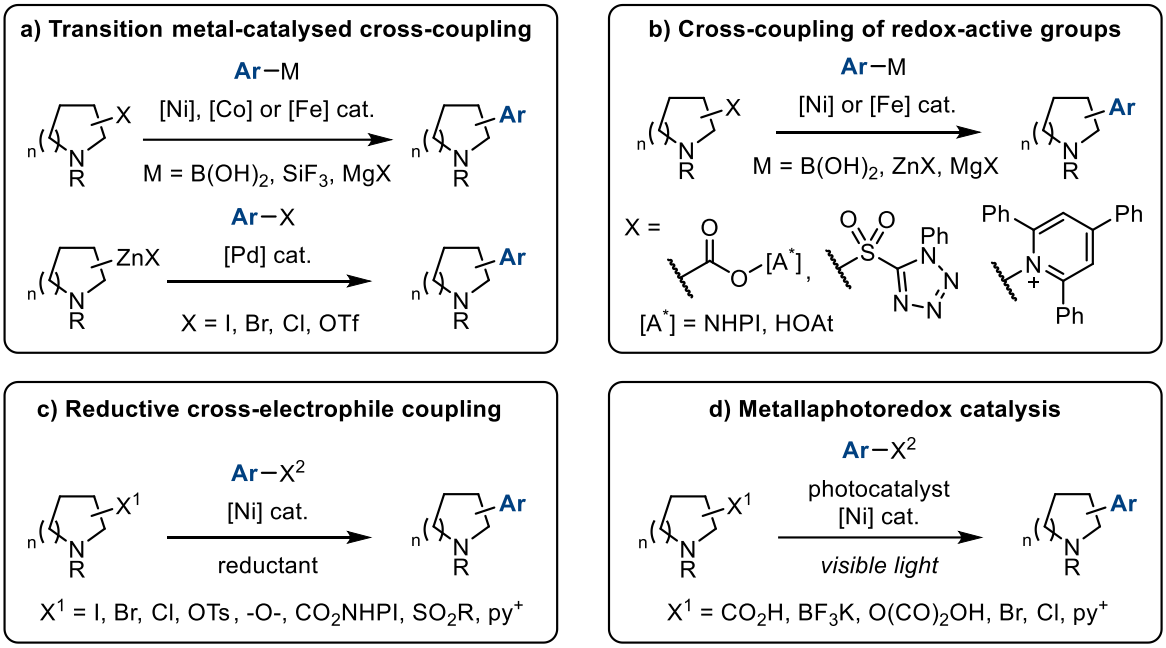
Other classical routes towards functionalised pyrrolidine and piperidine rings involve hydrogenation of aromatic or unsaturated precursors, as well as cycloaddition processes.[46b,49,50] Both approaches offer high potential for rapid generation of complexity in a single synthetic step. However, controlling the chemo-, regio- and stereoselectivity of these transformations remains a significant challenge, subject to extensive investigations.[49a,50a]

On the other hand, the functionalisation of pre-existing saturated rings to produce the desired substitution pattern is a relatively less-explored, but rapidly growing field.[49b] The next sections will focus on this approach, with particular attention paid to methods that can install aromatic substituents.

1.3.1 Direct Functionalisation on the Intact Ring

Conceptually, the direct functionalisation of pre-existing N-heterocyclic rings is an attractive strategy for the rapid modular synthesis of analogues as required in drug discovery programs.

In recent years, several methods have been developed that enable the direct installation of aromatic groups at different ring positions, typically taking advantage of preinstalled reactive handles, such as halides, alcohols or carboxylic acid functionalities (Scheme 1.1).



Scheme 1.1 Common methods for the direct arylation of saturated N-heterocycles using preinstalled functional groups.

One of the most successful approaches to arylate pyrrolidines and piperidines is the transition metal-catalysed cross-coupling of halogenated substrates (Scheme 1.1a).[49b] Since seminal works by Fu and co-workers in early 2000s describing the Ni-catalysed Suzuki[51] and Hiyama[52] couplings of secondary alkyl halides, this field has expanded rapidly.[53] Specific ligands have been designed to avoid β-hydride elimination and enable the Pd-catalysed Negishi reactions of aryl halides with alkylzinc reagents, including various piperidine examples.[54] Recently, Buchwald developed a Pd-catalysed in-water arylation of heterocyclic alkylzinc compounds, generated in-situ from the corresponding bromides.[55] Kumada couplings of Grignard reagents with secondary alkyl halides have also been successfully applied to the arylation of N-heteroaliphatic rings, involving Ni-,[56] Co-[57,58] or Fe-catalysis.[57b,59]

In 2016, Baran uncovered the use of carboxylic acids as halide surrogates in Ni- and Fe-catalysed couplings of alkyl groups, through the expedient formation of redox active esters (Scheme 1.1b).[60] *N*-Hydroxyphthalimide (NHPI) and *N*[1]-hydroxy-7-azabenzotriazole (HOAt) esters were shown to undergo SET fragmentation, enabling decarboxylative cross-couplings with (hetero)aryl zincs, boronic acids and Grignard reagents.[61] This strategy allowed for the efficient arylation of several N-heteroaliphatic carboxylic acids, including tertiary examples.[62] Furthermore, phenyl-tetrazole sulfones and pyridinium salts have been identified as alternative

redox-active handles for desulfonative and deaminative Ni-catalysed C(sp^3)–C(sp^2) couplings, demonstrating high functional group tolerance.[63,64]

Recently, the reductive coupling of two different electrophiles has emerged as an important alternative for the arylation of saturated N-heterocycles, avoiding the use of stoichiometric organometallic nucleophiles (Scheme 1.1c).[49b] The use of air-stable Ni(II) catalysts, in combination with various nitrogen-based ligands, allowed for the arylation of a wide range of electrophiles. These included N-heterocyclic alkyl bromides,[65,66] tosylates,[67] epoxides,[68] as well as redox-active esters,[69] pyridinium salts[70] and sulfones.[71] The requirement for super-stoichiometric reductants (typically Zn or Mn) remains an important drawback in these transformations, although innovative electrochemical protocols have been developed to overcome this issue.[72]

In recent years, ground-breaking advances in photoredox catalysis have been reported, enabling arylation of saturated N-heterocycles under mild, visible light conditions (Scheme 1.1d). Pioneering works from the groups of Doyle, MacMillan and Molander, demonstrated the use of a double iridium/nickel catalytic system for the arylation of carboxylic acids and trifluoroborates alkyl-radical precursors, circumventing classical cross-coupling problems such as β-hydride elimination or difficult transmetallation.[73] Following these seminal works, the scope of metallaphotoredox C(sp^3)–C(sp^2) couplings was extended to other radical precursors, including for instance oxalates,[74] alkyl halides[75] and pyridinium salts.[76] Finally, (hetero)arylation of pyrrolidine and piperidine precursors has also been achieved through visible light-mediated couplings with arylnitriles[77] and Minisci-type reactions.[78]

Despite the undeniable success of the synthetic approaches described thus far, the general requirement for pre-functionalised substrates represents an important limitation. This reduces the efficiency of such protocols and limits the ring positions that can be arylated to those bearing the reactive functionality. On the other hand, using ubiquitous carbon-hydrogen (C–H) bonds as non-traditional functional groups represents an attractive conceptual alternative for the direct functionalisation of saturated N-heterocycles.[49b,79] This offers huge potential to probe different exit vectors from readily available unsubstituted precursors, allowing access to a large number of isomers and enabling the rapid construction of diverse collections of complex N-heterocycles.

1.3.2 C–H Bonds as Attractive Sites for Functionalisation

Over the past two decades, several strategies have been investigated to directly functionalise C(sp^3)–H bonds on N-heteroaliphatic rings. Most approaches have focused on the functionalisation of C–H bonds α- to the (protected) nitrogen atom, due to their inherent higher reactivity. These bonds are “activated” by the adjacent heteroatom, both for homolytic and

heterolytic cleavage, as evidenced by lower bond dissociation energy (BDE)[80] and pK_a (Figure 1.3).[81] On the other hand, selective functionalisation of unactivated methylene C–H bonds at remote positions from the heteroatom represents a distinct and underexplored challenge.

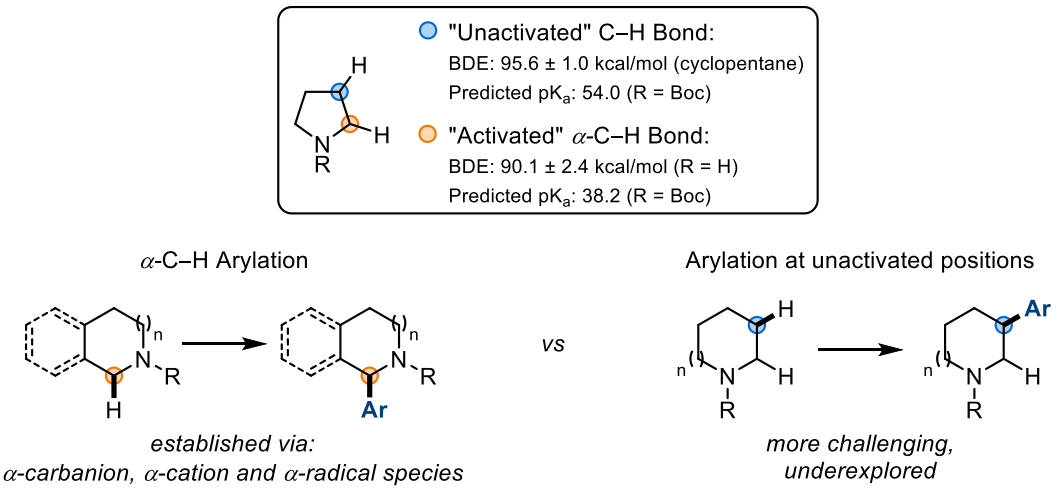
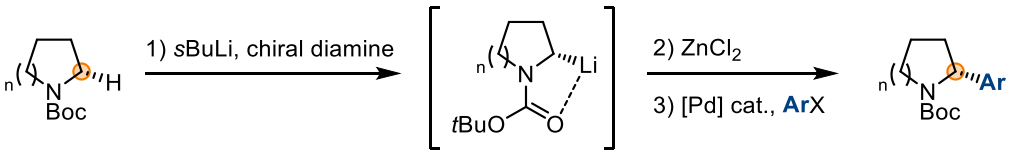


Figure 1.3 Activated *vs* Unactivated C–H bonds for the direct arylation of saturated N-heterocycles.

1.3.2.1 Functionalisation of the α-position to the heteroatom

α-C–H Arylation of saturated N-heterocycles has been achieved exploiting the generation of different reactive species, including α-carbanion, iminium ions and α-radical intermediates.[79]

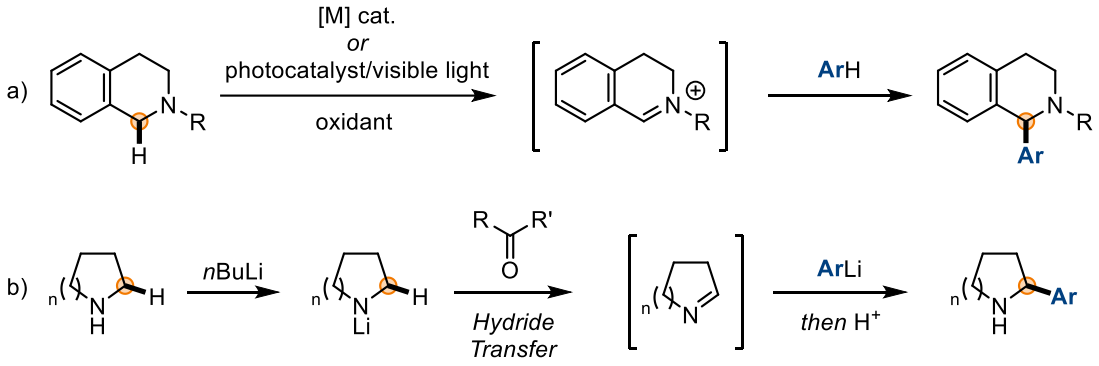
α-Carbanion Intermediate: At the beginning of 1990s, Beak and co-workers described the asymmetric deprotonation of *N*-Boc pyrrolidine with *sec*-BuLi and (–)-sparteine to form a configurationally-stable α-lithiated intermediate.[82] Since this pioneering work, this strategy has been extensively applied to the α-functionalisation of saturated N-heterocycles with various electrophiles.[49b,79] In particular, Campos developed the enantioselective α-arylation of *N*-Boc pyrrolidine, involving lithium-zinc transmetallation and subsequent Pd-catalysed Negishi cross-coupling with aryl bromides (Scheme 1.2).[83,84]



Scheme 1.2 α-C–H Arylation of saturated N-heterocycles *via* lithiation/cross-coupling sequence.

Related conditions were later reported to enable α-C–H arylation of the corresponding piperidine ring.[85] Highly regio- and diastereoselective arylation of substituted *N*-Boc piperidines was also achieved through a similar lithiation/transmetallation/coupling sequence.[86]

α-Cation Intermediate: Cross-Dehydrogenative-Coupling (CDC) has provided a useful strategy for the α-functionalisation of N-heteroaliphatic rings.[49b,79] This involves the generation of an iminium ion intermediate followed by reaction with different nucleophiles. A vast majority of these works has focused on the C(sp^3)–H functionalisation of tetrahydroisoquinolines (THIQ) at the α-benzylic position (Scheme 1.3a). Arylation of these substrates has been demonstrated *via* Fridel-Crafts reaction with electron-rich arenes, in the presence of Cu-, Fe- or V-catalysts and an external oxidant (typically *t*BuO_2H or O_2).[87] Metal-free and photochemical oxidation protocols were also developed enabling Friedel-Crafts arylation of this system.[88,89] Furthermore, the scope of coupling partners in the Cu-catalysed α-arylation of THIQs could also be extended to aryl boronic acids.[90]



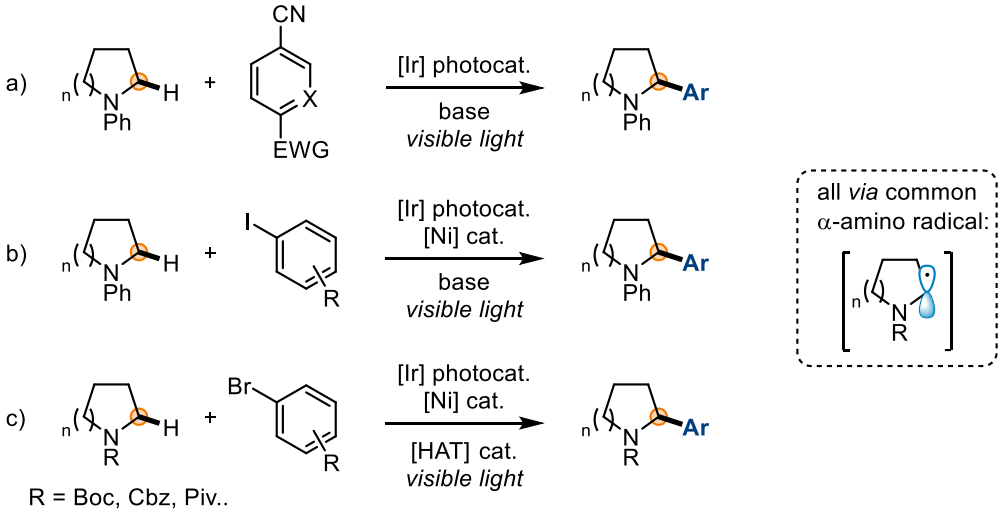
Scheme 1.3 α-C–H Arylation of saturated N-heterocycles *via* a) CDC coupling or b) intermolecular hydride transfer.

Redox-neutral processes have also emerged as an attractive alternative for the generation of iminium species, without the requirement for metal-catalysts or stoichiometric oxidants.[91] This methodology involves hydride transfer to generate the reactive intermediate, followed by intra- or intermolecular nucleophilic trapping. For example, α-arylation of *N*-substituted pyrrolidines and piperidines could be achieved through intramolecular hydride transfer, promoted by catalytic Lewis- or Brønsted acids, followed by reaction with aryl nucleophiles.[92] In addition, Seidel and co-workers demonstrated a novel intermolecular hydride transfer from *N*-deprotonated cyclic amines, using an external carbonyl acceptor (Scheme 1.3b). This formed endocyclic imine intermediates, which provided access to α-arylated unprotected N-heterocycles upon reaction with various organolithium reagents.[93] Very recently, this protocol was also extended to enable β-C–H alkylation, as well as di- and tri-functionalisation of unprotected 6-membered N-heterocycles.[94]

α-Radical Intermediate: The generation of α-amino radicals represents another important approach to functionalise α-C(sp^3)–H bonds in saturated cyclic amines. For instance, Nakamura reported an Fe-catalysed arylation of pyrrolidines and piperidines bearing an *N*-(2-

iodobenzyl) group. This proceeded *via* intramolecular 1,5-hydrogen atom transfer (HAT), followed by coupling with aryl zinc or Grignard reagents.[95]

In 2011, MacMillan reported the first example of photoredox catalysed α-C(sp^3)–H arylation of saturated N-heterocycles (Scheme 1.4a).[96] Oxidation by SET in the presence of an iridium photocatalyst and visible light was suggested to generate an *N*-centred radical cation. Subsequent deprotonation produced the α-amino radical species, which reacted with a radical anion formed from the cyanoarene coupling partner. However, the requirement for an *N*-aryl substituent limits the synthetic applicability of this approach. Very recently, Ellman used similar conditions to achieve α-arylation of poly-functionalised piperidines with very high diastereoselectivity (>95:5 *dr*).[97] Efficient α-C–H arylation was also demonstrated with a diverse range of electrophilic aryl chlorides, through homolytic aromatic substitution.[98]



Scheme 1.4 Strategies for the α-C–H arylation of saturated N-heterocycles involving photoredox-mediated generation of an α-amino radical intermediate.

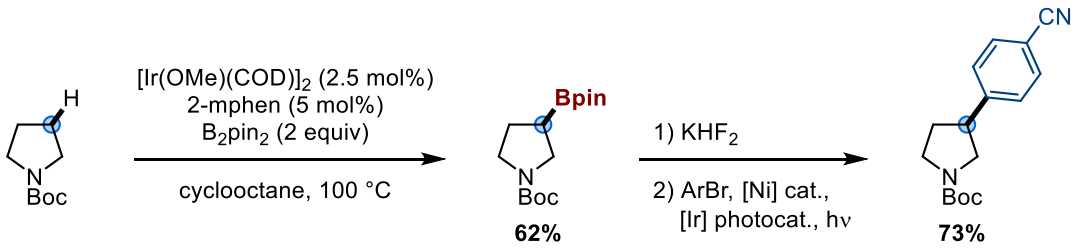
In 2016, Doyle and MacMillan independently reported the combination of Ir-photocatalysis and Ni-catalysed cross-coupling for the α-C–H arylation of N-heteroaliphatic rings with aryl halides.[99,100] In the former case, the α-amino radical was generated through similar Ir-catalysed oxidation/deprotonation of *N*-phenyl cyclic amines (Scheme 1.4b).[99] On the other hand, MacMillan's procedure involved the additional use of a HAT catalyst (3-acetoxyquinuclidine) in combination with Ir- and Ni-catalysis (Scheme 1.4c).[100] Upon oxidation by the excited state of the Ir(III)-photocatalyst, the resulting radical cation was key to generate the α-amino radical by hydrogen atom transfer. Importantly, this allowed the use of easily removable *N*-protecting groups, such as Boc or Cbz.

Finally, photoredox catalysed Minisci reaction has also been reported for the coupling of α-amino radicals in saturated cyclic amines with electron-deficient heteroarenes.[101] Interestingly,

this methodology was shown to be amenable to nanoscale high-throughput experimentation and scale-up using continuous-flow technology, offering high potential for applications in the pharmaceutical industry. However, the requirement for a superstoichiometric amount of cyclic amines remains an important limitation of this protocol.

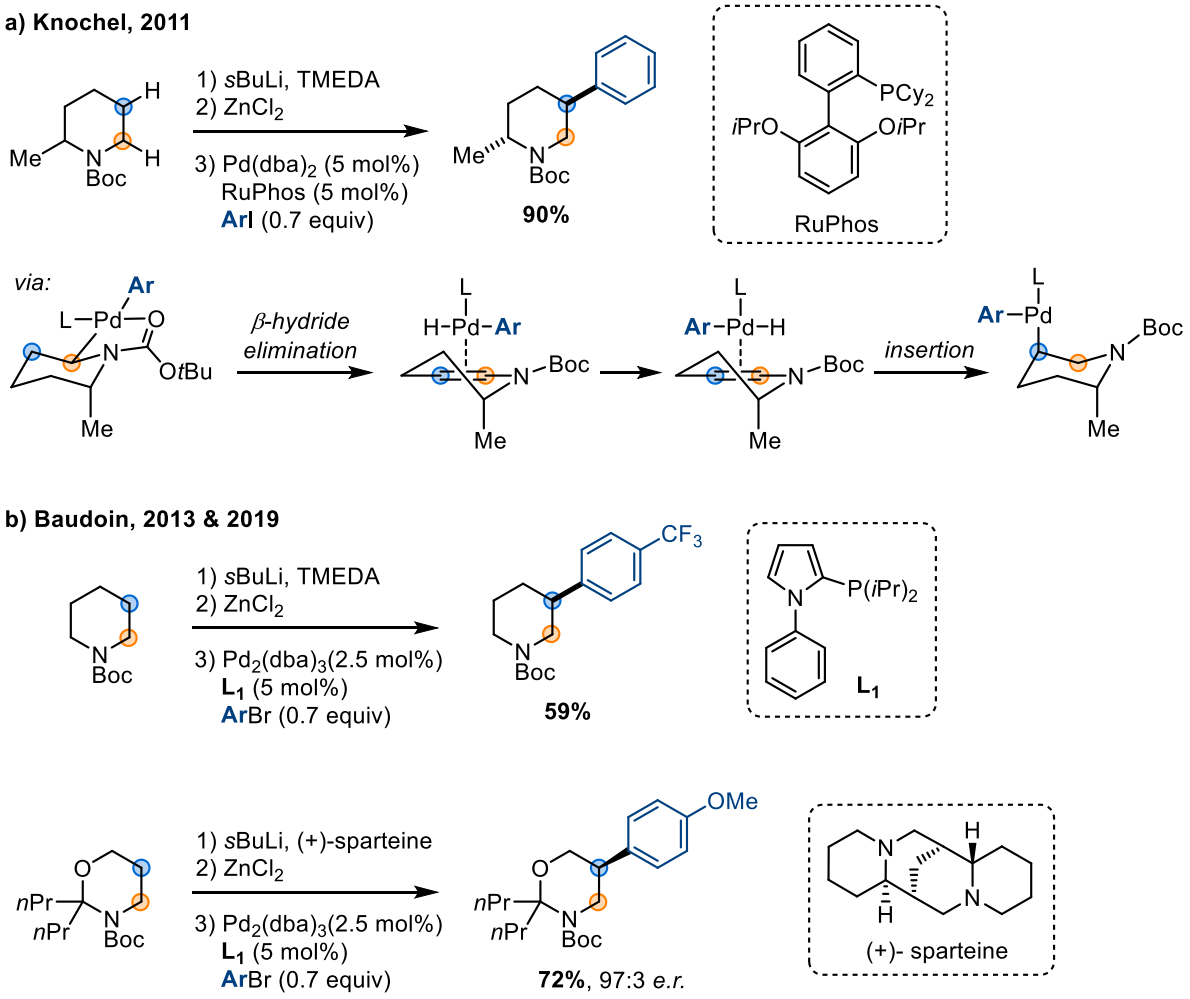
1.3.2.2 Functionalisation at unactivated positions

Although much less explored, the selective C–H functionalisation of unactivated positions on saturated N-heterocycles has recently attracted significant attention. Methods have been reported that allow alkylation,[94,102] oxidation[103] and trifluoromethylation[104] of these less reactive C–H bonds. Very recently, Hartwig described a powerful Ir-catalysed protocol for the C–H borylation of saturated O- and N-heterocycles.[105] In the presence of a uniquely effective 2-methylphenanthroline ligand, these substrates were borylated with high selectivity for the unactivated β-position. Upon installation, the β-boryl group was used as further synthetic handle for functionalisation, including arylation of a pyrrolidine ring (Scheme 1.5).



Scheme 1.5 Ir-catalysed C(sp^3)–H borylation at the β-position of *N*-Boc pyrrolidine.

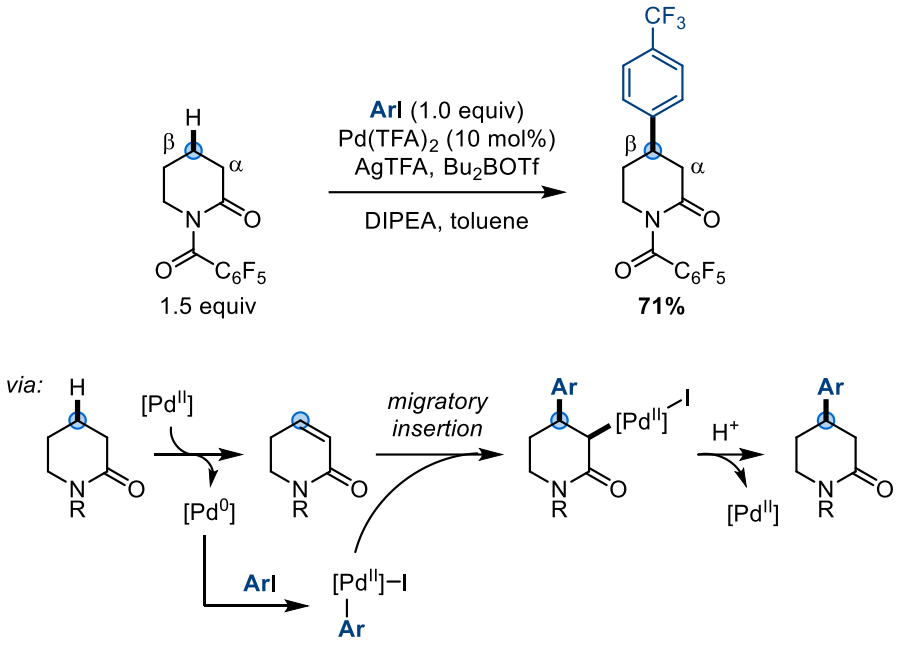
However, strategies for the direct installation of aromatic substituents remain scarce. During their investigations on the diastereoselective α-arylation of piperidine rings, Knochel and co-workers found that treatment of *N*-Boc 2-methyl-piperidine under lithiation/Negishi conditions exclusively formed *trans*-5-arylated products (Scheme 1.6a).[86] This was proposed to proceed through Pd(II) migration from the α- to the β-position, involving initial α-lithiation/transmetallation followed by β-hydride elimination of the Pd moiety. Rotation of the resulting π-complex, followed by migratory insertion, formed a new C–Pd bond at the least hindered β-position. Baudoin later developed a related C–H arylation protocol, where high β-selectivity was achieved using less sterically hindered pyrrole phosphine ligands (Scheme 1.6b).[106] More recently, the same group reported the asymmetric β-arylation of *N*-Boc 1,3-oxazinanes, combining enantioselective α-deprotonation in the presence of a chiral diamine with ligand-controlled stereospecific Pd-migration.[107]



Scheme 1.6 Selective β-C(sp^3)–H arylation of piperidine and 1,3-oxazinane rings *via* α-lithiation, followed by a) substrate-controlled or b) ligand-controlled migratory Negishi cross-coupling.

Finally, Dong recently reported a Pd(II)-catalysed protocol for the β-C(sp^3)–H arylation of *N*-substituted lactams (Scheme 1.7).[108] Pd(II)-catalysed lactam oxidation was proposed to occur in the presence of a boron Lewis acid species. Subsequent Pd(0) reoxidation with aryl iodides was followed by migratory insertion into the resulting lactam enone. Protonation of the corresponding Pd(II)-enolate finally yielded the arylated product.

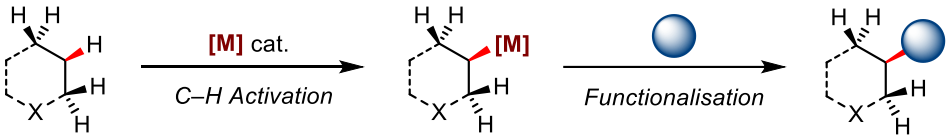
An alternative strategy for the arylation of unactivated C(sp^3)–H bonds in saturated N-heterocycles is represented by the direct C–H functionalisation using transition-metal catalysts. This approach will be the main focus of this thesis and will be discussed in detail in the following section.



Scheme 1.7 Dong's Pd(II)-catalysed β-C(sp^3)–H arylation of lactams with aryl iodides.

1.4 Transition Metal-Catalysed C–H Functionalisation

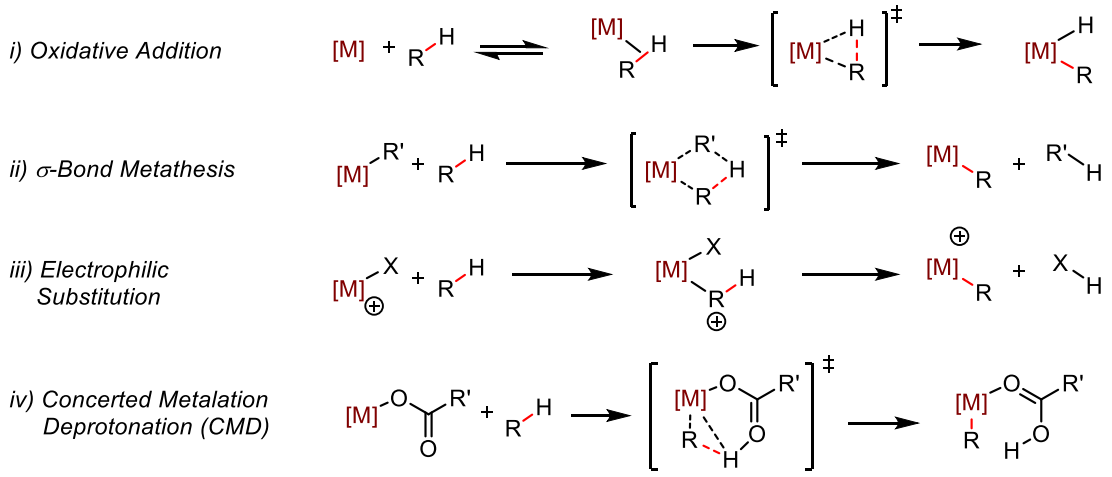
The concept of "transition metal-catalysed C–H functionalisation" has emerged and very rapidly expanded over the last 2 decades, transforming the way organic chemistry disconnections are envisaged.[109] This approach involves the use of a transition metal catalyst to "activate" typically inert C–H bonds, defined here as being through the formation of discrete carbon-metal bonds that does not involve radical, carbanion or carbocation intermediates (Scheme 1.8). The resulting organometallic species can then undergo functionalisation, reacting with various coupling partners to form new C–C or C–heteroatom bonds. As such, this strategy has high potential for the iterative and divergent synthesis of analogues, as well as for the late-stage functionalisation of complex biorelevant compounds.



Scheme 1.8 Schematic representation of transition metal-catalysed C–H functionalisation.

C–H Bond cleavage in the presence of transition metals has been proposed to occur through several mechanistic pathways (Scheme 1.9).[110] These include: *i)* oxidative addition at electron-rich complexes of low-valent late transition metals; *ii)* σ-bond metathesis, prevalent for early transition metals, typically bearing alkyl or hydride ligands; *iii)* electrophilic substitution, observed at electron-deficient late transition metals in strong polar solvents; and *iv)* redox-neutral concerted metalation deprotonation (CMD). The latter has been proposed as the C–H

activation mechanism in several transformations catalysed by Group 8-10 transition metals, including the Pd^{II}-catalytic systems discussed in this thesis (*vide infra*).

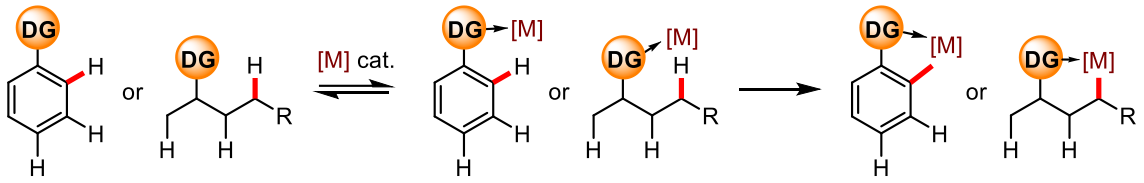


Scheme 1.9 Prevalent mechanisms for organometallic C–H bond activation.

The CMD mechanism involves a highly ordered transition state, in which concerted C–M bond formation and C–H cleavage are assisted by a base, typically carboxylate, carbonate or phosphate.[111] These groups can coordinate to the metal centre either in a mono- or bidentate fashion, allowing both stabilisation of the metal complex and intramolecular (or inner-sphere) deprotonation. In addition, they can also act as external bases, resulting in outer-sphere C–H activation (not shown).[112] A seminal computational study by Davies and Macgregor on the C–H palladation of dimethylbenzylamine suggested the initial formation of an agostic interaction with the Pd centre, which polarises the C–H bond and increases its acidity, prior to carboxylate-assisted CMD.[113]

In order to exploit C–H bond activation in synthetically viable catalytic C–H functionalisation, important challenges need to be overcome. These mainly include the inherent low reactivity of C–H bonds compared to traditional functional groups, and the complex site-selectivity. Given the ubiquity of C–H bonds in organic molecules, achieving efficient discrimination among many positions with similar reactivity is a very challenging task.

Since early 2000s, several strategies have been developed to overcome these issues and achieve regioselective transformations, involving in particular the use of directing groups (DGs).[114] These are Lewis-basic groups, able to coordinate to the metal centre allowing the catalyst to be positioned in close proximity to the desired C–H bond (Scheme 1.10). This allows C–H activation to occur at the site of interest, forming a thermodynamically stable metallacyclic intermediate.



Scheme 1.10 Regioselective C–H functionalisation using directing groups (DG).

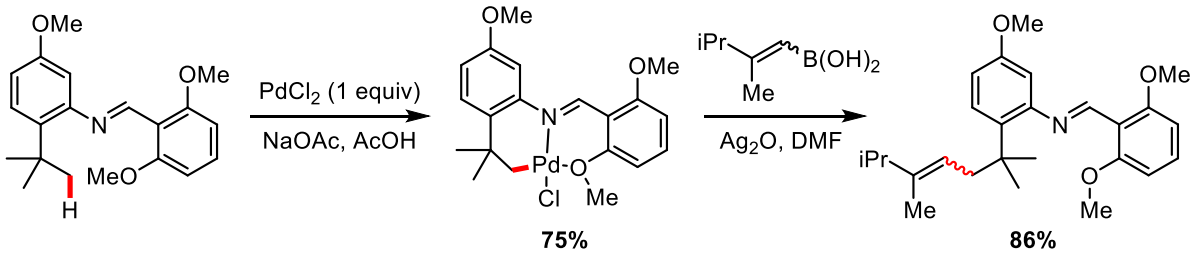
The directing groups approach has enabled huge progress in the catalytic C–H fuctionalisation of both aromatic and aliphatic substrates. C(sp^2)–H functionalisation of (hetero)arenes have been extensively investigated with a wide range of DGs and transition metals, allowing various functional groups to be installed *ortho*- to the directing auxiliary.[114,115] Furthermore, recent advances using bespoke DGs have enabled remote functionalisation of *meta*- and *para*-positions, although this will not be discussed here.[116]

On the other hand, the catalytic C–H functionalisation of aliphatic substrates is less well-developed and has taken significant strides only more recently.[117] This is likely due to additional problems of regio- and stereocontrol, as well as to the lower reactivity of C(sp^3)–H bonds. These are less acidic than their aromatic counterparts and lack suitable orbitals (*e.g.* π or π^*) that can readily interact with the metal centre. Important advances in this field have mainly relied on the use of removable directing groups and will be described in the next section. Other powerful strategies for selective C(sp^3)–H functionalisation, including intramolecular C–H activation of organohalide substrates,[118] catalyst-controlled C–H insertion of metal carbenes,[119] as well as methods that exploit minute differences in C–H bond reactivity[120] will not be discussed.

1.4.1 C(sp^3)–H Functionalisation Using Removable Directing Groups

A broad range of structurally different directing groups have been used to enable intermolecular C(sp^3)–H functionalisation. These can vary extensively in size and design, but generally contain one (monodentate) or two (bidentate) coordinating functionalities (*e.g.* nitrogen and sulfur moieties). Although methods have been developed using earth-abundant metals (Fe, Co, Ni, Cu), the directed functionalisation of C(sp^3)–H bonds has mainly relied on the use of noble transition metals, and of palladium in particular.[117,121]

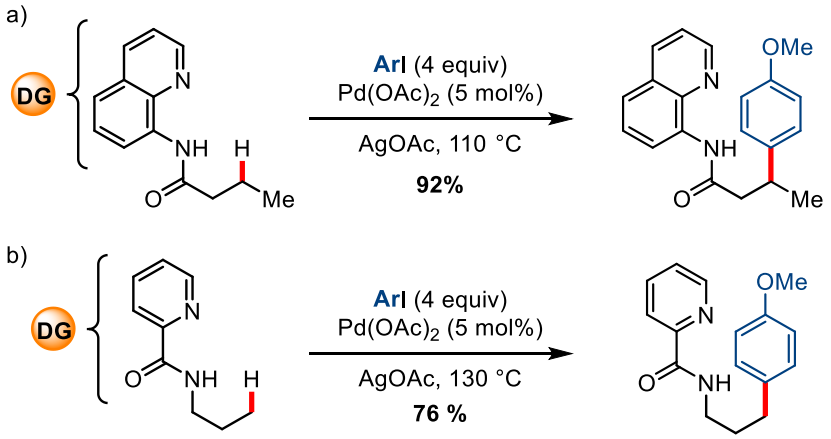
Very early examples of C(sp^3)–H functionalisation involved the use of stoichiometric amounts of palladium.[122] In a seminal example, Sames and co-workers applied this concept to the synthesis of Teleodocin B-4's core (Scheme 1.11).[122a] A bidentate imine-methoxy directing group was used for C(sp^3)–H activation on the adjacent *t*-butyl group in the presence of stoichiometric $PdCl_2$. Isolation of the resulting palladacycle was followed by treatment with a vinyl boronic acid to produce the alkenylated product in 86% yield.



Scheme 1.11 Stoichiometric C(sp^3)–H functionalisation in the synthesis of Teleodocin B-4's core.

Subsequent efforts to develop catalytic transformations have demonstrated the use of N-heterocycles (*e.g.* pyridine) as monodentate non-removable DGs for C–C bond formation.[123]

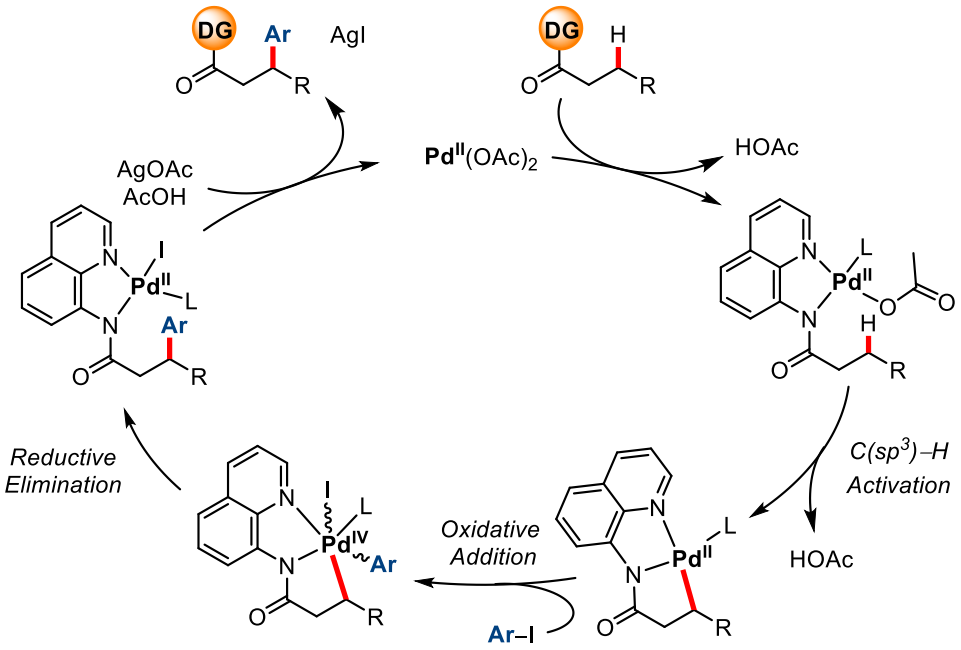
A major breakthrough in the field was reported by the group of Daugulis in 2005, describing the first example of catalytic intermolecular arylation of unactivated C(sp^3)–H bonds using removable DGs.[124] β-Arylation of carboxylic acid derivatives was achieved using 8-aminoquinoline (AQ) amide as directing group in combination with Pd-catalysis and excess silver(I) acetate (Scheme 1.12a). Similar conditions were also effective in the γ-C–H arylation of amine derivatives, using an inverted picolinamide (PA) auxiliary. The bidentate chelation mode of these DGs, involving the weakly acidic amide NH and the distal quinoline or pyridine nitrogen, was critical for the stabilisation of high-valent Pd intermediates and for the success of the reaction.



Scheme 1.12 Daugulis' bidentate auxiliary approach for C(sp^3)–H arylation using a) 8-aminoquinoline amide, and b) picolinamide DGs.

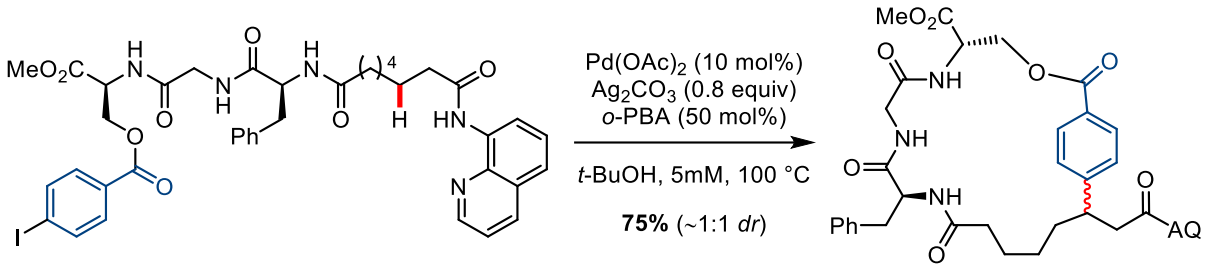
The reaction was proposed to proceed *via* a Pd^{II}/Pd^{IV} catalytic cycle (Scheme 1.13).[124,125] Initial coordination to the bidentate DG is followed by C–H activation, likely through carboxylate-assisted CDM,[126] to form a 5,5-bicyclic palladacyclic intermediate. Subsequent oxidative addition with the aryl iodide was proposed to generate a Pd(IV) intermediate,[127] that can undergo reductive elimination to form the new C–C bond. Final protodemetalation and halide abstraction by the silver salt liberate the product and regenerate the active catalyst. This

mechanistic proposal was supported by the isolation and characterisation of a related Pd(IV) complex, obtained by treating an AQ-bound cyclopalladated intermediate with Br_2 at –78 °C (a more detailed discussion will be given in section 5.1).[125]



Scheme 1.13 Proposed Pd^{II}/Pd^{IV} redox cycle for C(sp^3)–H arylation directed by 8-AQ auxiliary.

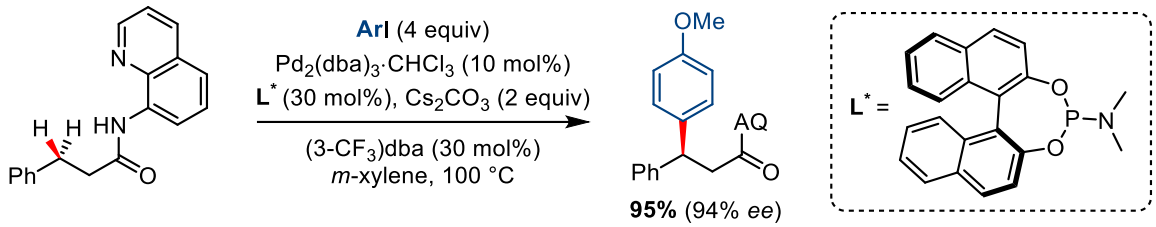
Since this seminal work, the use of bidentate directing groups has expanded tremendously, providing a robust and efficient strategy for selective C(sp^3)–H functionalisation.[128] Daugulis' 8-aminoquinoline has been shown to be a powerful and versatile directing group in several transformations. For instance, this has enabled the β-arylation of *N*-protected aminoacids,[129] cyclopropanes[130] and other cycloalkanes,[131,132] and has been successfully applied to the synthesis of several natural products.[129a,129c,131] Chen recently developed an 8-AQ-assisted intramolecular C(sp^3)–H arylation protocol to access cyclophane-braced peptide macrocycles, highlighting the ability of this DG to coordinate the metal catalyst also in the presence of many other competing polar functionalities (Scheme 1.14).[133]



Scheme 1.14 Chen's macrocyclization *via* 8-AQ-directed intramolecular C(sp^3)–H arylation.

The mechanism by which Pd-catalysed 8-AQ-assisted reactions can occur is not limited to Pd^{II}/Pd^{IV} catalytic cycles. For example, an alternative Pd^0/Pd^{II} pathway was demonstrated in

the enantioselective arylation of benzylic methylene positions, using a chiral BINOL-phosphoramidite (P^{III}) ligand (Scheme 1.15).[134] In this case, oxidative addition of the aryl halide to Pd^0 was proposed to occur prior to enantioselective C−H activation (*vide infra*).



Scheme 1.15 Pd(0)-catalysed enantioselective benzylic C–H arylation.

Inspired by the success of Daugulis' 8-AQ and PA auxiliaries, different bidentate DGs have been developed, typically involving an amide linkage.[128] Important auxiliaries for the C(sp^3)–H arylation of carboxylic acids include 2-pyridylisopropylamine and related DGs (a),[135] triazolyldimethylmethylamine (b),[136] oxazoline amine (c),[137] 2-methylthioaniline (d),[125,138] 2-sulfanylaniline (e),[139] and many others (Figure 1.4).[140,141]

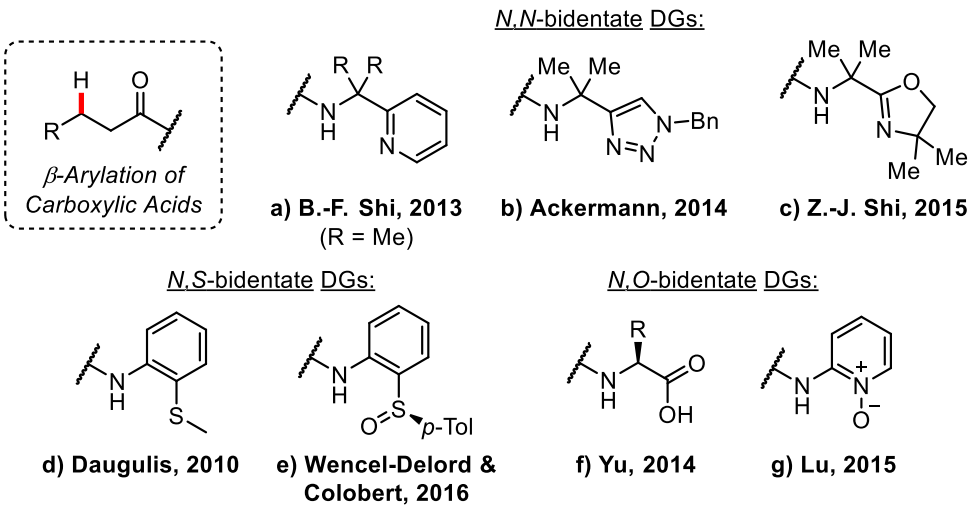


Figure 1.4 Bidentate directing groups used in the C(sp^3)–H arylation of carboxylic acid derivatives.

In addition, various amide-linked bidentate DGs have enabled the γ-arylation of amine derivatives.[124,142] More recently, β- and γ-arylation of aliphatic alcohols have also been demonstrated through the use of aldoxime-based bidentate DGs.[143]

Despite the success of these directing auxiliaries, their removal after C–H functionalisation can often be challenging mainly due to the strong amide bond. Nonetheless, aminoquinoline cleavage has been demonstrated under a variety of hydrolytic and oxidative conditions to uncover acid, amide or ester functionalities (for a more detailed discussion see section 3.5).[125,129c,131,144,145] Furthermore, recent advances in the field have uncovered the use of

transient bidentate DGs, which typically involve a reversible imine linkage to avoid installation and removal of covalent auxiliaries.[146] However, this approach will not be discussed here.

Monodentate DGs, such as perfluorinated aniline amide and trifluoromethyl-sufonamide, have also been extensively used for the functionalisation of unactivated C(sp^3)–H bonds.[117a,147] These weakly-coordinating auxiliaries are typically used in combination with fine-tuned ligands, designed and optimised for different substrates and reaction classes, to stabilise the metal centre and assist in the C–H activation step. Bespoke ligands have enabled very powerful transformations, including enantioselective variants.[148] However, the high ligand specificity represents an important limitation to the general applicability of the monodentate DG approach. Since pioneering work by Yu on the Pd-catalysed C–H arylation of pivalic acid,[149] using the free acid as DG, this strategy has been successfully applied to the functionalisation of methyl and methylene C(sp^3)–H bonds, through both Pd^{II}/Pd^{IV} and Pd^{II}/Pd^{0} catalysis (*vide infra*).[150] Very recently, native carboxylic acid and amine functionalities have been shown as suitable monodentate DGs for aliphatic C–H arylation, with no requirement for exogeneous directing auxiliaries.[151,152] To date, however, the scope of the latter transformations is mainly limited to methyl, cyclopropyl and cyclobutyl C(sp^3)–H bonds.

The directing group strategy has been successfully applied to the C(sp^3)–H arylation of saturated N-heterocycles, despite the additional challenges represented by the protected nitrogen atom. This can compete with the DG and result in unproductive catalyst coordination. The most relevant examples of N-heterocycle C(sp^3)–H arylation will be presented in the next section, classified based on the ring position being functionalised.

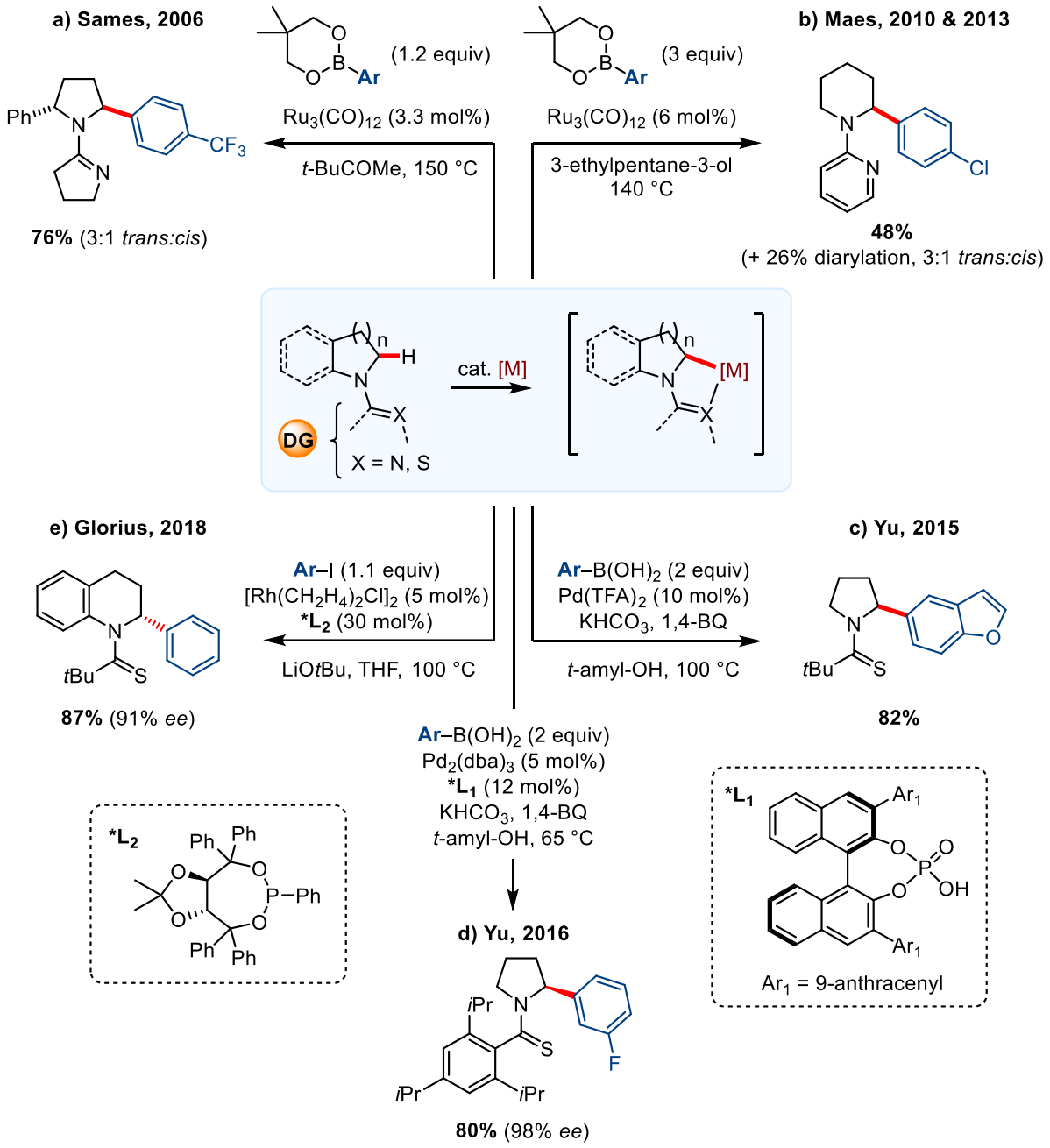
1.4.2 Directed C(sp^3)–H Arylation of Saturated N-Heterocycles

A comprehensive review on directed C(sp^3)–H functionalisation of saturated heterocycles up to the end of 2018 can be found in *Synthesis*.[153]

1.4.2.1 α-C(sp^3)–H Arylation using N-linked directing groups

Most of the methods reported to date have focused on the functionalisation of the activated α-C(sp^3)–H bond with various noble metal catalyst (Rh, Ru and Pd).[153] This has typically been achieved using an *N*-linked monodentate directing group to form a 5-membered metallacycle intermediate at the α-position (Scheme 1.16).

The first example of α-C–H arylation on pyrrolidine rings was reported by Sames in 2006, using Ru catalysis in combination with an amidine DG (Scheme 1.16a).[154] In this case, Ru(0) oxidative addition into the α-C–H bonds was followed by transmetallation with the arylboronate coupling partner. The arylated product was then yielded after final reductive elimination.

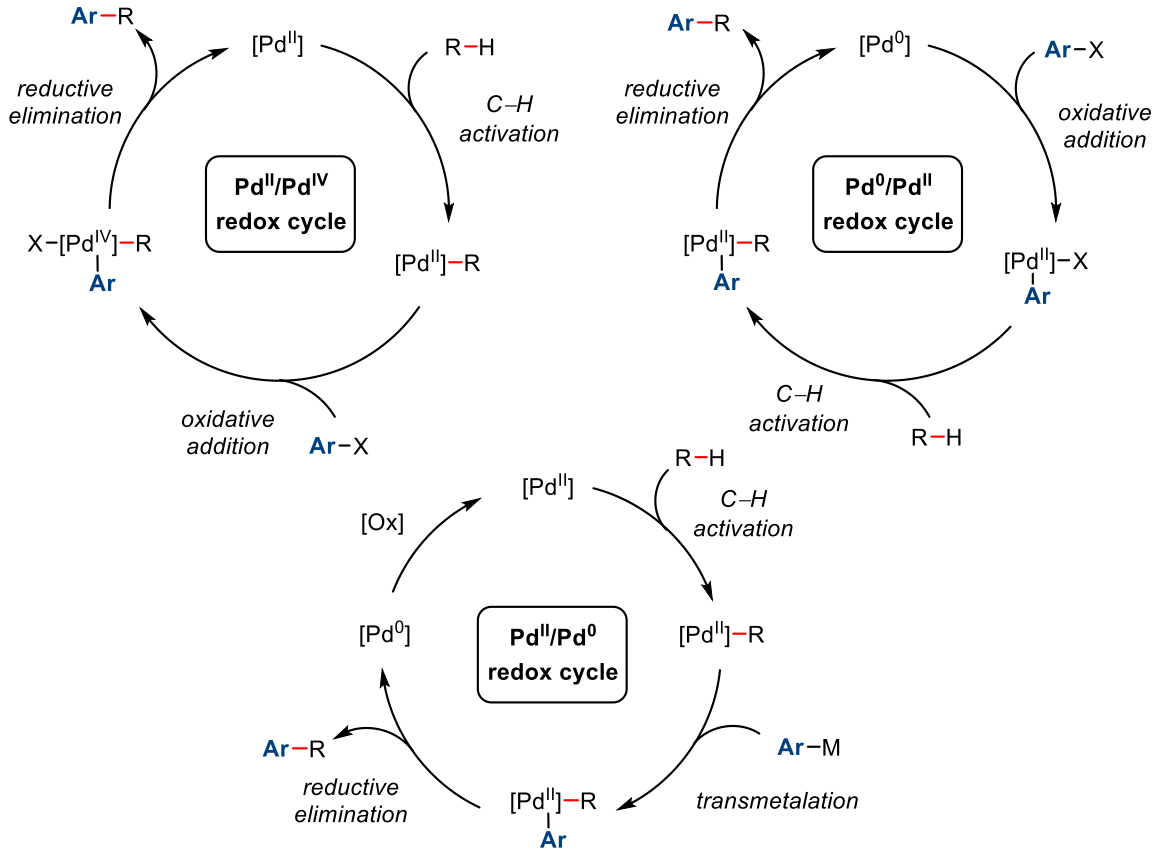


Scheme 1.16 α-C(sp^3)–H arylation of saturated N-heterocycles using *N*-linked directing groups.

However, very poor selectivity for mono- *vs* bis-arylation was obtained with unsubstituted substrates, and only low to moderate diastereoselectivity (*trans:cis*) was observed in case of disubstitution. Later Maes, extended this work to the 6-membered piperidine ring, using an *N*-2-pyridinyl DG, with similar selectivity outcomes (Scheme 1.16b).[155]

In 2015, Yu reported the first example of Pd-catalysed α-C–H arylation of N-heteroaliphatic rings.[156] The use of an *N*-thiopivaloyl auxiliary enabled efficient arylation of 5-, 6- and 7-membered rings with a broad range of arylboronic acids (Scheme 1.16c). In contrast to previous Ru-catalysed approaches, high mono-selectivity and *trans*-diastereoselectivity (for

disubstituted derivatives) were achieved under these conditions. The same strategy also enabled a powerful enantioselective variant, using a chiral phosphoric acid and a bulkier thioamide DG (Scheme 1.16d).[157] The reaction was proposed to proceed through a Pd^{II}/Pd^{0} redox cycle. In comparison with Pd^{II}/Pd^{IV} and Pd^{0}/Pd^{II} mechanistic scenarios, this strategy critically relies on the use of an external oxidant (*e.g.* 1,4-benzoquinone) to regenerate the active Pd(II) species after CMD, transmetallation and reductive elimination (Scheme 1.17).



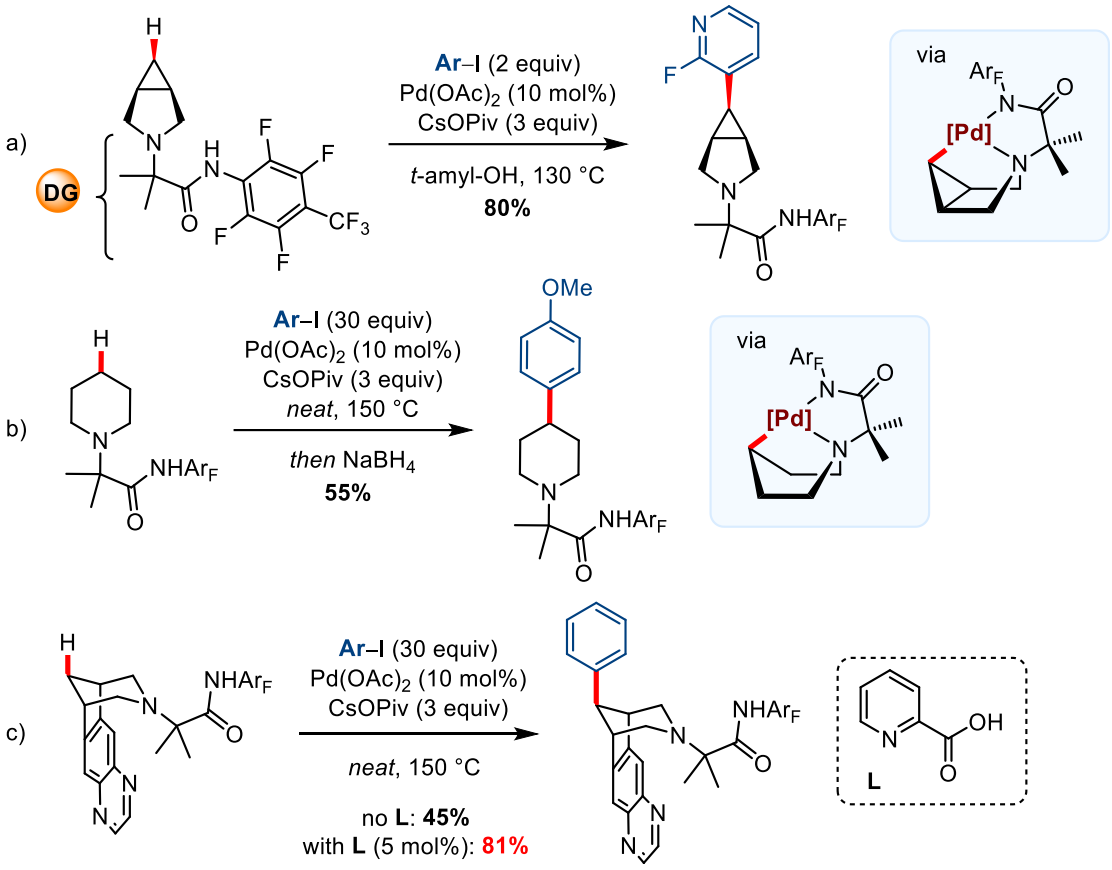
Scheme 1.17 Schematic comparison of Pd^{II}/Pd^{IV}, Pd^{0}/Pd^{II} and P^{II}/Pd^{0} catalysis for C–H arylation.

More recently, the use of *N*-thioamide DGs has been demonstrated in other enantioselective protocols. Excellent asymmetric induction was achieved under Pd^{II}/Pd^{0} catalysis using a chiral Co(III) anionic complex in combination with a chiral phosphoramidite ligand.[158] Furthermore, enantioselective α-C–H arylation of THIQ and other N-heterocycles with aryl iodides was reported using a Rh(I)-precatalysts and a chiral phosphonite ligand (Scheme 1.16e).[159]

1.4.2.2 Remote C(sp^3)–H arylation enabled by N-linked directing group

In addition to the methods described thus far, *N*-linked directing groups have also been used to enable C–H arylation at remote unactivated ring positions. In 2016, Sanford reported a Pd-catalysed protocol for the transannular C(sp^3)–H arylation of fused bicyclic N-heterocycles with aryl iodides (Scheme 1.18a).[160] The use of a bidentate DG, incorporating the nitrogen atom of the heterocycle, was crucial for the success of this challenging transformation. In particular,

the DG was proposed to position the Pd(II) catalyst in close proximity to the distal C(4)–H bond in a boat-like conformation. Extensive mechanistic studies confirmed this proposal, suggesting a Pd^{II}/Pd^{IV} catalytic cycle, which featured a turnover-limiting CMD step occurring in boat conformation.[161] Remarkably, this protocol could be extended to simple piperidine derivatives, although this required higher temperature and a very large excess of aryl iodide (Scheme 1.18b).[160] This was ascribed to the unfavourable chair-boat isomerisation necessary for the desired remote C–H activation. Furthermore, competing formation of aminal by-products was observed, and a reductive work-up was used to maximise the yield of the desired product.



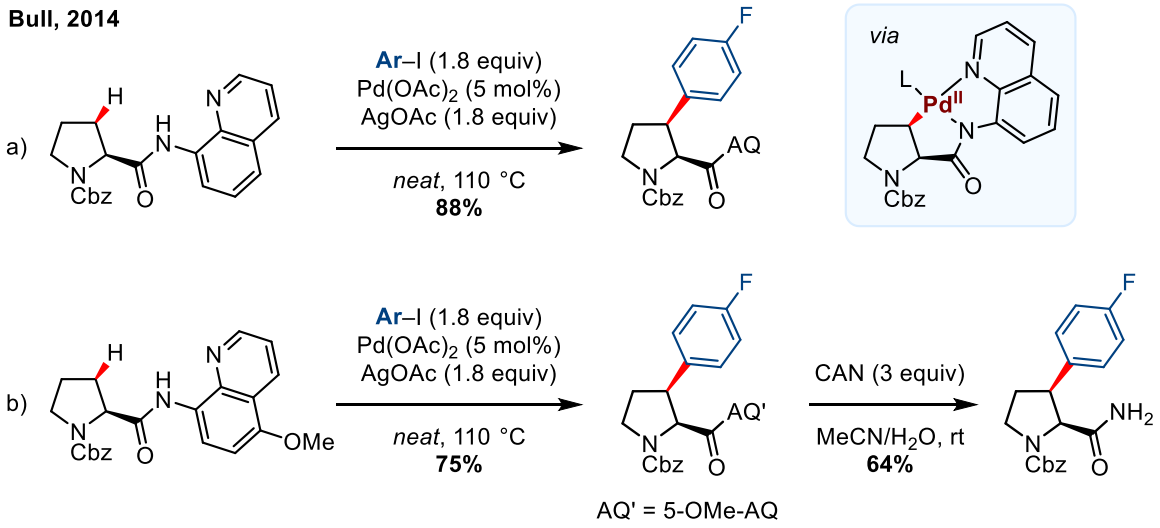
Scheme 1.18 Sanford's transannular remote C(sp^3)–H arylation of saturated N-heterocycles.

More recently, Sanford found that simple pyridine- or quinoline-carboxylic acid ligands improved the efficiency of the transannular C–H arylation.[162] By avoiding catalyst deactivation pathways, these ligands provided higher yields and reaction rates, and resulted in a broader substrate scope (Scheme 1.18c).[162,163] The transannular arylation was also recently applied to the synthesis of a small library of fragment-like molecules highlighting the potential utility of this transformation in drug discovery.[164]

1.4.2.3 C(sp^3)–H arylation at unactivated positions using C-linked directing groups

Despite the advances outlined in the previous section, functionalisation of unactivated C–H bonds in saturated N-heterocycles has been significantly less explored than the activated α-position. Examples to date have mainly focused on Pd-catalysis in combination with *C*-linked mono- or bidentate directing groups.[153] Depending on the position of the DG, different substitution patterns were obtained through regioselective β- or γ-functionalisation of carboxylic acid, amine and (most recently) alcohol derivatives.

In 2014, Bull reported the first example of Pd-catalysed C–H arylation of *L*-proline derivatives with aryl iodides.[165] Daugulis' 8-aminoquinoline was installed at C(2) through amide bond formation. This enabled C(sp^3)–H arylation at the unactivated 3-position *via* a Pd^{II}/Pd^{IV} catalytic cycle (Scheme 1.19a). The reaction was found to be highly diastereoselective for the *cis*-isomer, likely because of the formation of a strained 5,5,5-tricyclic fused palladacycle intermediate. This proceeded with complete retention of the enantiomeric excess of the starting proline amide, affording enantiopure *cis*-2,3-disubstituted products. Independent deuteration studies on the same substrate supported this proposal for a preferential C–H activation event *cis*- to the directing auxiliary.[166] The choice of *N*-protecting group was critical for the reaction, with *N*-Cbz providing the best results. On the other hand, *N*-Boc protected proline was much less reactive and required more forcing conditions.[167,168]



Scheme 1.19 Pd-catalysed C(3)–H arylation of proline derivatives with a) AQ or b) 5-OMe-AQ directing groups at C(2). Products isolated as single enantiomers (> 98% *ee*) and *cis*-diastereomers.

Due to the high steric congestion around the amide bond in the arylated products, 8-AQ cleavage was unsuccessful under several hydrolytic conditions. However, 5-methoxy-8-aminoquinoline amide, originally developed by Chen,[144c] was found to be similarly effective in the reaction and was more easily cleaved by treatment with ceric(IV) ammonium nitrate (CAN,

Scheme 1.19b). Subsequent Cbz removal afforded arylated NH proline amides that well-fit fragment-like criteria (see section 1.2.1.3). Furthermore, the utility of this transformation in medicinal chemistry projects was recently highlighted in the synthesis of antagonists for ionotropic glutamate receptors.[169]

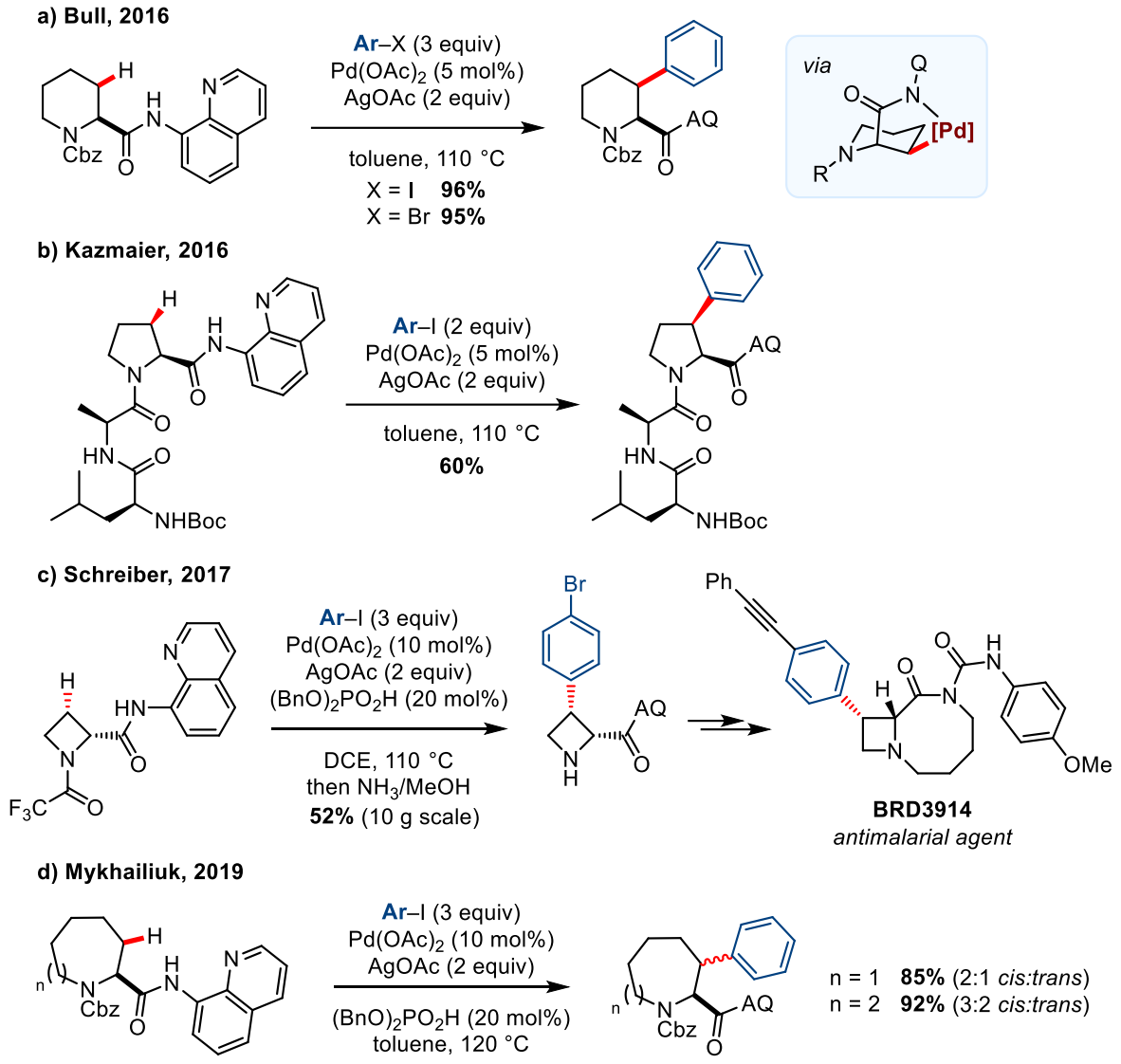
Since this original work, the C–H arylation of various saturated N-heterocycles has been investigated, focusing prevalently on C(3)–H functionalisation using the 8-AQ auxiliary at C(2). Related conditions were used in most cases, typically involving catalytic $Pd(OAc)_2$, aryl iodides and stoichiometric silver(I) salts.[153]

In 2016, Bull reported the directed C(3)–H arylation of piperidine-2-AQ amides (Scheme 1.20a).[167] The higher reactivity observed for the 6-membered ring enabled the use of both *N*-Cbz and *N*-Boc protecting groups. In addition, aryl bromides were also found as suitable coupling partners. In contrast to the corresponding 6-membered oxygen-heterocycles, featuring more variable stereochemical outcome,[167,170] excellent *cis*-selectivity was invariably observed for piperidine C(3)–H arylation. Despite the higher flexibility compared to the 5-membered pyrrolidine ring, the high *cis*-diastereoselectivity likely derived from the *N*-carbamate group forcing the DG in an axial position to minimise 1,3-allylic strain.[171]

Wu independently reported similar conditions for piperidine C(3)–H arylation and applied this to the synthesis of (–)-preclamol, a dopaminergic autoreceptor agonist.[172] Furthermore, Kazmaier demonstrated the C(3)–H arylation of pyrrolidine and piperidine cores in small di- and tripeptides using a similar Pd-catalysed approach (Scheme 1.20b).[173]

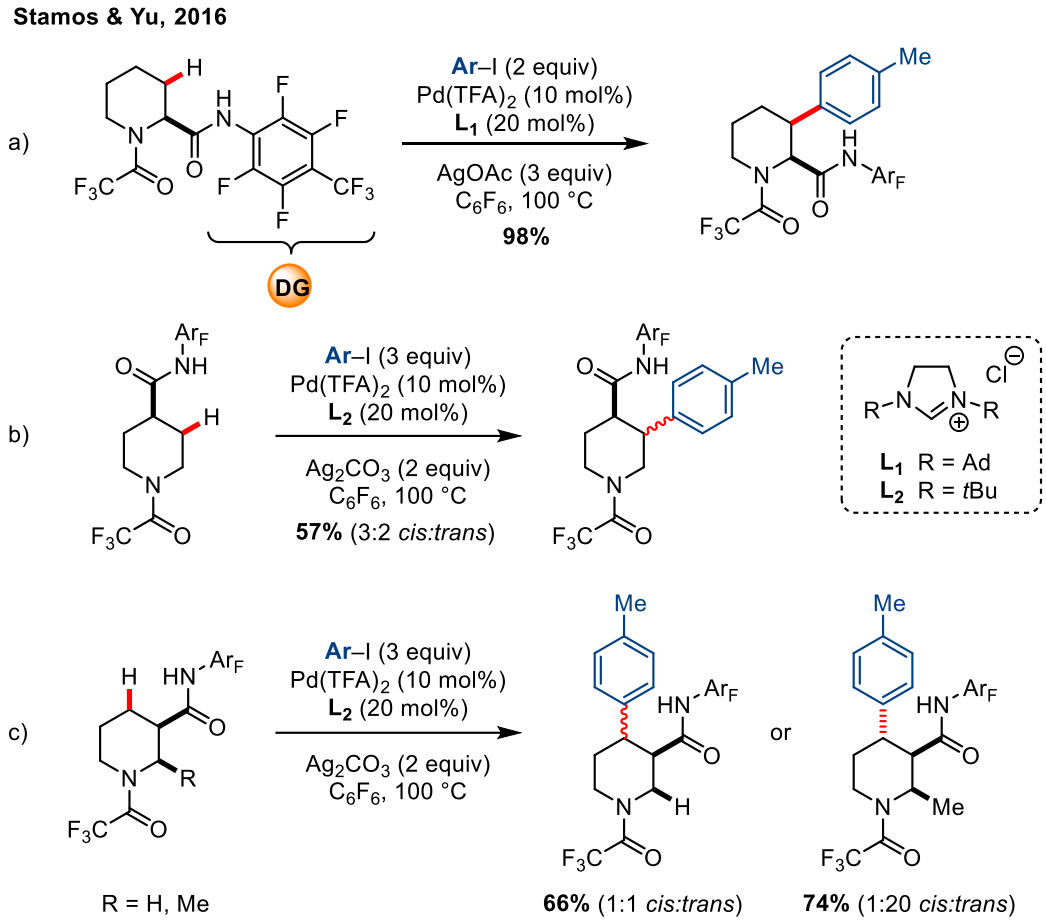
Later Schreiber extended the scope of 8-AQ-assisted C(3)–H arylation to pyroglutamic acid[174] and *N*-trifluoroacetyl azetidine derivatives.[175] In the latter case, the addition of a phosphate ester additive was key to facilitate the CMD step on the strained 4-membered ring, and this was used to streamline the synthesis of a potent azetidine-containing antimalarial agent (Scheme 1.20c).[175] More recently, this strategy has been applied to the synthesis of structurally diverse azetidines with antimalarial activity,[176] and to the preparation of a DNA-encoded library (DEL) containing chiral 2,3-disubsituted azetidines and pyrrolidines.[177]

In 2019, Mykhailiuk investigated in detail the effect of different substituents and conformational changes on pyrrolidine C(3)–H arylation.[178] In particular, aryl- and alkyl-substituents at C(4) and C(5) positions resulted in a slower C–H arylation, but this could be overcome by using a $(BnO)_2PO_2H$ additive. On the other hand, *trans*-C(3)-substituents, EWG groups such as fluorine, and conformational restrictions drastically hampered the reactivity. Furthermore, the scope of the reaction was extended to 7- and 8-membered rings. These could be arylated at C(3) in high yields, albeit with scarce diastereoselectivity due to the higher conformational flexibility (Scheme 1.20d).[178]



Scheme 1.20 8-AQ-assisted Pd-catalysed C(3)–H arylation of saturated N-heterocycles.

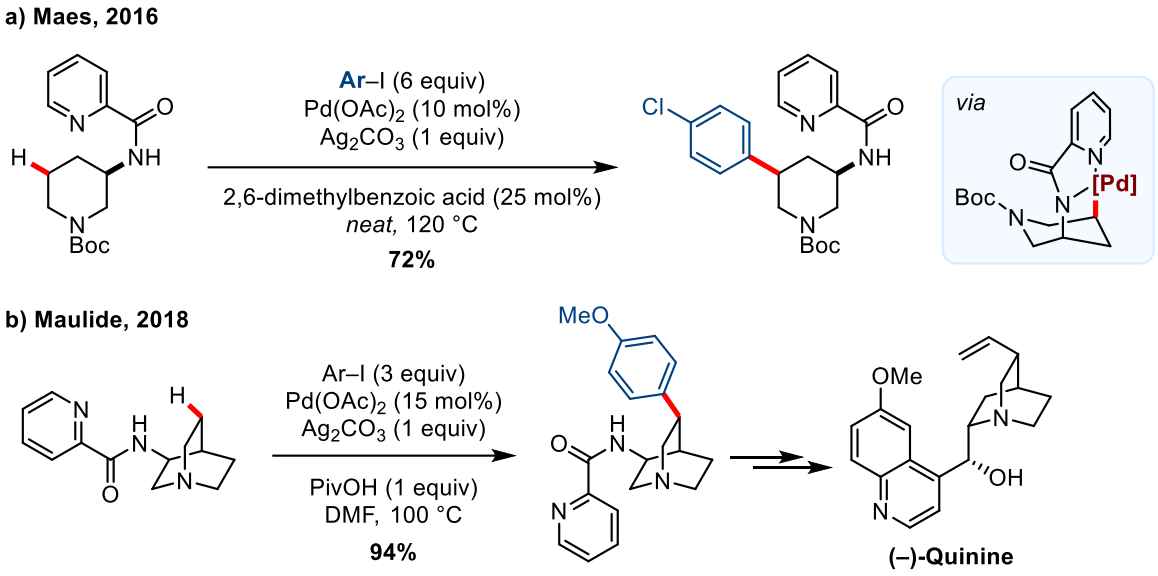
Apart from the 8-aminoquinoline, few other directing groups have been investigated in the C(sp^3)–H arylation of saturated N-heterocycles at unactivated positions. In 2016, Stamos and Yu developed an important alternative approach for the Pd-catalysed C(3)–H arylation of piperidine rings.[179] This involved the use of a monodentate amide DG at C(2) in combination with a bulky NHC ligand, and was similarly proposed to proceed through a Pd^{II}/Pd^{IV} mechanism (Scheme 1.21a). Few examples of piperidine C–H arylation were also described using C(3)- and C(4)-linked directing groups. This allowed the aromatic substituent to be installed with high monoselectivity at the 4- or 3-position, β- to the respective DG (Scheme 1.21b and c). Interestingly, when a C(3)-auxiliary was used, the 4-position was selectively arylated over the activated C(2)–H bond (Scheme 1.21c). This result, observed also for the corresponding tetrahydropyran derivative, was tentatively ascribed to the heteroatom lone pair hindering the formation of a partial negative charge on the α-carbon during C–H activation.



Scheme 1.21 Use of monodentate amide DG in the Pd-catalysed C–H arylation at unactivated positions on *N*-trifluoroacetyl piperidine derivatives.

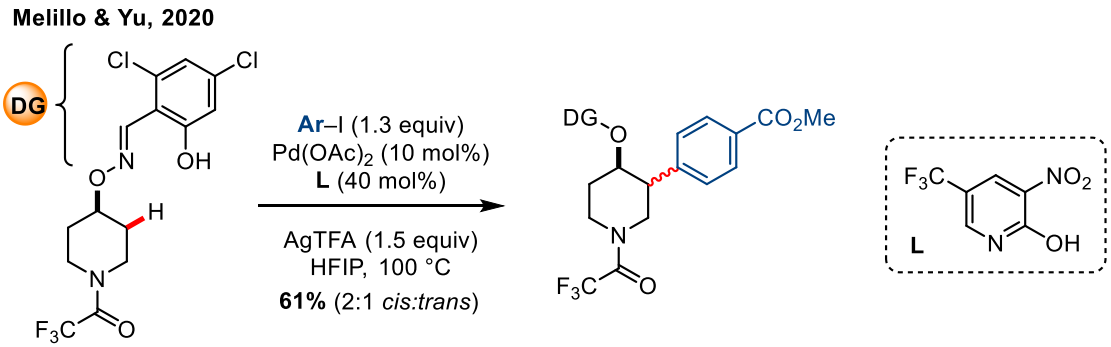
Despite providing the first example of C–H arylation of saturated N-heterocycles at positions different from C(3), this resulted in lower yield and much poorer stereoselectivity (*cis:trans*), compared to the corresponding C(3)–H arylation. In fact, high *trans*-diastereoselectivity was only obtained when the system was biased by the presence of a pre-installed *cis*-substituent at C(2) (Scheme 1.21c). In addition, no example of pyrrolidine C–H arylation with a C(3)-DG was reported.

At a similar time, Maes described the C(5)–H functionalisation of *N*-Boc piperidine-3-amine, using a picolinamide (PA) auxiliary and Pd-catalysis.[180,181] Arylation occurred γ- to the native amine functionality, *via* formation of a bridged 5-membered palladacycle intermediate, and proceed with high *cis*-diastereoselectivity (Scheme 1.22a). A similar approach was more recently developed by Maulide to achieve regio- and stereoselective C–H arylation of the quinuclidine core, as part of the total synthesis of (–)-quinine alkaloid and related arylated analogues (Scheme 1.22b).[182]



Scheme 1.22 PA-assisted Pd-catalysed C–H arylation of piperidine and quinuclidine rings.

Finally, Melillo and Yu most recently reported the use of an aldoxime bidentate DG for the β-arylation of methylene C(sp^3)–H bonds in aliphatic alcohols, including a few examples of saturated N-heterocycles (Scheme 1.23).[143a]



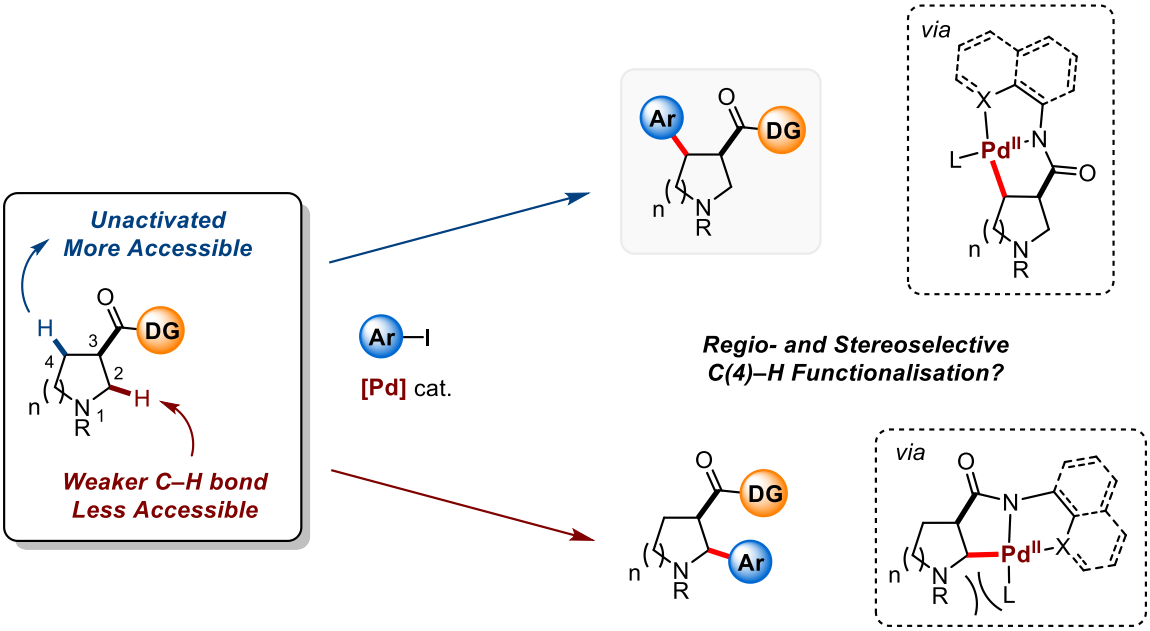
Scheme 1.23 Pd-catalysed β-C–H arylation of N-heterocyclic alcohol derivatives.

In summary, the catalytic C(sp^3)–H functionalisation of N-heteroaliphatic rings has generated significant interest in recent years. The directed Pd-catalysed C–H arylation of unactivated positions has been successfully used to access N-heterocycles with various substitution patterns and stereochemistry that would be challenging to prepare by other methods. Until late 2016, when the research described in this thesis started, such studies had mostly focused on C(3)–H arylation using an AQ bidentate auxiliary. In addition, no example of pyrrolidine arylation at the unactivated 4-position had been reported, despite such transformation would allow access to attractive derivatives for pharmaceutical screenings. Furthermore, apart from a single example of piperidine C(4)–H arylation reported by Yu (Scheme 1.21 c),[179] there had been no study on N-heterocycles which pose a regioselectivity question with β-hydrogens in different environments.

2. Project Aims

The research in this thesis aims at developing an efficient Pd-catalysed C(4)–H functionalisation method to access arylated pyrrolidines and piperidines as valuable fragments and building blocks for drug discovery.

The use of a C(3)-linked bidentate DG was envisaged to open underexplored synthetic opportunities and access 3,4-disubstituted derivatives with defined *cis*-stereochemistry. However, this poses a challenging regioselectivity question with both C(2)–H and C(4)–H bonds, β- to the DG, being available to undergo functionalisation through formation of 5-membered palladacycle intermediates (Scheme 2.1). The C(2)–H bond, electronically activated by the adjacent heteroatom, is more sterically hindered by the *N*-protecting group. On the other hand, the C(4)–H bond is relatively unactivated, but more sterically accessible.



Scheme 2.1 Regio- and stereoselective C–H arylation of pyrrolidines and piperidines using C(3)-DGs.

The initial goals of this research were:

i) to investigate whether efficient discrimination between these different steric and electronic environments could be achieved through Pd^{II}/Pd^{IV} catalysis, by taking advantage of the steric sensitivity of C–H activation and/or oxidative addition steps;

ii) to develop an optimal set of reaction conditions that can achieve regioselective arylation at the unactivated 4-position, while providing high stereocontrol and functional groups tolerance;

iii) to develop a general methodology that could also be extended to the corresponding 6-membered ring.

Another major aim of this research was to develop a rapid and divergent synthesis of pyrrolidine and piperidine derivatives for potential use in drug discovery. Efficient strategies to remove the directing auxiliary and unmask polar functionalities, that could be used for downstream elaboration, were therefore targeted as an essential requirement of the method. In addition, the use of readily removable *N*-protecting groups such as Boc and Cbz was envisaged. This would allow for important applications in drug discovery settings, such as the synthesis of drug analogues and the preparation of libraries of fragment-like compounds.

Despite the significant advances in synthetic C–H functionalisation, the mechanistic understanding of the factors that govern the selectivity features of these transformations remains scarce. Therefore, the final aim of this research was to investigate in detail the mechanism of the reaction, through a combination of computational and experimental studies. This would lead to useful insight into the regio-and stereoselectivity, that could help overcome synthetic limitations and ultimately aid the design of future transformations.

The next chapter will present the development of the Pd-catalysed C(4)–H arylation of pyrrolidines and piperidines using C(3) directing groups, including strategies for DG removal.

3. C–H Arylation of Pyrrolidines and Piperidines using C(3)-Directing Groups

A concise account of this work, including section 4.1, can be found in *Organic Letters*.[183]

3.1 4-Aryl Pyrrolidines and Piperidines in Bioactive Compounds

3,4-Disubstituted pyrrolidines and piperidines bearing an aromatic substituent at the 4-position are prevalent pharmacophores and structural elements in a wide range of bioactive compounds (Figure 3.1). These include commercial drugs, such as anti-rheumatic Upadacitinib,[184] anti-depressant Paroxetine[185] and anti-histamine Levocabastine ,[186] as well as various compounds currently under investigation as potential therapeutics.[187,188,189,190] Although in most cases the N-heteroaliphatic ring featured a *trans*-configuration, few examples of bioactive *cis*-3,4-disubstituted pyrrolidines and piperidines have been reported (*e.g.* Upadacitinib and Alvocidib).

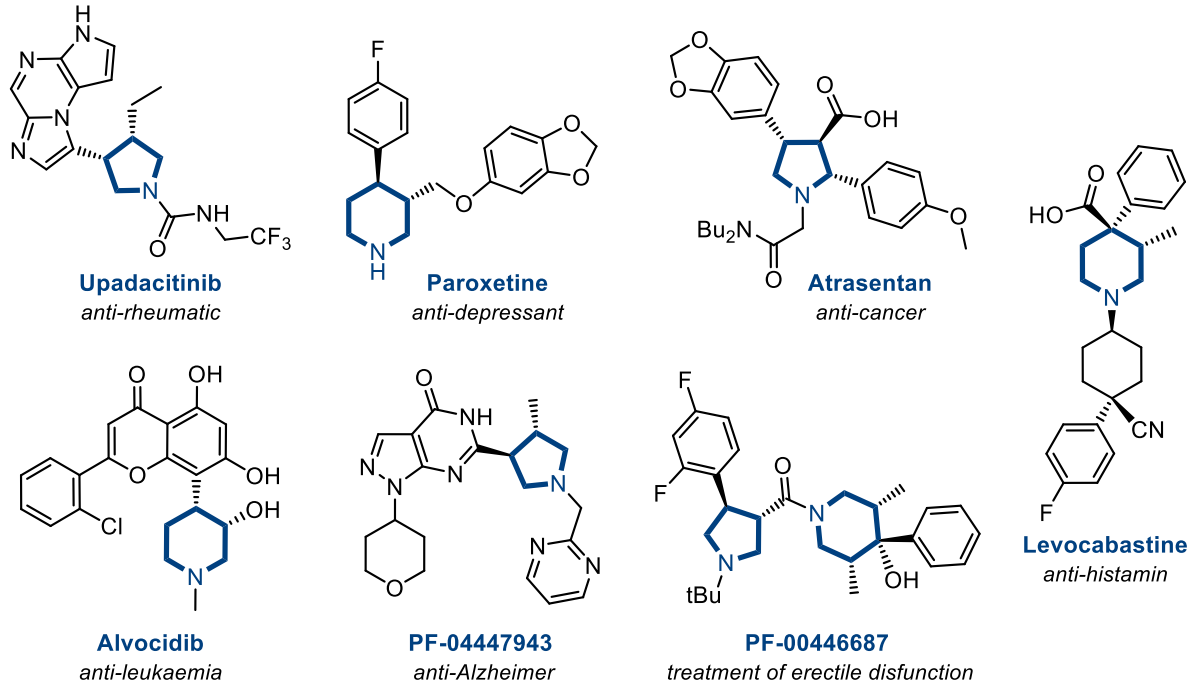


Figure 3.1 Selected examples of approved and investigational drug compounds containing arylated 3,4-disubstituted pyrrolidines and piperidines.

Recent studies have also demonstrated the potential of 4-aryl pyrrolidines and piperidines in various therapeutic areas, including the treatment of multiple sclerosis,[191] malaria,[192] schizophrenia[193] and blood clotting complications.[194] In particular, lead compounds possessing a 4-aryl-pyrrolidine-3-carboxamide core have been identified as potent thrombin inhibitors[194] and antimalarial agents (Figure 3.2).[192b] As such, arylated 3,4-disubstituted pyrrolidines and piperidines represent highly desirable targets for pharmaceutical screenings.

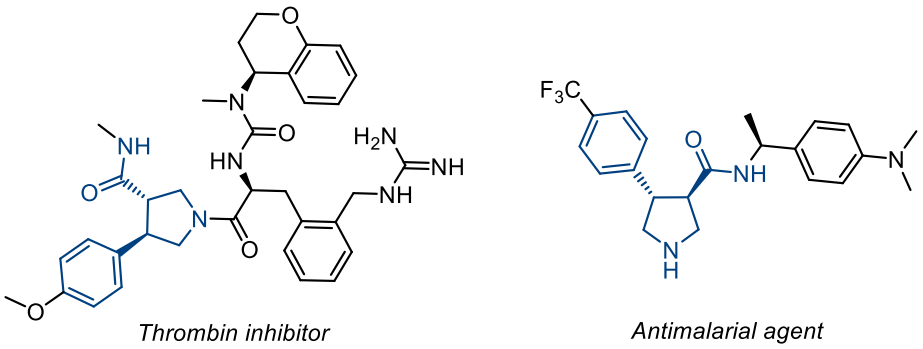
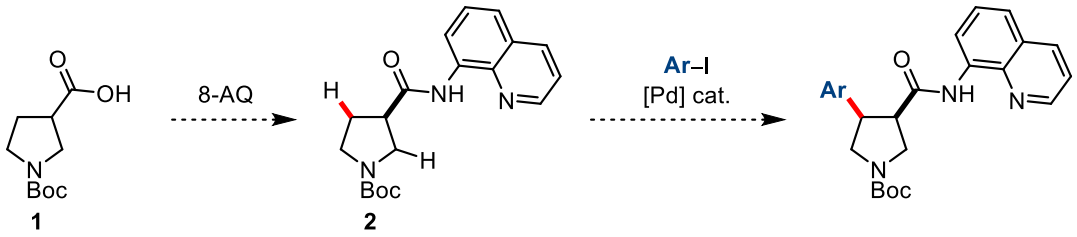


Figure 3.2 Examples of 4-aryl-pyrrolidines-3-carboxamides in recently identified bioactive compounds.

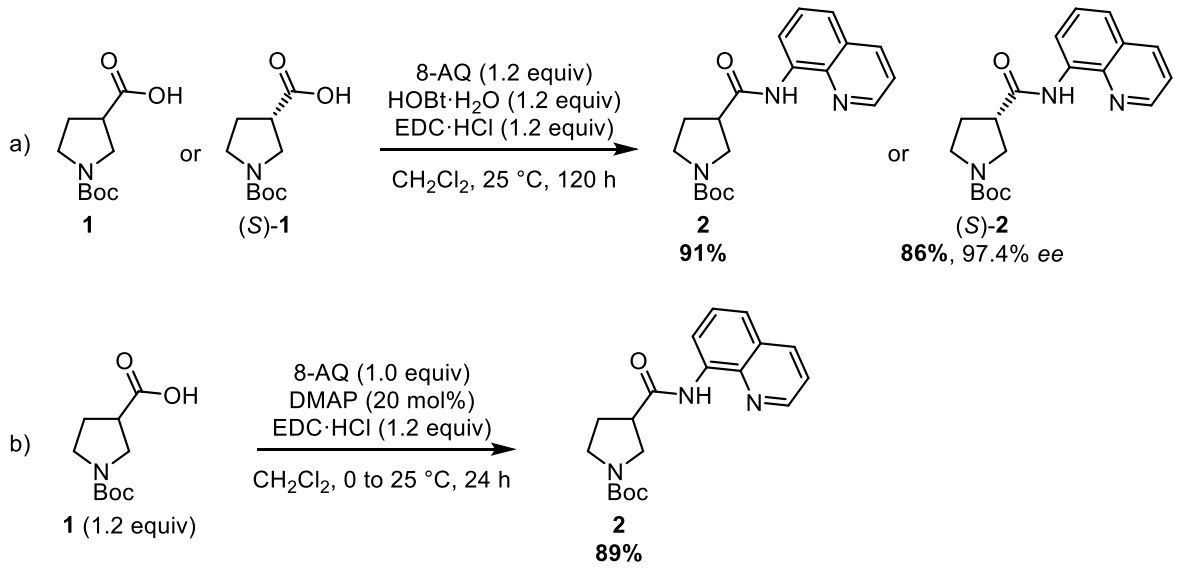
Building on previous work by Bull on the C(3)–H arylation of proline derivatives (Scheme 1.19, section 1.4.2.3),[165] Pd-catalysed C–H arylation was envisaged as an attractive method for the modular synthesis of diverse 4-aryl-3-substituted pyrrolidines and piperidines. It was reasoned that regioselective arylation at C(4) could be achieved using an amide-linked bidentate DG at C(3) alongside a bulky *N*-protecting group. The postulated formation of a sterically demanding palladacycle intermediate was anticipated to lead selectively to *cis*-configured products. Taking advantage of the acidic C–H bond α- to the carboxamide DG, these could also be converted into the corresponding *trans*-derivatives *via* base-mediated epimerisation, providing divergent access to both geometric isomers (*vide infra*). Based on these considerations, readily available *N*-Boc pyrrolidine-3-carboxylic acid **1** was selected as model substrate for this investigation. Furthermore, given the success of Daugulis' 8-aminoquinoline DG in the Pd-catalysed arylation of methylene C(sp^3)–H bonds,[123,125,165] this auxiliary was selected as a suitable starting point to probe the feasibility of this transformation (Scheme 3.1).



Scheme 3.1 Proposed regio- and stereoselective C(4)–H arylation of *N*-Boc pyrrolidine derivatives.

3.2 Development of Regio- and Stereoselective C(4)–H Arylation

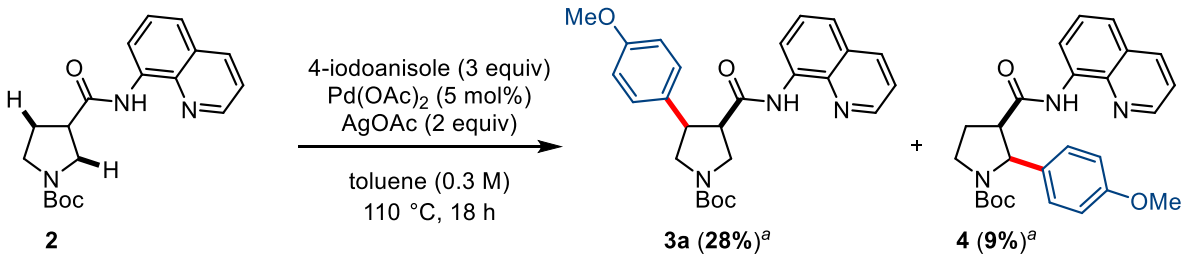
The directing auxiliary was easily installed at the 3-position by amide bond coupling using EDC in combination with HOBt (Scheme 3.2a). The same strategy was applied to the synthesis of enantioenriched derivative (*S*)-**2** from commercially available (*S*)-pyrrolidine-3-carboxylic acid (*S*)-**1**, proceeding with no loss in enantiomeric excess. Alternative conditions, involving the use of DMAP instead of HOBt, reduced the reaction time to 24 h, affording 4.7 g of pyrrolidine **2** in 89% yield (Scheme 3.2b).



Scheme 3.2 Synthesis of *N*-Boc pyrrolidines **2** and (*S*)-**2**, bearing the AQ auxiliary at the 3-position.

3.2.1 Initial Screenings and Products Identification

With pyrrolidine-3-carboxamide **2** in hand, the viability of selective C(4)–H arylation was evaluated. Initial reaction conditions were based on literature precedents for 8-AQ-assisted C(sp^3)–H arylation, particularly on N-heterocyclic substrates.[165,167] Treating pyrrolidine **2** with 3 equivalents of 4-iodoanisole, 2 equivalents of AgOAc and catalytic $Pd(OAc)_2$ in toluene, gave 2 different arylated products (Scheme 3.3). Pleasingly, the major derivative, formed in 28% NMR yield, was assigned as the 4-arylated pyrrolidine **3a**. In this product, no peak was observed in the region δ 5.50–4.50 ppm by ^{1}H NMR, which would be expected for the NC*H*Ar proton if arylation had occurred at the 2-position.[195] In addition, no signal (apart for the Boc group) was observed below δ 3.50 (^{1}H NMR), and δ 40.0 ppm (^{13}C NMR), which would be expected from the NCH_2CH_2 protons in case of C(2)-arylation.



Scheme 3.3 Initial attempt of Pd-catalysed C(4)–H arylation of pyrrolidine-3-carboxamide **2**. [a] Yield calculated by ^{1}H NMR using 1,3,5-trimethoxybenzene (TMB) as internal standard.

4-Arylated pyrrolidine **3a** was also formed as a single diastereoisomer. Unfortunately, the relative configuration could not be determined by simple analysis of coupling constants due to complex overlapping of peaks in the ^{1}H NMR spectrum. This issue was observed even when

the NMR experiment was performed at 100 °C in order to simplify the rotameric signals otherwise obtained at rt. Nonetheless, **3a** was finally assigned as a *cis*-configured derivative based on selective NOE experiments after Boc deprotection. More details on this will be given in section 3.4.2.

While unreacted starting material accounted for most of the mass balance, the formation of a minor arylated derivative (9%) was also observed in the C–H arylation of pyrrolidine **2** (Scheme 3.2). Although it could not be isolated pure, this was identified as the 2-arylated pyrrolidine **4**, through spectroscopic analysis of an inseparable 95:5 mixture of **3a** and **4**. In particular, signals consistent with C(2)-arylation were observed by ^{1}H NMR at 100 °C in DMSO-d_6 (Figure 3.3).

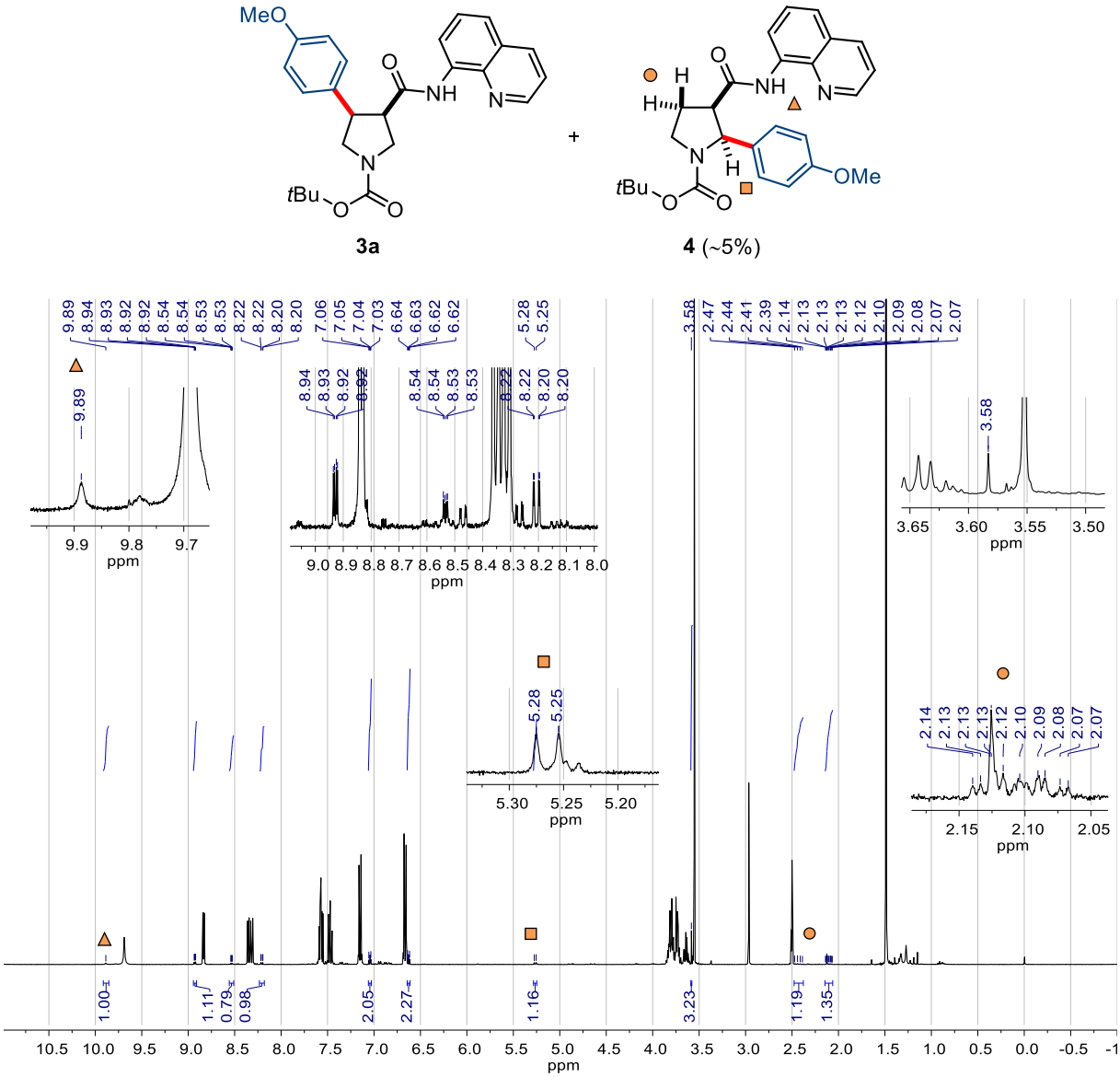


Figure 3.3 ^{1}H NMR spectrum (400 MHz, DMSO-d_6, 373 K) of a 95:5 mixture of **3a** and **4**.

Diagnostic peaks included a broad singlet at δ 9.89 (CONH), a doublet at δ 5.27 (NC*H*Ar)[195] and two multiplets below δ 2.50 ppm (NCH$_2$C*H*$_2$ protons). In addition, the doublet at δ 5.27 ppm

featured a coupling constant of J = 8.2 Hz, suggestive of a *cis*-configuration. This is consistent with values of J = 8.1–8.5 Hz reported by Holladay for *cis*-*N*-acetyl-3-propylproline derivatives.[196] In contrast, values of J = 4.4–6.2 Hz were reported for the corresponding *trans*-isomer, whose configuration was confirmed by X-ray spectroscopy.[196]

This preliminary evidence confirmed that Pd-catalysed C–H arylation occurred preferentially at the unactivated 4-position, using an 8-AQ directing group at C(3). Optimisation of the reaction conditions was then undertaken in order to: *i)* maximise the yield of *cis*-3,4-disubstituted pyrrolidine **3a**; *ii)* minimise competing C(2)-arylation and *iii)* avoid the use of expensive Ag(I) salts. Given the heterogenous nature of the reaction mixture, scale, stirring rate (1000 rpm), stir bar and reaction vessel size were all kept constant throughout the optimisation process.

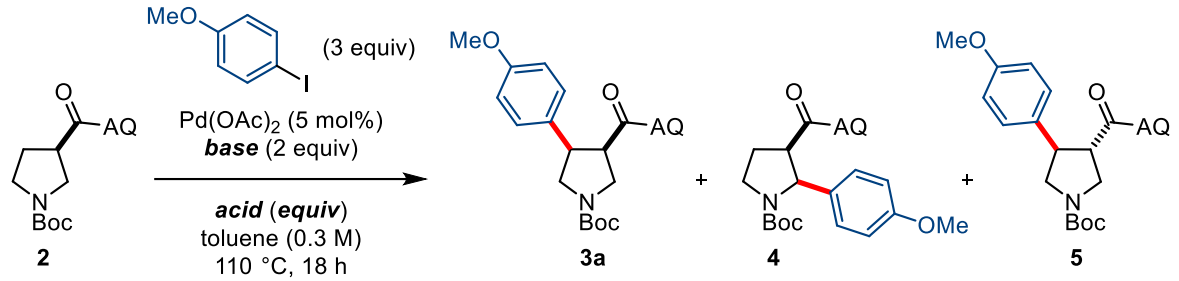
3.2.2 Optimisation of Regio- and Stereoselective C(4)–H Arylation

Initially, the effect of different acetate and carbonate bases in combination with various carboxylic acid additives was investigated (Table 3.1).

Although the carbonate (or bicarbonate) anion has itself potential to play an active role in the C–H cleavage,[112] carbonate bases have often been used in combination with soluble carboxylic acid ligands, particularly pivalic acid (PivOH). Pioneering work by Fagnou demonstrated a crucial role played by PivOH in the Pd-catalysed C(sp^2)–H arylation of benzene.[197] Based on experimental and computational evidence, the pivalate anion was suggested to lower the energy of C−H bond cleavage, enabling efficient inner sphere CMD by a pivalate-bound palladium catalyst. In addition, this was proposed to act as a catalytic proton shuttle from the substrate to the stoichiometric K_2CO_3 base. PivOH has since been shown as an important additive/co-catalyst in various Pd-catalysed C–H functionalisation reactions on both sp^2 and sp^3 systems, enabling the development of Ag-free conditions.[198] Furthermore, more sterically demanding carboxylic acids have been recently developed to enable intra- and intermolecular Pd-catalysed C(sp^2)–H arylation under mild conditions.[199] Therefore, carbonate bases were initially tested both alone and in combination with a PivOH additive.

The use of Ag_2CO_3 gave similar results to AgOAc, while an increase in yield was observed upon addition of 30 mol% PivOH (entries 1–3). Using CsOAc gave 47% of the desired product, although this was accompanied by a higher proportion of 2-arylation (entry 4). On the other hand, Cs_2CO_3 was found to promote epimerisation of the product forming 10% of *trans*-arylated pyrrolidine **5** (entry 5, *vide infra*). *In-situ* formation of 2 equivalents of CsOPiv using equimolar amounts of Cs_2CO_3 and PivOH led to an important increase in yield, without noticeable epimerisation (entry 6). K_2CO_3 gave a comparable result to Ag_2CO_3, and the addition of PivOH was similarly beneficial (entries 2–3 *vs* 7–8). Furthermore, using 2 equivalents of PivOH,

resulted in 50% yield of the desired product, while preserving high C(4)-regioselectivity (entry 9).



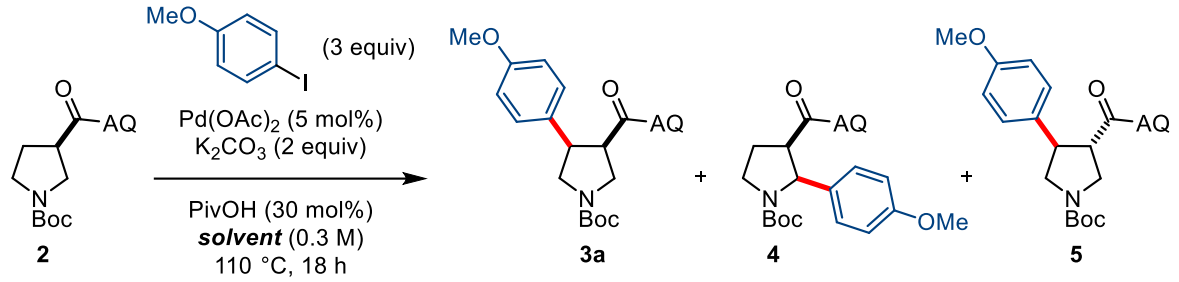
entry	base	acid (equiv)	yield[a] (%)				
			3a	4	5	2	tot
1	AgOAc	/	28	9	/	58	95
2[b]	Ag_2CO_3	/	29	4	/	56	89
3[b]	Ag_2CO_3	PivOH (0.3)	37	7	/	44	88
4	CsOAc	/	47	11	/	23	81
5	Cs_2CO_3	/	3	/	10	72	85
6	Cs_2CO_3	PivOH (2.0)	51	9	/	28	88
7	K_2CO_3	/	26	4	/	59	89
8	**K_2CO_3**	**PivOH (0.3)**	**36**	**5**	**/**	**53**	**94**
9	K_2CO_3	PivOH (2.0)	50	5	/	32	87
10	$KHCO_3$	PivOH (0.3)	25	6	/	69	100
11	PivOK	/	31	9	/	50	90
12	K_2CO_3	AcOH (0.3)	20	2	/	69	91
13	K_2CO_3	$EtCO_2H$ (0.3)	22	2	/	67	91
14	K_2CO_3	*i*$PrCO_2H$ (0.3)	37	4	/	47	88
15	K_2CO_3	1-Ad-CO_2H (0.3)	36	4	/	55	95
16	K_2CO_3	2-Mes-CO_2H (0.3)	36	2	/	50	88
17	K_2CO_3	TFA (0.3)	7	/	/	92	99
18	K_2CO_3	$(BnO)_2PO_2H$ (0.3)	15	3	trace	75	93

Table 3.1 Screening of bases and carboxylic acids for C–H arylation of *N*-Boc pyrrolidine **2**. Reaction scale: 0.2 mmol. [a] Calculated by ^{1}H NMR using 1,3,5-TMB as internal standard. [b] 1 equiv of Ag_2CO_3.

Interestingly, both $KHCO_3$ and preformed PivOK were less efficient in promoting the reaction (entries 10 and 11). Based on these results, inexpensive K_2CO_3 was selected as suitable base for further screening of various acid additives. An additive loading of 30 mol% was used for comparison, with the possibility to increase this at later stages in the optimisation process. AcOH and $EtCO_2H$ performed poorly in comparison to PivOH (entries 12 and 13). On the other

hand, more sterically demanding acids, such as 1-adamantyl carboxylic acid and 2-mesitylene carboxylic acid, all gave similar yields to PivOH, suggesting a beneficial effect played by steric hindrance on the reaction outcome (entries 14–16). Finally, trifluoroacetic acid and dibenzyl phosphate were both found to hinder the reaction (entries 17 and 18).

As no improvement was observed with different acids, PivOH was selected to continue the optimisation, with the screen of various solvents (Table 3.2).



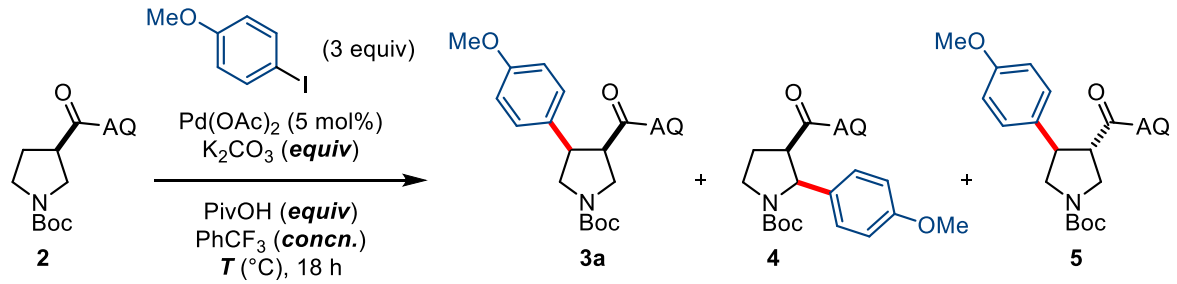
entry	solvent	yield (%)[a]				
		3a	**4**	**5**	**2**	**tot**
1	toluene	36	5	/	53	94
2	/	29	/	trace	68	97
3	1,2-DCE	38	<3	/	53	94
4	1,4-dioxane	25	3	/	62	90
5	*t*-amyl-OH	11	/	7	75	93
6	*t*-amyl-OH/H_2O (4:1)	6	/	7	86	99
7	2-Me-THF	12	/	trace	71	83
8	EtOAc	21	/	trace	76	97
9	DMF	/	/	/	100	100
10	MeCN	18	/	4	88	100
11	*n*-hexane	17	/	/	76	93
12	*m*-xylene	35	4	/	58	97
13	*o*-DCB	24	3	/	69	96
14	**$PhCF_3$**	**46**	**6**	**/**	**42**	**94**

Table 3.2 Solvent screen for C–H arylation of *N*-Boc pyrrolidine **2**. Reaction scale: 0.2 mmol. [a] Calculated by ^1H NMR using 1,3,5-TMB as internal standard.

While running the reaction in absence of solvent gave a reduced yield, the use of 1,2-DCE gave similar results to the initial toluene conditions (entries 1–3). On the other hand, more polar coordinating solvents were all found highly detrimental for the reaction outcome (entries 4–10). Notably, using *t*-amyl-OH, product epimerisation was also observed (entries 5 and 6). Higher

reactivity was restored with less polar aromatic solvents, such as *m*-xylene (entry 12). Using α,α,α-trifluorotoluene gave 46% of the desired product. Therefore, this solvent was taken further in the optimisation.

Having fixed the discrete variables of the reaction, continuous factors were then evaluated, such as the loadings of base and additive, the temperature and the concentration (Table 3.3).



entry	equiv K_2CO_3	equiv PivOH	concn. (M)	temp (°C)	yield (%)[a]				
					3a	4	5	2	tot
1	2.0	0.3	0.3	110	46	6	/	42	94
2	3.0	0.3	0.3	110	40	4	/	49	93
3	1.0	0.3	0.3	110	48	4	/	36	88
4	1.0	1.0	0.3	110	49	5	/	44	98
5	1.0	2.0	0.3	110	27	9	/	56	92
6	1.0	1.0	0.1	110	32	6	/	53	91
7	1.0	1.0	1.0	110	66	3	/	22	91
8[b]	**1.0**	**1.0**	**1.0**	**110**	**71 (64)**	**6**	**/**	**22**	**99**
9	1.0	1.0	2.0	110	65	3	/	24	92
10	2.0	2.0	1.0	110	50	3	/	38	91
11[c]	1.0	1.0	1.0	110	62	4	traces	24	90
12	1.0	1.0	1.0	80	39	2	/	59	100
13	1.0	1.0	1.0	120	61	5	3	20	89
14	1.0	1.0	1.0	130	60	6	5	20	91

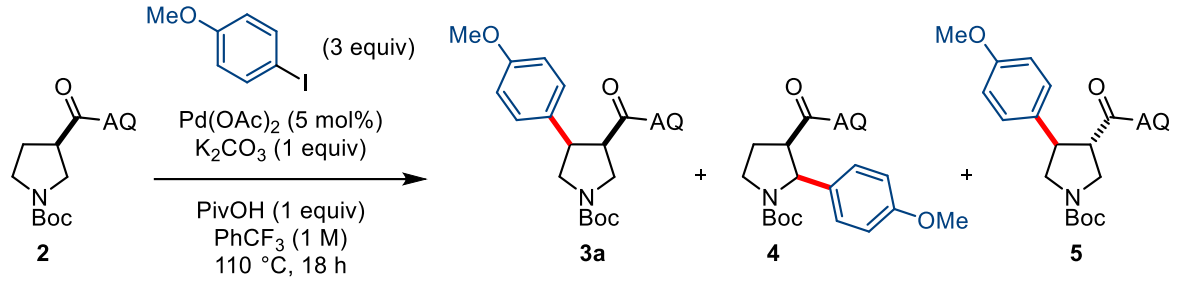
Table 3.3 Optimisation of continuous factors for C–H arylation of *N*-Boc pyrrolidine **2**. Reaction scale: 0.2 mmol. [a] Calculated by ^{1}H NMR using 1,3,5-TMB as internal standard. [b] 0.5 mmol scale. [c] 36 h. Isolated yield reported in brackets.

Increasing the loading of K_2CO_3 up to 3.0 equivalents resulted in a slightly reduced yield (entry 2). On the other hand, this could be reduced to just 1.0 equiv without any detrimental effect on the reaction outcome (entries 1 *vs* 3). Using an equimolar amount of PivOH, previously observed to be beneficial, did not provide higher reactivity, although better mass recovery was

obtained (entry 4). On the other hand, a significant drop in yield was observed when PivOH was used in excess compared to K_2CO_3 (entry 5). This was ascribed to the excess pivalic acid neutralising the $KHCO_3$ to form CO_2 and H_2O, that could in turn hinder the reaction. Reducing the concentration to 0.1 M was also found to have a negative effect on the reaction (entry 6). In contrast, when the concentration was raised to 1 M, a higher yield of 66% was observed (entry 7). Pleasingly, running the same conditions on a slightly higher 0.5 mmol scale afforded the desired product in 71% yield (entry 8). Increasing further the concentration, the equivalents of base/additive or the reaction time did not give better results (entries 9–11). Although product formation was still observed at temperatures as low as 80 °C, this resulted in a significant reduction in reactivity (entry 12). On the other hand, running the reaction at 120 or 130 °C increased the proportion of epimerisation, without improving the yield of desired product (entries 13 and 14). Therefore, the conditions reported in entries 7 and 8 were selected for further investigation.

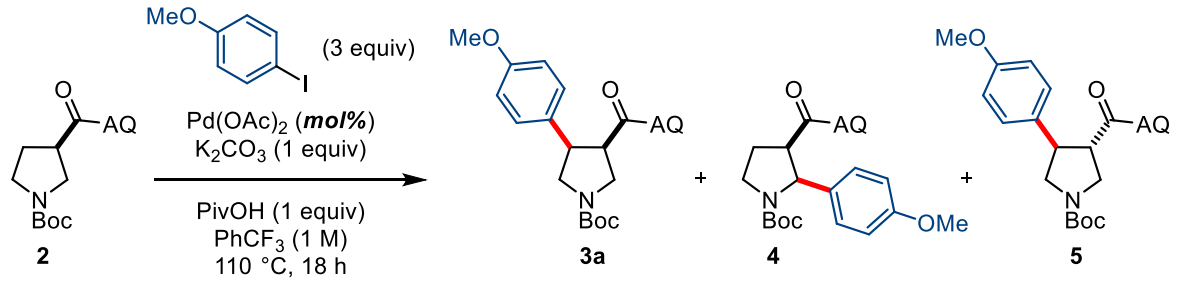
At this stage in the study, variable yields started to be observed under identical conditions. Considering that, despite being run under inert atmosphere (Ar), the reactions were not set-up in glovebox, this issue was ascribed to variations in the degree of ambient humidity. In particular, the effect of moisture was systematically evaluated comparing different levels of "dry" conditions (Table 3.4). Entry 1 outlines the results obtained with relative humidity = 45%, when no particular precaution was taken during the reaction set-up, apart from the use of flame-dried glassware. In comparison, a 10% reduction in yield was obtained in the presence of higher humidity (70%, entry 2). A slight increase in yield, under the same humidity conditions, was observed when K_2CO_3 was flame-dried before being added to the reaction vial (entry 3). When K_2CO_3 was flame-dried directly in the reaction vessel, an improved yield of 65%, comparable to entry 1, was obtained (entry 4). The addition of 1 equivalent of water, under this modified set-up, did not seem to affect significantly the reaction outcome (entry 5). On the other hand, 10 equivalents of H_2O resulted in a reduced 56% yield, similar to that observed without the additional flame-drying procedure (entries 2 *vs* 6). Finally, a slight increase in the base loading did not improve the reaction under otherwise equal conditions (entry 7). These results confirmed the sensitivity of the reaction to variations in ambient humidity. This could be controlled by flame-drying the carbonate base, which became standard operational procedure in the reaction set-up.

Following this, the loading of Pd-catalyst was investigated under the new reaction set-up (Table 3.5). Reducing the catalyst loading to 2.5 mol% gave a lower yield (entry 2). On the other hand, using 10.0 mol% did not improve the reaction, and only resulted in lower mass recovery (entry 3). Finally, the use of different Pd(II) pre-catalysts gave comparable results to $Pd(OAc)_2$ and were not investigated further (entries 4 and 5).



entry	yield (%)[a]				
	3a	4	5	2	tot
1[b]	**66**	**3**	**/**	**22**	**91**
2	57	3	/	32	92
3[c]	60	3	/	30	93
4[d]	**65**	**3**	**/**	**27**	**93**
5[d,e]	62	2	/	25	89
6[d,f]	56	2	/	37	95
7[d,g]	64	2	/	18	84

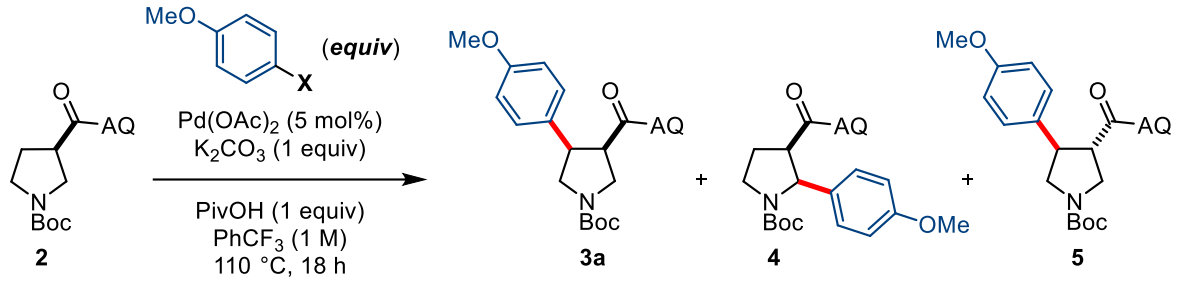
Table 3.4 Effect of ambient humidity on C–H arylation of *N*-Boc pyrrolidine **2**. Reaction scale: 0.2 mmol. Relative humidity measured by hygrometer: 70%, unless otherwise stated. [a] Calculated by ^{1}H NMR using 1,3,5-TMB as internal standard. [b] Relative humidity: 45%. [c] Flame-dried K_2CO_3. [d] K_2CO_3 was flame-dried directly in the reaction vessel. [e] 1 equiv of H_2O added. [f] 10 equiv of H_2O added. [g] 1.2 equiv of K_2CO_3.



entry	cat. loading (mol%)	yield (%)[a]				
		3a	4	5	2	tot
1	**5.0**	**66**	**3**	**/**	**22**	**91**
2	2.5	45	2	/	47	94
3	10	61	5	/	15	81
4[c]	5.0	66	3	/	24	94
5[d]	5.0	62	traces	/	21	84

Table 3.5 Optimisation of catalyst loading for C–H arylation of *N*-Boc pyrrolidine **2**. Reaction scale: 0.2 mmol. [a] Calculated by ^{1}H NMR using 1,3,5-TMB as internal standard. [c] $Pd(TFA)_2$. [d] $Pd(OPiv)_2$.

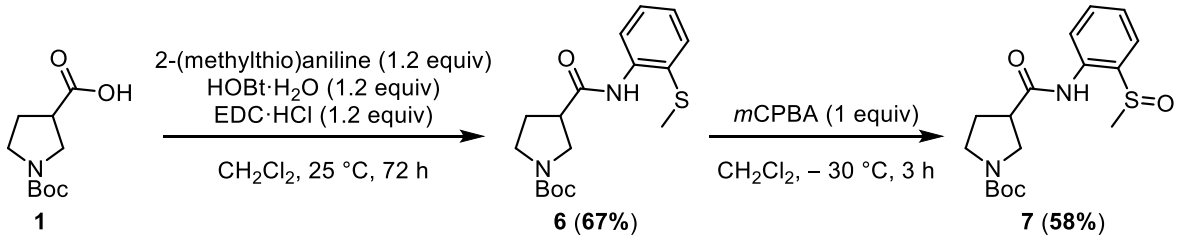
Finally, the loading of aryl iodides and the use of aryl bromides as alternative coupling partners was evaluated (Table 3.6). Reducing the equivalents of 4-iodoanisole to 2.5 and 2 equivalents, had a negative impact on the reaction outcome (entries 2 and 3). Furthermore, replacing the iodide for a bromide coupling partner gave the 4-arylated product in only 12% yield, despite the use of more forcing 2 M conditions (entry 4). This was ascribed to a more difficult oxidative addition to form the high valent Pd^{IV} species. Therefore, 3 equivalents of aryl iodide were maintained as optimal loading of coupling partner.



entry	X (equiv)	yield (%)[a]				
		3a	4	5	2	tot
1	**I (3.0)**	**66**	**3**	**/**	**22**	**91**
2	I (2.5)	59	4	/	37	100
3	I (2.0)	53	3	/	39	95
4[b]	Br (3.0)	12	/	/	81	93

Table 3.6 Investigations into different coupling partners. Reaction scale: 0.2 mmol. [a] Calculated by ^{1}H NMR using 1,3,5-TMB as internal standard. [b] Concentration = 2.0 M.

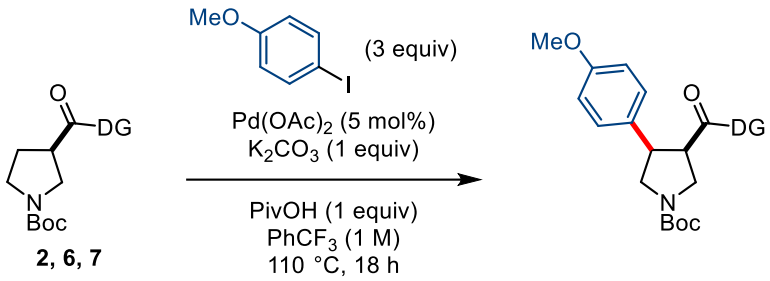
To better understand the effect of the 8-AQ auxiliary, the performance of different bidentate DGs was also investigated. In particular, 2-(methylthio)aniline DG was installed through amide bond formation and the desired product **6** was isolated in 67% yield (Scheme 3.4). Subsequent oxidation with *m*CPBA afforded the corresponding 2-sulfinyl aniline derivative **7** in 58% yield.



Scheme 3.4 Synthesis of *N*-Boc pyrrolidine-3-carboxamides **6** and **7**.

With pyrrolidine derivatives **6** and **7** in hand, the directing ability of these alternative sulfur-based DGs was evaluated (Table 3.7). However, both failed in providing useful reactivity. While very small conversion was observed with thioaniline **6**, the use of sulfoxide **7** only resulted in

unreacted staring material being recovered (entries 2 and 3). This confirmed the crucial role played by the AQ directing group in enabling the regio- and stereoselective C(4)–H arylation of pyrrolidine-3-carboxylic acid derivatives.



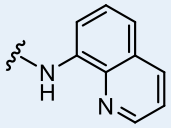
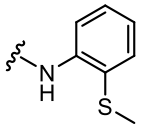
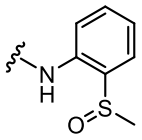
entry	DG	RSM (%)[a]	Product yield (%)[a]
1		**2** (27)	65
2		**6** (83)	<10
3		**7** (96)	/

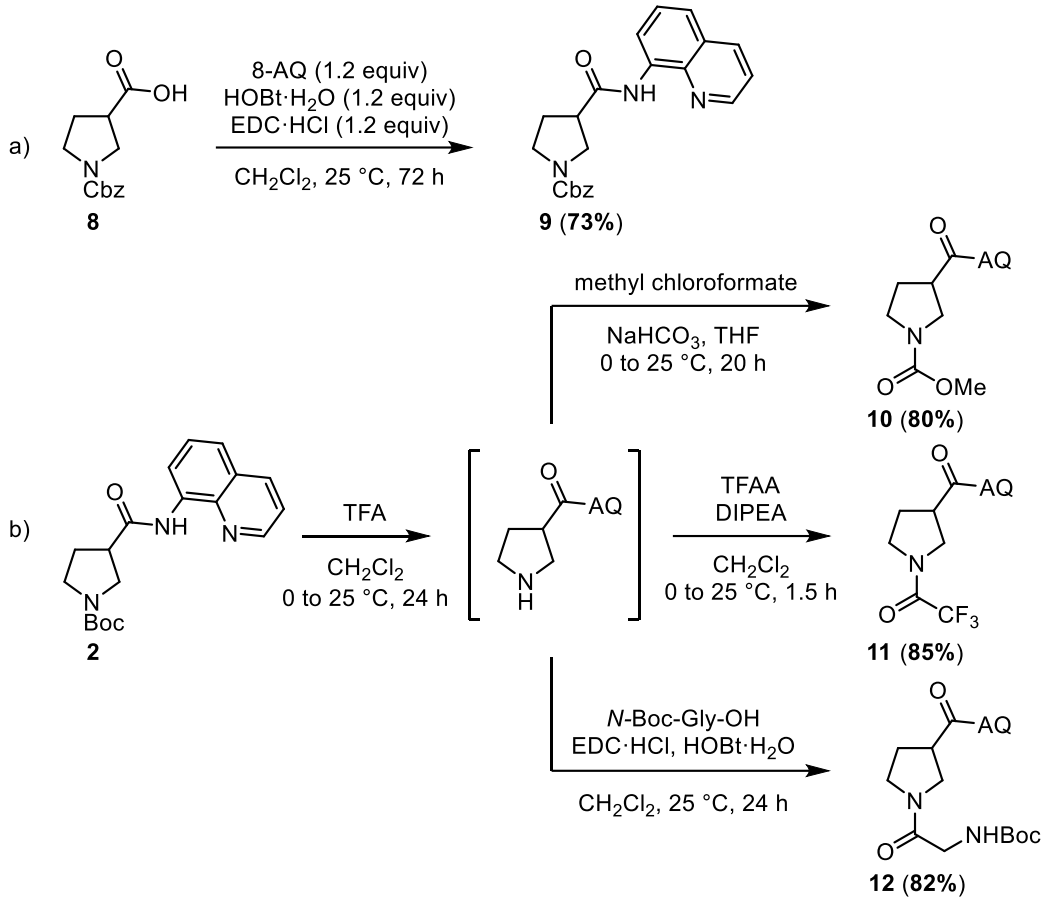
Table 3.7 Comparison of different bidentate directing groups. Reaction scale: 0.2 mmol. [a] Calculated by ^{1}H NMR spectroscopy using 1,3,5-TMB as internal standard.

All efforts described above to force the reaction by increasing temperature, reaction time or catalyst loading were unsuccessful in promoting the formation of *cis*-derivative **3a**, and only resulted in increased epimerisation or lower overall mass recovery. Therefore, the conditions described in Table 3.3, entry 8, involving the use of 3 equivalents of aryl iodide, 5 mol% $Pd(OAc)_2$, 1 equivalent of K_2CO_3 and PivOH in $PhCF_3$ (1 M) at 110 °C were selected to evaluate the scope of the reaction.

3.3 Scope of Pyrrolidine C(4)–H Arylation

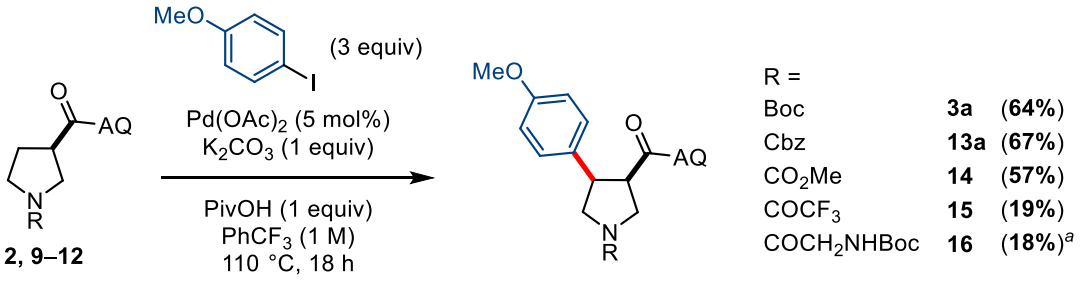
3.3.1 Variation of *N*-Protecting Groups

First, the *N*-protecting group varied. *N*-Cbz pyrrolidine-3-carboxamide **9** was synthesised by amide bond formation from the corresponding carboxylic acid **8** in 73% yield (Scheme 3.5a). On the other hand, *N*-substituted pyrrolidines **10**–**12** were accessed from carboxamide **2**, through Boc-deprotection followed by reaction with methyl chloroformate, TFAA or *N*-Boc glycine (Scheme 3.5b).



Scheme 3.5 Synthesis of *N*-substituted pyrrolidines **9**–**12**.

With these derivatives in hand, the effect of changing the *N*-protecting group was investigated (Scheme 3.6). Different carbamate protecting groups were well tolerated, with *N*-Cbz (**9**) giving similar results to *N*-Boc in the reaction with 4-iodoanisole. 4-Arylated pyrrolidine **13a** was isolated in 67% yield as a single *cis*-diastereomer. Excellent *cis*-stereoselectivity and high C(4) selectivity were observed also with a smaller methyl carbamate group (**10**), affording pyrrolidine **14** in 57% yield.



Scheme 3.6 Scope of *N*-protecting groups for pyrrolidine C–H arylation. Reaction scale: 0.5 mmol. Products isolated as single *cis*-diastereomers and < 5% C2-arylation. [a] 5 equiv of 4-iodoanisole, 48 h.

On the other hand, trifluoroacetamide **11** and *N*-Boc glycine amide **12** were found to be much less reactive and resulted in low yield of 4-arylation. Although the basis of this detrimental

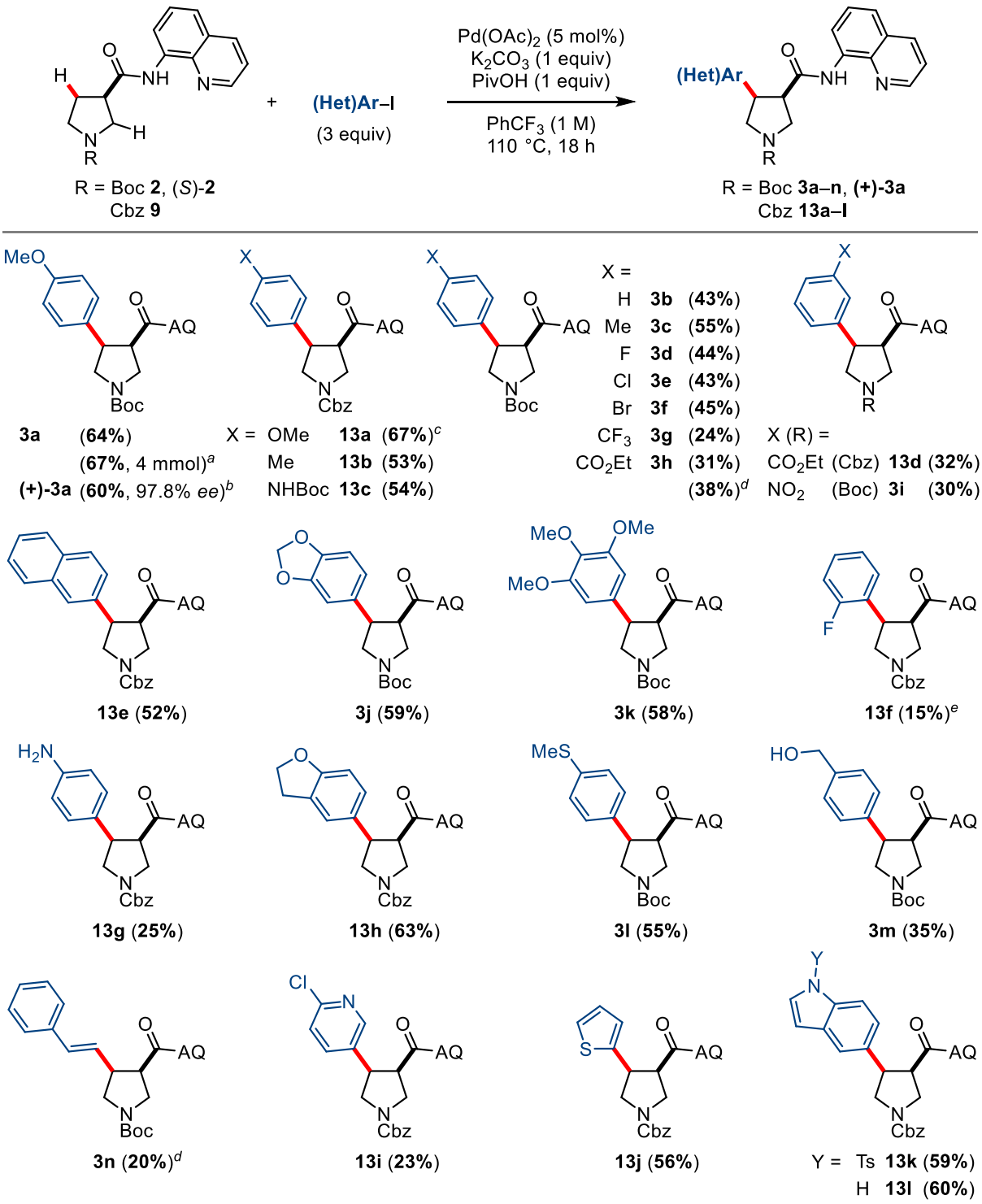
effect is not well understood yet, the change in nitrogen hybridisation might result in a less reactive conformation.[200]

Given the success obtained with both *N*-Boc and *N*-Cbz protecting groups, these were used interchangeably to investigate the scope of aryl iodides, as described in the next section.

3.3.2 Variation of Aryl Iodide Coupling Partners

In all cases when evaluating the iodide scope, the reaction proceeded with high regioselectivity for the 4-position and complete *cis*-selectivity, with unreacted starting material accounting for the remaining mass balance (Scheme 3.7). The reaction with 4-iodoanisole could be scaled up to 4 mmol by increasing the concentration to 2 M. This afforded arylated pyrrolidine **3a** in > 1 g with no reduction in yield compared to 0.5 mmol scale. Furthermore, complete retention of enantiomeric excess was observed when using enantioenriched substrate (*S*)-**2**. In this case, no racemisation of either the starting amide or the arylated product occurred under the C−H arylation conditions, and pyrrolidine **(+)-3a** was obtained in 60% yield as a single enantiomer.

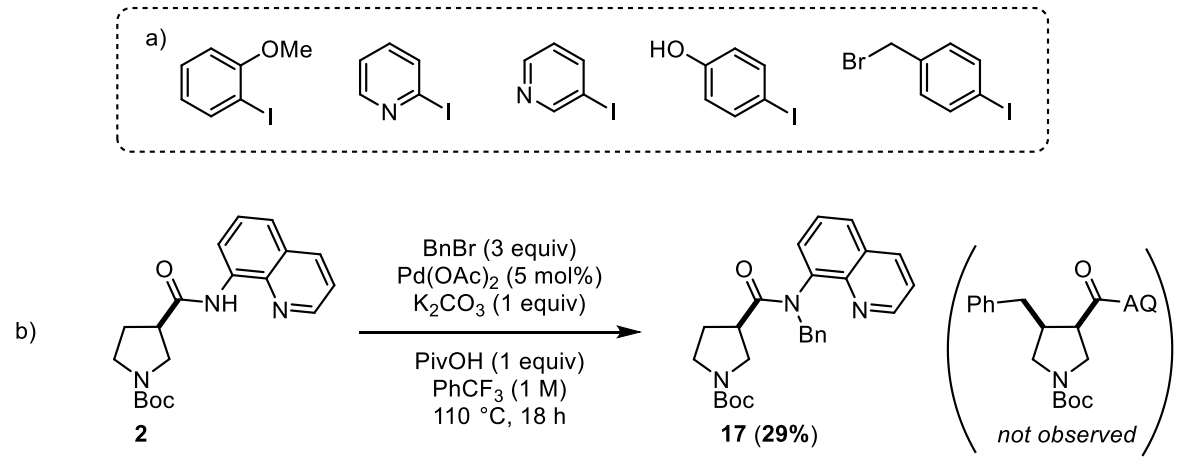
Under the optimised conditions, various *para*-substituted aromatic groups could be installed (**3a–h**, **13a–c**). Higher yields were generally observed for more electron-rich aryl iodides. This was suggestive of a challenging reductive elimination step, which becomes more difficult with electron-poorer arenes, and will be discussed in greater detail in chapter 5. Electron-donating substituents at the *para*-position, such as methoxy (**3a**, **13a**), methyl (**3c**, **13b**) and *N*-Boc amine (**13c**), resulted in up to 67% yield of the desired 4-arylated products. Halogens were also well tolerated (**3d–f**), and high chemoselectivity for the iodide functionality was observed in the reaction with 4-chloro- and 4-bromo-iodobenzene, providing useful handles for potential downstream elaboration. Lower yields were obtained with electron-withdrawing 4-CF_3 and 4-CO_2Et groups (**3g** and **3h**, 24% and 31% respectively). In the latter case, a slight increase in yield was observed using more forcing conditions. *meta*-Substituents gave similar outcomes (**3i–k**, **13d–e**). While electron-withdrawing groups at the *meta*-position led to low reactivity (**3i**, **13d**), electron-rich 2-naphthalene, benzodioxole and trimethoxybenzene functionalities could be installed in high yield (**3j–j, 13e**). On the other hand, *ortho*-substitution was not tolerated: pyrrolidine **13f** was isolated in just 15% using 4 equivalents of 2-fluoroiodobenzene. Importantly, in absence of silver(I) additives, groups sensitive to oxidation, including unprotected aniline, dihydrobenzofuran, methyl sulfide, and benzyl alcohol functionalities, could be successfully installed (**3l–m, 13g–h**). The scope of coupling partners was also extended to alkenyl iodides, though resulting in lower conversion. For instance, alkenylated pyrrolidine **3n** was isolated in 20% yield using (*E*)-β-styryl iodide, with retention of the initial alkene configuration.



Scheme 3.7 Scope of aryl iodides for pyrrolidine C–H arylation. Reaction scale: 0.5 mmol, unless otherwise stated. Products isolated as single *cis*-diastereomers and < 5% C2-arylation. [a] 2 M concentration. [b] Using (*S*)-**2** substrate. [c] 0.2 mmol. [d] 4 equiv ArI, 48 h. [e] 4 equiv ArI, 72 h.

Heteroaryl iodides proved also to be successful coupling partners. 2-Chloro-5-iodopyridine was installed in 23% yield (**13i**), while the electron-rich nature of 2-iodothiophene resulted in higher 56% yield (**13j**). Finally, the reaction was successful with both *N*-Ts and free *N*-H 5-iodoindole derivatives, affording products **13k** and **13l** in 59% and 60% yield respectively.

Alongside these successful examples, few other aryl iodides were tested, but failed in providing the corresponding 4-arylated derivatives in synthetically useful yield (Scheme 3.8a). Only traces of product formation (3–10% conversion) were observed with 2-iodoanisole, 2- and 3-iodopyridine, and 4-iodophenol. In the first case, this can be ascribed to the sensitivity of the reaction to steric hindrance, while the failure of 2- and 3-iodopyridine might result from the combination of low electron density and unproductive coordination to the Pd catalyst. Similarly, the poor reactivity of 4-iodophenol might be due its strong coordinating ability. Finally, reaction with 4-iodo-benzyl bromide also did not afford any 4-arylated product. However, formation of a different derivative in ~30% was observed. Although isolation attempts have been unsuccessful, the product signals in the crude NMR appeared to be consistent with a *N*-benzylated derivative. To confirm this, benzyl bromide was directly tested as coupling partner. This formed a similar product, which could be isolated in 29% yield as the *N*-benzylated pyrrolidine amide **17** (Scheme 3.8b).



Scheme 3.8 a) Unsuccessful aryl iodides. b) Reaction with benzyl bromide.

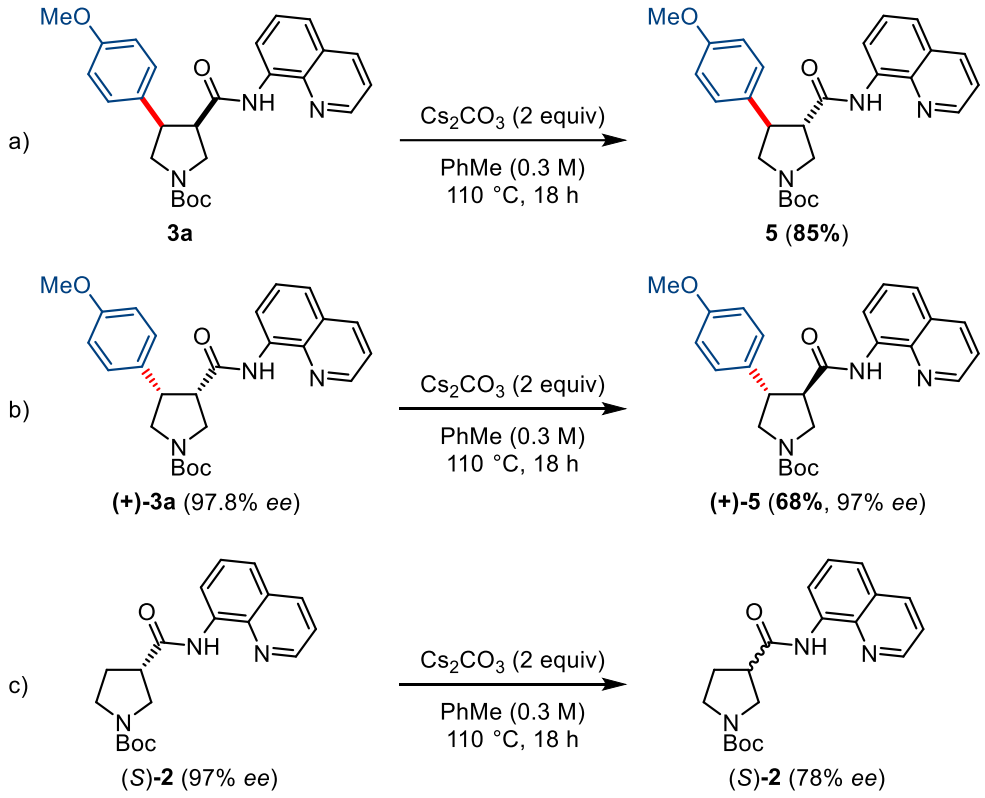
3.4 Base-Mediated Epimerisation for the Formation of *trans*-Isomers

3.4.1 Synthesis of *trans*-3,4-Disubstituted Pyrrolidines

During the process of optimisation of the reaction, a small degree of *cis*-to-*trans* isomerisation was noticed when using high temperature or alcohol solvents (*e.g. t*-amyl-OH). Furthermore, a small amount of *trans*-2,3-disubstituted pyrrolidine **5** was also formed in the presence of a suitable base such as cesium carbonate (Section 3.2.2, Table 3.1). Encouraged by these observations, the viability of a base-mediated epimerisation process to access *trans*-3,4-disubstituted pyrrolidines was investigated.

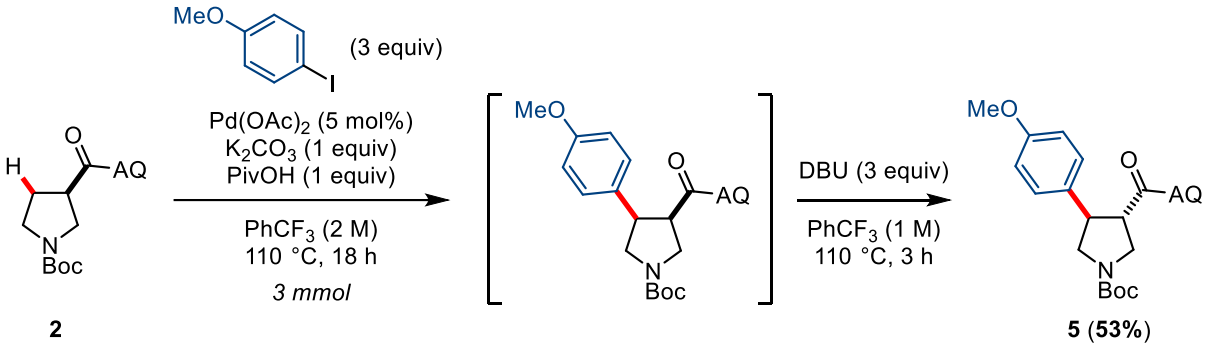
Epimerisation occurred readily when **3a** was treated with excess Cs_2CO_3 in toluene at 110 °C, and *trans*-diastereomer **5** was obtained in 85% yield (Scheme 3.9a). Furthermore, subjecting enantioenriched *cis*-pyrrolidine **(+)-3a** to the same conditions afforded *trans*-derivative **(+)-5** in

68% yield with full retention of *ee* (Scheme 3.9b). This confirmed the epimerisation of a single centre in **3a** and **(+)-3a**, likely *via* formation of a cesium enolate intermediate. Treating monosubstituted enantioenriched pyrrolidine (*S*)-**2** with Cs_2CO_3, only a partial loss of enantiopurity was observed (78% *ee*). This supports a key role played by the additional *cis*-substituent in promoting effective C(3)-epimerisation of **3a** to form thermodynamically favoured *trans*-derivative **5** (Scheme 3.9c).



Scheme 3.9 Base-mediated epimerisation of a) *cis*-pyrrolidine **3a**, b) enantioenriched pyrrolidine **(+)-3a** and c) pyrrolidine amide (*S*)-**2**.

Based on these positive results, the possibility to access directly *trans*-configured pyrrolidines, without isolating the *cis*-isomers, was investigated. Performing the C–H arylation with Cs_2CO_3 in place of K_2CO_3 resulted in similar overall reactivity, with *trans*-pyrrolidine **5** being formed in just 8% NMR yield alongside 61% of *cis*-arylated product **3a** (not shown). The poor epimerisation was ascribed to the stoichiometric reaction of Cs_2CO_3 with PivOH, forming less basic CsOPiv and $CsHCO_3$ species. Alternatively, a simple one-pot procedure was envisaged to provide direct access to the *trans*-diastereomer, involving the use of DBU as a strong organic-soluble base (Scheme 3.10). The isomerisation could be promoted by simple addition of DBU to the crude C–H arylation mixture, with no need for work-up procedures or chromatographic purification, resulting in complete conversion of *cis*-pyrrolidine **3a** to the *trans*-diastereomer **5** in just 3 h at 110 °C. This *trans*-C–H arylation protocol could be scaled up to 3 mmol scale, affording the desired pyrrolidine **5** as a single *trans*-diastereomer in 53% yield.

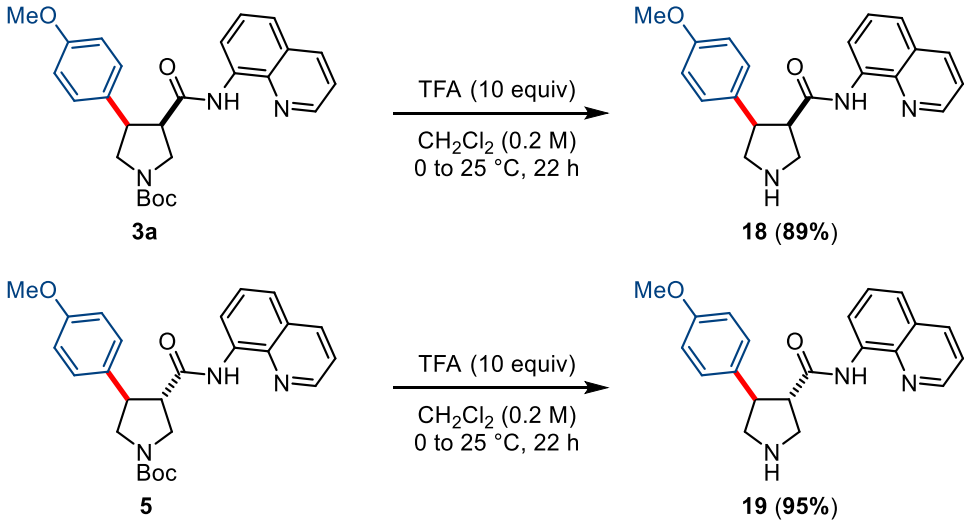


Scheme 3.10 Synthesis of *trans*-configured pyrrolidine **5** *via* one-pot C(4)–H arylation/epimerisation.

Having access to both *cis*-and *trans*-3,4-disubstituted pyrrolidines, these could be tested for further arylation. However, subjecting both isomers to the standard C–H arylation conditions did not lead to any noticeable *bis*-arylation (not shown). Furthermore, being able to compare both isomers by NMR spectroscopy, allowed the relative configuration of pyrrolidine derivatives **3a** and **5** to be assigned as described in the next section.

3.4.2 Boc Deprotection and Stereochemical Assignments

Stereochemical assignment of 3,4-disubstituted pyrrolidine derivatives **3a** and **5** was possible after Boc deprotection to give compounds **18** and **19** (Scheme 3.11).



Scheme 3.11 Boc deprotection on *cis*- and *trans*-arylated pyrrolidines **3a** and **5**.

The geometric configuration around the ring was assigned based on NOE experiments on both N-H pyrrolidines **18** and **19**. Selective NOE spectroscopy on both derivatives indicated spatial correlations between aromatic proton H_a and nearby protons on the pyrrolidine ring (Figures 3.4 and 3.5). However, no interaction was observed between H_a (δ 7.20 ppm) and CH_bCO (δ 3.38–3.29 ppm) in pyrrolidine **18**, consistent with a *cis*-configuration of this derivative (Figure 3.4).

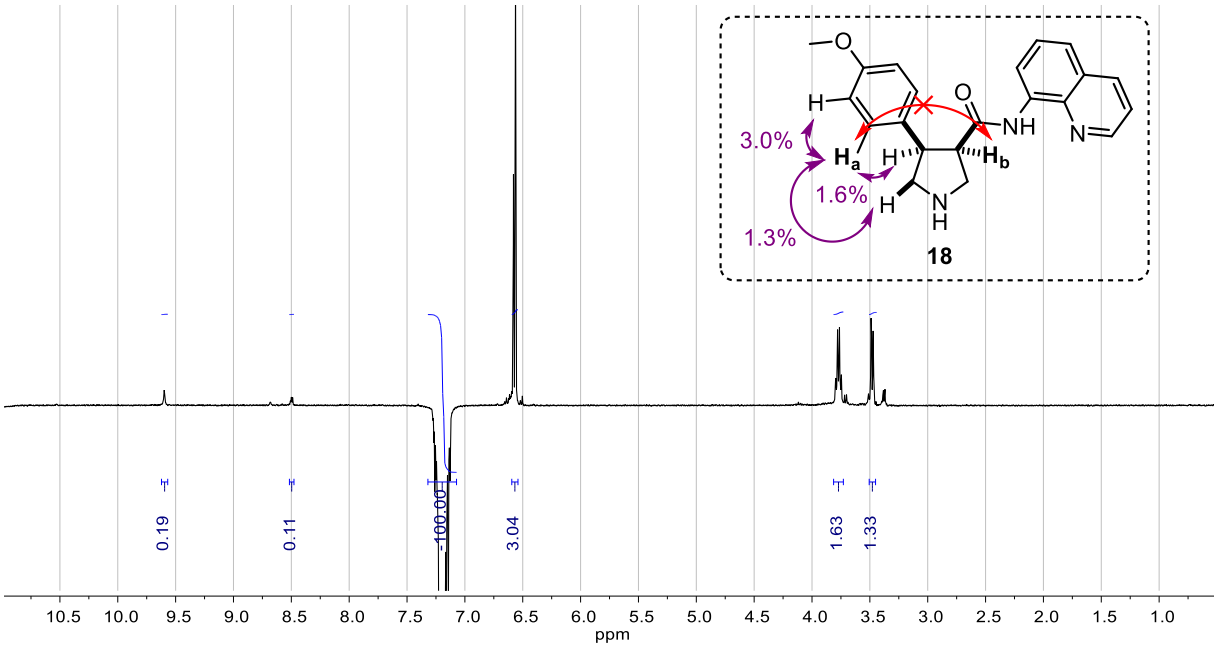


Figure 3.4 NOE spectrum for pyrrolidine **18**, in which proton H_a (δ 7.20 ppm) was selectively irradiated (500 MHz, $CDCl_3$, 298 K).

In contrast, a non-negligible NOE correlation (0.8%) was observed between H_a (δ 7.27 ppm) and CH_bCO (δ 3.21–3.14 ppm) for pyrrolidine **19**, supporting a *trans*-configuration of this compound (Figure 3.5).

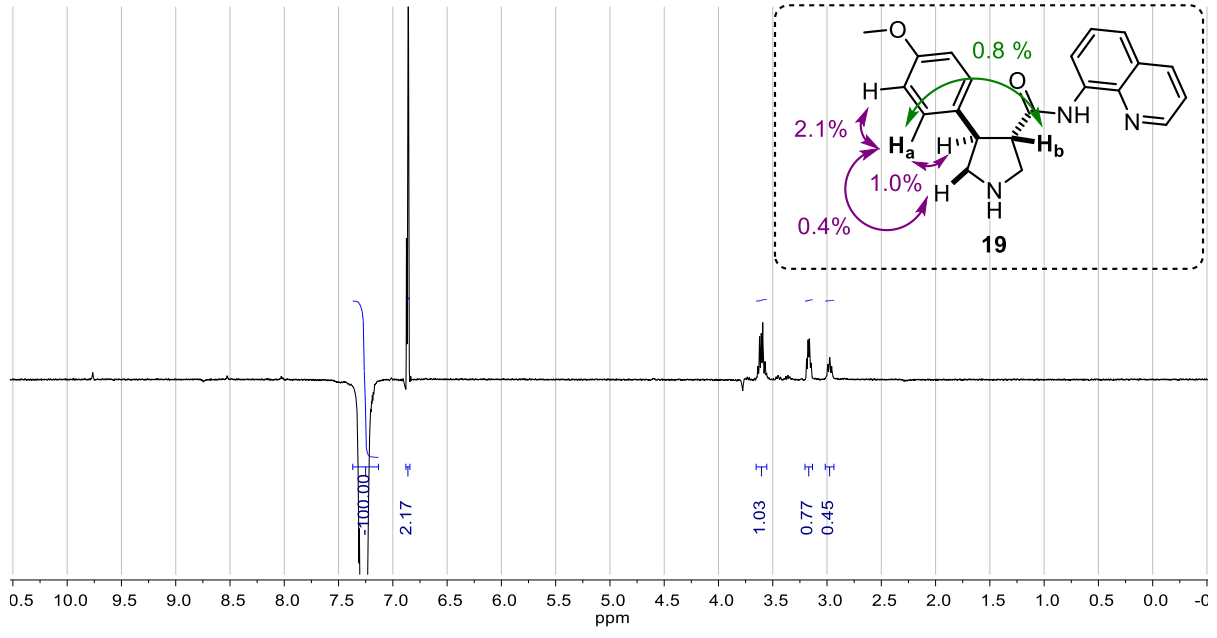
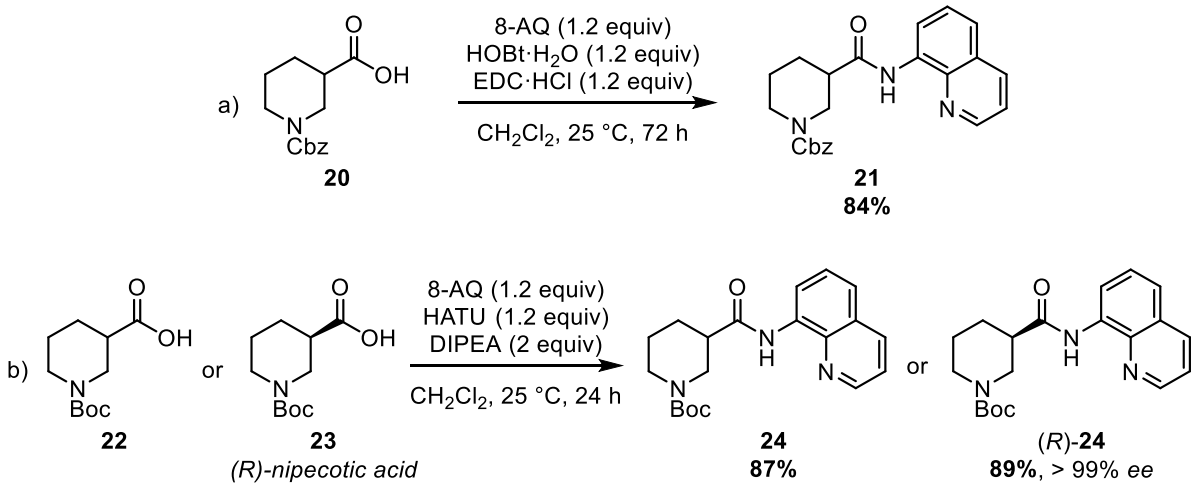


Figure 3.5 NOE spectrum for pyrrolidine **19**, in which proton H_a (δ 7.27 ppm) was selectively irradiated (500 MHz, $CDCl_3$, 298 K).

3.5 Piperidine C(4)–H Arylation

Following the study on pyrrolidine functionalisation, C–H arylation of 6-membered piperidine was investigated.

N-Cbz piperidine-3-carboxamide **21** was synthesised using the same EDC-mediated protocol used for the pyrrolidine ring (Scheme 3.12a). However, this set of conditions gave lower yield of the corresponding *N*-Boc derivative. In the latter case, a modified procedure was devised, involving the use of HATU and DIPEA, to access piperidine-3-carboxamide **24** in high yield (Scheme 3.12b). Furthermore, the same conditions could be used to install the aminoquinoline on *N*-Boc (*R*)-nipecotic acid **23** in 89% yield with no loss of enantiomeric excess.

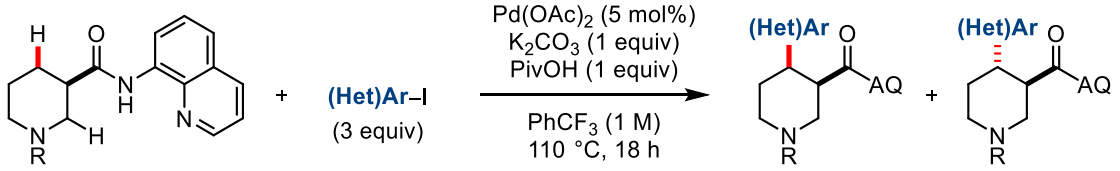


Scheme 3.12 Synthesis of *N*-Boc and *N*-Cbz piperidines-3-carboxamide **21**, **24** and (*R*)-**24**.

With these compounds in hand, the Pd-catalysed C(4)–H arylation of piperidines was evaluated.

3.5.1 Scope of *N*-Protecting Groups and Aryl Iodides

The same Pd-catalysed conditions used in the C(4)–H arylation of pyrrolidines also proved suitable for the corresponding piperidine AQ amides **21** and **24**. As for pyrrolidines, the reaction proceeded with high regioselectivity for the 4-position, affording 3,4-disubstituted piperidines (Table 3.8). However, in this case, the formation of minor *trans*-derivatives was observed alongside the expected *cis*-configured products. Although the crude *dr* could only be roughly estimated due to complex overlapping of proton signals, both diastereomers could be separated by flash column chromatography, affording isolated diastereomeric ratios ranging between 6:4 and 7:3 (*cis:trans*). This represents an interesting improvement in stereoselectivity compared to Yu's monodentate DG approach, which only gave a 1:1 mixture of *cis*- and *trans*-isomers (Section 1.4.2.3, Scheme 1.21).[179]



R = Boc **24**
Cbz **21**

Major (cis)
R = Boc **25a–g**
Cbz **27a–c**

Minor (trans)
R = Boc **26a–g**
Cbz **28a–c**

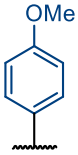
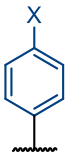
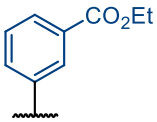
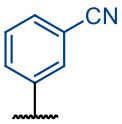
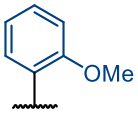
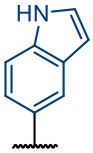
entry	R	(Het)Ar	*cis* (%)[a]	*trans* (%)[a]	*cis* + *trans* (%)[b]	*dr*[c]
1	Boc		**25a** (44) (52)[d]	**26a** (20) (16)[d]	64 (68)[d]	69:31 (76:24)[d]
2	Cbz		**27a** (50)	**28a** (19%)	69	72:28
3	Boc		X =			
			Me	**25b** (35)	**26b** (21)	56	63:57
			F	**25c** (42)	**26c** (16)	58	72:28
			Cl	**25d** (30)	**26d** (14)	44	68:32
4	Cbz		**27b** (25)	/ [e]	25	n.d.
5	Boc		**25e** (25)	**26e** (13)	38	66:34
6	Boc		**25f** (44)	/ [e]	44	n.d.
7	Boc		**25g** (41)	**26g** (24)	65	63:37
8	Cbz		**27c** (47)	**28c** (19)	66	71:29

Table 3.8 Scope of *N*-protecting groups and aryl iodides for piperidine C–H arylation. Reaction scale: 0.5 mmol, unless otherwise stated. [a] Isolated yield of single diastereomers. [b] Overall yield. [c] Isolated *dr* (*cis:trans*). [d] 3.4 mmol scale, 2 M concentration. [e] *trans*-Isomer inseparable from unreacted **21**/**24**.

Both *N*-Boc and *N*-Cbz protecting groups gave similar yield and *dr* of 4-methoxy derivatives (entries 1 and 2). As for the 5-membered ring, increasing the concentration to 2 M enabled the successful scale-up of the reaction to > 3 mmol (entry 1). Various aryl iodides, with either *para*- or *meta*-substitution, could be installed in 25% to 69% combined yields (entries 3–5). The

different reactivity was again dependent on the electronic nature of the substituents, with higher yield observed for more electron rich examples. For instance, *p*-tolyl and *p*-fluorophenyl groups were introduced in 56% and 58% overall yield respectively, while 4-chloroiodobenzene gave a lower 44% combined yield (entry 3). Interestingly, previously unsuccessful *o*-iodobenzene could now be installed in 44% yield, suggesting a lower sensitivity to steric hindrance compared to the 5-membered ring (entry 6). Finally, electron rich heteroaryl iodides, such as 2-iodothiophene and N-H 5-iodoindole, were well tolerated, affording 65% and 66% overall yield respectively (entries 7 and 8).

3.5.2 Stereochemical Assignment

The relative *cis*-configuration of 3,4-disubstitued piperidine **25a** was assigned based on ^{1}H NMR and NOESY experiments. These were run at 100 °C in DMSO-d_6 to simplify the spectra by promoting coalescence of rotameric signals.

The ^{1}H chemical shifts (δ) and coupling constant values (*J*) for piperidine **25a** indicate a chair conformation in which the amide substituent occupies the axial position, while the aromatic group is equatorial (Figure 3.6a,b). This is consistent with the higher A-value for a phenyl substituent on cyclohexane (3.0 kcal/mol), compared to a CO_2Me group (1.3 kcal/mol).[201] Only equatorial-equatorial (*J* ~ 2.5 Hz) and axial-equatorial (*J* ~ 3–5 Hz) couplings were observed for proton CH_aCO, while proton CH_bAr clearly featured a larger axial-axial coupling (*J* ~ 12 Hz). Furthermore, axial proton H_c (δ 2.68 ppm) resonated at lower field than equatorial H_d (δ 1.69 ppm), in contrast to what is expected for methylene positions both in cyclohexane and piperidine rings.[202] This was ascribed to the deshielding anisotropic effect of the axial carbonyl group.[203]

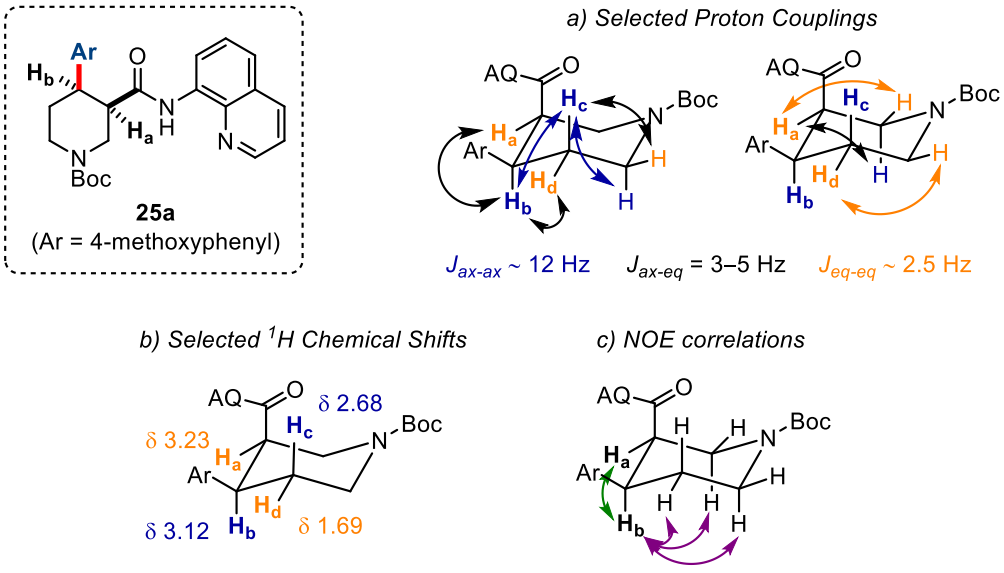


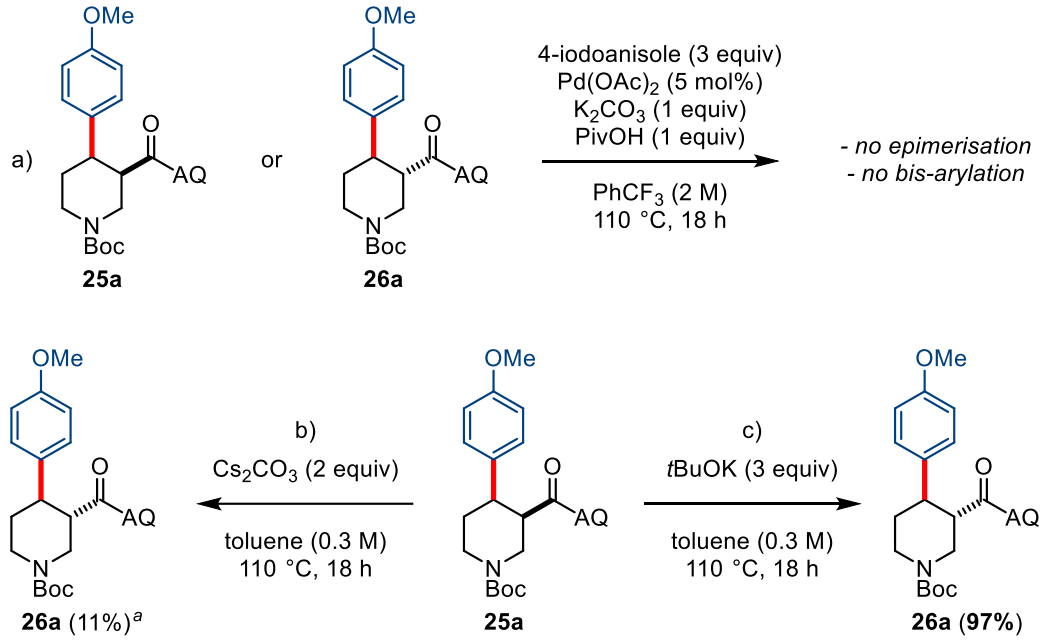
Figure 3.6 Stereochemical assignment of *cis*-piperidine **25a** by ^{1}H NMR and NOESY experiments.

In addition to the observed coupling constants, the *cis*-configuration of piperidine **25a** was confirmed by NOE spectroscopy. In particular, proton CH_bAr was found to correlate exclusively to nearby protons on the same face of the ring, including CH_aCO (Figure 3.6c).

3.5.3 Studies into Epimerisation and Stereochemical Outcome

3.5.3.1 Base-mediated epimerisation of 3,4-disubstituted piperidines

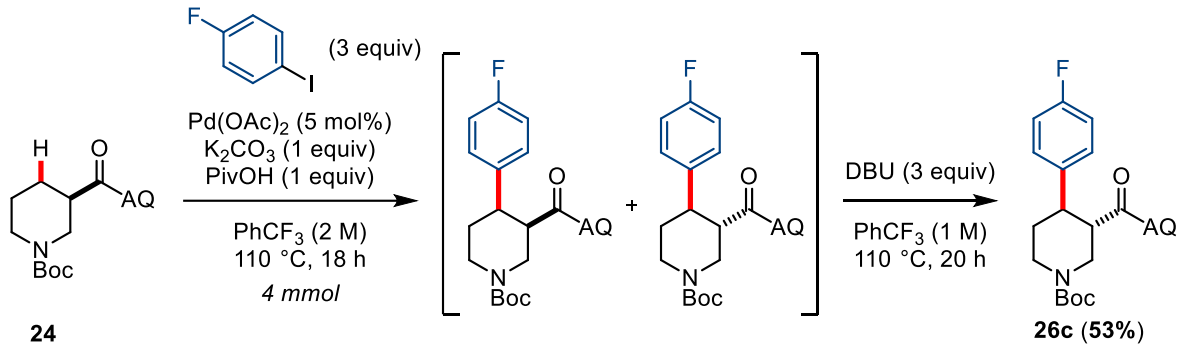
In order to gain insight into the formation of the minor *trans*-isomer, *cis*- and *trans*-piperidines **25a** and **26a** were resubjected to the C–H arylation conditions (Scheme 3.13a). Both isomers did not give any detectable *bis*-arylation and were found to be configurationally stable. The absence of any detectable epimerisation of *cis*-derivative **25a** suggested that *trans*-piperidine **26a** was not formed through *cis*-to-*trans* isomerisation under the standard reaction conditions. Instead, the *trans*-diastereomer is more likely to derive directly from a discrete *trans*-palladacycle intermediate (*vide infra*).



Scheme 3.14 a) Control experiments on the configurational stability of *cis*-and *trans*-piperidines **25a** and **26a**. b) and c) Base-mediated epimerisation of *cis*-derivative **25a**. [a] Yield calculated by ^{1}H NMR using 1,3,5-TMB as internal standard.

In comparison to the corresponding pyrrolidine, *cis*-3,4-disubstituted piperidine **25a** was less prone to epimerisation, likely because of a lower degree of steric clash between the *cis*-substituents. For instance, the use of Cs_2CO_3 was ineffective in promoting *cis*-to-*trans* isomerisation, resulting in only 11% conversion by ^{1}H NMR (Scheme 3.13b). Nonetheless, complete conversion could be achieved in the presence of stronger bases. Treating *cis*-piperidine **25a** with excess *t*-BuOK in toluene at 100 °C afforded the corresponding *trans*-isomer **26a** in 97% yield after simple aqueous work-up (Scheme 3.13c).

Alternatively, DBU could also be used to promote efficient epimerisation, giving the opportunity to develop a 2-steps, one-pot protocol for the *trans*-C(4)–H arylation of piperidine rings. This was exemplified in the reaction with 4-fluoroiodobenzene, which gave *trans*-piperidine derivative **26c** in 53% yield on a 4 mmol scale (Scheme 3.14). A longer epimerisation time was required, due to the lower reactivity of the 6-membered substrate in comparison with the pyrrolidine ring. However, this strategy offered the additional advantage to avoid separation of the diastereomers formed by C–H arylation, affording exclusively the *trans*-isomer after a single purification step.

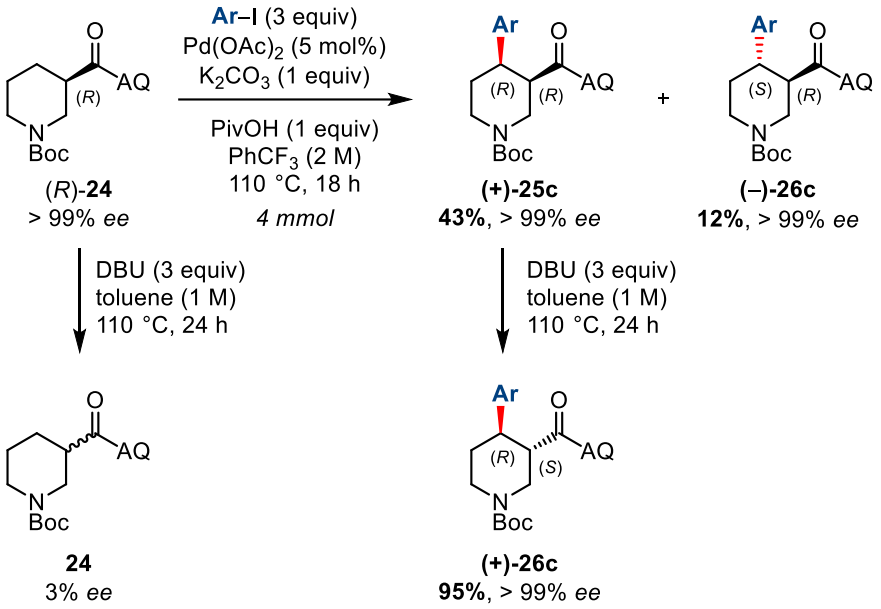


Scheme 3.14 Synthesis of *trans*-configured piperidine **26c** *via* one-pot C(4)–H arylation/epimerisation.

3.5.3.2 C–H Arylation on enantioenriched piperidine substrate

To provide further understanding of the origin of the diastereomeric mixture observed with piperidine substrates, Pd-catalysed C–H arylation was performed on enantioenriched piperidine amide (*R*)-**24** (Scheme 3.15). Reaction with 4-fluoroiodobenzene was carried out on a 4 mmol scale, giving *cis*- and *trans*-derivatives **(+)-25c** and **(–)-26c** in 55% combined yield (43% + 12% isolated yield, respectively). Chiral HPLC analysis on both diastereomeric products revealed that these were formed as single enantiomers, each in > 99% *ee*, supporting the configurational stability of both substrate and arylated products under the arylation conditions.

DBU-mediated epimerisation of the isolated *cis*-derivative **(+)-25c** formed *trans*-piperidine **(+)-26c** as the dextrorotatory enantiomer in 95% yield and > 99% *ee*. Complete racemisation of piperidine (*R*)-**24** was observed under identical conditions, suggesting a viable epimerisation of the C(3) centre. Furthermore, the absolute configuration of **(–)-26c** and **(+)-26c** was confirmed after DG removal by comparison with literature compounds (see Section 4.1.4). Importantly, the opposite sign of optical rotation found for *trans*-piperidines **(–)-26c** and **(+)-26c** is consistent with the proposed formation of a *trans*-palladacycle leading to *trans*-diastereomer **(–)-26c**.



Scheme 3.15 C–H Arylation and base-mediated epimerisation on enantioenriched piperidine derivatives. Ar = 4-fluorophenyl.

3.5.3.3 trans-Palladacycle as proposed reaction intermediate

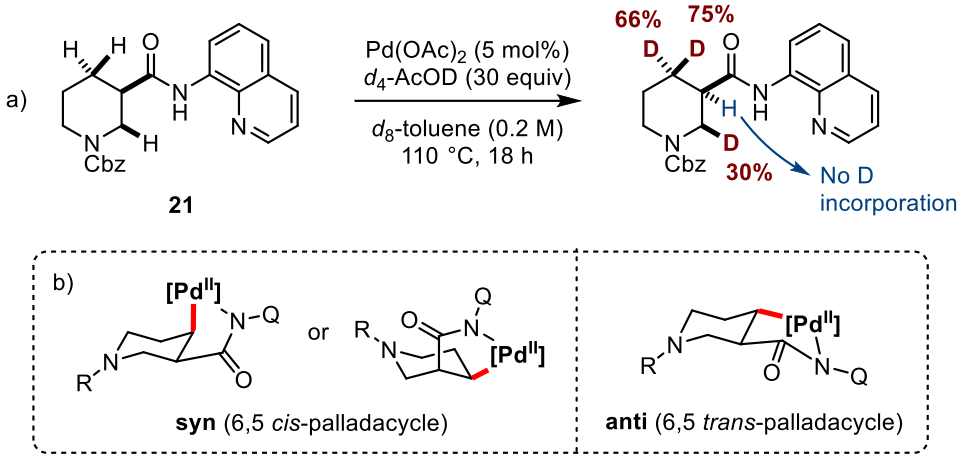
In order to probe the viability of a reversible *trans*-C–H activation, Pd-catalysed deuteration of piperidine amide **21** was attempted. The *N*-Cbz protecting group was used, due to its acid-resistance, to undergo treatment with catalytic $Pd(OAc)_2$ and AcOD-d_4 (Scheme 3.16a). The percentage of deuterium incorporation (% D) was determined after filtration through Celite, by quantitative ^{1}H NMR (400 Hz) at 100 °C in DMSO-d_6, using a delay time d_1 = 70 s.*

Consistent with the regioselectivity of C–H arylation, deuteration occurred preferentially at the 4-position. Importantly, a similar % D was observed at both *cis*- and *trans*-C(4)–H positions (75% D and 66% D, respectively). No deuterium incorporation was observed at C(3), excluding enol formation and epimerisation occurring under the acidic conditions. This evidence supports the possible formation of both *cis*- and *trans*-palladacycle intermediates at C(4), leading to the observed diastereomeric mixture of piperidine products (Scheme 3.16b). This is consistent with the proposed formation of related *trans*-palladacycles in the reported C–H functionalisation of 6-membered cyclohexane and tetrahydropyran rings.[166,170,204]

On the other hand, the 2-position was also deuterated, although in a lower extent (30% D). This occurred exclusively *cis*- to the directing group, likely due to the *N*-protecting group hindering *trans*-C–H activation. This would suggest the possibility for the α-C–H bond to undergo Pd-catalysed CMD, at least under the conditions used for D incorporation. However,

* To account for the longest relaxation time (T_1 ≈ 13 s) of an aromatic Cbz proton resonating at δ 7.30 ppm. This was determined by Peter Haycock (Imperial College London).

activation of this C–H bond appears to be disfavoured in comparison with *cis*- and *trans*-C(4) positions. Furthermore, a C(2)-palladacycle might undergo more difficult oxidative additive or reductive elimination steps, contributing to the C(4) regioselectivity.



Scheme 3.16 a) Pd-catalysed C–H deuteration of *N*-Cbz piperidine amide **21**. b) Proposed reactive Pd(II) intermediates formed through concerted metalation deprotonation (CMD).

The position of protons relative to the directing group in **21** was assigned by ^{1}H NMR, based on chemical shifts and coupling constants values. In particular, monosubstituted piperidine **21** was found to adopt a preferential chair conformation with the C(3)-amide in equatorial position (Figure 3.7). This was supported by the axial-axial (J ~ 10 Hz) and axial-equatorial (J ~ 4 Hz) couplings observed for proton H_a (δ 2.85 ppm). In a similar way, the signal at δ 3.23 ppm (dd, J = 13.2, 10.0 Hz) was assigned as axial proton H_b (*cis* to the DG). Equatorial protons (γ to the heteroatom) in unsubstituted N-H piperidine are more deshielded than the corresponding axial protons, due to the anisotropic effect of the adjacent C–C bonds.[202b] Based on this consideration, multiplets at δ 2.14–2.06 ppm and δ 1.85–1.73 ppm were assigned respectively as equatorial H_d (*trans* to DG) and axial H_e (*cis* to DG), despite their complex multiplicity.

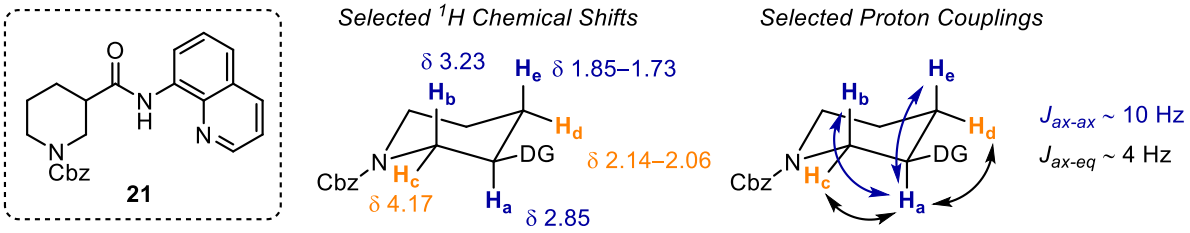


Figure 3.7 Stereochemical assignment of *N*-Cbz piperidine **21** by ^{1}H NMR (DMSO-d_6, 100 °C).

3.6 Towards Medicinal Chemistry Applications: Divergent Removal of the Directing Group

The possibility to remove the directing auxiliary after C–H arylation is of fundamental importance to access compounds of pharmaceutical interest. In particular, strategies to replace the DG with polar functionalities, such as carboxylic acid, amide or alcohol groups, followed by simple *N*-deprotection, would provide access to building blocks and fragment-like molecules in a desirable range of M_W (< 250) and lipophilicity (clogP < 2).[35] These functional groups not only offer the potential to develop specific binding interaction with biological targets, but also provide useful handles for further synthetic elaboration (*e.g.* fragment growth into lead-like compounds). In addition, a divergent strategy to access various derivatives after a single C–H arylation step would be highly beneficial for the rapid construction of diverse collections of pyrrolidine and piperidine fragments.

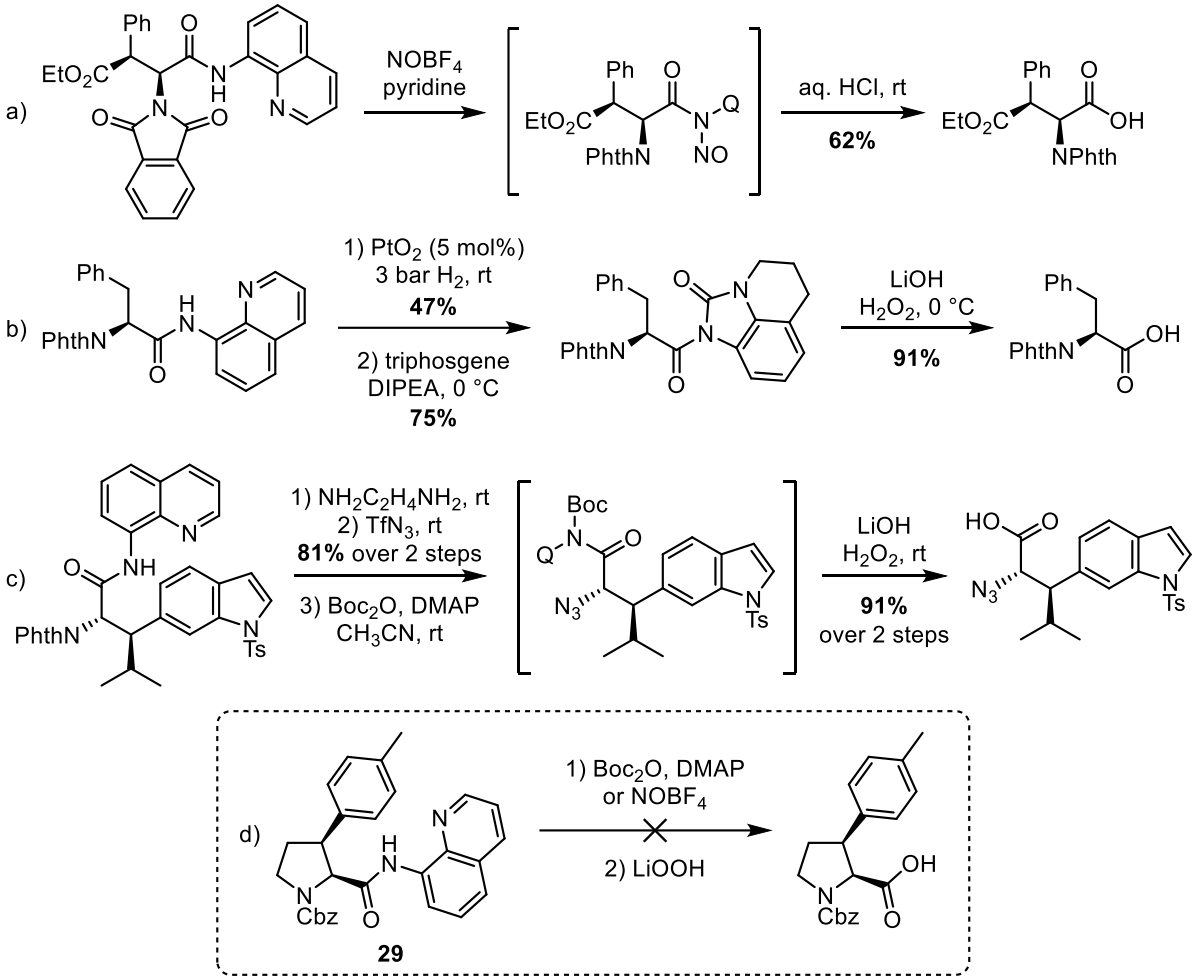
Due to the strong amide bond, AQ cleavage has often proved problematic, typically requiring the use of strong acids (*e.g.* H_2SO_4 or TfOH) or bases (*e.g.* NaOH) at high temperature (100–130 °C).[125,205,206] Notwithstanding the success of these protocols and their utility to access different stereochemistry on specific substrates,[167] such conditions can limit dramatically the functional group tolerance of the DG removal step. In the specific case discussed here, preserving the *cis*-configuration of the arylated pyrrolidines and piperidines would likely be very challenging under such forcing conditions. Furthermore, the presence of either *N*-Boc or *N*-Cbz protecting groups was an additional concern, as preserving these groups would allow higher synthetic flexibility for downstream elaboration. Therefore, milder conditions were investigated to achieve divergent AQ removal and access carboxylic acid, amide and alcohol derivatives, while preserving both *cis*-stereochemistry and *N*-protecting group.

3.6.1 Carboxylic Acid Derivatives

Useful methods for the cleavage of strong amide bonds involve amide activation, by increasing the electrophilicity of the carbonyl group and/or forcing geometrical distortion to disrupt the amide conjugation. This then allows the use of mild hydrolytic conditions to form the corresponding carboxylic acid derivatives.

Following seminal studies on amide activation/hydrolysis by Grieco and Evans,[207] AQ removal has been successfully achieved on various substrates. Activation of AQ amides has been demonstrated through nitrosylation[145e] or quinoline hydrogenation followed by treatment with triphosgene to form an activated cyclic urea (Scheme 3.17a,b).[145a] However, the most common approach to AQ amide activation arguably involves reaction with Boc_2O to form a labile imide functionality, that can be cleaved with LiOOH at room temperature.[114a] Despite allowing the use of mild conditions, the latter approach is typically limited by high sensitivity to steric

hindrance. For instance, conversion of the bulky α-*N*-phthalimide group into a smaller α-azido functionality was key to cleave the AQ amide in Chen's total synthesis of Celogentin C (Scheme 3.17c).[129c]

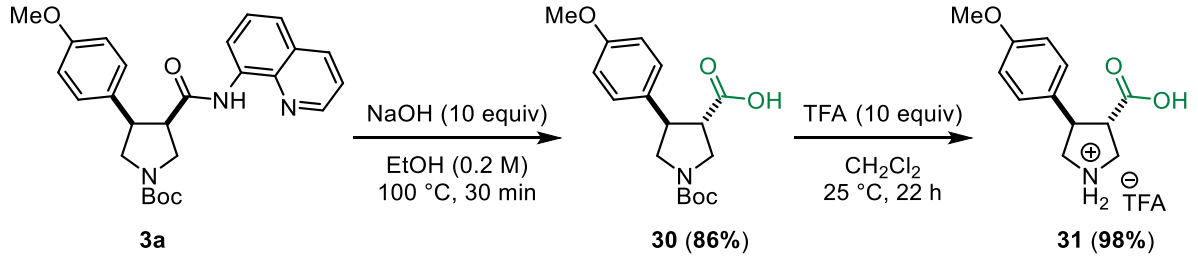


Scheme 3.17 a)–c) Literature examples of amide activation/hydrolysis strategies to remove the aminoquinoline DG. d) Unsuccessful hydrolysis of the AQ amide on proline derivative **29**.

Unfortunately, the amide activation/hydrolysis strategy was unsuccessful in removing the AQ auxiliary from sterically demanding 3-arylated proline derivative **29**, regardless of the method used for amide activation (Scheme 3.17d).[208] Therefore, the AQ removal on *cis*-3,4-disubstituted pyrrolidines represented a major concern at the start of this investigation.

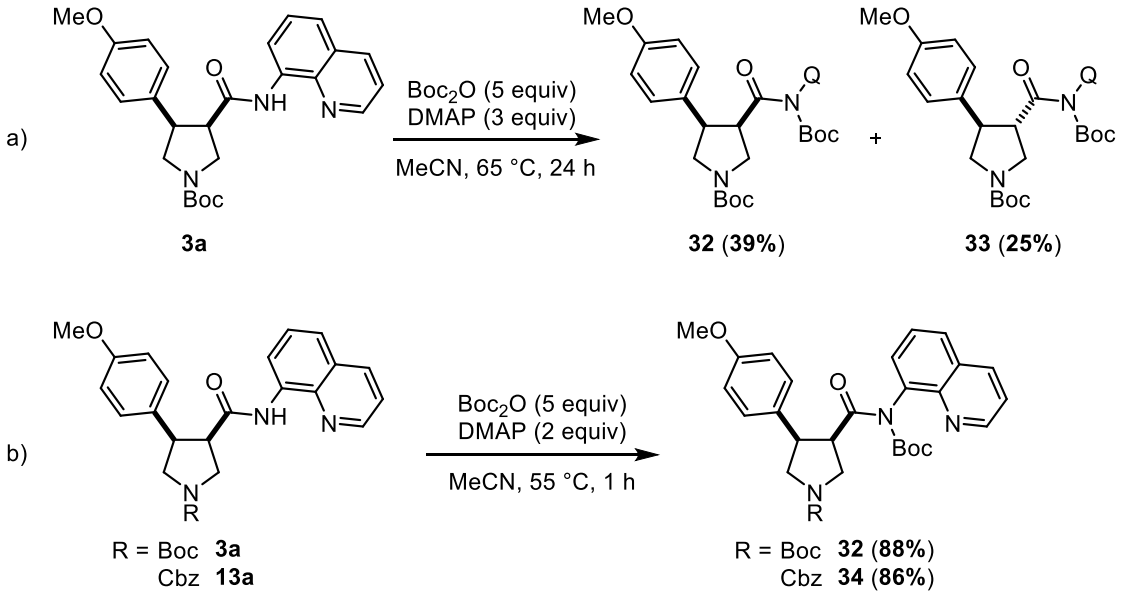
In order to probe the viability of AQ removal on these substrates, *N*-Boc arylated derivative **3a** was initially treated under strong basic conditions, involving the use of 10 equivalents of NaOH in EtOH at 100 °C. Full conversion was achieved after just 30 min reaction, and *N*-Boc pyrrolidine carboxylic acid **30** was isolated in 86% yield after simple acid/base work-up (Scheme 3.18). Unsurprisingly, complete epimerisation was observed under the reaction conditions, and pyrrolidine **30** was formed as a single *trans*-diastereomer. Subsequent

treatment with TFA afforded unnatural β-aminoacid **31** as the corresponding TFA salt in 98% yield. Although this approach provides access to *trans*-arylated pyrrolidine acids with no need for a separate epimerisation step, a complementary strategy that preserves the initial *cis*-configuration would be highly beneficial to enable biological evaluation of both isomers.



Scheme 3.18 One-pot AQ removal/epimerisation of *cis*-3,4-disubstituted pyrrolidine **3a**, followed by Boc deprotection to form *trans*-configured β-aminoacid **31**.

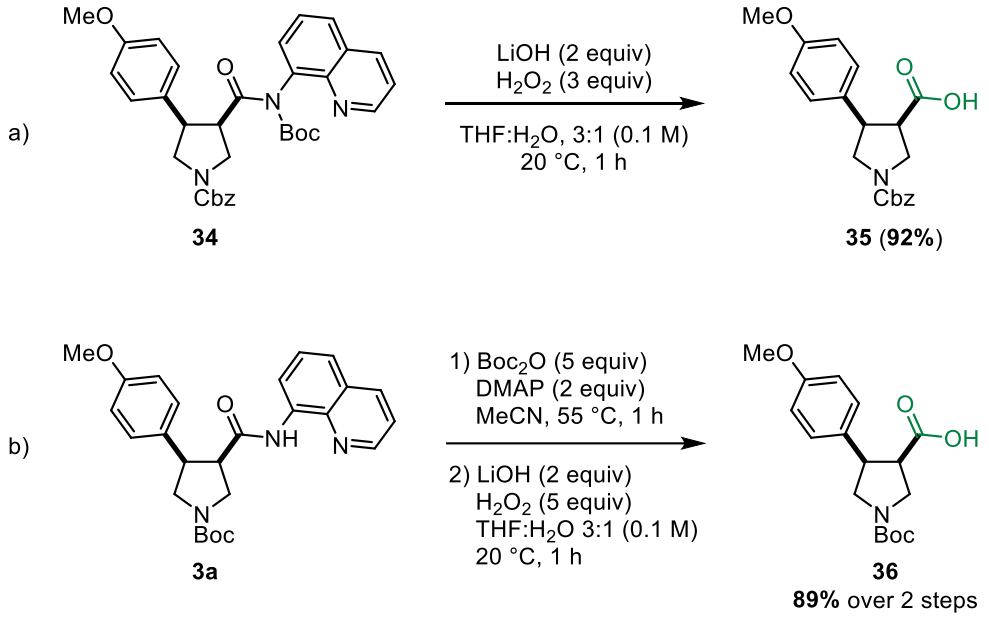
Therefore, the use of a milder amide activation/hydrolysis sequence was evaluated, involving carbamoylation with Boc_2O, followed by hydrolysis with LiOOH. Although initial attempts to activate pyrrolidine amide **3a** in the presence of excess Boc_2O and DMAP showed promising conversion, the corresponding Boc-protected product was found to be particularly sensitive to epimerisation. A mixture of *cis*- and *trans*-derivatives **32** and **33** was observed when the reaction was stirred at 65 °C for 24 h (Scheme 3.19a). Reasoning that this could be due to DMAP-mediated isomerisation, the loading of DMAP, the temperature and the reaction time were reduced. Under these conditions, carbamoylation of both *N*-Boc and *N*-Cbz pyrrolidines **3a** and **13a** proceeded in high yield, without any noticeable epimerisation (Scheme 3.19b).



Scheme 3.19 a) Initial attempt and b) final conditions for the Boc protection of *cis*-3,4-disubstituted pyrrolidines **3a** and **13a** to form activated imides **32** and **34**.

Pleasingly, subsequent reaction with LiOOH, formed *in-situ* from H_2O_2 and LiOH, proceeded smoothly in just 1 h at rt, affording *cis*-pyrrolidine acid **35** in excellent yield as a single diastereomer (Scheme 3.20a). In order to minimise the chances of epimerisation, LiOOH was preformed and reacted under argon atmosphere to avoid potential reaction of LiOH and/or LiOOH with CO_2 generating lithium carbonate. Importantly, the Cbz protecting group was well tolerated under these mild hydrolytic conditions.

Isolation of the Boc-protected amide intermediate was not necessary for the success of the reaction, as demonstrated in the synthesis of *N*-Boc *cis*-pyrrolidine acid **36**. This derivative was isolated in 89% yield in a telescoped process, in which the crude Boc-protection mixture was directly treated with LiOOH (Scheme 3.20b).



Scheme 3.20 a) Stepwise and b) telescoped AQ-removal *via* Boc-protection/hydrolysis to access *cis*-pyrrolidine carboxylic acids **35** and **36**.

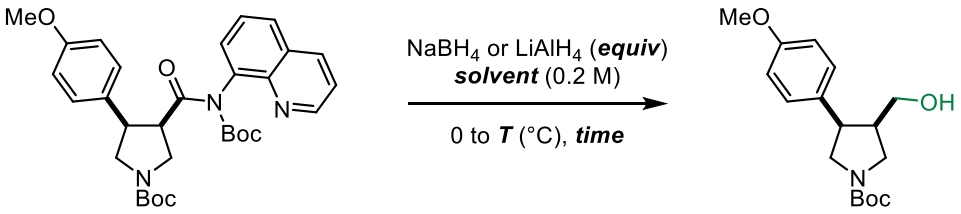
Based on these promising results, it was envisaged that Boc-protected amides **32** and **34** could be used as valuable common intermediates to access various derivatives. Therefore, the use of different nucleophiles, including hydride, alcohols or amines, was investigated.

3.6.2 Alcohol, Methyl Ester and Secondary Amide Derivatives

3.6.2.1 Hydride reduction towards alcohol products

Inspired by the reaction of acylimidodicarbonates with $NaBH_4$ for the reduction of primary amides reported by Ragnarsson,[209] the possibility to convert the Boc-protected AQ amide to a primary alcohol was evaluated. Given the poor solubility of *N*-Cbz derivatives in EtOH (*vide infra*), *N*-Boc pyrrolidine **32** was selected as a suitable substrate for this study. $NaBH_4$ was

initially evaluated to access alcohol derivative **37** by reduction of the activated amide (Table 3.9). Using 2 equiv of $NaBH_4$ at rt afforded the reduced product **37** in 20% yield with a small degree of epimerisation (entry 1). The use of MeOH as solvent was unsuccessful even in the presence of 5 equivalents of $NaBH_4$ (entry 2). Increasing the temperature to 40 °C, gave the desired product in 45% yield as an inseparable mixture of *cis*- and *trans*-isomers (7:3 *dr,* entry 3). The discrepancy between high conversion and low isolated yield, as well as the epimerisation, were likely due to a slow reduction of a configurationally labile aldehyde intermediate. Accordingly, increasing the loading of $NaBH_4$ at 40 °C resulted in complete consumption of starting material (entry 4). The desired alcohol was isolated in 81% yield, although with only a small improvement in *dr*. Reasoning that a faster reduction of the aldehyde intermediate could avoid epimerisation, $LiAlH_4$ was evaluated. Pleasingly, this gave the desired *cis*-alcohol product **37** in 76% as a single diastereomer after just 30 min reaction at 25 °C (entry 5). This represented the first example of direct reduction of an activated AQ amide to form a primary alcohol derivative.



32 **37**

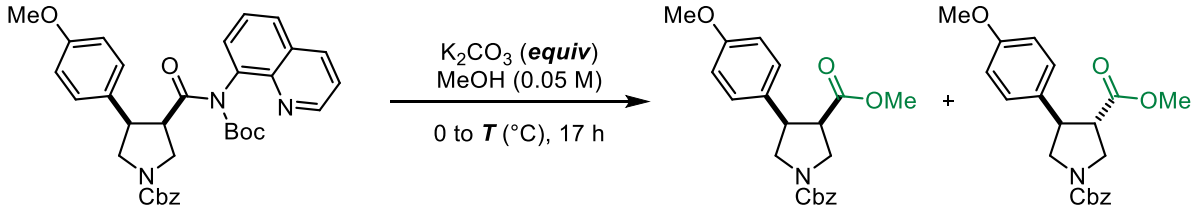
entry	hydride source (equiv)	solvent	T (°C)	time (h)	conversion (%)[a]	37 (%)[b]	*dr* cis:trans[c]
1	$NaBH_4$ (2.0)	EtOH	25	24	29	20	9:1
2	$NaBH_4$ (5.0)	MeOH	25	24	3	-	-
3	$NaBH_4$ (2.0)	EtOH	40	24	80	45	7:3
4	$NaBH_4$ (5.0)	EtOH	40	24	91	81	8:2
5	**$LiAlH_4$ (4.0)**	**THF**	**25**	**0.5**	**> 95**	**76**	**> 50:1**

Table 3.9 Optimisation of the reduction of *N*-Boc amide **32**. Relative configuration of major and minor components of the isolated mixtures was confirmed by NOE spectroscopy. [a] Calculated by ^{1}H NMR spectroscopy on the crude reaction mixture. [b] Isolated yield. [c] Calculated by ^{1}H NMR spectroscopy on the isolated product.

3.6.2.1 Methanolysis towards methyl ester products

The conversion of AQ amides into ester derivatives through direct alcoholysis have been the subject of recent investigations. In 2017, Oshima reported the esterification of unactivated AQ amides catalysed by a Ni(II)-diketonate complex.[145c] At a similar time, Mashima developed a

one-pot protocol involving propylene oxide ring-opening, followed by Zn-catalysed esterification of the resulting *N*-β-hydroxyethylamides.[145d] However, the requirement for high temperatures (80–100 °C) and/or strong basic conditions (*e.g.* NaH) limited the functional group compatibility of these strategies. On the other hand, Chen demonstrated the methanolysis of Boc-activated AQ amides with MeOH and K_2CO_3 under mild conditions.[210] This was envisaged as an attractive alternative for the formation of methyl ester pyrrolidine derivatives (Table 3.10). Although the Cbz group was well tolerated in the reaction of pyrrolidine amide **34**, partial epimerisation was observed even at room temperature, with *cis*- and *trans*-pyrrolidine esters **38** and **39** being isolated in 56% and 29% yield respectively (entry 1). Reducing the temperature to 0 °C did not lead to useful conversion of the starting material, while halving the loading of K_2CO_3 resulted in lower overall conversion and lower *dr* (entry 2 and 3).



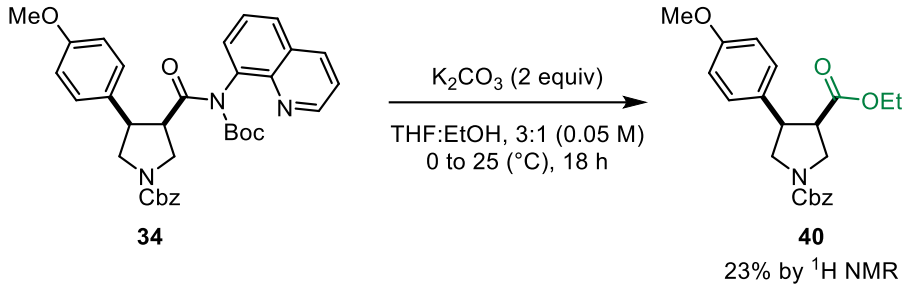
entry	K_2CO_3 equiv	T (°C)	SM conversion (%)[a]	*dr* (*cis:trans*)[a]	38 (%)[b]	39 (%)[b]	tot (%)[b]
1	**2.0**	**25**	**94**	**7:3**	**56**	**29**	**85**
2[c]	2.0	0	-	-	-	-	-
3	1.0	25	51	6:4	-	-	-

Table 3.10 Optimisation of the methanolysis of *N*-Boc amide **34**. The relative configuration of both diastereomeric products was confirmed by NOE spectroscopy. [a] Calculated by ^{1}H NMR spectroscopy on the crude reaction mixture. [b] Isolated yield. [c] 2 h.

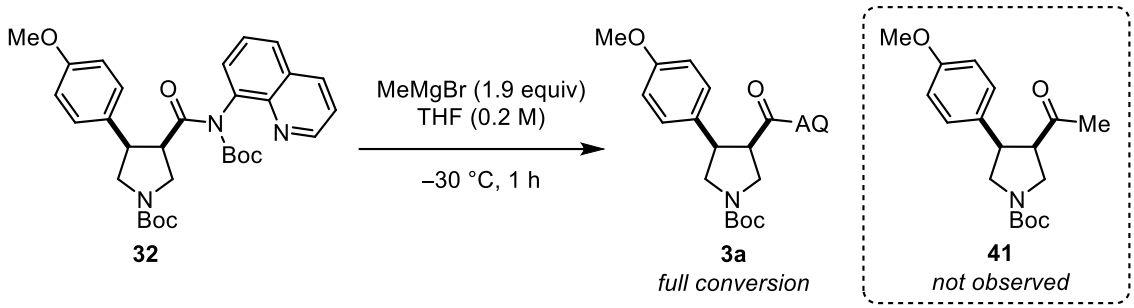
The formation of the corresponding ethyl ester derivative was unsuccessful, due to the very poor solubility of pyrrolidine **34** in EtOH. However, using a 3:1 mixture of THF:EtOH, formation of the desired ethyl ester pyrrolidine **40** was observed, though in low conversion (Scheme 3.21). Although this reaction requires further optimisation, this result offers a proof of concept for the potential formation of different ester derivatives other than methyl.

Following this, the reactivity of carbamoylated amide **32** in the presence of MeMgBr was also investigated. It was envisaged that this activated amide could react with the Grignard reagent in a Weinreb amide-like fashion to afford the correspondent methyl ketone **41**. However, after 1 h reaction at –30 °C, full conversion to the deprotected pyrrolidine amide **3a**, with loss of the Boc group, was observed (Scheme 3.22). This likely derived from a preferential nucleophilic

attack the Boc group and was not further investigated. Instead, transamidation with amine reagents was evaluated.



Scheme 3.21 Preliminary evidence for esterification of pyrrolidine amide **34** with EtOH.

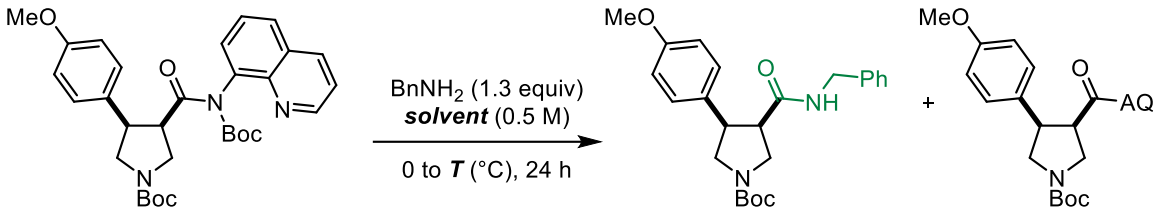


Scheme 3.22 Attempted reaction of *N*-Boc amide **32** with Grignard reagents.

3.6.2.2 Transamidation towards secondary amide products

In 2017, Szostak described the metal-free transamidation of activated secondary amides with primary and secondary amines.[211] Although no AQ examples were reported, a similar approach was investigated to achieve transamidation on *N*-Boc protected AQ amide **32** with $BnNH_2$. Szostak's conditions involved the use of 3 equivalents of Et_3N in CH_2Cl_2 to promote the reaction. In applying to pyrrolidine **32**, the additional base was avoided to preserve the *cis*-configuration. Furthermore, the loading of benzylamine was reduced from 3 to 1.3 (Table 3.11). Under these modified conditions, only traces of product were observed after 18 h reaction at 25 °C (entry 1). Performing the reaction at 45 °C led to approximately 50% conversion, but a significant proportion of Boc-deprotected amide **3a** was observed by ^{1}H NMR (entry 2). Benzyl amide **42** was isolated in 44% yield after 24 h at 60 °C (entry 3). Switching the solvent to toluene finally gave the desired product **42** in 69% yield, although a small amount of Boc deprotection could not be avoided (entry 4).

While this study was carried out, a similar set of conditions was reported by Verho for the metal-free transamidation of aminoquinoline amides.[145b] This work confirmed that the chemoselectivity for transamidation over competing Boc-deprotection is highly dependent on steric hindrance, with *ortho*-substituted benzamides being unsuccessful substrates.

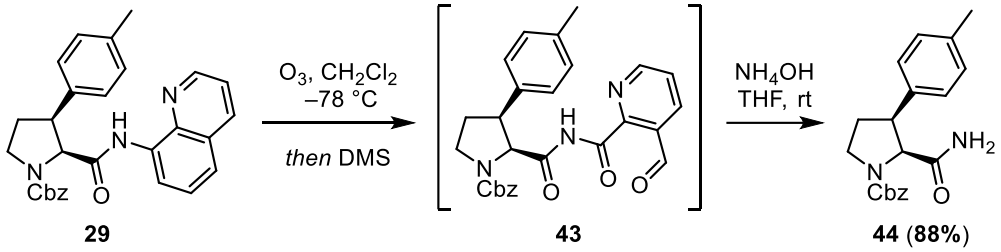


entry	T (°C)	solvent	32 (%)[a]	42 (%)[a]	3a (%)[a]
1	25	CH_2Cl_2	> 95	traces	-
2	45	CH_2Cl_2	37	37	25
3	60	CH_2Cl_2	27	44 (44)[b]	29
4[c]	**60**	**toluene**	**3**	**71 (69)[b]**	**26**

Table 3.11 Optimisation of the transamidation of *N*-Boc amide **32** with $BnNH_2$. [a] Relative composition of the crude reaction mixture by ^1H NMR spectroscopy. [b] Isolated yield. [c] 1.5 equiv of benzylamine.

3.6.3 Primary Amide Derivatives

In 2016, an alternative strategy to remove the AQ auxiliary with high tolerance to steric congestion was reported by Maulide.[144b] This involved an ozonolytic fragmentation of the aminoquinoline DG, to form a labile imide intermediate (**43**). Subsequent reaction of this activated species with NH_3 or LiOOH afforded the corresponding primary amide or carboxylic acid derivatives. This innovative approach enabled efficient AQ removal also on very hindered substrates, unreactive under typical hydrolytic conditions, including proline amide **29** which could be deprotected in high yield (Scheme 3.23).

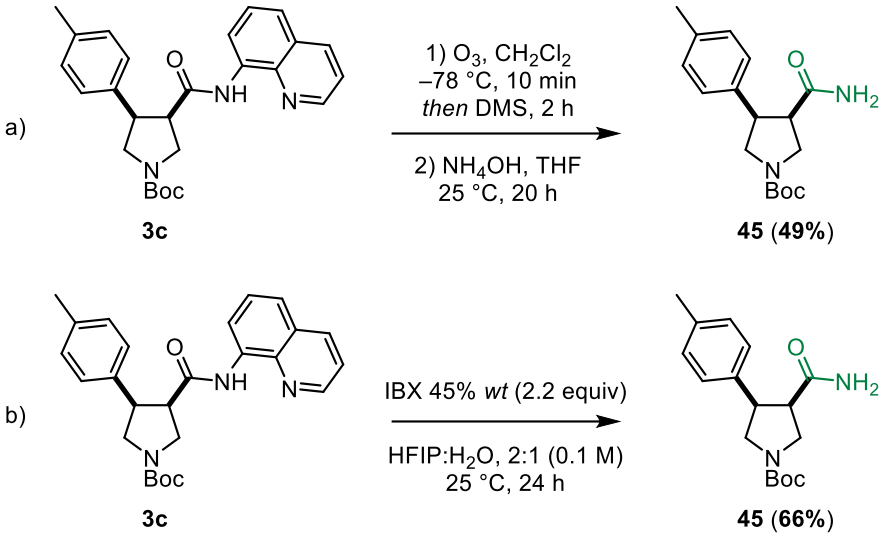


Scheme 3.23 Maulide's ozonolytic cleavage of the aminoquinoline DG on sterically demanding proline amide **29**.

Furthermore, in 2018, Zhang described the use of 2-iodoxybenzoic acid (IBX) for the oxidative cleavage of *N*-aryl secondary amides, though without any AQ example.[212]

Given the attractive potential of these oxidative protocols to access primary amides functionalities, both strategies were evaluated for AQ removal on *cis*-pyrrolidine amide **3c**. Pleasingly, treating this derivative under Maulide's ozonolytic conditions gave the desired

pyrrolidine amide **45** in 49% isolated yield, without any sign of epimerisation (Scheme 3.24a). In addition, Zhang's conditions also proved to be successful, and the same amide product could be isolated in 66% after reaction with IBX at 25 °C (Scheme 3.24b).



Scheme 3.24 AQ cleavage to form primary amide **45** under a) ozone- or b) IBX-mediated oxidation.

Later, the use of IBX for specific AQ removal has been systematically studied by Chen, showing that a set of conditions similar to Zhang's original one could be used to remove the AQ auxiliary on various substrates.[144a]

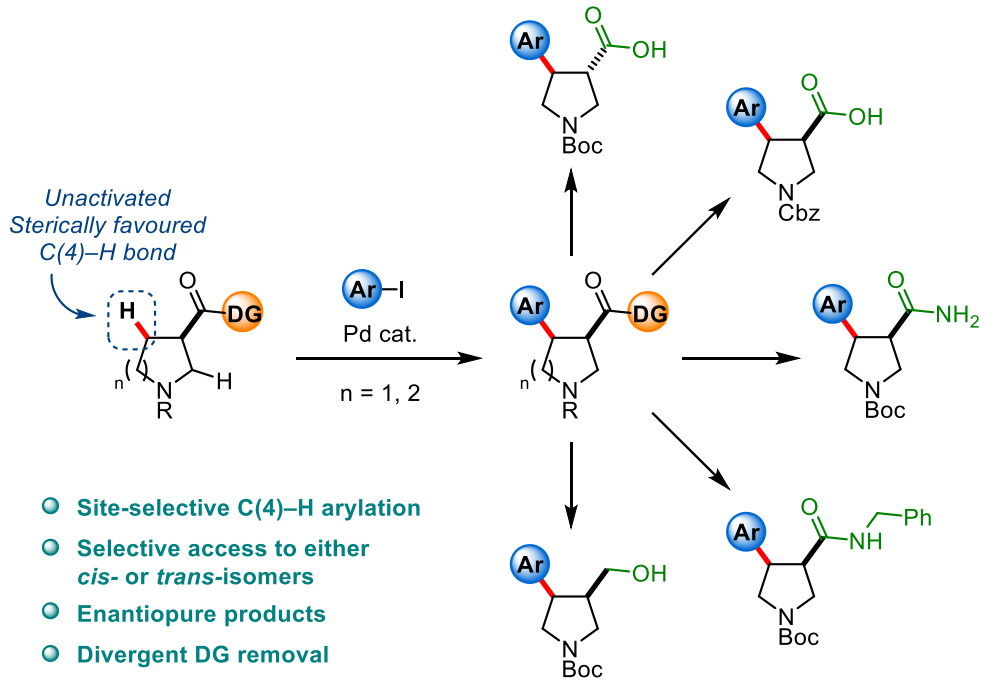
3.7 Conclusions

In conclusion, a highly regio- and stereoselective Pd-catalysed C(sp^3)–H arylation of pyrrolidines and piperidines was developed (Scheme 3.25).

High regioselectivity for the unactivated C(4)-position over competing C(2) was achieved using an aminoquinoline DG at C(3) in combination with *N*-carbamate protecting groups. Conditions were optimised that avoided stoichiometric Ag-salts, using low catalyst loading and inexpensive K_2CO_3 and PivOH, to provide high functional group tolerance. The reaction was scalable up to 1 g and allowed access to 3,4-disubstituted pyrrolidines with excellent *cis*-diastereoselectivity. No racemisation of substrate or product occurred under the reaction conditions, enabling the formation of enantiopure arylated products. Various (hetero)aryl iodides and *N*-protecting groups were successful, allowing the isolation of 30 examples of arylated pyrrolidines in up to 67% yield.

The same conditions were successful for the C–H arylation of the 6-membered piperidine ring, giving similarly high C(4)-regioselectivity, and additional 10 examples of 3,4-disubstituted piperidines were isolated in up to 69% overall yield. In this case, *trans*-configured derivatives were also formed as minor reaction products. Based on epimerisation and C–H deuteration

experiments, this was proposed to derive from the formation of a discrete *trans*-palladacycle intermediate alongside the favoured *cis*-configured species. Formation of enantiopure *cis*- and *trans*-arylated piperidines was also demonstrated.



Scheme 3.25 Regio- and stereoselective Pd-catalysed C(4)–H arylation of pyrrolidines and piperidines followed by divergent DG removal to access pharmaceutically relevant compounds.

Base-mediated epimerisation gave access to the corresponding *trans*-3,4-disubstituted pyrrolidine and piperidine derivatives. Furthermore, a one-pot protocol was developed for the direct *trans*-C–H arylation of both substrates. This involved a sequential C–H arylation/DBU-mediated epimerisation, avoiding additional purification steps.

Finally, a divergent strategy for the removal of the aminoquinoline DG was developed, to provide the potential to deliver various biologically relevant fragments and building blocks, containing amide, carboxylic acid, ester and alcohol functionalities. Different conditions for AQ removal were optimised on *cis*-3,4-disubstituted pyrrolidine amides, to achieve high control over the stereochemical outcome while preserving the *N*-protecting group.

The use of similar DG removal strategies for the piperidine derivatives will be discussed in detail in the next chapter. This will describe the application of the C(4)–H arylation in various drug discovery settings, including the synthesis of piperidine-based drug compounds and the construction of a library of arylated pyrrolidine and piperidine fragments.

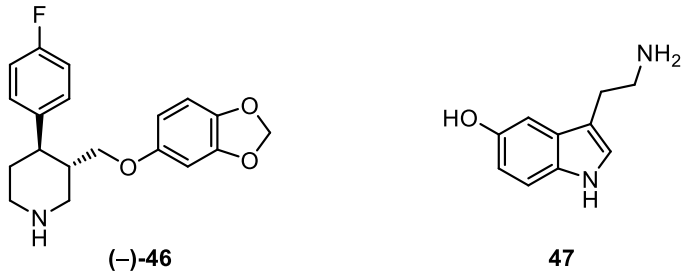
4. Applications of C(4)–H Arylation in Drug Discovery

Having uncovered a method that enables the regio- and stereoselective arylation of pyrrolidines and piperidines at the 4-position, its synthetic potential for drug discovery was investigated. The combination of C(4)–H arylation and DG removal was first envisaged as an attractive approach for the stereocontrolled synthesis of antidepressant drug (–)-paroxetine, which features a 4-aryl piperidine core.

4.1 Stereocontrolled Synthesis of (–)-Paroxetine

4.1.1 Antidepressant (–)-Paroxetine: An Overview

(–)-Paroxetine **(–)-46** is a potent selective serotonin reuptake inhibitor (SSRI, Figure 4.1).[185]



(–)-46
(–)-Paroxetine

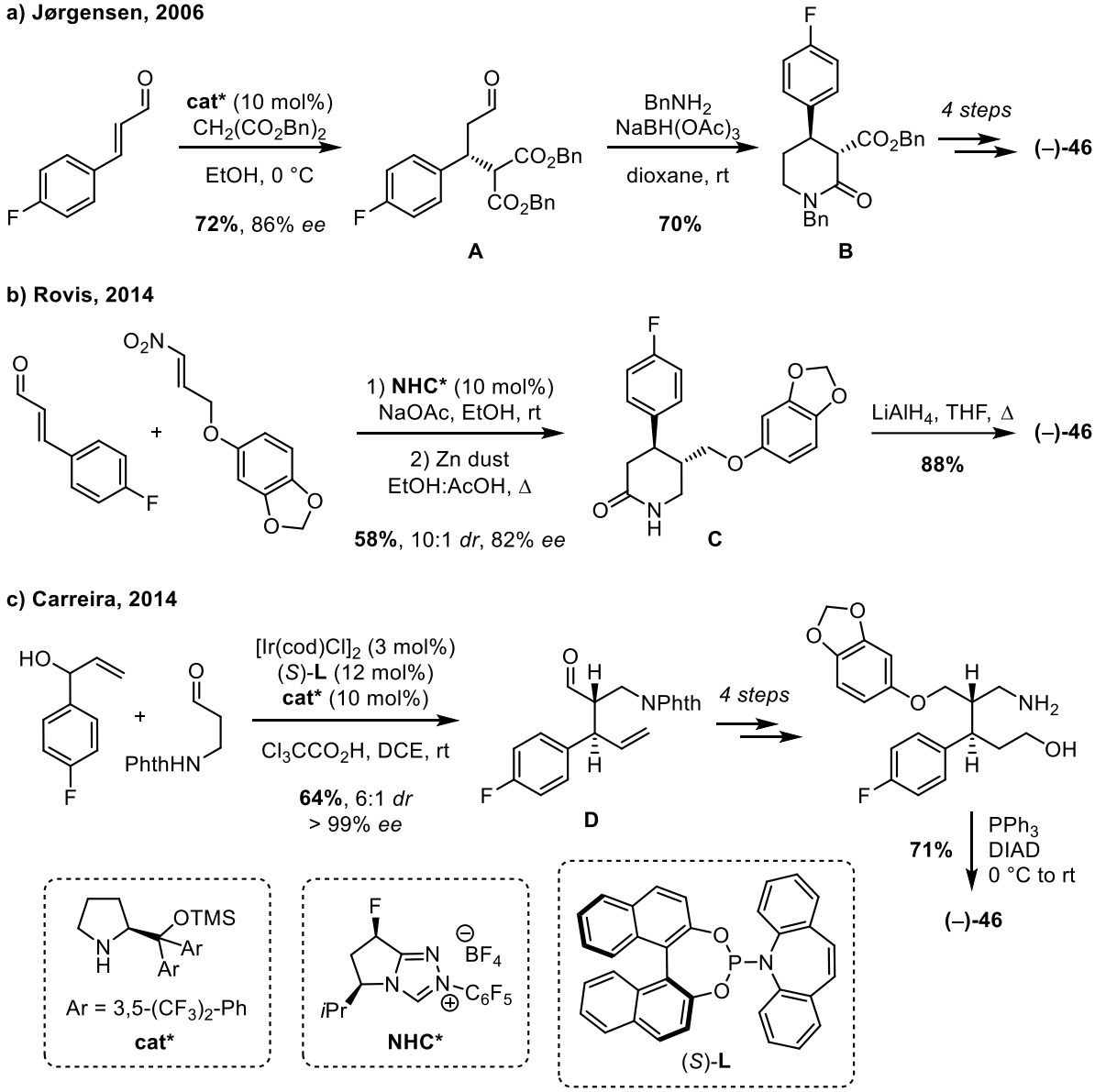
47
Serotonin (5-HT)

Figure 4.1 Antidepressant (–)-paroxetine, a selective serotonin reuptake inhibitor (SSRI).

Serotonin (**47**) or 5-hydroxytryptamine (5-HT) is a crucial neurotransmitter and hormone, which modulates an extremely broad range of physiological and behavioural processes.[213] In the central nervous system, these effects include the regulation of body temperature, movements and sleep, as well as mood, appetite and stress responses among many others.[213] Released in the synaptic space between neurons, serotonin exerts its biological activity by binding to 5-HT receptors and activating signaling response in postsynaptic neurons. The serotoninergic transmission is terminated by the action of transmembrane serotonin transporters (SERT), which remove 5-HT from the synaptic cleft, transporting it back into presynaptic neurons.[214] (–)-Paroxetine binds with high affinity and selectivity to SERT, preventing 5-HT binding and blocking its active reuptake.[214,215] In turn, this enhances serotoninergic neuronal activity. Based on this mechanism of action, (–)-paroxetine is indicated in the treatment of depression, anxiety and obsessive-compulsive disorders, post-traumatic stress disorder and for the management of menopause symptoms.[185] In 2017, (–)-paroxetine was the 68th most frequently prescribed drug in the U.S. with over 11 million prescriptions.[216] Based on this important therapeutic activity, the synthesis of (–)-paroxetine has attracted significant attention over the last few decades.

4.1.2 Recent Advances in the Synthesis of (–)-Paroxetine

Several synthetic approaches have been developed to access the bioactive (–)-enantiomer of paroxetine.[217] Most strategies involve the late-stage construction of the piperidine ring, after a stereoselective step has established the appropriate stereochemistry. For instance, in 2006, Jørgensen reported an organocatalytic enantioselective Michael addition of malonates to α,β-unsaturated aldehydes as the key step in the synthesis of (–)-paroxetine **(–)-46**.[218] Reaction between *trans*-(4-fluoro)-cinnamaldehyde and dibenzyl malonate afforded the addition product **A** in 72% yield and 86% *ee* (Scheme 4.1a). Subsequent reductive amination and lactamisation provided lactam **B** as suitable (–)-paroxetine precursor.

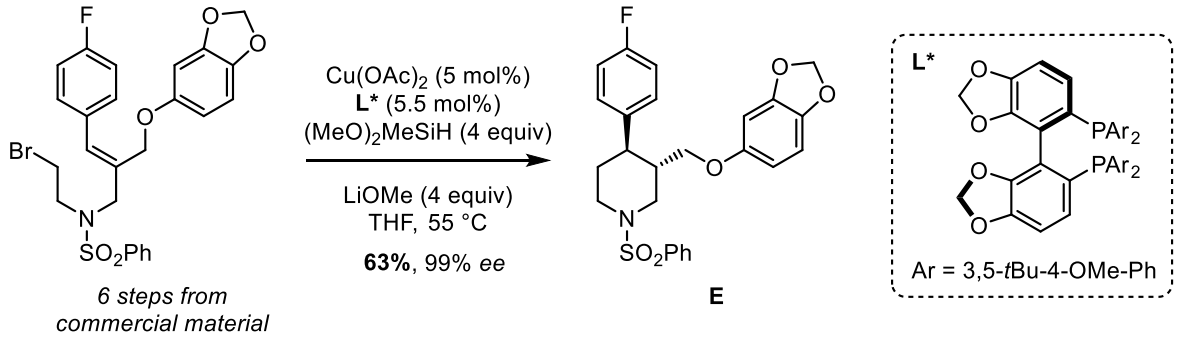


Scheme 4.1 Selected examples of (–)-paroxetine synthesis involving the enantioselective formation of acyclic precursors followed by ring-closing cyclisation.

More recently, various asymmetric conjugate additions have been used to install the correct stereochemistry prior to ring-forming cyclisation.[219] These include the asymmetric addition of malonates, imidomalonates or nitroalkanes to α,β-unsaturated aldehydes, pyrazoleamides and nitro compounds.[220] Furthermore, Rovis described the use of chiral NHC catalysts in the enantioselective addition of enals to nitroalkenes, to form δ-nitroesters. This strategy, followed by one-pot reduction of the nitro functionality, afforded lactam **C** in 58% yield. In turn, this could be readily converted into (–)-paroxetine **(–)-46** upon lactam reduction (Scheme 4.1b).[221]

Other strategies to access optically pure acyclic precursors of (–)-paroxetine have used phase-transfer catalysis for the enantioselective monoalkylation of malonamide esters,[222] or Pd-catalysed asymmetric cross-coupling of allyl acetates with allyl boronic esters.[223] In 2014, Carreira developed a powerful dual catalytic approach for the enantio- and diastereoselective α-allylation of aldehydes.[224] Two contiguous stereocentres could be fixed in a single step, using $[Ir(cod)Cl]_2$ and prolinol ether catalysts, in combination with a chiral phosphoramidite ligand. Under these conditions, aldehyde **D** was synthesised in 64% yield with high enantio- and diastereoselectivity (Scheme 4.1c). This was then converted into (–)-paroxetine **(–)-46** in 5 steps, involving aldehyde elaboration, hydroboration/oxidation and a final ring-closing Mistunobu reaction.

An alternative approach for the synthesis of (–)-paroxetine was reported by Buchwald in 2015. This involved the Cu-catalysed enantioselective intramolecular hydroalkylation of halogenated styrene derivatives.[225] Although several synthetic steps were required to access the desired styrene precursor, *N*-substituted piperidine **E** was then formed in a single enantioselective cyclisation step, using a chiral copper hydride complex generated *in-situ* (Scheme 4.2). (–)-Paroxetine was finally accessed by SmI_2-mediated *N*-deprotection (61%, not shown).

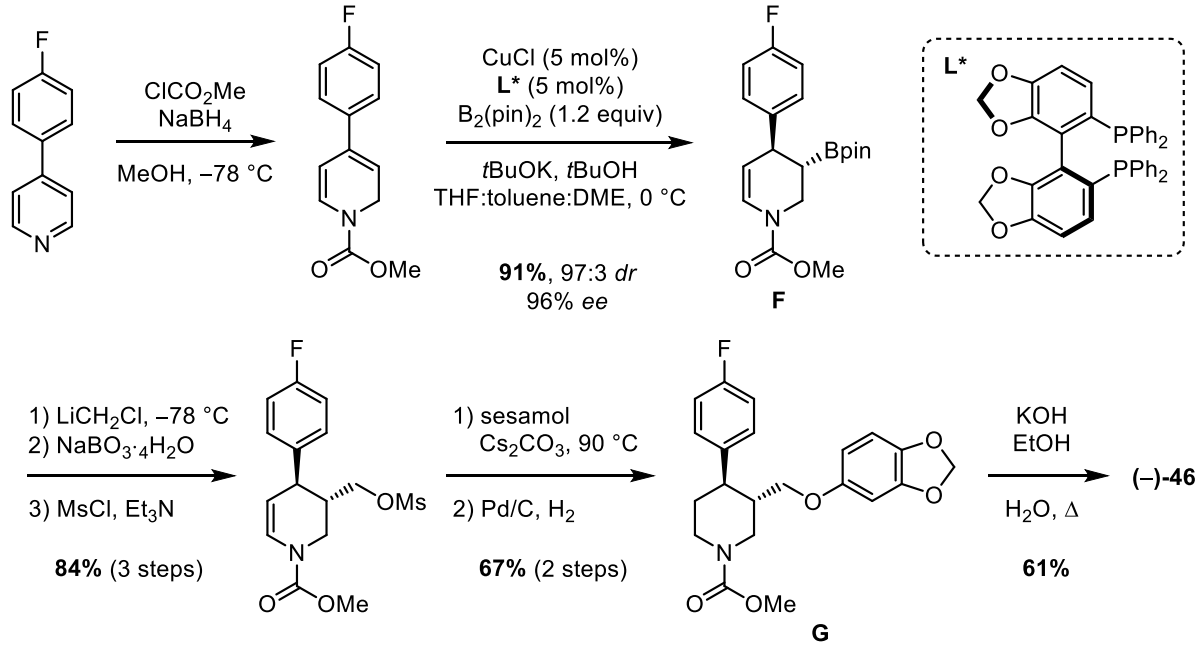


Scheme 4.2 Buchwald's synthesis of (–)-paroxetine through CuH-catalysed enantioselective hydroalkylation.

On the other hand, strategies that could provide stereocontrolled access to (–)-paroxetine through direct functionalisation of readily available pre-existent ring systems are significantly more limited. In 2014, Linclau reported the synthesis of racemic paroxetine through Co-

catalysed diastereoconvergent Kumada coupling.[57c] However, several steps were required to access the desired piperidine bromide precursor from commercially available substrate, and this strategy did not allow access to the enantiopure drug.

More recently, Ito developed a stepwise dearomatisation and enantioselective Cu-catalysed borylation of pyridine rings to access enantiopure piperidine derivatives.[226] Using CuCl in the presence of a chiral bisphosphine ligand, boryl tetrahydropyridines were synthesised in high yield and excellent enantioselectivity, including derivative **F** (Scheme 4.3). One carbon homologation, followed by oxidation, *O*-alkylation and reduction afforded piperidine **G** as a single enantiomer. Final *N*-deprotection gave (–)-paroxetine **(–)-46** in 61% yield.

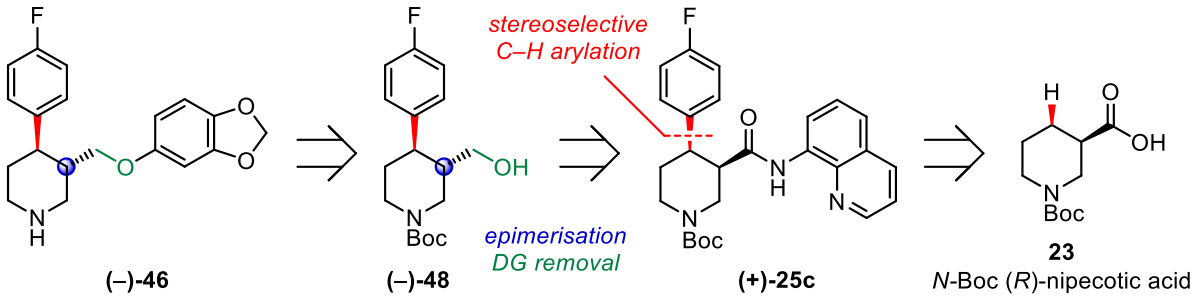


Scheme 4.3 Ito's synthesis of (–)-paroxetine **(–)-46** through the enantioselective dearomatisation/ borylation of 4-aryl pyridines.

4.1.3 Retrosynthetic Analysis and Proposed Strategy

Despite the success of the methods described above, these typically require the 4-fluorophenyl group to be present prior to stereoselective steps and/or ring formation. This reduces the flexibility of such protocols, limiting their potential to provide rapid access to different (–)-paroxetine analogues through variation of the aromatic substituent. In contrast, the C(4)–H arylation on pre-existing piperidine rings was envisaged as a more modular approach to vary this functionality with inherent enantiocontrol. Furthermore, both dextro- and levorotatory enantiomers of the final drug could be easily accessed by selecting the appropriate configuration of the starting substrate. In order to demonstrate these concepts, the synthesis of (–)-paroxetine was first investigated.

(–)-Paroxetine **(–)-46** could be formed from *trans*-hydroxymethyl derivative **(–)-48** through a known 3-steps sequence involving mesylation, S_N2 reaction with sesamol and Boc-deprotection (Scheme 4.4).[227] On the other hand, formation of enantiopure key intermediate **(–)-48** was envisaged from commercially available *N*-Boc (*R*)-nipecotic acid **23** through diastereoselective Pd-catalysed C(4)–H arylation, followed by selective C(3)-epimerisation and reductive AQ removal.



Scheme 4.4 Retrosynthetic analysis of (–)-paroxetine **(–)-46** from readily available **23**, featuring stereoselective C(4)–H arylation, C(3)-epimerisation and DG removal as key synthetic steps.

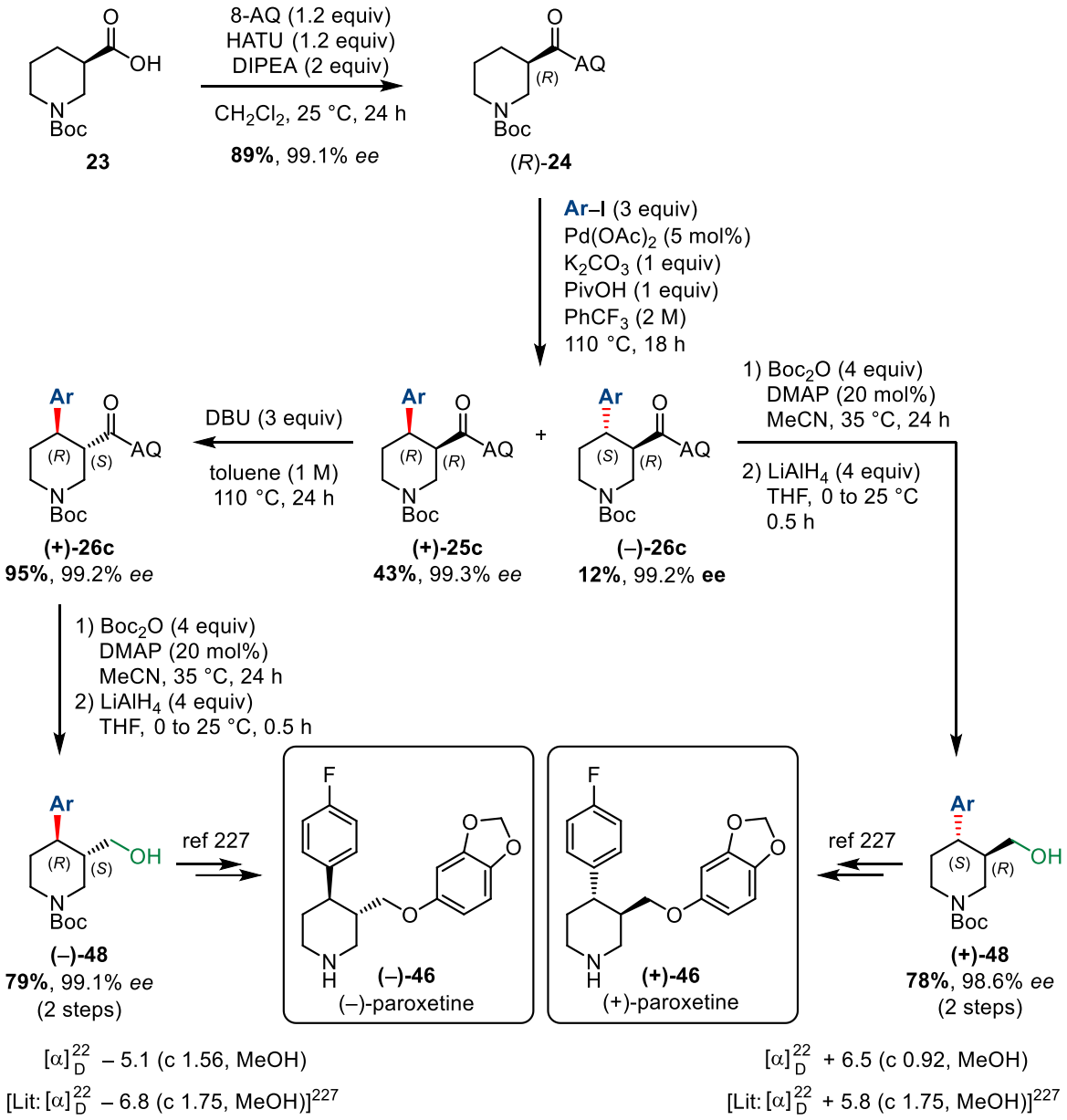
Although (+)-paroxetine could be formed in the same way starting from (*S*)-nipecotic acid, access to the dextrorotatory enantiomer was also envisaged from the *trans*-4-arylated piperidine formed as minor C(4)–H arylation product (*vide infra*).

4.1.4 Stereocontrolled Formal Synthesis of (+)- and (–)-Paroxetine

Based on this proposed strategy, the formal synthesis of (+)- and (–)-paroxetine **(+)-46** and **(–)-46** was attempted (Scheme 4.5).

As previously discussed in section 3.5 (Schemes 3.12 and 3.15), enantiopure piperidine-3-AQ amide (*R*)-**24** could be formed from commercially available *N*-Boc (*R*)-nipecotic acid **23** with no loss in *ee*. In particular, approximately 5.5 g (~ 15.4 mmol) of amide (*R*)-**24** was obtained (89%, >99% *ee*) using HATU as amide coupling reagent. Subsequent reaction with 4-fluoro-iodobenzene was carried out on a 4 mmol scale under the Pd-catalysed conditions previously developed (section 3.2). The desired *cis*-arylated piperidine **(+)-25c** was formed in 43% yield as a single enantiomer (>99% *ee*) alongside 12% of enantiopure *trans*-isomer **(–)-26c**.

After chromatographic separation of these derivatives, the viability of AQ removal was first investigated on *trans*-piperidine **(–)-26c**.



Scheme 4.5 Stereocontrolled formal synthesis of (+)- and (–)-paroxetine **(+)-46** and **(–)-46**. Ar = 4-fluorophenyl.

Boc-activation of the AQ amide occurred smoothly in the presence of Boc_2O and catalytic DMAQ. Pleasingly, using the same conditions optimised for the 5-membered ring (section 3.6.2.1), the resulting activated amide was readily converted into hydroxymethyl piperidine **(+)-48** in 78% yield over the telescoped 2-step process. Comparison of the experimental optical rotation with the literature value, confirmed the absolute *3R,4S* stereochemistry of derivative **(+)-48**, which represents a known intermediate in the synthesis of (+)-paroxetine **(+)-46**.[227]

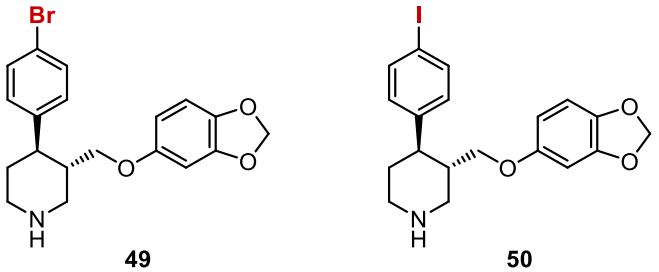
Encouraged by these promising results, base-mediated epimerisation of *cis*-piperidine **(+)-25c** was used to form *trans*-diastereoisomer **(+)-26c** as the correct enantiomer for the synthesis of (–)-paroxetine drug. Initial attempts using *t*BuOK were unsuccessful, leading to partial AQ

hydrolysis. Nonetheless, selective C(3)-epimerisation could be effectively promoted by DBU, forming derivative **(+)-26c** in 95% and >99% *ee*. Finally, AQ removal under the same reductive conditions afforded key alcohol intermediate **(–)-48** as a single enantiomer in 79% (2 steps), thus completing the formal synthesis of antidepressant (–)-paroxetine **(–)-46**.[227]

Following this, the possibility to use the same Pd-catalysed C(4)–H arylation approach to access (–)-paroxetine analogues was evaluated.

4.2 Total Synthesis of Br- and I-Analogues of (–)-Paroxetine

In collaboration with Eric Gouaux at Oregon Health & Science University, (–)-paroxetine analogues whereby the terminal fluorine atom is substituted with either bromine (**49**) or iodine (**50**) were targeted (Figure 4.2). These derivatives were envisaged as useful ligands to generate unambiguous X-ray and cryo-EM data, in order to elucidate the structure of the active site and the (–)-paroxetine binding mode to SERT protein. These structural studies were performed by J. Coleman, V. Navratna and D. Yang and are outside the scope of this thesis. However, a detailed account of this work including full biochemical and spectroscopic data can be found in *eLife*.[228]



49 Br-(–)-Paroxetine **50** I-(–)-Paroxetine

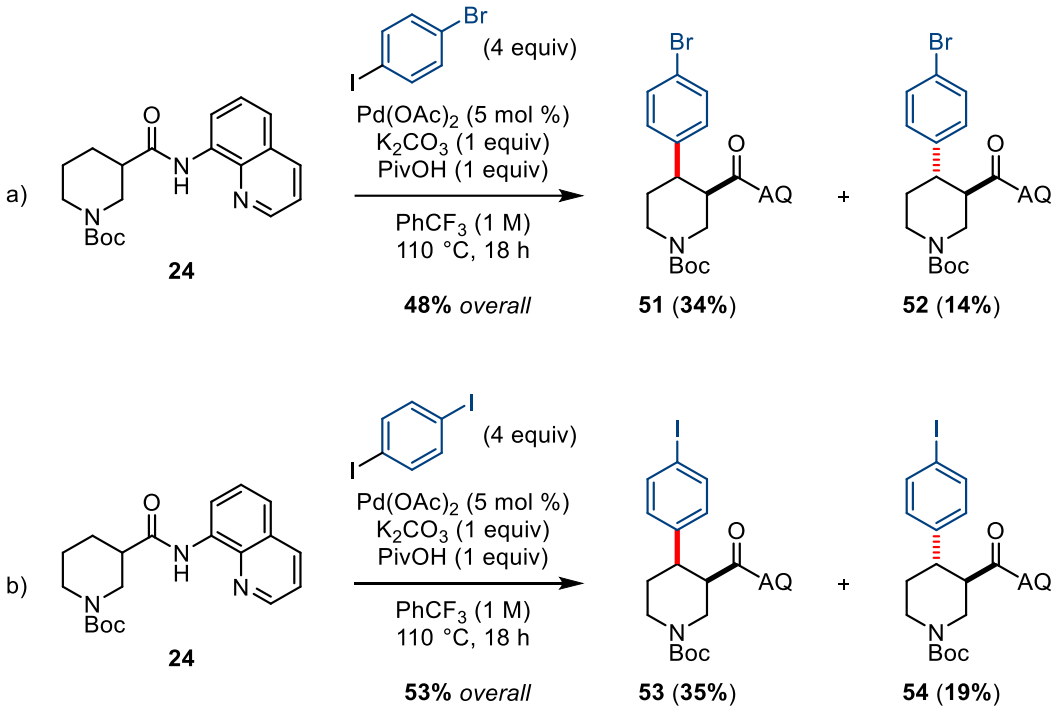
Figure 4.2 Targeted Br- and I-(–)-paroxetine analogues.

At the outset of this investigation, no synthesis had previously been reported for either Br- or I-(–)-paroxetine analogues, and a synthetic strategy to access these derivatives was devised involving a key stereocontrolled Pd-catalysed C(4)–H arylation step. Similarly to the synthesis of (–)-paroxetine described above, this approach was based on the formation of hydroxymethyl piperidine derivatives after reductive AQ cleavage. However, two main challenges were identified for the direct translation of an identical synthetic sequence to the targeted Br- and I-derivatives. The first involved the use of 1,4-diiodobenzene in the C–H arylation step towards I-(–)-paroxetine **50**, which could lead to competing dialkylation. The second concern derived from a possible aromatic dehalogenation in the presence of $LiAlH_4$ during the DG removal step.[229]

With these considerations in mind, the synthesis of Br- and I-(–)-paroxetine **49** and **50** was attempted.

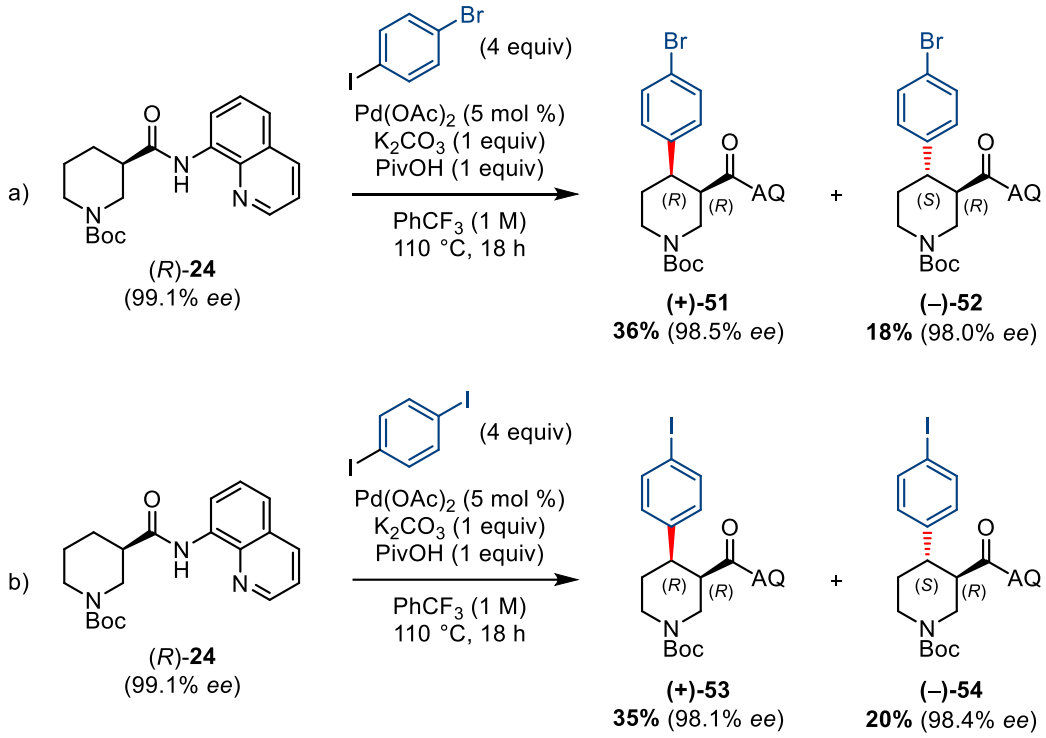
4.2.1 C(4)–H Arylation Step

Initially, the C(4)–H arylation with both 4-bromo-iodobenzene and 1,4-diiodobenzene was tested on racemic piperidine-3-carboxamide **24** (Scheme 4.6). 1,4-Diiodobenzene was used in a larger excess (4 equivalents) to avoid undesired dimerisation. Pleasingly, the C(4)–H arylation was successful with both coupling partners resulting in 48% and 53% overall yield respectively. Furthermore, no noticeable double alkylation was observed in the reaction with 1,4-diiodobenzene. *cis*-Br-piperidine **51** was isolated in 34% yield, alongside 14% of *trans*-isomer **52**, and similar results were obtained for I-derivatives **53** and **54**.



Scheme 4.6 Pd-catalysed C–H arylation of racemic piperidine amide **24** with a) 4-bromo-iodobenzene, and b) 1,4-diiodobenzene. Reaction scale: 0.5 mmol.

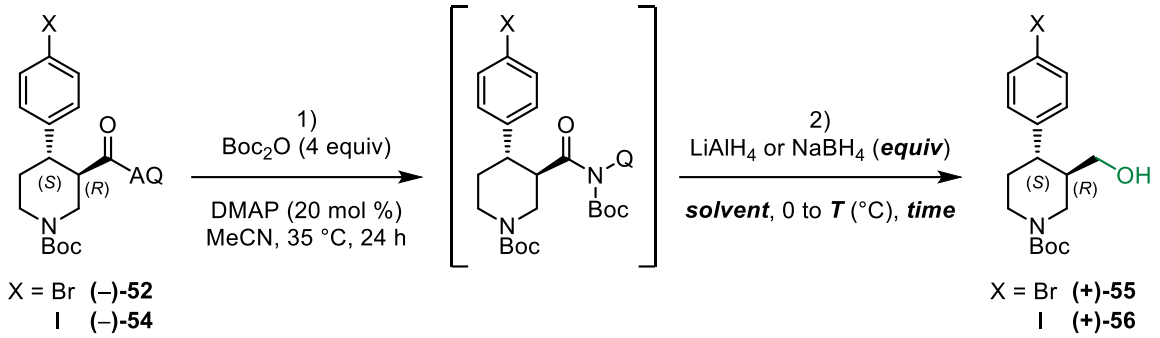
Subsequently, C(4)–H arylation on enantioenriched piperidine amide (*R*)-**24** was performed on a 4 mmol scale. In this case, *cis*-Br-arylated product **(+)-51** was isolated in 36% yield as a single enantiomer (> 98% *ee*), while the minor *trans*-derivative **(–)-52** was obtained in 18% (Scheme 4.7a). 1,4-Diiodobenzene gave similar reactivity, with no dialkylation observed when increasing the reaction scale. In particular, the desired *cis*-I-piperidine derivative **(+)-53** was obtained in 35% yield and > 98% *ee* (Scheme 4.7b).



Scheme 4.7 Pd-catalysed C–H arylation of enantioenriched piperidine amide (*R*)-**24** with a) 4-bromo-iodobenzene, and b) 1,4-diiodobenzene. Reaction scale: 4 mmol.

4.2.2 Synthesis of Key Alcohols Intermediates

Different deprotection conditions were first tested on *trans*-(3*R*,4*S*)-piperidines **(–)-52** and **(–)-54**. In particular, milder reductive conditions were investigated after Boc-protection, in order to reduce the risk of potential dehalogenation.[229] $NaBH_4$ was found to be significantly less effective than $LiAlH_4$, resulting in just 20% conversion after 24 h at 55 °C (Table 4.1, entry 1). On the other hand, the equivalents of $LiAlH_4$ could be reduced from 4, as initially used in the synthesis of (–)-paroxetine, to 2 equivalents with no detrimental effect (entry 2). The desired Br-hydroxymethyl derivative **(+)-55** was obtained in 70% yield over 2 steps, with complete retention of *ee* and without any competing debromination. Pleasingly, I-piperidine **(–)-54** was also successfully converted into hydroxymethyl derivative **(+)-56** using 2 equivalents of $LiAlH_4$ after amide activation (entry 3). In this case, enantiopure **(+)-56** was isolated in 63% yield over 2 steps, though containing a small amount (~10%) of inseparable deiodinated derivative. Reducing the loading of $LiAlH_4$ to 1 equivalent resulted in just 37% conversion (entry 4). Therefore, the use of 2 equivalents of $LiAlH_4$ was maintained, as giving an acceptable balance between reactivity and chemoselectivity.



X = Br **(–)-52**
I **(–)-54**

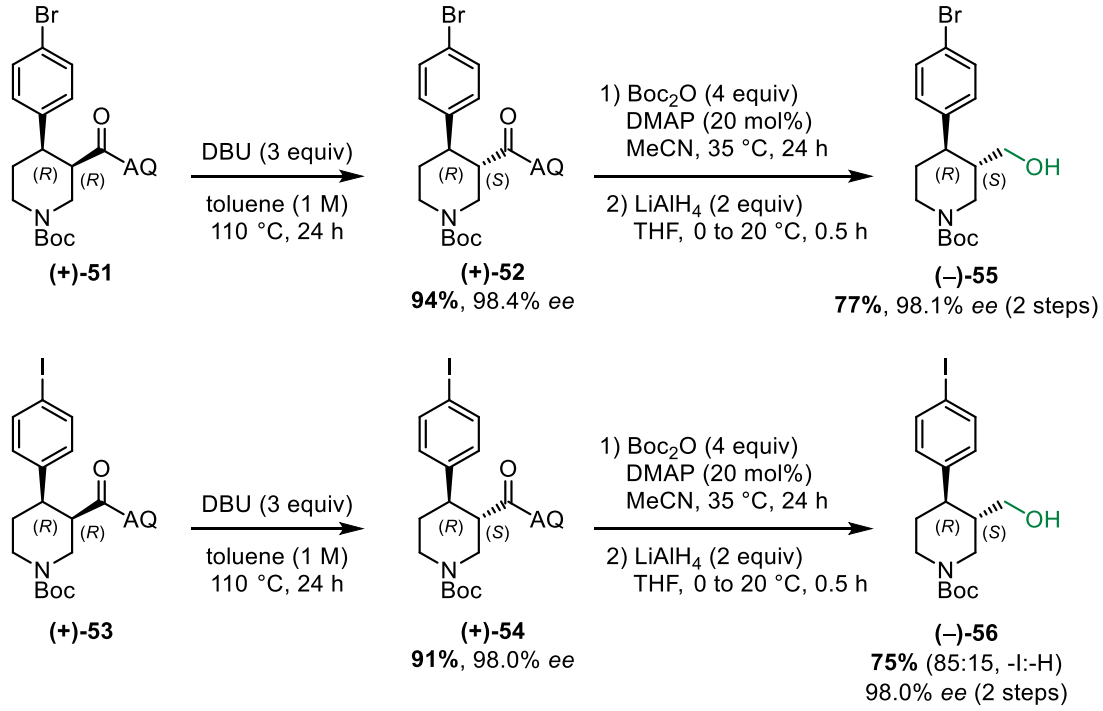
X = Br **(+)-55**
I **(+)-56**

entry	X	hydride source (equiv)	solvent	T (°C)	time (h)	conv. (%)[a]	yield (%)[b]	*ee* (%)[c]
1	Br	$NaBH_4$ (5.0)	EtOH	55	24	20	-	-
2	Br	$LiAlH_4$ (2.0)	THF	20	0.5	> 95	**(+)-55** (70)	98.1
3	I	$LiAlH_4$ (2.0)	THF	20	0.5	> 95	**(+)-56** (63)[d]	98.1
4	I	$LiAlH_4$ (1.0)	THF	20	0.5	37	-	-

Table 4.1 Optimisation of the reductive AQ removal from enantiopure Br- and I-piperidine amides **(–)-52** and **(–)-54**. [a] Calculated by ^1H NMR spectroscopy on the crude reaction mixture. [b] Isolated yield over 2 steps. [c] Measured by chiral HPLC on the isolated derivative. [d] Containing ~10% of deiodinated hydroxymethyl derivative.

In order to access the correct enantiomer of the key hydroxymethyl intermediates, DBU was used to promote C(3)-epimerisation of *cis*-arylated piperidines **(+)-51** and **(+)-53**. This proceeded smoothly in both cases, affording enantiopure *trans*-(3*S*,4*R*)-derivatives **(+)-52** and **(+)-54** in 94% and 91% yield (Scheme 4.8). Subsequent carbamoylation followed by reduction with $LiAlH_4$ was used to remove the DG and unmask the desired alcohol functionality. Pleasingly, under the optimised conditions, Br-derivative **(–)-55** was obtained in 77% yield and > 98% *ee* over 2 steps. On the other hand, an inseparable 85:15 mixture of hydroxymethyl derivative **(–)-56** and the corresponding dehalogenated product was isolated in 75% yield for the iodine series (corresponding to ~68% of desired product). Reasoning that the dehalogenated impurity might be removed more easily after *O*-alkylation, this mixture was used in the next step without further purification.

Furthermore, in absence of enolisable protons, the high enantiopurity was expected to be retained in the next synthetic steps, as demonstrated in literature precedents for (–)-paroxetine synthesis.[227] Therefore, the synthesis was continued exclusively on left-handed enantiomers **(–)-55** and **(–)-56** without further determination of enantiomeric excess.



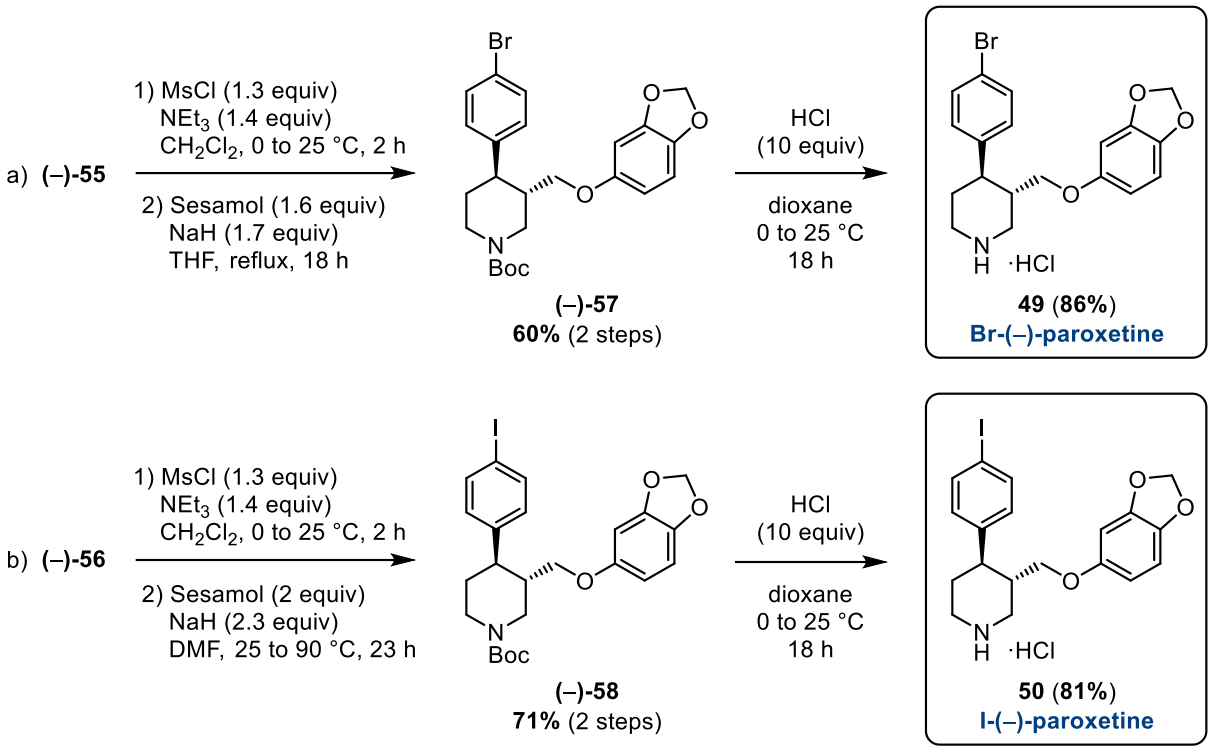
Scheme 4.8 Reductive AQ removal on *trans*-(3*S*,4*R*)-piperidines **(+)-52** and **(+)-54**.

4.2.3 Final Steps

With the key hydroxymethyl derivatives **(–)-55** and **(–)-56** in hand, the final steps in the synthesis of Br- and I-(–)-paroxetine were evaluated. Treatment of Br-derivative **(–)-55** with MsCl, followed by nucleophilic displacement with sesamol in the presence of NaH, afforded ether derivative **(–)-57** in 60% yield over two steps (Scheme 4.9a). Despite a quantitative mesylation step, the subsequent S_N2 reaction was found to be more sluggish, with unreacted -OMs substrate accounting for most of the remaining mass balance. To improve the conversion in the I-series, the solvent was switched to DMF and the temperature was raised to 90 °C (Scheme 4.9b). Pleasingly full conversion was observed in this case, and the desired alkylated product **(–)-58** was isolated in 71% yield over 2 steps, after effective separation from the deiodinated contaminant.

Finally, Boc-deprotection with HCl in dioxane afforded the targeted Br- and I-(–)-paroxetine **49** and **50** as the corresponding hydrochloride salts in 86% and 81% yield respectively (Scheme 4.9). This completed the total synthesis of both Br- and I-(–)-paroxetine drug analogues in 8 steps from commercial material and 12% overall yield.

During the preparation of this work, an alternative 7-step synthesis of Br-(–)-paroxetine **49** was reported using Jørgensen's enantioselective conjugate addition strategy.[218,230] However, this was not demonstrated for the corresponding I-(–)-paroxetine, with the route described in this thesis representing the first synthesis of this derivative.



Scheme 4.9 Final steps in the synthesis of a) Br- (**49**) and b) I- (**50**) (–)-paroxetine drug analogues.

Following the successful synthesis of antidepressant (–)-paroxetine drug and its Br- and I-analogues by C(4)–H arylation, the synthetic utility of this strategy was further evaluated in the construction of a small library of pyrrolidine and piperidine fragments.

4.3 Preparation of a Library of Pyrrolidine and Piperidine Fragments by C–H Arylation

4.3.1 Fragment-Based Drug Discovery

Over the last 20 years, fragment-based drug discovery (FBDD) has rapidly emerged as a very powerful tool for the development of new therapeutics.[231] This approach focuses on the early screening of low-M_W fragments to provide "high-quality hits" that can be optimised into potent lead molecules (Figure 4.3a). As such, FBDD offers high potential to reduce pharmaceutical late-stage attrition, and to modulate typically intractable targets, such as protein-protein interactions (PPIs).[231b]

In recent years, FBDD has enabled the discovery of a broad range of drug candidates currently in phase I–III of clinical trials.[232] Furthermore, the success of this approach is highlighted by the recent FDA approval of Vemurafenib,[233,234] Venetoclax[235,236,237] and Erdafitinib[238] antineoplastic drugs, originally discovered through FBDD campaigns (Figure 4.3b).

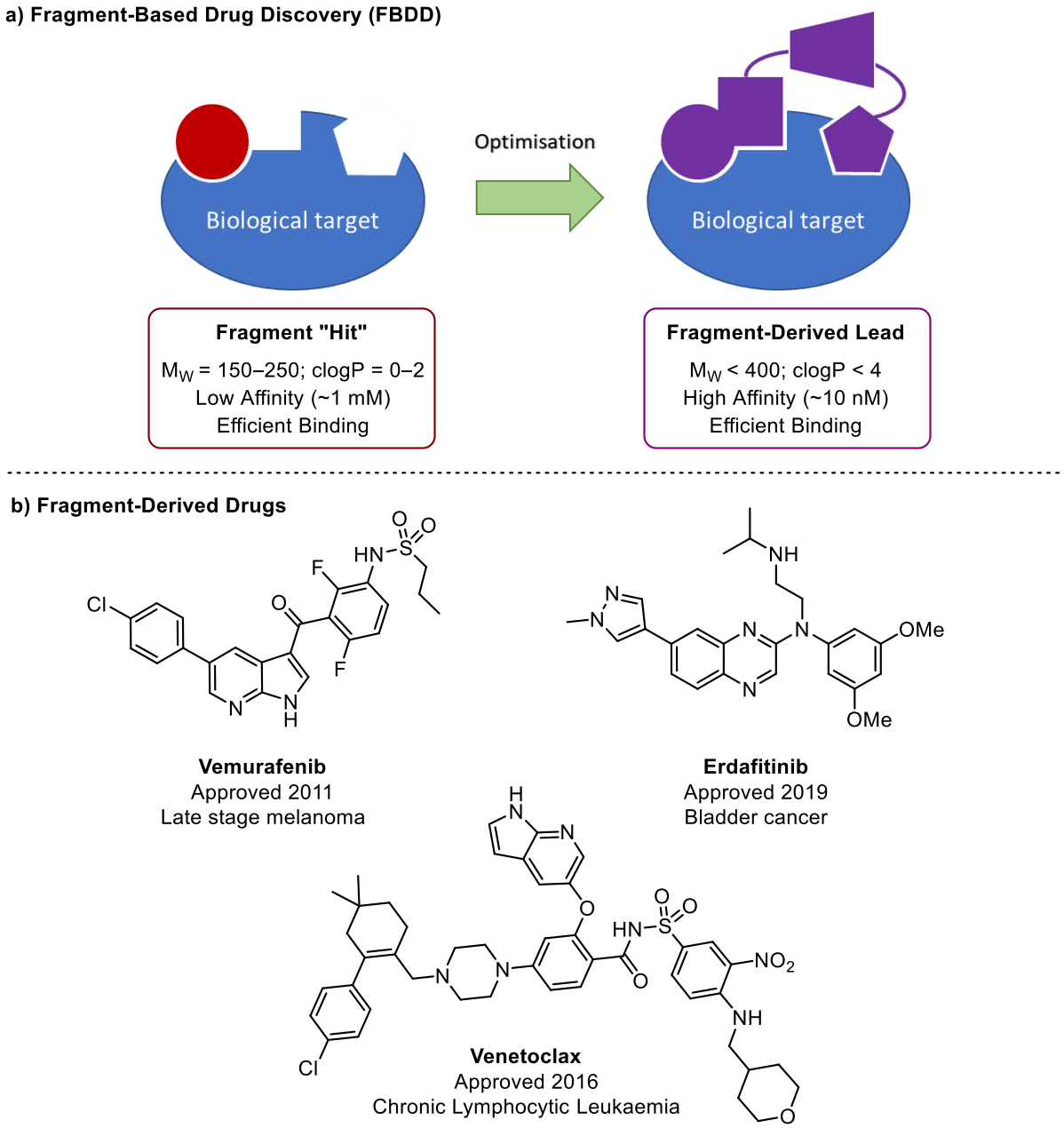


Figure 4.3 a) Schematic representation of Fragment-Based Drug Discovery (FBDD). b) Structures of recently approved drugs discovered through FBDD.

By virtue of their small size, fragments can form efficient binding interactions with biological targets, albeit with low potency.[231b] Pioneering work from Jencks showed that the binding of a small molecule to a biological target is accompanied by a significant entropic cost, that is largely independent on molecular size.[239,240] As such, small fragments need to form higher quality interactions with the target, compared to larger drug-like molecules, in order to overcome this entropic barrier and have measurable affinity. These interactions will likely be maintained during the fragment optimisation, offering high potential for a successful lead identification campaign.

Furthermore, the use of low-M_W fragments enables a more efficient exploration of chemical space, in comparison with typical lead-like compounds.[231b,241] Raymond calculated that the number of "drug-like" molecules with ≤ 11 non-H atoms is in the magnitude order of 10^7.[242] However, this increases dramatically with the molecular size, with 10^{11} possible compounds having ≤ 17 heavy atoms being enumerated.[243] It derives that screening smaller compounds would sample a larger proportion of chemical space, increasing the chances to identify efficiently binding hits.

Once a fragment hit has been identified through sensitive biophysical techniques, such as NMR or X-ray crystallography, it can be optimised to generate a more potent lead (Figure 4.3a). This can involve the use of various methodologies, such as fragment growth and/or fragment linking for compounds that bind on adjacent sites.[231a,232] In either case, the presence of synthetic handles for elaboration along different vectors is an essential requirement to ensure optimal fragment developability.

The success of a FBDD program is strictly linked to the quality of the compounds being screened. As described in section 1.2.1.3, simple guidelines can be used to aid the design of suitable screening libraries. In particular, scientists at Astex suggested that desirable criteria for fragment-like molecules include M_W = 140–230, clogP = 0–2, NROT ≤ 3, HBA ≤ 3, HBD ≤ 3 and PSA ≤ 60 Å^2.[33,35] In addition, the construction of fragment libraries with higher 3-dimensional character has recently attracted significant attention. Higher degree of saturation can increase the number and direction of growth vectors, providing more opportunities to develop productive binding interactions.[35] This has been proposed to be particularly advantageous for complex biological targets, such as PPIs.[35,241] Furthermore, the use of topologically diverse and more 3-dimensional fragments would provide access to less "flat" and more soluble lead molecules, which has in turn been proposed to reduce the risk of late-stage attrition (see section 1.2.1.2).[25,28] However, increasing the 3-dimensional shape while maintaining the small size and the efficient sampling advantages of fragment compounds, remains an important challenge in organic synthesis.

Various methods have recently been used to access 3D fragments, with a particular attention paid to the synthesis of small saturated *N*-heterocycles as a strategy to achieve high three-dimensionality.[244,245] In particular, C–H functionalisation has also been exploited to form diverse collections of 3D fragments. For instance, Sanford reported the synthesis of a small library of bicyclic *N*-heterocycles through Pd-catalysed transannular C–H arylation (see section 1.4.2.2).[160,164] Very recently, Spring also reported the use of auxiliary-assisted C(sp^3)–H arylation to access cyclobutane-based fragments.[246]

In this context, it was envisaged that the Pd-catalysed C–H functionalisation approach, including subsequent DG removal as developed in the previous chapter, would provide efficient and rapid access to diverse sp^3-rich pyrrolidine and piperidine fragments.

4.3.2 Design of Pyrroline and Piperidine Fragments

4.3.2.1 Target 3,4-disubstituted pyrrolidines and piperidines

In this study, 3,4-disubstituted pyrrolidines and piperidines were targeted to be included in a larger library of 3-dimensional N-heterocyclic compounds for screening in FBDD. These derivatives were designed to include: *i)* either a pyrrolidine or piperidine core scaffold; *ii)* an aromatic substituent bearing either a *p*-methoxy or *p*-fluorine group; *iii)* a polar functional group such as carboxylic acid, primary alcohol or primary amide; and *iv)* either *cis*- or *trans*-configuration (Figure 4.4).[†]

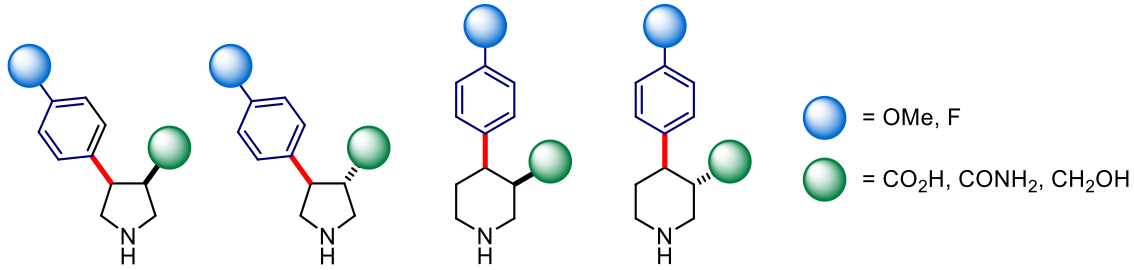


Figure 4.4 3,4-Disubstituted pyrrolidine and piperidine fragments targeted in this study.

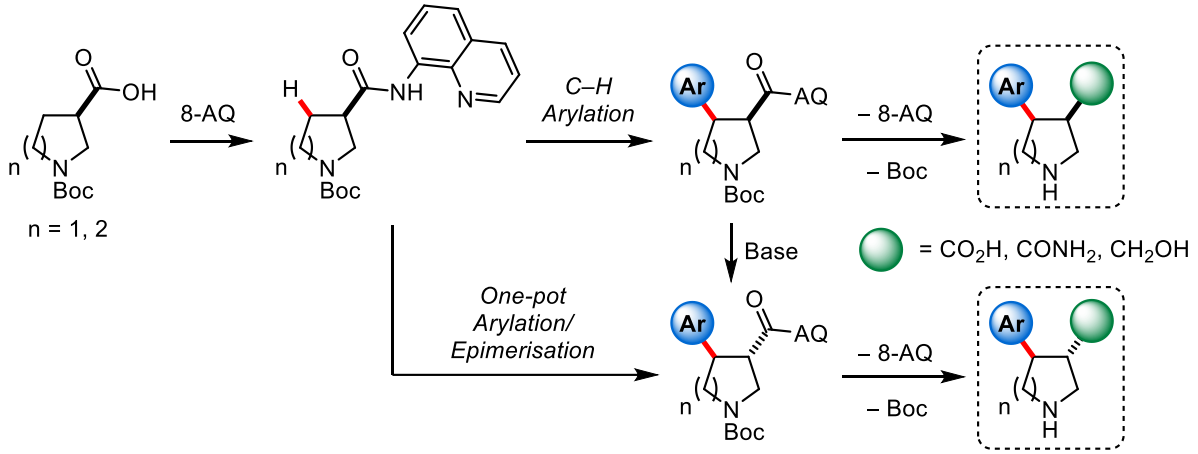
Combinations of these elements were anticipated to provide access to an attractive collection of small polar saturated N-heterocycles, that fit well in fragment-like space (M_W < 250, clogP < 2, NROT ≤ 3, HBD ≤ 3, etc.) and feature diverse topologies, to increase the shape diversity of the library. Furthermore, these would possess various structural elements to promote binding interactions, as well as to provide options for synthetic elaboration along different vectors. To retain potential affinity to the largest possible number of proteins, racemic fragments were targeted. Finally, 50–100 mg of each fragment compound were targeted to provide enough material for biological screenings.

With the typical time and financial constraints of pharmaceutical research, synthetic tractability is of pivotal importance to rapidly access fragment libraries in FBDD. As such, a suitable synthetic route to a fragment compound should involve the lowest possible number of steps (preferentially ≤ 4–5) from commercial material.[35]

[†] Compounds designed by A.-S. Piticari, J. A. Bull (Imperial College London) and M. Webster (AbbVie Pharmaceuticals).

4.3.2.2 Proposed synthetic strategy

With all these considerations in mind, a synthetic strategy towards 3,4-disubstituted pyrrolidine and piperidine fragments was devised, involving a key C–H functionalisation step (Scheme 4.10). In order to minimise the number of chromatographic purification steps and increase synthetic tractability, the use of one-pot or telescoped processes was included whenever possible. After DG installation, stereoselective C(4)–H arylation would provide access to *cis*-arylated pyrrolidines and piperidines.



Scheme 4.10 Proposed synthetic strategy towards 3,4-disubstituted N-heterocycle fragments.

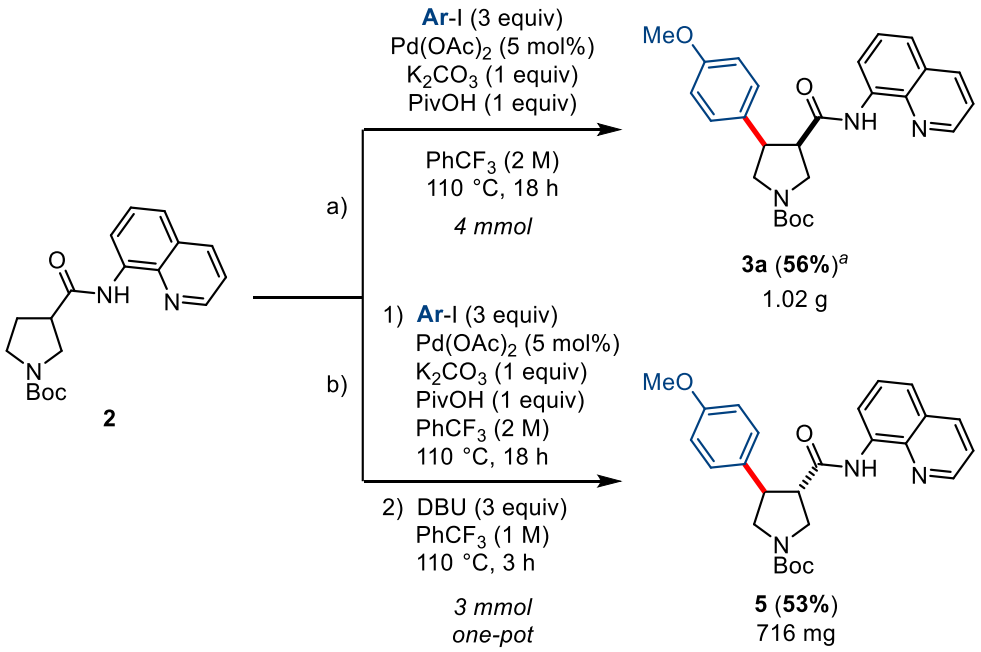
The corresponding *trans*-isomer could be formed from the same substrate *via* one-pot arylation/epimerisation, or from the *cis*-arylated derivative through a separate epimerisation step. Divergent DG removal, under the conditions developed in section 3.6, would then allow modification of the right-hand side of the ring and lead to the targeted acid, alcohol and amide functionalities. Boc-deprotection would finally afford the desired pyrrolidine and piperidine fragments in 4–6 synthetic steps.

Based on this proposed route, the synthesis of the targeted fragments was investigated.

4.3.3 Synthesis of Target Fragments

4.3.3.1 Pyrrolidine and piperidine C(4)–H arylation

The synthesis of *cis*- and *trans*-3,4-disubstituted pyrrolidines **3a**, **3d**, **5** and **59** was performed *via* Pd-catalysed C(4)–H arylation as previously discussed in chapter 3. Reaction of pyrrolidine-3-carboxamide **2** with 4-iodoanisole proceeded well on 4 mmol scale using a 2 M concentration. This afforded *cis*-arylated pyrrolidine **3a** in 56% yield (> 1 g), upon purification by automated column chromatography (Scheme 4.11a).



Scheme 4.11 Large scale synthesis of a) *cis*- and b) *trans*-3,4-disubstituted pyrrolidines **3a** and **5** with 4-iodoanisole. [a] Isolated by automated column chromatography.

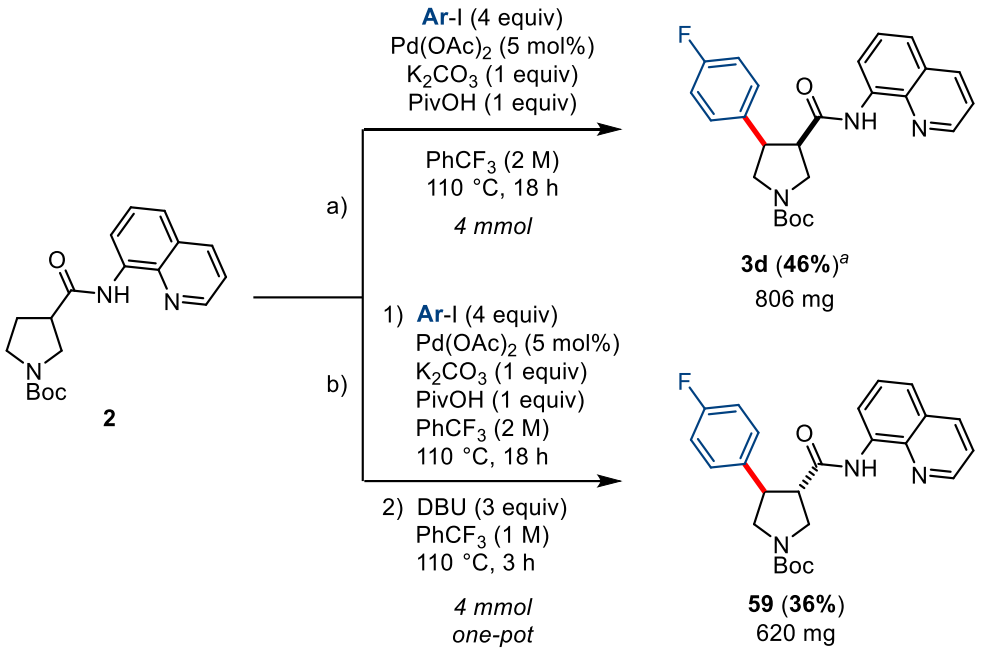
On the other hand, a *one-pot* arylation/epimerisation procedure was used to access the corresponding *trans*-diastereomer **5** (Scheme 4.11b). In this case, Pd-catalysed C(4)–H arylation followed by DBU-mediated epimerisation was performed on 3 mmol scale, affording *trans*-3,4-disubstituted pyrrolidine **5** in 53% yield (> 700 mg).

Similarly, the 4-fluorophenyl group was installed, providing the corresponding *cis*- *a*nd *trans*-derivatives **3d** and **59** in 46% and 36% yield respectively (Scheme 4.12). To increase the yield with this more electron-poor aryl iodide, 4 equiv of the coupling partner were used. The lower yield observed for *trans*-pyrrolidine **59** was due to a more difficult chromatographic separation.

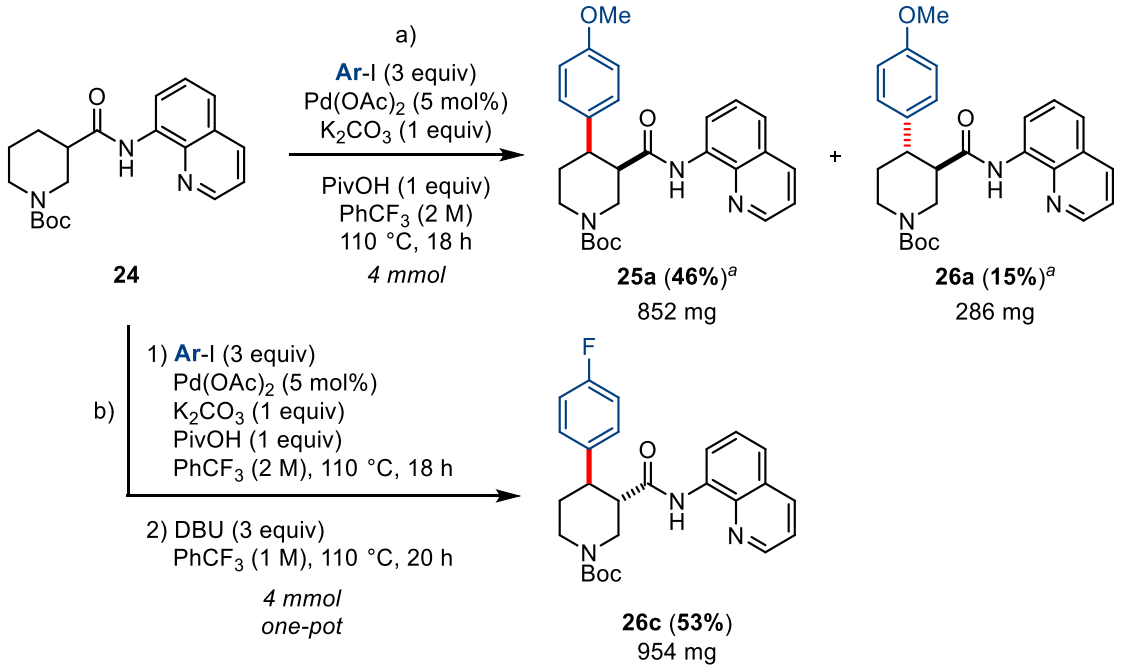
In order to access *cis*-derivative **3d** in a larger amount for the following deprotection steps, the same C–H arylation procedure was performed on a second batch of pyrrolidine amide **2** (3 mmol scale, not shown) affording *cis*-pyrrolidine derivative **3d** in 44% yield (~600 mg).

Subsequently, C(4)–H arylation of piperidine-3-carboxamide **24** was conducted on a 4 mmol scale, under the same conditions used for the 5-membered ring. Arylation with 4-iodoanisole furnished 46% of the major *cis*-configured piperidine **25a** with an additional 15% of minor *trans*-isomer **26a** (Scheme 4.13a).

To access both diasteroisomers in larger amount, the reaction was repeated on a second batch of amide **24** (3.4 mmol scale), affording *cis*- and *trans*-piperidine derivatives **25a** and **26a** in 52% (821 mg) and 16% (253 mg) yield respectively (not shown).



Scheme 4.12 Large scale synthesis of a) *cis*- and b) *trans*-3,4-disubstituted pyrrolidines **3d** and **59** with 4-fluoroiodobenzene. [a] Isolated by automated column chromatography.



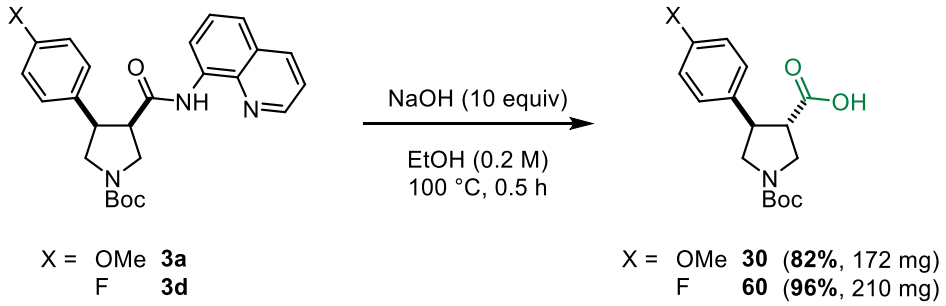
Scheme 4.13 Large scale synthesis of *cis*- and *trans*-4-arylated piperidines with a) 4-iodoanisole (**25a** and **26a**) and b) 4-fluoro-iodobenzene (**26c**). [a] Isolated by automated column chromatography.

Finally, 4-fluorophenyl piperidine **26c** was obtained through *one-pot* arylation/epimerisation in 53% yield as a single *trans*-diastereoisomer (Scheme 4.13b).

4.3.3.2 Directing group removal: carboxylic acid derivatives

Several conditions were employed to cleave the AQ auxiliary and uncover the corresponding carboxylic acid functionality (see section 3.6.1).

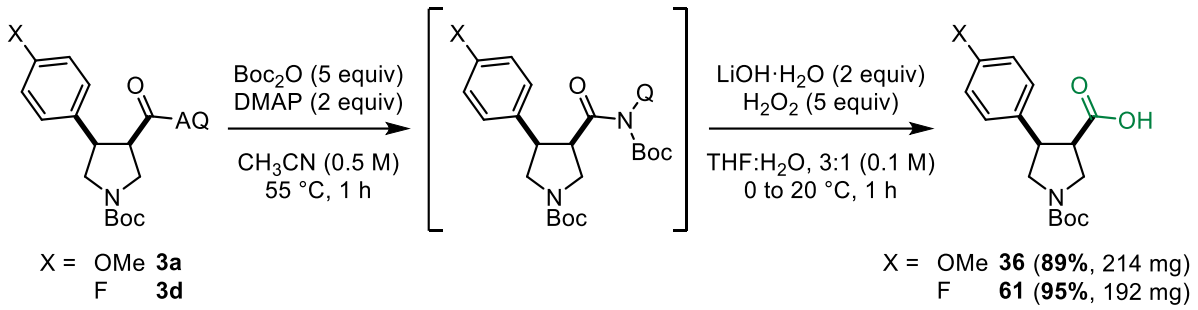
trans-Pyrrolidine-3-carboxylic acids **30** and **60** were obtained in a single step from *cis*-configured pyrrolidines **3a** and **3d** (Scheme 4.14). Treating arylated pyrrolidine-3-AQ amide **3a** with NaOH at 100 °C in EtOH, afforded 4-methoxyphenyl derivative **30** in 82% yield as a single *trans*-diastereoisomer. The same procedure was successful in forming the corresponding 4-fluorophenyl derivative **60** in 96% yield. In both cases, the acid products were isolated by acid/base work-up without the need for chromatographic purification.



Scheme 4.14 Synthesis of *trans*-pyrrolidine-3-carboxylic acids **30** and **60** *via* one-pot epimerisation/AQ removal.

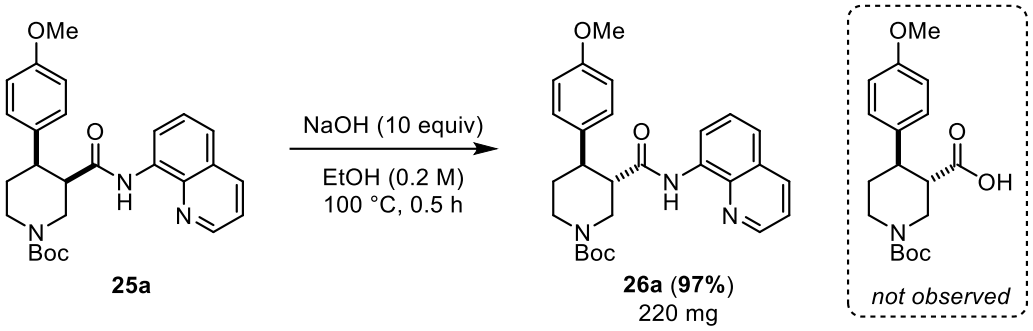
On the other hand, *cis*-configured pyrrolidine acids **36** and **61** were prepared using a telescoped process involving initial carbamoylation of the AQ amide with Boc_2O, followed by hydrolysis with LiOOH. This afforded the desired 4-methoxy- and 4-fluorophenyl derivatives **36** and **61** in excellent yields, after simple acid/base work-up (Schemes 3.20b and 4.15).

Unfortunately, treating *cis*-arylated piperidine **25a** with NaOH in EtOH failed to deliver the expected *trans*-carboxylic acid derivative, despite the success of this approach for the corresponding 5-membered ring (Scheme 4.16). While full conversion to the epimerised *trans*-isomer **26a** was observed after just 30 min at 100 °C, longer reaction times resulted in undesired Boc deprotection. Nonetheless, this provided a more efficient protocol for piperidine epimerisation compared to previous approaches involving overnight treatment with DBU or *t*BuOK in toluene at reflux (see section 3.5.3).



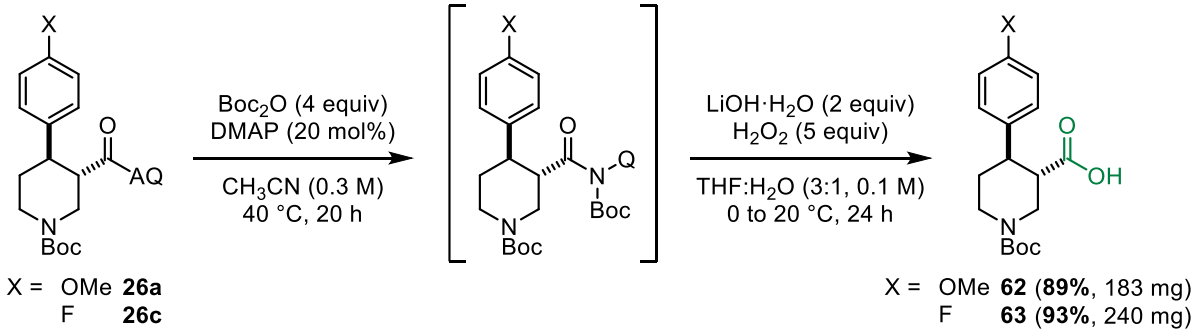
Scheme 4.15 AQ cleavage to form *cis*-pyrrolidine-3-carboxylic acids **36** and **61**.

Therefore, epimerisation with NaOH was used to access more *trans*-piperidine amide **26a**, that was obtained in almost quantitative yield with no need for chromatographic purification (Scheme 4.16).



Scheme 4.16 Epimerisation of *cis*-arylated piperidine **25a** using NaOH.

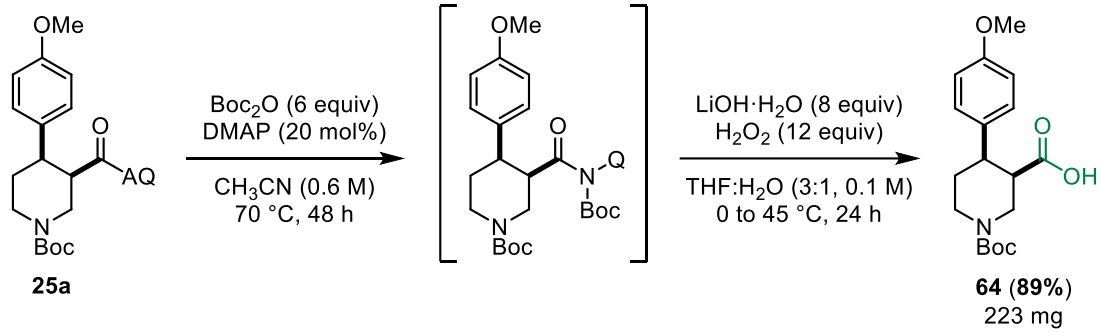
The targeted *trans*-piperidine-3-carboxylic acids **62** and **63** were instead obtained from the corresponding *trans*-piperidine amides **26a** and **26c** using the Boc-activation/hydrolysis strategy. This afforded the desired products in 89% (**62**) and 93% yield (**63**) over 2 steps (Scheme 4.17).



Scheme 4.17 AQ cleavage to form *trans*-piperidine carboxylic acids **62** and **63**.

Following these positive results, AQ removal on *cis*-configured piperidine amide **25a** was investigated through the same 2-steps route. However, this substrate was found to be poorly reactive in both Boc protection and hydrolysis steps. This was ascribed to a higher degree of steric congestion around the amide functionality either compared to the *trans*-isomer or the

corresponding *cis*-pyrrolidine derivative. In this case, only < 40% conversion was observed after 24 h under otherwise identical conditions to those used for pyrrolidine carbamoylation (see Scheme 4.15). Increasing the temperature to 70 °C provided better results, with ~80% conversion observed after 72 h (not shown). However, purification of the Boc-protected intermediate was complicated by a significant degree of instability on silica. Therefore, a telescoped process was finally devised, involving the use of higher temperature and reagent loadings for both amide activation and hydrolysis steps (Scheme 4.18). Pleasingly, the use of these forcing conditions gave *cis*-pyrrolidine-3-carboxylic acid **64** in 89% yield over 2 steps.

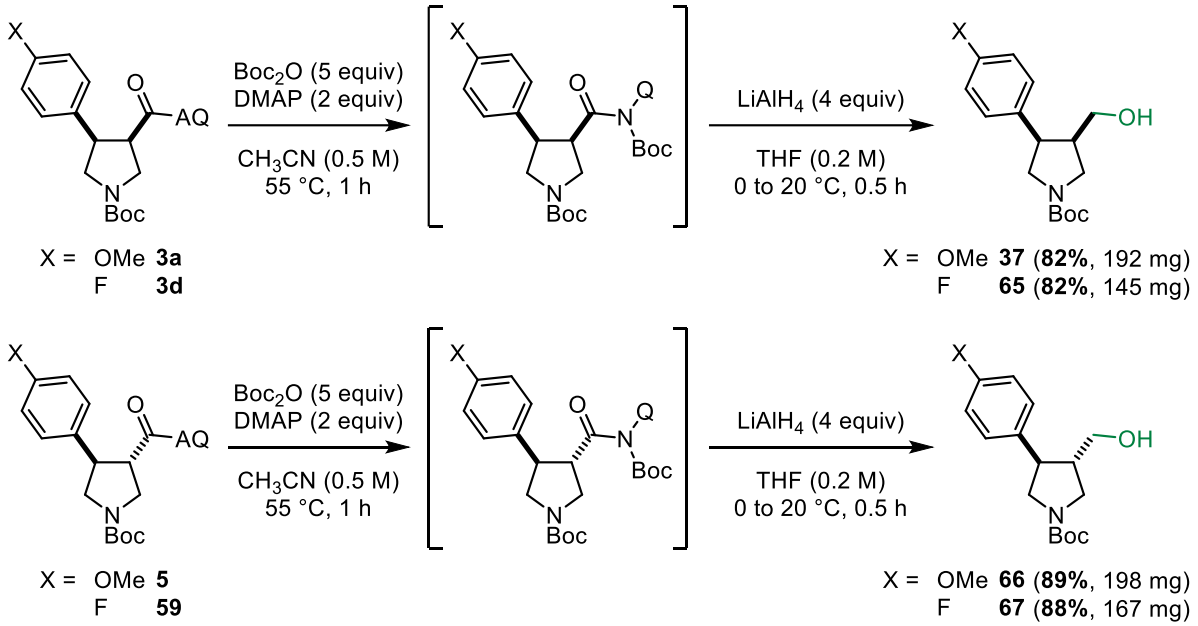


Scheme 4.18 AQ cleavage to form *cis*-piperidine carboxylic acid **64**.

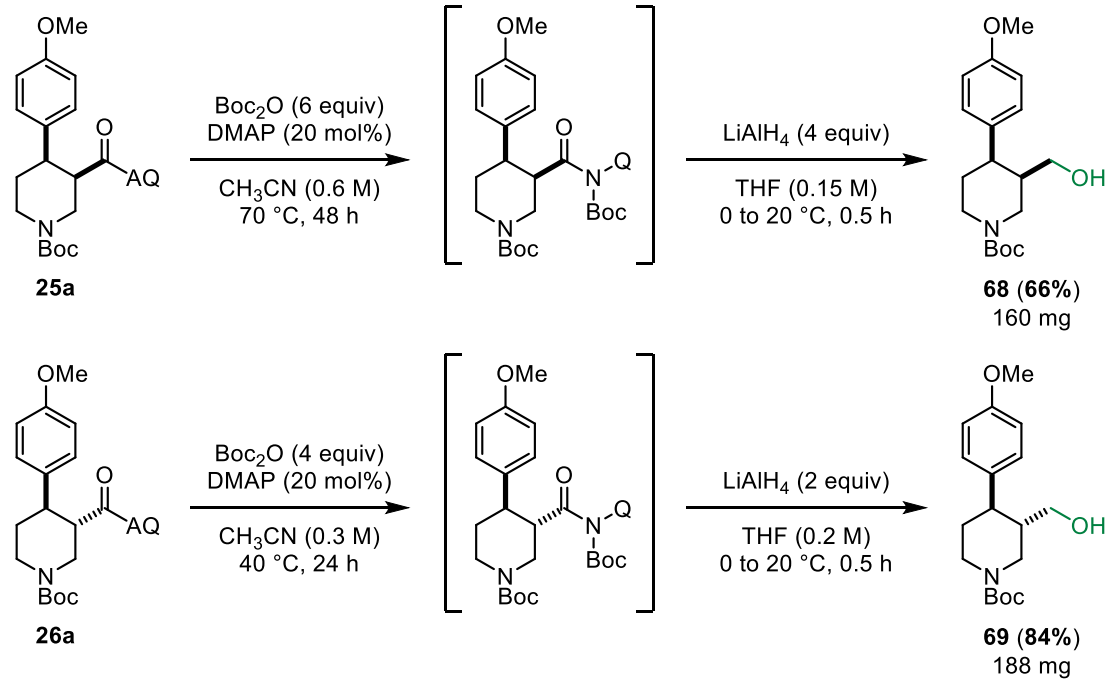
4.3.3.3 Directing group removal: primary alcohol derivatives

3-Hydroxymethyl pyrrolidine and piperidine derivatives were prepared using a similar telescoped 2-step protocol, involving amide activation, followed by reduction with $LiAlH_4$ (see sections 3.6.2 and 4.1.4). The reaction proceeded smoothly with both *cis*- and *trans*-pyrrolidine derivatives, affording the desired alcohol products **37**, **65–67** in 82–89% yield over 2 steps (Scheme 4.19).

The same strategy was also successful for the reduction of *cis*- and *trans*-piperidine-AQ amides **25a** and **26a** (Scheme 4.20). Higher temperature, reaction time and loading of Boc_2O were again used to achieve effective carbamoylation of the *cis*-configured derivative **25a**. Pleasingly, *cis*- and *trans*-3-hydroxymethyl piperidines **68** and **69** were isolated in 66% and 84% yield respectively.



Scheme 4.19 Reductive AQ removal affording *cis*- and *trans*-hydroxymethyl pyrrolidines **37**, **65–67**.



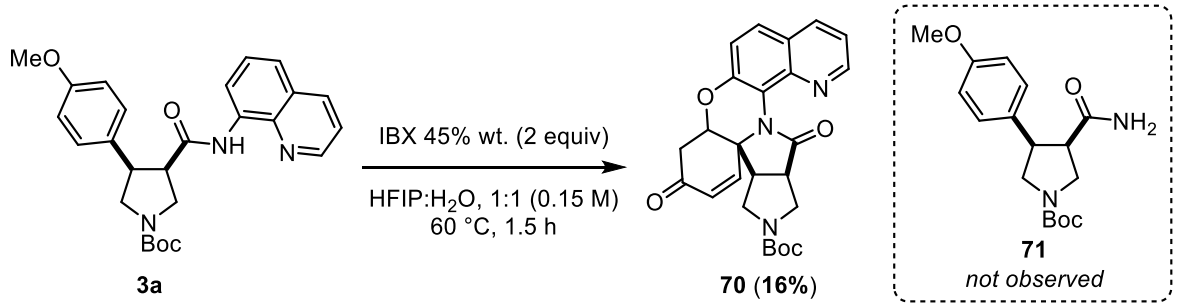
Scheme 4.20 Reductive AQ removal affording *cis*- and *trans*-hydroxymethyl piperidines **68** and **69**.

4.3.3.4 Directing group removal: primary amide derivatives

At this stage in the investigation, attention turned to the synthesis of primary amide derivatives, through oxidative cleavage of the AQ. The viability of this transformation was previously demonstrated on *p*-tolyl substituted pyrrolidine substrates either using ozonolytic fragmentation[144b] or IBX-mediated oxidation protocols (see section 3.6.3).[144a,212] Unfortunately, attempts to use Maulide's ozonolytic cleavage in the presence of electron-rich aromatic substituents (*i.e.* 4-methoxyphenyl) were unsuccessful, likely because of competing

overoxidation.[144b] Alternatively, the use of IBX under the conditions specifically optimised by Zhang and Chen for AQ removal was evaluated in order to access pyrrolidine and piperidine amide derivatives.[212]

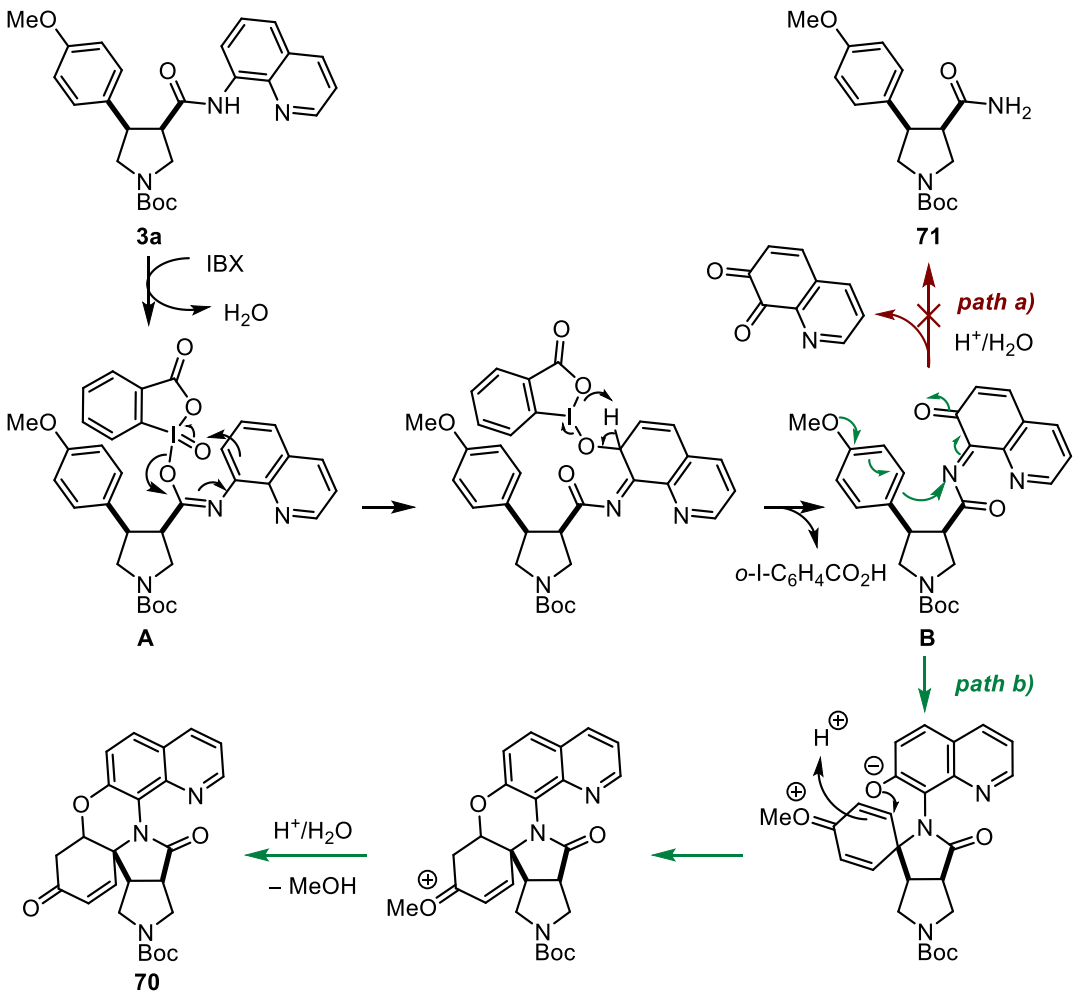
Accordingly, *cis*-pyrrolidine-AQ amide **3a** was treated with IBX in a mixture of HFIP and H_2O at 60 °C for 1.5 h (Scheme 4.21). Although full conversion of the starting substrate was observed under these conditions, the resulting NMR was of difficult interpretation. Furthermore, the ^{1}H NMR singlet expected for the -OMe group was not observed, indicating the absence of desired amide product **71**. Purification by flash column chromatography afforded a single derivative in 16% yield. This was identified as polycyclic compound **70**, based on ^{1}H and ^{13}C NMR spectroscopy, in combination with 2D NMR experiments and HRMS. While the *cis*-stereochemistry of the pyrrolidine ring was assigned by analogy with the starting material, the relative configuration of the CHO and quaternary CN centres was not determined. A similar IBX-mediated spirocyclisation was observed by Chen when attempting AQ removal on indole-tethered derivatives.[212,247] Unfortunately, no improvement was obtained when repeating the reaction at lower temperature (25 °C for 18 h, not shown), with spirolactam derivative **70** similarly formed as major product.



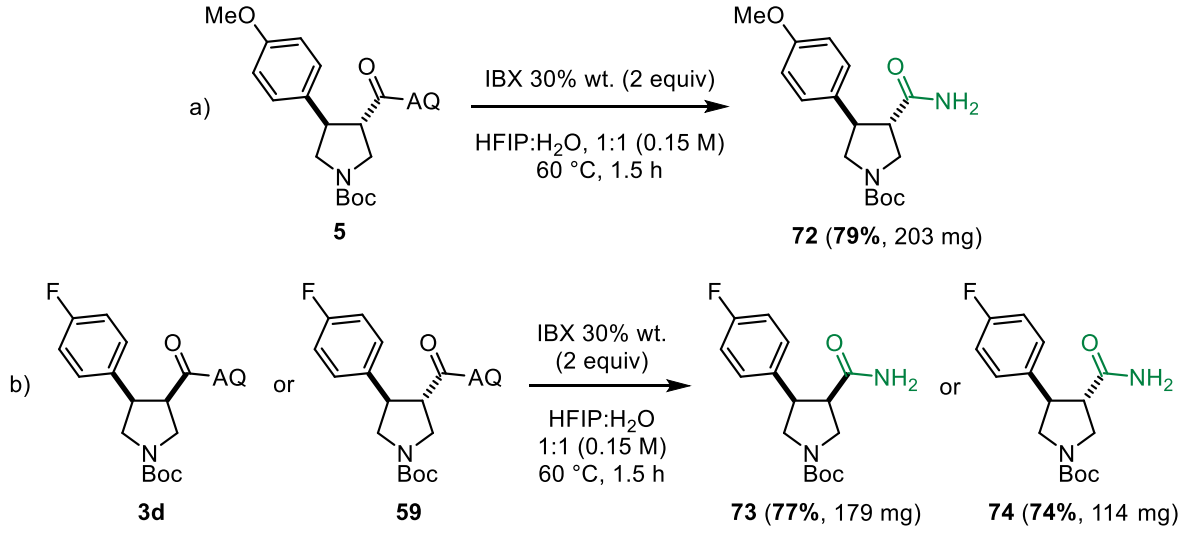
Scheme 4.21 IBX-mediated amide spirocyclisation of *cis*-4-methoxyphenyl pyrrolidine derivative **3a**.

A plausible mechanism for this transformation involves an initial formation of iodoimidate **A,** followed by oxidative dearomatisation of the AQ auxiliary at the 7-position, forming imine intermediate **B** (Scheme 4.22). At this point, spirocyclisation (path b) could occur preferentially over the desired hydrolysis pathway (path a), likely due to the proximity between the 4-methoxyphenyl and amide substituents in *cis*-pyrrolidine **3a**. Subsequent conjugate addition and hydrolysis would deliver the observed spirolactam derivative **70**.

Based on this mechanistic proposal, it was reasoned that path b could be geometrically disfavoured for *trans*-configured pyrrolidine **5**, thus promoting the desired formation of amide **72**. Pleasingly, treating *trans*-4-methoxyphenyl derivative **5** under identical oxidative conditions afforded *trans*-configured pyrrolidine amide **72** in 79% yield (Scheme 4.23a).



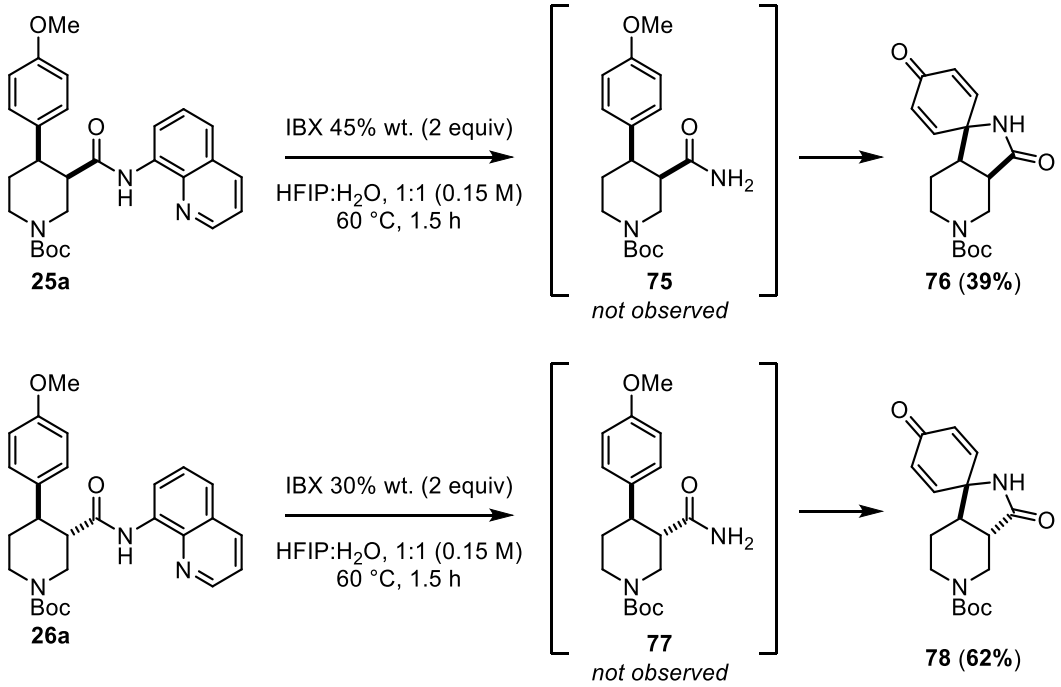
Scheme 4.22 Proposed mechanism for IBX-mediated spirocyclisation of *cis*-4-methoxyphenyl-pyrrolidine amide **3a**.



Scheme 4.23 IBX-mediated AQ cleavage on a) *trans*-4-methoxyphenyl pyrrolidine **5**, and b) *cis*- and *trans*-4-fluorophenyl pyrrolidines **3d** and **59**.

Furthermore, the oxidative AQ cleavage proceeded smoothly in the absence of electron donating groups. In particular, this was successful for both *cis*- and *trans*-4-fluorophenyl pyrrolidine derivatives **3d** and **59**, affording deprotected pyrrolidine amides **73** and **74** in high yield (Scheme 4.23b).

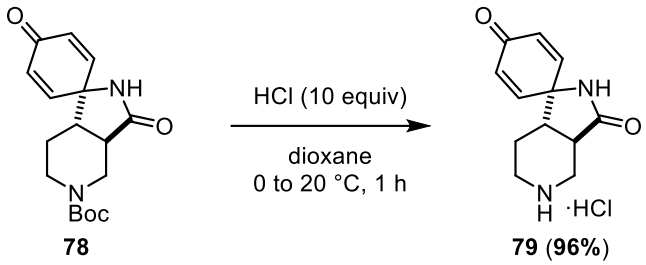
Following this, the same oxidative approach was investigated for the deprotection of *cis*- and *trans*-4-methoxyphenyl piperidines **25a** and **26a**. Unfortunately, the reaction was unsuccessful in both cases, forming exclusively spirocyclic lactam products **76** and **78**, isolated in 39% and 62% yield respectively (Scheme 4.24). In contrast to the corresponding *cis*-pyrrolidine amide, spirocyclisation likely occurred *via* overoxidation of piperidine-3-carbamoyl derivatives **75** and **77**, after complete removal of the AQ group. A similar outcome was observed by Chen in the presence of a 4-methoxyphenyl substituent, although the corresponding spirolactams was only formed as minor side product alongside the desired primary amide.[212] Kita reported a related catalytic spirolactamisation of secondary amides tethered to 4-methoxy- and 4-fluorophenyl groups, in the presence of a hypervalent iodine(III) species generated in trifluoroethanol.[248] This was proposed to occur *via* formation of a reactive nitrenium ion, although the generation of a radical cation species was not excluded.



Scheme 4.24 IBX-mediated AQ cleavage/spirocyclisation of *cis*- and *trans*-4-methoxyphenyl piperidines **25a** and **26a**.

The *trans*-configuration of spirolactam **78** was confirmed after Boc-deprotection with 4 N HCl in dioxane (Scheme 4.25). In particular, the coupling constant values observed by ^{1}H NMR

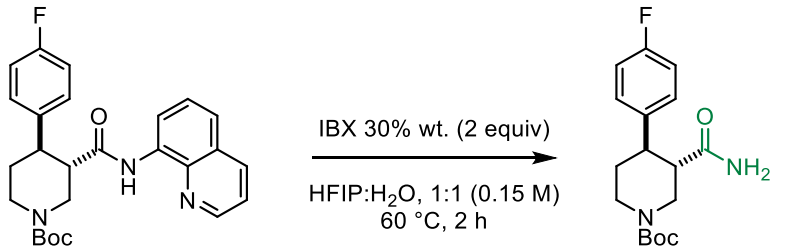
spectroscopy of N-H derivative **79** indicated both piperidine protons at the ring junction to be in an axial position, consistent with a *trans*-configuration.



78 **79** (**96%**)

Scheme 4.25 Boc-deprotection of *trans*-spirocyclic lactam **78**.

Although piperidine amides bearing a 4-methoxyphenyl group could not be accessed by this route, the synthesis of the corresponding *trans*-fluorine analogue was attempted. Pleasingly, upon treatment of substrate **26c** with IBX, *trans*-4-fluorophenyl piperidine amide **80** was obtained in 65% yield, without any detectable spirocyclisation (Scheme 4.26).

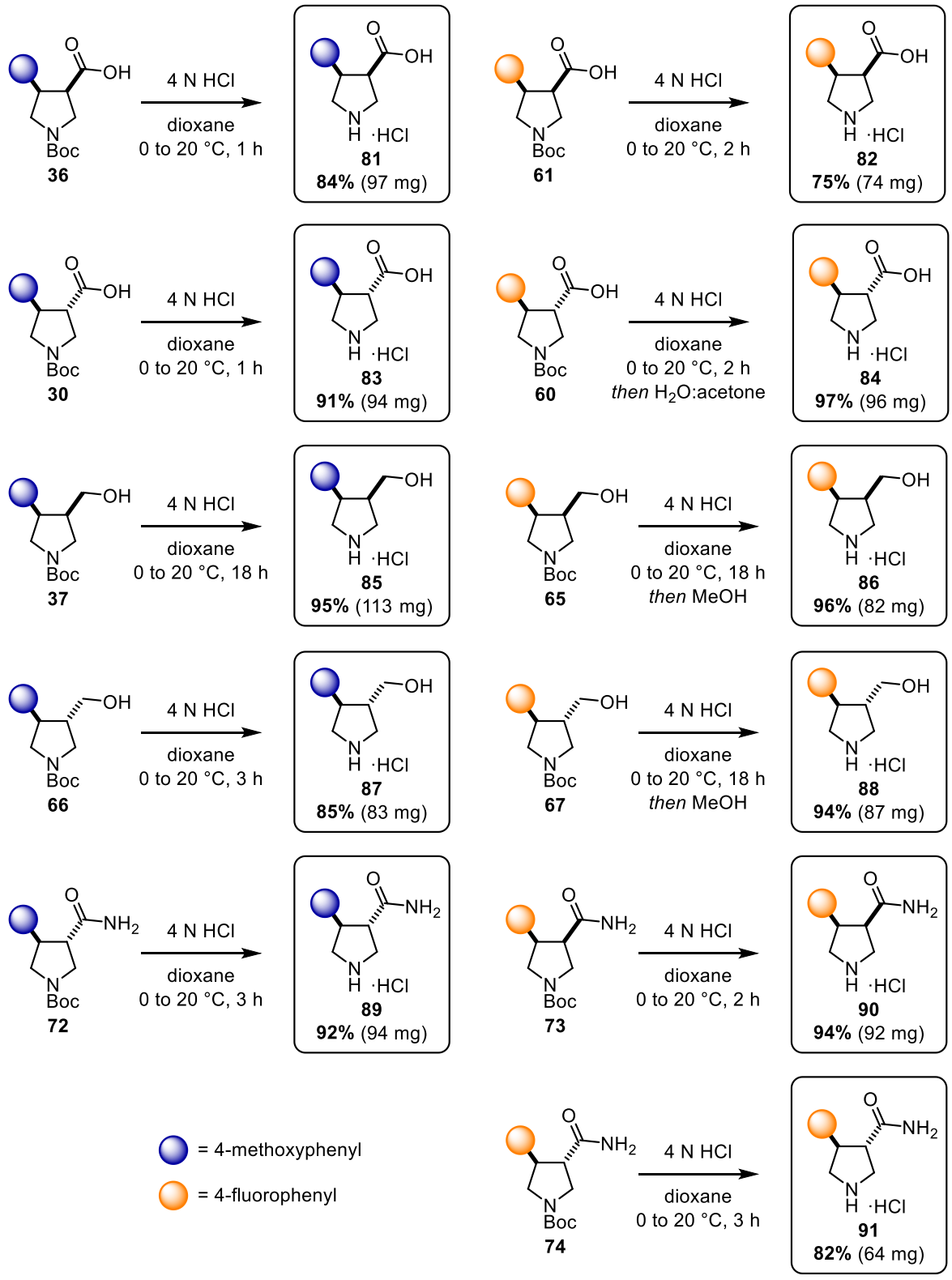


26c **80** (**65%**, 211 mg)

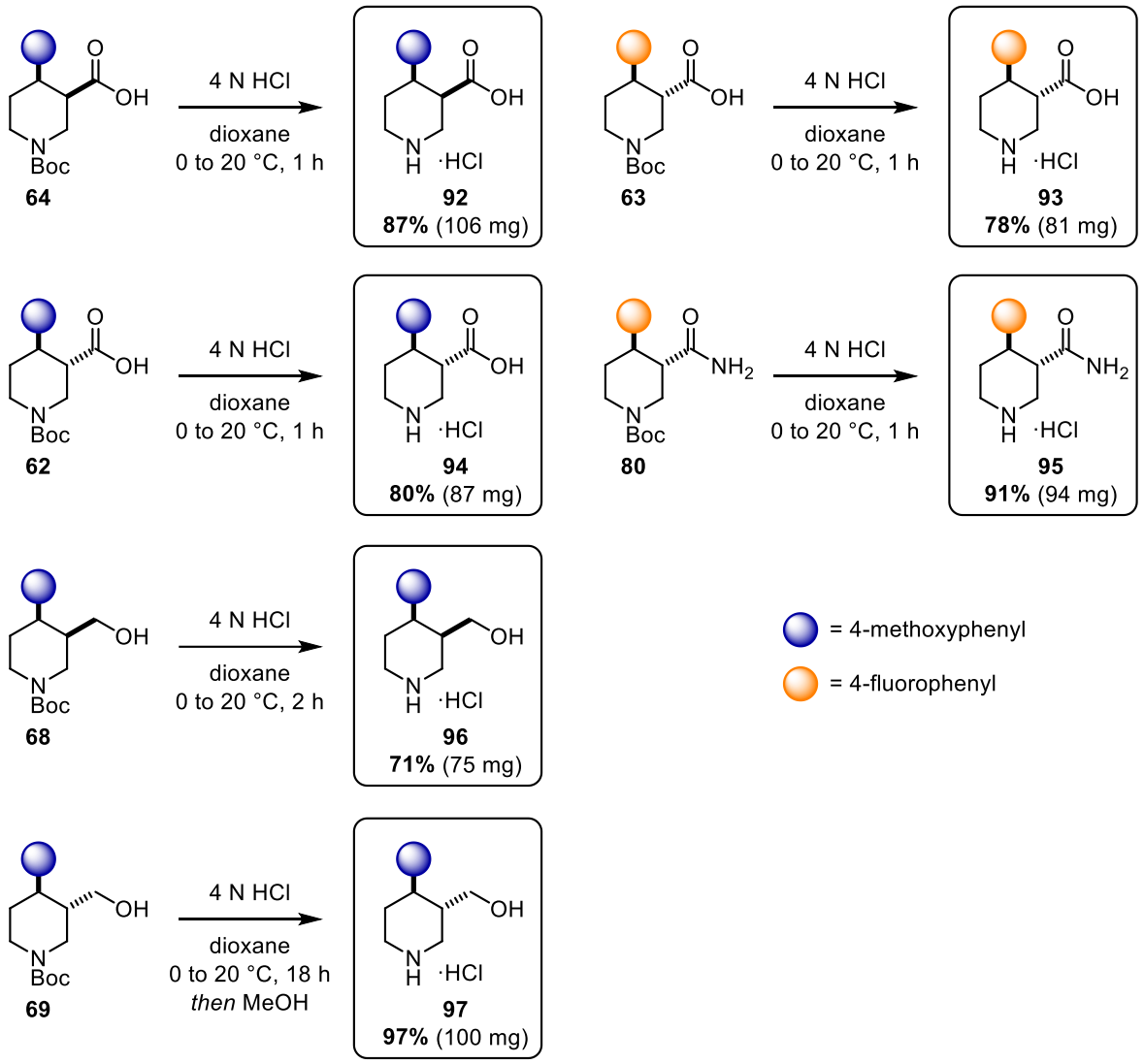
Scheme 4.26 IBX-mediated AQ cleavage on *trans*-4-fluorophenyl piperidine **26c**.

4.3.3.5 Endgame: Boc deprotection

Finally, pyrrolidine and piperidine fragments **81–91** and **92–97** were obtained by Boc-deprotection as the corresponding hydrochloride salts (Schemes 4.27 and 4.28). Removal of the *N*-protecting group provided the desired products in high to excellent yields (71%–97%). In most cases, the HCl salts crashed out of solution within 1–3 h, and pure fragments **81–83**, **85**, **87** and **89–96** could be obtained after simple filtration and wash with ice-cold Et_2O, with no need for further purification. A few derivatives containing the hydroxymethyl functionality (pyrrolidines **86**, **88** and piperidine **97**) were found to be highly hygroscopic and quickly turned into a paste during the filtration. Thus, the material was recovered in MeOH and the solvent removed under reduced pressure to afford the final products. However, this strategy was unsuccessful for *trans*-4-(4-fluorophenyl)-pyrrolidine 3-carboxylic acid **84**. In this case, rapid conversion to the corresponding methyl ether was observed upon concentration from MeOH (compound **S3** in experimental part 8). Alternatively, pyrrolidine hydrochloride salt **84** could be obtained in 97% yield, using a 1:1 mixture of H_2O:acetone to recover the hygroscopic material after Boc-deprotection.



Scheme 4.27 Boc-deprotection to afford 3,4-disubstituted pyrrolidine fragments **81–91**.



Scheme 4.28 Boc-deprotection to afford 3,4-disubstituted piperidine fragments **92–97**.

With these 3,4-disubstituted pyrrolidine and piperidine fragments in hand, their physico-chemical and structural properties were analysed as described in the following section.

4.3.4 Physicochemical Properties Analysis

The library was evaluated against physicochemical descriptors and molecular shape in order to: *i)* assess its suitability for use in FBDD programs; *ii)* evaluate the degree of 3-dimensional character of the fragments; and *iii)* estimate the properties of lead-like compounds that could be derived from such library. This analysis was performed using the Lead-Likeness and Molecular Analysis (LLAMA) platform developed by Marsden and Nelson.[249,250] The relevant physicochemical parameters for each fragment are presented in Figure 4.5, while the average set of descriptors across the whole library is given in Table 4.2.

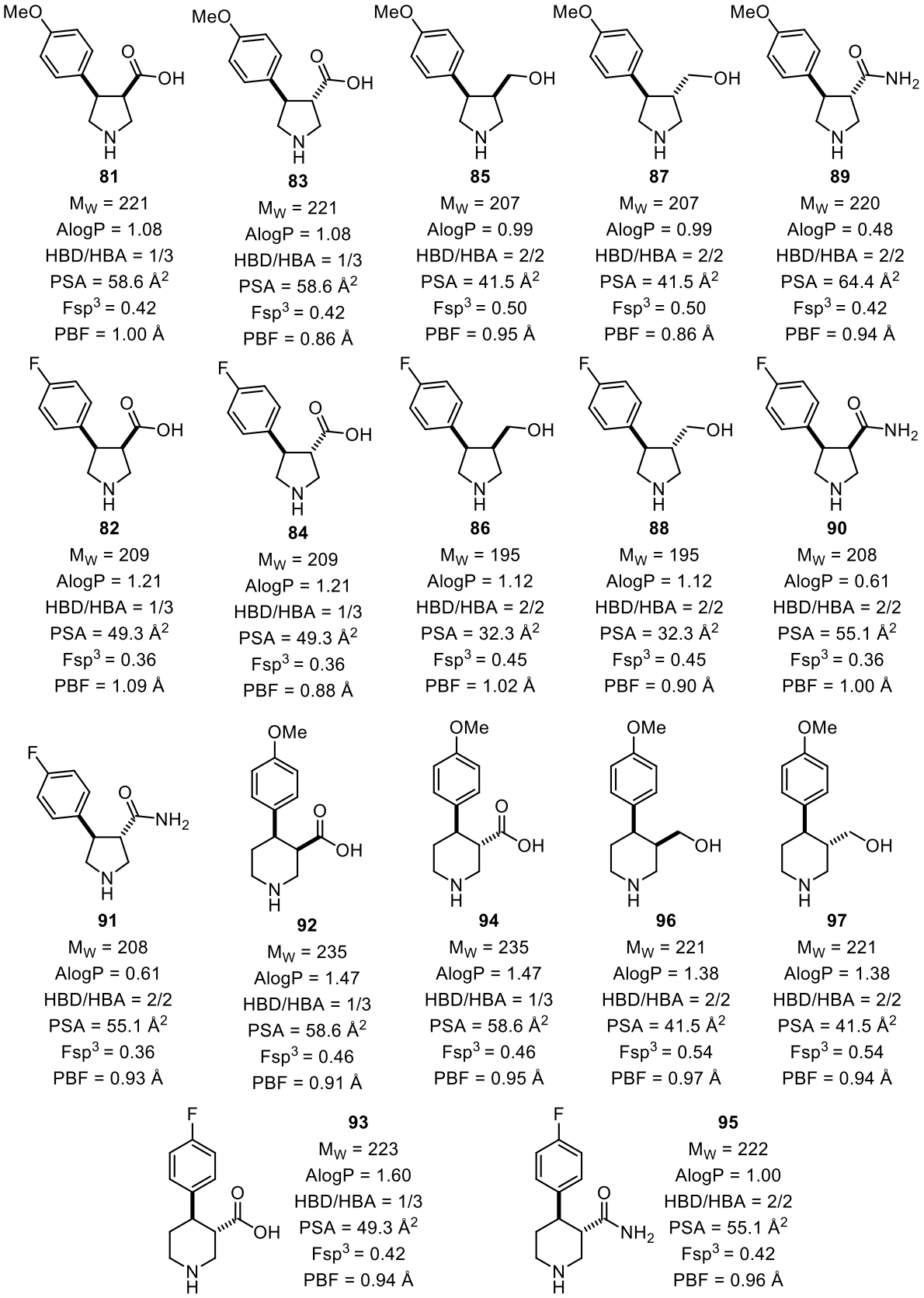


Figure 4.5 Physicochemical properties for pyrrolidine and piperidine fragments **81–97**.

Pleasingly, these compounds were all found to be within Astex's ideal fragment chemical space.[33,35] The M_W varied from 195 to 235 g·mol^{-1}, with an average at 215 g·mol^{-1}. Similarly, optimal lipophilicity was estimated, with a mean AlogP of 1.14 (calculated by addition of individual atomic clogP contributions).[249]

entry	property	fragment set average[a]
1	M_W	215 g·mol^{-1}
2	AlogP	1.14
3	HBD[b]	1–2
4	HBA[b,c]	2–3
5	PSA	49.2 Å^2
6	Fsp^3	0.44
7	PBF	0.95 Å
8	NROT	2–3

Table 4.2 Average physicochemical properties for the 17-membered library of fragments **81–97**. [a] Calculated using LLAMA computation tool. [b] Calculated using Marvin 19.27.0 (ChemAxon). [c] The fluorine atom was included in the HBA count.

The number of hydrogen bond donors and acceptors were calculated using Marvin 19.27.0 (ChemAxon), considering the corresponding ionised form at physiological pH = 7.4, and were both found to be ≤ 3.[81] Furthermore, PSA ≤ 60 Å^2 and NROT ≤ 3 were observed across the collection, as desired for fragment-like molecules.[33]

Finally, the degree of 3-dimensionality was evaluated using different parameters, including for instance the fraction of sp^3 carbon atoms (Fsp^3) originally proposed by Lovering.[25] Pleasingly, a relatively high mean Fsp^3 value of 0.44 was observed across the fragment set.

In addition, the shape distribution of these derivatives was analysed by construction of a principal moments of inertia (PMI) plot (Figure 4.6).[251] This triangular plot gives the distribution of molecular geometries relative to the linear, spherical and disc-like extreme shapes, represented at the three corners by acetylene, adamantane and benzene molecules respectively. Upon selection of the lowest-energy conformers, the LLAMA tool calculated the corresponding moments of inertia in the three dimensions (x, y and z axis). In turn, this gave coordinates I1 [inertia(x)/inertia(z)] and I2 [inertia(y)/inertia(z)] for each compound, used to build the PMI plot. Based on this analysis, fragments **81–97** were found to move away from the rod-like-disc-like axis, often overpopulated in screening libraries.[39b] Interestingly, significant differences in shape were observed between diastereoisomers, with *cis*-pyrrolidines generally having a higher spherical character than their *trans*-equivalents (Figure 4.6). On the other

hand, an increased disk-like shape was observed for *trans*-configured piperidines, compared to their *cis*-counterparts. Compounds exhibiting higher 3D shape, moving towards the right hand-side of the plot, were invariably *cis*-configured pyrrolidines.

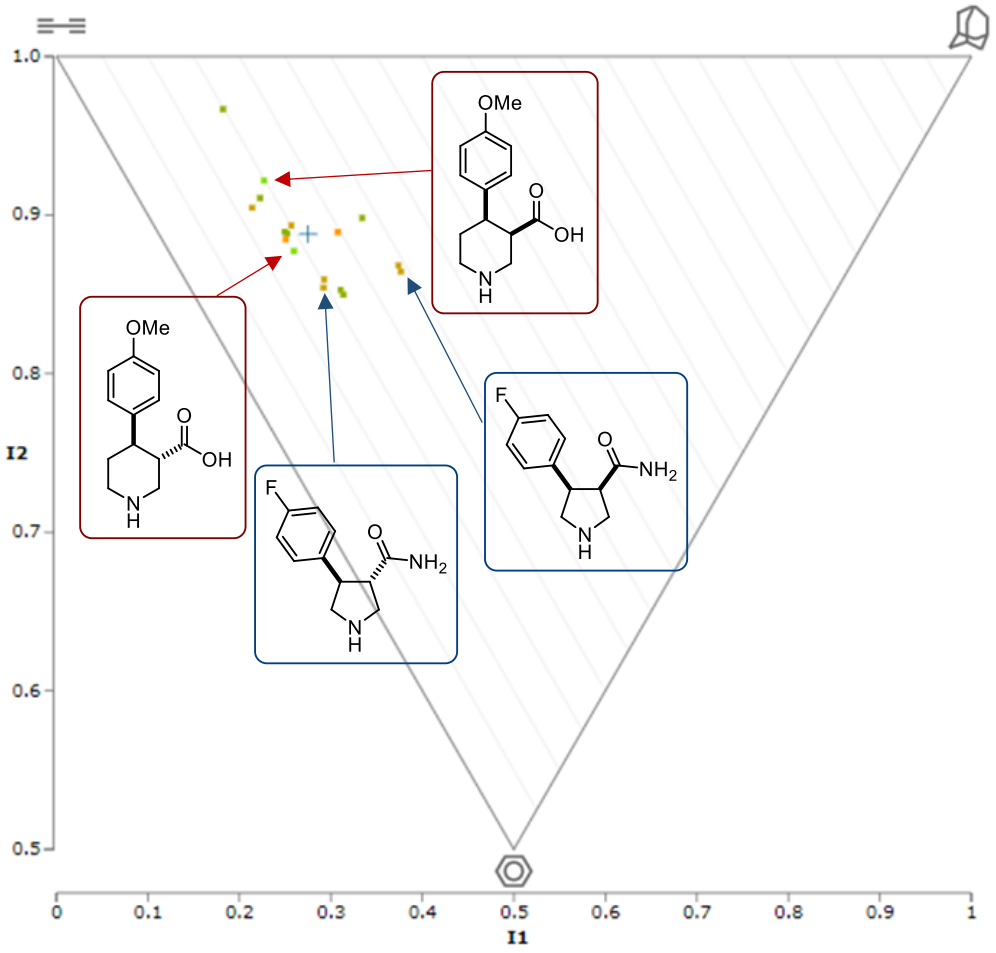


Figure 4.6 PMI plot for pyrrolidine and piperidine fragments **81–97** calculated by LLAMA. Mean PMI coordinates: I1 = 0.275, I2 = 0.888 (denoted by +).

In 2012, Brown and Blagg introduced the plane of best fit (PBF) as an additional topological descriptor to evaluate molecular shape.[252] The PBF is a theoretical plane passing through the molecule, calculated to minimise its distance from each atom. The largest atomic distance corresponds to the PBF score, which can be used to estimate the degree of molecular 3-dimensionality. In particular, it was proposed that compounds with PBF ≥ 0.6 Å and the sum of mean PMI coordinates I1+I2 ≥ 1.07 have a good degree of 3D character.[252] With an average PBF score of 0.95 Å and a combined mean PMI value of 1.16, good 3-dimensionality was thus estimated for N-heterocycle fragments **81–97**.

Finally, the LLAMA platform was used to perform a virtual decoration of this library, in order to evaluate its potential for the generation of a wider array of lead- and drug-like molecules. A LLAMA default set of 44 reactants was used to elaborate the pyrrolidine and piperidine

scaffolds through reactions commonly used in medicinal chemistry, such as reductive amination, amide formation and alcohol functionalisation (for a full list of reactants and reactions, see Appendix I).

Permitting up to 2 reactions on each scaffold, a total of 3,369 compounds were generated. The 1st round of virtual elaboration generated 393 pyrrolidine- and piperidine-containing molecules, with higher molecular size and lipophilicity (Figure 4.7a,b).

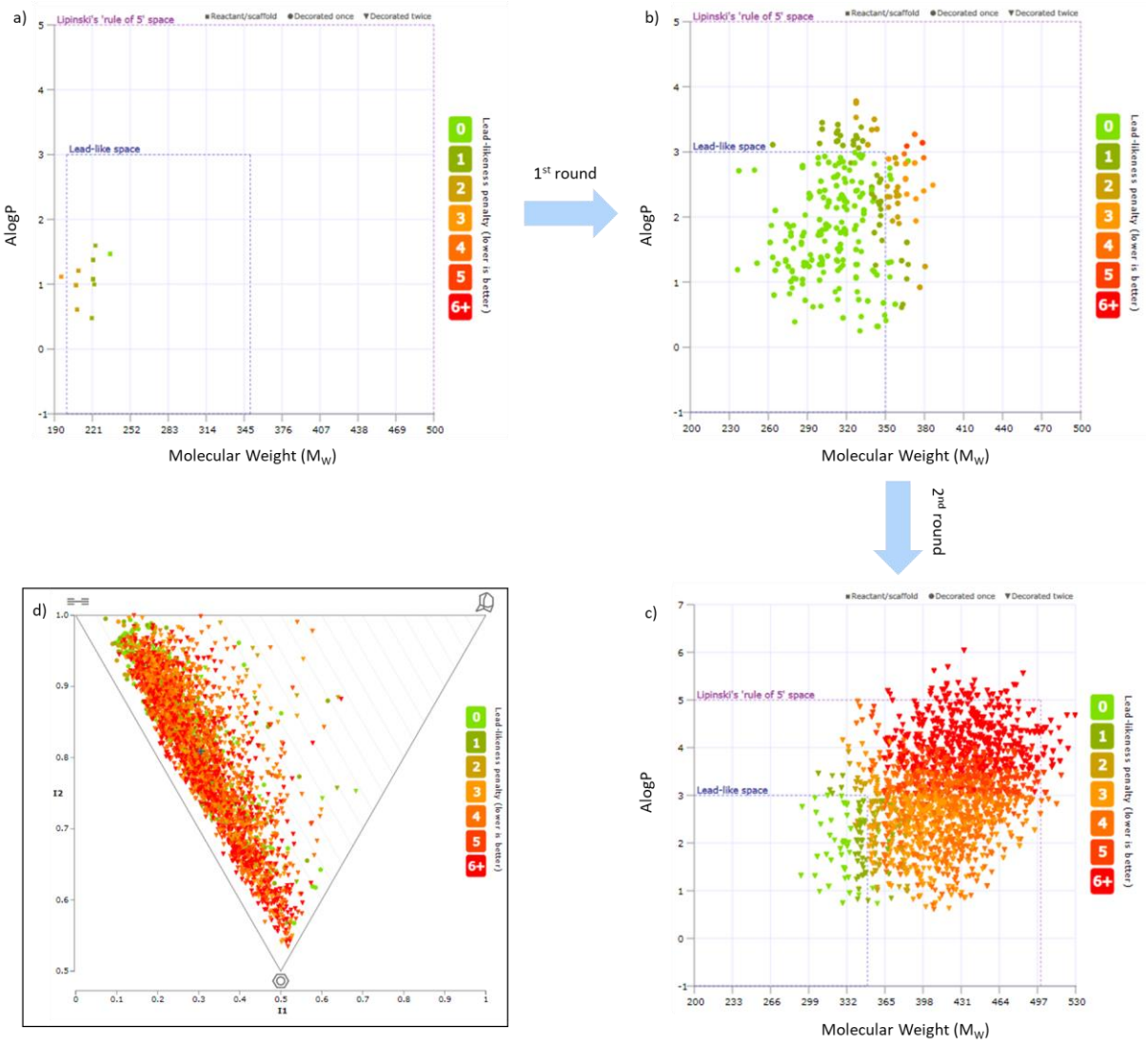


Figure 4.7 a) AlogP *vs* M_W plot for pyrrolidine and piperidine fragments **81–97**. b) AlogP *vs* M_W plot for compounds deriving from the 1st round virtual decoration. c) AlogP *vs* M_W plot for compounds deriving from the 2nd round of virtual decoration. d) PMI plot for the full set of decorated compounds; mean PMI coordinates: I1 = 0.305, I2 = 0.809 (denoted by +). Calculated by LLAMA.

The LLAMA platform assigned to each compound a Lead-Likeness Penalty, in order to give an indication of how far outside this ideal space such derivatives lay. Lower score (green colour) indicates higher lead-likeness of the selected compound. Pleasingly, 72% of the 1st

round compounds fell in optimal lead-like space, with $M_W \leq 350$ g·mol^{-1} and AlogP ≤ 3 (Figure 4.7b).

Upon a 2nd round of decoration, additional 2,976 compounds were generated, now efficiently exploring drug-like space, delimited by the Lipinski's rule of 5 constraints ($M_W \leq 500$ Da and AlogP ≤ 5, Figure 4.7c).

Finally, a PMI plot of the elaborated compounds showed that the full set displayed highly varied topologies, despite most of the compounds remains close to the region along the rod-like–disk-like axis (Figure 4.7d).

4.4 Conclusions

In conclusion, the synthetic potential of Pd-catalysed C(4)–H arylation of pyrrolidines and pyrrolidines was demonstrated in various medicinal chemistry applications.

This approach enabled the concise stereocontrolled formal synthesis of antidepressant drug (–)-paroxetine, involving C(4)–H arylation followed by reductive DG removal as key steps.

The same strategy was applied to the total synthesis of enantiopure Br- and I-(–)-paroxetine analogues, for structural elucidation studies on SERT protein. Synthetic challenges such as potential dialkylation of 1,4-diiodobenzene and poor compatibility of these halides with strong reductive conditions were addressed, completing the synthesis of both derivatives in 12% yield over 8 steps from commercial substrates.

Furthermore, the C(4)–H arylation approach was applied to the synthesis of a library of 17 pyrrolidine and piperidine fragments for potential screening in FBDD. These were synthesised through sequential C(4)–H arylation (and epimerisation), DG cleavage and final Boc deprotection. This provided divergent access to acid-, alcohol- or amide-containing C(4)-arylated N-heterocycles with either *cis*- or *trans*-configuration. In all cases, 50–100 mg of the final fragment was obtained in 4–6 synthetic steps and no more than 3 chromatographic purifications.

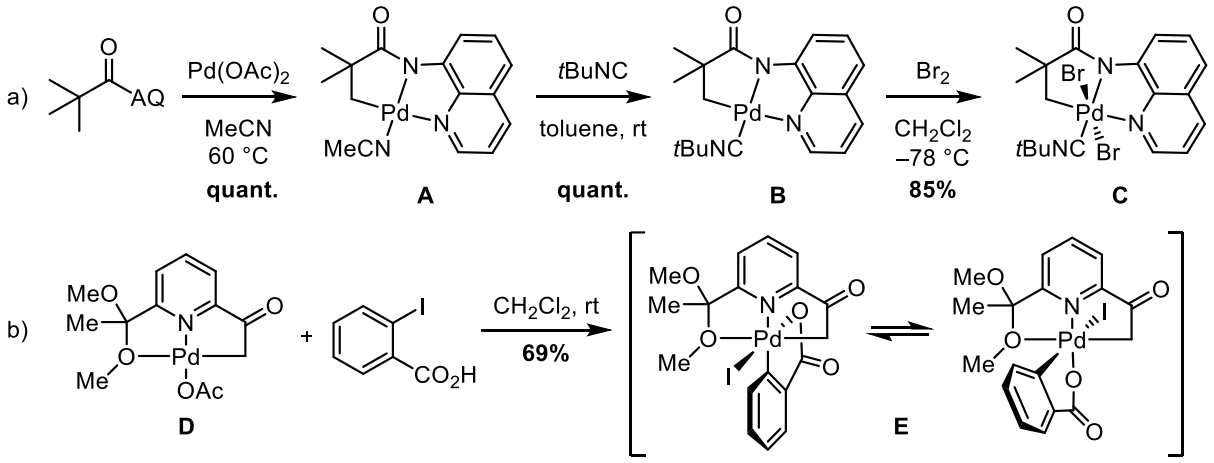
The library was analysed against physicochemical properties and molecular shape through Nelson and Marsden's LLAMA computational tool. Pleasingly, these derivatives well fitted in the ideal fragment-like chemical space, featuring good degree of three-dimensional character while maintaining low M_W. These displayed various molecular topologies, dependent on ring size and stereochemical configuration. Finally, virtual decoration of the fragments demonstrated the potential of this library to generate a broad array of lead- and drug-like molecules.

Despite the successful applicability of this protocol in drug discovery settings, the moderate yields often observed in the C–H arylation step represented an important limitation throughout these projects. In order to solve this issue and to gain useful insight into the requirements for the regio- and stereoselectivity of the transformation, detailed mechanistic studies were undertaken as discussed in the next chapter.

5. Mechanism and Selectivity of Pd-Catalysed C(4)–H Arylation

5.1 Mechanism of C(sp^3)–H Functionalisation *via* Pd^{II}/Pd^{IV} Catalytic Cycle

The Pd-catalysed arylation of unactivated C(sp^3)–H bonds with aryl halides, assisted by bidentate DGs, has typically been proposed to proceed *via* a Pd^{II}/Pd^{IV} redox cycle (see sections 1.4.1 and 1.4.2).[128] Daugulis proposed this mechanism to be operative in the β-C(sp^3)–H arylation of AQ-amide derivatives, as supported by the isolation of Pd(IV) complex **C** (Scheme 5.1a).[124,125] In this study, the stoichiometric reaction of AQ pivalamide with $Pd(OAc)_2$ in MeCN formed monomeric Pd(II) complex **A** in quantitative yield. This was found to react with 4-iodotoluene at rt to form a mixture of mono- and diarylated derivatives (not shown). Arylation of **A** was proposed to occur *via* oxidative addition generating a high valent Pd(IV) intermediate, followed by C–C bond-forming reductive elimination.[253] Although the postulated aryl-Pd(IV) complex could not be isolated, ligand exchange with *tert*-butyl isonitrile, followed by oxidation with Br_2 at –78 °C, formed species **C** in 85% yield. This featured an octahedral geometry with a *trans*-arrangement of the bromine ligands as observed by X-ray diffraction.

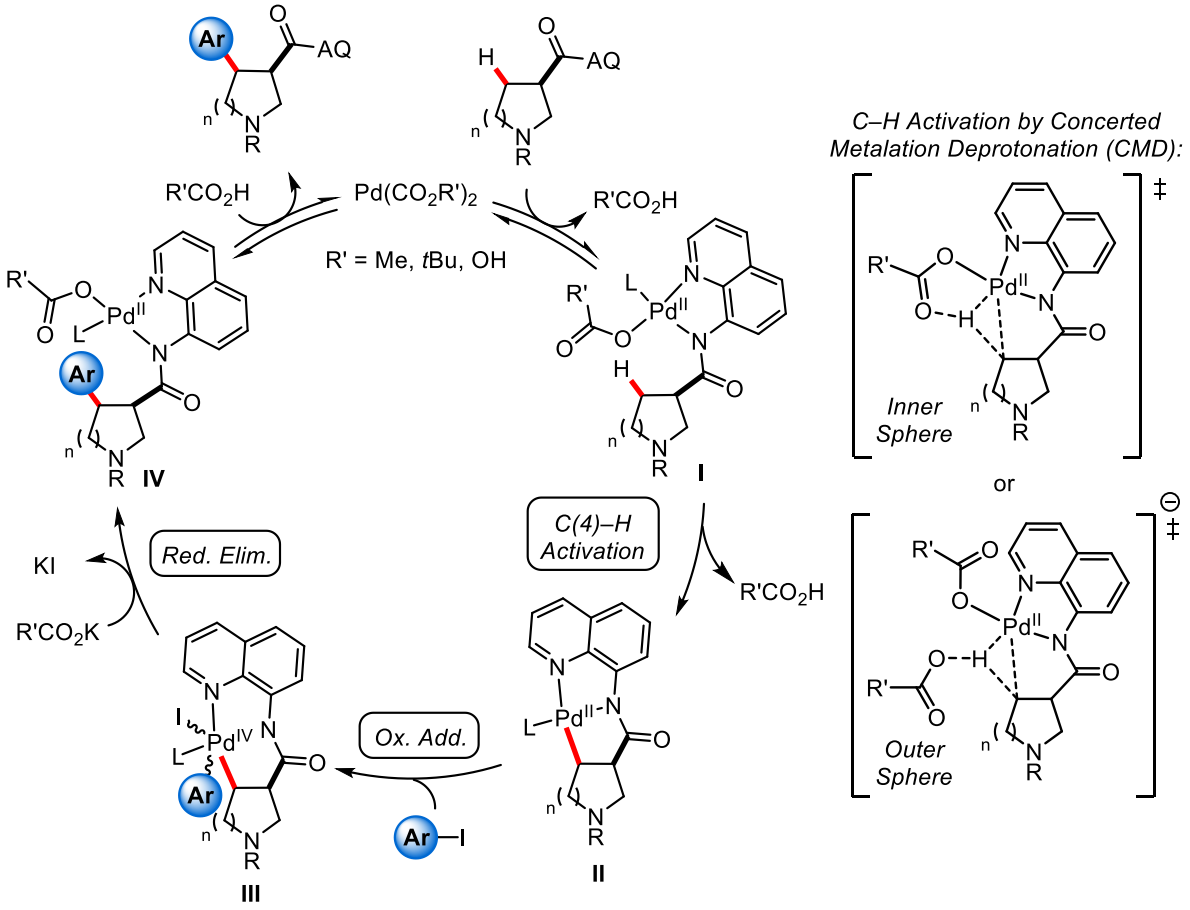


Scheme 5.1 Literature precedents for the stoichiometric formation of Pd(IV) complexes involving the use of a) an AQ amide ligand and b) an aryl iodide oxidant.

The isolation of an aryl-Pd(IV) complex was later achieved by Vicente through oxidative addition of 2-iodobenzoic acid to Pd(II) complex **D**, using a monoanionic tridentate pincer ligand (Scheme 5.1b).[127] Initial coordination through the benzoate moiety, in combination with an *ortho*-EWG group, allowed proximity-induced oxidative addition to occur at rt. Although the stability of Pd(IV) complex **E** was strictly dependent on the chelating benzoate, this demonstrated the possible formation of Pd(IV) intermediates in the reaction with aryl halides.

More recently, computational studies by Wu and Zeng demonstrated the viability of a Pd^{II}/Pd^{IV} catalytic cycle in the AQ-assisted functionalisation of unactivated C(sp^3)–H bonds with aryl bromides.[126]

Based on these literature precedents, the Pd-catalysed C(4)–H arylation of pyrrolidines and piperidines with aryl iodides was proposed to involve a related Pd^{II}/Pd^{IV} catalytic cycle (Scheme 5.2). In this mechanistic scenario, initial catalyst coordination to the aminoquinoline DG would be followed by C–H activation to form palladacycle **II**, likely occurring through an inner- or outer-sphere concerted-metalation-deprotonation pathway (CMD, see section 1.4).[111,112,126] Oxidative addition to an aryl iodide would generate Pd(IV) complex **III**, which would subsequently undergo concerted reductive elimination to form the new $C(sp^3)$–$C(sp^2)$ bond. Halide abstraction and protodemetalation were finally envisaged to liberate the arylated product and regenerate the active catalytic species.



Scheme 5.2 Initial proposal for the C(4)–H arylation of pyrrolidines and piperidines via Pd^{II}/Pd^{IV} mechanism.

Such catalytic cycle is consistent with various empirical observations collected during the process of optimisation of the reaction (see section 3.2). In particular, the tolerance of the reaction for Ag(I) salts and the poor reactivity of aryl bromides would exclude the involvement of an active low valent Pd(0) species (*e.g.* in a Pd^0/Pd^{II} catalytic scenario). On the other hand, the involvement of bimetallic Pd(III) complexes could not be excluded, although this has been

typically observed for C(sp^2)–H functionalisation using monodentate DGs in the presence of stronger iodine(III) oxidants.[254]

At this stage, this simplistic representation of the catalytic cycle did not provide any information on the selectivity features of this transformation, as well as on more intimate details of the reaction mechanism (*e.g.* the presence of product inhibition and/or catalyst deactivation). The possible formation of a *trans*-palladacycle intermediate in the C(4)–H functionalisation of piperidines has already been discussed in section 3.5.3. However, the understanding of factors that govern the regio- and stereoselectivity of the reaction, particularly for 5-membered rings, remained very limited. This also derived from the scarce literature precedent for mechanistic investigations into the directed C–H functionalisation of related substrates, whereby multiple C–H bonds are potentially available.[166,170] Therefore, experimental and computational studies were envisaged to gain better insight into the regio- and stereoselectivity of C(4)–H arylation, with a particular focus on the pyrrolidine system. A better mechanistic understating could aid in overcoming synthetic limitations, such as the low reactivity of electron-poor aryl iodides. Furthermore, more general mechanistic information could benefit the design of regio- and stereoselective transformations on both cyclic and acyclic systems.

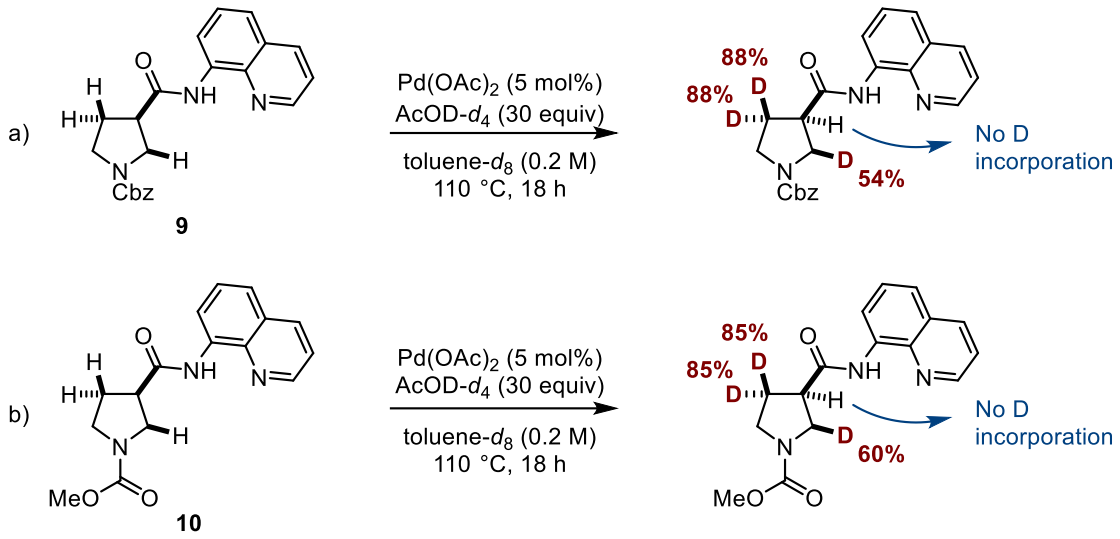
With these considerations in mind, the C–H activation step was first investigated.

5.2 Investigations into the C–H Activation Step

5.2.1 Deuterium Labelling Experiments on Pyrrolidine-3-AQ Amide

Pd-catalysed C–H deuteration was used to study the C–H activation step separately from the overall catalytic cycle. *N*-Cbz pyrrolidine-3-AQ amide **9** was treated with catalytic $Pd(OAc)_2$ and AcOD-d_4, under the same conditions previously used for the corresponding piperidine system (section 3.5.3.3). In this case, reaction at C(4) was similarly favoured over C(2), with the latter position being deuterated in 54%, exclusively *cis*- to the DG (Scheme 5.3a).[§] On the other hand, in contrast with the excellent *cis*-diastereoselectivity observed in the C–H arylation of this substrate, both *cis*- and *trans*-C(4)–H bonds were deuterated by the Pd(II) catalyst in 88%. A very similar result was observed for pyrrolidine amide **10**, suggesting the regio- and stereochemical outcomes of deuteration to be independent of the *N*-protecting group (Scheme 5.3b).

[§] The position of protons relative to the DG was assigned based on 2D NOESY NMR experiments at 100 °C. In particular, CHCO was found to correlate exclusively with protons on the same face of the pyrrolidine ring.

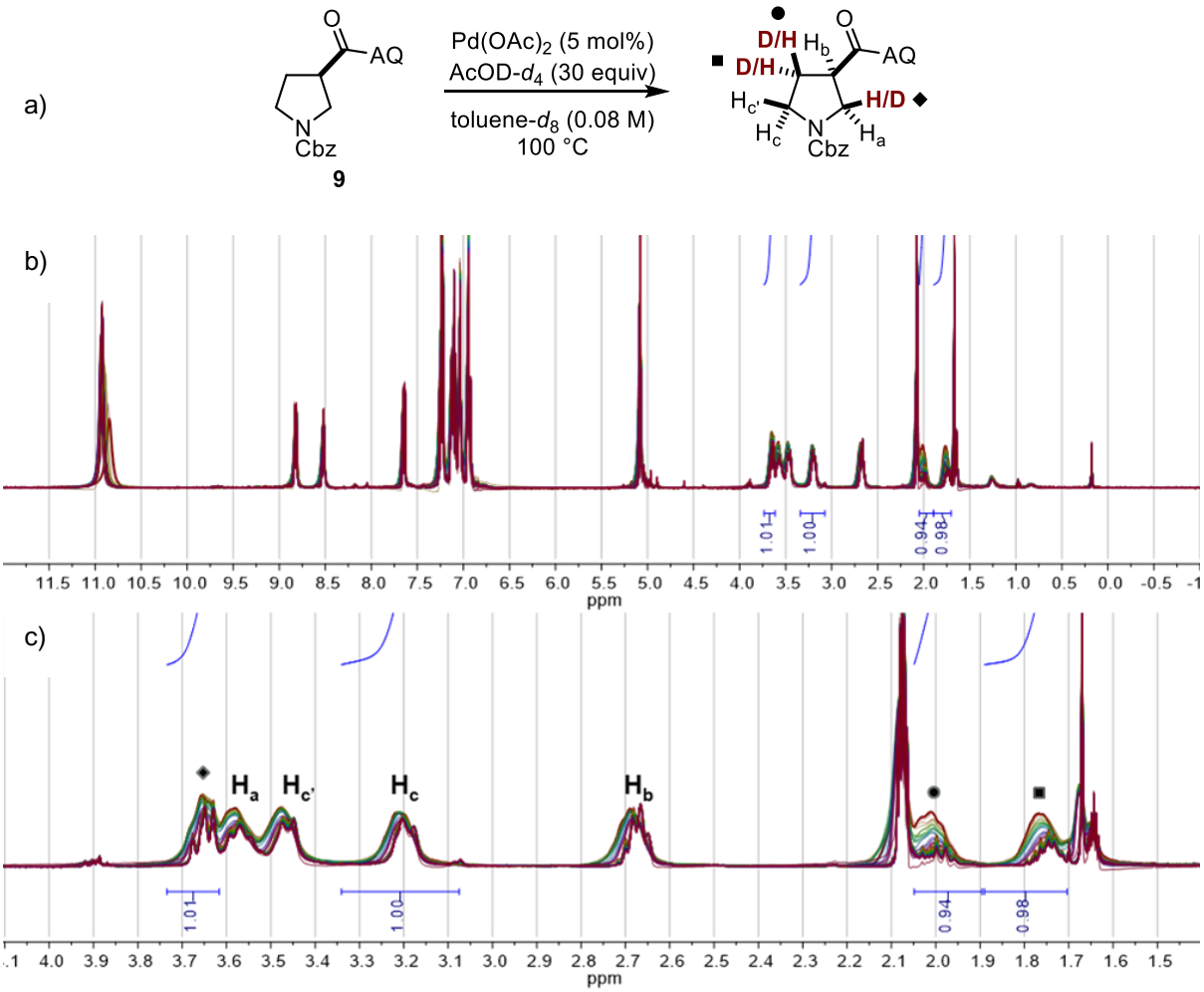


Scheme 5.3 a) Pd-catalysed C–H deuteration of *N*-Cbz pyrrolidine amide **9**. Deuterium incorporation (%) determined by quantitative ^{1}H NMR (400 Hz) at 100 °C in DMSO-d_6, using a delay time d_1 = 70 s. b) Pd-catalysed C–H deuteration of pyrrolidine amide **10**. Deuterium incorporation (%) determined by quantitative ^{1}H NMR (500 Hz) at 100 °C in DMSO-d_6, using a delay time d_1 = 1 s.

Potential epimerisation occurring under the acidic conditions was excluded based on the absence of deuteration at the enolisable C(3) position. In addition, no isotopic labelling occurred in the absence of $Pd(OAc)_2$ (not shown). These results are thus suggestive of a non-stereodetermining C–H activation step, with the potential to form both *cis*- and *trans*-configured palladacycle intermediates also for the 5-membered pyrrolidine ring. Pd-catalysed deuteration of both *cis*- and *trans*-β-C–H bonds have previously been observed for cyclopentane-AQ amide, while exclusive *cis*-C(3)–H deuteration was reported for *N*-Cbz proline-2-AQ amide.[166] This indicates that the stereochemical outcome of C–H activation for 5-membered rings is strictly dependent on the substitution pattern and on the conformational accessibility of different C–H bonds.

The kinetics of C–H deuteration at the different positions was then investigated, following the C–H deuteration of pyrrolidine **9** over time (Scheme 5.4a). The reaction was run in a J-Young NMR tube at 100 °C, allowing collection of consecutive ^{1}H NMR spectra every 5 min for the 1st hour, and every 15 min over the following 20 h.[**] The signal at δ 3.27–3.13 ppm, assigned as NCH_cHCH$_2$, was used for integral normalisation, as not involved in the reaction. Deuterium incorporation (%) at the different time points (t) was extrapolated from the relative integral values for signals at δ 3.70–3.62 ppm (NC$H_{(cis)}$HCHCO), δ 2.05–1.93 ppm (NCH$_2$C$H_{(cis)}$H) and δ 1.81–1.70 ppm (NCH$_2$CH$H_{(trans)}$).

[**] NMR experiment performed by Peter Haycock (Imperial College London). Raw kinetic data can be found in Appendix II.



Scheme 5.4 a) Pd-catalysed C–H deuteration of *N*-Cbz pyrrolidine **9** followed over time. b) Stacked ^{1}H NMR spectra collected at different time points (400 MHz, toluene-d_8, 100 °C, 6 scans, d_1 = 1 s). c) Magnified region at δ 4.1–1.4 ppm. Integral values for the spectrum collected at t = 5 min are shown.

Under these conditions, a similar rate of deuteration was observed at *cis*- and *trans*-C(4) positions (Figure 5.1, blue and orange profiles respectively). The data obtained during the 1st hour were used to estimate the initial k_{obs} for both positions, and *cis*-C(4) deuteration was found to be 1.7 times quicker than *trans*-C(4). On the other hand, the low deuterium incorporation at *cis*-C(2) resulted in noisier data, particularly in the initial stages of the reaction, and the corresponding k_{obs} was not determined. Nonetheless, this appeared to be much slower than for both C(4) positions, and resulted in lower overall D incorporation at the end of the reaction (grey profile).

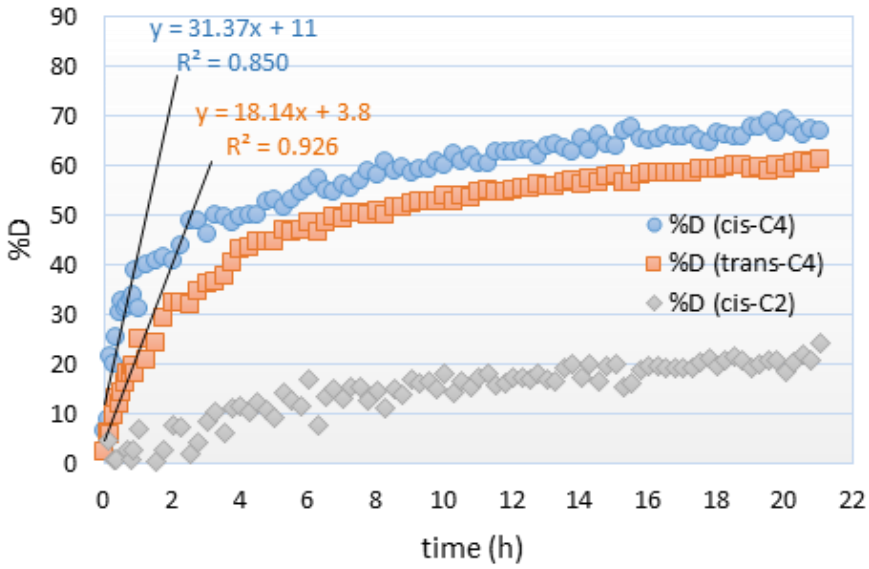
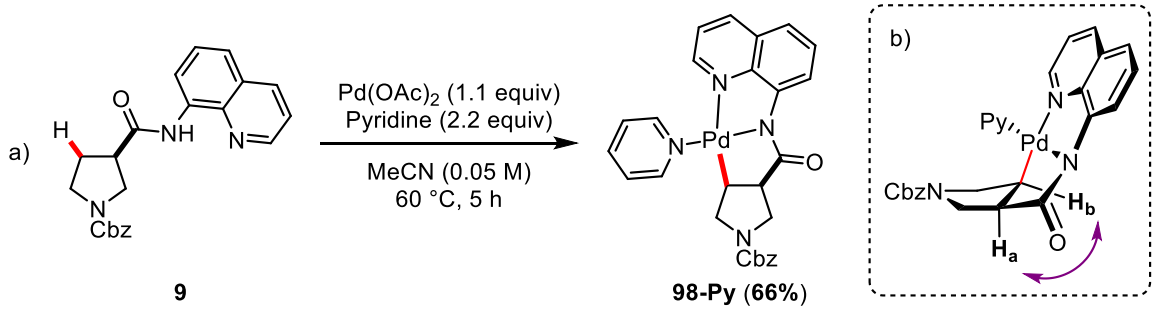


Figure 5.1 Pd-catalysed C–H deuteration (%) of pyrrolidine 3-carboxamide **9** as a function of time.

5.2.2 Synthesis and Reactivity of 5,5-*cis*-Palladacycle Complexes

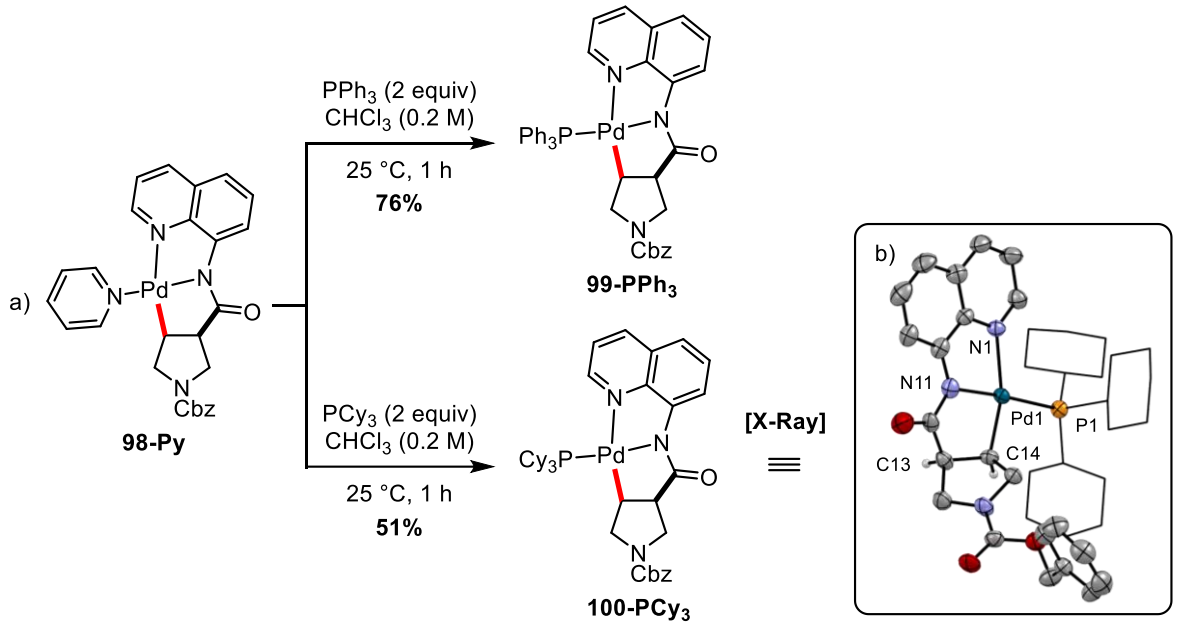
Following these deuteration studies, the isolation of relevant palladacycle intermediates, formed by C–H activation, was investigated. Initial attempts involving the stoichiometric reaction of *N*-Cbz pyrrolidine **9** with $Pd(OAc)_2$ in MeCN were unsuccessful, likely due to the resulting organopalladium derivative being less stable than the starting materials. Pleasingly, the addition of 2.2 equivalents of pyridine as a stabilising ligand,[139b,166] enabled the isolation of monomeric Pd(II)-complex **98-Py** in 66% yield as a single *cis*-C(4)-diastereomer (Scheme 5.5a).



Scheme 5.5 a) Synthesis of 5,5-*cis*-palladacycle complex **98-Py**. b) Diagnostic NOE correlations for stereochemical assignment (500 MHz, toluene-d_8, 25 °C).

Palladacycle **98-Py** could be isolated by silica column chromatography and was found to be stable at rt under air for > 7 days. The relative *cis*-configuration of the pyrrolidine ring was initially assigned based on 2D NOESY experiments in toluene-d_8 at 25 °C.[255] In particular, a strong NOE correlation was found between CH_aCO (δ 3.47 ppm) and CH_bPd (δ 2.02 ppm), consistent with a *cis*-configuration of the ring (Scheme 5.5b).

Initial attempts to confirm this stereochemical assignment by X-ray crystallography were unsuccessful due to the low crystallinity of complex **98-Py**. Therefore, ligand exchange with either PPh_3 or PCy_3 was evaluated to increase packing interactions and crystallinity. This afforded phosphine-complexes **99-PPh$_3$** and **100-PCy$_3$** in 76% and 51% yield respectively (Scheme 5.6a). Pleasingly, an X-ray structure could be obtained for **100-PCy$_3$**, confirming the *cis*-configuration of this derivative (Scheme 5.6b).[††] Interestingly, an envelope conformation was observed for the pyrrolidine ring, with the DG and the Pd-atom occupying pseudo-axial and pseudo-equatorial positions respectively. Furthermore, a slightly distorted square planar geometry was observed for the Pd(II) centre ($C_{14}PdN_{11}$ bond angle = 81.6°), confirming the bidentate binding mode of the AQ auxiliary.

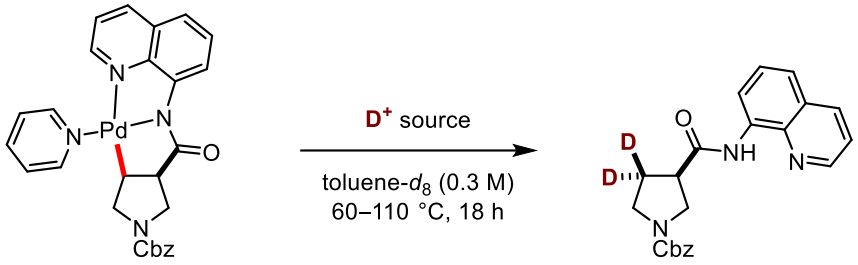


Scheme 5.6 a) Synthesis of 5,5-*cis*-palladacycles **99-PPh$_3$** and **100-PCy$_3$** by ligand exchange. b) ORTEP-diagram of palladacycle **100-PCy$_3$** (ellipsoids drawn at 50% probability level). Hydrogens are omitted for clarity, except for those at the bridgehead pyrrolidine carbons (C13 and C14).

With *cis*-palladacycle **98-Py** in hand, its reactivity was evaluated in deuteration experiments, with particular attention paid to the stereochemical outcome. Unfortunately, treating **98-Py** with DCl (35% wt. in D_2O) at rt resulted in complete degradation of the starting material, likely by pyrrolidine ring-opening (not shown). Therefore, the use of milder deuteration conditions was evaluated. However, no reaction was observed heating **98-Py** at reflux in CD_3OD for 18 h (Table 5.1, entry 1). On the other hand, deuteration of both *cis*- and *trans*-C(4) positions was obtained using either AcOD-d_4 or HFIP-d_2 in toluene-d_8 at 110 °C (entries 2 and 3). In the

[††] Performed by Andrew White (Imperial College London). Full details on bond lengths and angles can be found in Appendix III.

former case, this stereochemical outcome could be ascribed to the in-situ formation of $Pd(OAc)_2$, which could promote deuteration at both *cis*- and *trans*-C(4)-positions, as previously observed. In contrast, deuterium incorporation at the *trans*-position in the presence of HFIP-d_2 might derive from direct deuteration occurring with inversion.

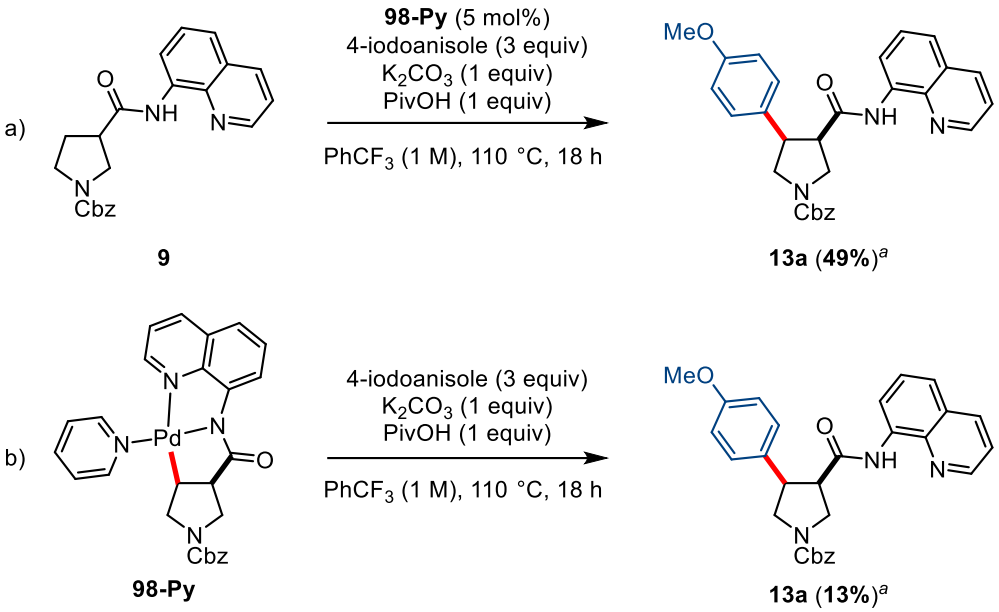


98-Py **9-d_x**

entry	D^+ source (equiv)	T (°C)	9-d_x (%)[a]	% D[b]	
				C4-*cis*	C4-*trans*
1[c]	CD_3OD (0.07 M)	60	-	-	-
2	AcOD-d_4 (2)	110	27	40	25
3	HFIP-d_2 (10)	110	16	54	40

Table 5.1 Stoichiometric deuteration of palladacycle **98-Py**. [a] Isolated yield. [b] % D determined by ^{1}H NMR (400 Hz, d_1 = 70 s) at 100 °C in DMSO-d_6. [c] CD_3OD used as solvent instead of toluene-d_8. Unreacted starting material was recovered (> 95%).

Following this, the reactivity of organopalladium derivative **98-Py** was investigated both in catalytic and stoichiometric arylation experiments. Pleasingly, **98-Py** was found to be a competent catalyst for pyrrolidine C(4)–H arylation, promoting the formation of *cis*-arylated product **13a** in 49% yield (Scheme 5.7a). In addition, palladacycle **98-Py** could react with stoichiometric 4-iodoanisole, affording exclusively *cis*-arylated pyrrolidine **13a** in 13% yield (Scheme 5.7b). No unreacted starting material was observed by crude ^{1}H NMR, suggesting significant substrate decomposition, likely due to the stoichiometric amount of pyridine hampering the arylation in favour of other decomposition pathways.



Scheme 5.7 a) Use of **98-Py** as pre-catalyst in the C–H arylation of pyrrolidine **9**. b) Stoichiometric arylation of palladacycle **98-Py** with 4-iodoanisole. [a] Yield calculated by ^{1}H NMR using 1,3,5-TMB as internal standard.

Overall, these results suggested that closely related Pd(II) species, bearing AcOH or PivOH ligands in place of pyridine, are likely active intermediates in the catalytic C–H arylation and deuteration of pyrrolidine 3-carboxamide.

Following these investigations into the C–H activation step, the turnover-limiting step of pyrrolidine C(4)–H arylation was investigated using various kinetic studies.

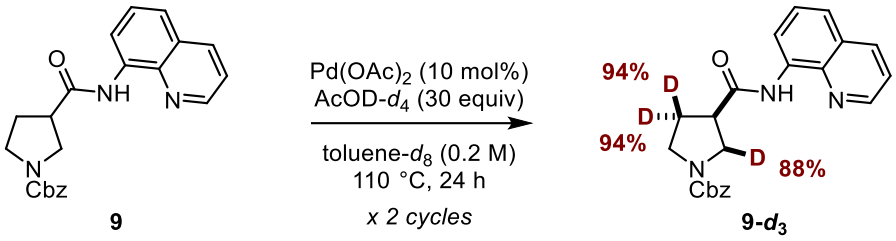
5.3 Kinetic Analysis to Determine the Turnover-Limiting Step

5.3.1 Evaluation of Kinetic Isotope Effect

Being able to deuterate the reactive position on the pyrrolidine substrate, the effect of deuterium substitution on the rate of C–H arylation was investigated to determine the Kinetic Isotope Effect (KIE).

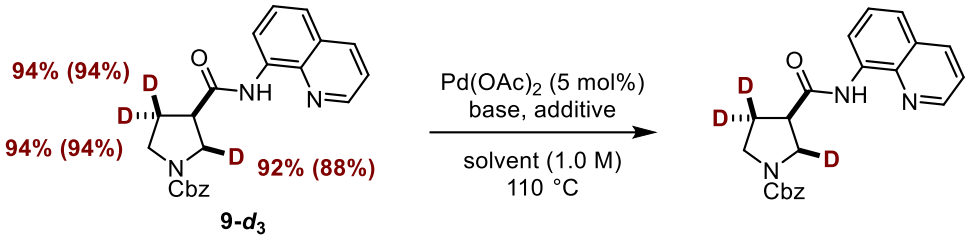
5.3.1.1 Substrate synthesis and preliminary considerations on H/D scrambling

First, full deuteration of the reactive C–H bonds was achieved by subjecting pyrrolidine **9** to 2 consecutive C–H deuteration cycles, leading to derivative **9-*d*$_3$** in 83% yield and ~ 90% D at *cis*-C(2), *cis*-C(4) and *trans*-C(4) (Scheme 5.8). An isotopic profile consistent with *bis*- (18.4%) and *tris*-deuteration (81.6%) was observed for derivative **9-*d*$_3$** by HRMS.



Scheme 5.8 Synthesis of deuterated pyrrolidine **9-*d*$_3$** *via* Pd-catalysed C–H deuteration. Reaction scale: 1.3 mmol. % D determined by quantitative ^{1}H NMR (500 Hz, DMSO-d_6, 100 °C, d_1 = 70 s).

To obtain meaningful data in the KIE experiments, H/D scrambling under the reaction conditions should be minimised. However, erosion of % D was observed when treating deuterated pyrrolidine **9-*d*$_3$** under the standard arylation conditions in the absence of aryl iodide (Table 5.2, entry 1). This is consistent with a reversible C–H activation step and could lead to unpredictable variations in the % D affecting the KIE analysis. Reducing the reaction time to 5 h resulted in slightly higher, but not complete, retention of % D (entry 2). H/D scrambling was also obtained when using PivOK in place of K_2CO_3/PivOH either in $PhCF_3$ or toluene-d_8 (entries 3 and 4). Similarly, treatment of protic pyrrolidine **9** with $Pd(OAc)_2$ and K_2CO_3/AcOD-d_4 in toluene-d_8, did not result in any detectable deuterium incorporation (not shown).

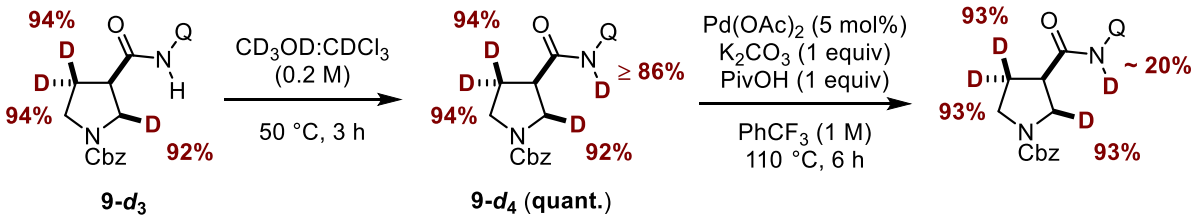


entry	base/additive (equiv)	solvent (conc.)	time (h)	% D[a]		
				***cis*-C(4)[b]**	***trans*-C(4)[b]**	***cis*-C(2)**
1	K_2CO_3 (1) PivOH (1)	$PhCF_3$ (1 M)	18	75 (66)	75 (78)	92 (86)
2	K_2CO_3 (1) PivOH (1)	$PhCF_3$ (1 M)	5	85	85	93
3	PivOK (2)	$PhCF_3$ (1 M)	18	70	70	93
4	PivOK (2)	toluene-d_8 (1 M)	18	68	68	93

Table 5.2 H/D Scrambling experiments on derivative **9-*d*$_3$**. [a] % D determined by ^{1}H NMR at 25 °C in $CDCl_3$ with d_1 = 1 s. When applicable, % D determined by ^{1}H NMR at 100 °C in DMSO-d_6 with d_1 = 70 s is reported in brackets. [b] For measurements in $CDCl_3$, average % D of *cis*- and *trans*-C(4) positions is reported due to overlap of proton signals.

Reasoning that the NH amide might play an important role as proton source, pyrrolidine **9-*d*$_3$** was stirred in CD_3OD:$CDCl_3$ (4:1) at 50 °C to form deuterated derivative **9-*d*$_4$** in quantitative yield and ≥ 86% D at the amide position (Scheme 5.9). The addition of $CDCl_3$ as cosolvent

was necessary due to the poor solubility of the substrate in CD_3OD. Pleasingly, no H/D scrambling was observed upon treatment of **9-*d*$_4$** under the standard arylation conditions in absence of ArI, despite the use of PivOH (Scheme 5.9). Therefore, this derivative was further used in the intermolecular KIE experiments.



Scheme 5.9 Synthesis of deuterated pyrrolidine **9-*d*$_4$** and subsequent H/D scrambling experiment. % D determined by ^{1}H NMR ($CDCl_3$, 25 °C, d_1 = 1 s).

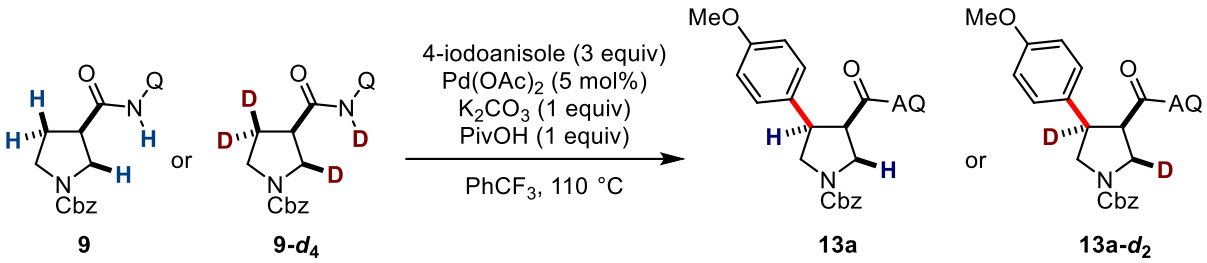
5.3.1.2 Intermolecular KIE determined by parallel experiments

With deuterated pyrrolidine **9-*d*$_4$** in hand, the intermolecular KIE was evaluated by comparing the initial rate of C–H arylation between proteo- and deutero-substrates **9** and **9-*d*$_4$** in independent experiments (Table 5.3 and Figure 5.2). The high concentration and the highly heterogeneous nature of the reaction mixture made it difficult to sample representative aliquots, or to monitor in situ the progress of the reaction. Therefore, discrete reactions (0.1 mmol scale) were stopped and worked-up at different time points over the first 45 min of the reaction, corresponding to 13–15% conversion. More details on the reproducibility of discrete reactions to build a reaction profile will be given in next section.

Reasoning that the change in concentration of the aryl iodide would be small enough not to influence the rate, and that no significant catalyst deactivation would occur in the early stages of the reaction (*vide infra*), overall zero-order kinetics was assumed at early time points. Therefore, the slope of the straight line ($R^2 > 0.99$), obtained plotting the [SM] as a function of time, was used to estimate the kinetic constants k_H and k_D (Figure 5.2).

Finally, the intermolecular KIE was calculated as the ratio between k_H and k_D (Equation 1). A similar rate was observed for both substrates, resulting in a small KIE value of 1.19.

$$\mathbf{KIE} = \frac{k_{\mathrm{H}}}{k_D} = \frac{1.186}{0.993} = 1.19 \qquad (1)$$



entry	SM	P	time (min)	SM (%)[a]	P (%)[a]	tot (%)[a]	[SM] (mM)[b]	[P] (mM)[b]
1			5	96	6	102	422	26
2			10	94	8	102	413	35
3	**9**	**13a**	20	92	10	102	404	44
4			30	89	12	100	390	52
5			45	85	15	100	373	66
6			5	94	4	98	412	18
7			10	93	6	99	408	26
8	**9-*d*$_4$**	**13-*d*$_2$**	20	90	8	98	395	35
9			30	88	10	98	386	44
10			45	85	13	98	373	57

Table 5.3 Raw kinetic data for the determination of intermolecular KIE through individual kinetics. Each entry corresponds to a discrete reaction (0.1 mmol). [a] Calculated by ^{1}H NMR using 1,3,5-TMB as internal standard. [b] A corrected volume of 228 μL, accounting for both the solvent (100 μL) and the volume occupied by the reagents as measured with a volumetric flask, was used to derive concentration values.

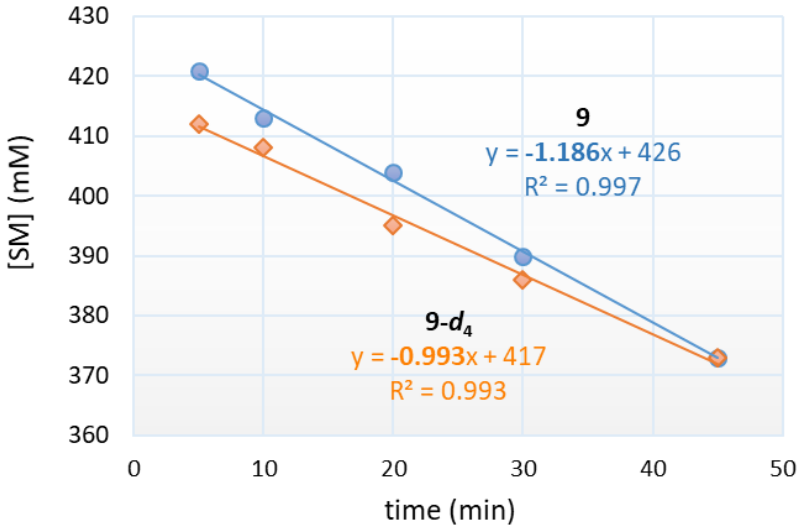
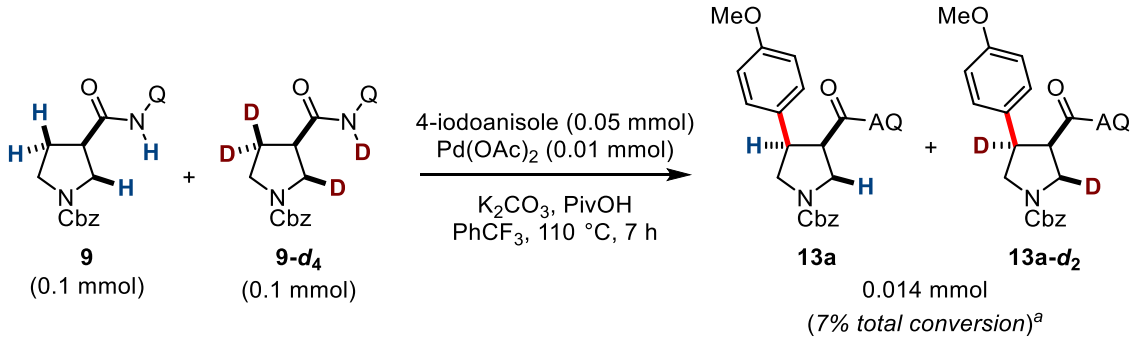


Figure 5.2 Profile of starting material consumption over time (0–45 min) for proteo- and deutero-pyrrolidines **9** and **9-*d*$_4$**. Each time point corresponds to a discrete reaction.

5.3.1.3 Intermolecular KIE determined by one-pot competition

The KIE was also evaluated by one-pot intermolecular competition. In this case, pyrrolidine amides **9** and **9-*d*$_4$** were used in a 1:1 mixture to compete for a limiting amount of ArI. This would allow the KIE to be calculated from the relative amount of product formed by functionalisation of the C(4)–H and C(4)–D bonds.[256] Using 25 mol% of 4-iodoanisole gave arylated pyrrolidines **13a** and **13a-*d*$_2$** in an overall 7% yield after 7 h reaction (Scheme 5.10).



Scheme 5.10 KIE determination by one-pot intermolecular competition. [a] Calculated by ^{1}H NMR using 1,3,5-TMB as internal standard.

Unfortunately, no signal could be used for the direct quantification of products distribution, due to complex overlap of substrate and product signals in the crude ^{1}H NMR. Alternatively, this was extrapolated from the relative amount of unreacted starting materials **9** and **9-*d*$_4$**. In particular, the multiplet centred at δ 2.36 ppm in the ^{1}H NMR spectrum (NCH$_2$C*H*$_2$ protons) was used as diagnostical signal to determine [**9**] and [**9-*d*$_4$**]. On the other hand, the multiplet centred at δ 3.30 ppm (NCHCO proton, not involved in the reaction) was used for integral normalisation (Figure 5.3).

The values for unreacted [**9**] and [**9-*d*$_4$**] at t = 7 h were found resolving Equations 2 and 3:

$$\frac{[\mathbf{9}]}{[\mathbf{9}\text{-}\boldsymbol{d_4}]} = \frac{int_{t=7}}{int_{t=0}} \qquad (2)$$

$$[\mathbf{9}]_0 - [\mathbf{9}] + [\mathbf{9}\text{-}\boldsymbol{d_4}]_0 - [\mathbf{9}\text{-}\boldsymbol{d_4}] = [\mathrm{P}]_{\mathrm{tot}} \qquad (3)$$

From these, it was possible to calculate the KIE as described in Equation 4. This gave the same value of 1.19 previously observed by comparison of individual reaction rates.

$$\mathbf{KIE} = \frac{[\mathrm{P}]_{\mathrm{H}}}{[\mathrm{P}]_{\mathrm{D}}} = \frac{[\mathbf{9}]_0 - [\mathbf{9}]}{[\mathbf{9}\text{-}\boldsymbol{d_4}]_0 - [\mathbf{9}\text{-}\boldsymbol{d_4}]} = 1.19 \qquad (4)$$

The absence of a large primary isotope effect in both KIE experiments indicated that the C–H bond cleavage is not turnover-limiting in the catalytic C(4)–H arylation.[256] Furthermore, the

small value observed can be ascribed to an equilibrium isotope effect, consistent with a reversible C–H activation scenario.[256]

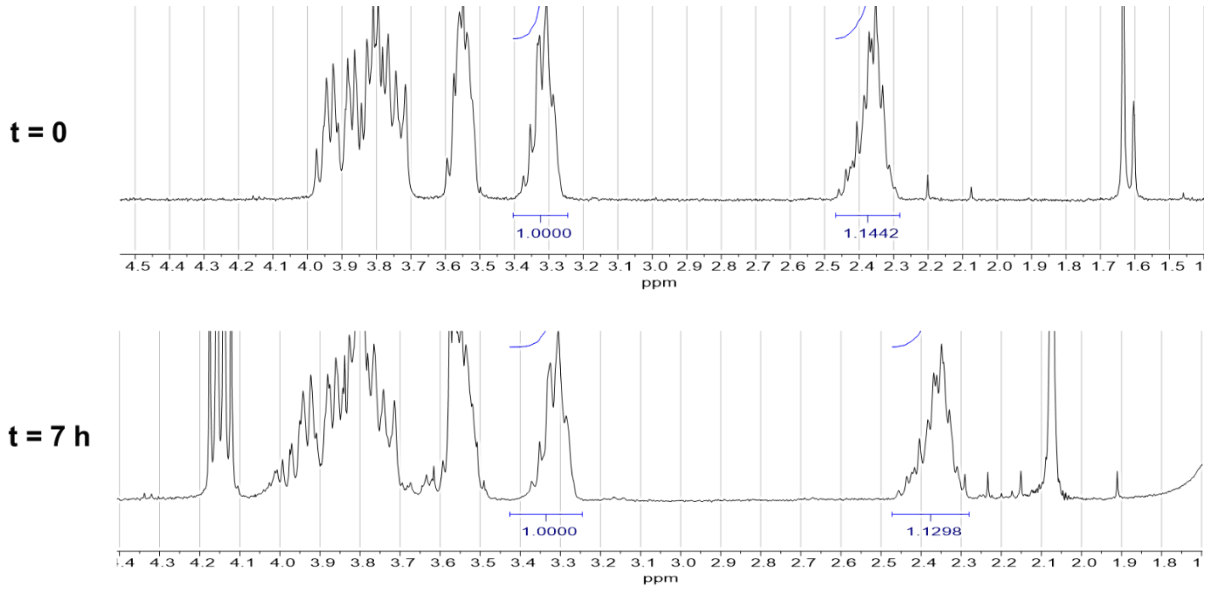


Figure 5.3 Top row: ^{1}H NMR (400 MHz, $CDCl_3$, 25 °C, d_1 = 1 s, magnified region at δ 4.5–1.4 ppm) of a 1:1 mixture of **9** and **9-*d*$_4$** at t =0. Bottom row: ^{1}H NMR (400 MHz, $CDCl_3$, 25 °C, d_1 = 1 s, magnified region at 4.4–1.7 ppm) of the crude reaction mixture (t = 7 h).

5.3.2 Kinetic Order in Reaction Components

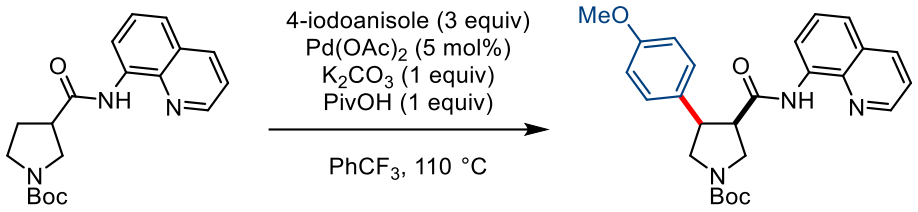
5.3.2.1 Variable Time Normalisation Analysis

In order to improve the understanding of the reaction, the use of Variable Time Normalisation Analysis (VTNA), developed by Burés in 2016,[257,258] was envisaged to determine the order in palladium catalyst and other reaction components. This strategy is based on the visual comparison of concentration profiles run at different initial loadings of a specific reagent or catalyst, after mathematic normalisation of the time scale. In comparison with more traditional kinetic analysis, VTNA offers the attractive advantage to use concentration data with no need to extrapolate rate values.[257] Furthermore, this can enable efficient determination of kinetic orders even when fewer and/or noisier data points are used, as it is based on intuitive visual comparison of reaction profiles.[257]

Before applying this kinetic analysis to the Pd-catalysed C(4)–H arylation, a standard reaction profile was constructed, and its reproducibility was evaluated.

5.3.2.2 Standard reaction profile and considerations on the reproducibility of kinetic data

The progress of the arylation of *N*-Boc pyrrolidine **2** with 4-iodoanisole was followed over time by quenching independent reactions, each run under standard conditions, at different time points (Table 5.4 and Figure 5.4a).



2 **3a**

entry	time (h)	2 (%)[a]	3a (%)[a]	tot (%)[a]	[SM] (M)[b]	[P] (M)[b]
1	0.08	95	7	102	0.418	0.031
2	0.25	92	12	104	0.404	0.053
3	0.5	86	19	105	0.378	0.084
4	1	75	26	101	0.330	0.114
5	1.5	69	32	101	0.303	0.141
6	2	58	38	96	0.255	0.167
7	3	48	47	95	0.211	0.207
8	4	44	52	96	0.193	0.229
9	5	44	53	97	0.193	0.233
10	6	42	56	98	0.185	0.246
11	18	27	62	89	0.118	0.272

Table 5.4 Raw kinetic data for the C(4)–H arylation of pyrrolidine **2** over time. Each entry corresponds to a discrete reaction (0.2 mmol, 440 mM). [a] Calculated by ^{1}H NMR using 1,3,5-TMB as internal standard. [b] A corrected volume of 455 μL, accounting for both the solvent (200 μL) and the volume occupied by the reagents, was used to derive concentration values.

The reaction was found to be relatively quick at early stages, with approx. 20% yield of product **3a** being formed after just 30 min. However, the conversion rate progressively decreased reaching a plateau at 6 h and 50–55% yield (Figure 5.4a). After this point, only a marginal increase in the yield of pyrrolidine **3a** was observed (62% after 18 h), despite the presence of a significant amount of unreacted starting material. This was suggestive of either product inhibition or catalyst deactivation pathways, as will be discussed in more detail in section 5.5. For the purposes of determining the kinetic order in different reagents, the profiles analysed here will therefore focus on the first 6 hours of the reaction.

Small variations from this profile were observed when using different batches of pyrrolidine **2**, likely due to a variable amount of impurities undetectable by ^{1}H NMR. On the other hand, when the same batch of amide **2** was used, excellent reproducibility of the kinetic data was achieved. In particular, this was demonstrated by repeating various data points in the early stages of the reaction, when the largest variations were expected (Figure 5.4.b). This resulted in a low standard deviation (≤ 0.006 M) for each data point. In order to ensure high reliability of the data, the same batch of starting material was therefore used for each comparison of reaction profiles presented herein.

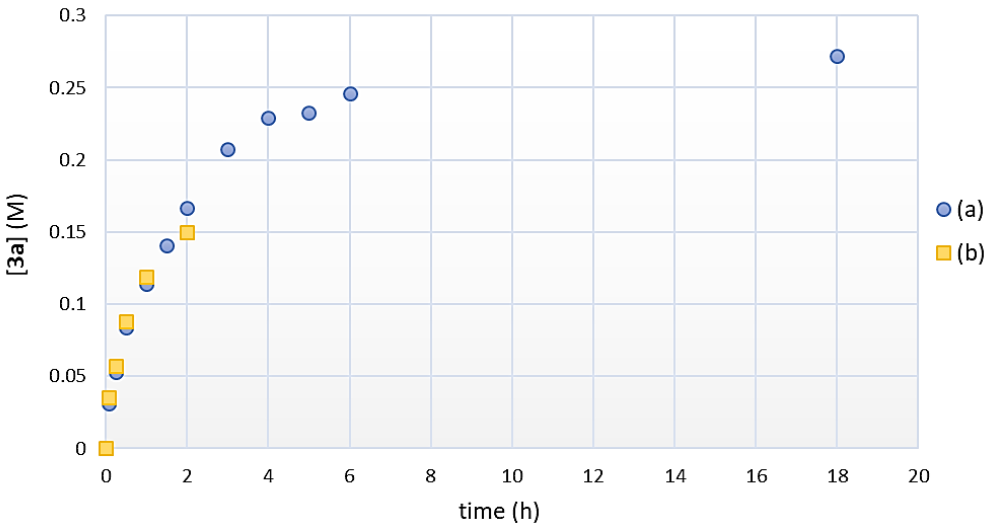


Figure 5.4 a) Formation of arylated pyrrolidine **3a** as a function of time. b) Data points repeated using the same batch of pyrrolidine amide **2**. Each time point corresponds to a discrete reaction.

Finally, the effect of different stirring rates on the reproducibility of the reaction was evaluated. This did not affect significantly the reaction outcome, suggesting mass-transfer was not a limiting factor for this heterogenous transformation (for more details see Appendix IV). Therefore, 1000 rpm was maintained as constant stirring rate throughout the investigations described below.

5.3.2.2 Order in $Pd(OAc)_2$

With these considerations in mind, the order in $Pd(OAc)_2$ was evaluated using Burés' VTNA analysis. The formation of arylated pyrrolidine **3a** was evaluated over time using different initial loadings of $Pd(OAc)_2$, namely 3.5, 5.0, 7.5 and 10 mol%, while the concentration of all other components was kept constant (Figure 5.5a). The use of lower catalyst loading (2.5 mol%) was excluded from this comparison as it resulted in higher variation of the kinetic data, likely due to more significant catalyst deactivation.[259]

As described by Burès, the different profiles can be visually compared after normalisation of the time scale to $\Delta t \cdot [cat]_0^n$ (on the abscissa axis).[257b] The arbitrary power *n* can be adjusted until all concentration profiles overlay, at which point the value of *n* will correspond to the kinetic order in catalyst.[257b] This normalisation method is based on the assumption that the catalyst concentration remains constant during the reaction.[257b]

Although catalyst deactivation was suspected to affect the Pd-catalysed C(4)–H arylation, this is less likely at the start of the reaction, where it would be possible to assume a constant catalyst concentration. Therefore, early time points (0–45 min) were considered to determine the order in $Pd(OAc)_2$, and a faster reaction was observed when using higher catalyst loadings (Figure 5.5a).

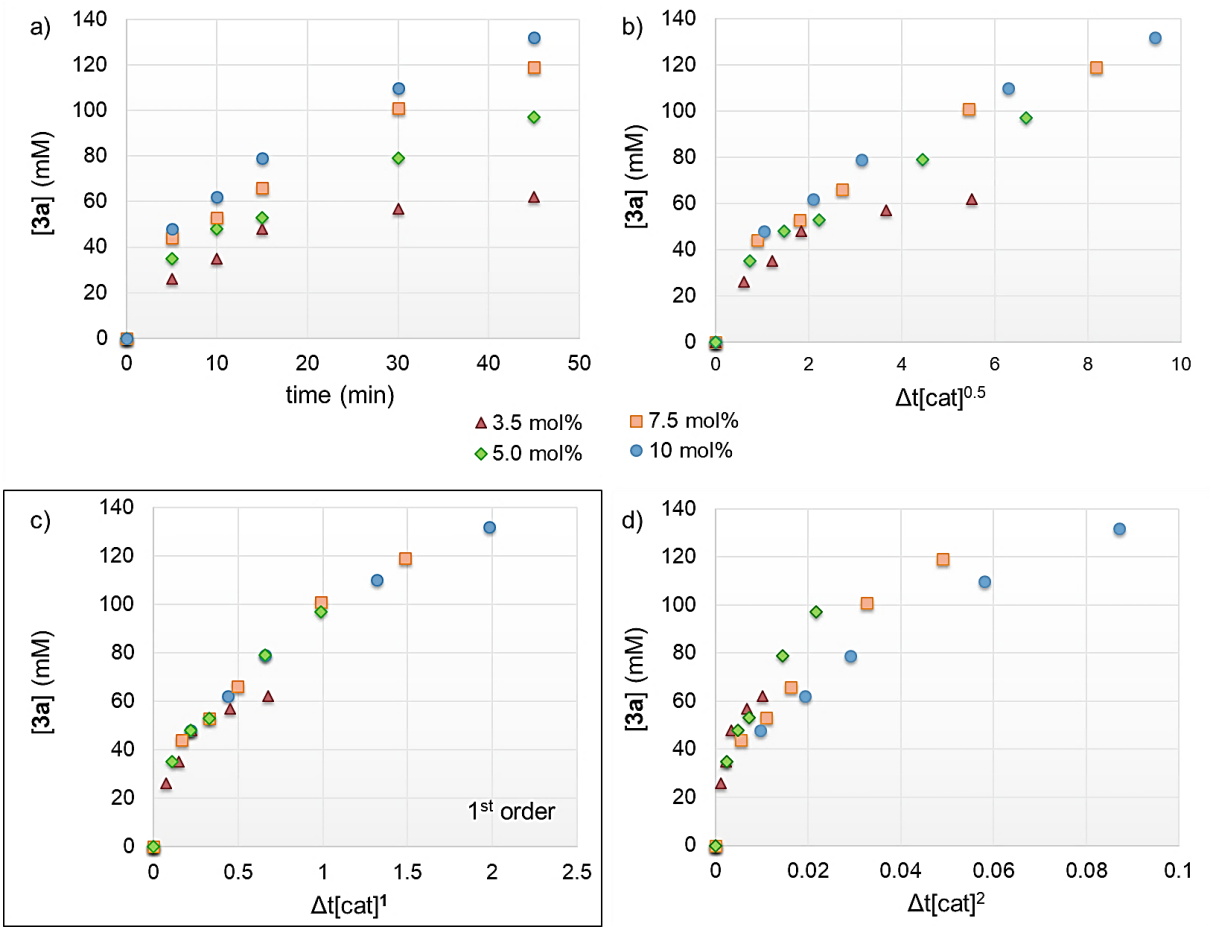


Figure 5.5 Use of VTNA to determine the kinetic order in $Pd(OAc)_2$. Each profile corresponds to different initial catalyst loadings in the reaction of pyrrolidine **2** with 4-iodoanisole. Each data point corresponds to a discrete reaction. The profile obtained under standard arylation conditions is represented by green diamonds. Reaction conditions: **2** (0.2 mmol), ArI (0.6 mmol), $Pd(OAc)_2$ (7–20 μmol), K_2CO_3 (0.2 mmol), PivOH (0.2 mmol), $PhCF_3$ (200 μL), 110 °C.

The different reaction profiles were compared after time scale normalisation for n = 0.5, 1 and 2 (Figure 5.5b–d). The best overlap was observed for a power n = 1, suggesting a first order dependence in $Pd(OAc)_2$. This is consistent with a mononuclear Pd species being involved in the turnover-limiting step, supporting the absence of kinetically-relevant bimetallic Pd(III) complexes.[254c]

5.3.2.3 Order in aryl iodide

A similar strategy was used to determine the order in the aryl iodide coupling partner. Four concentration profiles for product formation were obtained using 2.25, 3.00, 3.75 and 4.50 equivalents of 4-iodoanisole, and considering the first 6 h of reaction (Figure 5.6a).

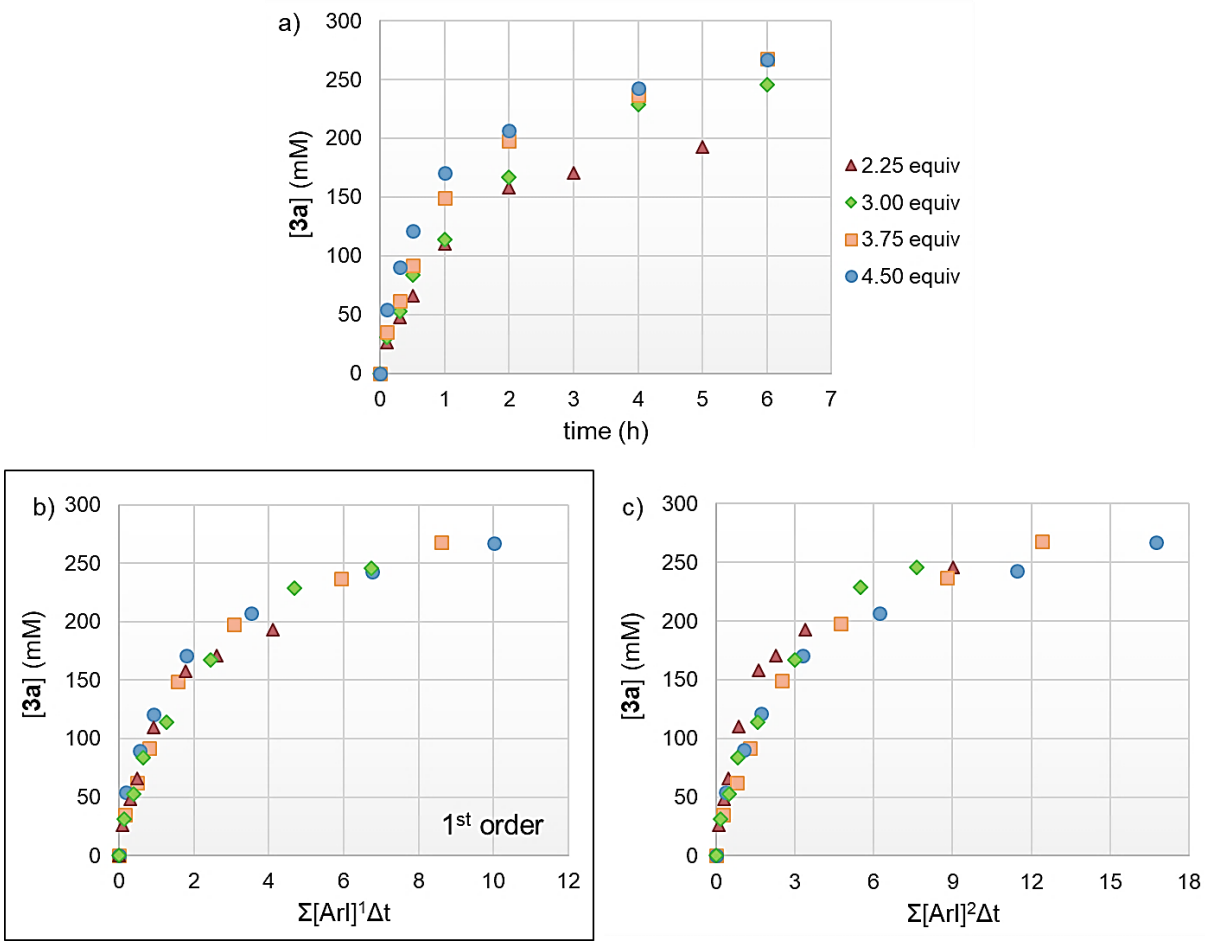


Figure 5.6 Use of VTNA to determine the kinetic order in aryl iodide. Each profile corresponds to different initial concentrations of 4-iodoanisole in the reaction of pyrrolidine **2**. Each data point corresponds to a discrete reaction. The profile obtained under standard arylation conditions is represented by green diamonds. Reaction conditions: **2** (0.2 mmol), ArI (0.45–0.9 mmol), $Pd(OAc)_2$ (10 μmol), K_2CO_3 (0.2 mmol), PivOH (0.2 mmol), $PhCF_3$ (200 μL), 110 °C.

The aryl iodide was found to be a kinetically relevant species, as no overlap between the profiles was observed before time scale adjustment. Instead, faster formation of product **3a** was observed when increasing the iodide loading.

To account for the variation in iodide concentration during the reaction, a different mathematical normalisation of the time scale developed by Burès was applied (Equation 5).[257a]

$$\sum_{i=0}^{n} \left(\frac{[\mathrm{ArI}]_i + [\mathrm{ArI}]_{i-1}}{2} \right)^{\alpha} (t_i - t_{i-1}) \qquad (5)$$

Using this formula, the different reaction profiles were visually compared for α = 1 and 2, with the former resulting in an optimal fitting of all profiles (Figure 5.6b,c). This indicates a first order kinetic in the aryl iodide, suggesting that either oxidative addition (OA) or reductive elimination (RE) is the turnover-limiting step of the reaction.

5.3.2.4 Order in Pyrrolidine Substrate and K_2CO_3/PivOH

Following this, the order in pyrrolidine **2** was investigated (Figure 5.7). In this case, two profiles were compared using a different initial loading of *N*-Boc pyrrolidine amide **2**: 0.20 mmol and 0.15 mmol. Despite the different initial substrate loading, the same rate of product formation (**3a**) was observed up to approximately 4 h (Figure 5.7a). From this point forward the profiles started to diverge, likely due to the lower concentration of substrate available for the reaction to proceed in one of the 2 cases (orange profile).

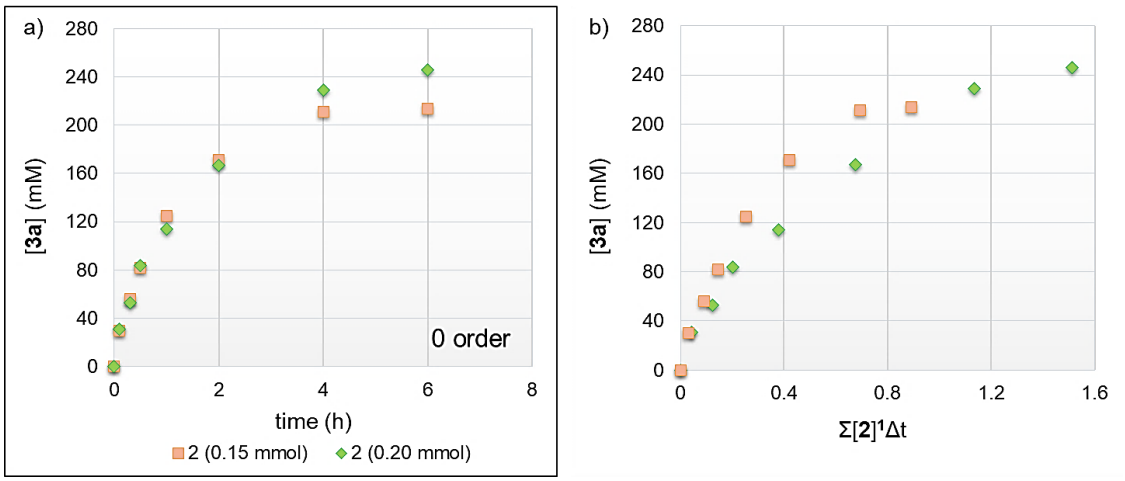


Figure 5.7 Use of VTNA to determine the kinetic order in pyrrolidine amide **2**. Each profile corresponds to a different initial loading of pyrrolidine **2** in the reaction with 4-iodoanisole. Each data point corresponds to a discrete reaction. The profile obtained under standard arylation conditions is represented by green diamonds. Reaction conditions: **2** (0.15–0.2 mmol), ArI (0.6 mmol), $Pd(OAc)_2$ (10 μmol), K_2CO_3 (0.2 mmol), PivOH (0.2 mmol), $PhCF_3$ (200 μL), 110 °C.

On the other hand, this initial overlap was lost when normalising the time scale for the concentration of **2** and changing the arbitrary power to $\alpha = 1$, (Figure 5.7b). This outcome indicates a zero-order dependence in pyrrolidine **2**, likely the result of catalyst saturation under the synthetically relevant conditions.

Finally, given the important role played by the combination of K_2CO_3 and PivOH in providing higher reaction yields, the kinetic influence of these reaction components was investigated. In particular, the rate of formation of arylated pyrrolidine **3a** was evaluated using either 1.0 or 0.5 equivalents of both K_2CO_3 and PivOH (Figure 5.8). By comparison of these concentration profiles, without time scale normalisation, the same reaction rate was observed up to approximately 2 h. After this point the reaction with half the amount of base and acid (orange profile) started to plateau. Thus, it can be concluded that neither K_2CO_3 nor PivOH are involved in the turnover-limiting step, but they are required for the reaction to proceed.

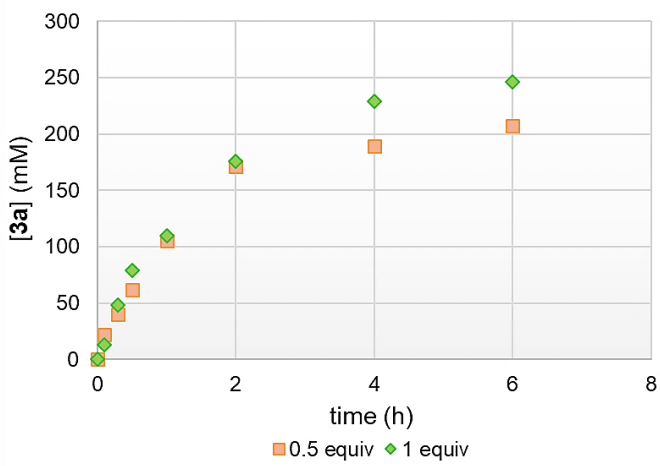


Figure 5.8 Study on the kinetic effect of K_2CO_3 and PivOH. Each profile corresponds to different initial loadings of K_2CO_3 and PivOH in the reaction of pyrrolidine **2** with 4-iodoanisole. Each data point corresponds to a discrete reaction. The profile obtained under standard arylation conditions is represented by green diamonds. Reaction conditions: **2** (0.2 mmol), ArI (0.6 mmol), $Pd(OAc)_2$ (10 μmol), K_2CO_3 (0.1–0.2 mmol), PivOH (0.1–0.2 mmol), $PhCF_3$ (200 μL), 110 °C.

In summary, a first order dependency in palladium catalyst and aryl iodide was determined using a VTNA approach, as the only kinetically relevant species in the reaction. This resulted in the empirical power law depicted in Equation 6:

$$\boldsymbol{rate} = k[\text{cat.}][\text{ArI}] = k'[\text{ArI}] \ (\text{if } [\text{cat.}] = \text{const.}) \qquad (6)$$

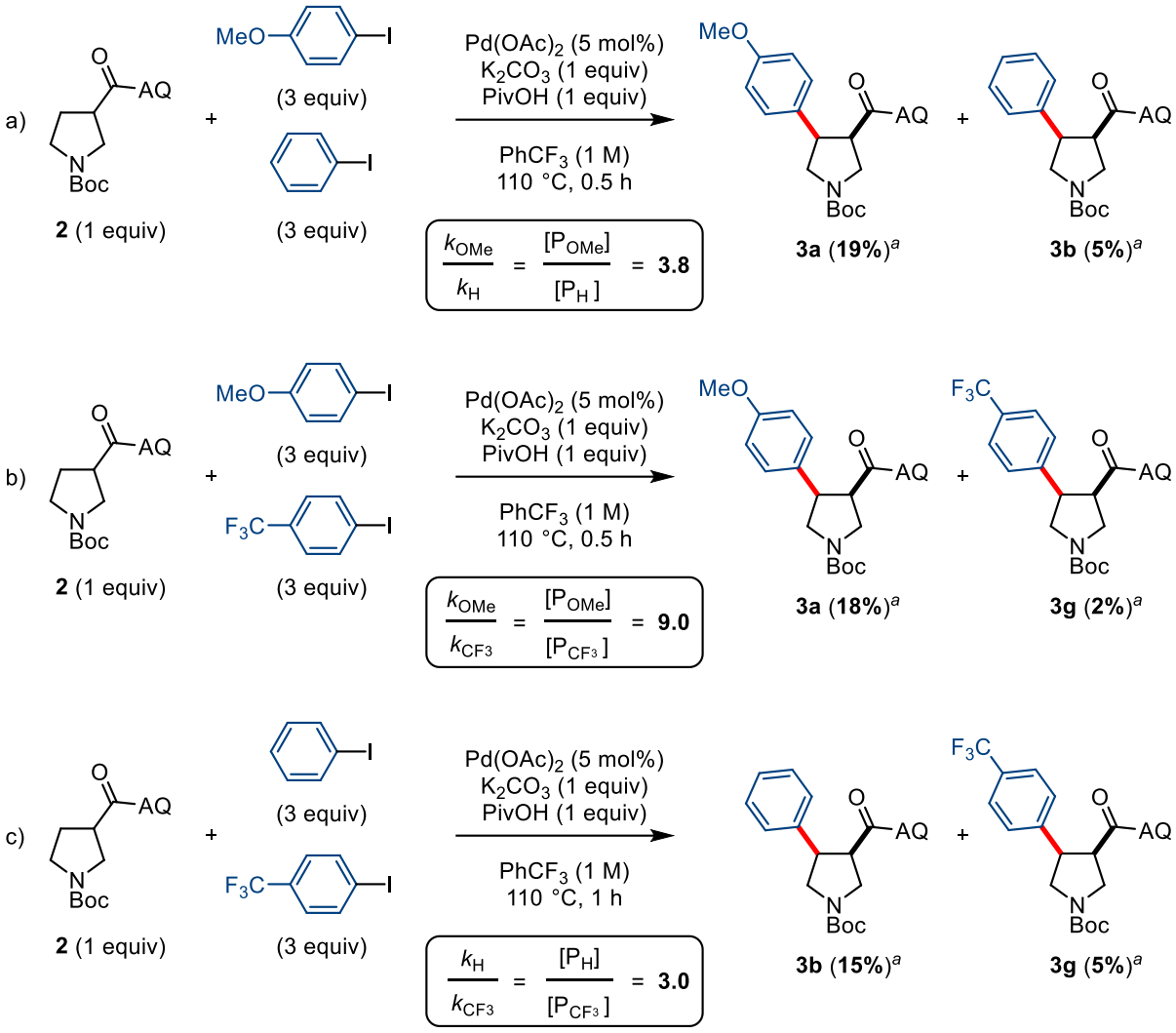
Such kinetic scenario would be consistent with a turnover-liming OA or RE step, following an initial low-barrier cyclometallation.

In order to discriminate between OA and RE as the turnover-limiting step, the electronic effect of different *para*-substituted aryl iodides on the reaction rate was evaluated.

5.3.3 Electronic Effect of the Aryl Iodides on the Reaction Rate

5.3.3.1 Competition experiments

First, competition experiments were performed, in which two different aryl iodides had to compete for a limiting amount of pyrrolidine **2**. In particular, the kinetic preference between 4-iodoanisole, iodobenzene and 4-iodobenzotrifluoride was evaluated (Scheme 5.11). The reactions were stopped after 0.5–1 h, corresponding to approx. 20% conversion, and the kinetic effect of the substituents was estimated from the relative amount of product formed. Consistent with the higher yield observed in the presence of electron-donating substituents (see section 3.3.2), higher reactivity was observed for more electron-rich iodides, with 4-iodoanisole reacting 4 and 9 times faster than iodobenzene and 4-iodobenzotrifluoride, respectively (Scheme 5.11a,b).



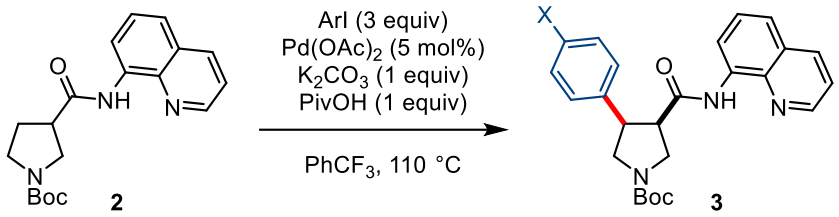
Scheme 5.11 Competition experiments with different *para*-substituted aryl iodides. [a] Calculated by ^{1}H NMR using 1,3,5-TMB as internal standard.

A faster reaction was also observed for iodobenzene in the competition with 4-iodobenzotrifluoride, likely due to its higher electron density (Scheme 5.11c).

To further confirm this trend, the individual kinetic profiles for the reaction with various *para*-substituted aryl iodides were evaluated.

5.3.3.2 Hammett plot from individual kinetics

Similarly to the KIE experiment, discrete reactions on 0.1 mmol scale were stopped at different time points in order to evaluate the initial rate of arylation with different iodides. Assuming zero-order kinetics at early time points, the first 20–60 min of reaction were considered, corresponding in all cases to 10–15% conversion (Table 5.5 and Figure 5.9). Six *para*-substituted aryl iodides were evaluated under otherwise identical conditions, and the corresponding kinetic constants k_X were estimated from the slope of the straight lines ($R^2 \geq 0.97$) obtained plotting the [**2**] (mM) as a function of time (min) (Figure 5.9).



entry	X	time (min)	2 (%)[a]	3 (%)[a]	tot (%)[a]	[2] (mM)[b]	[3] (mM)[b]
1	OMe (**3a**)	5	92	6	98	404	26
2		10	89	9	98	390	40
3		15	86	12	98	377	53
4		20	84	14	98	368	61
5	Me (**3c**)	5	92	6	98	404	26
6		10	90	7	97	395	31
7		15	88	8	96	386	35
8		20	86	9	95	377	40
9		30	84	11	95	368	48
10	H (**3b**)	5	96	3	99	421	13
11		10	95	5	100	417	22
12		20	93	6	99	408	26
13		30	91	7	98	399	31
14		45	87	10	97	382	44
15	Cl (**3e**)	6	93	5	98	408	22
16		10	91	5	96	399	22
17		21	88	8	96	386	35
18		30	85	10	95	373	44
19		45	82	12	94	360	53
20	CO_2Et (**3h**)	5	93	7	100	408	31
21		15	88	8	96	395	35
22		30	87	11	98	0.382	48
23		45	85	13	98	0.373	57
25	CF_3 (**3g**)	5	97	2	99	425	9
26		15	95	3	98	417	13
27		30	93	5	98	408	22
28		45	90	6	96	395	26
29		60	89	7	96	390	31

Table 5.5 Raw kinetic data for the C(4)–H arylation of pyrrolidine **2** with different aryl iodides. Each entry corresponds to a discrete reaction (0.1 mmol). [a] Calculated by ^{1}H NMR using 1,3,5-TMB as internal standard. [b] A corrected volume of 228 μL, accounting for both solvent (100 μL) and the volume occupied by the reagents, was used to derive concentration values.

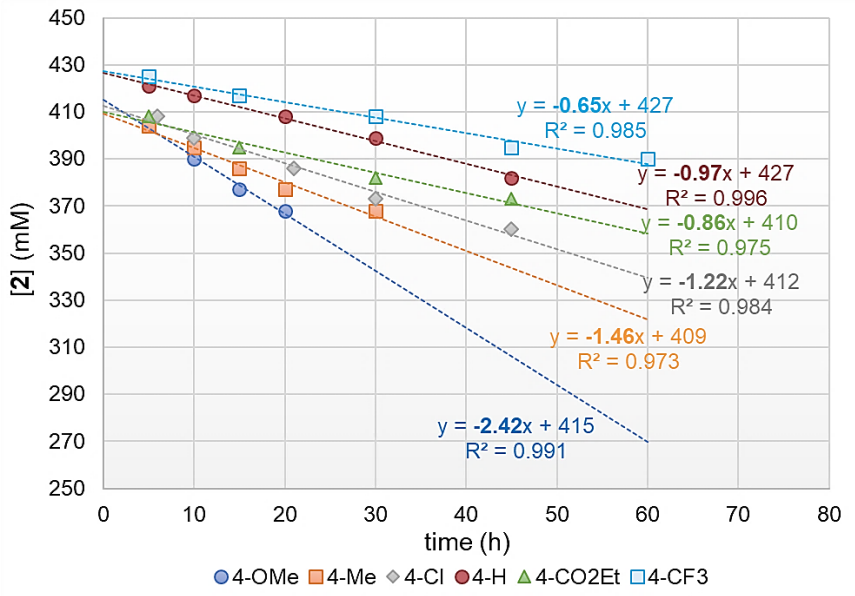


Figure 5.9 Individual initial rates of C–H arylation of pyrrolidine **2** (substrate consumption over time) with different *para*-substituted aryl iodides. Each time point corresponds to a discrete reaction.

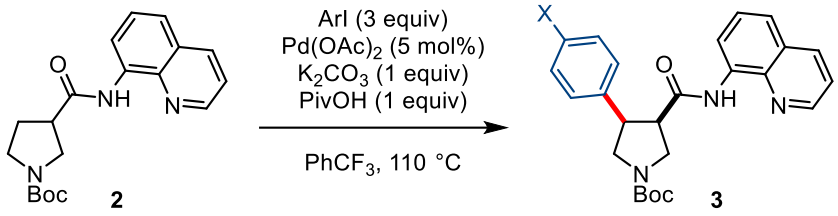
A faster reaction rate was again observed for more electron-rich aryl iodides, with 4-iodoanisole (dark blue profile) found to be the most reactive coupling partner. Interestingly, the use of 4-chloro-iodobenzene resulted in a faster reaction compared to the unsubstituted system (grey and red profiles, respectively), likely due to the π-donating effect of the chlorine substituent. This suggests an impact of mesomeric effects on the initial reaction rate.

This kinetic data was then used to quantify the correlation between the observed initial rates (k_{obs}) and the electronic effect of different groups, expressed by the substituent constants σ, through the Hammett equation (Equation 7).[260,261]

$$\textbf{Hammett Equation:}\quad \log\frac{k_X}{k_H} = \rho\sigma \qquad (7)$$

Substituent constants σ_p, experimentally derived from the effect of *para*-substituents on the ionisation equilibrium of benzoic acid,[260,261] were first used to construct an Hammett plot for the Pd-catalysed C(4)–H arylation of pyrrolidine **2** (Table 5.6 and Figure 5.10a). Despite a modest correlation (R^2 = 0.757), a negative linear dependence was observed, accounting for a faster reaction with more electron-rich iodides. On the other hand, when electrophilic substituent constants σ_p+ were used, a better correlation for the linear regression was obtained (R^2 = 0.927, Figure 5.10b). Electrophilic σ_p+ values are based on the rate of S_N1 reaction of *t*-cumyl chlorides with water.[261,262] As such, these can offer better correlations when the substituents are in conjugation with the reaction centre, providing mesomeric stabilisation of a (partial) positive charge. In the specific case of pyrrolidine **2**, the negative slope of the Hammett plot (ρ = – 0.35) suggested the formation of a partial positive charge in the turnover-limiting

transition state, which can be stabilised by EDG substituents in direct conjugation. In turn, this is consistent with the reductive elimination (RE) being the turnover-limiting step.



entry	X	σ_p^{261}	σ_p+^{261}	k_{obs} (mM/min)	log(k_X/k_H)
1	OMe (**3a**)	– 0.27	– 0.78	– 2.42	+ 0.380
2	Me (**3c**)	– 0.17	– 0.31	– 1.46	+ 0.146
3	H (**3b**)	0.00	0.00	– 0.97	0.000
4	Cl (**3e**)	+ 0.23	+ 0.11	– 1.22	+ 0.079
5	CO_2Et (**3h**)	+ 0.45	+ 0.48	– 0.86	– 0.046
6	CF_3 (**3g**)	+ 0.54	+ 0.61	– 0.65	– 0.155

Table 5.6 Evaluation of the aryl iodide electronic effects on reaction rate.

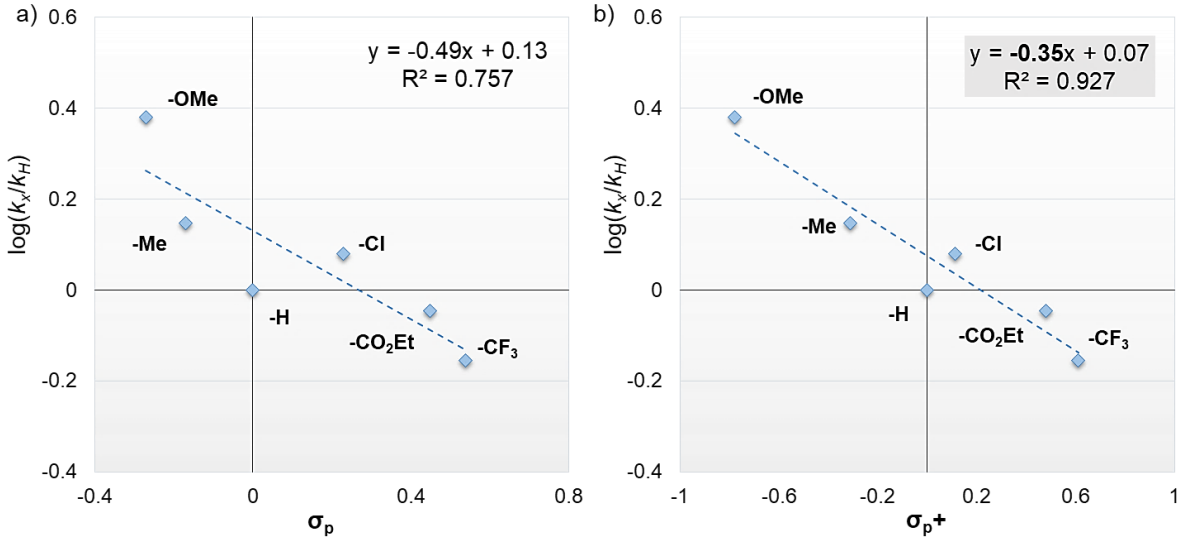


Figure 5.10 Evaluation of the aryl iodide electronic effects on reaction rate: Hammett plot of log(k_X/k_H) as a function of a) σ_p and b) σ_p+.

5.4 Computational Modelling of Reaction Mechanism

At this stage in the investigation, the reaction mechanism was modelled through density-functional theory (DFT) calculations. This computational study was carried out by Luis Casarrubios (Universidad Complutense de Madrid), and an analysis of the results obtained is presented here.

For this study, a simpler model was chosen to represent the experimental system, involving the use of $Pd(OAc)_2$ as catalyst, without considering the potential for *in-situ* formation of $Pd(OPiv)_2$ in the presence of K_2CO_3 and PivOH. Toluene was used as model solvent instead of $PhCF_3$, and the temperature was fixed at 25 °C. Finally, methyl carbamate was selected as representative *N*-protecting group. This was shown to give comparable results to *N*-Boc and *N*-Cbz groups without affecting the regio- and stereochemical outcomes in both arylation and deuteration experiments (see sections 3.3.1 and 5.2.1). Furthermore, several possible conformations of the pyrrolidine and piperidine rings were evaluated in the optimisation of reaction intermediates and transition states, and all free energy values (ΔG) reported herein refer to the most stable conformation found in each case.

Initial catalyst coordination to the AQ auxiliary in pyrrolidine amide **10** resulted in the formation of Pd complex **I-1**, 11.6 kcal·mol^{-1} downhill compared to the mixture of **10** and $Pd(OAc)_2$ (Figure 5.11). This was taken as the starting point to investigate the C–H activation mechanism, and all ΔG values in the following section will be given with reference to this intermediate.

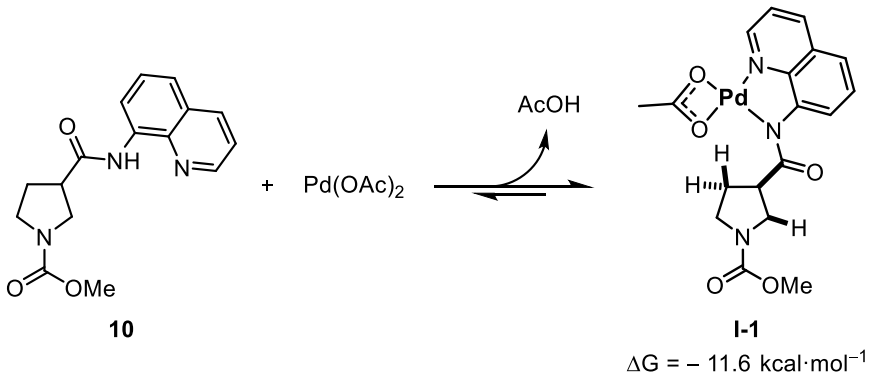


Figure 5.11 Exothermic formation of intermediate **I-1** from a mixture of pyrrolidine **10** and $Pd(OAc)_2$. Calculated at DFT/m062x/Def2svpp.[263]

5.4.1 DFT Study on the C–H Activation Step

First, the feasibility of an inner-sphere CDM mechanism[111] was evaluated on Pd-intermediate **I-1**, in order to gain insight into the stereoselectivity observed at C(4) (Figure 5.12). Consistent with the stereochemical outcome of deuteration, a viable C–H activation event was found at both *cis*- and *trans*-C(4)–H positions, with very similar energetic barriers for the corresponding transition states **TS-1/2*cis*** and **TS-1/2*trans*** (24.3 and 24.0 kcal·mol^{-1} respectively). In these 6-membered transition states, the acetate ligand was found to play an essential role in abstracting either the *cis*- or *trans*-C(4)–H proton with simultaneous formation of the C–Pd bond.[111] The Pd centre was found to interact with both the carbon and hydrogen atoms, indicating an agostic interaction that weakens the C–H bond and allows cyclometallation to occur. Only one ring conformation with the DG in a pseudo-equatorial orientation was

compatible with a *trans*-C–H activation (**TS-1/2**$_{trans}$, Figure 5.13a). On the other hand, both axial and equatorial orientations of the DG were possible for *cis*-C(4)–H activation. However, the lowest energy pathway was found to involve the AQ auxiliary in a pseudo-axial orientation (**TS-1/2**$_{cis}$, Figure 5.13b).

Activation of the C–H bond afforded the corresponding *cis*- and *trans*-5,5-palladacycle intermediates **I-2**$_{cis}$ and **I-2**$_{trans}$ (Figure 5.14). Both calculated palladacycles exhibited a pseudo-equatorial orientation of the DG and a slightly distorted square-planar geometry at the Pd centre. The different conformation of **I-2**$_{cis}$ in comparison with *cis*-palladacycle **100-PCy$_3$**, where the DG occupied a pseudo-axial position (see section 5.2.2), could be ascribed to the formation of a weak H-bond interaction between the AcOH ligand and the pyrrolidine nitrogen in **I-2**$_{cis}$ (Figure 5.14b). Nonetheless, the distortion from the square-planar geometry observed in **100-PCy$_3$** was very similar to the one calculated for **I-2**$_{cis}$ (C_4PdN bond angle equal to 83.3° in **I-2**$_{cis}$ and 81.6° in **100-PCy$_3$**).

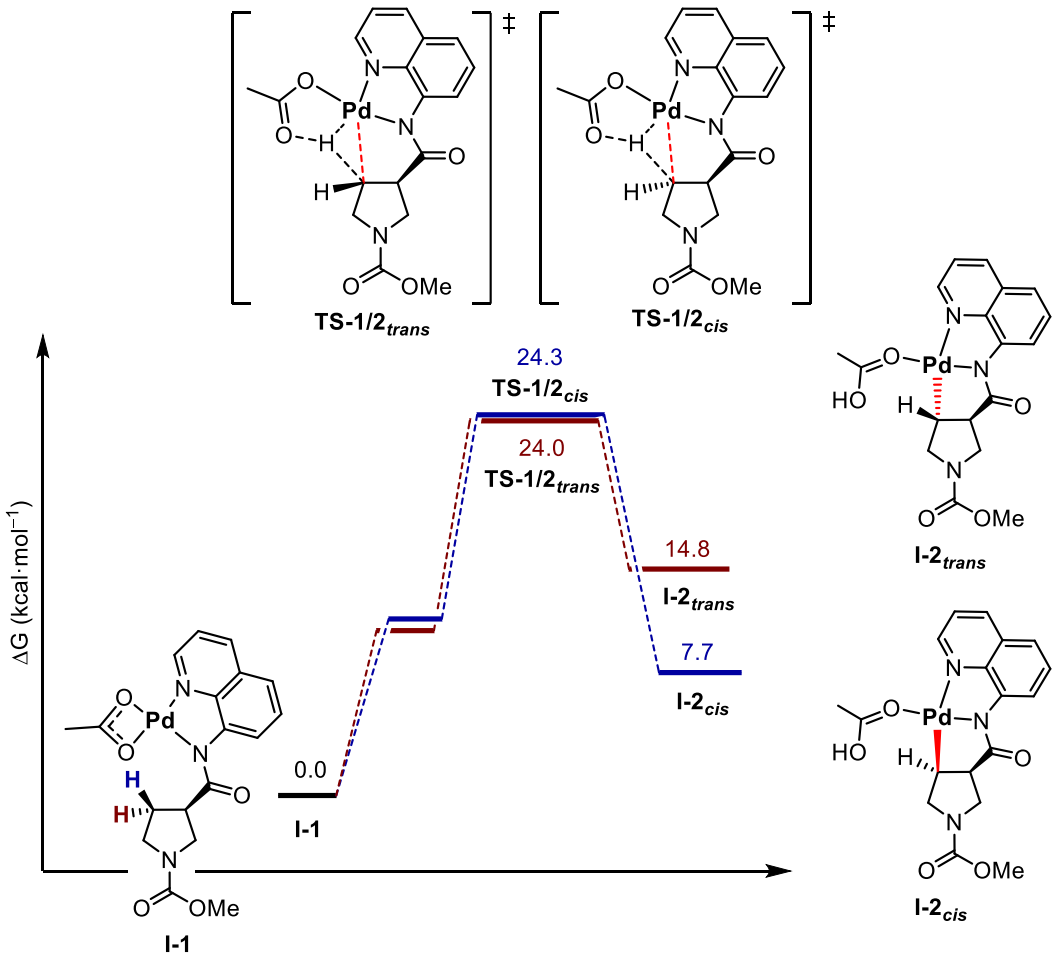


Figure 5.12 Computational modelling of inner-sphere CMD at *cis*- and *trans*-C(4) positions of pyrrolidine **I-1**. Calculated at DFT/m062x/Def2svpp.[263]

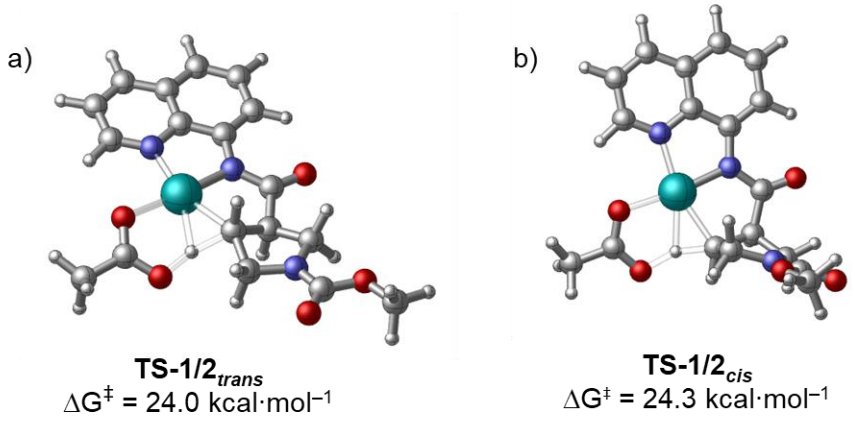


Figure 5.13 Calculated transition states for *cis*- and *trans*-C(4)–H activation, **TS-1/2*trans*** and **TS-1/2*cis***. Images rendered with CYLview v1.0 Beta.

Both cyclopalladated derivatives **I-2*cis*** and **I-2*trans*** were found to be significantly less stable than intermediate **I-1**, supporting a reversible character of the C–H activation step biased towards the starting material. This would explain the difficulty to isolate any palladacycle intermediate in absence of a stabilising ligand. Furthermore, the thermodynamic preference for intermediate **I-2*cis*** (7.1 kcal·mol^{-1} more stable than **I-2*trans***) is consistent with the exclusive formation of *cis*-palladacycle **98-Py** in stoichiometric experiments (see section 5.2.2).

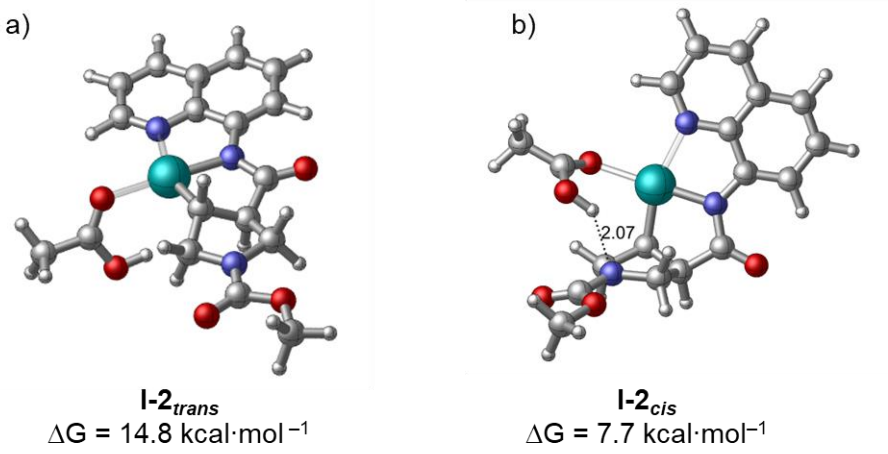


Figure 5.14 Calculated structures for palladacycle intermediates **I-2*cis*** and **I-2*trans***. Images rendered with CYLview v1.0 Beta.

Next, the possibility for an inner-sphere CMD event at *cis*-C(2) was investigated. Unfortunately, no conclusive energetic discrimination between the transition states relative to *cis*-C(4)–H (**TS-1/2*cis***) and *cis*-C(2)–H bond cleavage (**TS-1/3*cis***) could be observed. Only a small energy difference ($\Delta\Delta G^{‡}$ = 0.8 kcal·mol^{-1}) was obtained in favour of the *cis*-C(4) pathway when performing the calculations at the m062x/Def2tzvpp level of theory (Figure 5.15). This difference was lower than the standard error of the method (~ 1 kcal·mol^{-1}) and no significant

discrimination could thus be inferred. Interestingly, C(2)-palladacycle **I-3**$_{cis}$ was 2.1 kcal·mol^{-1} downhill compared to **I-1**. This was likely due to the stabilising effect of an intramolecular hydrogen-bond between the pendant AcOH ligand and the *N*-protecting group (atomic distance = 1.49 Å). Despite the calculated thermodynamic stability of this derivative, formation of a similar H-bond would likely be disrupted in a strong coordinating solvent such as MeCN and would not be preserved using a pyridine ligand. In turn, this could account for the C(4)-regioselectivity observed in the stoichiometric palladacycle formation (see section 5.2.2). On the other hand, the formation of stable **I-3**$_{cis}$ would result in a higher kinetic barrier for a reverse CMD process at C(2), which could contribute to the slower rate of deuteration at this position in toluene-d_8. However, no evidence for the formation of such derivative was observed by ^{1}H NMR during the catalytic C–H deuteration of pyrrolidine **9** (see section 5.2.1).

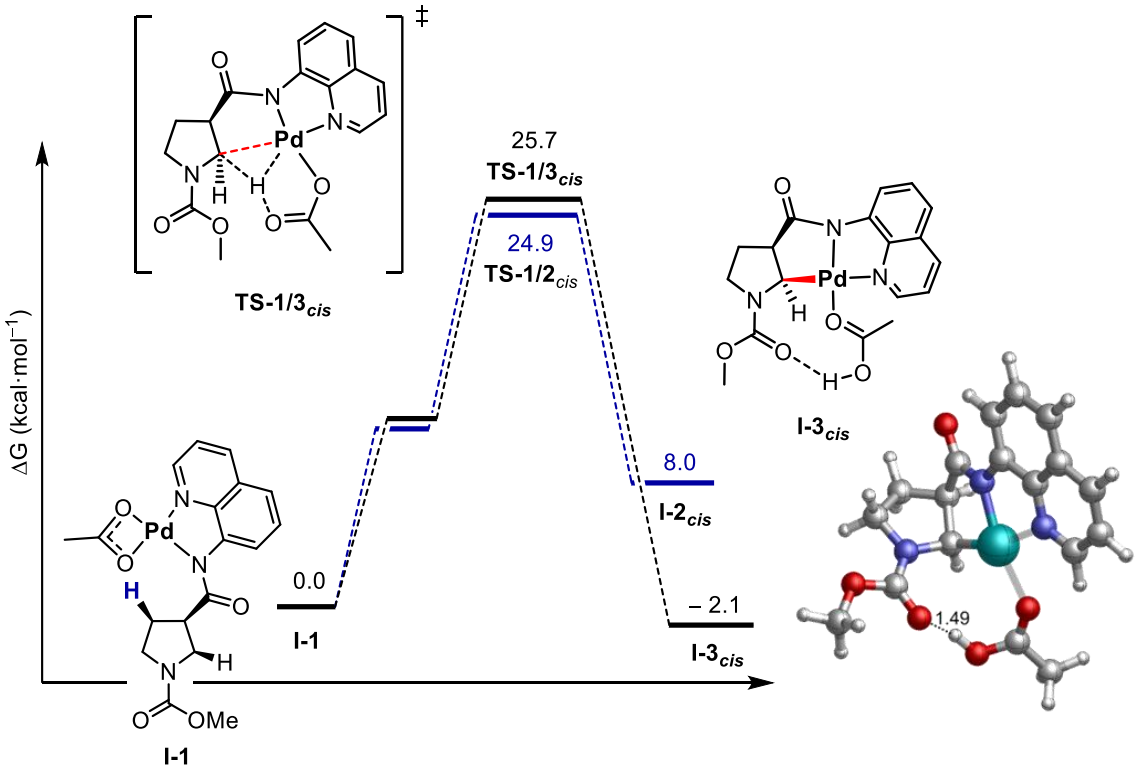


Figure 5.15 Computational modelling of inner-sphere CMD at *cis*-C(4)- and *cis*-C(2)-positions. Calculated at DFT/m062x/Def2tzvpp.[263] Structure of **I-3**$_{cis}$ rendered with CYLview v1.0 Beta.

Although an alternative outer-sphere CMD pathway[112] was also found to be viable at the different C–H bonds (not shown), this did not provide any additional insight into the regio- and stereoselectivity of C–H activation.

5.4.2 Stereodetermining Oxidative Addition

Following this investigation into the C–H activation step, iodobenzene was selected as model aryl iodide to investigate the subsequent OA and RE processes. As the aryl iodide could

undergo OA and RE with the iodine atom either on the same or opposite side relative to the pyrrolidine ring, all possible combinations of these 2 orientations and ring conformations were calculated. Expecting the energetic barriers for ligand exchange and isomerisation processes to be negligible in comparison with those for OA or RE steps, all ΔG values reported below refer to the lowest energy found in each case.

Oxidative addition to iodobenzene was first investigated with C(4)-palladacycles **I-2**$_{cis}$ and **I-2**$_{trans}$ (Figures 5.16 and 5.17). Initial exchange of the AcOH ligand for the PhI coupling partner, coordinated through the iodine atom, allowed oxidative addition to occur through transition states **TS-2/4**$_{cis}$ and **TS-2/4**$_{trans}$. These featured a distorted square pyramidal geometry at the Pd centre, and led to the formation of penta-coordinated Pd(IV) intermediates **I-4**$_{cis}$ and **I-4**$_{trans}$. Subsequent AcOH reassociation could occur to stabilise the Pd(IV) complexes in an octahedral geometry, forming intermediates **I-5**$_{cis}$ and **I-5**$_{trans}$.

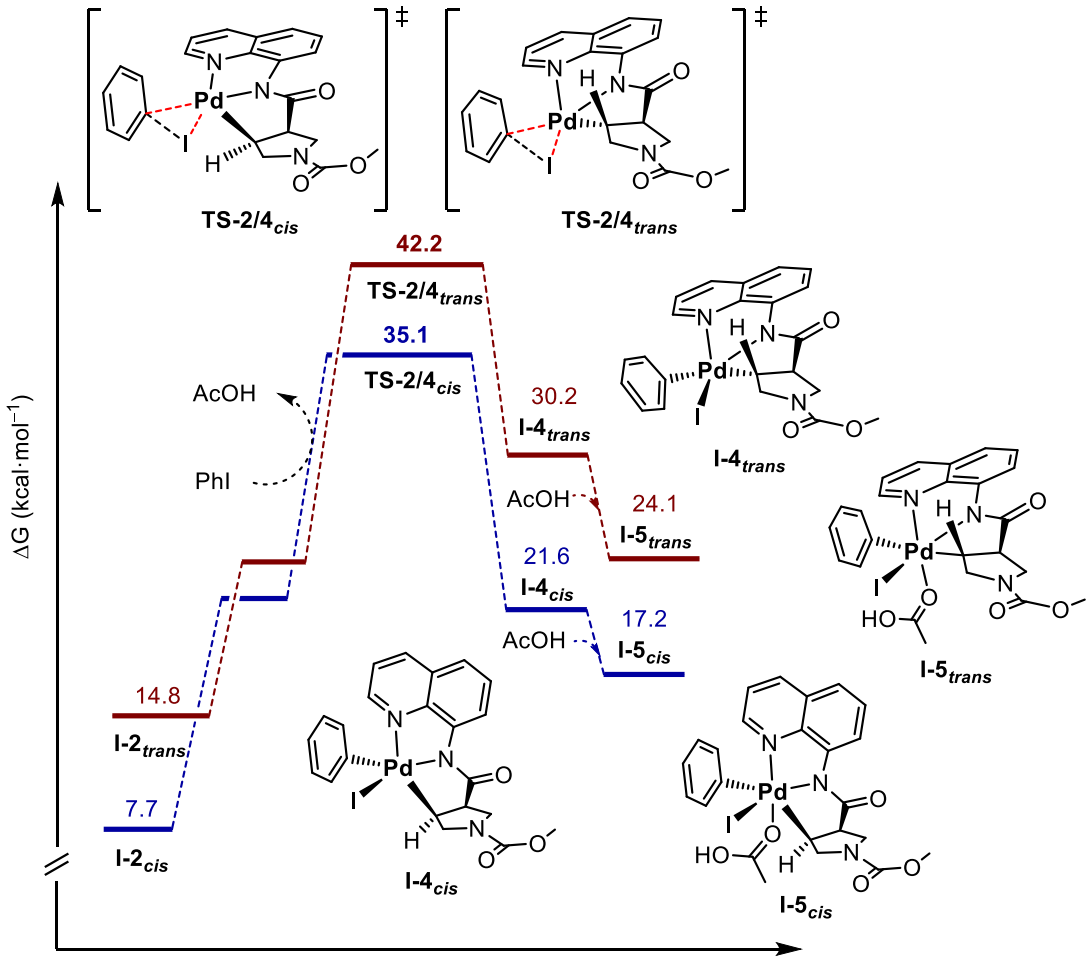


Figure 5.16 Computational modelling of oxidative addition of iodobenzene to palladacycles **I-2**$_{cis}$ and **I-2**$_{trans}$. Calculated at DFT/m062x/Def2svpp.[263]

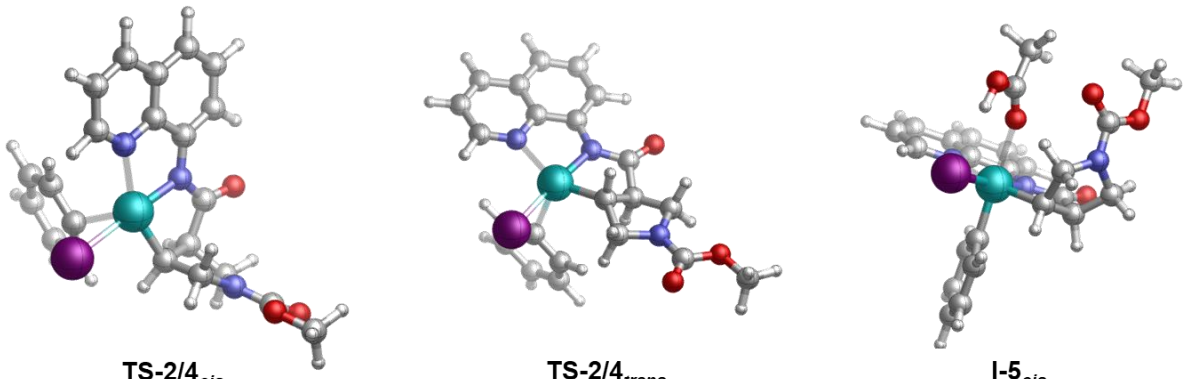


Figure 5.17 Structures of OA transition states **TS-2/4*cis*** and **TS-2/4*trans***, as well as of octahedral Pd(IV) intermediate **I-5*cis***. Images rendered with CYLview v1.0 Beta.

Importantly, a significant energetic difference of 7.1 kcal·mol^{-1} was observed between **TS-2/4*cis*** and **TS-2/4*trans***, in favour of the *cis*-pathway. The same ΔΔG value was found between *cis*- and *trans*-palladacycles **I-2*cis*** and **I-2*trans***, suggesting that this difference derives from the higher strain associated with the *trans*-geometry. This result strongly suggested the OA to be the stereodetermining step in the C(4)–H arylation of pyrrolidine-3-carboxamides, allowing the exclusive formation of *cis*-arylated products. Therefore, the computation data given below for the following RE step will focus exclusively on the *cis* pathway.

Dissociation of AcOH from intermediate **I-5*cis*** allowed RE to occur through unsaturated square-pyramidal transition state **TS-5/6*cis*** (Figure 5.18). This formed the new C–C bond and led to intermediate **I-6*cis***, which could in turn afford the *cis*-arylated pyrrolidine product upon halide abstraction and protodemetalation. The RE for the *cis*-pathway was associated to an energetic barrier of ΔG‡ = 35.3 kcal·mol^{-1}, very similar to the activation energy found for the corresponding OA step (ΔG‡ = 35.1 kcal·mol^{-1}, Figure 5.16). Nonetheless, recalculating the OA (**TS-2/4*cis***) and RE transition states (**TS-5/6*cis***) at m062x/Def2tzvpp resulted in a better discrimination. In particular, a higher energetic barrier was observed for the RE (ΔG‡ = 33.8 kcal·mol^{-1}) *vs* the OA steps (ΔG‡ = 32.3 kcal·mol^{-1}), thus supporting the kinetic evidence for a turnover-limiting RE (not shown).

At this point, oxidative addition and reductive elimination were also evaluated at *cis*-C(2), in an attempt to rationalise the C(4)-regioselectivity observed in arylation experiments. Unfortunately, a similar energetic barrier (ΔΔG‡ = 0.9 kcal·mol^{-1}) was found for OA processes at *cis*-C(2) and *cis*-C(4), while a favourable RE step was observed at C(2) (not shown). As no conclusive information could be obtained computationally, this was not further investigated (for full reaction profile see Appendix V).

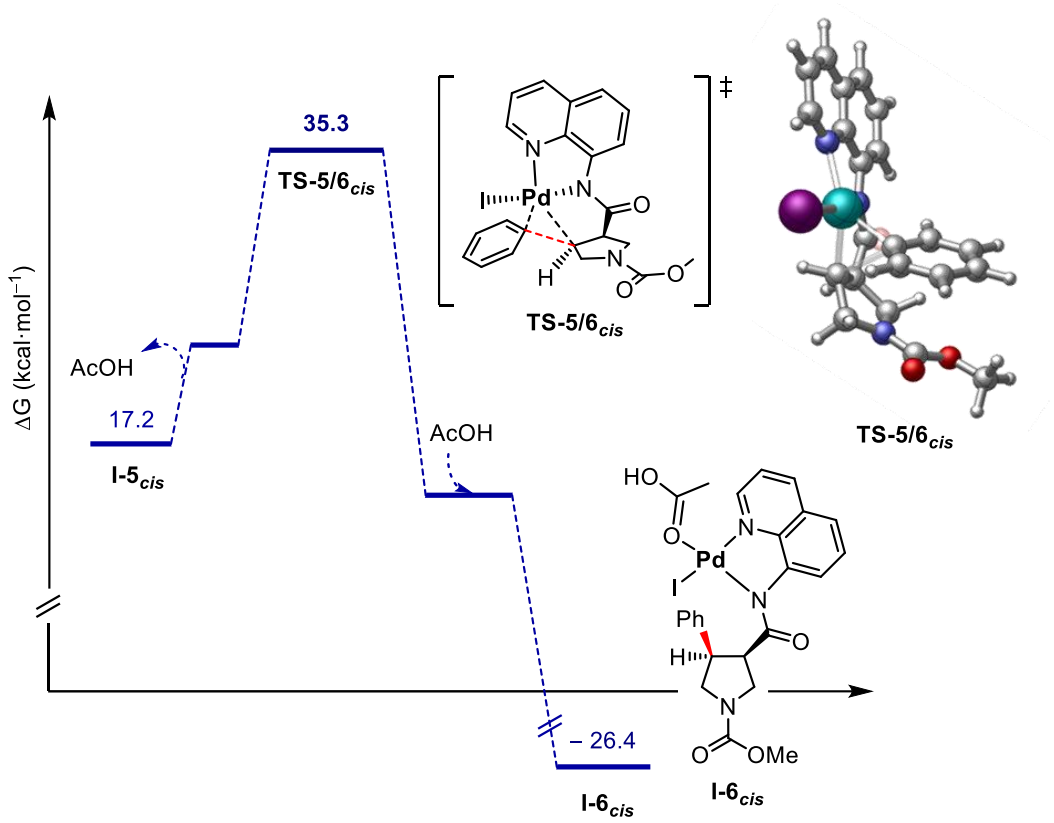


Figure 5.18 Computational modelling of reductive elimination *cis*-to the AQ auxiliary. Calculated at DFT/m062x/Def2svpp.[263] Structure of **TS-5/6*cis*** rendered with CYLview v1.0 Beta.

On the other hand, the DFT calculations discussed in this section have been successful in providing important computational support for the stereoselectivity observed in the arylation of pyrrolidine-3-carboxamides, suggesting a stereodetermining OA step. Furthermore, the calculations were in agreement with the kinetic studies, supporting turnover-limiting RE step.

Finally, in order to compare the arylation mechanism between different ring sizes, the C–H arylation of the corresponding piperidine system was evaluated.

5.4.3 The Case of Piperidine-3-Carboxamide

Similarly to the 5-membered ring, a methyl carbamate *N*-protecting group was used to model the reaction mechanism for piperidine-3-AQ amides, starting from chelated Pd-intermediate **I-7**. In this case, an inner sphere CMD process was again found to be equally feasible at both *cis*- and *trans*-C(4) positions (Figure 5.19). However, the resulting *cis*- and *trans*-palladacycle intermediates **I-8*cis*** and **I-8*trans*** were found to be much more similar in energy ($\Delta\Delta G$ = 0.7 kcal·mol^{-1}) than for the pyrrolidine system. Subsequent oxidative addition occurred preferentially on *cis*-palladacycle **I-8*cis***, with the transition state for the *trans*-pathway (**TS-8/9*trans***) being 2.8 kcal·mol^{-1} higher in energy than the corresponding *cis*-one (**TS-8/9*cis***). On the other hand, an easier RE step was observed for a *trans*-geometry ($\Delta\Delta G^{‡}$ = 2.9 kcal·mol^{-1}).

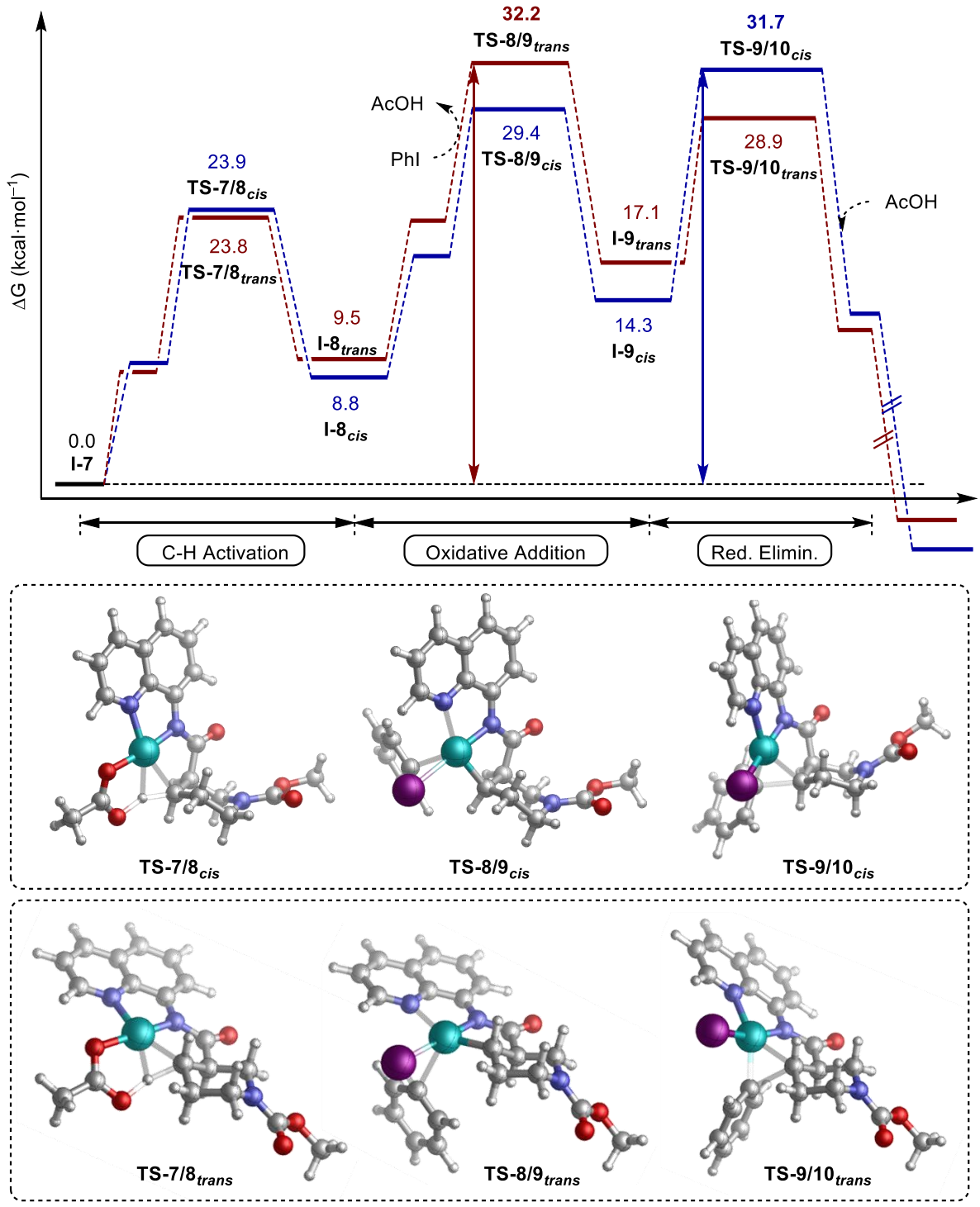


Figure 5.19 Computational modelling of C(4)–H arylation on piperidine-3-AQ amide. Calculated at DFT/B3LYP/6-31G**/Pd,I LANL2DZ.[263] Transition state structures rendered with CYLview v1.0 Beta.

This indicated a different turnover-limiting step for piperidine C–H arylation, that is dependent on the geometry of the system. The highest energetic barrier for the formation of *trans*-arylated products was observed for the OA step ($\Delta G^{\ddagger}$ = 32.2 kcal·mol^{-1}), while the formation of *cis*-derivatives was limited by the RE process ($\Delta G^{\ddagger}$ = 31.7 kcal·mol^{-1}). Overall, a very similar

activation energy was observed for both pathways, consistent with the formation of both *cis*- and *trans*-arylated products in the arylation of piperidine-3-carboxamides.

Having analysed the mechanism of the reaction by DFT calculations to gain insight into the selectivity features of C(4)–H arylation, potential product inhibition and catalyst deactivation were then investigated.

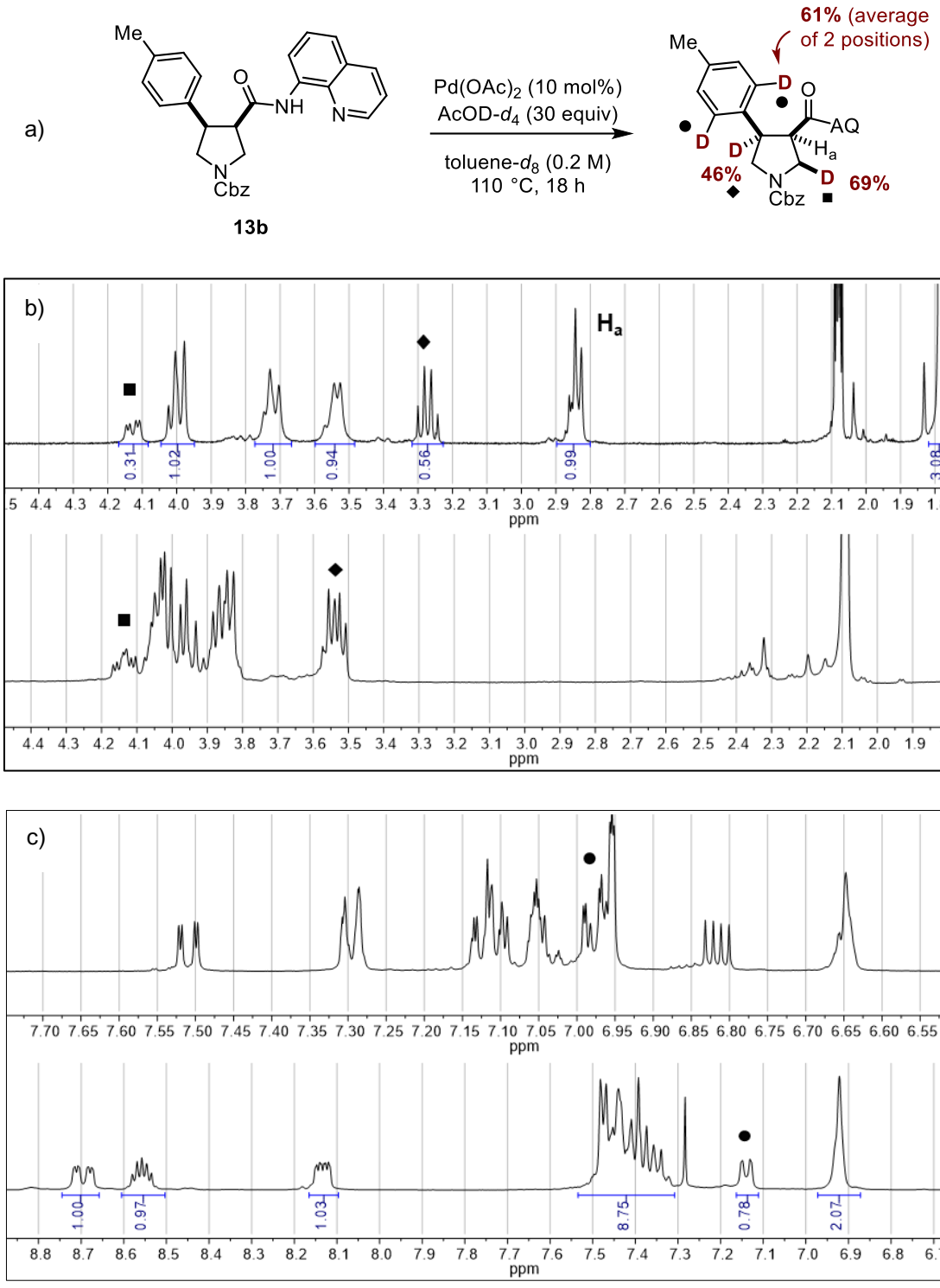
5.5 Investigations into Product Inhibition and Catalyst Deactivation

The profile for pyrrolidine arylation over time showed a progressive decrease in reaction rate until a plateau in product formation was reached at about 50–60% conversion (see section 5.3.2). This occurred despite the presence of a significant amount of unreacted starting material in the reaction mixture. Reasoning that this might be due to either product inhibition[264] or irreversible catalyst deactivation processes,[162,265] both possibilities were investigated through a combination of deuteration and kinetic experiments.

5.5.1 Deuteration Studies on 4-Arylated Pyrrolidine Product

Initially, the potential for 3,4-disubstituted pyrrolidine products to interact with the Pd catalyst was explored. C–H deuteration of *N*-Cbz 4-tolyl-pyrrolidine **13b** was attempted in the presence of catalytic $Pd(OAc)_2$, to evaluate whether such derivative could undergo reversible cyclometallation (Scheme 5.12a). Using 10 mol% $Pd(OAc)_2$ in the presence of AcOD-d_4, deuterium incorporation was observed at three different sites on pyrrolidine **13b**: *i)* at *cis*-C(2) in 69% D; *ii)* at the tertiary benzylic *trans*-C(4) position in 46% D; and *iii)* at the *ortho*-position on the aromatic ring (61% D, average of 2 positions being deuterated). The latter result was particularly interesting, suggesting a reversible C(sp^2)–H bond activation to form a larger 7-membered palladacycle intermediate.[264a,266] The deuterium incorporation was determined by quantitative ^{1}H NMR (d_1 = 70 s) in both $CDCl_3$ at 25 °C and toluene-d_8 at 100 °C (Figure 5.12b,c). The use of toluene-d_8 was necessary to resolve the signals in the aliphatic region, particularly the one relative to the $ArCH_{trans}$ proton at δ 3.2 ppm (Figure 5.12b).[‡‡] On the other hand, the relevant aromatic signals overlapped with protons from the Cbz group and the residual toluene solvent. Therefore, deuteration of this position was quantified from the rt NMR in $CDCl_3$ (Figure 5.12c).

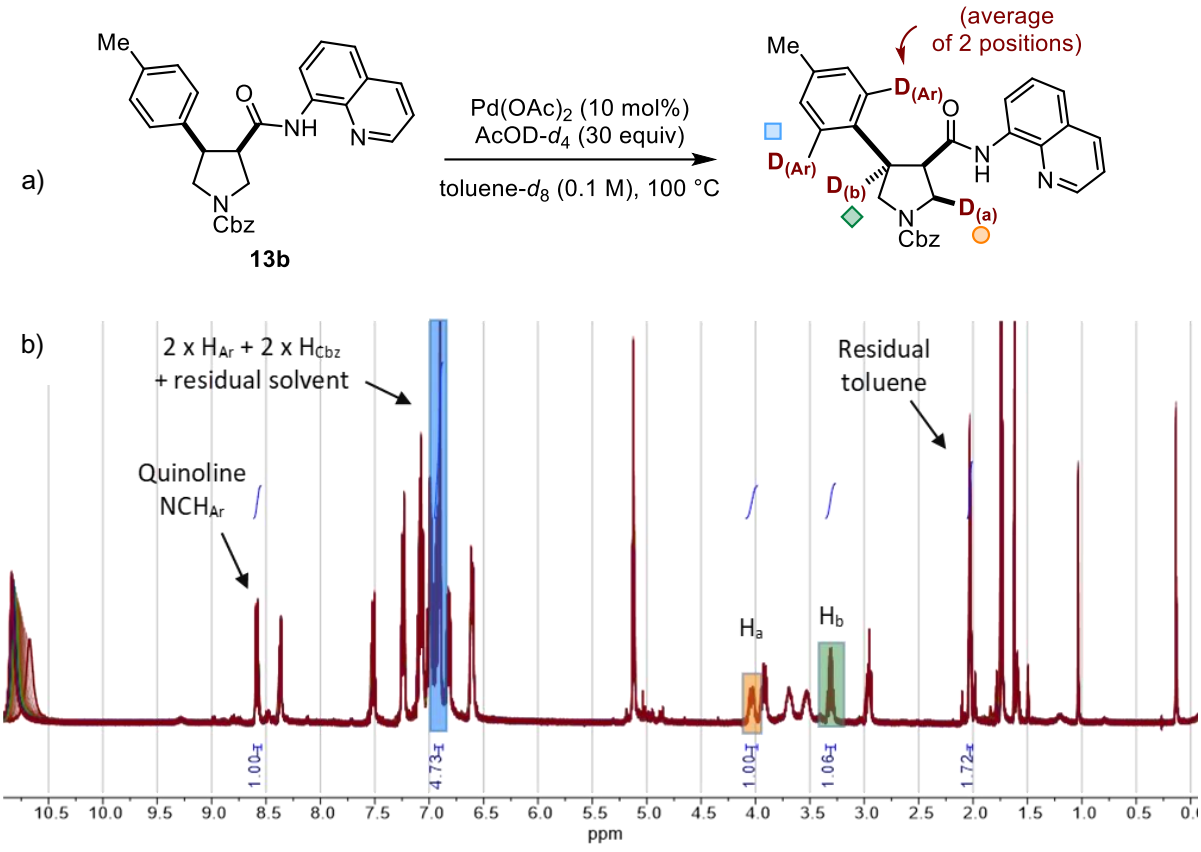
[‡‡] The position of aliphatic protons relative to the DG was assigned based on 2D NOESY NMR experiments at 100 °C. In particular, CHCO was found to correlate exclusively with protons on the same face of the pyrrolidine ring.



Scheme 5.12 a) Pd-catalysed C–H deuteration of 4-tolyl-pyrrolidine **13b**. b) Top row: ^{1}H NMR in toluene-d_8, 100 °C (400 MHz, d_1 = 70 s), magnified region at δ 4.5–1.5 ppm. Bottom row: ^{1}H NMR in $CDCl_3$, 25 °C (400 MHz, d_1 = 70 s), magnified region at δ 4.5–1.5 ppm; c) Top row: ^{1}H NMR in toluene-d_8, 100 °C, magnified region at δ 7.8–6.4 ppm. Bottom row: ^{1}H NMR in $CDCl_3$, 25 °C, magnified region at δ 8.9–6.4 ppm.

Importantly, no D incorporation was observed at C(3), and no reaction occurred either at rt or in the absence of $Pd(OAc)_2$ (not shown). This supported the proposed formation of discrete palladacycle intermediates, through temperature-dependent C–H activation.

Following this, deuteration of 4-tolyl-pyrrolidine **13b** was monitored over time by ^{1}H NMR, in order to have a better understanding of the relative rate of reaction at the different positions. The C–H deuteration was run in a J-Young NMR tube at 100 °C, and ^{1}H NMR spectra were generated every 5 min over a period of 12 h (Scheme 5.13a). [§§] Deuteration at the aromatic position was estimated subtracting from the observed integral at δ 6.91 ppm the value derived from the residual toluene solvent (2 protons) and the contribution from the Cbz group (2 protons). The residual toluene signal at δ 2.08 ppm was used as reference to estimate the integral value relative to the solvent in the aromatic region (Scheme 5.13b).



Scheme 5.13 a) Pd-catalysed C–H deuteration of 4-tolyl-pyrrolidine **13b** followed over time. b) Stacked ^{1}H NMR spectra collected at different time points (400 MHz, toluene-d_8, 100 °C, 1 scan, d_1 = 70 s). Integral values for the spectrum collected at t = 5 min are shown.

Quinoline NCH_{Ar} signal at δ 8.58 ppm was used for integral normalisation.

[§§] NMR experiment performed by Peter Haycock (Imperial College London). Raw kinetic data can be found in Appendix II.

Plotting the calculated deuterium incorporation values (%) as a function of time, a similar rate of deuteration was observed for *cis*-C(2) and *o*-CH_{Ar} positions, with the reaction being only slightly quicker at the proximal C(sp^3)–H bond (Figure 5.20). Both positions were deuterated up to 30–35% D after 12 h. On the other hand, deuteration at *trans*-C(4) appeared to be ~ 1.5–2 times slower, and resulted in just 20% D at the end of the observation period. The lower % D compared to the reaction run in a sealed vial was likely due to the lack of accurate control over stirring and water content deriving from running the reaction in an NMR tube and using a non-anhydrous solvent.

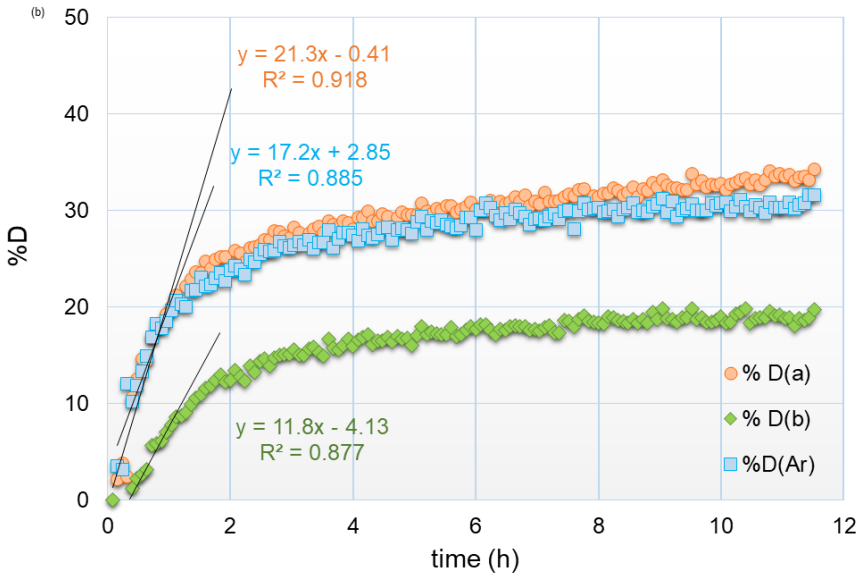
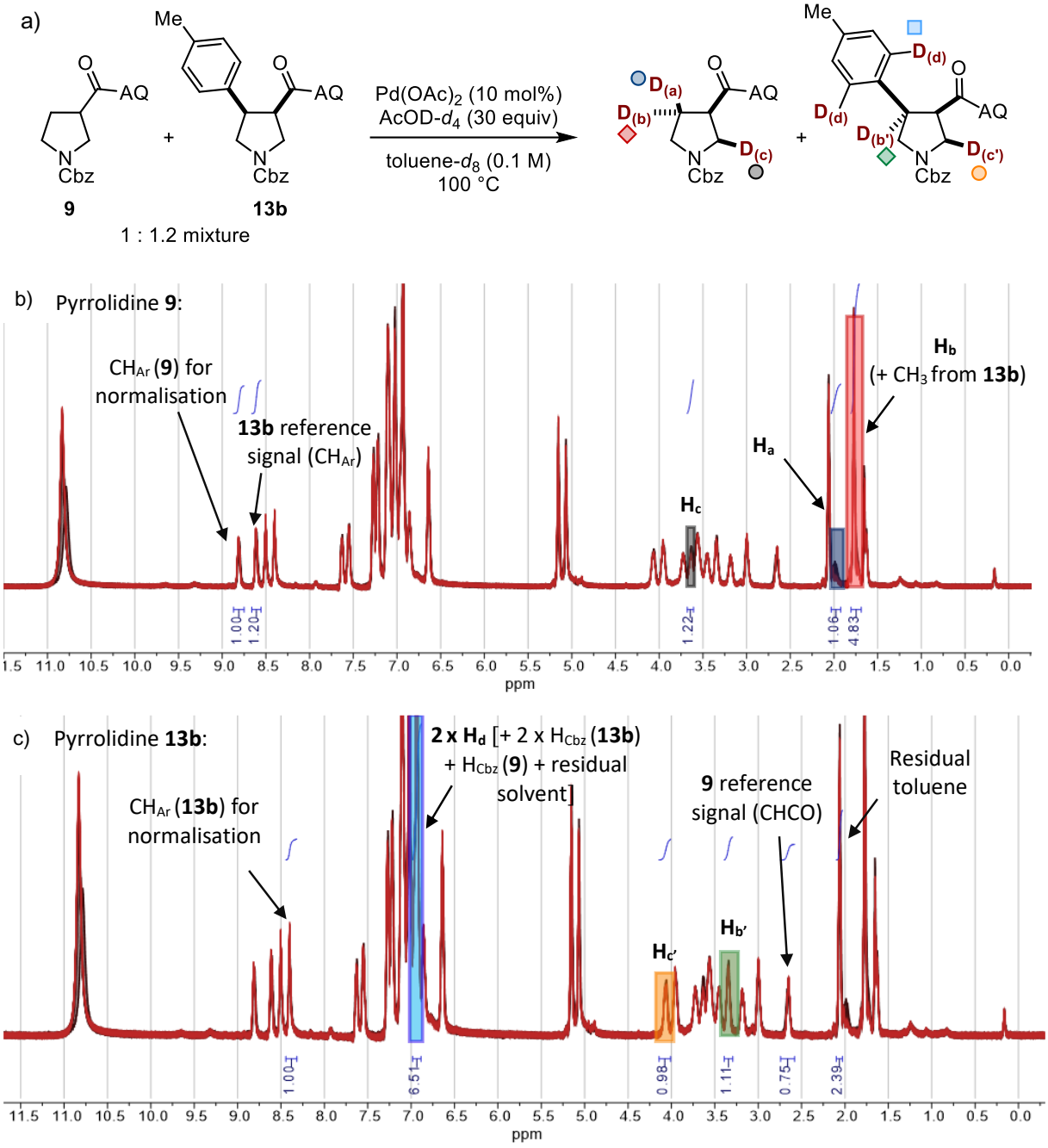


Figure 5.20 Pd-catalysed C–H deuteration (%) of 4-tolyl-pyrrolidine **13b** as a function of time.

This result confirmed the possibility for 4-aryl-pyrrolidine derivatives to interact with the Pd catalyst, undergoing C–H activation at various positions. In turn, this might lead to product inhibition, if the arylated product was to outcompete the substrate in the coordination to a limited amount of catalyst in the reaction mixture. This competition would be more evident at higher conversion, slowing down and eventually stopping the desired reaction. On the other hand, if preferential coordination of the Pd centre to the substrate could be obtained (*e.g.* in case of higher affinity), a product inhibition effect might be reduced or completely avoided. In order to have a better indication for the potential of the product to compete with the substrate, an additional NMR experiment was performed. A 1:1.2 mixture of pyrrolidine **9** and arylated derivative **13b** was treated with 10 mol% of $Pd(OAc)_2$ and AcOD-d_4 in toluene-d_8 at 100 °C, and the deuteration of both substrates was monitored by ^{1}H NMR.[***] Most proton signals were well resolved from each other and could be integrated separately to determine % D (Scheme

[***] NMR experiment performed by Corey Fulop (Imperial College London). Raw kinetic data can be found in Appendix II.

5.14b,c). In the few cases where the signals of **9** and **13b** overlapped with each other (or with the residual solvent), the percentage of deuteration was estimated subtracting the relevant contributions from the observed integral.



Scheme 5.14 a) Pd-catalysed C–H deuteration of a 1:1.2 mixture of pyrrolidine-3-carboxamide **9** and 4-tolyl-pyrrolidine **13b** followed over time. b) Stacked ^{1}H NMR spectra collected at different time points (500 MHz, toluene-d_8, 100 °C, 8 scans, d_1 = 1 s). Integral values for pyrrolidine **9** at t = 5 min are shown. c) Integral values for pyrrolidine **13b** at t = 5 min are shown.

Plotting the % D in function of time, preferential deuteration of monosubstituted pyrrolidine **9** was observed, despite the presence of a small excess of arylated derivative **13b** (Figure 5.21).

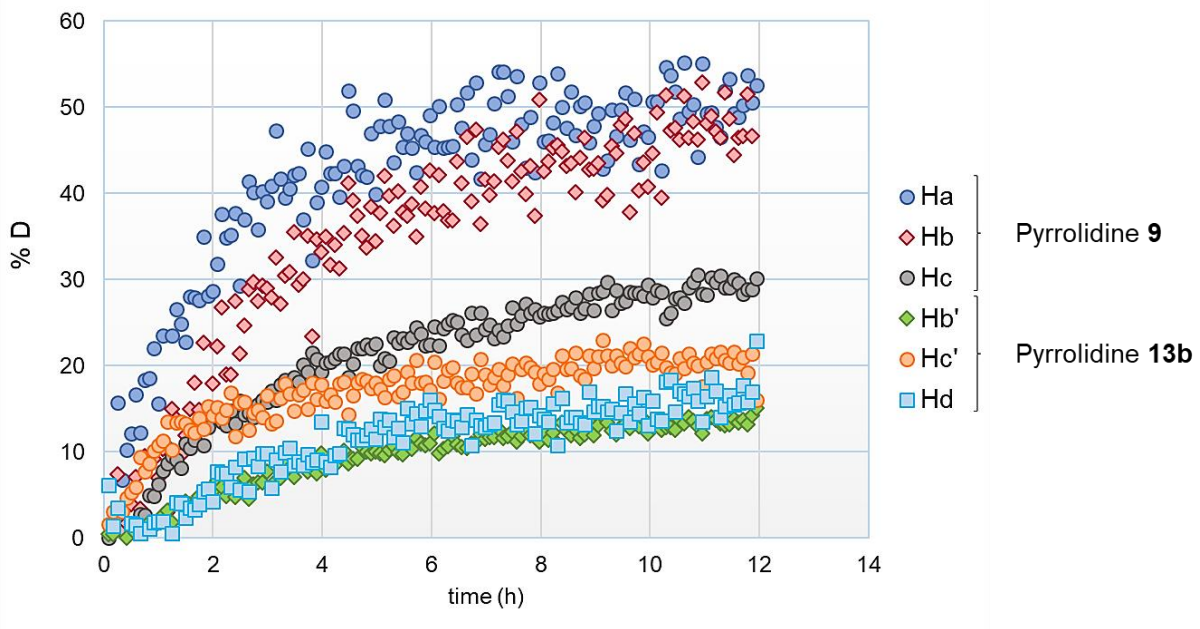


Figure 5.21 Pd-catalysed C–H deuteration (%) of a 1:1.2 mixture pyrrolidine-3-carboxamide **9** and 4-tolyl-pyrrolidine **13b** as a function of time.

The fastest reaction was observed at both *cis*- and *trans*-C(4) positions in the starting material ($D_{(a)}$ and $D_{(b)}$, respectively) followed by *cis*-C(2) on the same substrate. On the other hand, an overall lower reactivity was found for pyrrolidine **13b**. Although the *cis*-C(2) position of **13b** ($D_{(c')}$, orange profile) initially reacted at a similar rate to the corresponding position in the starting material ($D_{(c)}$, grey profile), it reached a faster plateau, resulting in approx. 20% overall deuteration against 30% D observed for pyrrolidine **9**. This result indicated that the pyrrolidine-3-carboxamide substate can outcompete an equimolar amount of *cis*-arylated product for reaction with the palladium catalyst, thus suggesting low likelihood of product inhibition. To further confirm this hypothesis, reaction progress kinetic analysis (RPKA), in the form of a "same excess" protocol, was performed.

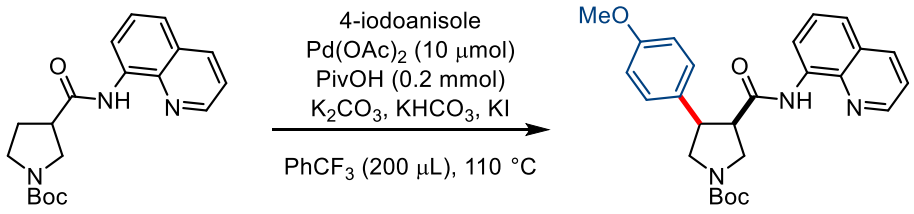
5.5.2 Reaction Progress Kinetic Analysis (RPKA)

Pioneered by Blackmond in early 2000s, RPKA has rapidly been established as a powerful approach to study the mechanism of complex catalytic reactions.[267] Based on the monitoring of the entire course of a reaction, RPKA offers the potential to study mechanistic features, such as induction periods, product inhibition and catalyst deactivation, that would be difficult to identify with other kinetic analysis (*e.g.* initial rates). The utility of this approach was further extended by Blackmond in 2012, demonstrating the use of visual comparison of concentration profiles to allow RPKA studies, without requiring the mathematic extraction of rate data.[264b] In

this case, the use of a "same excess" protocol enabled the identification of product inhibition for a Pd-catalysed C(sp^2)–H olefination reaction.

The term "excess" corresponds to the difference in concentration of two reagents, which remains constant throughout the course of a reaction.[264b,267] As such, the reaction rate at a given concentration of one of the reagents is a function of its excess. Based on this, "same excess" experiments use lower initial concentrations of two reaction components, while maintaining the same excess between them, to mimic the reaction at a later time point.[264b,267]

In the specific case of pyrrolidine C(4)–H arylation, the same excess protocol was applied to evaluate the presence of product inhibition or catalyst deactivation. In particular, t = 1 h was chosen as reference time point for this study, corresponding approximately to half of the total conversion of pyrrolidine **2** into 4-methoxyphenyl derivative **3a**. At this stage in the progress of the reaction, approximately 30% of product **3a** was expected alongside 70% of unreacted **2**. A "same excess" profile was thus constructed using lower initial loadings of amide **2** and 4-iodoanisole to match their concentrations in the standard reaction at t = 1 h, while keeping a constant excess between them (Table 5.7, entry 2). As K_2CO_3 is also stoichiometrically consumed during the reaction, forming $KHCO_3$ and KI, the amount of base in the same excess experiment was corrected by addition of the expected amount of $KHCO_3$ being formed at t = 1 h. On the other hand, the loadings of $Pd(OAc)_2$ and PivOH were kept constant.



2 **3a**

entry	run	2 (mmol)	ArI (mmol)	3a (mmol)	KI (mmol)	K_2CO_3 (mmol)	$KHCO_3$ (mmol)
1	standard	0.20	0.60	0.00	0.00	0.20	0.00
2	"same-excess"	0.13	0.53	0.00	0.00	0.13	0.07
3	"same-excess" + **3a**	0.13	0.53	0.07	0.00	0.13	0.07
4	"same-excess" + KI	0.13	0.53	0.00	0.07	0.13	0.07

Table 5.7 Initial reagent loadings for standard and "same-excess" RPKA experiments.

To evaluate the presence of product inhibition, additional “same excess” profiles were built upon addition of either 4-aryl-pyrrolidine **3a** or KI in the amount expected at t = 1 h (entries 3 and 4).

The resulting profiles, constructed in each case from discrete reaction quenched at different time points, could be compared after time-scale adjustment to match the 1 h reference point (Figure 5.22). The same excess profile, run at smaller initial concentrations of the two reagents, showed a higher rate compared to the standard reaction (Figure 5.22a). This could be due either to the absence of product, or to the fewer number of catalyst turnover, indicating product inhibition or catalyst deactivation scenarios respectively.

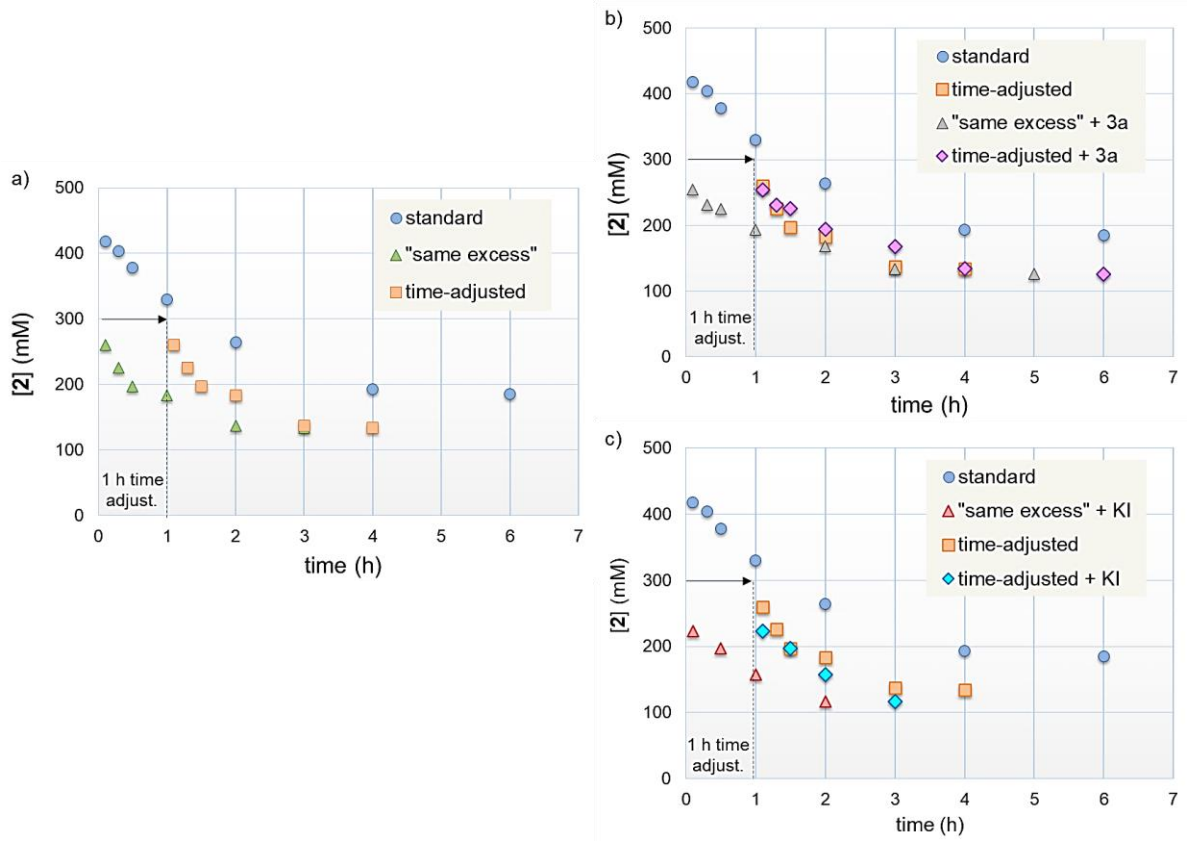


Figure 5.22 a) Comparison of standard and “same-excess” plots, before and after time-adjustment, for the [**2**] (mM) in function of time (h). b) Comparison of standard and “same-excess” plots in the presence of product **3a**, before and after time-adjustment. c) Comparison of standard and “same-excess” plots in the presence of KI, before and after time-adjustment. Each data point corresponds to a discrete reaction.

Importantly, no decrease in reaction rate for the same excess profile was observed in the presence of product **3a** (Figure 5.22b). The same result was obtained using an uncorrected amount of K_2CO_3, without any added $KHCO_3$ (not shown). The lack of overlap between the standard and same excess profile in the presence of **3a** indicated the absence of a product inhibition effect.

Finally, no visual overlap of the profiles was observed in the presence of by-product KI (Figure 5.22c). This would suggest the absence of KI-mediated catalyst inhibition under the synthetically relevant conditions, likely due to the poor solubility of KI in $PhCF_3$ (*vide infra*).

Having excluded the possibility of a product inhibition process, the alternative possibility of an irreversible catalyst deactivation pathway was evaluated.

5.5.3 Estimation of Catalyst Deactivation Profile

In 2019, Burés extended the VTNA approach to enable the study of catalyst deactivation when is not possible to quantify directly the [active cat.] in the reaction mixture.[268] This was based on the mathematic manipulation of kinetic data to maximise the linearity of VTNA profiles. VTNA allows the kinetic effect of a reagent to be removed from concentration profiles, upon time scale normalisation for the correct order in that reagent.[257a] Therefore, a straight line should be expected once the time scale is normalised by all the kinetically relevant reagents whose concentration changes during the reaction.[257a] When this is not observed, for instance in the presence of catalyst deactivation, a manual linearisation of the plot was demonstrated to provide an indirect way to estimate the amount of active catalyst present at different time points.[268]

In the case of pyrrolidine C(4)–H arylation, the palladium catalyst and the aryl iodide were found as the only kinetically relevant species, exhibiting an order ≠ 0 (see section 5.3.2). In the absence of catalyst deactivation, only the concentration of aryl iodide is expected to change during the reaction. Therefore, the temporal profile should become a straight line after normalisation of the time scale for the sole concentration of ArI. However, a non-linear plot was observed, suggesting an irreversible catalyst deactivation process that varies the concentration of active catalyst during the reaction (blue profile, Figure 5.23a). The concentration of [active cat.] at different time points was thus estimated through mathematic linearisation of the VTNA profile. According to Burés' procedure, Microsoft Excel's add-in Solver was used, imposing as the only constraint that the catalyst concentration cannot increase over time.[268] Based on this, the software calculated a series of catalyst concentration values to give a straight line with $R^2 = 0.999$ (orange profile, Figure 5.23a).

Plotting the solution given by Solver as the percentage of residual active catalyst as a function of time, a catalyst deactivation profile was obtained (Figure 5.23b). Unfortunately, very fast catalyst deactivation was observed, with < 20% [active cat.] being left after 2 h.

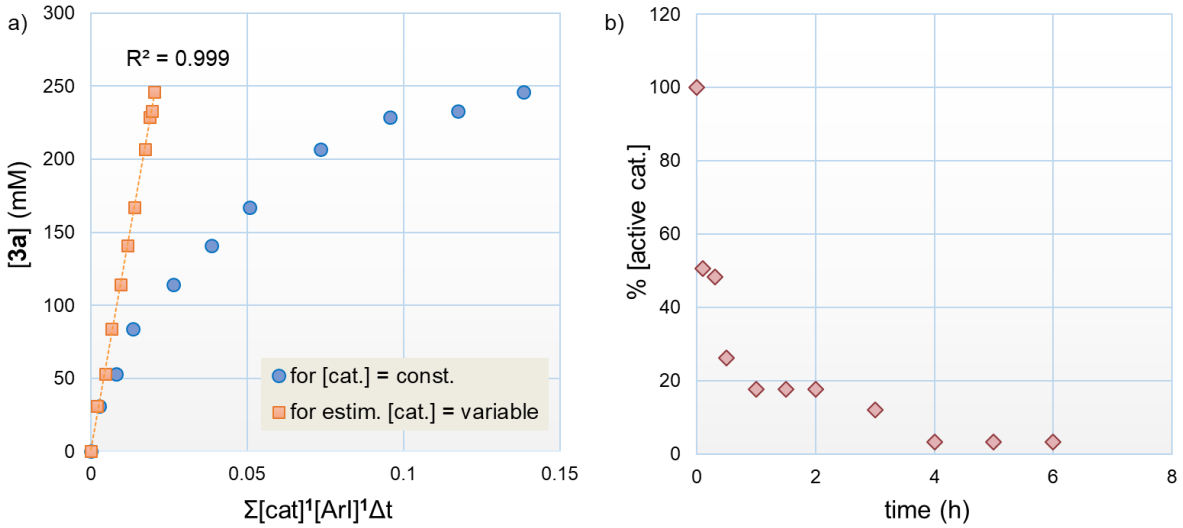
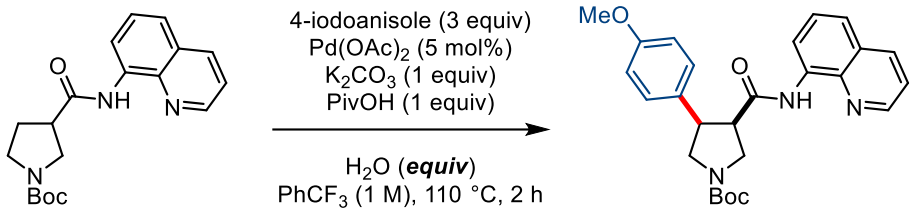


Figure 5.23 a) Concentration profiles for the formation of **3a** after time scale normalisation. In blue: original VTNA profile assuming the [cat.] to be constant during the reaction and equal to the initial [$Pd(OAc)_2$]. In orange: linearised VTNA profile obtained through mathematic estimation of [cat.] at each time point. b) Estimated catalyst deactivation profile.

In order to overcome this limitation, possible causes of deactivation were examined.

During the process of optimisation of the reaction, this was found to be sensitive to variations in the relative ambient humidity (see section 3.2.2). Reasoning that H_2O could form *in-situ* by decomposition of $KHCO_3$, which has been reported to occur at temperatures as low as 91 °C,[269] the effect of water as source of deactivation was first investigated. In particular, discrete reactions were run in the presence of different equivalents of H_2O and stopped after 2 h, arbitrarily selected as representative time point (Table 5.8). Small amount of water seemed to not affect the reaction, with similar yield of product **3a** being observed in the presence of 0–5 equivalents of water (entries 1–4), while 10 equivalents only resulted in a slight decrease in yield (entry 5). A significant reduction in reactivity was only observed upon addition of ~ 110 μL of water (30 equiv), but these conditions were not considered to be synthetically relevant, as the standard loading of K_2CO_3 is 1 equivalent. This suggested that the small amount of water potentially formed during the reaction is not likely to be the cause of catalyst deactivation.



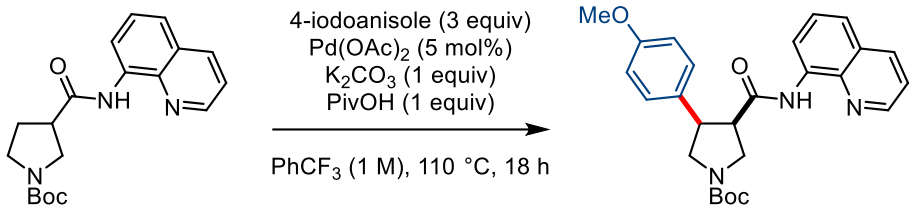
2 **3a**

entry	H_2O (equiv)	2 (%)[a]	3a (%)[a]	tot (%)[a]
1	0	59	37	96
2	0.5	54	40	94
3	1.0	55	39	94
4	5.0	56	37	93
5	10	63	34	98
6	30	71	26	97

Table 5.8 Effect of added H_2O on the C(4)–H arylation of pyrrolidine **2**. Reaction scale: 0.2 mmol.
[a] Calculated by ^1H NMR using 1,3,5-TMB as internal standard.

Following this, the potential for the iodide ions formed during the reaction to poison the catalyst was evaluated. The RPKA studies above suggested the absence of catalyst inhibition upon external addition of insoluble KI. However, if the extraction of iodide ions from solution was not efficient enough, catalyst deactivation could derive from the generation of unreactive PdI_2.[270,271]

To investigate this hypothesis, various control experiments were performed (Table 5.9). First, the reaction was run in the presence of tetrabutylammonium iodide (TBAI), to mimic the addition of soluble iodide ions (entries 2 and 3). This was found to inhibit the reaction completely, with no conversion observed when using as low as 30 mol% of TBAI (entry 3). Using Bu_4NOAc also had a detrimental effect on the conversion, although traces of product formation were observed (entry 4). This is suggestive of an initial catalytic activity, followed by immediate catalyst deactivation, likely due to the tetrabutylammonium cation stopping the formation of insoluble KI. On the other hand, addition of 1 equivalent of KI was confirmed not to affect the reaction outcome, likely because of its low solubility (entry 5). Similarly, the addition of Me_4NCl, which has been reported to form insoluble iodide salts,[271] did not result in any reduction in yield (entry 6).



entry	variation from "standard"	2 (%)[a]	3a (%)[a]	tot (%)[a]
1	none	22	67	89
2	TBAI (1 equiv)	99	-	99
3	TBAI (30 mol%)	99	-	99
4	Bu_4NOAc (1 equiv)	99	traces	99
5	KI (1 equiv)	30	62	92
6	Me_4NCl (1 equiv)	21	61	82
7	PdI_2 (no K_2CO_3 and PivOH)	99	-	99
8	PdI_2 (no PivOH)	91	7	98
9	no K_2CO_3 and PivOH	98	4	102
10	no PivOH	70	28	98
11	PdI_2	22	64	86

Table 5.9 Effect of different iodide sources on catalyst turnover in the C(4)–H arylation of pyrrolidine **2**. [a] Determined by ^1H NMR using 1,3,5-TMB as internal standard.

Next, the catalytic activity of PdI_2 was investigated. Using PdI_2 in place of $Pd(OAc)_2$ and in the absence of K_2CO_3 and PivOH, no product formation was observed (entry 7). Furthermore, when PivOH was exclusively removed, product **3a** was obtained in just 7% yield (entry 8). In comparison, the use of $Pd(OAc)_2$ in the absence of both K_2CO_3 and PivOH gave **3a** in 4% yield, suggestive of one catalyst turnover, while a higher 28% conversion was observed upon addition of K_2CO_3 (entries 9 and 10). Taken together, these results suggested an intrinsic activity of $Pd(OAc)_2$, while K_2CO_3 and PivOH were essential to allow catalyst turnover. On the other hand, PdI_2 was likely an unreactive pre-catalyst, which could be activated upon ligand exchange with CMD-active pivalate or carbonate anions, accompanied by the formation of insoluble KI. In addition, although the carbonate base has potential to promote the CMD step, the addition of PivOH was found to be important to regenerate a more active, carboxylate-bound catalytic species. Finally, when both K_2CO_3 and PivOH were used in the presence of catalytic PdI_2 the reactivity of the system was fully restored (entry 11). Therefore, it can be concluded that soluble iodide ions are indeed able to inhibit the reaction by formation of unreactive PdI_2. However, the combination of K_2CO_3 and PivOH appeared to enable efficient catalyst turnover.

During the preparation of this work, similar observations concerning a catalyst deactivation process were described for a Pd-catalysed C(sp^2)–H arylation reaction occurring in the presence of K_2CO_3 and PivOH.[265] In this case, the deactivation was ascribed to the entrapment of the Pd catalyst during the crystallisation of the product and/or KI, although this was not supported by direct evidence. Nonetheless, a similar physical effect could be responsible for the catalyst deactivation process observed in the C(4)–H functionalisation of saturated N-heterocycles.

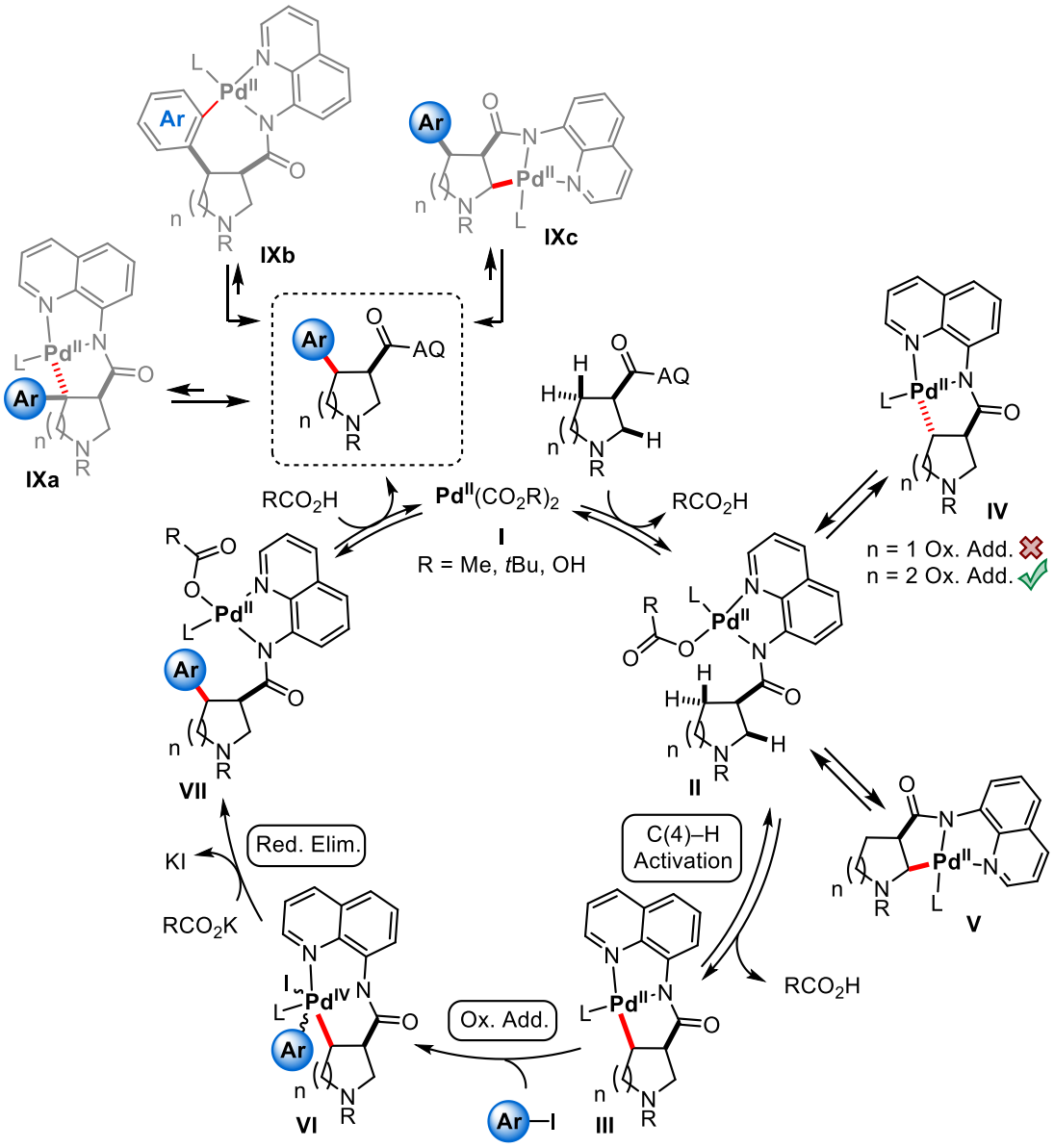
5.7 Conclusions: Proposed Catalytic Cycle

In conclusion, the mechanism of Pd-catalysed C(sp^3)–H arylation of pyrrolidines and piperidines was investigated in detail through a combination of experimental and computational studies. This provided important insight into the selectivity features of this transformation, allowing a revised Pd^{II}/Pd^{IV} catalytic cycle to be proposed (Scheme 5.15).

Following the initial formation of chelated intermediate **II**, evidence for a reversible, non-stereodetermining C–H activation step was observed in deuteration experiments and computational studies. Furthermore, the absence of a large primary kinetic isotope effect indicated the C–H activation process to be not turnover-limiting, as confirmed by the low energetic barrier observed computationally. Reversible cyclometallation was found to be feasible at both *cis*- and *trans*-C(4) positions on 5- and 6-membered rings, leading to the corresponding palladacycle species **III** and **IV**. The involvement of *cis*-palladacycle **III** was further supported by the stochiometric isolation of a closely related pyridine-complex. While the following OA step was found energetically viable for both diastereomeric derivatives in the case of piperidine-3-carboxamide, only *cis*-palladacycle **III** could undergo stereodetermining OA for the smaller pyrrolidine ring. From intermediate **II**, reversible C–H activation could also occur at *cis*-C(2) forming palladacycle **V**. While a conclusive rationale for the observed C(4)-regioselectivity could not be inferred computationally, this might derive from a similarly disfavoured OA process at C(2).

Oxidative addition on palladacycle **III** formed Pd(IV) intermediate **VI**, which could then undergo C–C bond forming reductive elimination. This was found to be the turnover-limiting step for the overall transformation, based on competition experiments, Hammett analysis and DFT calculations. Furthermore, this was consistent with a first order kinetic dependence in $Pd(OAc)_2$ and ArI found through VTNA studies.

Although it was not possible to unambiguously determine whether halide abstraction occurred before or after turnover-limiting RE, this was found to be important for catalyst turnover. In particular the combination of K_2CO_3 and PivOH is believed to play a critical role to regenerate the active catalyst while sequestering detrimental iodide by-product as insoluble KI.



Scheme 5.15 Proposed catalytic cycle for the Pd-catalysed C(4)–H arylation of pyrrolidines and piperidines-3-AQ amides.

Finally, the limitations of the reaction were analysed. The arylated product formed from protodemetalation of intermediate **VII** was able to interact with the Pd catalyst, undergoing reversible C–H activation at three different sites. These included *cis*-C(2) and *trans*-C(4), as well as the *ortho*-positions on the aromatic substituent. Nonetheless, a product inhibition effect was excluded based on competition experiments and RPKA studies. On the other hand, VTNA studies identified a fast catalyst deactivation as an intrinsic limitation of the method. While significant catalyst deactivation by H_2O and KI was excluded under the synthetically relevant conditions, this might be due to the physical sequestration of the catalyst from the reaction.

Strategies to overcome this catalyst deactivation and increase the efficiency of the reaction will be discussed in detail in the next chapter.

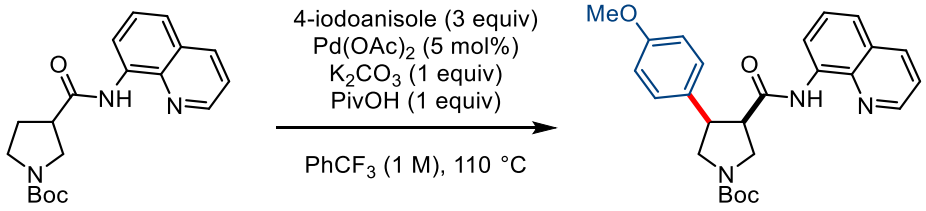
6. Discovery of Dimethylaminoquinolinyl (DMAQ) Amide as an Improved Directing Group

6.1 Initial Attempts to Overcome Catalyst Deactivation

A fast catalyst deactivation was found to limit the efficiency of the Pd-catalysed C(4)–H arylation of pyrrolidine and piperidine rings. In order to overcome this issue, various strategies were initially evaluated, including: *i)* spiking experiments with fresh catalyst, *ii)* use of stabilising ligands, and *iii)* use of alternative reaction conditions.

6.1.1 Spiking Experiments

Different spiking experiments were first investigated aiming to achieve full conversion. This involved the addition of fresh catalyst, with or without additional K_2CO_3 and PivOH, to the reaction mixture at an arbitrary time point. As the kinetic data suggested < 20% of the initial catalyst loading to be left in the reaction after 2 h (see section 5.5.3), this was selected as a suitable time point for the spiking experiments. The effect of adding fresh reaction components was then evaluated after further 2 h (Table 6.1).



2 **3a**

entry	spiking experiment[a]	tot. reaction time (h)	2 (%)[b]	3a (%)[b]	tot (%)[b]
1	none	4 h	55	40	95
2	$Pd(OAc)_2$ (5 mol%)	4 h	29	64	93
3	K_2CO_3 (1 equiv) PivOH (1 equiv)	4 h	43	49	92
4	$Pd(OAc)_2$ (5 mol%) K_2CO_3 (1 equiv) PivOH (1 equiv)	4 h	24	59	83
5	$Pd(OAc)_2$ (5 mol%)	24 h	13	69	82
6[c]	2 x $Pd(OAc)_2$ (5 mol%)	24 h	11	63	78

Table 6.1 Effect of spiking experiments on the C(4)–H arylation of pyrrolidine **2**. Reaction scale: 0.2 mmol. [a] Spiking time = 2 h. [b] Determined by ^{1}H NMR using 1,3,5-TMB as internal standard. [c] Double addition of $Pd(OAc)_2$ at t = 2 h and t = 4 h.

Adding 5 mol% of fresh $Pd(OAc)_2$ resulted in a significant increase in yield compared to the control reaction and afforded product **3a** in 64% NMR yield (entries 1 and 2). Interestingly, this was comparable to the yield of **3a** obtained after 18 h under the standard arylation conditions. On the other hand, just a slight increase in yield was observed upon addition of fresh K_2CO_3 and PivOH (entry 3). Similarly, spiking with all three components did not give an improved outcome compared to the single addition of $Pd(OAc)_2$, suggesting no advantage in spiking with K_2CO_3 and PivOH (entry 4).

Based on these encouraging results, the yield after 24 h was then evaluated using different sequential additions of $Pd(OAc)_2$. Unfortunately, adding 5 mol% of $Pd(OAc)_2$ at 2 h, and stopping the reaction after additional 22 h, did not result in an increased yield, but did reduce the recovery of the substrate (entry 5). A similar outcome was found with 2 sequential additions of Pd catalyst at 2 and 4 h time points (entry 6). Despite the lower mass balance, no different product or new component was identified by ^{1}H NMR. Similar results were previously observed during the process of optimisation of the reaction, when using a higher catalyst loading from t = 0 (Table 3.5, section 3.2.2).

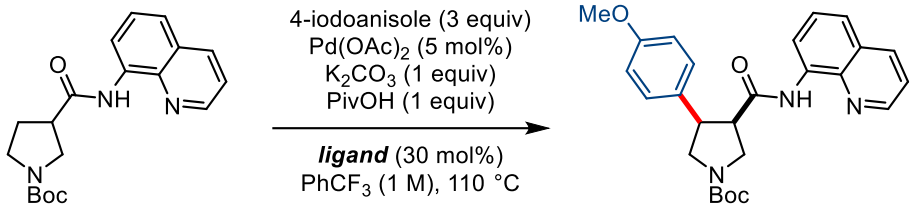
To investigate the possibility of the lower mass balance being due to the formation of insoluble organopalladium complexes at the higher catalyst concentration, a spiking experiment was performed, adding additional $Pd(OAc)_2$ after 6 h (not shown). The reaction was stopped after a total of 18 h, diluted with MeOH and concentrated without any filtration step. Unfortunately, while product **3a** was formed in a similar 60 % yield, low recovery of pyrrolidine **2a** was again observed (total mass recovery = 74%). This suggested that the use of higher catalyst loading, either from the start of the reaction or from sequential additions at various time points, would promote unproductive degradation pathways, and was therefore no longer investigated.

6.1.2 Ligand Screening

At this point, a different strategy to overcome catalyst deactivation was evaluated, based on the use of ligands to stabilise on-cycle Pd species while avoiding off-cycle irreversible processes. In 2018, Sanford reported the use of pyridine- and quinoline-2-carboxylate ligands to avoid reversible and irreversible catalyst deactivation in the transannular Pd-catalysed C–H arylation of bicyclic N-heterocycles (see section 1.4.2.2).[162] Although the causes of catalyst deactivation could not be conclusively identified, these ligands were found to be particularly effective in restoring optimal catalytic activity.

As such, the effect of these ligands on the C(4)–H arylation of pyrrolidines and piperidines was investigated. In addition, monoprotected aminoacid and pyridone ligands, known to promote the CMD step,[272,273] as well as simpler monodentate pyridine ligands used to stabilise the

palladium complex intermediates,[150d] were also evaluated. A loading of 30 mol% was used for the comparison of these different ligands (Table 6.2).



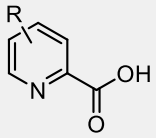
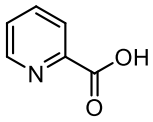
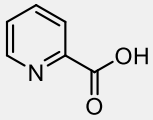
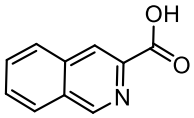
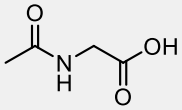
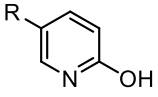
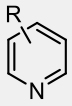
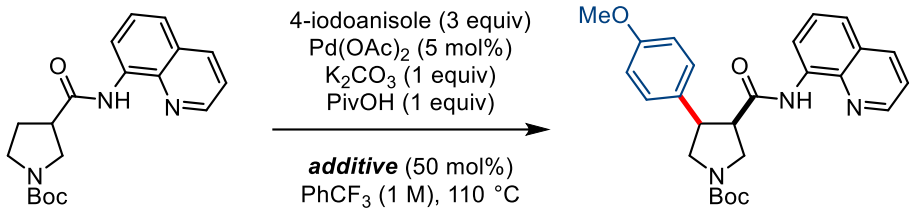
entry	ligand			2 (%)[a]	3a (%)[a]	tot (%)[a]
1	none			22	66	88
2		R =	H	65	36	101
3			5-CF_3	41	42	83
4			4-OMe	101	/	101
5[b]				45	45	90
6[c]				72	15	97
7				57	43	100
8				24	53	80
9		R =	H	66	14	80
10[c]			H	101	/	101
11			CF_3	97	/	97
12		R =	2-Me	52	37	89
13			2-OMe	24	60	84
14			2,6-OMe	32	66	98

Table 6.2 Ligand screening for the C(4)–H arylation of pyrrolidine **2**. Reaction scale: 0.2 mmol. [a] Determined by ^{1}H NMR using 1,3,5-TMB as internal standard. [b] 1.5 equiv of K_2CO_3 used. [c] No PivOH added.

Unfortunately, the use of picolinic acid-based ligands resulted in a general reduction in yield, with no product observed when using an electron-rich 4-methoxy derivative (entries 2–7). To account for the additional acidic protons, the reaction with 2-picolinic acid was also repeated using 1.5 equiv of K_3CO_3 (entry 5). Although this appeared to be beneficial compared to entry

2, lower conversion than in the absence of ligand was still observed. The reaction was also repeated in the absence of PivOH to evaluate the ligand ability to promote a CMD process, but this gave only 15% yield of product **3a** (entry 6). The use of *N*-Ac-Gly had a lower negative effect on the reaction outcome but did not result in improved reactivity (entry 8). On the other hand, the use of 2-pyridone ligands was found to be highly detrimental, overall resulting in very low or no conversion (entries 9–11). Finally, monodentate pyridine ligands were also unsuccessful in promoting the reaction. While using 2-picoline gave a reduction in yield (entry 12), more electron-rich 2-methoxy and 2,6-dimethoxy derivatives resulted in 60% and 66% yield, respectively (entries 13 and 14). Despite representing an improvement compared to the other ligands tested, no advantage was found in comparison to the standard reaction (entry 1).

The effect of various additives on the yield of product **3a** was then studied. Coordinating additives that could stabilise on-cycle Pd-species, including sulfide and sulfoxide ligands,[274] as well as oxidants, additional halide scavengers and electron-withdrawing anionic ligands that could promote the RE step (*e.g* fluoride and trifluoroacetate) were evaluated (Table 6.3). However, no improvement in the reaction outcome was observed in any case. The use of coordinating additives, such as DMSO, methyl *p*-tolylsulfide, DMF and NMP, all resulted in a significant reduction in yield (entries 2–5). On the other hand, HFIP was tolerated, but did not result in improved conversion (entry 6). Oxidants, such as 1,4-BQ and copper(II) acetate gave reduced yields, while manganese(II) acetate was better tolerated (entries 7–9). The addition of fluoride salts did not affect the reaction, while silver(I) additives were found to have a detrimental effect (entries 10,11 and 13,14). Based on these unsuccessful results, alternative reaction conditions were then examined to avoid catalyst deactivation.



2 **3a**

entry	additive	2 (%)[a]	3a (%)[a]	tot (%)[a]
1	none	24	66	94
2	DMSO	44	44	90
3	methyl *p*-tolyl-sulfide	59	37	96
4	DMF	82	16	98
5	NMP	47	46	95
6	HFIP	27	58	85
7	1,4-BQ	55	36	91
8	$Cu(OAc)_2$	45	45	90
9	$Mn(OAc)_2$	36	54	92
10	KF	31	57	91
11	CsF	37	57	97
12	LiCl	72	23	95
13[b]	AgF	52	35	87
14[b]	AgTFA	47	35	82
15[b]	K_2HPO_4	26	57	83

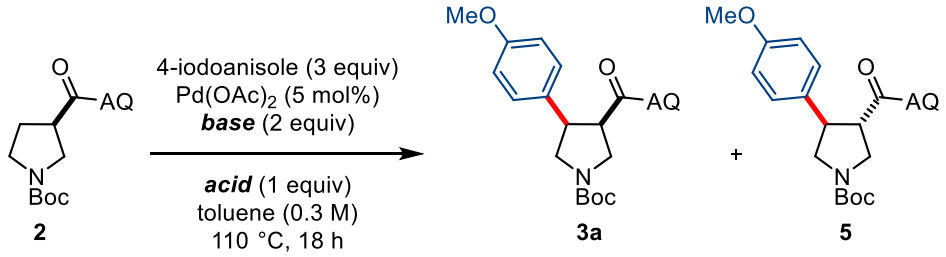
Table 6.3 Additive screening for the C(4)–H arylation of pyrrolidine **2**. Reaction scale: 0.2 mmol. [a] Determined by ^{1}H NMR using 1,3,5-TMB as internal standard. [b] 1.0 equiv of additive used.

6.1.3 Alternative Reaction Conditions

Reasoning that the decrease in catalytic activity might derive from a physical entrapment of the catalyst in the crystalline KI formed during the reaction,[265] the use of different arylating agents was investigated. Aryl bromides were previously found to be much less reactive than the corresponding iodides. Therefore, more electrophilic coupling partners, diaryliodonium and aryldiazonium salts, was evaluated (not shown). Unfortunately, both were unsuccessful in promoting C–H arylation of pyrrolidine **2** under various conditions, resulting in low conversion and/or substrate decomposition.

Following this, the use of Cs_2CO_3 in place of the corresponding potassium base was examined in order to change the physical properties of the heterogenous reaction mixture. This has been previously reported as a successful strategy to avoid catalyst deactivation in the presence of

K_2CO_3 and PivOH, while preserving effective catalyst turnover.[265] However, the use Cs_2CO_3 or CsOPiv, either alone or in combination with K_2CO_3, did not result in higher yield of *cis*-arylated pyrrolidine **3a** (Table 6.4). Instead, the simultaneous formation of small amounts of the corresponding *trans*-isomer **5** was observed, likely due to the Lewis acidity of the cesium ion promoting *in-situ* epimerisation. Therefore, this strategy was not investigated further.



entry	base	acid	yield (%)[a]			
			2	3a	5	tot
1	K_2CO_3	PivOH	22	67	/	89
2	Cs_2CO_3	PivOH	13	61	6	80
3	CsOPiv	/	23	49	4	76
4[b]	K_2CO_3 + Cs_2CO_3	PivOH	16	61	4	81

Table 6.4 Screening of cesium bases for the C–H arylation of *N*-Boc pyrrolidine **2**. Reaction scale: 0.2 mmol. [a] Calculated by ^{1}H NMR using 1,3,5-TMB as internal standard. [b] K_2CO_3 (0.5 equiv) and Cs_2CO_3 (0.5 equiv) were used.

As none of the strategies discussed above resulted in an improved reactivity, a last approach was envisaged, involving the modification of the aminoquinoline DG.

6.2 Evaluation of Steric and Electronic Effects on the Directing Group

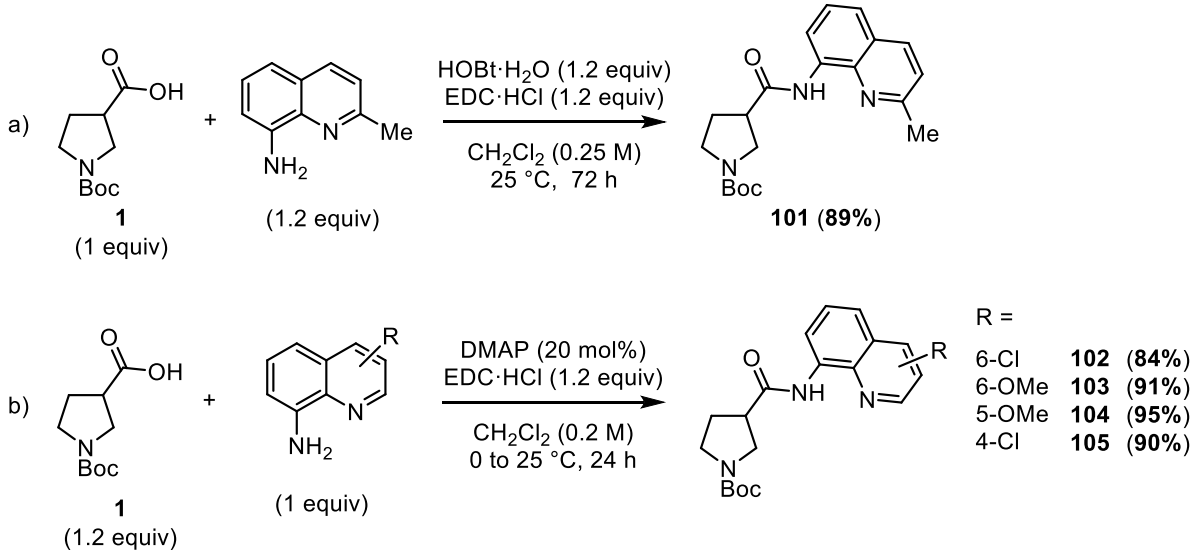
At this point in the investigation, it was considered that a change in steric and/or electronic properties of the DG could provide a solution to overcome the limitations observed in the C(4)–H arylation reaction. These included both catalyst deactivation and a sluggish reductive elimination which resulted in the poor performance of electron-poor aryl iodides. In particular, the installation of different electron-donating or -withdrawing substituents at various positions on the AQ auxiliary was envisaged to evaluate whether: *i)* increasing the steric hindrance around the distal (quinoline nitrogen) or proximal (amide NH) binding sites could promote reductive elimination; *ii*) changing the pK_a and coordinating ability of the amide NH could influence the binding affinity to the Pd centre, slowing down or avoiding catalyst deactivation pathways; and *iii)* varying the basicity and σ-donation properties of the distal quinoline nitrogen would result in any difference in reactivity. In addition to these considerations, it was

appreciated that each DG modification could have different effects on more than one step in the catalytic cycle, resulting in a complex influence on the overall reaction outcome.[275]

Finally, the use of a longer acylhydrazide linker, in place of the amide, was also targeted to study the effect of a 6- *vs* 5-membered chelation of the Pd centre on the reaction outcome.

6.2.1 Synthesis of Pyrrolidine Substrates

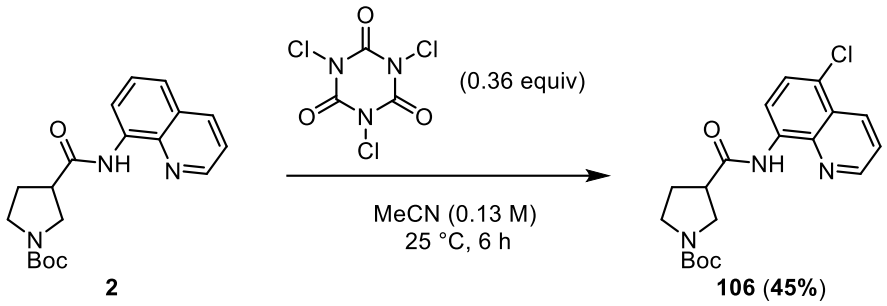
First, 2-methyl-8-aminoquinoline derivative **101** was synthesised from pyrrolidine-3-carboxylic acid **1** in 89% yield by EDC-mediated amide bond formation (Scheme 6.1a). A similar strategy, involving the use of DMAP in place of HOBt, was used to access 6-Cl-, 6-OMe-, 5-OMe-, and 4-Cl-derivatives **102–105** from the corresponding substituted 8-aminoquinolines (Scheme 6.1b). These were used as limiting reagents, affording the desired pyrrolidine amide products in 84–95% yield.



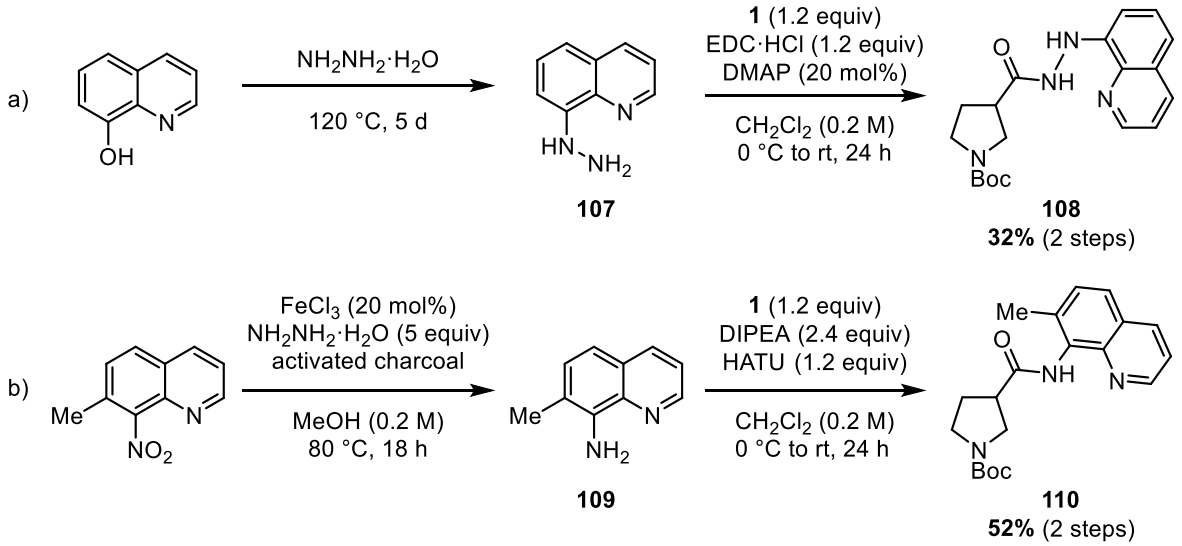
Scheme 6.1 Synthesis of pyrrolidine amides **101**–**105** by amide bond formation.

Pyrrolidine amide **106**, bearing a 5-chloro substituent, was synthesised from pyrrolidine-3-carboxamide **2** *via* direct C(5)–H chlorination of the AQ ring (Scheme 6.2). Trichloroisocyanuric acid was used as chlorinating agent,[276] affording pyrrolidine **106** in 45% yield.

On the other hand, acyl hydrazide **108** and 7-methyl-8-AQ amide **110** were respectively formed from commercially available 8-hydroxyquinoline and 7-methyl-8-nitroquinoline (Scheme 6.3). In the former case, condensation with hydrazine monohydrate formed 8-hydrazinoquinoline **107**,[277] which was directly used in the reaction with acid **1**, affording hydrazide **108** in 32% yield (Scheme 6.3a). Similarly, after an initial reduction of the nitro functionality,[278] amide coupling of 7-methyl-8-aminoquinoline **109** in the presence of HATU and DIPEA formed sterically hindered pyrrolidine amide **110** in 52% over 2 steps (Scheme 6.3b).



Scheme 6.2 Synthesis of pyrrolidine amide **106** from pyrrolidine-3-AQ amide **2**.

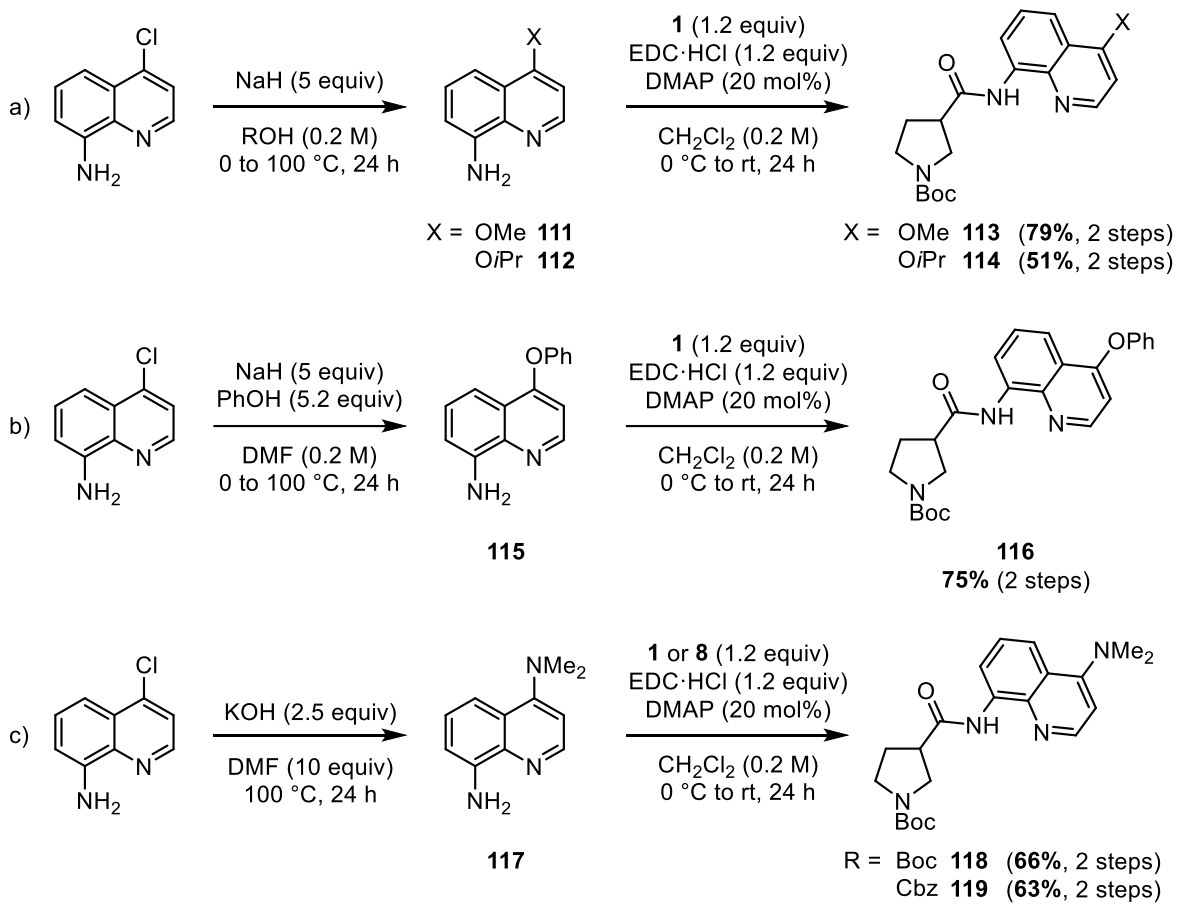


Scheme 6.3 Synthesis of acyl hydrazide **107** and pyrrolidine amide **110** from 8-hydroxyquinoline and 7-methyl-8-nitroquinoline.

Following this, 4-substituted 8-aminoquinoline substrates were synthesised *via* nucleophilic aromatic substitution (S_NAr). 4-Methoxy-8-aminoquinoline **111** was obtained treating the corresponding 4-chloro derivative with NaH and MeOH at reflux (Scheme 6.4a). Subsequent amide bond formation afforded the desired pyrrolidine amide **113** in 79% yield over 2 steps. A similar 2-step telescoped sequence was used to access 4-O*i*Pr and 4-OPh derivatives **114** and **116** (Scheme 6.4a,b).

Finally, *N*-Boc and *N*-Cbz 4-dimethylamino derivative **118** and **119** were obtained in 63–66% yield by means of a similar S_NAr strategy, where 4-chloro-8-aminoquinoline was treated with KOH in DMF at 100 °C to form dimethylquinoline-4,8-diamine **117** (Scheme 6.4c).[279]

With these AQ amide derivatives in hand, their effect on the C(4)–H arylation was evaluated.

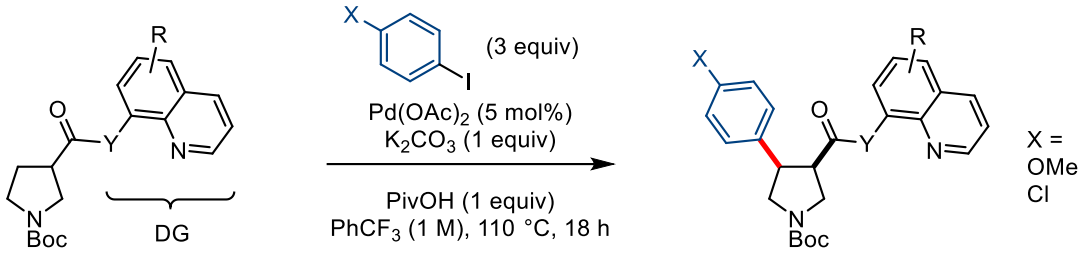


Scheme 6.4 2-Step synthesis of 4-substituted-8-AQ substrates **113**, **114**, **116**, **118** and **119** from 4-chloro-8-aminoquinoline.

6.2.2 Directing Group Effect on Reaction Outcome

The efficiency of the various DGs was compared in the reaction with both 4-iodoanisole and 4-chloro-iodobenzene under identical conditions to those optimised in chapter 3. This was to ensure the reaction outcome to be independent of the electronic properties of the aryl iodide. First, the effect of modifications affecting the proximal binding site was investigated (Table 6.5).

No reaction was observed when using a hydrazide linker, and unreacted starting material **108** was fully recovered (entry 2). This supported an essential role played by the bidentate 5-membered chelation mode of the AQ amide to promote a productive reaction. Similarly, increasing the steric hindrance around the proximal binding site by addition of a 7-Me group, resulted in no conversion, likely due to more difficult C–H activation and/or OA steps (entry 3). Decreasing the electron density by installation of a chloride functionality either at the 6- or 5-position resulted in lower yields of the corresponding arylated products, in comparison to the unsubstituted system (entries 4 and 5). The higher conversion observed in the reaction with 4-iodoanisole (**122a** and **123a**) suggested a turnover-limiting RE step also in the presence of this less electron-rich DG.



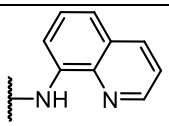
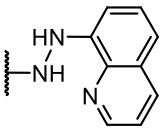
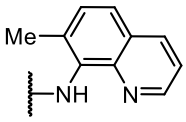
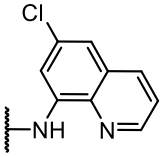
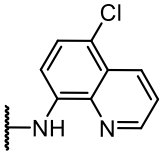
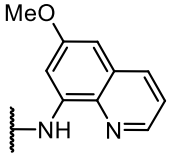
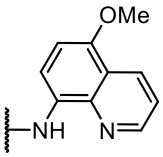
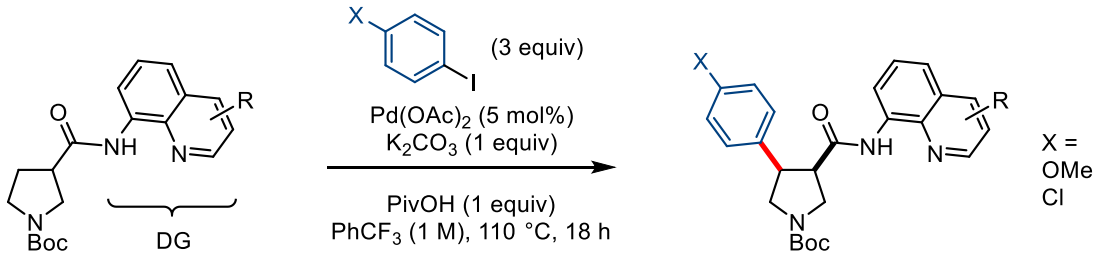
entry	DG	SM	X	yield (%)[a]			
				product		RSM	tot
1		**2**	OMe	**3a**	65	27	92
			Cl	**3e**	45	44	89
2		**108**	OMe	**120a**	-	> 95	> 95
			Cl	**120b**	n.d.	n.d.	n.d.
3		**110**	OMe	**121a**	-	> 95	> 95
			Cl	**121b**	n.d.	n.d.	n.d.
4		**102**	OMe	**122a**	41	49	90
			Cl	**122b**	10	72	82
5		**106**	OMe	**123a**	33	61	94
			Cl	**123b**	19	81	100
6		**103**	OMe	**124a**	72	15	87
			Cl	**124b**	56	40	96
7		**104**	OMe	**125a**	68	25	93
			Cl	**125b**	52	47	99

Table 6.5 Investigation into the steric and electronic properties of the proximal binding site on the DG. Reaction scale: 0.2 mmol. [a] Calculated by ^{1}H NMR using 1,3,5-TMB as internal standard.

On the other hand, higher reactivity was restored upon introduction of electron-donating 6- and 5-methoxy substituents (entries 6 and 7). However, these did not result in any significant improvement compared to the parent DG, although slightly higher yields were observed in the reaction with 4-chloro-iodobenzene.

The effect of similar structural modifications affecting the distal binding site was then examined (Table 6.6). Introducing a methyl group at the 2-position, adjacent to the coordinating nitrogen, resulted in full recovery of unreacted substrate **101** (entry 2). This was likely due to the increase in steric hindrance, preventing an efficient coordination to the Pd centre.



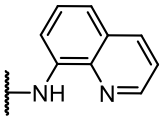
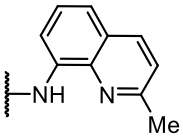
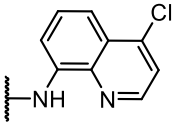
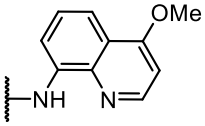
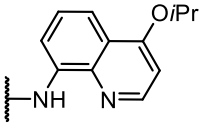
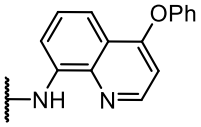
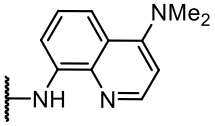
entry	DG	SM	X	yield (%)[a]			
				product		RSM	tot
1		**2**	OMe	**3a**	65	27	92
			Cl	**3e**	45	44	89
2		**101**	OMe	**126a**	-	> 95	> 95
			Cl	**126b**	n.d.	n.d.	n.d.
3		**105**	OMe	**127a**	49	45	92
			Cl	**127b**	29	68	97
4		**113**	OMe	**128a**	83	13	96
			Cl	**128b**	63	34	96
5		**114**	OMe	**129a**	76	11	87
			Cl	**129b**	60	38	98
6		**116**	OMe	**130a**	75	19	94
			Cl	**130b**	53	44	97
7		**118**	OMe	**131a**	**81** (71)[b]	**4** (18)[b]	**85** (92)[b]
			Cl	**131b**	**76**	**19**	**97**

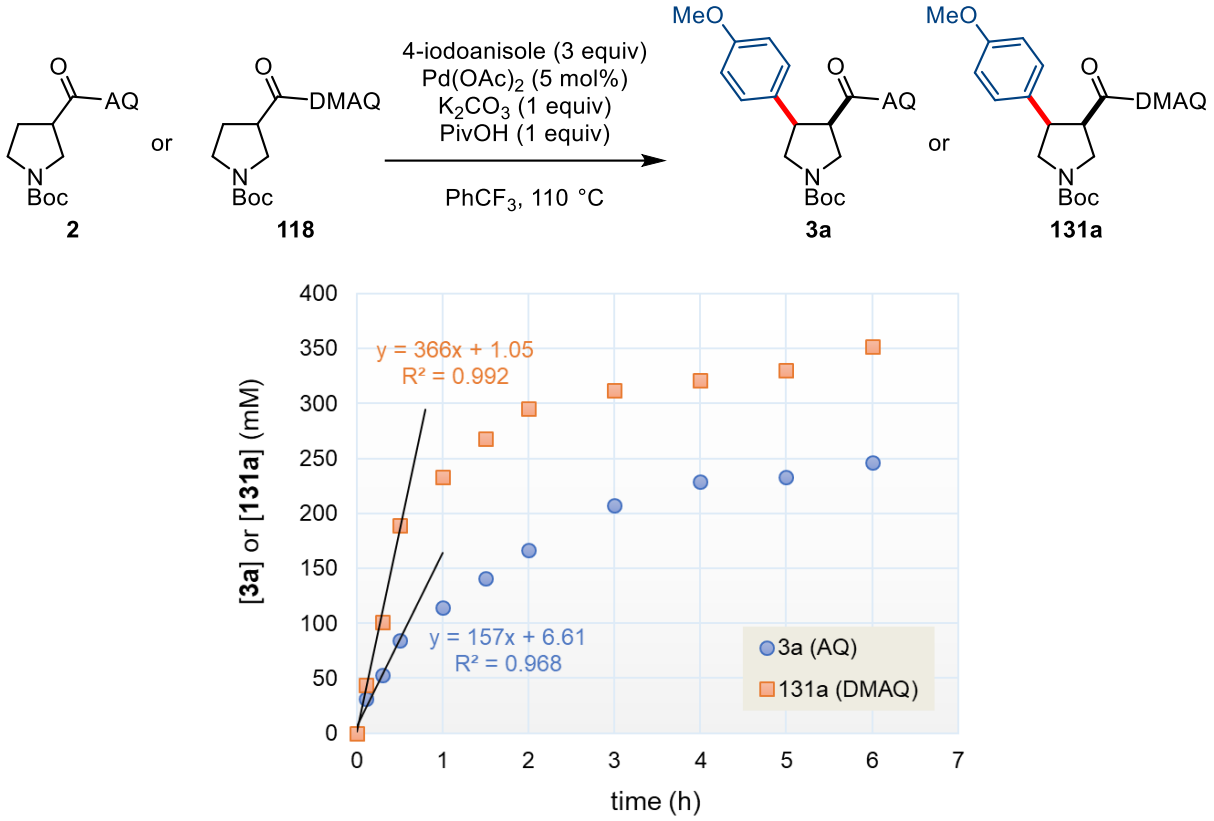
Table 6.6 Investigation into the steric and electronic properties of the distal binding site on the DG. Reaction scale: 0.2 mmol. [a] Calculated by ^{1}H NMR using 1,3,5-TMB as internal standard. [b] ^{1}H NMR yields obtained using 1 equivalent of ArI are reported in brackets.

Similarly to the results for the proximal binding site, the introduction of an electron-withdrawing substituent at the quinoline 4-position resulted in lower yields of both *p*-chloro- and *p*-methoxyphenyl pyrrolidine products **127a** and **127b** (entry 3). Nonetheless, a decreased detrimental effect was observed in comparison with either the 6-Cl or 5-Cl substitution patterns. On the other hand, when a methoxy group was installed at the 4-position, a significant increase in reactivity was observed (entry 4). Using this electron-rich DG, arylated pyrrolidine products **128a** and **128b** were obtained in 83% and 63% NMR yield respectively, corresponding to an increase of about 20% in both cases, compared to the unsubstituted AQ auxiliary.

Encouraged by this promising result, the electronic properties of the distal binding site were further explored. Increasing slightly the electron-donating character of the 4-substituent (-O*i*Pr) did not result in any improvement (entry 5). On the other hand, a small reduction in the yield of *p*-chlorophenyl derivative **130b** was observed when using a less electron-donating 4-phenoxy group (entry 6). Finally, in the presence of an even more electron-donating dimethylamino substituent ($\sigma_p[NMe_2] = –0.87$ *vs* $\sigma_p[OMe] = –0.27$),[261] 4-arylated pyrrolidines **131a** and **131b** were obtained in 81% and 76% NMR yield respectively (entry 7). This represented a substantial improvement compared to the original AQ system, particularly in the reaction with 4-chloro-iodobenzene. In addition, using this DG, the equivalents of 4-iodoanisole could be reduced from 3 to 1, resulting in just 10% decrease in NMR yield of **131a** (entry 7). Therefore, this novel 4-dimethylamino-8-quinolinyl (DMAQ) amide DG was selected for further investigations.

First, the rate of C–H arylation was evaluated. A reaction profile for the formation of product **131a** was constructed and compared with the one previously obtained using the unsubstituted AQ system, under otherwise identical conditions (Scheme 6.5). Pleasingly, a 2-fold increase in the initial rate of arylation was observed with the new DG. This allowed higher yields of the arylated product to be obtained in shorter reaction times, despite the progressive plateauing of the reaction. As such, approximately 80% NMR yield of pyrrolidine derivative **131a** could be obtained after just 6 h reaction.

Next, the scope and limitations of the C(4)–H arylation reaction with DMAQ directing group were investigated.



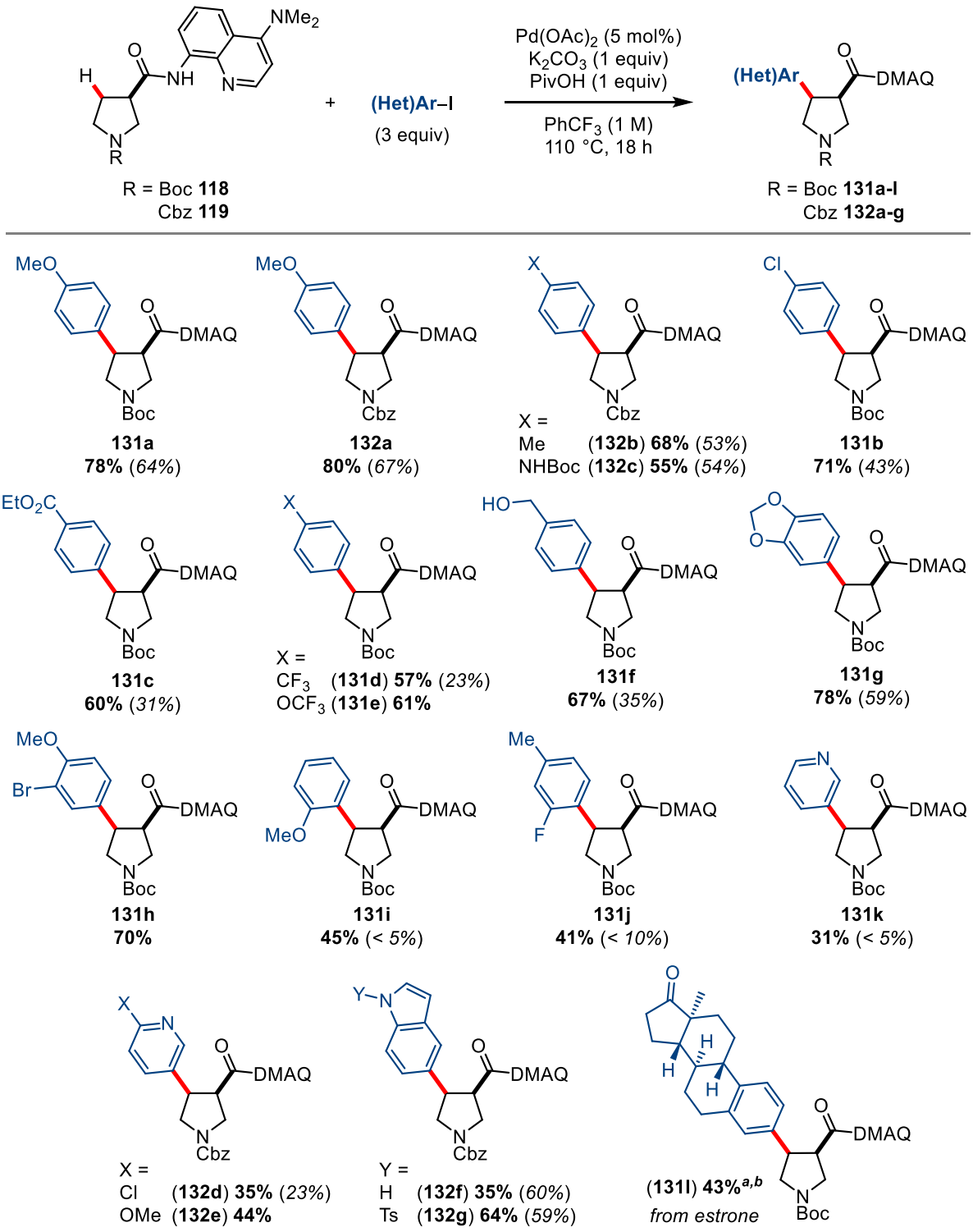
Scheme 6.5 Comparison of temporal profiles for product formation using either AQ or DMAQ directing groups. Each time point corresponds to a discrete reaction.

6.3 Scope of Pyrrolidine C(4)–H Arylation with DMAQ Directing Group

The reaction scope was evaluated varying both *N*-protecting groups and aryl iodide coupling partners (Scheme 6.6). Particular attention was paid to functionalities that were poorly tolerated under the previous AQ system, including electron-poor as well as *ortho*-substituted iodides.

First, Boc and Cbz *N*-protecting groups were investigated in the reaction with 4-iodoanisole. Pleasingly, DMAQ amides **118** and **119** showed similar reactivity, affording *cis*-3,4-disubstituted pyrrolidines **131a** and **132a** in 78% and 80% yield respectively. While the regio- and stereoselectivity of the transformation were identical to those observed with the 1st generation system, the DMAQ auxiliary allowed the desired arylated products to be formed in significantly higher yields. Furthermore, the higher conversion enabled an easier chromatographic separation from the unreacted substrate.

Under the same conditions previously optimised for pyrrolidine-3-AQ derivatives, *para*-substituted aromatic groups could be installed in 55–80% yields (**131a–f**, **132a–c**). This corresponded to an important improvement compared to 23–67% yields previously found for the same iodide reagents.



Scheme 6.6 Scope of *N*-protecting groups and aryl iodides for pyrrolidine C–H arylation using DMAQ directing group. When applicable, yields obtained for the same aryl iodide with the AQ system are reported in brackets. Reaction scale: 0.2 mmol. Products isolated as single *cis*-diastereomers and < 5% C2-arylation. [a] 1 equiv ArI. [b] Isolated as 1:1 mixture of *cis*-3,4-diastereomers.

More electron-rich arenes were again characterised by higher reactivity (**131a**, **132a–b**), suggesting RE to remain the turnover-limiting step. Nonetheless, the most striking

improvement associated to the new DG was observed in the presence of electron-withdrawing substituents (**131b–131e**). A ~30% higher yield was obtained in the reaction with 4-chloro-iodobenzene, forming 4-aryl pyrrolidine derivative **131b** in 71% yield. An increase in reactivity of similar magnitude was found for electron-withdrawing 4-CO_2Et and 4-CF_3 groups (**131c,d**), which were installed in 60% and 57% yield respectively, against 32% and 23% previously observed. Furthermore, trifluromethoxy and benzyl alcohol functionalities were well-tolerated, affording the corresponding pyrrolidine products **131e,f** in good yields. *meta*-Substituted aryl iodides reacted well under the optimised conditions, affording benzodioxole and 3-bromo-4-methoxyphenyl derivatives in 70–78% yield (**131g,h**).

Pleasingly, the new DG enabled the scope of coupling partners to finally include more sterically hindered *ortho*-substituted aryl iodides. Reaction with 2-iodoanisole, completely unsuccessful with the AQ auxiliary, now afforded pyrrolidine **131i** in 45% yield. The reaction was also tolerant of more electron-withdrawing functionalities at the *ortho*-position, giving 2-fluoro derivative **131j** in good yield. Importantly, the reaction scope could be extended to electron-poor heteroaromatic groups, which could not be installed under the 1st generation system. In particular, 4-(3-pyridyl)-pyrrolidine derivative **131k** was isolated in synthetically useful 31% yield. This was likely due to the stronger chelating ability of the DMAQ auxiliary compared to the AQ, which could outcompete the unproductive coordination from the pyridine coupling partner. Despite this encouraging result, the reaction was still limited with very electron-poor pyridyl iodides, and only a minor improvement was observed in the reaction with 2-chloro-5-iodopyridine (**132d**). On the other hand, higher reactivity was observed with more electron-rich pyridyl rings, including 2-methoxy-pyridine derivative **132e** formed in 44% yield.

Interestingly, unprotected 5-iodoindole gave a reduced yield of compound **132f** in comparison with the AQ system. This indicated that the use of highly electron-rich aryl iodides might result in lower performances with the DMAQ auxiliary, suggesting a higher barrier for the oxidative addition step. On the other hand, good reactivity was restored upon reduction of the electron density by NH protection, affording *N*-tosyl indole derivative **132g** in 64% yield.

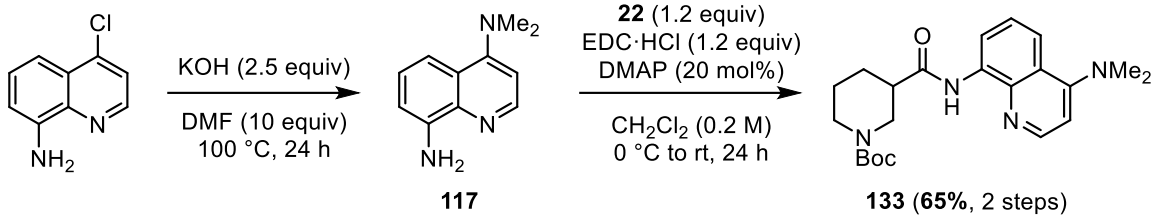
Finally, offering the potential to reduce the equivalents of aryl iodides while preserving good reactivity, the new DG could promote the efficient installation of more complex and less readily available aromatic substituents. This was exemplified in the synthesis of alkylated estrone derivative **131l**, which could be obtained in 43% yield using just 1 equivalent of estrone-derived aryl iodide.[†††]

[†††] Aryl iodide synthesised by Alexander Boddy (Imperial College London).

Following this study on pyrrolidine arylation, the C(4)–H functionalisation of piperidine rings in the presence of DMAQ directing group was evaluated.

6.4 Piperidine C(4)–H Arylation with DMAQ Directing Group

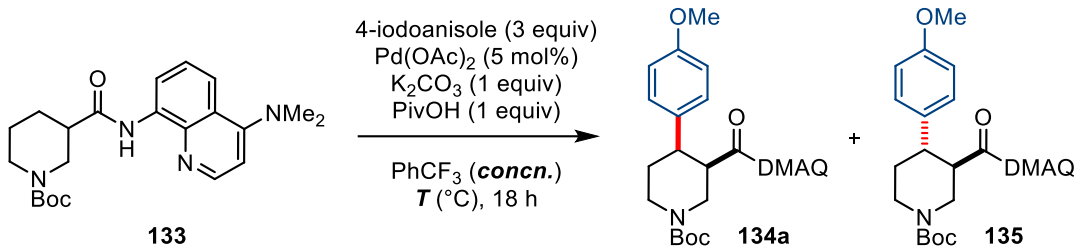
N-Boc piperidine-3-DMAQ amide **133** was synthesised through the same 2-step telescoped sequence use for the corresponding pyrrolidine ring, involving treatment with KOH and DMF, followed by amide bond formation (Scheme 6.7). With this derivative in hand, the Pd-catalysed C(4)–H arylation was investigated.



Scheme 6.7 2-Step synthesis of piperidine-3-carboxamide substrate **133** from 4-chloro-8-aminoquinoline.

Pleasingly, reaction with 4-iodoanisole proceeded well, affording *cis*- and *trans*-4-arylated piperidine derivatives **134a** and **135** in 77% combined yield by ^{1}H NMR (Table 6.7, entry 1). Although the formation of a small amount of unidentified side-products was observed, this represented a good improvement from the 1st generation AQ system, which gave the corresponding derivatives in 64% overall yield (Table 3.8, section 3.5.1). Furthermore, an interesting improvement in *cis*-diastereoselectivity was observed with the DMAQ directing group, resulting in a 82:18 *dr* (*cis:trans*) against 66:34 *dr* previously obtained. This might be ascribed to the new DG having an opposite influence on OA and RE steps, which were found to limit the formation of *trans*- and *cis*-piperidine products, respectively (see section 5.4.3).

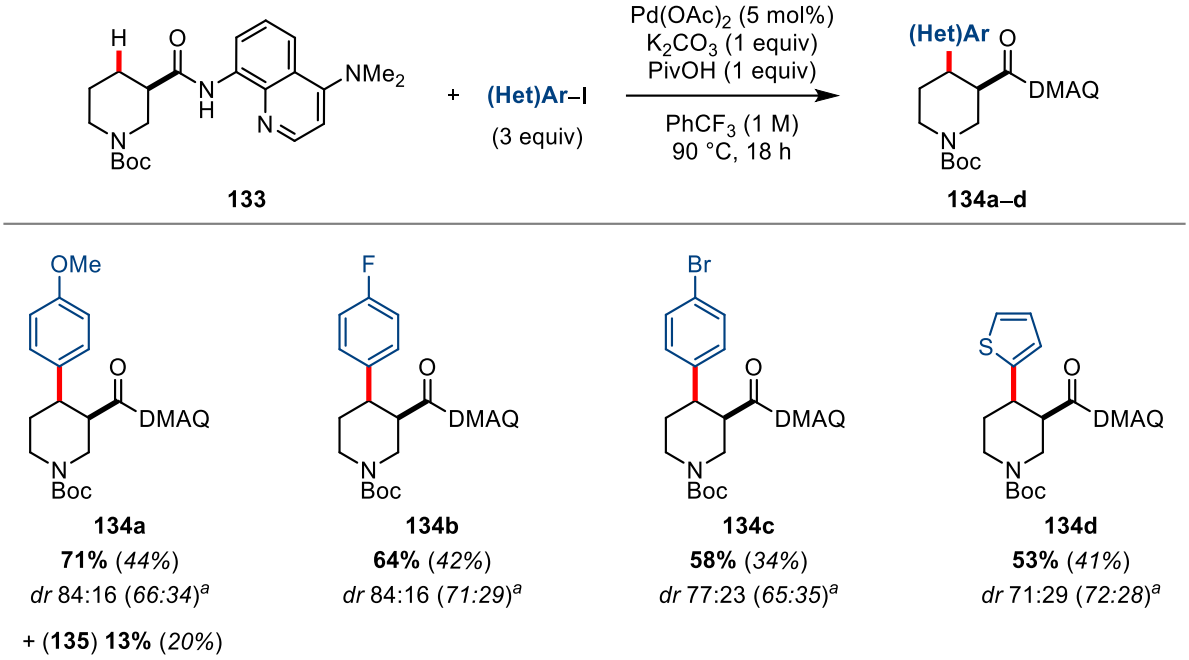
Encouraged by this promising result, continuous variables such as concentration and reaction temperature were screened, in order to improve the mass recovery and/or the diastereoselectivity (Table 6.7). Halving the concentration to 0.5 M resulted in lower overall conversion, while similar mass recovery and *dr* were observed (entry 2). On the other hand, lowering the temperature to 90 °C gave a higher combined yield of piperidine derivatives **134a** and **135**, due to reduced side-products formation (entry 3). Finally, lower temperatures of 80 or 70 °C resulted in poorer substrate conversion, while not providing any significant improvement in diastereoselectivity (entries 4 and 5). Therefore, 90 °C was selected as optimum temperature to evaluate the aryl iodide scope for piperidine C(4)–H arylation.



entry	temp (°C)	conc. (M)	133 (%)[a]	134a + 135 (%)[a,b]	tot (%)[a]	dr[c]
1	110	1.0	9	77	86	82:18
2	110	0.5	15	69	84	84:16
3	90	1.0	9	81	90	84:16
4	80	1.0	22	69	91	83:17
5	70	1.0	37	60	97	87:13

Table 6.7 Screening of continuous variables for the C–H arylation of *N*-Boc piperidine amide **133**. Reaction scale: 0.2 mmol. [a] Calculated by ^{1}H NMR using 1,3,5-TMB as internal standard. [b] Combined NMR yield of *cis*- and *trans*-arylated derivatives **134a** and **135**. [c] *dr* (*cis:trans*) estimated by ^{1}H NMR.

As a result of higher reactivity and better stereoselectivity, *cis*-configured *p*-methoxyphenyl piperidine **134a** was isolated in 71% yield (*vs* 44% previously obtained), alongside 13% of *trans*-isomer **135** (Scheme 6.8). Similarly higher yields (58–64%) were found for *cis*-piperidine derivatives **134b** and **134c**, potential intermediates in the synthesis of paroxetine and Br-paroxetine, respectively (see chapter 4). Finally, heteroaromatic groups were well-tolerated, as exemplified in the reaction with 2-iodothiophene, though no increase in *dr* was observed in this case (**134d**).



Scheme 6.8 Scope of aryl iodides for the C–H arylation of piperidne-3-DMAQ amide **133**. Yields and *dr* obtained for the same aryl iodide with the AQ system are reported in brackets. Reaction scale: 0.2 mmol. Products isolated as single diastereomers and < 5% C2-arylation. [a] *dr* (*cis:trans*) estimated by ^{1}H NMR on the crude reaction mixture.

6.5 Mechanistic Rationale for the Improvement in Reactivity

At this point in the study, the effect of the DMAQ directing group on the reaction mechanism was investigated to understand better the improvement in reactivity observed for both pyrrolidine and piperidine rings.

Reasoning that the higher efficiency of the DMAQ-directed arylation might result from a slower catalyst deactivation, this possibility was first examined.

6.5.1 Estimation of Catalyst Deactivation with DMAQ Directing Group

Initially, the kinetic order in pyrrolidine-3-DMAQ amide **118** was evaluated using Burès VTNA analysis (Figure 8.1 in Experimental part 8.2.6).[257a] As for the previous AQ auxiliary, a zero-order dependency in pyrrolidine substrate was observed, suggesting no variation in the overall rate law when incorporating the DMAQ directing group.

Therefore, the catalyst deactivation profile was estimated through the same mathematical linearisation approach previously used (see chapter 5.5.3).[268] After normalisation of the time scale for the sole concentration of ArI, a non-linear plot was again observed (not shown). This was linearised (R^2 = 0.997) using Microsoft Excel's add-in Solver to estimate the concentration of active catalyst at the different time points. Plotting the percentage of residual active catalyst

over time for the two DGs, a slightly slower catalyst deactivation was observed for the DMAQ auxiliary in the early stages of the reaction (Figure 6.1). Nonetheless, the two profiles started to overlap at t = 1 h, and < 20% active catalyst was estimated to be left after 2 h in both cases. Reasoning that the difference in the early time points might be a simple artefact deriving from mathematic manipulation of the kinetic data, no significant difference in catalyst deactivation is likely present between the two DGs.

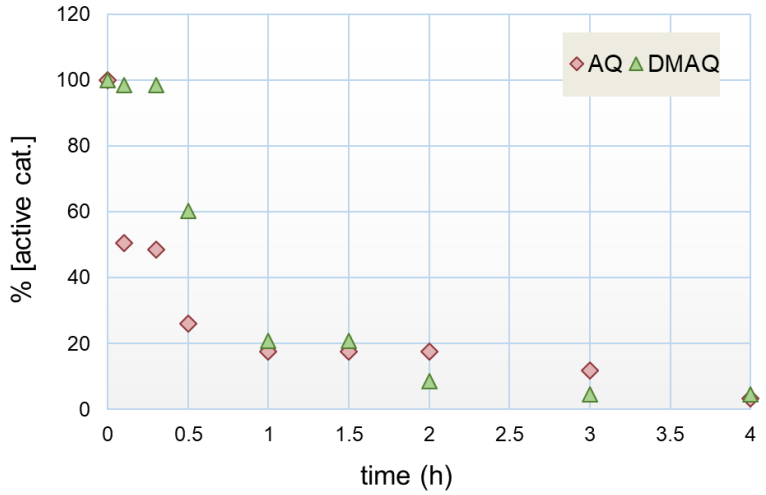


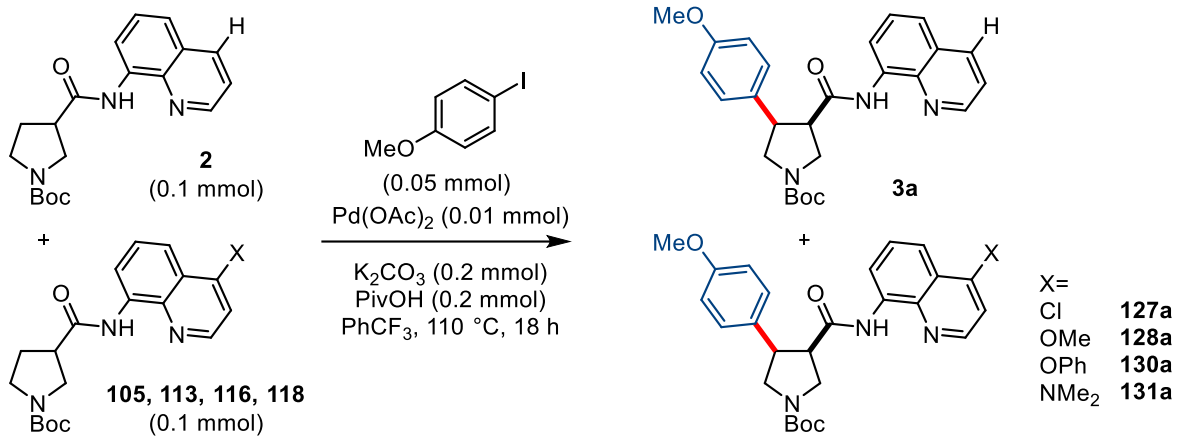
Figure 6.1 Comparison of catalyst deactivation profiles for AQ and DMAQ directing groups.

Following this, additional kinetic and computational studies were undertaken to investigate the mechanistic origin of the beneficial effect of DMAQ directing group.

6.5.2 Kinetic Effect of 4-Substituents on the Directing Group

Although 5-substituted AQ derivatives have been used in the literature either to provide a more easily removable DG (*e.g.* 5-OMe-AQ),[144c] or to avoid competing S_EAr at the activated 5-position (*e.g.* 5-Cl-AQ),[280] no example of 4-substituted AQ directing group have previously been reported in C–H functionalisation reactions. As such, to gain more insight into this substitution pattern, the kinetic effect of different groups at the 4-position was investigated.

First, competition experiments were performed, in which two substrates, bearing different 4-substituted DGs had to compete for a limiting amount of 4-iodoanisole. In particular, the kinetic preference between any of 4-NMe_2, 4-OMe, 4-OPh and 4-Cl substrates and the corresponding unsubstituted system was evaluated (Table 6.8).



entry	X	σ_p[261]	3a (%)[a]	Product (%)[a]	k_X/k_H	log(k_X/k_H)
1	NMe_2 (**118**)	– 0.83	1	**131a** (33)	33	+ 1.519
2	OMe (**113**)	– 0.27	7	**128a** (28)	4.0	+ 0.602
3	OPh (**116**)	– 0.03	11	**130a** (20)	1.8	+ 0.260
4	Cl (**105**)	+ 0.23	18	**127a** (8)	0.5	– 0.301

Table 6.8 Evaluation of 4-substituted DGs in competition experiments.

As only 0.5 equiv of aryl iodide were used, the reactions were stopped after 18 h in order to obtain suitable conversion (~30%). The kinetic effect of the substituents was estimated from the relative amount of product formed. Higher reactivity was observed for more electron-donating substituents, with pyrrolidine-3-DMAQ amide **118** reacting 33 times faster than unsubstituted AQ amide **2** (entry 1). Smaller kinetic ratio of 4 and 1.8 were respectively observed for 4-OMe and 4-OPh substituted substrates (entries 2 and 3). In contrast, a slower reaction compared to pyrrolidine **2** was observed in the presence of an electron-withdrawing chloride substituent (entry 4).

Representing this data as a function of substituent parameters σ_p gave a linear Hammett plot with a negative slope, corresponding to a reaction constant $\rho = -1.72$ (Figure 6.2).[260,261] A similar linear regression was obtained when using the electrophilic substituent constants σ_p+ (not shown).[261,262]

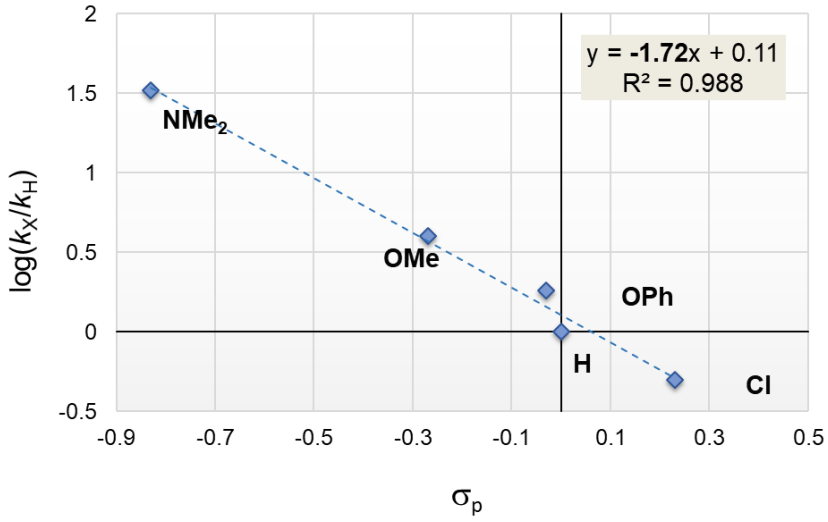


Figure 6.2 Hammett plot for competition experiments with different 4-substituted AQ directing groups.

Despite the high correlation (R^2) observed, it was reasoned that this Hammett correlation might result from a preferential coordination of the catalyst to stronger σ-donating DGs, rather than from a direct effect of the substituents on the energy of the turnover-limiting transition state.[275] Therefore, individual kinetic profiles for the reaction with various 4-substituted DGs were evaluated.

Discrete reactions on 0.1 mmol scale were stopped at different time points in the first 0–30 min of reaction, in order to evaluate the initial rate of arylation with various 4-substituted DGs. Four DGs bearing different substituents at the 4-position (NMe_2, OMe, H and Cl) were evaluated under otherwise identical conditions. The corresponding kinetic constants k_{obs} were estimated from the slope of the straight lines ($R^2 > 0.95$) obtained plotting the product concentration (mM) as a function of time (min) (Figure 6.3 and Table 6.9, also see Scheme 6.5). A faster reaction was again observed for more electron-donating substituents in the order NMe_2 > OMe > H > Cl. Nonetheless, a significant reduction in the relative rate of arylation between pyrrolidine-3-DMAQ amide **118** and unsubstituted substrate **2** was observed in comparison with the competition experiment (k_{DMAQ}/k_{AQ} = 2.1 and 33, respectively). This is consistent with a preferred coordination to the DMAQ directing group increasing the relative arylation rate in competition experiments.

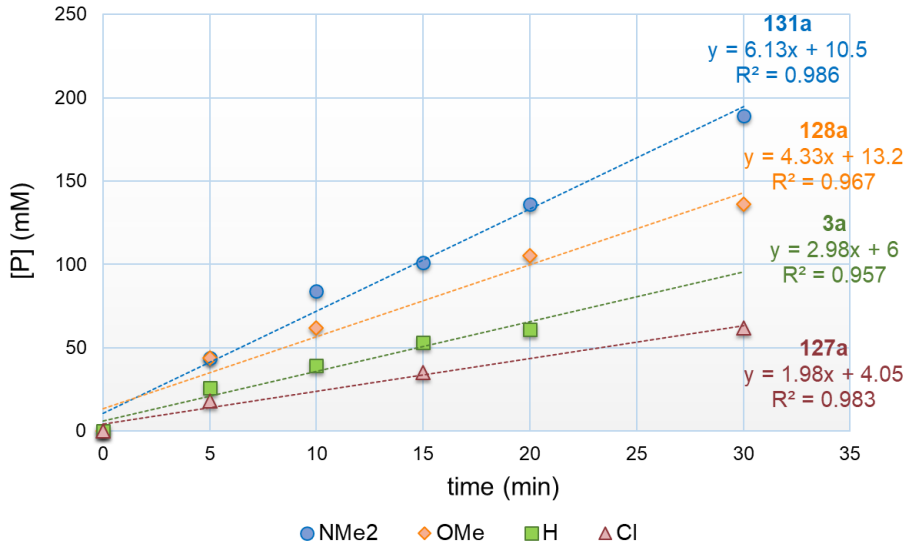
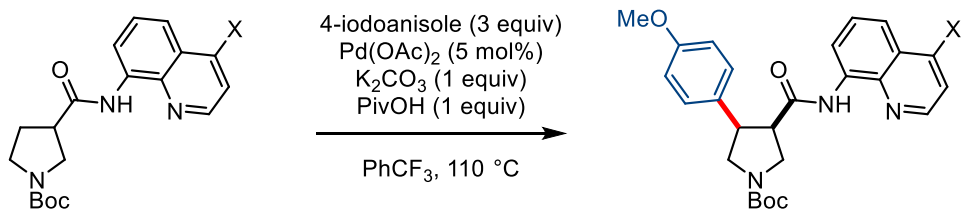


Figure 6.3 Individual initial rates of C–H arylation with different 4-substituted DGs. Each time point corresponds to a discrete reaction.



2, 105, 113, 118 **3a, 127a, 128a, 131a**

entry	X	σ_p[261]	k_{obs} (mM/min)	log(k_X/k_H)
1	NMe_2 (**118**)	– 0.83	+ 6.13	+ 0.314
2	OMe (**113**)	– 0.27	+ 4.33	+ 0.162
3	H (**2**)	0.00	+ 2.98	0.00
4	Cl (**118**)	+ 0.23	+ 1.98	– 0.178

Table 6.9 Individual kinetics of C(4)–arylation using different 4-substituted DGs.

Finally, construction of the corresponding Hammett plot revealed a negative linear dependence with $\rho = -0.45$ (Figure 6.4). This suggested that higher σ-donation character of the distal nitrogen binding site could reduce the activation energy of the turnover-limiting RE step. This is consistent with the higher reactivity observed with electron-poor aryl iodides in the DMAQ-directed C(4)–H arylation. Such effect might be speculatively ascribed to an increased structural *trans*-effect (STE) due to the stronger σ-donation of the quinoline ligand, weakening the *trans*-C–Pd bond on Pd(IV) intermediates and thus facilitating RE.[281]

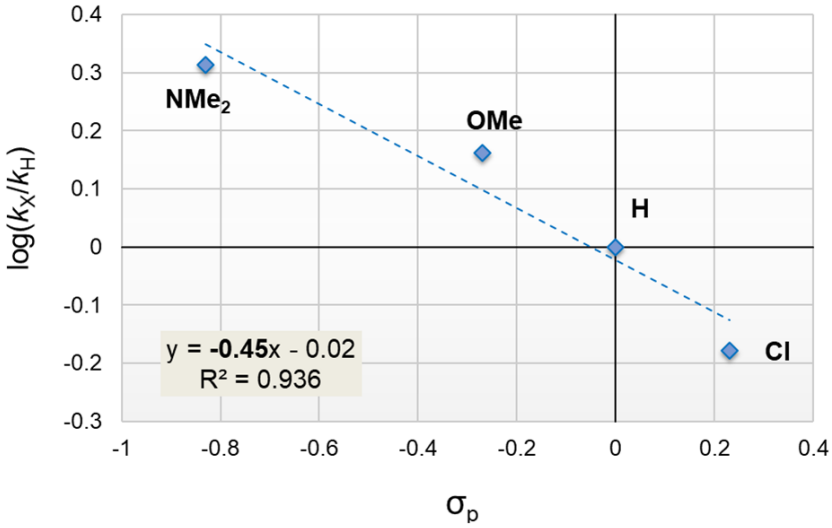


Figure 6.2 Hammett plot for individual kinetics of C–H arylation using different 4-substituted AQ directing groups.

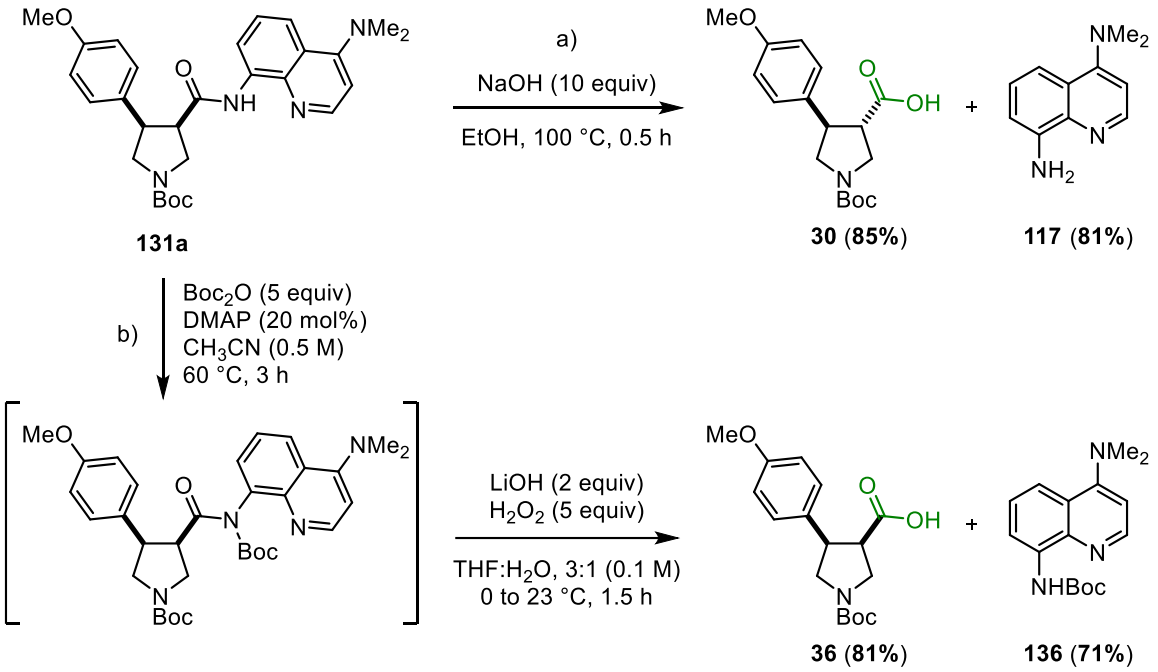
DFT calculations were performed by Luis Casarrubios (Universidad Complutense de Madrid) to support this mechanistic hypothesis. Unfortunately, no significant difference in the energetic barrier for the RE step could be observed between the DMAQ and AQ directing groups ($\Delta\Delta G^{\ddagger}$ = 0.5 kcal·mol^{-1}). As such, no conclusive rationale could be obtain computationally (for full reaction profile, see Appendix VI).

6.6 Removal of DMAQ Directing Group

To demonstrate the synthetic utility of the new DG, various strategies for its removal were examined.

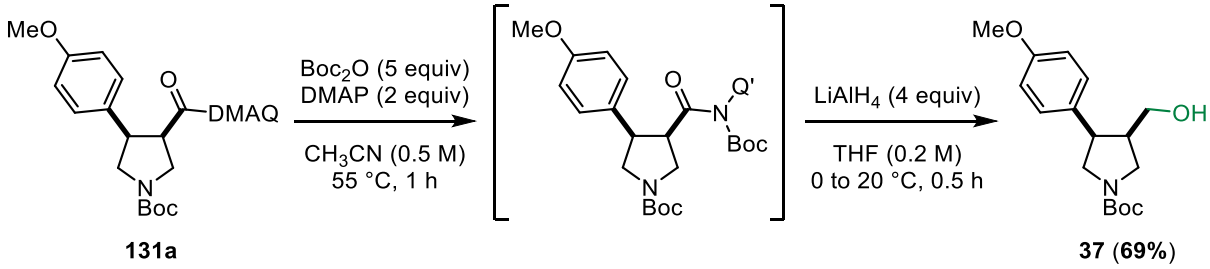
Unfortunately, the direct oxidative cleavage of the DMAQ auxiliary in the presence of IBX was unsuccessful, resulting in full recovery of unreacted pyrrolidine **131b** (not shown). Nonetheless, DMAQ removal was demonstrated under different conditions, allowing access to carboxylic acid- and alcohol-containing pyrrolidine building blocks (Scheme 6.9).

Treating arylated pyrrolidine-3-DMAQ amide **131a** with NaOH at 100 °C in EtOH afforded 4-methoxyphenyl derivative **30** in 85% yield as a single *trans*-diastereoisomer, upon acid/base work-up (Scheme 6.9a). Furthermore, DMAQ amine **117** could be recovered in 81% yield after chromatographic purification of the resulting organic phase, allowing the DG to be recycled. On the other hand, amide activation followed by hydrolysis with LiOOH provided access to *cis*-carboxylic acid derivative **36** in similarly high yield (Scheme 6.9b). In this case, the removed DG was recovered as Boc-protected DMAQ amide **136** in 71% yield.



Scheme 6.9 DMAQ removal to access *trans*- and *cis*-carboxylic acid derivatives **30** and **36**, allowing recovery of the DG.

Finally, the synthesis of hydroxymethyl pyrrolidine derivative **37** was demonstrated from **131a** using the same Boc-protection/reduction sequence previously developed for AQ removal (Scheme 6.10).

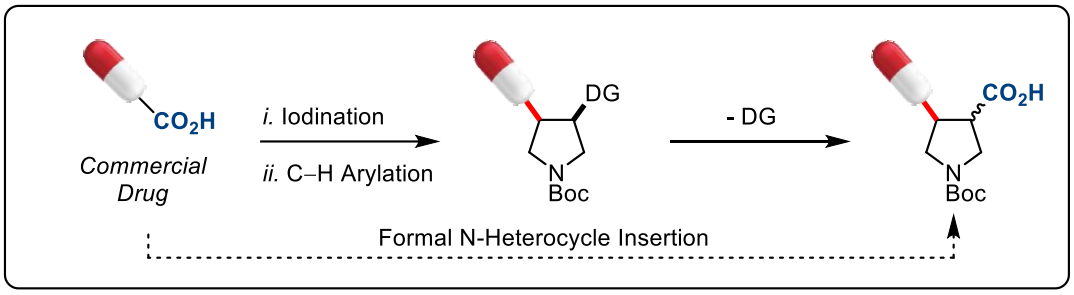


Scheme 6.10 Access to hydroxymethyl pyrrolidine derivative **37** by reductive DMAQ removal. Q' = dimethylaminoquinolin-8-yl.

Following this study, the synthetic potential of the improved DMAQ directing group was evaluated in the late-stage functionalisation of pharmaceutically relevant compounds.

6.7 Medicinal Chemistry Applications: Late-Stage Functionalisation of Acid-Containing Drugs

It was reasoned that the improved C(4)–H arylation using the DMAQ auxiliary could open new opportunities for the late-stage functionalisation of complex biorelevant molecules. In particular, a combination of C–H arylation and recent decarboxylative iodination methods was envisaged to provide rapid access to N-heterocyclic derivatives of benzoic acid-containing drugs (Scheme 6.11).

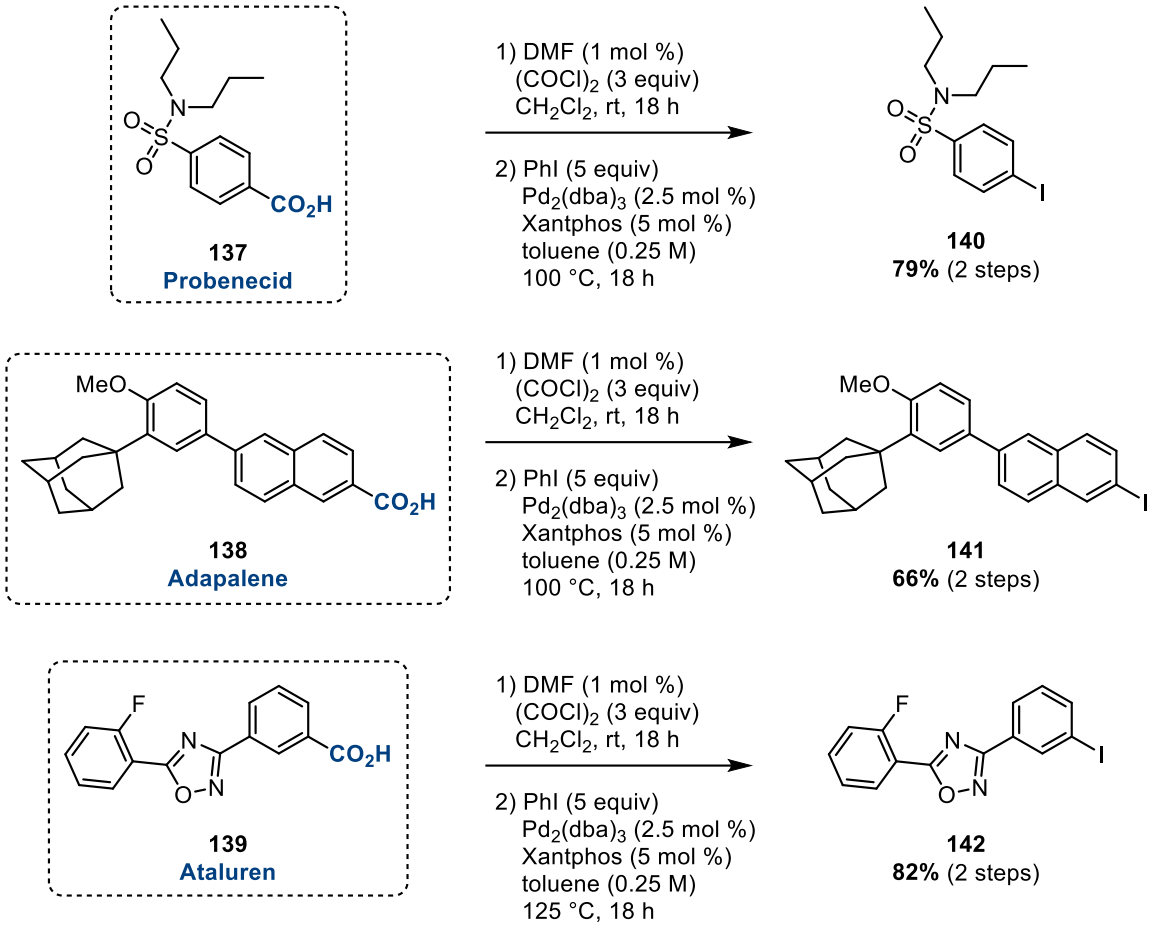


Scheme 6.11 Proposed synthetic strategy for the late-stage functionalisation of acid-containing drugs.

In 2018, Morandi reported a powerful Pd-catalysed functional group metathesis for the direct conversion of aroyl chlorides into aryl iodides, including various late-stage functionalisation examples.[282] A similar strategy was envisaged to access complex aryl iodides from commercial drugs compounds. These could then be used as coupling partners in the C(4)–H functionalisation of pyrrolidine rings with just 1 equivalent, avoiding the usual requirement for large excess. Final DG removal would regenerate the carboxylic acid functionality, representing overall a formal N-heterocycle insertion into the original pharmacophore.

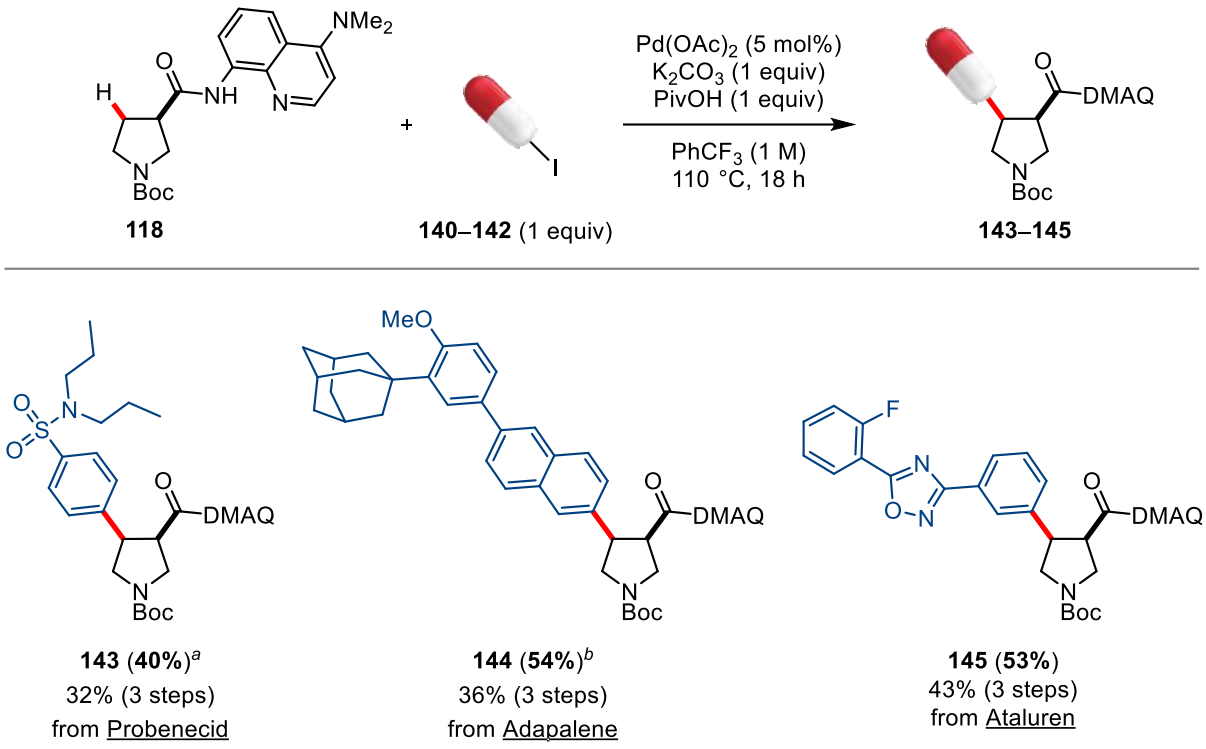
As such, this transformation would open new opportunities for late-stage structure-activity relationship (SAR) studies in drug discovery. In particular, with the possibility to access both *cis*- and *trans*-derivatives, different orientations of the acid group could be explored, offering the potential to develop new binding interactions with the biological targets.

With this proposal in mind, three benzoic acid-containing drugs were targeted to access the corresponding aryl iodides: anti-hyperuricemic Probenecid **137**,[283] anti-acne Adapalene **138**,[284] and Ataluren **139**, recently approved for the treatment of Duchenne muscular dystrophy.[285] Pleasingly, using Morandi's decarboxylative iodination conditions,[282] the corresponding aryl iodides **140–142** were formed in high yields (66–82% over 2 steps), without requiring the controlled atmosphere of a glovebox (Scheme 6.12).



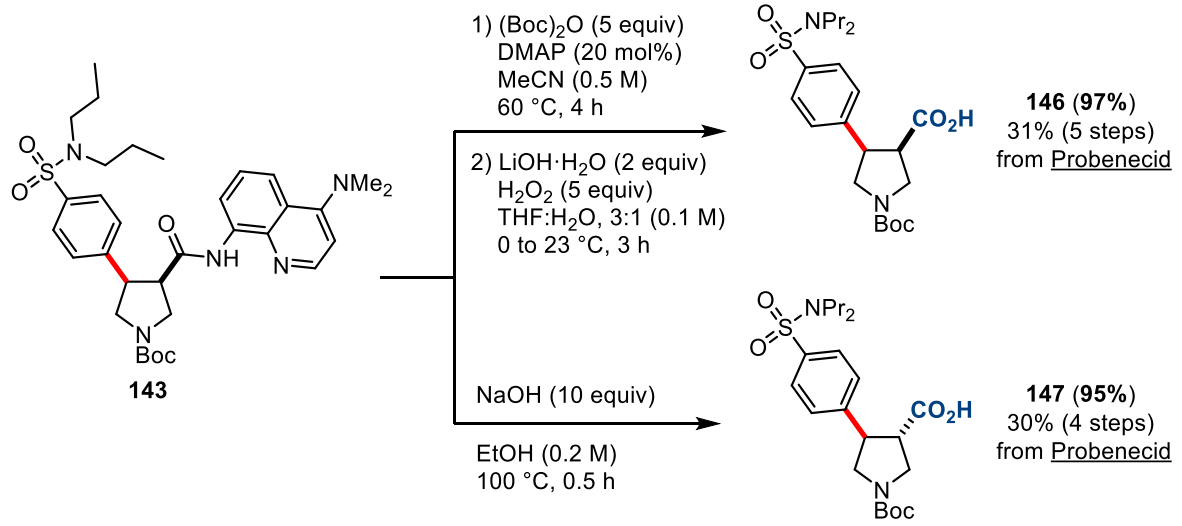
Scheme 6.12 Synthesis of aryl iodides **140**, **141** and **142**, from Probenecid, Adapalene and Ataluren drugs.

With these derivatives in hand, the following C(4)–H arylation step was investigated (Scheme 6.13). Using a 1:1 ratio of iodide **140** and pyrrolidine **118**, 4-arylated product **143** was obtained in 40% yield on a 1 mmol scale, corresponding to 32% over 3 steps from Probenecid drug. Despite the modest yield observed, a similar transformation would not have been possible with the previous AQ system, considering the use of just 1 equivalent of coupling partner and the electron-poor nature of Probenecid derivative **140**. On the other hand, Adapalene and Ataluren derivatives **141** and **142** were better tolerated, and could be respectively installed in 54% and 53% yields, highlighting the high functional group tolerance of the C(4)–H arylation protocol. Pleasingly, this corresponded to 36% and 43% yield over 3 steps from the respective drug compounds. The use of lower concentration (0.75 M) and different order of addition in the reaction set-up (ArI added last) were crucial to obtain good reactivity with Adapalene iodide **141**, due to the very poor solubility of this derivative.



Scheme 6.13 Pd-catalysed C(4)–H arylation of pyrrolidine **118** with aryl iodides **140–142** derived from commercial drug compounds. Reaction scale: 0.2 mmol, unless otherwise stated. [a] 1.0 mmol scale, 2 M concentration. [b] 0.75 M concentration.

Finally, DG removal to uncover the carboxylic acid functionality was demonstrated on pyrrolidine **143** (Scheme 6.14). Pleasingly, both *cis*- and *trans*-pyrrolidine acids **146** and **147** were formed with almost quantitative conversion, providing access to N-heterocyclic Probenecid derivatives in 4–5 steps and 30%–31% overall yields.



Scheme 6.14 Synthesis of *cis*- and *trans*-configured Probenecid derivatives **146** and **147**.

6.8 Conclusions

In conclusion, a novel 4-dimethylamino-8-quinolinyl (DMAQ) amide directing group was developed to improve the regio- and stereoselective C(4)–H arylation of pyrrolidine and piperidine rings.

This allowed *cis*-3,4-disubstituted pyrrolidine derivatives to be formed in higher yields, up to 80%, while expanding the scope of aryl iodide coupling partners. Significantly higher reactivity was observed with electron-poor aryl iodides, resulting in ~30% increase in yield in comparison with the AQ system. *ortho*-Substituted and electron deficient heteroaryl iodides, which were not previously tolerated, could be successfully installed. Furthermore, the loading of coupling partner could be reduced to 1 equivalent, without a significant detrimental effect on the reaction outcome, enabling the use of more complex and less readily available aryl iodides.

A similar increase in reactivity, accompanied by higher *cis*-diastereoselectivity, was observed for the corresponding 6-membered ring. This allowed *cis*-4-arylated piperidine derivatives, including intermediates in the synthesis of paroxetine drug and its Br-paroxetine analogue, to be accessed with higher efficiency.

In addition, the new DG resulted in a 2-fold increase in the reaction rate, although mechanistic studies excluded a slower catalyst deactivation as the rationale for this improvement. On the other hand, kinetic analysis into the unprecedent 4-substitution pattern of the DG suggested a stronger coordination to the Pd centre, and an easier turnover-limiting reductive elimination.

Efficient removal of DMAQ auxiliary was also demonstrated under different conditions to access carboxylic acid and hydroxymethyl pyrrolidine building blocks, offering the potential for application of this new DG to the synthesis of N-heterocycle fragment compounds.

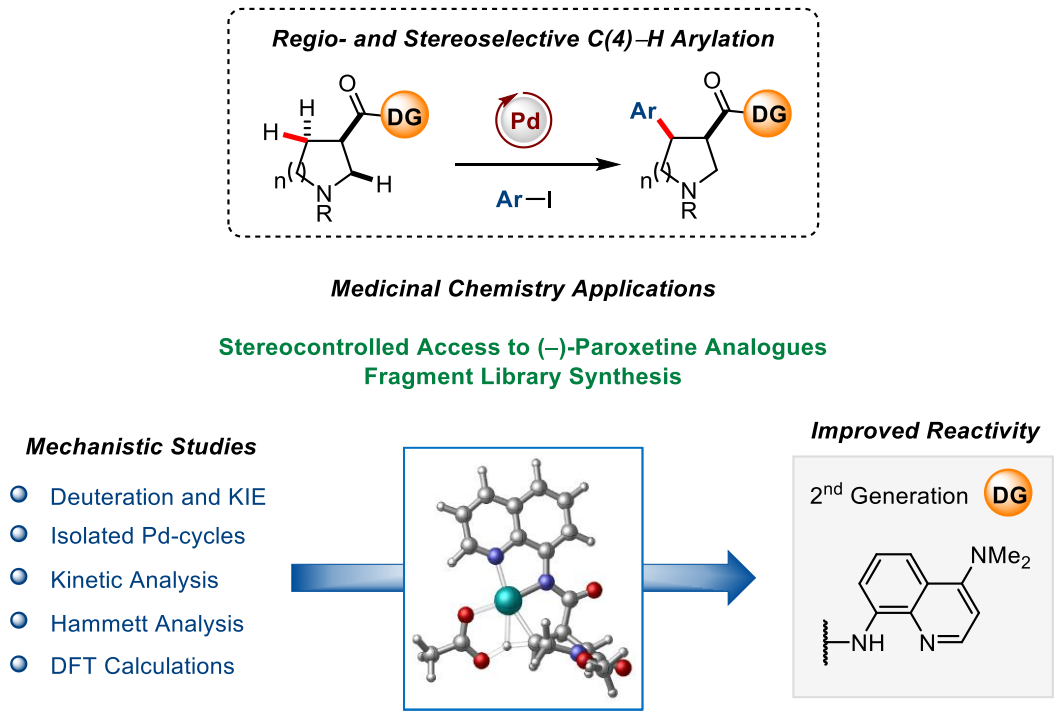
Finally, the synthetic utility of the improved DG was showcased in the late-stage functionalisation of various benzoic-acid containing drugs, opening new opportunities for late-stage SAR studies in drug discovery programs.

7. Conclusions and Future Work

Saturated N-heterocycles are highly attractive structures for pharmaceutical screenings. Pyrrolidine and piperidine rings, in particular, are low-M_W, 3-dimensional, polar scaffolds, prevalent in a wide range of bioactive compounds. As such, these offer high potential as fragments and building blocks in drug discovery programs.

The development of new synthetic methods that can provide access to such valuable compounds, with reliable regio- and stereocontrol, would thus be of important value for the discovery of new therapeutics. Offering high potential for the iterative and divergent synthesis of analogues, the direct C–H functionalisation of readily available heterocyclic precursors is an attractive strategy for the preparation of N-heterocycles with diverse substitution patterns and defined stereochemistry.

In this thesis, a highly regio- and stereoselective Pd-catalysed C(sp^3)–H arylation of pyrrolidines and piperidines at the unactivated 4-position was developed. This was achieved using a bidentate DG at the 3-position, allowing selective access to 3,4-disubstituted N-heterocyclic derivatives with defined *cis*-stereochemistry (Scheme 7.1).



Scheme 7.1 Overview of the research on the regio- and stereoselective C(4)–H arylation of saturated N-heterocycles described in the this thesis.

Subsequent DG removal enabled various applications of this methodology in drug discovery settings. This included the stereocontrolled synthesis of piperidine-based drug compounds and the construction of a library of arylated pyrrolidine and piperidine fragments. Important insights

into the mechanism and selectivity of the transformation were obtained through a combination of experimental and computational studies. This ultimately led to the development of a novel improved DG that provided a faster reaction rate, higher yields and a broader substrate scope.

Using an 8-AQ amide directing group at C(3), a set of silver-free conditions was first developed that allowed highly regioselective arylation of pyrrolidine rings at the unactivated C(4)-position over competing C(2). This occurred with excellent *cis*-diastereoselectivity, and also enabled the formation of enantiopure products from enantioenriched substrates. Various (hetero)aryl iodides and carbamate *N*-protecting groups were successful using $Pd(OAc)_2$ as catalyst in combination with K_2CO_3 and PivOH. However, low reactivity was generally observed for electron-poor and/or *ortho*-substituted aryl iodides. The corresponding piperidine ring could also be selectively arylated at the unactivated 4-position under identical conditions. In this case, *trans*-configured derivatives were formed as minor reaction products, deriving from a *trans*-palladacycle intermediate. In addition, direct access to *trans*-3,4-disubstituted pyrrolidine and piperidine products was achieved through sequential C(4)–H arylation and base-mediated epimerisation in one-pot.

Different strategies for the removal of the aminoquinoline DG were developed, providing divergent access to carboxylic acid, ester, amide and alcohol derivatives. Conditions were optimised to achieve high control over the stereochemical outcome and preserve the *N*-protecting groups. This enabled the concise stereocontrolled formal synthesis of antidepressant drug (–)-paroxetine, and the total synthesis of enantiopure Br- and I-paroxetine analogues. This was completed in 8 steps from commercial material, involving C(4)–H arylation followed by reductive DG removal as key synthetic steps.

Furthermore, the synthetic potential of the C(4)–H arylation approach was demonstrated in the synthesis of a library of pyrrolidine and piperidine fragments for potential screening in FBDD. C(4)-Arylated acid, alcohol or amide derivatives, with either *cis*- or *trans*-configuration, were accessed in 4–6 steps, involving C(4)–H arylation (and epimerisation), DG cleavage and final Boc deprotection. These compounds featured various molecular topologies with good degree of 3D character, while satisfying the desirable criteria of low M_W and lipophilicity for fragment-like molecules.

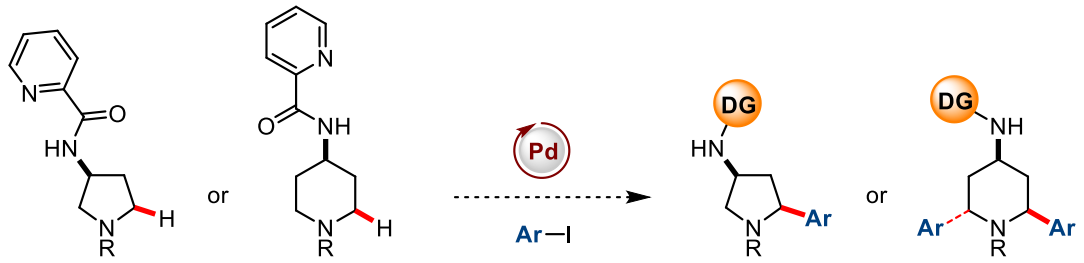
Based on experimental and computation investigations into the mechanism of the reaction, this was proposed to proceed through a Pd^{II}/Pd^{IV} catalytic cycle. The C–H activation step was found to be neither turnover-limiting nor stereodetermining, with reversible CMD shown to be feasible at both *cis*- and *trans*-C(4) positions on pyrrolidine and piperidine rings. The following oxidative addition step was found to be energetically viable for both diastereomeric intermediates in the piperidine case, consistent with the lower diastereoselectivity of arylation.

On the other hand, only the *cis*-palladacycle could undergo stereodetermining oxidative addition for the corresponding 5-membered ring, explaining the exclusive formation of *cis*-arylated pyrrolidine products. The high C(4)-regioselectivity of arylation might also derive from a disfavoured oxidative addition process at C(2), although this could not be confirmed computationally. The following C–C bond-forming reductive elimination was identified as the turnover-limiting step for the transformation, based on kinetic analysis and DFT calculations. Furthermore, K_2CO_3 and PivOH were found play an important role in regenerating the active catalyst by formation of insoluble KI.

While a product inhibition effect was excluded based on deuteration experiments and RPKA studies, a fast catalyst deactivation was found to impair significantly the methodology. In order to overcome this limitation, a novel removable 4-dimethylamino-8-quinolinyl (DMAQ) amide DG was developed. This allowed *cis*-3,4-disubstituted pyrrolidine derivatives to be formed in 20–30% higher yields, while expanding the scope of coupling partners to *ortho*-substituted and electron-deficient (hetero)aryl iodides. A similar increase in reactivity, accompanied by higher *cis*-diastereoselectivity, was found for the corresponding piperidine ring. Using this DG, a 2-fold increase in reaction rate was observed, likely deriving from an easier reductive elimination step. Finally, the increase in reactivity allowed the iodide loading to be lowered to just 1 equivalent without a significant reduction in yield, enabling the late-stage functionalisation of complex natural products and pharmaceuticals.

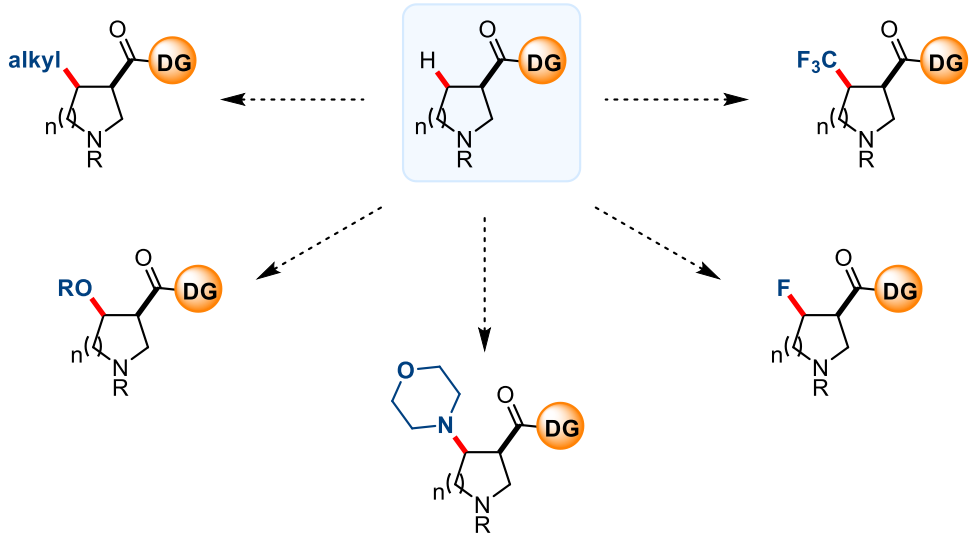
The next stage of this research will be to expand the diversity of saturated N-heterocycles that can be accessed *via* C–H functionalisation approaches, both in terms of substitution pattern and nature of the substituent. This would greatly expand the type of structures that could be included in pharmaceutical screening libraries or used as building blocks in drug discovery. Ultimately, it is hoped that all possible exit vectors from the ring system can be accessed selectively, in order to probe the full 3D space around any potential fragment hit or lead compound.

For example, a study on the desymmetrisation of piperidine-4-carboxylic acids by C(3)–H arylation is ongoing within the Bull group (not shown). Furthermore, the use of amine-linked DGs can be envisaged as an additional strategy to access N-heterocyclic derivatives with different substitution patterns (Scheme 7.2). In particular, installing a picolinamide DG at the 3- or 4-position of pyrrolidine or piperidine derivatives respectively, would allow γ-C–H functionalisation to occur at the acidic C(2)-position. Promising preliminary results were obtained by Ahmed Carter and Thomas Larribeau (Imperial College London),[286] and future work will focus on the optimisation of this approach to form 4-amino-2-aryl piperidine and 3-amino-2-aryl-pyrrolidine derivatives.



Scheme 7.2 Future work 1 – γ-C(2)–H functionalisation of pyrrolidine and piperidine derivatives.

On the other hand, the use of different coupling partners would allow access to new classes of N-heterocyclic fragments. Reaction with alkyl iodides will be investigated with both AQ and DMAQ directing groups in order to access new 3,4-disubstituted pyrrolidine and piperidine derivatives (Scheme 7.3). Similarly, the potential for C–H acetoxylation, alkoxylation and trifluoromethylation could be evaluated in the presence of different oxidants, with in turn could result in different regio- and stereochemical outcomes.



Scheme 7.3 Future work 2 – Expanding the scope of C(4)–H functionalisation for heterocycle diversification.

Finally, the DMAQ directing group will be evaluated in order to promote difficult C–heteroatom bond-forming reductive elimination processes. These include intermolecular C–H amination reactions, which would be of particular interest to access attractive structures for drug discovery applications. *O*-Benzoyl hydroxylamine reagents have been reported to promote intermolecular C(sp^3)–H amination through a Pd^{II}/Pd^{IV} catalytic cycle.[287] However, this was strictly limited to primary centres. As such, the use of the DMAQ directing group might prove beneficial to expand this transformation to unactivated methylene positions, both in linear and cyclic substrates, by promoting C–N bond-forming reductive elimination.

8. Experimental

8.1 General Experimental Considerations

All non-aqueous reactions were carried out under an inert atmosphere (argon) with flame-dried glassware, using standard techniques, unless specified. Anhydrous solvents were obtained by filtration through drying columns (THF, DMF, EtOH, MeCN, CH_2Cl_2, toluene) or used as supplied (1,4-dioxane, HFIP, α,α,α-trifluorotoluene, MeOH, *i*PrOH, $CHCl_3$). Reactions in sealed tubes were run in Biotage microwave vials (2–5 mL or 10–20 mL). Aluminium caps equipped with molded butyl/PTFE septa were used for reactions in toluene and α,α,α-trifluorotoluene, while simple butyl septa were used for reactions in MeCN or alcoholic solvents.

Flash column chromatography was performed using 230–400 mesh silica, with the indicated solvent system according to standard techniques. Automated flash chromatography using Biotage® Selekt system was performed under the indicated conditions. Analytical thin-layer chromatography (TLC) was performed on precoated glass-backed silica gel plates. Visualisation of the developed chromatogram was performed by UV absorbance (254 nm) and stained with aqueous potassium permanganate solution, phosphomolybdic acid solution, or ninhydrin solution in ethanol.

IR spectra were recorded as solids or neat liquids on an Agilent Cary 630 FT-IR spectrometer and are reported in reciprocal centimetres (ν_{max}, cm^{-1}).

Nuclear magnetic resonance spectra were recorded on 400 or 500 MHz spectrometers. Chemical shifts for ^1H NMR spectra are recorded in parts per million (ppm) from tetramethylsilane with the solvent resonance as the internal standard ($CDCl_3$: δ = 7.27 ppm, DMSO-d_6: δ = 2.50 ppm, MeOD-d_4: δ = 3.35 ppm, toluene-d_8: δ = 2.08 ppm). Data is reported as follows: chemical shift (multiplicity [s = singlet, d = doublet, t = triplet, q = quartet, p = pentet, h = heptet, m = multiplet and br = broad], coupling constant (in Hz), integration and assignment). ^{13}C NMR spectra were recorded with complete proton decoupling. Chemical shifts are reported in parts per million from tetramethylsilane with the solvent resonance as the internal standard ($^{13}CDCl_3$: δ = 77.0 ppm, $(^{13}CD_3)_2SO$: δ = 39.5 ppm, $^{13}CD_3OD$: δ = 49.0 ppm, $^{13}(CD_3)_2CO$: δ = 29.8 ppm, $^{13}C_6D_5{}^{13}CD_3$: δ = 20.4 ppm). Assignments of ^1H and ^{13}C spectra were based upon the analysis of δ and *J* values, as well as DEPT, COSY, NOESY, HSQC and HMBC experiments where appropriate. ^{19}F and ^{31}P NMR spectra were recorded with or without complete proton decoupling. Decoupling is indicated as $^{19}F\{^1H\}$ and $^{31}P\{^1H\}$ and where relevant this is stated in each assignment. ^{19}F and ^{31}P NMR spectra are

indirectly referenced to $CFCl_3$ and H_3PO_4 automatically *via* direct measurement of the absolute frequency of the deuterium lock signal by the spectrometer hardware.

All Boc, Cbz, methyl carbamate and TFA containing compounds appeared as a mixture of rotamers in the NMR spectra at rt; therefore, NMR experiments for these compounds were carried out at 373 K to coalesce the signals, which is indicated in parentheses where appropriate.

Melting points were determined in open glass capillaries using Optimelt MPA100 apparatus and are uncorrected.

HPLC analyses were carried out on an Agilent 1260 Infinity Series system, employing Daicel Chiracel columns, under the indicated conditions.

Observed optical rotations (α') were measured at the indicated temperature (T °C) and were converted to the corresponding specific rotations $[\alpha]_D^T$ in deg cm^2 g^{-1}, concentration (*c*) in g per 100 mL.

The high-resolution mass spectrometry (HRMS) analyses were performed using electrospray ion source (ESI), atmospheric pressure chemical ionisation (APCI) or pneumatically assisted nanospray ionisation (pNSI). ESI was performed using a Waters LCT Premier equipped with an ESI source operated in positive or negative ion mode. In most cases the software used was MassLynx 4.1. This software does not account for the electron and the calibrations/references are calculated accordingly, *i.e.* $[M+H]^+$ is detected and the mass is calibrated to output [M+H]. APCI was performed using an Orbitrap XL or Xevo G2S. pNSI was performed using an Orbitrap XL in positive ion mode.

Reagents: Commercial reagents were used as supplied or purified by standard techniques where necessary. K_2CO_3 was purchased from Sigma-Aldrich Company Ltd and was flame-dried before use as part of reaction set-up. $Pd(OAc)_2$ and 8-Aminoquinoline were purchased from Fluorochem Ltd and used as supplied. PivOH and α,α,α-trifluorotoluene were purchased from Sigma-Aldrich Company Ltd and used as supplied.

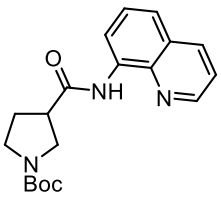
Purity: $Pd(OAc)_2$, > 98%; PivOH, 99%; K_2CO_3, ≥ 98% (powder, -325 mesh). 2-Iodoxybenzoic acid (IBX) was purchased as a mixture of the title compound (30 wt.% or 45 wt.%) and 2 stabilisers, namely isophthalic acid and benzoic acid. The mixture was used as supplied without any further purification.

8.2 Experimental Details and Characterisation Data

8.2.1 Compounds for Chapter 3

*8.2.1.1 Pyrrolidine Amide Substrates **2–9***

tert-Butyl (±)-3-(quinolin-8-ylcarbamoyl)pyrrolidine-1-carboxylate (2)



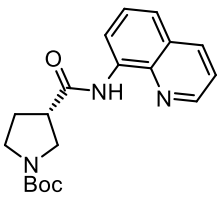
HOBt hydrate (2.56 g, 16.7 mmol) was added to a solution of *N*-Boc-pyrrolidine-3-carboxylic acid **1** (3.00 g, 14.0 mmol) and 8-aminoquinoline (2.41 g, 16.8 mmol) in dry CH_2Cl_2 (55 mL) at 25 °C, and was stirred for 5 min. EDC·HCl (3.20 g, 16.8 mmol) was then added and the solution was stirred for 5 days. The reaction was diluted with CH_2Cl_2 (75 mL), then a solution of sat. aq. $NaHCO_3$ (75 mL) was added and the aqueous layer was extracted with CH_2Cl_2 (3 × 150 mL). The combined organic extracts were dried over Na_2SO_4 and filtered. The solvent was removed under reduced pressure. The crude material was purified by flash column chromatography (15% to 50% EtOAc/pentane), the product containing fractions were combined and the solvent was removed under reduced pressure. Et_2O (20 mL) and pentane (20 mL) were added and the solvent was removed under reduced pressure to afford amide **2** as a white solid (4.30 g, 91%). R_f 0.23 (25% EtOAc/pentane); mp = 110–113 °C (from Et_2O/pentane); ν_{max} (film)/cm^{-1} 3343 (NH), 2972, 1738, 1693 (C=O carbamate), 1672 (C=O amide), 1536, 1487, 1398, 1362, 1223, 1164, 1125, 1082, 986, 874, 821, 782, 686; ^{1}H NMR (400 MHz, DMSO-d_6, 373 K) δ 10.02 (br s, 1 H, NH), 8.91 (dd, J = 4.2, 1.7 Hz, 1 H, HC_{Ar}), 8.58 (dd, J = 7.7, 1.3 Hz, 1 H, HC_{Ar}), 8.36 (dd, J = 8.3, 1.7 Hz, 1 H, HC_{Ar}), 7.65 (dd, J = 8.2, 1.3 Hz, 1 H, HC_{Ar}), 7.60 (dd, J = 8.3, 4.2 Hz, 1 H, HC_{Ar}), 7.56 (t, J = 7.9 Hz, 1 H, HC_{Ar}), 3.63 (dd, J = 10.4, 7.5 Hz, 1 H, NC*H*HCHCO), 3.55–3.44 (m, 3 H, NCH*H*CHCO, CHCO, NC*H*HCH$_2$), 3.34 (ddd, J = 10.5, 7.5, 7.5 Hz, 1 H, NCH*H*CH$_2$), 2.27–2.19 (m, 1 H, NCH$_2$C*H*H), 2.18–2.09 (m, 1 H, NCH$_2$CH*H*), 1.43 (s, 9 H, C(CH$_3$)$_3$); ^{13}C NMR (101 MHz, DMSO-d_6, 373 K) δ 171.0 (C=O amide), 153.2 (C=O carbamate), 148.4 (C_{Ar}), 138.0 (C_{Ar} quat), 136.0 (C_{Ar}), 133.9 (C_{Ar} quat), 127.5 (C_{Ar} quat), 126.4 (C_{Ar}), 121.6 (C_{Ar}), 121.5 (C_{Ar}), 116.5 (C_{Ar}), 78.0 (*C*(CH$_3$)$_3$), 48.1 (N*C*H$_2$CHCO), 44.9 (N*C*H$_2$CH$_2$), 44.1 (*C*HCO), 28.5 (NCH$_2$*C*H$_2$), 27.8 (C(*C*H$_3$)$_3$); HRMS (ESI$^+$) *m*/*z* Calculated for $C_{19}H_{24}N_3O_3$ [M+H] 342.1818; Found 342.1829.

Procedure for the synthesis of amide 2 using EDC·HCl and DMAP:

EDC·HCl (3.60 g, 18.7 mmol) was added to a solution of *N*-Boc-pyrrolidine-3-carboxylic acid **1** (4.00 g, 18.7 mmol) and 8-aminoquinoline (2.20 g, 15.6 mmol) in anhydrous CH_2Cl_2 (80 mL) at 0 °C. DMAP (70.1 mg, 0.6 mmol) was then added and the solution was stirred at 25 °C for 24 h. The reaction was diluted with CH_2Cl_2 (80 mL), then a solution of sat. aq. $NaHCO_3$ (80 mL) was added and the aqueous layer was extracted with CH_2Cl_2 (3 × 100 mL). The combined

organic extracts were dried over Na_2SO_4 and filtered. The solvent was removed under reduced pressure. The crude material was purified by flash column chromatography (50% to 70% Et_2O/pentane) to afford amide **2** as a pale yellow solid (4.74 g, 89%). R_f 0.19 (50% Et_2O/pentane). Characterisation data was the same as above.

***tert*-Butyl (–)-(*S*)-3-(quinolin-8-ylcarbamoyl)pyrrolidine-1-carboxylate ((*S*)-2)**

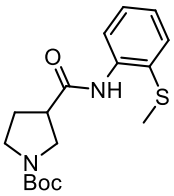


HOBt hydrate (430 mg, 2.80 mmol) was added to a solution of (*S*)-*N*-Boc-pyrrolidine-3-carboxylic acid (*S*)-**1** (500 mg, 2.33 mmol) and 8-aminoquinoline (404 mg, 2.80 mmol) in dry CH_2Cl_2 (9.0 mL) at 25 °C, and was stirred for 5 min. EDC·HCl (537 mg, 2.80 mmol) was then added and the solution was stirred for 5 days. The reaction was diluted with CH_2Cl_2 (12 mL), then a solution of sat. aq. $NaHCO_3$ (12 mL) was added and the aqueous layer was extracted with CH_2Cl_2 (3 × 30 mL). The combined organic extracts were dried over Na_2SO_4 and filtered. The solvent was removed under reduced pressure. The crude material was purified by flash column chromatography (15% to 40% EtOAc/hexane), the product containing fractions were combined and the solvent was removed under reduced pressure. Et_2O (10 mL) and pentane (10 mL) were added and the solvent was removed under reduced pressure to afford amide (*S*)-**2** as a white solid (684 mg, 86%, 97.4% *ee*). $[\alpha]_D^{25}$ –7.7 (*c* 1.00, $CHCl_3$).

Characterisation data identical to that reported for racemic amide **2** (page 197).

HPLC Conditions: Chiralpak IA 3-column, 90:10 *n*-hexane:*i*-PrOH, flow rate: 1 mL·min^{-1}, 35 ºC. UV detection wavelength: 210.4 nm. Retention times: 11.5 min (*S* enantiomer), 12.6 min (*R* enantiomer).

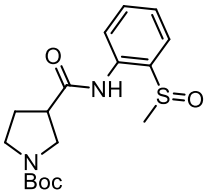
***tert*-Butyl (±)-3-((2-(methylthio)phenyl)carbamoyl)pyrrolidine-1-carboxylate (6)**



HOBt hydrate (2.60 g, 16.8 mmol) was added to a solution of *N*-Boc-pyrrolidine-3-carboxylic acid **1** (3.00 g, 14.0 mmol) and 2-(methylthio)aniline (2.1 mL, 16.8 mmol) in dry CH_2Cl_2 (55 mL) at rt, and was stirred for 5 min. EDC·HCl (3.20 g, 16.8 mmol) was then added and the solution was stirred for 5 days. The reaction was diluted with CH_2Cl_2 (70 mL), then a solution of sat. aq. $NaHCO_3$ (70 mL) was added and the aqueous layer was extracted with CH_2Cl_2 (3 × 150 mL). The combined organic extracts were dried over Na_2SO_4 and filtered. The solvent was removed under reduced pressure. Purification by flash column chromatography (30% EtOAc/hexane) afforded amide **6** as an orange oil (3.17 g, 67%). R_f 0.17 (30% EtOAc/hexane); ν_{max} (film)/cm^{-1} 3260 (NH), 2975, 2881, 1687 (C=O), 1661 (C=O), 1579, 1513, 1402, 1364, 1163, 1118, 1072, 879, 745; ^{1}H NMR (400 MHz, DMSO-d_6, 373 K) δ 9.05 (br s, 1 H, NH), 7.54–7.47 (m, 1 H, HC_{Ar}), 7.43–7.36 (m, 1 H, HC_{Ar}), 7.24–7.16 (m, 2 H, HC_{Ar}), 3.57 (dd, *J* = 10.8,

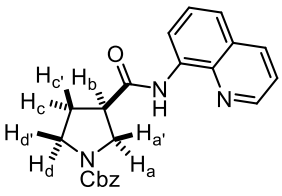
8.0 Hz, 1 H, NC*H*HCHCO), 3.52–3.38 (m, 2 H, NCH*H*CHCO, NC*H*HCH$_2$), 3.30 (ddd, *J* = 10.5, 7.5, 7.5 Hz, 1 H, NCH*H*CH$_2$), 3.23 (dddd, *J* = 7.5, 7.5, 7.5, 7.5 Hz, 1 H, CHCO), 2.42 (s, 3 H, CH$_3$), 2.18–2.04 (m, 2 H, NCH$_2$C*H*$_2$), 1.44 (s, 9 H, C(CH$_3$)$_3$); ^{13}C NMR (101 MHz, DMSO-*d*$_6$, 373 K) δ 170.7 (C=O amide), 153.0 (C=O carbamate), 135.7 (C$_{Ar}$ quat), 132.2 (SC$_{Ar}$ quat), 127.8 (C$_{Ar}$), 125.5 (C$_{Ar}$), 125.4 (C$_{Ar}$), 125.0 (C$_{Ar}$), 77.8 (*C*(CH$_3$)$_3$), 47.9 (N*C*H$_2$CHCO), 44.8 (N*C*H$_2$CH$_2$), 43.0 (*C*HCO), 28.2 (NCH$_2$*C*H$_2$), 27.7 (C(*C*H$_3$)$_3$), 15.5 (SCH$_3$); HRMS (ESI$^+$) *m*/*z* Calculated for C$_{17}$H$_{25}$N$_2$O$_3$S [M+H] 337.1586; Found 337.1588.

***tert*-Butyl (±)-3-((2-(methylsulfinyl)phenyl)carbamoyl)pyrrolidine-1-carboxylate (7)**



A solution of *m*-CPBA (256 mg, 1.49 mmol) in CH$_2$Cl$_2$ (3.0 mL) was added dropwise to a solution of starting carboxamide **6** (500 mg, 1.49 mmol) in CH$_2$Cl$_2$ (6.0 mL) at –30 °C. The reaction mixture was stirred at –30 °C for 3 h, then sat. aq. NaHCO$_3$ (10 mL) was added and the reaction mixture was stirred at 25 °C for 30 min. The phases were separated, and the aqueous layer was extracted with CH$_2$Cl$_2$ (3 × 25 mL). The combined organic extracts were dried over Na$_2$SO$_4$ and filtered. The solvent was removed under reduced pressure. Purification by flash column chromatography (EtOAc) afforded amide **7** as a colourless oil (305 mg, 58%, 1:1 *dr*). *R*$_f$ 0.11 (EtOAc); ν$_{max}$ (film)/cm^{-1} 3242 (NH), 2976, 2884, 1685 (C=O), 1587, 1525, 1475, 1403, 1163, 1120, 1014, 955, 879, 756; ^{1}H NMR (400 MHz, DMSO-*d*$_6$, 373 K) δ 9.96 (br s, 1 H, NH), 7.77 (dd, *J* = 7.8, 1.6 Hz, 1 H, HC$_{Ar}$), 7.59 (dd, *J* = 8.0, 1.3 Hz, 1 H, HC$_{Ar}$), 7.52 (ddd, *J* = 8.0, 7.3, 1.6, Hz, 1 H, HC$_{Ar}$), 7.43 (ddd, *J* = 7.8, 7.3, 1.4, Hz, 1 H, HC$_{Ar}$), 3.57 and 3.55 (2 × dd, *J* = 10.9, 7.9 Hz, 1 H, NC*H*HCHCO), 3.52–3.38 (m, 2 H, NCH*H*CHCO, NC*H*HCH$_2$), 3.305 and 3.301 (2 × ddd, *J* = 10.5, 7.5, 7.5 Hz, 1 H, NCH*H*CH$_2$), 3.17 (dddd, *J* = 7.4, 7.4, 7.4, 7.4 Hz, 1 H, CHCO), 2.774 and 2.771 (2 × s, 3 H, SCH$_3$), 2.22–2.03 (m, 2 H, NCH$_2$C*H*$_2$), 1.44 and 1.43 (2 × s, 9 H, C(CH$_3$)$_3$); ^{13}C NMR (101 MHz, DMSO-*d*$_6$, 373 K) δ 171.3 and 171.2 (C=O amide), 153.0 (C=O carbamate), 138.6 (SC$_{Ar}$ quat), 135.1 (C$_{Ar}$ quat), 130.8 (C$_{Ar}$), 125.8 (C$_{Ar}$), 125.0 and 124.9 (C$_{Ar}$), 124.0 (C$_{Ar}$), 77.8 (*C*(CH$_3$)$_3$), 47.7 and 47.6 (N*C*H$_2$CHCO), 44.7 (N*C*H$_2$CH$_2$), 43.2 (*C*HCO), 41.6 (SCH$_3$), 28.1 and 27.9 (NCH$_2$*C*H$_2$), 27.7 (C(*C*H$_3$)$_3$); HRMS (ESI$^+$) *m*/*z* Calculated for C$_{17}$H$_{25}$N$_2$O$_4$S [M+H] 353.1535; Found 353.1523.

Benzyl (±)-3-(quinolin-8-ylcarbamoyl)pyrrolidine-1-carboxylate (9)‡‡‡



HOBt hydrate (2.20 g, 14.4 mmol) was added to a solution of *N*-Cbz-pyrrolidine-3-carboxylic acid **8** (3.00 g, 12.0 mmol) and 8-aminoquinoline (1.70 g, 12.0 mmol) in dry CH_2Cl_2 (45 mL) at 25 °C, and was stirred for 5 min. EDC·HCl (2.70 g, 14.4 mmol) was then added and the solution was stirred for 3 days. The reaction was diluted with CH_2Cl_2 (40 mL), then a solution of sat. aq. $NaHCO_3$ (40 mL) was added and the aqueous layer was extracted with CH_2Cl_2 (3 × 60 mL). The combined organic extracts were dried over Na_2SO_4 and filtered. The crude material was purified by flash column chromatography (70% to 100% Et_2O/pentane). The product containing fractions were combined and the solvent was removed under reduced pressure to afford amide **9** as a white solid (3.30 g, 73%). R_f 0.15 (70% Et_2O/pentane); mp = 124–125 °C (from Et_2O/pentane); ν_{max} (film)/cm^{-1} 3342 (NH), 2888, 1685 (C=O), 1524, 1484, 1422, 1365, 1335, 1181, 1133, 956, 877, 823, 786, 727, 686;

<u>*Characterisation in DMSO-d_6*</u>: ^{1}H NMR (400 MHz, DMSO-d_6, 373 K) δ 10.06 (br s, 1 H, NH), 8.91 (dd, *J* = 4.2, 1.7 Hz, 1 H, HC_{Ar}), 8.59 (dd, *J* = 7.6, 1.4 Hz, 1 H, HC_{Ar}), 8.37 (dd, *J* = 8.3, 1.7 Hz, 1 H, HC_{Ar}), 7.66 (dd, *J* = 8.3, 1.4 Hz, 1 H, HC_{Ar}), 7.61 (dd, *J* = 8.3, 4.2 Hz, 1 H, HC_{Ar}), 7.57 (t, *J* = 8.0 Hz, 1 H, HC_{Ar}), 7.40–7.33 (m, 4 H, HC_{Ar}), 7.33–7.28 (m, 1 H, HC_{Ar}), 5.12 (s, 2 H, OCH_2Ph), 3.73 (dd, *J* = 10.6, 7.8 Hz, 1 H, NCH_aHCHCO), 3.63 (dd, *J* = 10.6, 6.5 Hz, 1 H, NCH$H_{a'}$CHCO), 3.61–3.50 (m, 2 H, CH_bCO, NC$H_{d'}$HCH$_2$), 3.44 (ddd, *J* = 10.5, 7.5, 7.5 Hz, 1 H, NCHH_dCH$_2$), 2.28 (dddd, *J* = 12.5, 7.4, 7.4, 5.2 Hz, 1 H, NCH_2CH_cH), 2.18 (dddd, *J* = 12.4, 7.6, 7.6, 7.6 Hz, 1 H, NCH_2CH*$H_{c'}$*); ^{13}C NMR (101 MHz, DMSO-d_6, 373 K) δ 170.8 (C=O amide), 153.5 (C=O carbamate), 148.3 (C_{Ar}), 137.9 (C_{Ar} quat), 136.7 (C_{Ar} quat), 135.9 (C_{Ar}), 133.9 (C_{Ar} quat), 127.8 (2 × C_{Ar}), 127.4 (C_{Ar} quat), 127.1 (C_{Ar}), 126.8 (2 × C_{Ar}), 126.3 (C_{Ar}), 121.5 (C_{Ar}), 121.4 (C_{Ar}), 116.5 (C_{Ar}), 65.4 (OCH_2Ph), 48.1 (NCH_2CHCO), 45.1 (NCH_2CH_2), 44.0 (*C*HCO), 28.4 (NCH_2CH_2);

<u>*Characterisation in toluene-d_8*</u>: ^{1}H NMR (400 MHz, toluene-d_8, 373 K) δ 9.65 (br s, 1 H, NH), 8.92 (dd, *J* = 7.7, 1.3 Hz, 1 H, HC_{Ar}), 8.48 (dd, *J* = 4.2, 1.7 Hz, 1 H, HC_{Ar}), 7.59 (dd, *J* = 8.3, 1.7 Hz, 1 H, HC_{Ar}), 7.29–7.18 (m, 3 H, HC_{Ar}), 7.15–7.00 (m, 4 H, HC_{Ar}), 6.88 (dd, *J* = 8.3, 4.2 Hz, 1 H, HC_{Ar}), 5.09 (s, 2 H, OCH_2Ph), 3.68 (dd, *J* = 10.9, 7.4 Hz, 1 H, NC$H_{a'}$HCHCO), 3.54 (dd, *J* = 10.9, 7.9 Hz, 1 H, NCHH_aCHCO), 3.50–3.41 (m, 1 H, NC$H_{d'}$HCH$_2$), 3.16 (ddd, *J* = 10.5, 7.6, 7.6 Hz, 1 H, NCHH_dCH$_2$), 2.51 (ddddd, *J* = 7.6, 7.6, 7.6, 7.6, 7.6 Hz, 1 H, CH_bCO),

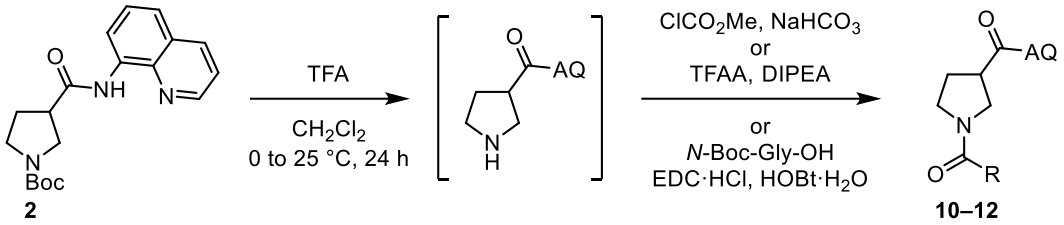
‡‡‡ To allow interpretation of the deuteration studies described in chapter 5, *N*-Cbz pyrrolidine **9** was characterised at 373 K in both DMSO-d_6 and toluene-d_8, as well as at 298 K in $CDCl_3$. Full characterisation in each solvent is reported here to enable direct comparison.

1.98 (dddd, J = 12.5, 8.2, 8.2, 8.2 Hz, 1 H, NCH_2CH_cH), 1.66 (dddd, J = 12.2, 7.4, 7.4, 4.6 Hz, 1 H, NCH_2CHH_c); ^{13}C NMR (101 MHz, toluene-d_8, 373 K) δ 170.4 (C=O amide), 154.7 (C=O carbamate), 148.2 (C_{Ar}), 139.4 (C_{Ar} quat), 138.4 (C_{Ar} quat), 136.4 (C_{Ar}), 135.7 (C_{Ar} quat), 128.7 (C_{Ar}), 128.6 (C_{Ar} quat), 128.4 (2 × C_{Ar}), 128.0 (C_{Ar}), 127.9 (2 × C_{Ar}), 121.6 (C_{Ar}), 121.5 (C_{Ar}), 117.4 (C_{Ar}), 67.0 (OCH_2Ph), 49.4 (NCH_2CHCO), 46.3 ($CHCO$), 46.1 (NCH_2CH_2), 29.6 (NCH_2CH_2);

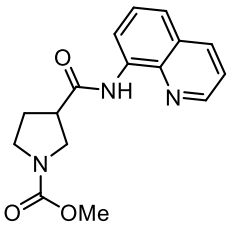
<u>*Characterisation in $CDCl_3$*</u>: ^1H NMR (400 MHz, $CDCl_3$, 298 K, observed as a mixture of rotamers) δ 9.97 (br s, 1 H, NH), 8.80 (dd, J = 4.3, 1.7 Hz, 1 H, HC_{Ar}), 8.76 (dd, J = 6.1, 2.9 Hz, 1 H, HC_{Ar}), 8.18 (dd, J = 8.3, 1.7 Hz, 1 H, HC_{Ar}), 7.59–7.51 (m, 2 H, HC_{Ar}), 7.48 (dd, J = 8.3, 4.2 Hz, 1 H, HC_{Ar}), 7.43–7.28 (m, 5 H, HC_{Ar}), 5.23–5.13 (m, 2 H, OCH_2Ph), 3.98–3.67 (m, 3 H, NCH_2CHCO, $NCHHCH_2$), 3.60–3.47 (m, 1 H, $NCHHCH_2$), 3.37–3.23 (m, 1 H, CH_bCO), 2.46–2.25 (m, 2 H, NCH_2CH_2); ^{13}C NMR (101 MHz, $CDCl_3$, 298 K, observed as a mixture of rotamers) δ 170.6 and 170.5 (C=O amide), 154.6 (C=O carbamate), 148.2 (C_{Ar}), 138.2 (C_{Ar} quat), 136.84 and 136.79 (C_{Ar} quat), 136.4 (C_{Ar}), 134.0 (C_{Ar} quat), 128.4 (2 × C_{Ar}), 128.0 (C_{Ar} quat), 127.88 (C_{Ar}), 127.85 (2 × C_{Ar}), 127.3 (C_{Ar}), 121.8 (C_{Ar}), 121.7 (C_{Ar}), 116.6 (C_{Ar}), 66.8 (OCH_2Ph), 49.1 and 48.6 (NCH_2CHCO), 46.3 and 45.5 ($CHCO$), 46.0 and 45.3 (NCH_2CH_2), 29.7 and 29.1 (NCH_2CH_2);

HRMS (ESI^+) m/z Calculated for $C_{22}H_{22}N_3O_3$ [M+H] 376.1661; Found 376.1662.

*8.2.1.2 N-Substituted Pyrrolidine Amides **10–12***

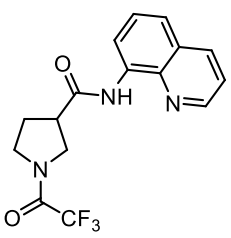


Methyl (±)-3-(quinolin-8-ylcarbamoyl)pyrrolidine-1-carboxylate (10)



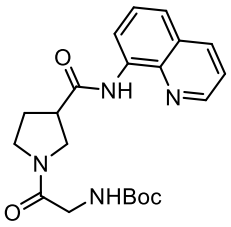
Trifluoroacetic acid (6.5 mL) was added dropwise to a solution of Boc-protected pyrrolidine **2** (3.00 g, 8.79 mmol) in dry CH_2Cl_2 (43 mL) at 0 °C. The reaction was allowed to warm up and stirred at 25 °C for 24 h. The reaction mixture was then diluted with CH_2Cl_2 (15 mL) and quenched with sat. aq. $NaHCO_3$ (30 mL). The organic and aqueous phases were separated, and the aqueous layer was extracted with CH_2Cl_2 (4 × 60 mL). The combined organic layers were dried over Na_2SO_4 and the solvent was removed under reduced pressure, affording *N*-(quinolin-8-yl)pyrrolidine-3-carboxamide (2.40 g), which was used in the next step without further purification. A portion of *N*-(quinolin-8-yl)pyrrolidine-3-carboxamide (362 mg, 1.50 mmol) was solubilised in THF (2.0 mL), and sat. aq. $NaHCO_3$ (2.0 mL) was added. The resulting solution was stirred for 5 min at 0 °C. Methyl chloroformate (232 μL, 3.00 mmol) was then added and the solution was stirred at 25 °C for 20 h. The reaction was diluted with EtOAc (5 mL) and sat. aq. $NaHCO_3$ (2 mL). The organic layer was separated, and the aqueous layer was extracted with EtOAc (3 × 15 mL). The combined organic extracts were dried over Na_2SO_4 and filtered. The solvent was removed under reduced pressure. Purification by flash column chromatography (30% to 60% EtOAc/pentane) afforded amide **10** as a white paste (360 mg, 80% over two steps). R_f 0.09 (40% EtOAc/hexane); ν_{max} (film)/cm^{-1} 3340 (NH), 2953, 2883, 1678 (C=O), 1523, 1485, 1448, 1425, 1383, 1323, 1259, 1187, 1164, 1119, 826, 791, 767; ^{1}H NMR (400 MHz, DMSO-d_6, 373 K) δ 10.05 (br s, 1 H, NH), 8.92 (dd, *J* = 4.2, 1.7 Hz, 1 H, HC_{Ar}), 8.59 (dd, *J* = 7.6, 1.4 Hz, 1 H, HC_{Ar}), 8.37 (dd, *J* = 8.3, 1.7 Hz, 1 H, HC_{Ar}), 7.66 (dd, *J* = 8.3, 1.4 Hz, 1 H, HC_{Ar}), 7.61 (dd, *J* = 8.3, 4.2 Hz, 1 H, HC_{Ar}), 7.56 (t, *J* = 7.9 Hz, 1 H, HC_{Ar}), 3.68 (dd, *J* = 10.3, 7.6 Hz, 1 H, NC*H*HCHCO), 3.64 (s, 3 H, OCH_3), 3.61–3.48 (m, 3 H, NCH*H*CHCO, CHCO, NC*H*HCH_2), 3.39 (ddd, *J* = 10.4, 7.4, 7.4 Hz, 1 H, NCH*H*CH_2), 2.31–2.21 (m, 1 H, NCH_2C*H*H), 2.21–2.11 (m, 1 H, NCH_2CH*H*); ^{13}C NMR (101 MHz, DMSO-d_6, 373 K) δ 170.8 (C=O amide), 154.0 (C=O carbamate), 148.2 (C_{Ar}), 137.9 (C_{Ar} quat), 135.9 (C_{Ar}), 133.9 (C_{Ar} quat), 127.4 (C_{Ar} quat), 126.2 (C_{Ar}), 121.43 (C_{Ar}), 121.41 (C_{Ar}), 116.4 (C_{Ar}), 51.3 (OCH_3), 48.0 (NCH_2CHCO), 45.0 (NCH_2CH_2), 44.0 (*C*HCO), 28.4 (NCH_2CH_2); HRMS (ESI$^+$) *m*/*z* Calculated for $C_{16}H_{18}N_3O_3$ [M+H] 300.1348; Found 300.1342.

(±)-*N*-(Quinolin-8-yl)-1-(2,2,2-trifluoroacetyl)pyrrolidine-3-carboxamide (11)



Trifluoroacetic acid (6.5 mL) was added dropwise to a solution of Boc-protected pyrrolidine **2** (3.00 g, 8.79 mmol) in dry CH_2Cl_2 (43 mL) at 0 °C. The reaction was allowed to warm up and stirred at 25 °C for 24 h. The reaction mixture was then diluted with CH_2Cl_2 (15 mL) and quenched with sat. aq. $NaHCO_3$ (30 mL). The organic and aqueous phases were separated, and the aqueous layer was extracted with CH_2Cl_2 (4 × 60 mL). The combined organic layers were dried over Na_2SO_4 and the solvent was removed under reduced pressure, affording *N*-(quinolin-8-yl)pyrrolidine-3-carboxamide (2.40 g), which was used in the next step without further purification. A portion of *N*-(quinolin-8-yl)pyrrolidine-3-carboxamide (724 mg, 3.00 mmol) was dissolved in dry CH_2Cl_2 (10 mL), and DIPEA (1.5 mL, 8.76 mmol) was added. This solution was stirred for 5 min at 25 °C and then cooled at 0 °C. Trifluoroacetic anhydride (542 μL, 3.90 mmol) was then added and the solution was stirred at 0 °C for 30 min, warmed to 25 °C and stirred for 1 h. The reaction was diluted with CH_2Cl_2 (5 mL) and acidified with 1 M HCl to pH ~ 2. The organic layer was separated, and the aqueous layer was extracted with CH_2Cl_2 (3 × 30 mL). The combined organic extracts were dried over Na_2SO_4 and filtered. The solvent was removed under reduced pressure. The crude material was purified by flash column chromatography (30% EtOAc/hexane), the product containing fractions were combined and the solvent was removed under reduced pressure. Et_2O (10 mL) and pentane (10 mL) were added and the solvent was removed under reduced pressure to afford amide **11** as a white solid (863 mg, 85% over two steps). R_f 0.18 (30% EtOAc/hexane); mp = 84–87 °C (from Et_2O/pentane); ν_{max} (film)/cm^{-1} 3348 (NH), 1690 (C=O), 1671 (C=O), 1523, 1485, 1427, 1380, 1321, 1238, 1201, 1143, 863, 830, 800, 755, 703, 676; ^{1}H NMR (400 MHz, DMSO-d_6, 373 K, observed as a mixture of rotamers) δ 10.14 (br s, 1 H, NH), 8.93 (dd, *J* = 4.2, 1.7 Hz, 1 H, HC_{Ar}), 8.58 (dd, *J* = 7.6, 1.4 Hz, 1 H, HC_{Ar}), 8.38 (dd, *J* = 8.3, 1.7 Hz, 1 H, HC_{Ar}), 7.67 (dd, *J* = 8.3, 1.4 Hz, 1 H, HC_{Ar}), 7.61 (dd, *J* = 8.3, 4.2 Hz, 1 H, HC_{Ar}), 7.57 (t, *J* = 7.9 Hz, 1 H, HC_{Ar}), 4.04–3.66 (m, 4 H, NC*H*$_2$CHCO, CHCO, NC*H*HCH$_2$), 3.65–3.54 (m, 1 H, NCH*H*CH$_2$), 2.48–2.14 (m, 2 H, NCH$_2$C*H*$_2$); ^{13}C NMR (101 MHz, DMSO-d_6, 373 K, observed as a mixture of rotamers) δ 170.4 and 170.0 (C=O amide), 153.7 (q, J_{CF} = 35.6 Hz, CF_3*C*=O), 148.3 (C_{Ar}), 138.0 (C_{Ar} quat), 135.9 (C_{Ar}), 133.8 (C_{Ar} quat), 127.4 (C_{Ar} quat), 126.2 (C_{Ar}), 121.6 (C_{Ar}), 121.4 (C_{Ar}), 116.7 (C_{Ar}), 115.7 (q, J_{CF} = 288.4 Hz, CF_3), 49.4 and 46.4 (N*C*H$_2$CHCO), 48.2 and 45.5 (N*C*H$_2$CH$_2$), 44.6 and 41.9 (*C*HCO), 29.4 and 26.7 (NCH$_2$*C*H$_2$) ^{19}F NMR (376 MHz, DMSO-d_6, 373 K) δ –71.3; HRMS (ESI$^+$) *m*/*z* Calculated for $C_{16}H_{15}N_3O_2F_3$ [M+H] 338.1116; Found 338.1105.

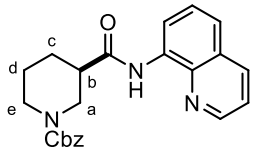
***tert*-Butyl (±)-(2-oxo-2-(3-(quinolin-8-ylcarbamoyl)pyrrolidin-1-yl)ethyl)carbamate (12)**



Trifluoroacetic acid (6.5 mL) was added dropwise to a solution of Boc-protected pyrrolidine **2** (3.00 g, 8.79 mmol) in dry CH_2Cl_2 (43 mL) at 0 °C. The reaction was allowed to warm up and stirred at 25 °C for 24 h. The reaction mixture was then diluted with CH_2Cl_2 (15 mL) and quenched with sat. aq. $NaHCO_3$ (30 mL). The organic and aqueous phases were separated, and the aqueous layer was extracted with CH_2Cl_2 (4 × 60 mL). The combined organic layers were dried over Na_2SO_4 and the solvent was removed under reduced pressure, affording *N*-(quinolin-8-yl)pyrrolidine-3-carboxamide (2.40 g), which was used in the next step without further purification. A portion of *N*-(quinolin-8-yl)pyrrolidine-3-carboxamide (362 mg, 1.50 mmol) was solubilised in dry CH_2Cl_2 (6.0 mL) and HOBt hydrate (276 mg, 1.80 mmol) and *N*-(*tert*-butoxycarbonyl)glycine (315 mg, 1.80 mmol) were added. The resulting solution was stirred for 5 min at 25 °C. EDC·HCl (345 mg, 1.80 mmol) was then added and the solution was stirred for 24 h. The reaction was diluted with CH_2Cl_2 (10 mL), then a solution of sat. aq. $NaHCO_3$ (10 mL) was added and the aqueous layer was extracted with CH_2Cl_2 (3 × 20 mL). The combined organic extracts were dried over Na_2SO_4 and filtered. The crude material was purified by flash column chromatography (3% MeOH/CH_2Cl_2), the product containing fractions were combined and the solvent was removed under reduced pressure. Et_2O (10 mL) and pentane (10 mL) were added and the solvent was removed under reduced pressure to afford amide **12** as a white solid (4.88 mg, 82%). R_f 0.44 (5% MeOH/CH_2Cl_2); mp = 62–67 °C (from Et_2O/pentane); ν_{max} (film)/cm^{-1} 3339 (NH), 2974, 1686 (C=O), 1648 (C=O), 1525, 1486, 1439, 1425, 1390, 1365, 1324, 1246, 1162, 1053, 865, 827, 792, 760; ^{1}H NMR (400 MHz, $CDCl_3$, 298 K, observed as a mixture of rotamers) δ 9.98 and 9.96 (2 × br s, 1 H, NH_{AQ}), 8.81 and 8.80 (2 × dd, *J* = 4.4, 1.7 Hz, 1 H, HC_{Ar}), 8.76–8.69 (m, 1 H, HC_{Ar}), 8.19 and 8.17 (2 × dd, *J* = 3.9, 1.7 Hz, 1 H, HC_{Ar}), 7.58–7.51 (m, 2 H, HC_{Ar}), 7.48 and 7.47 (2 × dd, *J* = 8.3, 4.2 Hz, 1 H, HC_{Ar}), 5.51 and 5.49 (2 × br s, 1 H, NHBoc), 4.05–3.65 (m, 5 H, C*H*$_2$NHBoc, NC*H*$_2$CHCO, NC*H*HCH$_2$), 3.64–3.46 (m, 1 H, NCH*H*CH$_2$), 3.40 and 3.28 (2 × dddd, *J* = 7.5, 7.5, 7.5, 7.5 Hz, 1 H, CHCO), 2.55–2.26 (m, 2 H, NCH$_2$C*H*$_2$), 1.46 and 1.45 (2 × s, 9 H, C(CH$_3$)$_3$); ^{13}C NMR (101 MHz, $CDCl_3$, 298 K, observed as a mixture of rotamers) δ 170.4 and 169.8 (CH*C*=O amide), 166.9 (CH$_2$*C*=O amide), 155.8 (C=O carbamate), 148.31 and 148.27 (C_{Ar}), 138.3 (C_{Ar} quat), 136.44 and 136.40 (C_{Ar}), 134.0 and 133.9 (C_{Ar} quat), 127.9 (C_{Ar} quat), 127.3 (C_{Ar}), 122.0 and 121.9 (C_{Ar}), 121.74 and 121.71 (C_{Ar}), 116.70 and 116.67 (C_{Ar}), 79.6 (*C*(CH$_3$)$_3$), 48.9 and 47.8 (N*C*H$_2$CHCO), 46.4 and 44.4 (*C*HCO), 45.6 and 44.9 (N*C*H$_2$CH$_2$), 43.1 and 43.0 (*C*H$_2$NHBoc), 29.8 and 28.5 (NCH$_2$*C*H$_2$), 28.3 (C(*C*H$_3$)$_3$); HRMS (ESI$^+$) *m*/*z* Calculated for $C_{21}H_{27}N_4O_4$ [M+H] 399.2032; Found 399.2052.

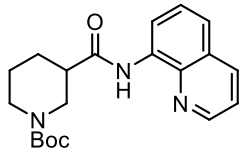
*8.2.1.3 Piperidine Amide Substrates **21–24***

Benzyl (±)-3-(quinolin-8-ylcarbamoyl)piperidine-1-carboxylate (21)



HOBt hydrate (670 mg, 4.60 mmol) was added to a solution of *N*-Cbz-piperidine-3-carboxylic acid **20** (1.00 g, 3.80 mmol) and 8-aminoquinoline (657 mg, 4.60 mmol) in CH_2Cl_2 (15 mL) at 25 °C, and was stirred for 5 min. EDC·HCl (874 mg, 4.60 mmol) was then added and the solution was stirred for 3 days. The reaction was diluted with CH_2Cl_2 (20 mL), then a solution of sat. aq. $NaHCO_3$ (20 mL) was added and the aqueous layer was extracted with CH_2Cl_2 (3 × 30 mL). The combined organic extracts were dried over Na_2SO_4 and filtered. The solvent was removed under reduced pressure. The crude material was purified by flash column chromatography (15% to 40% EtOAc/pentane), the product containing fractions were combined and the solvent was removed under reduced pressure. Et_2O (10 mL) and pentane (10 mL) were added and the solvent was removed under reduced pressure to afford amide **21** as a white solid (1.20 g, 84%). R_f 0.08 (20% EtOAc/hexane); mp = 110–111 °C (from Et_2O/pentane); ν_{max} (film)/cm^{-1} 3347 (NH), 2936, 2858, 1679 (C=O), 1522, 1485, 1423, 1383, 1326, 1234, 1136, 949, 825, 790, 756, 696; ^{1}H NMR (400 MHz, DMSO-d_6, 373 K) δ 10.02 (br s, 1 H, NH), 8.89 (dd, J = 4.2, 1.7 Hz, 1 H, HC_{Ar}), 8.59 (dd, J = 7.6, 1.4 Hz, 1 H, HC_{Ar}), 8.36 (dd, J = 8.3, 1.7 Hz, 1 H, HC_{Ar}), 7.65 (dd, J = 8.3, 1.4 Hz, 1 H, HC_{Ar}), 7.60 (dd, J = 8.3, 4.2 Hz, 1 H, HC_{Ar}), 7.56 (t, J = 7.9 Hz, 1 H, HC_{Ar}), 7.38–7.26 (m, 5 H, HC_{Ar}), 5.12 (s, 2 H, OCH_2Ph), 4.17 (dddd, J = 13.2, 4.2, 1.5, 1.5 Hz, 1 H, $C_aH_{(trans)}H$), 3.94–3.87 (m, 1 H, $C_eH_{(trans)}H$), 3.23 (dd, J = 13.2, 10.0 Hz, 1 H, $C_aHH_{(cis)}$), 3.02 (ddd, J = 13.3, 11.2, 3.2 Hz, 1 H, $C_eHH_{(cis)}$), 2.90–2.81 (m, 1 H, C_bHCO), 2.15–2.05 (m, 1 H, $C_cH_{(trans)}H$), 1.86–1.75 (m, 2 H, $C_cHH_{(cis)}$, C_dHH), 1.62–1.47 (m, 1 H, C_dHH); ^{13}C NMR (101 MHz, DMSO-d_6, 373 K) δ 171.1 (C=O amide), 154.1 (C=O carbamate), 148.2 (C_{Ar}), 137.9 (C_{Ar} quat), 136.6 (C_{Ar} quat), 135.9 (C_{Ar}), 133.8 (C_{Ar} quat), 127.7 (2 × C_{Ar}), 127.3 (C_{Ar} quat), 127.1 (C_{Ar}), 126.8 (2 × C_{Ar}), 126.2 (C_{Ar}), 121.4 (C_{Ar}), 121.3 (C_{Ar}), 116.2 (C_{Ar}), 65.8 (OCH_2Ph), 45.6 (NCH_2CHCO), 43.4 (NCH_2CH_2), 42.5 ($CHCO$), 26.8 ($N(CH_2)_2CH_2$), 23.2 (NCH_2CH_2); HRMS (ESI$^+$) *m*/*z* Calculated for $C_{23}H_{24}N_3O_3$ [M+H] 390.1818; Found 390.1816.

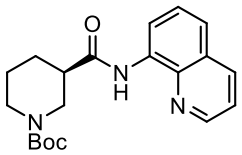
***tert*-Butyl (±)-3-(quinoline-8-ylcarbamoyl)piperidine-1-carboxylate (24)**



DIPEA (3.0 mL, 17.4 mmol) was added to a solution of *N*-Boc-piperidine-3-carboxylic acid **22** (2.00 g, 8.70 mmol) and HATU (3.97 g, 10.4 mmol) in CH_2Cl_2 (40 mL) at 0 °C, and was stirred for 5 min. 8-Aminoquinoline (1.50 g, 10.4 mmol) was then added and the solution was stirred for 24 h at 25 °C. The reaction was diluted with CH_2Cl_2 (40 mL), then a solution of sat. aq. $NaHCO_3$ (40 mL) was added and the aqueous layer was extracted with CH_2Cl_2 (3 × 50 mL). The combined organic extracts were dried over Na_2SO_4 and filtered. The solvent was removed

under reduced pressure. The crude material was purified by flash column chromatography (10% to 20% EtOAc/pentane), the product containing fractions were combined and the solvent was removed under reduced pressure. Et_2O (20 mL) and pentane (20 mL) were added and the solvent was removed under reduced pressure to afford amide **24** as a pale brown solid (2.73 g, 87%). R_f 0.14 (15% EtOAc/pentane); mp = 124–128 °C (from Et_2O/pentane); ν_{max} (film)/cm^{-1} 3350 (NH), 2936, 1682 (C=O), 1525, 1486, 1423, 1389, 1366, 1327, 1257, 1241, 1163, 1147, 826, 792, 760; ^{1}H NMR (400 MHz, DMSO-d_6, 373 K) δ 10.00 (br s, 1 H, NH), 8.91 (dd, J = 4.2, 1.7 Hz, 1 H, HC_{Ar}), 8.60 (dd, J = 7.6, 1.4 Hz, 1 H, HC_{Ar}), 8.36 (dd, J = 8.3, 1.7 Hz, 1 H, HC_{Ar}), 7.64 (dd, J = 8.3, 1.4 Hz, 1 H, HC_{Ar}), 7.60 (dd, J = 8.3, 4.2 Hz, 1 H, HC_{Ar}), 7.56 (t, J = 7.9 Hz, 1 H, HC_{Ar}), 4.15–4.06 (m, 1 H, NC*H*HCHCO), 3.88–3.80 (m, 1 H, NC*H*HCH$_2$), 3.11 (dd, J = 13.1, 10.1 Hz, 1 H, NCH*H*CHCO), 2.94–2.86 (m, 1 H, NCH*H*CH$_2$), 2.84–2.75 (m, 1 H, CHCO), 2.12–2.04 (m, 1 H, N(CH$_2$)$_2$C*H*H), 1.81–1.70 (m, 2 H, N(CH$_2$)$_2$CH*H*, NCH$_2$C*H*H), 1.53–1.46 (m, 1 H, NCH$_2$CH*H*), 1.42 (s, 9 H, C(CH$_3$)$_3$); ^{13}C NMR (101 MHz, DMSO-d_6, 373 K) δ 171.2 (C=O amide), 153.5 (C=O carbamate), 148.2 (C_{Ar}), 137.8 (C_{Ar} quat), 135.9 (C_{Ar}), 133.9 (C_{Ar} quat), 127.3 (C_{Ar} quat), 126.3 (C_{Ar}), 121.4 (C_{Ar}), 121.2 (C_{Ar}), 116.1 (C_{Ar}), 78.3 (*C*(CH$_3$)$_3$), 45.7 (N*C*H$_2$CHCO), 43.3 (N*C*H$_2$CH$_2$), 42.7 (*C*HCO), 27.6 (C(*C*H$_3$)$_3$), 26.9 (N(CH$_2$)$_2$*C*H$_2$), 23.3 (NCH$_2$*C*H$_2$); HRMS (ESI$^+$) *m*/*z* Calculated for $C_{20}H_{26}N_3O_3$ [M+H] 356.1974; Found 356.1986.

***tert*-Butyl (–)-(*R*)-3-(quinolin-8-ylcarbamoyl)piperidine-1-carboxylate ((*R*)-24)**

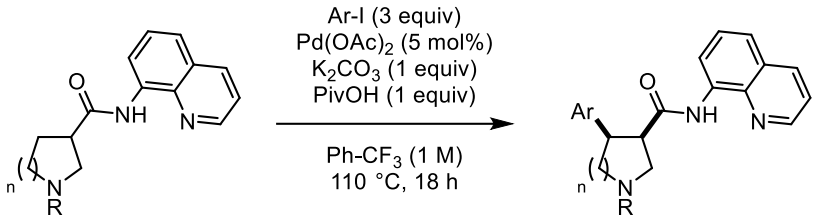


N-Ethyl-*N*-isopropylpropan-2-amine (6.0 mL, 34.9 mmol) was added to a solution of *(R)*-1-(*tert*-butoxycarbonyl)piperidine-3-carboxylic acid **23** (4.0 g, 17.4 mmol) and HATU (8.00 g, 20.9 mmol) in CH_2Cl_2 (90 mL) at 0 °C, and was stirred for 5 min. 8-Aminoquinoline (3.0 g, 20.9 mmol) was then added and the solution was stirred for 24 h at 25 °C. The reaction was diluted with CH_2Cl_2 (90 mL), then a solution of sat. aq. $NaHCO_3$ (90 mL) was added and the aqueous layer was extracted with CH_2Cl_2 (3 × 150 mL). The combined organic extracts were dried over Na_2SO_4 and filtered. The solvent was removed under reduced pressure. The crude material was purified by flash column chromatography (10% to 20% EtOAc/pentane), the product containing fractions were combined and the solvent was removed under reduced pressure. Et_2O (30 mL) and pentane (30 mL) were added and the solvent was removed under reduced pressure to afford amide (*R*)-**24** as a pale brown solid (5.49 g, 89%, 99.1% *ee*). $[\alpha]_D^{25}$ –8.5 (*c* 1.41, $CHCl_3$).

Characterisation data identical to that reported for racemic amide **24**.

HPLC Conditions: Chiralpak IA 3-column, 95:5 *n*-hexane:*i*-PrOH, flow rate: 1 mL·min^{-1}, 35 ºC. UV detection wavelength: 210.4 nm. Retention times: 14.4 min (*S* enantiomer), 15.7 min (*R* enantiomer).

8.2.1.4 ***General Procedure A*** *for C–H Arylation of Pyrrolidines and Piperidines*

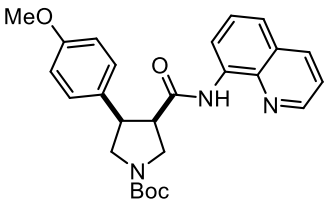


n = 1, 2
R = Boc, Cbz, CO_2Me, TFA, $COCH_2NHBoc$

A reaction tube was charged with K_2CO_3 (69.1 mg, 0.50 mmol), flame-dried, and allowed to cool under argon. The starting carboxamide (0.50 mmol), the requisite aryl iodide (1.50 mmol), $Pd(OAc)_2$ (5.60 mg, 25.0 μmol) and PivOH (51.2 mg, 0.50 mmol) were added sequentially. The reaction vessel was sealed and purged with argon, then $PhCF_3$ (500 μL, 1.0 M) was added by syringe. The reaction tube was then placed in a preheated oil bath and stirred at 110 ºC for 18 h. The reaction mixture was then allowed to cool to rt and EtOAc (10 mL) was added. The resulting mixture was filtered through a pad of Celite, eluting with further EtOAc (2 × 10 mL). The solvent was removed under reduced pressure, and the crude material was purified by flash column chromatography under the specified conditions. The product containing fractions were combined and the solvent was removed under reduced pressure. Et_2O (5 mL) and pentane (5 mL) were added and the solvent was removed under reduced pressure to afford the 3-arylated derivative.

*8.2.1.5 Pyrrolidine C–H Arylation: Scope of N-Protecting Groups and Aryl Iodides (**3a–n, 13a–l**):*

tert-Butyl _cis_-(±)-3-(4-methoxyphenyl)-4-(quinolin-8-ylcarbamoyl)pyrrolidine-1-carboxylate (3a)



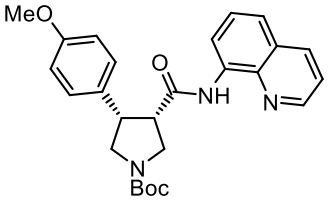
Prepared according to **General Procedure A** using *tert*-butyl 3-(quinoline-8-ylcarbamoyl)pyrrolidine-1-carboxylate **2** (171 mg) and 4-iodoanisole (351 mg). Purification by flash column chromatography (5% to 20% acetone/pentane) afforded arylated pyrrolidine **3a** as a yellow solid (143 mg, 64%). R_f 0.20 (20% acetone/pentane); mp = 62–65 °C (from Et_2O/pentane); ν_{max} (film)/cm^{-1} 3346 (NH br), 2976, 1681 (C=O), 1525, 1515, 1486, 1402, 1365, 1324, 1248, 1163, 1114, 1033, 912, 791, 758, 729; ^{1}H NMR (400 MHz, DMSO-d_6, 373 K) δ 9.69 (br s, 1 H, NH), 8.83 (dd, J = 4.2, 1.7 Hz, 1 H, HC_{Ar}), 8.35 (dd, J = 7.6, 1.4 Hz, 1 H, HC_{Ar}), 8.31 (dd, J = 8.3, 1.7 Hz, 1 H, HC_{Ar}), 7.60–7.55 (m, 2 H, HC_{Ar}), 7.47 (t, J = 7.9 Hz, 1 H, HC_{Ar}), 7.19–7.11 (m, 2 H, HC_{Ar}), 6.71–6.64 (m, 2 H, HC_{Ar}), 3.86–3.76 (m, 3 H, CHCO, CHAr, NC*H*HCHCO), 3.76–3.71 (m, 2 H, NC*H*$_2$CHAr), 3.67–3.60 (m, 1 H, NCH*H*CHCO), 3.55 (s, 3 H, OCH_3), 1.49 (s, 9 H, $C(CH_3)_3$); ^{13}C NMR (101 MHz, DMSO-d_6, 373 K) δ 169.4 (C=O amide), 157.7 (OC_{Ar} quat), 153.2 (C=O carbamate), 147.9 (C_{Ar}), 137.6 (C_{Ar} quat), 135.7 (C_{Ar}), 133.6 (C_{Ar} quat), 129.9 (C_{Ar} quat), 128.0 (2 × C_{Ar}), 127.2 (C_{Ar} quat), 126.1 (C_{Ar}), 121.2 (C_{Ar}), 121.1 (C_{Ar}), 116.0 (C_{Ar}), 113.3 (2 × C_{Ar}), 78.0 (*C*$(CH_3)_3$), 54.4 (OCH_3), 49.8 (N*C*H_2CHAr), 49.2 (*C*HCO), 47.4 (N*C*H_2CHCO), 44.8 (*C*HAr), 27.8 (C(*C*$H_3)_3$); HRMS (ESI$^+$) *m*/*z* Calculated for $C_{26}H_{30}N_3O_4$ [M+H] 448.2236; Found 448.2238.

Gram scale C–H Arylation for the Preparation of Pyrrolidine Derivative 3a:

A large microwave vial (10–20 mL recommended volume) was charged with K_2CO_3 (553 mg, 4.00 mmol), flame-dried, and allowed to cool under argon. *tert*-Butyl 3-(quinolin-8-ylcarbamoyl)pyrrolidine-1-carboxylate **2** (1.37 g, 4.00 mmol), 4-iodoanisole (2.81 g, 12.0 mmol), $Pd(OAc)_2$ (45.1 mg, 0.20 mmol) and PivOH (409 mg, 4.00 mmol) were added sequentially. The reaction vessel was sealed and purged with argon, then $PhCF_3$ (2.0 mL, 2.0 M) was added by syringe. The reaction tube was then placed in a preheated oil bath and stirred at 110 ºC for 18 h. The reaction mixture was then allowed to cool to rt and EtOAc (20 mL) was added. The resulting mixture was filtered through a pad of Celite, eluting with further EtOAc (2 × 50 mL). The solvent was removed under reduced pressure. The reaction mixture was purified by flash column chromatography (20% acetone/hexane). The product containing fractions were combined and the solvent was removed under reduced pressure. Et_2O (20 mL) and pentane (20 mL) were added and the solvent was removed under reduced

pressure to afford arylated pyrrolidine **3a** as a yellow solid (1.20 g, 67%). Characterisation data identical to that reported on 0.5 mmol scale.

***tert*-Butyl (+)-(3*S*,4*S*)-3-(4-methoxyphenyl)-4-(quinolin-8-ylcarbamoyl)pyrrolidine-1-carboxylate ((+)-3a)**

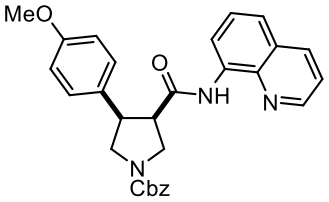


Prepared according to **General Procedure A** using amide (*S*)-**2** (171 mg), and 4-iodoanisole (351 mg). Purification by flash column chromatography (5% to 20% acetone/pentane) afforded arylated pyrrolidine **(+)-3a** as a yellow solid (134 mg, 60%, 97.8% *ee*). $[\alpha]_D^{25}$ +92 (*c* 0.40, $CHCl_3$).

Characterisation data identical to that reported for racemic pyrrolidine **3a** (page 208).

HPLC Conditions: Chiralpak IF 3-column, 80:20 *n*-hexane:*i*-PrOH, flow rate: 1 mL·min^{-1}, 35 ºC. UV detection wavelength: 210.4 nm. Retention times: 15.7 min (3*R*,4*R* enantiomer), 18.2 min (3*S*,4*S* enantiomer).

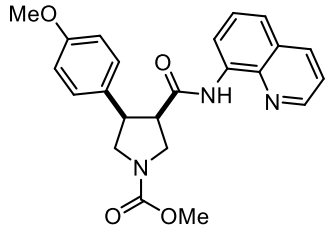
Benzyl *cis*-(±)-3-(4-methoxyphenyl)-4-(quinolin-8-ylcarbamoyl)pyrrolidine-1-carboxylate (13a)



A reaction tube was charged with K_2CO_3 (27.6 mg, 0.20 mmol), flame-dried, and allowed to cool under argon. Amide **9** (75.1 mg, 0.20 mmol), 4-iodoanisole (140 mg, 0.6 mmol), $Pd(OAc)_2$ (2.20 mg, 10.0 μmol) and PivOH (20.5 mg, 0.20 mmol) were added sequentially. The reaction vessel was sealed and purged with argon, then $PhCF_3$ (200 μL, 1.0 M) was added by syringe. The reaction tube was then placed in a preheated oil bath and stirred at 110 ºC for 18 h. The reaction mixture was then allowed to cool to rt and EtOAc (5 mL) was added. The resulting mixture was filtered through a pad of Celite, eluting with further EtOAc (2 × 5 mL). The solvent was removed under reduced pressure and the crude material was purified by flash column chromatography (0% to 20% acetone/hexane). The product containing fractions were combined and the solvent was removed under reduced pressure. Et_2O (5 mL) and pentane (5 mL) were added and the solvent was removed under reduced pressure to afford arylated pyrrolidine **13a** as a yellow solid (65.1 mg, 67%). R_f 0.10 (20% acetone/hexane); mp = 54–60 °C (from Et_2O/pentane); ν_{max} (film)/cm^{-1} 3342 (NH br), 2955, 1685 (C=O), 1525, 1417, 1324, 1248, 1181, 1110, 1030, 826, 756, 697; ^{1}H NMR (400 MHz, DMSO-d_6, 373 K): δ 9.70 (br s, 1 H, NH), 8.82 (dd, *J* = 4.2, 1.7 Hz, 1 H, HC_{Ar}), 8.35 (dd, *J* = 7.7, 1.4 Hz, 1 H, HC_{Ar}), 8.31 (dd, *J* = 8.3, 1.7 Hz, 1 H, HC_{Ar}), 7.54–7.48 (m, 2 H, HC_{Ar}), 7.47 (t, *J* = 8.0 Hz, 1 H, HC_{Ar}), 7.44–7.35 (m, 4 H, HC_{Ar}), 7.35–7.29 (m, 1 H, HC_{Ar}), 7.18–7.14 (m, 2 H, HC_{Ar}), 6.69–6.63 (m, 2 H, HC_{Ar}), 5.18 (s, 2H, OCH_2Ph), 3.90

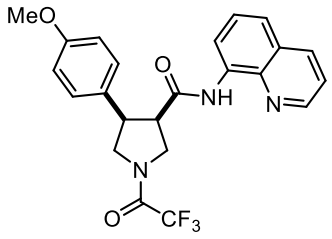
(dd, *J* = 10.5, 3.8 Hz, 1 H, NC*H*HCHCO), 3.88–3.80 (m, 4 H, CHCO, CHAr, NC*H*$_2$CHAr), 3.76–3.70 (m, 1 H, NCH*H*CHCO), 3.55 (s, 3 H, OCH_3);^{13}C NMR (101 MHz, DMSO-d_6, 373 K) δ 169.3 (C=O amide), 157.8 (OC_{Ar} quat), 153.6 (C=O carbamate), 147.9 (C_{Ar}), 137.7 (C_{Ar} quat), 136.8 (C_{Ar}, quat), 135.7 (C_{Ar}), 133.6 (C_{Ar} quat), 129.7 (C_{Ar} quat), 128.0 (2 × C_{Ar}), 127.8 (2 × C_{Ar}), 127.2 (C_{Ar} quat), 127.1 (C_{Ar}), 126.8 (2 × C_{Ar}), 126.1 (C_{Ar}), 121.2 (C_{Ar}), 121.1 (C_{Ar}), 116.0 (C_{Ar}), 113.3 (2 × C_{Ar}), 65.5 (OCH_2Ph), 54.4 (OCH_3), 49.8 (N*C*H$_2$CHAr), 49.1 (*C*HCO), 47.7 (N*C*H$_2$CHCO), 44.9 (CHAr); HRMS (ESI$^+$) *m*/*z* Calculated for $C_{29}H_{28}N_3O_4$ [M+H] 482.2080; Found 482.2072.

Methyl *cis*-(±)-3-(4-methoxyphenyl)-4-(quinolin-8-ylcarbamoyl)pyrrolidine-1-carboxylate (14)



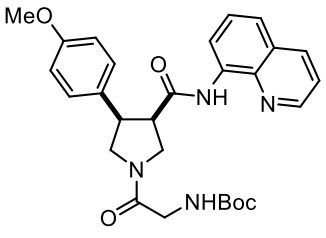
Prepared according to **General Procedure A** using methyl 3-(quinolin-8-ylcarbamoyl)pyrrolidine-1-carboxylate **10** (154 mg) and 4-iodoanisole (351 mg). Purification by flash column chromatography (30% to 35% acetone/hexane) afforded arylated pyrrolidine **14** as a pale pink solid (118 mg, 57%). R_f 0.18 (30% acetone/hexane); mp = 60–65 °C (from Et_2O/pentane); ν_{max} (film)/cm^{-1} 3336 (NH br), 2954, 1683 (C=O), 1525, 1486, 1451, 1386, 1324, 1248, 1182, 1116, 1032, 827, 792, 769; ^{1}H NMR (400 MHz, DMSO-d_6, 373 K) δ 9.70 (br s, 1 H, NH), 8.83 (dd, *J* = 4.2, 1.7 Hz, 1 H, HC_{Ar}), 8.35 (dd, *J* = 7.7, 1.4 Hz, 1 H, HC_{Ar}), 8.31 (dd, *J* = 8.3, 1.7 Hz, 1 H, HC_{Ar}), 7.60–7.54 (m, 2 H, HC_{Ar}), 7.47 (t, *J* = 8.0 Hz, 1 H, HC_{Ar}), 7.19–7.13 (m, 2 H, HC_{Ar}), 6.70–6.65 (m, 2 H, HC_{Ar}), 3.88–3.76 (m, 5 H, CHCO, CHAr, NC*H*HCHCO, NC*H*$_2$CHAr), 3.72–3.7 (m, 4 H, NCH*H*CHCO, CO_2CH_3), 3.55 (s, 3 H, OCH_3); ^{13}C NMR (101 MHz, DMSO-d_6, 373 K) δ 169.4 (C=O amide), 157.7 (OC_{Ar} quat), 154.2 (C=O carbamate), 147.9 (C_{Ar}), 137.7 (C_{Ar} quat), 135.7 (C_{Ar}), 133.6 (C_{Ar} quat), 129.7 (C_{Ar} quat), 128.0 (2 × C_{Ar}), 127.2 (C_{Ar} quat), 126.1 (C_{Ar}), 121.3 (C_{Ar}), 121.1 (C_{Ar}), 116.0 (C_{Ar}), 113.3 (2 × C_{Ar}), 54.4 (OCH_3), 51.4 (CO_2CH_3), 49.7 (N*C*H$_2$CHAr), 49.1 (*C*HCO), 47.6 (N*C*H$_2$CHCO), 44.9 (*C*HAr); HRMS (ESI$^+$) *m*/*z* Calculated for $C_{23}H_{24}N_3O_4$ [M+H] 406.1767; Found 406.1771.

***cis*-(±)-4-(4-Methoxyphenyl)-*N*-(quinolin-8-yl)-1-(2,2,2-trifluoroacetyl)pyrrolidine-3-carboxamide (15)**



Prepared according to **General Procedure A** using *N*-(quinolin-8-yl)-1-(2,2,2-trifluoroacetyl) pyrrolidine-3-carboxamide **11** (189 mg) and 4-iodoanisole (351 mg). Purification by flash column chromatography (20% to 30% acetone/hexane) afforded arylated pyrrolidine **15** as a pale yellow solid (43.0 mg, 19%, containing 6% of inseparable impurity). R_f 0.26 (30% acetone/pentane); mp = 111–115 °C (from Et_2O/pentane); ν_{max} (film)/cm^{-1} 3332 (NH br), 1681 (C=O), 1531, 1515, 1488, 1456, 1424, 1325, 1245, 1197, 1127, 1035, 940, 826, 788, 755, 689; ^{1}H NMR (400 MHz, DMSO-d_6, 373 K, observed as a mixture of rotamers) δ 9.74 (br s, 1 H, NH), 8.83 (dd, J = 4.2, 1.7 Hz, 1 H, HC_{Ar}), 8.39–8.29 (m, 2 H, HC_{Ar}), 7.60 (dd, J = 8.3, 1.4 Hz, 1 H, HC_{Ar}), 7.57 (dd, J = 8.3, 4.2 Hz, 1 H, HC_{Ar}), 7.48 (t, J = 7.9 Hz, 1 H, HC_{Ar}), 7.21–7.16 (m, 2 H, HC_{Ar}), 6.71–6.66 (m, 2 H, HC_{Ar}), 4.21–3.82 (br m, 6 H, CHCO, CHAr, NCH_2CHCO, NCH_2CHAr), 3.55 (s, 3 H, OCH_3); ^{13}C NMR (101 MHz, DMSO-d_6, 373 K, observed as a mixture of rotamers) δ 169.3 and 168.8 (C=O amide), 158.0 (OC_{Ar} quat), 153.8 (q, J_{CF} = 35.5 Hz, CF_3C=O), 148.0 (C_{Ar}), 137.7 (C_{Ar} quat), 135.7 (C_{Ar}), 133.5 (C_{Ar} quat), 128.6 and 128.4 (C_{Ar} quat), 128.0 (2 × C_{Ar}), 127.2 (C_{Ar} quat), 126.1 (C_{Ar}), 121.4 (C_{Ar}), 121.3 (C_{Ar}), 116.3 and 116.2 (C_{Ar}), 115.8 (q, J_{CF} = 287.7 Hz, CF_3), 113.4 (2 × C_{Ar}), 54.5 (OCH_3), 50.7 and 49.4 (NCH$_2$CHAr), 49.60 and 47.0 (*C*HCO), 49.55 and 48.1 (NCH$_2$CH$_2$CO), 45.6 and 43.0 (CHAr); ^{19}F NMR (376 MHz, DMSO-d_6, 373 K, observed as a mixture of rotamers) δ –71.16, –71.21; HRMS (ESI$^+$) *m*/*z* Calculated for $C_{23}H_{21}N_3O_3F_3$ [M+H] 444.1535; Found 444.1543.

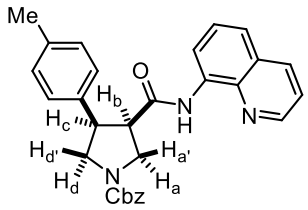
***tert*-Butyl *cis*-(±)-(2-(3-(4-methoxyphenyl)-4-(quinolin-8-ylcarbamoyl)pyrrolidin-1-yl)-2-oxoethyl)carbamate (16)**



Prepared according to **General Procedure A** using *tert*-butyl (±)-(2-oxo-2-(3-(quinolin-8-ylcarbamoyl)pyrrolidin-1-yl)ethyl)carbamate **12** (199 mg) and 4-iodoanisole (585 mg, 2.50 mmol). The reaction was stirred at 110 °C for 48 h. Purification by flash column chromatography (2% MeOH/CH_2Cl_2) afforded arylated pyrrolidine **16** as a pale yellow solid (44.3 mg, 18%). R_f 0.47 (5% MeOH/CH_2Cl_2); mp = 155–160 °C (from Et_2O/pentane); ν_{max} (film)/cm^{-1} 3407 (NH), 3325 (NH), 2974, 1706 (C=O), 1685 (C=O), 1645 (C=O), 1529, 1488, 1440, 1326, 1246, 1163, 1035, 826, 789, 705; ^{1}H NMR (400 MHz, $CDCl_3$, 298 K, observed as a mixture of rotamers) δ 9.48 and 9.46 (2 × br s, 1 H, NH_{AQ}), 8.68 and 8.67 (2 × dd, J = 4.2, 2.1 Hz, 1 H, HC_{Ar}), 8.58–8.45 (m, 1 H, HC_{Ar}), 8.12 and 8.10 (2 × dd, J = 3.4, 1.7 Hz, 1 H, HC_{Ar}), 7.49–7.43 (m, 2 H, HC_{Ar}), 7.42 and

7.41 (2 × dd, J = 8.5, 4.4 Hz, 1 H, HC_{Ar}), 7.19–7.10 (m, 2 H, HC_{Ar}), 6.67–6.59 (m, 2 H, HC_{Ar}), 5.57 (br t, J = 4.3 Hz, 1 H, NHBoc), 4.22 (dd, J = 12.4, 3.2 Hz, 0.6 H, NC*H*HCHCO), 4.12–3.96 (m, 3.4 H, NC*H*HCHCO, C*H*$_2$NHBoc, NC*H*HCHAr), 3.91–3.72 (m, 3 H, NCH*H*CHAr, CHAr, NCH*H*CHCO), 3.63–3.56 (m, 0.4 H, CHCO), 3.54 and 3.53 (2 × s, 3 H, OCH_3), 3.50–3.44 (m, 0.6 H, CHCO), 1.48 (s, 9 H, $C(CH_3)_3$); ^{13}C NMR (101 MHz, $CDCl_3$, 298 K, observed as a mixture of rotamers) δ 169.4 and 168.7 (CH*C*=O amide), 167.1 (CH_2*C*=O amide), 158.9 and 158.8 (OC_{Ar} quat), 155.8 (C=O carbamate), 148.0 (C_{Ar}), 138.2 and 138.1 (C_{Ar} quat), 136.1 (C_{Ar}), 133.8 and 133.7 (C_{Ar} quat), 128.6 and 128.5 (2 × C_{Ar}), 128.1 (C_{Ar} quat), 127.7 (C_{Ar} quat), 127.2 (C_{Ar}), 121.7 (C_{Ar}), 121.5 (C_{Ar}), 116.5 and 116.4 (C_{Ar}), 114.1 and 114.0 (2 × C_{Ar}), 79.6 (*C*$(CH_3)_3$), 55.0 and 54.9 (OCH_3), 51.6 and 50.0 (*C*HCO), 49.8 and 49.1 (N*C*H_2CHAr), 48.5 and 47.21 (N*C*H_2CHCO), 47.15 and 45.2 (CHAr), 43.2 and 43.0 (CH_2NHBoc), 28.4 (C(*C*$H_3)_3$); HRMS (ESI$^+$) *m*/*z* Calculated for $C_{28}H_{33}N_4O_5$ [M+H] 505.2451; Found 505.2457.

Benzyl *cis*-(±)-3-(quinolin-8-ylcarbamoyl)-4-(*p*-tolyl)pyrrolidine-1-carboxylate (13b)‡‡‡



Prepared according to **General Procedure A** using amide **9** (187 mg) and 4-iodotoluene (327 mg). Purification by flash column chromatography (5% to 10% MeCN/CH_2Cl_2) afforded arylated pyrrolidine **13b** as a pale brown solid (123 mg, 53%). R_f 0.53 (10% MeCN/CH_2Cl_2); mp = 56–59 °C (from Et_2O/pentane); ν_{max} (film)/cm^{-1} 3347 (NH br), 1694 (C=O), 1523, 1485, 1415, 1358, 1324, 1167, 1112, 824, 790, 765, 732, 696;

Characterisation in DMSO-d_6: ^{1}H NMR (400 MHz, DMSO-d_6, 373 K): δ 9.73 (br s, 1 H, NH), 8.82 (dd, J = 4.2, 1.7 Hz, 1 H, HC_{Ar}), 8.34 (dd, J = 7.7, 1.4 Hz, 1 H, HC_{Ar}), 8.31 (dd, J = 8.3, 1.7 Hz, 1 H, HC_{Ar}), 7.62–7.52 (m, 2 H, HC_{Ar}), 7.47 (t, J = 8.0 Hz, 1 H, HC_{Ar}), 7.46–7.33 (m, 4 H, HC_{Ar}), 7.36–7.27 (m, 1 H, HC_{Ar}), 7.17–7.09 (m, 2 H, HC_{Ar}), 6.95–6.87 (m, 2 H, HC_{Ar}), 5.18 (s, 2 H, OCH_2Ph), 3.94–3.82 (br m, 5 H, NC*H*$_{a'}$HCHCO, CH_bCO, CH_cAr, NC*H*$_2$CHAr), 3.74 (dd, J = 10.3, 5.9 Hz, 1 H, NCH*H*$_a$CHCO), 2.07 (s, 3 H, CH_3); ^{13}C NMR (101 MHz, DMSO-d_6, 373 K) δ 169.3 (C=O amide), 153.6 (C=O carbamate), 147.9 (C_{Ar}), 137.7 (C_{Ar} quat), 136.7 (C_{Ar}, quat), 135.7 (C_{Ar}), 135.2 (C_{Ar} quat), 134.7 (C_{Ar} quat), 133.6 (C_{Ar} quat), 128.1 (2 × C_{Ar}), 127.7 (2 × C_{Ar}), 127.2 (C_{Ar} quat), 127.1 (C_{Ar}), 126.83 (2 × C_{Ar}), 126.80 (2 × C_{Ar}), 126.1 (C_{Ar}), 121.2 (C_{Ar}), 121.1 (C_{Ar}), 116.0 (C_{Ar}), 65.5 (OCH_2Ph), 49.7 (N*C*H_2CHAr), 49.0 (*C*HCO), 47.7 (N*C*H_2CHCO), 45.2 (CHAr), 19.7 (CH_3);

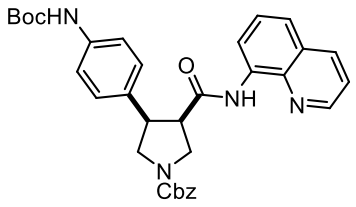
‡‡‡ To allow interpretation of the deuteration studies described in chapter 5, pyrrolidine **13b** was characterised at 373 K in both DMSO-d_6 and toluene-d_8, as well as at 298 K in $CDCl_3$. Full characterisation in each solvent is reported here to enable direct comparison.

Characterisation in toluene-d_8: ^{1}H NMR (500 MHz, toluene-d_8, 373 K): δ 9.33 (br s, 1 H, NH), 8.72 (dd, *J* = 7.7, 1.3 Hz, 1 H, HC_{Ar}), 8.39 (dd, *J* = 4.2, 1.7 Hz, 1 H, HC_{Ar}), 7.51 (dd, *J* = 8.3, 1.7 Hz, 1 H, HC_{Ar}), 7.31–7.28 (m, 2 H, HC_{Ar}), 7.14–7.09 (m, 3 H, HC_{Ar}), 7.00–6.94 (m, 4 H, HC_{Ar}), 6.82 (dd, *J* = 8.3, 4.2 Hz, 1 H, HC_{Ar}), 6.95 (d, *J* = 7.9 Hz, 2 H, HC_{Ar}), 5.17 (s, 2 H, OCH_2Ph), 4.13 (dd, *J* = 11.3, 4.3 Hz, 1 H, NCH_aHCHCO), 4.00 (dd, *J* = 10.5, 8.3 Hz, 1 H, NCH_dHCH$_2$), 3.73 (dd, *J* = 9.1, 9.1 Hz, 1 H, NCHH_dCH$_2$), 3.55 (dd, *J* = 9.1, 9.1 Hz, 1 H, NCHH_aCHCO), 3.28 (ddd, *J* = 7.6, 7.6, 7.6 Hz, 1 H, CH_cAr), 2.86 (ddd, *J* = 7.2, 7.2, 4.4 Hz, 1 H, CH_bCO), 1,79 (s, 3 H, CH_3); ^{13}C NMR (101 MHz, toluene-d_8, 373 K) δ 169.4 (C=O amide), 155.0 (C=O carbamate), 147.9 (C_{Ar}), 139.2 (C_{Ar} quat), 138.5 (C_{Ar} quat), 136.8 (C_{Ar}), 135.5 (C_{Ar} quat), 135.4 (C_{Ar} quat), 129.5 (2 × C_{Ar}), 128.7 (C_{Ar}, C_{Ar} quat), 128.4 (2 × C_{Ar}, C_{Ar} quat), 128.2 (2 × C_{Ar}), 128.0 (C_{Ar}), 127.8 (2 × C_{Ar}), 121.3 (C_{Ar}), 121.2 (C_{Ar}), 117.1 (C_{Ar}), 67.2 (OCH_2Ph), 51.8 (*C*HCO), 51.0 (N*C*H$_2$CHAr), 49.0 (N*C*H$_2$CHCO), 47.5 (CHAr), 20.7 (CH_3);

Characterisation in $CDCl_3$: ^{1}H NMR (400 MHz, $CDCl_3$, 298 K, observed as a mixture of rotamers): δ 9.56 and 9.53 (2 × br s, 1 H, NH amide), 8.70 and 8.67 (2 × dd, *J* = 4.2, 1.7 Hz, 1 H, HC_{Ar}), 8.59–8.50 (m, 1 H, HC_{Ar}), 8.13 and 8.11 (2 × dd, *J* = 4.4, 1.7 Hz, 1 H, HC_{Ar}), 7.50–7.29 (m, 8 H, HC_{Ar}), 7.13 (d, *J* = 8.0 Hz, 2 H, HC_{Ar}), 6.11 (d, *J* = 7.7 Hz, 2 H, HC_{Ar}), 5.31–5.17 (m, 2 H, OCH_2Ph), 4.17–4.08 (m, 1 H, NCH_aHCHCO), 4.08–3.91 (m, 2 H, NCH_2CHAr), 3.91–3.78 (m, 2 H, NCHH_aCHCO, CH_cAr), 3.58–3.48 (m, 1 H, CH_bCO), 2.08 and 2.07 (2 × s, 3 H, CH_3); ^{13}C NMR (101 MHz, $CDCl_3$, 298 K, observed as a mixture of rotamers) δ 169.4 and 169.2 (C=O amide), 154.7 (C=O carbamate), 147.91 and 147.88 (C_{Ar}), 138.1 (C_{Ar} quat), 136.84 and 136.80 (C_{Ar} quat), 136.1 (C_{Ar}), 134.2 and 134.1 (C_{Ar} quat), 133.9 (C_{Ar} quat), 129.2 (2 × C_{Ar}), 128.4 (2 × C_{Ar}), 128.0–127.7 (m, 3 × C_{Ar}, C_{Ar} quat), 127.7 (C_{Ar} quat), 127.4 (2 × C_{Ar}), 127.2 (C_{Ar}), 121.5 (C_{Ar}), 121.4 (C_{Ar}), 116.40 and 116.36 (C_{Ar}), 66.9 (OCH_2Ph), 51.5 and 50.7 (*C*HCO), 50.4 and 49.9 (N*C*H$_2$CHAr), 48.4 and 47.7 (N*C*H$_2$CHCO), 47.1 and 46.2 (CHAr), 20.8 (CH_3);

HRMS (ESI$^+$) *m*/*z* Calculated for $C_{29}H_{28}N_3O_3$ [M+H] 466.2131; Found 466.2123.

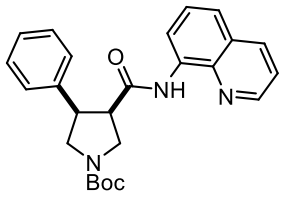
Benzyl *cis*-(±)-3-(4-((tert-butoxycarbonyl)amino)phenyl)-4-(quinolin-8-ylcarbamoyl)-pyrrolidine-1-carboxylate (13c)



Prepared according to **General Procedure A** using amide **9** (187 mg) and *tert*-butyl (4-iodophenyl)carbamate (479 mg). The crude material was purified by flash column chromatography (20% to 30% acetone/hexane), the product containing fractions were combined and the solvent was removed under reduced pressure. CH_2Cl_2 (5 mL) and pentane (5 mL) were added and the solvent was removed under reduced pressure to afford arylated compound **13c** as a yellow solid (153 mg, 54%). R_f 0.30 (30% acetone/hexane); mp = 92–97 °C (from CH_2Cl_2/pentane); ν_{max} (film)/cm^{-1} 3280 (NH br),

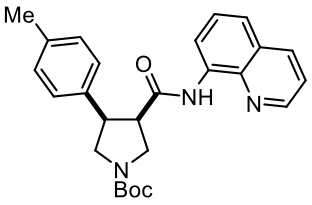
1674 (C=O), 1537, 1419, 1315, 1196, 1156, 1113, 1047, 1031, 789, 754, 695; ^{1}H NMR (400 MHz, $CDCl_3$, 298 K, observed as a mixture of rotamers): δ 9.57 and 9.54 (2 × br s, 1 H, NH amide), 8.70 and 8.67 (2 × dd, *J* = 4.2, 1.7 Hz, 1 H, HC_{Ar}), 8.58–8.49 (m, 1 H, HC_{Ar}), 8.12 and 8.10 (2 × dd, *J* = 4.1, 1.7 Hz, 1 H, HC_{Ar}), 7.49–7.29 (m, 8 H, HC_{Ar}), 7.16 (d, *J* = 8.6 Hz, 2 H, HC_{Ar}), 7.11 (d, *J* = 8.4 Hz, 2 H, HC_{Ar}), 6.28 (br s, 1 H, NH carbamate), 5.30–5.15 (m, 2 H, OCH_2Ph), 4.15–4.06 (m, 1 H, NC*H*HCHCO), 4.06–3.89 (m, 2 H, NC*H*$_2$CHAr), 3.89–3.76 (m, 2 H, NCH*H*CHCO, CHAr), 3.57–3.46 (m, 1 H, CHCO), 1.45 (br s, 9 H, $C(CH_3)_3$);^{13}C NMR (101 MHz, $CDCl_3$, 298 K, observed as a mixture of rotamers) δ 169.4 and 169.1 (C=O amide), 154.8 and 154.7 (C=O Cbz), 152.4 (C=O Boc), 148.1 and 148.0 (C_{Ar}), 138.1 (C_{Ar} quat), 137.5 (C_{Ar} quat), 136.8 (C_{Ar} quat), 136.1 (C_{Ar}), 133.8 (C_{Ar} quat), 131.7 and 131.5 (C_{Ar} quat), 128.4 (2 × C_{Ar}), 128.2 (2 × C_{Ar}), 127.9 (2 × C_{Ar}), 127.8 (C_{Ar}), 127.7 (C_{Ar} quat), 127.2 (C_{Ar}), 121.6 (C_{Ar}), 121.5 and 121.4 (C_{Ar}), 118.3 (2 × C_{Ar}), 116.5 and 116.4 (C_{Ar}), 80.3 (*C*$(CH_3)_3$), 66.9 (OCH_2Ph), 51.4 and 50.6 (*C*HCO), 50.4 and 49.9 (N*C*H_2CHAr), 48.4 and 47.7 (N*C*H_2CHCO), 46.9 and 46.0 (CHAr), 28.2 (C(*C*$H_3)_3$); HRMS (ESI$^+$) *m*/*z* Calculated for $C_{33}H_{35}N_4O_5$ [M+H] 567.2607; Found 567.2617.

tert-Butyl _cis_-(±)-3-phenyl-4-(quinolin-8-ylcarbamoyl)pyrrolidine-1-carboxylate (3b)



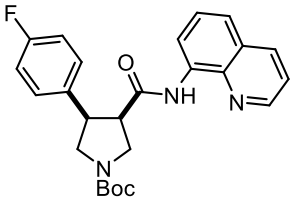
Prepared according to **General Procedure A** using amide **2** (171 mg) and iodobenzene (306 mg). Purification by flash column chromatography (10% MeCN/CH_2Cl_2) afforded arylated pyrrolidine **3b** as a white solid (89.6 mg, 43%). R_f 0.42 (10% MeCN/CH_2Cl_2); mp = 65–68 °C (from Et_2O/pentane); ν_{max} (film)/cm^{-1} 3341 (NH br), 2976, 1682 (C=O), 1524, 1485, 1390, 1365, 1325, 1256, 1162, 1116, 874, 826, 790, 755, 698; ^{1}H NMR (400 MHz, DMSO-d_6, 373 K) δ 9.75 (br s, 1 H, NH), 8.85 (dd, *J* = 4.2, 1.7 Hz, 1 H, HC_{Ar}), 8.33 (dd, *J* = 3.8, 1.5 Hz, 1 H, HC_{Ar}), 8.31 (dd, *J* = 4.5, 1.5 Hz, 1 H, HC_{Ar}), 7.60–7.54 (m, 2 H, HC_{Ar}), 7.46 (t, *J* = 8.0 Hz, 1 H, HC_{Ar}), 7.27–7.22 (m, 2 H, HC_{Ar}), 7.15–7.09 (m, 2 H, HC_{Ar}), 7.05–7.00 (m, 1 H, HC_{Ar}), 3.92–3.85 (m, 2 H, CHCO, CHAr), 3.85–3.77 (m, 3 H, NC*H*HCHCO, NC*H*$_2$CHAr), 3.69–3.64 (m, 1 H, NCH*H*CHCO), 1.49 (s, 9 H, $C(CH_3)_3$); ^{13}C NMR (101 MHz, DMSO-d_6, 373 K) δ 169.3 (C=O amide), 153.2 (C=O carbamate), 148.0 (C_{Ar}), 138.1 (C_{Ar} quat), 137.7 (C_{Ar} quat), 135.7 (C_{Ar}), 133.6 (C_{Ar} quat), 127.5 (2 × C_{Ar}), 127.2 (C_{Ar} quat), 127.0 (2 × C_{Ar}), 126.1 (C_{Ar}), 126.0 (C_{Ar}), 121.3 (C_{Ar}), 121.1 (C_{Ar}), 116.0 (C_{Ar}), 78.0 (*C*$(CH_3)_3$), 49.7 (N*C*H_2CHAr), 49.0 (*C*HCO), 47.5 (N*C*H_2CHCO), 45.4 (CHAr), 27.8 (C(*C*$H_3)_3$); HRMS (ESI$^+$) *m*/*z* Calculated for $C_{25}H_{28}N_3O_3$ [M+H] 418.2131; Found 418.2136.

***tert*-Butyl *cis*-(±)-3-(quinolin-8-ylcarbamoyl)-4-(*p*-tolyl)pyrrolidine-1-carboxylate (3c)**



Prepared according to **General Procedure A** using amide **2** (171 mg) and 4-iodotoluene (327 mg). Purification by flash column chromatography (5% to 10% MeCN/CH_2Cl_2) afforded arylated pyrrolidine **3c** as a white solid (118 mg, 55%). R_f 0.22 (5% MeCN/CH_2Cl_2); mp = 60–64 °C (from Et_2O/pentane); ν_{max} (film)/cm^{-1} 3345 (NH br), 2974, 1685 (C=O), 1525, 1485, 1391, 1324, 1163, 1115, 874, 824, 791, 758; ^{1}H NMR (400 MHz, DMSO-d_6, 373 K) δ 9.71 (br s, 1 H, NH), 8.84 (dd, J = 4.2, 1.7 Hz, 1 H, HC_{Ar}), 8.34 (dd, J = 7.7, 1.4 Hz, 1 H, HC_{Ar}), 8.31 (dd, J = 8.3, 1.7 Hz, 1 H, HC_{Ar}), 7.60–7.53 (m, 2 H, HC_{Ar}), 7.47 (t, J = 8.0 Hz, 1 H, HC_{Ar}), 7.14–7.08 (m, 2 H, HC_{Ar}), 6.94–6.88 (m, 2 H, HC_{Ar}), 3.87–3.78 (m, 3 H, CHCO, CHAr, NC*H*HCHCO), 3.78–3.72 (m, 2 H, NCH_2CHAr), 3.69–3.61 (m, 1 H, NCH*H*CHCO), 2.07 (s, 3 H, CH_3), 1.49 (s, 9 H, $C(CH_3)_3$); ^{13}C NMR (101 MHz, DMSO-d_6, 373 K) δ 169.3 (C=O amide), 153.2 (C=O carbamate), 147.9 (C_{Ar}), 137.6 (C_{Ar} quat), 135.7 (C_{Ar}), 135.1 (C_{Ar} quat), 135.0 (C_{Ar} quat), 133.6 (C_{Ar} quat), 128.1 (2 × C_{Ar}), 127.2 (C_{Ar} quat), 126.8 (2 × C_{Ar}), 126.1 (C_{Ar}), 121.2 (C_{Ar}), 121.1 (C_{Ar}), 116.0 (C_{Ar}), 78.0 (*C*$(CH_3)_3$), 49.7 (N*C*H_2CHAr), 49.1 (*C*HCO), 47.5 (N*C*H_2CHCO), 45.2 (CHAr), 27.8 (C(*C*$H_3)_3$), 19.7 (CH_3); HRMS (ESI$^+$) m/z Calculated for $C_{26}H_{30}N_3O_3$ [M+H] 432.2287; Found 432.2304.

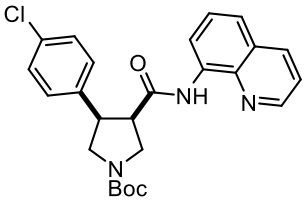
***tert*-Butyl *cis*-(±)-3-(4-fluorophenyl)-4-(quinolin-8-ylcarbamoyl)pyrrolidine-1-carboxylate (3d)**



Prepared according to **General Procedure A** using amide **2** (171 mg) and 4-fluoroiodobenzene (333 mg). Purification by flash column chromatography (5% to 15% acetone/pentane) afforded arylated pyrrolidine **3d** as a white solid (95.8 mg, 44%). R_f 0.12 (10% acetone/pentane); mp = 94–97 °C (from Et_2O/pentane); ν_{max} (film)/cm^{-1} 3334 (NH br), 2973, 1678 (C=O), 1526, 1486, 1391, 1324, 1226, 1164, 1119, 827, 791, 769; ^{1}H NMR (400 MHz, DMSO-d_6, 373 K) δ 9.73 (br s, 1 H, NH), 8.85 (dd, J = 4.2, 1.7 Hz, 1 H, HC_{Ar}), 8.33 (m, 1 H, HC_{Ar}), 8.31 (m, 1 H, HC_{Ar}), 7.61–7.55 (m, 2 H, HC_{Ar}), 7.47 (t, J = 8.0 Hz, 1 H, HC_{Ar}), 7.30–7.24 (m, 2 H, HC_{Ar}), 6.94–6.87 (m, 2 H, HC_{Ar}), 3.93–3.84 (m, 2 H, CHCO, CHAr), 3.84–3.71 (m, 3 H, NC*H*HCHCO, NCH_2CHAr), 3.66 (dd, J = 10.9, 6.7 Hz, 1 H, NCH*H*CHCO), 1.49 (s, 9 H, $C(CH_3)_3$); ^{13}C NMR (101 MHz, DMSO-d_6, 373 K) δ 169.3 (C=O amide), 160.4 (d, J_{CF} = 243.4 Hz, FC_{Ar} quat), 153.2 (C=O carbamate), 148.0 (C_{Ar}), 137.7 (C_{Ar} quat), 135.8 (C_{Ar}), 134.2 (d, J_{CF} = 3.3 Hz, F-*p*-C_{Ar} quat), 133.5 (C_{Ar} quat), 128.9 (d, J_{CF} = 8.1 Hz, 2 × F-*m*-C_{Ar}), 127.2 (C_{Ar} quat), 126.1 (C_{Ar}), 121.3 (C_{Ar}), 121.2 (C_{Ar}), 116.2 (C_{Ar}), 114.2 (d, J_{CF} = 21.0 Hz, 2 × F-*o*-C_{Ar}), 78.1 (*C*$(CH_3)_3$), 49.7 (N*C*H_2CHAr), 49.0 (*C*HCO), 47.4 (N*C*H_2CHCO), 44.8 (CHAr), 27.8 (C(*C*$H_3)_3$); ^{19}F NMR (471 MHz, DMSO-d_6, 373 K) δ –116.3

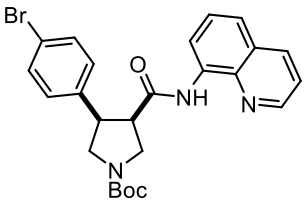
(tt, J_{HF} = 8.6, 5.8 Hz); HRMS (ESI$^+$) *m*/*z* Calculated for $C_{25}H_{27}N_3O_3F$ [M+H] 436.2036; Found 436.2053.

tert-Butyl _cis_-(±)-3-(4-chlorophenyl)-4-(quinolin-8-ylcarbamoyl)pyrrolidine-1-carboxylate (3e)



Prepared according to **General Procedure A** using amide **2** (171 mg) and 1-chloro-4-iodobenzene (358 mg). Purification by flash column chromatography (5% to 10% MeCN/CH_2Cl_2) afforded arylated pyrrolidine **3e** as a white solid (97.2 mg, 43%). R_f 0.17 (5% MeCN/CH_2Cl_2); mp = 152–155 °C (from Et_2O/pentane); ν_{max} (film)/cm^{-1} 3267 (NH br), 2982, 1674 (C=O), 1534, 1489, 1407, 1390, 1322, 1161, 1116, 1016, 871, 829, 799, 767; ^{1}H NMR (400 MHz, DMSO-d_6, 373 K) δ 9.75 (br s, 1 H, NH), 8.85 (dd, *J* = 4.2, 1.7 Hz, 1 H, HC_{Ar}), 8.35–8.29 (m, 2 H, HC_{Ar}), 7.62–7.55 (m, 2 H, HC_{Ar}), 7.47 (t, *J* = 8.0 Hz, 1 H, HC_{Ar}), 7.28–7.23 (m, 2 H, HC_{Ar}), 7.18–7.12 (m, 2 H, HC_{Ar}), 3.93–3.84 (m, 2 H, CHCO, CHAr), 3.84–3.71 (m, 3 H, NC*H*HCHCO, NCH_2CHAr), 3.70–3.62 (m, 1 H, NCH*H*CHCO), 1.48 (s, 9 H, C(CH_3)$_3$); ^{13}C NMR (101 MHz, DMSO-d_6, 373 K) δ 169.2 (C=O amide), 153.1 (C=O carbamate), 148.0 (C_{Ar}), 137.7 (C_{Ar} quat), 137.1 (C_{Ar} quat), 135.7 (C_{Ar}), 133.5 (C_{Ar} quat), 130.9 (C_{Ar} quat), 128.8 (2 × C_{Ar}), 127.4 (2 × C_{Ar}), 127.2 (C_{Ar} quat), 126.1 (C_{Ar}), 121.3 (2 × C_{Ar}), 116.2 (C_{Ar}), 78.1 (*C*(CH_3)$_3$), 49.5 (N*C*H_2CHAr), 48.9 (*C*HCO), 47.5 (N*C*H_2CHCO), 44.8 (CHAr), 27.8 (C(*C*H_3)$_3$); HRMS (ESI$^+$) *m*/*z* Calculated for $C_{25}H_{27}N_3O_3{}^{35}Cl$ [M+H] 452.1741; Found 452.1750.

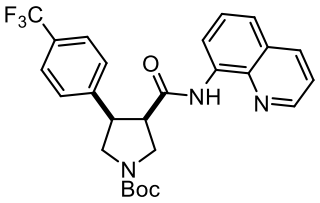
tert-Butyl _cis_-(±)-3-(4-bromophenyl)-4-(quinolin-8-ylcarbamoyl)pyrrolidine-1-carboxylate (3f)



Prepared according to **General Procedure A** using amide **2** (171 mg) and 1-bromo-4-iodobenzene (424 mg). Purification by flash column chromatography (10% MeCN/CH_2Cl_2) afforded arylated pyrrolidine **3f** as a pale pink solid (112 mg, 45%). R_f 0.34 (10% MeCN/CH_2Cl_2); mp = 159–161°C; ν_{max} (film)/cm^{-1} 3273 (NH br), 2980, 1674 (C=O), 1533, 1488, 1409, 1389, 1321, 1161, 1115, 1011, 870, 828, 798, 767; ^{1}H NMR (400 MHz, DMSO-d_6, 373 K) δ 9.75 (br s, 1 H, NH), 8.85 (dd, *J* = 4.2, 1.7 Hz, 1 H, HC_{Ar}), 8.33 (dd, *J* = 2.7, 1.5 Hz, 1 H, HC_{Ar}), 8.31 (t, *J* = 1.8 Hz, 1 H, HC_{Ar}), 7.61–7.56 (m, 2 H, HC_{Ar}), 7.47 (t, *J* = 8.0 Hz, 1 H, HC_{Ar}), 7.31–7.27 (m, 2 H, HC_{Ar}), 7.21–7.17 (m, 2 H, HC_{Ar}), 3.91–3.83 (m, 2 H, CHCO, CHAr), 3.83–3.71 (m, 3 H, NC*H*HCHCO, NCH_2CHAr), 3.69–3.63 (m, 1 H, NCH*H*CHCO), 1.48 (s, 9 H, C(CH_3)$_3$); ^{13}C NMR (101 MHz, DMSO-d_6, 373 K) δ 169.1 (C=O amide), 153.1 (C=O carbamate), 148.0 (C_{Ar}), 137.7 (C_{Ar} quat), 137.6 (C_{Ar} quat), 135.7 (C_{Ar}), 133.5 (C_{Ar} quat), 130.4 (2 × C_{Ar}), 129.2 (2 × C_{Ar}), 127.2 (C_{Ar} quat), 126.1 (C_{Ar}), 121.3 (2 × C_{Ar}),

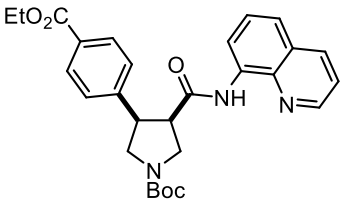
119.3 (C_{Ar} quat), 116.2 (C_{Ar}), 78.1 ($C(CH_3)_3$), 49.4 (NCH_2CHAr), 48.8 ($CHCO$), 47.5 (NCH_2CHCO), 44.9 (CHAr), 27.8 ($C(CH_3)_3$); HRMS (ESI^+) *m*/*z* Calculated for $C_{25}H_{27}N_3O_3Br$ [M+H] 496.1236; Found 496.1239.

***tert*-Butyl *cis*-(±)-3-(quinolin-8-ylcarbamoyl)-4-(4-(trifluoromethyl)phenyl)pyrrolidine-1-carboxylate (3g)**



Prepared according to **General Procedure A** using amide **2** (171 mg) and 1-iodo-4-(trifluoromethyl)benzene (408 mg). Purification by flash column chromatography (5% to 10% $MeCN/CH_2Cl_2$) afforded arylated pyrrolidine **3g** as a pale brown solid (59.0 mg, 24%). R_f 0.43 (10% $MeCN/CH_2Cl_2$); mp = 143–145 °C (from Et_2O/pentane); ν_{max} (film)/cm^{-1} 3274 (NH br), 2978, 1674 (C=O), 1532, 1488, 1408, 1369, 1328, 1161, 1117, 1070, 1019, 872, 841, 797, 765; ^1H NMR (400 MHz, DMSO-d_6, 373 K) δ 9.75 (br s, 1 H, NH), 8.83 (dd, *J* = 4.2, 1.7 Hz, 1 H, HC_{Ar}), 8.31 (dd, *J* = 8.3, 1.7 Hz, 1 H, HC_{Ar}), 8.28 (dd, *J* = 7.7, 1.3 Hz, 1 H, HC_{Ar}), 7.60–7.54 (m, 2 H, HC_{Ar}), 7.49–7.41 (m, 5 H, HC_{Ar}), 4.03–3.91 (m, 2 H, CHCO, CHAr), 3.86–3.78 (m, 3 H, $NCHHCHCO$, NCH_2CHAr), 3.69 (dd, *J* = 11.2, 7.0 Hz, 1 H, $NCHHCHCO$), 1.49 (s, 9 H, $C(CH_3)_3$); ^{13}C NMR (101 MHz, DMSO-d_6, 373 K) δ 169.1 (C=O amide), 153.1 (C=O carbamate), 148.0 (C_{Ar}), 143.0 (C_{Ar} quat), 137.7 (C_{Ar} quat), 135.7 (C_{Ar}), 133.4 (C_{Ar} quat), 127.9 (2 × C_{Ar}), 127.2 (C_{Ar} quat), 127.1 (q, J_{CF} = 30.1 Hz, F_3CC_{Ar} quat), 126.0 (C_{Ar}), 124.3 (q, J_{CF} = 3.9 Hz, 2 × C_{Ar}), 123.6 (q, J_{CF} = 271.9 Hz, CF_3 quat), 121.3 (C_{Ar}), 121.2 (C_{Ar}), 116.2 (C_{Ar}), 78.2 ($C(CH_3)_3$), 49.2 (NCH_2CHAr), 48.8 ($CHCO$), 47.6 (NCH_2CHCO), 45.2 ($CHAr$), 27.8 ($C(CH_3)_3$); ^{19}F NMR (376 MHz, DMSO-d_6, 373 K) δ –61.3; HRMS (ESI^+) *m*/*z* Calculated for $C_{26}H_{27}N_3O_3F_3$ [M+H] 486.2005; Found 486.2003.

***tert*-Butyl *cis*-(±)-3-(4-(ethoxycarbonyl)phenyl)-4-(quinolin-8-ylcarbamoyl)pyrrolidine-1-carboxylate (3h)**

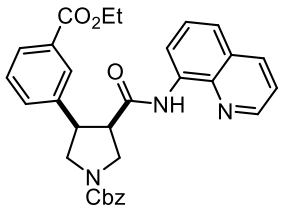


Prepared according to **General Procedure A** using amide **2** (171 mg) and ethyl 4-iodobenzoate (552 mg, 2.0 mmol). The reaction was stirred at 110 °C for 48 h. Purification by flash column chromatography (20% acetone/hexane) afforded arylated pyrrolidine **3h** as a white solid (76.3 mg, 38%). R_f 0.12 (20% acetone/hexane); mp = 69–71 °C (from Et_2O/pentane); ν_{max} (film)/cm^{-1} 3323 (NH br), 1689 (C=O), 1525, 1486, 1392, 1324, 1276, 1164, 1105, 826, 791, 759; ^1H NMR (400 MHz, DMSO-d_6, 373 K) δ 9.74 (br s, 1 H, NH), 8.82 (dd, *J* = 4.2, 1.7 Hz, 1 H, HC_{Ar}), 8.32–8.28 (m, 2 H, HC_{Ar}), 7.72–7.68 (m, 2 H, HC_{Ar}), 7.59–7.53 (m, 2 H, HC_{Ar}), 7.45 (t, *J* = 7.9 Hz, 1 H, HC_{Ar}), 7.40–7.35 (m, 2 H, HC_{Ar}), 4.22 (q, *J* = 7.1 Hz, 2 H, OCH_2CH_3), 4.02–3.88 (m, 2 H, CHCO,

CHAr), 3.85–3.79 (m, 3 H, NC*H*HCHCO, NC*H*$_2$CHAr), 3.68 (dd, *J* = 11.2, 6.9 Hz, 1 H, NCH*H*CHCO), 1.49 (s, 9 H, C(CH$_3$)$_3$), 1.25 (t, *J* = 7.1 Hz, 3 H, OCH$_2$C*H*$_3$); ^{13}C NMR (101 MHz, DMSO-*d*$_6$, 373 K) δ 169.1 (C=O amide), 164.8 (C=O ester), 153.2 (C=O carbamate), 147.9 (C$_{Ar}$), 143.6 (C$_{Ar}$ quat), 137.7 (C$_{Ar}$ quat), 135.7 (C$_{Ar}$), 133.5 (C$_{Ar}$ quat), 128.3 (2 × C$_{Ar}$), 128.2 (C$_{Ar}$ quat), 127.3 (2 × C$_{Ar}$), 127.2 (C$_{Ar}$ quat), 126.1 (C$_{Ar}$), 121.3 (C$_{Ar}$), 121.2(C$_{Ar}$), 116.2 (C$_{Ar}$), 78.1 (*C*(CH$_3$)$_3$), 59.8 (O*C*H$_2$CH$_3$), 49.3 (N*C*H$_2$CHAr), 48.9 (*C*HCO), 47.5 (N*C*H$_2$CHCO), 45.4 (CHAr), 27.8 (C(*C*H$_3$)$_3$), 13.4 (OCH$_2$*C*H$_3$); HRMS (ESI$^+$) *m*/*z* Calculated for C$_{28}$H$_{32}$N$_3$O$_5$ [M+H] 490.2342; Found 490.2346.

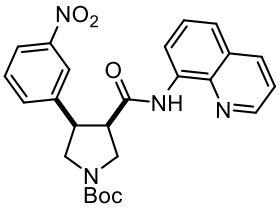
Pyrrolidine **3h** was isolated in 31% when using ethyl 4-iodobenzoate (414 mg, 1.5 mmol) and running the reaction for 18 h, under otherwise identical conditions. Identical characterisation data was observed.

Benzyl *cis*-(±)-3-(3-(ethoxycarbonyl)phenyl)-4-(quinolin-8-ylcarbamoyl)pyrrolidine-1-carboxylate (13d)



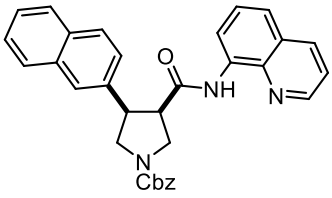
Prepared according to **General Procedure A** using amide **9** (187 mg) and ethyl 3-iodobenzoate (414 mg). Purification by flash column chromatography (30% acetone/hexane) afforded arylated pyrrolidine **13d** as a pale yellow solid (84.3 mg, 32%). *R*$_f$ 0.24 (30% acetone/hexane); mp = 47–53 °C (from Et$_2$O/pentane); ν$_{max}$ (film)/cm^{-1} 3332 (NH br), 2979, 1697 (C=O), 1524, 1486, 1416, 1324, 1275, 1193, 1108, 1021, 826, 791, 751, 695; ^{1}H NMR (400 MHz, DMSO-*d*$_6$, 373 K): δ 9.78 (br s, 1 H, NH), 8.79 (dd, *J* = 4.2, 1.7 Hz, 1 H, HC$_{Ar}$), 8.32–8.30 (m, 1 H, HC$_{Ar}$), 8.30–8.28 (m, 1 H, HC$_{Ar}$), 7.89–7.87 (m, 1 H, HC$_{Ar}$), 7.62–7.59 (m, 1 H, HC$_{Ar}$), 7.58–7.52 (m, 2 H, HC$_{Ar}$), 7.52–7.48 (m, 1 H, HC$_{Ar}$), 7.47–7.35 (m, 5 H, HC$_{Ar}$), 7.34–7.29 (m, 1 H, HC$_{Ar}$), 7.25 (t, *J* = 7.7 Hz, 1 H, HC$_{Ar}$), 5.20 (s, 2 H, OCH$_2$Ph), 4.16 (qd, *J* = 7.1, 1.6 Hz, 2 H, OC*H*$_2$CH$_3$), 4.03 (ddd, *J* = 7.4, 7.4, 7.4 Hz, 1 H, CHAr), 3.99–3.88 (m, 4 H, CHCO, NC*H*HCHCO, NC*H*$_2$CHAr), 3.81–3.74 (m, 1 H, NCH*H*CHCO), 1.17 (t, *J* = 7.1 Hz, 3 H, OCH$_2$C*H*$_3$);^{13}C NMR (101 MHz, DMSO-*d*$_6$, 373 K) δ 169.1 (C=O amide), 164.9 (C=O ester), 153.6 (C=O carbamate), 147.9 (C$_{Ar}$), 138.4 (C$_{Ar}$ quat), 137.7 (C$_{Ar}$ quat), 136.7 (C$_{Ar}$ quat), 135.7 (C$_{Ar}$), 133.4 (C$_{Ar}$ quat), 131.6 (C$_{Ar}$), 129.7 (C$_{Ar}$ quat), 127.9 (C$_{Ar}$), 127.81 (C$_{Ar}$), 127.75 (2 × C$_{Ar}$), 127.2 (C$_{Ar}$ quat), 127.1 (C$_{Ar}$), 126.9 (C$_{Ar}$), 126.8 (2 × C$_{Ar}$), 126.0 (C$_{Ar}$), 121.25 (C$_{Ar}$), 121.21 (C$_{Ar}$), 116.2 (C$_{Ar}$), 65.6 (OCH$_2$Ph), 59.8 (O*C*H$_2$CH$_3$), 49.6 (N*C*H$_2$CHAr), 48.9 (*C*HCO), 47.7 (N*C*H$_2$CHCO), 45.3 (CHAr), 13.3 (OCH$_2$*C*H$_3$); HRMS (ESI$^+$) *m*/*z* Calculated for C$_{31}$H$_{30}$N$_3$O$_5$ [M+H] 524.2185; Found 524.2196.

***tert*-Butyl *cis*-(±)-3-(3-nitrophenyl)-4-(quinolin-8-ylcarbamoyl)pyrrolidine-1-carboxylate (3i)**



Prepared according to **General Procedure A** using amide **2** (171 mg) and 1-iodo-3-nitrobenzene (374 mg). Purification by flash column chromatography (10% to 20% acetone/pentane) afforded arylated pyrrolidine **3i** as a white solid (70.5 mg, 30%). R_f 0.24 (20% acetone/pentane); mp = 76–79 °C (from Et_2O/pentane); ν_{max} (film)/cm^{-1} 3340 (NH br), 2974, 1682 (C=O), 1525 (NO_2), 1485, 1392, 1346 (NO_2), 1324, 1163, 1120, 873, 827, 792, 730, 681; ^{1}H NMR (400 MHz, DMSO-d_6, 373 K) δ 9.81 (br s, 1 H, NH), 8.80 (dd, J = 4.2, 1.7 Hz, 1 H, HC_{Ar}), 8.31 (dd, J = 8.3, 1.7 Hz, 1 H, HC_{Ar}), 8.25 (dd, J = 7.7, 1.3 Hz, 1 H, HC_{Ar}), 8.10 (t, J = 2.1 Hz, 1 H, HC_{Ar}), 7.84 (ddd, J = 8.2, 2.4, 1.0 Hz, 1 H, HC_{Ar}), 7.70–7.63 (m, 1 H, HC_{Ar}), 7.61–7.54 (m, 2 H, HC_{Ar}), 7.42 (dt, J = 16.0, 7.9 Hz, 2 H, HC_{Ar}), 4.07 (ddd, J = 7.3, 7.3, 7.3 Hz, 1 H, CHAr), 4.00 (ddd, J = 7.3, 7.3, 4.5 Hz, 1 H, CHCO), 3.88–3.78 (m, 3 H, NC*H*HCHCO, NC*H*$_2$CHAr), 3.69 (dd, J = 11.2, 7.3 Hz, 1 H, NCH*H*CHCO), 1.50 (s, 9 H, $C(CH_3)_3$); ^{13}C NMR (101 MHz, DMSO-d_6, 373 K) δ 169.0 (C=O amide), 153.1 (C=O carbamate), 148.0 (C_{Ar}), 147.4 (O_2NC_{Ar} quat), 140.5 (C_{Ar} quat), 137.8 (C_{Ar} quat), 135.7 (C_{Ar}), 133.6 (C_{Ar}), 133.3 (C_{Ar} quat), 128.9 (C_{Ar}), 127.2 (C_{Ar} quat), 126.0 (C_{Ar}), 121.9 (C_{Ar}), 121.4 (C_{Ar}), 121.3 (C_{Ar}), 120.9 (C_{Ar}), 116.4 (C_{Ar}), 78.3 (*C*$(CH_3)_3$), 49.3 (N*C*H_2CHAr), 48.8 (*C*HCO), 47.3 (N*C*H_2CHCO), 45.0 (CHAr), 27.8 (C(*C*$H_3)_3$); HRMS (ESI$^+$) *m*/*z* Calculated for $C_{25}H_{27}N_4O_5$ [M+H] 463.1981; Found 463.1980.

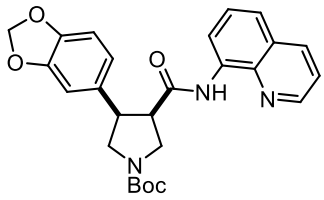
Benzyl *cis*-(±)-3-(naphthalen-2-yl)-4-(quinolin-8-ylcarbamoyl)pyrrolidine-1-carboxylate (13e)



Prepared according to **General Procedure A** using amide **9** (187 mg) and 2-iodonaphthalene (381 mg). Purification by flash column chromatography (5% to 10% MeCN/CH_2Cl_2) afforded arylated pyrrolidine **13e** as a pale orange solid (131 mg, 52%). R_f 0.34 (5% MeCN/CH_2Cl_2); mp = 59–64 °C (from Et_2O/pentane); ν_{max} (film)/cm^{-1} 3333 (NH br), 2951, 1681 (C=O), 1524, 1485, 1416, 1359, 1324, 1209, 1166, 1111, 824, 791, 746; ^{1}H NMR (400 MHz, DMSO-d_6, 373 K): δ 9.76 (br s, 1 H, NH), 8.67 (dd, J = 4.2, 1.7 Hz, 1 H, HC_{Ar}), 8.29–8.22 (m, 2 H, HC_{Ar}), 7.76–7.73 (m, 1 H, HC_{Ar}), 7.69–7.58 (m, 3 H, HC_{Ar}), 7.52 (dd, J = 8.3, 1.3 Hz, 1 H, HC_{Ar}), 7.48 (dd, J = 8.3, 4.2 Hz, 1 H, HC_{Ar}), 7.48–7.34 (m, 6 H, HC_{Ar}), 7.37–7.28 (m, 3 H, HC_{Ar}), 5.21 (s, 2 H, OCH_2Ph), 4.12 (ddd, J = 7.3, 7.3, 7.3 Hz, 1 H, CHAr), 4.07–3.94 (m, 4 H, CHCO, NC*H*HCHCO, NC*H*$_2$CHAr), 3.86–3.76 (m, 1 H, NCH*H*CHCO); ^{13}C NMR (101 MHz, DMSO-d_6, 373 K) δ 169.3 (C=O amide), 153.6 (C=O carbamate), 147.8 (C_{Ar}), 137.6 (C_{Ar} quat), 136.8 (C_{Ar} quat), 135.6 (C_{Ar}), 135.4 (C_{Ar} quat), 133.5

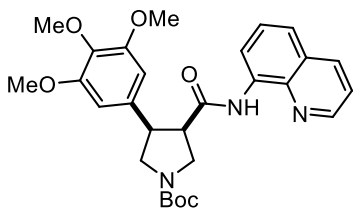
(C_{Ar} quat), 132.4 (C_{Ar} quat), 131.5 (C_{Ar} quat), 127.8 (2 × C_{Ar}), 127.1 (C_{Ar} quat, C_{Ar}), 127.0 (C_{Ar}), 126.83 (2 × C_{Ar}), 126.78 (C_{Ar}), 126.6 (C_{Ar}), 126.0 (C_{Ar}), 125.5 (C_{Ar}), 125.4 (C_{Ar}), 125.2 (C_{Ar}), 124.8 (C_{Ar}), 121.2 (2 × C_{Ar}), 116.1 (C_{Ar}), 65.5 (OCH_2Ph), 49.6 (NCH_2CHAr), 49.0 (*C*HCO), 47.9 (NCH_2CHCO), 45.6 (CHAr); HRMS (ESI$^+$) *m*/*z* Calculated for $C_{32}H_{28}N_3O_3$ [M+H] 502.2131; Found 502.2140.

tert-Butyl _cis_-(±)-3-(benzo[_d_][1,3]dioxol-5-yl)-4-(quinolin-8-ylcarbamoyl)pyrrolidine-1-carboxylate (3j)



Prepared according to **General Procedure A** using amide **2** (171 mg) and 5-iodo-1,3-benzodioxole (372 mg). Purification by flash column chromatography (20% acetone/pentane) afforded arylated pyrrolidine **3j** as a pale yellow solid (137 mg, 59%). R_f 0.18 (20% acetone/pentane); mp = 75–80 °C (from Et_2O/pentane); ν_{max} (film)/cm^{-1} 3328 (NH br), 2975, 1684 (C=O), 1526, 1486, 1400, 1324, 1240, 1164, 1120, 1039, 934, 874, 826, 791, 770; ^{1}H NMR (400 MHz, DMSO-d_6, 373 K) δ 9.69 (br s, 1 H, NH), 8.84 (dd, *J* = 4.2, 1.7 Hz, 1 H, HC_{Ar}), 8.37 (dd, *J* = 7.7, 1.3 Hz, 1 H, HC_{Ar}), 8.32 (dd, *J* = 8.3, 1.7 Hz, 1 H, HC_{Ar}), 7.61–7.55 (m, 2 H, HC_{Ar}), 7.48 (t, *J* = 7.9 Hz, 1 H, HC_{Ar}), 6.77 (d, *J* = 1.8 Hz, 1 H, HC_{Ar}), 6.70 (dd, *J* = 8.0, 1.8 Hz, 1 H, HC_{Ar}), 6.59 (d, *J* = 8.0 Hz, 1 H, HC_{Ar}), 5.75 (d, *J* = 1.0 Hz, 1 H, OC*H*HO), 5.71 (d, *J* = 1.0 Hz, 1 H, OCH*H*O), 3.84–3.76 (m, 3 H, CHCO, CHAr, NC*H*HCHCO), 3.76–3.66 (m, 2H, NCH_2CHAr), 3.66–3.59 (m, 1 H, NCH*H*CHCO), 1.48 (s, 9 H, $C(CH_3)_3$); ^{13}C NMR (101 MHz, DMSO-d_6, 373 K) δ 169.4 (C=O amide), 153.2 (C=O carbamate), 147.9 (C_{Ar}), 146.7 (OC_{Ar} quat), 145.4 (OC_{Ar} quat), 137.7 (C_{Ar} quat), 135.7 (C_{Ar}), 133.6 (C_{Ar} quat), 131.7 (C_{Ar} quat), 127.2 (C_{Ar} quat), 126.1 (C_{Ar}), 121.3 (C_{Ar}), 121.1 (C_{Ar}), 120.1 (C_{Ar}), 116.0 (C_{Ar}), 107.4 (C_{Ar}), 107.2 (C_{Ar}), 100.0 (OCH_2O), 78.0 ($C(CH_3)_3$), 49.6 (NCH_2CHAr), 49.2 (*C*HCO), 47.4 (NCH_2CHCO), 45.3 (CHAr), 27.8 ($C(CH_3)_3$); HRMS (ESI$^+$) *m*/*z* Calculated for $C_{26}H_{28}N_3O_5$ [M+H] 462.2029; Found 462.2032.

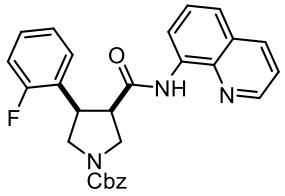
tert-Butyl _cis_-(±)-3-(quinolin-8-ylcarbamoyl)-4-(3,4,5-trimethoxyphenyl)pyrrolidine-1-carboxylate (3k)



Prepared according to **General Procedure A** using amide **2** (171 mg) and 1,3,5-trimethoxybenzene (441 mg). Purification by flash column chromatography (30% acetone/hexane) afforded arylated pyrrolidine **3k** as a yellow solid (147 mg, 58%). R_f 0.20 (30% acetone/hexane); mp = 156–161 °C (from Et_2O/pentane); ν_{max} (film)/cm^{-1} 3357 (NH br), 2971, 1692 (C=O), 1671 (C=O), 1589, 1521, 1485, 1464, 1406, 1366, 1323, 1239, 1169, 1120, 1015, 845, 828, 794; ^{1}H NMR (400 MHz, DMSO-d_6, 373 K) δ 9.66 (br s, 1 H, NH), 8.82 (dd, *J* = 4.2, 1.7 Hz, 1 H, HC_{Ar}), 8.42 (dd, *J* = 7.6, 1.4 Hz, 1 H, HC_{Ar}),

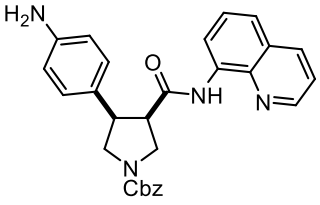
8.31 (dd, J = 8.3, 1.7 Hz, 1 H, HC_{Ar}), 7.59–7.53 (m, 2 H, HC_{Ar}), 7.48 (t, J = 7.9 Hz, 1 H, HC_{Ar}), 6.51 (s, 2 H, HC_{Ar}), 3.85–3.80 (m, 3 H, CHCO, CHAr, NC*H*HCHCO), 3.76–3.71 (m, 2H, NCH_2CHAr), 3.65–3.58 (m, 1 H, NCH*H*CHCO), 3.51 (s, 6 H, OCH_3), 3.31 (s, 3 H, OCH_3), 1.49 (s, 9 H, $C(CH_3)_3$); ^{13}C NMR (101 MHz, DMSO-d_6, 373 K) δ 169.4 (C=O amide), 153.1 (C=O carbamate), 152.2 (2 × OC_{Ar} quat), 147.9 (C_{Ar}), 137.5 (C_{Ar} quat), 136.9 (OC_{Ar} quat), 135.7 (C_{Ar}), 133.7 (C_{Ar} quat), 133.1 (C_{Ar} quat), 127.2 (C_{Ar} quat), 126.1 (C_{Ar}), 121.3 (C_{Ar}), 121.0 (C_{Ar}), 115.6 (C_{Ar}), 105.7 (2 × C_{Ar}), 78.0 ($C(CH_3)_3$), 59.0 (OCH_3), 55.4 (2 × OCH_3), 49.4 (*C*HCO), 49.2 (NCH_2CHAr), 47.2 (NCH_2CHCO), 45.7 (CHAr), 27.8 ($C(CH_3)_3$); HRMS (ESI$^+$) *m*/*z* Calculated for $C_{28}H_{34}N_3O_6$ [M+H] 508.2448; Found 508.2458.

Benzyl *cis*-(±)-3-(2-fluorophenyl)-4-(quinolin-8-ylcarbamoyl)pyrrolidine-1-carboxylate (13f)



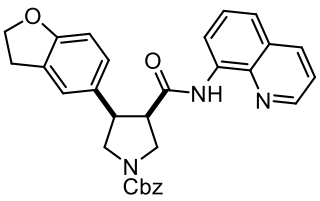
Prepared according to **General Procedure A** using amide **9** (187 mg) and 2-fluoroiodobenzene (444 mg, 2.0 mmol). The reaction was stirred at 110 °C for 72 h. Purification by flash column chromatography (5% to 10% MeCN/CH_2Cl_2) afforded arylated pyrrolidine **13f** as a brown solid (36.2 mg, 15%). R_f 0.54 (10% MeCN/CH_2Cl_2); mp = 50–54 °C; ν_{max} (film)/cm^{-1} 3345 (NH br), 2953, 1683 (C=O), 1524, 1486, 1416, 1380, 1324, 1210, 1103, 825, 791, 752, 696; ^{1}H NMR (400 MHz, DMSO-d_6, 373 K): δ 9.80 (br s, 1 H, NH), 8.83 (dd, J = 4.2, 1.7 Hz, 1 H, HC_{Ar}), 8.31 (td, J = 8.2, 1.5 Hz, 2 H, HC_{Ar}), 7.59–7.54 (m, 2 H, HC_{Ar}), 7.48–7.36 (m, 5 H, HC_{Ar}), 7.34–7.29 (m, 1 H, HC_{Ar}), 7.25 (td, J = 7.7, 1.5 Hz, 1 H, HC_{Ar}) 7.12–7.05 (m, 1 H, HC_{Ar}), 7.01–6.92 (m, 2 H, HC_{Ar}), 5.19 (s, 2 H, OCH_2Ph), 4.13 (ddd, J = 7.5, 7.5, 7.5 Hz, 1 H, CHAr), 3.95–3.88 (m, 4 H, NC*H*HCHCO, CHCO, NCH_2CHAr), 3.80 (dd, J = 12.1, 8.3 Hz, 1 H, NCH*H*CHCO); ^{13}C NMR (101 MHz, DMSO-d_6, 373 K) δ 169.1 (C=O amide), 160.0 (d, J_{CF} = 244.6 Hz, FC_{Ar} quat), 153.6 (C=O carbamate), 148.0 (C_{Ar}), 137.6 (C_{Ar} quat), 136.7 (C_{Ar}, quat), 135.7 (C_{Ar}), 133.5 (C_{Ar} quat), 128.0 (d, J_{CF} = 8.6 Hz, F-*m*-C_{Ar}), 127.9 (d, J_{CF} = 4.4 Hz, F-*m*-C_{Ar}), 127.8 (2 × C_{Ar}), 127.15 (C_{Ar} quat), 127.09 (C_{Ar}), 126.8 (2 × C_{Ar}), 126.1 (C_{Ar}), 124.7 (d, J_{CF} = 14.2 Hz, F-*o*-C_{Ar} quat), 123.5 (d, J_{CF} = 3.6 Hz, F-*p*-C_{Ar}), 121.3 (C_{Ar}), 121.2 (C_{Ar}), 115.9 (C_{Ar}), 114.5 (d, J_{CF} = 22.6 Hz, F-*o*-C_{Ar}), 65.5 (OCH_2Ph), 48.8 (NCH_2CHAr), 47.9 (*C*HCO, NCH_2CHCO), 38.8 (CHAr); ^{19}F NMR (471 MHz, DMSO-d_6, 373 K) δ –116.0 (m); HRMS (ESI) *m*/*z* Calculated for $C_{28}H_{25}N_3O_3F$ [M+H] 470.1880; Found 470.1893.

Benzyl *cis*-(±)-3-(4-aminophenyl)-4-(quinolin-8-ylcarbamoyl)pyrrolidine-1-carboxylate (13g)



Prepared according to **General Procedure A** using amide **9** (187 mg) and 4-iodoaniline (329 mg). The crude material was purified by flash column chromatography (30% to 40% acetone/hexane), the product containing fractions were combined and the solvent was removed under reduced pressure. CH_2Cl_2 (5 mL) and pentane (5 mL) were added and the solvent was removed under reduced pressure to afford arylated pyrrolidine **13g** as a pale orange solid (57.9 mg, 25%). R_f 0.28 (40% acetone/hexane); mp = 75–78 °C (from CH_2Cl_2/pentane); ν_{max} (film)/cm^{-1} 3347 (NH br), 2944, 1683 (C=O), 1624, 1521, 1485, 1419, 1358, 1324, 1166, 1114, 826, 791, 755, 697; ^{1}H NMR (500 MHz, DMSO-d_6, 373 K): δ 9.73 (br s, 1 H, NH amide), 8.84 (dd, J = 4.2, 1.7 Hz, 1 H, HC_{Ar}), 8.39 (dd, J = 7.7, 1.3 Hz, 1 H, HC_{Ar}), 8.32 (dd, J = 8.3, 1.8 Hz, 1 H, HC_{Ar}), 7.61–7.54 (m, 2 H, HC_{Ar}), 7.48 (t, J = 7.9 Hz, 1 H, HC_{Ar}), 7.43–7.35 (m, 4 H, HC_{Ar}), 7.34–7.29 (m, 1 H, HC_{Ar}), 6.97–6.86 (m, 2 H, HC_{Ar}), 6.39–6.32 (m, 2 H, HC_{Ar}), 5.17 (s, 2 H, OCH_2Ph), 4.49 (br s, 2 H, $ArNH_2$), 3.87 (dd, J = 10.8, 3.2 Hz, 1 H, NC*H*HCHCO), 3.83–3.66 (m, 5 H, NCH*H*CHCO, CHCO, CHAr, NC*H*$_2$CHAr); ^{13}C NMR (126 MHz, DMSO-d_6, 373 K) δ 169.4 (C=O amide), 153.6 (C=O carbamate), 148.0 (C_{Ar}), 146.5 ($C_{Ar}NH_2$ quat), 137.6 (C_{Ar} quat), 136.8 (C_{Ar} quat), 135.7 (C_{Ar}), 133.7 (C_{Ar} quat), 127.7 (2 × C_{Ar}), 127.4 (2 × C_{Ar}), 127.2 (C_{Ar} quat), 127.1 (C_{Ar}), 126.8 (2 × C_{Ar}), 126.1 (C_{Ar}), 124.9 (C_{Ar} quat), 121.3 (C_{Ar}), 121.0 (C_{Ar}), 115.9 (C_{Ar}), 113.5 (2 × C_{Ar}), 65.4 (OCH_2Ph), 50.1 (N*C*H$_2$CHAr), 49.2 (*C*HCO), 47.7 (N*C*H$_2$CHCO), 45.0 (CHAr); HRMS (ESI$^+$) *m*/*z* Calculated for $C_{28}H_{27}N_4O_3$ [M+H] 467.2083; Found 467.2090.

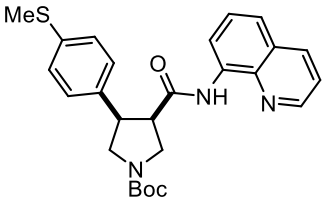
Benzyl *cis*-(±)-3-(2,3-dihydrobenzofuran-5-yl)-4-(quinolin-8-ylcarbamoyl)pyrrolidine-1-carboxylate (13h)



Prepared according to **General Procedure A** using amide **9** (187 mg) and 5-iodo-2,3-dihydrobenzofuran (369 mg). Purification by flash column chromatography (20% to 30% acetone/hexane) afforded arylated pyrrolidine **13h** as a pale yellow solid (156 mg, 63%). R_f 0.20 (30% acetone/hexane); mp = 58–65 °C (from Et_2O/pentane); ν_{max} (film)/cm^{-1} 3343 (NH br), 2891, 1683 (C=O), 1523, 1486, 1416, 1357, 1324, 1239, 1212, 1165, 1104, 982, 941, 825, 791, 758, 697; ^{1}H NMR (400 MHz, DMSO-d_6, 373 K): δ 9.64 (br s, 1 H, NH), 8.81 (dd, J = 4.2, 1.7 Hz, 1 H, HC_{Ar}), 8.37 (dd, J = 7.7, 1.4 Hz, 1 H, HC_{Ar}), 8.32 (dd, J = 8.3, 1.7 Hz, 1 H, HC_{Ar}), 7.62–7.52 (m, 2 H, HC_{Ar}), 7.48 (t, J = 8.0 Hz, 1 H, HC_{Ar}), 7.45–7.35 (m, 4 H, HC_{Ar}), 7.34–7.29 (m, 1 H, HC_{Ar}), 7.08–7.05 (m, 1 H, HC_{Ar}), 6.96 (dd, J = 8.2, 2.0 Hz, 1 H, HC_{Ar}), 6.45 (d, J = 8.2 Hz, 1 H, HC_{Ar}), 5.18 (s, 2 H, OCH_2Ph), 4.30–

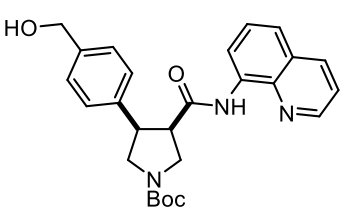
4.15 (m, 2 H, CH_2CH_2O), 3.91 (dd, *J* = 10.7, 3.7 Hz, 1 H, NC*H*HCHCO), 3.90–3.75 (m, 4 H, CHAr, CHCO, NCH_2CHAr), 3.71 (dd, *J* = 10.7, 6.8, 1 H, NCH*H*CHCO), 2.91–2.81 (m, 1 H, C*H*HCH$_2$O), 2.79–2.69 (m, 1 H, CH*H*CH$_2$O); ^{13}C NMR (101 MHz, DMSO-d_6, 373 K) δ 169.5 (C=O amide), 158.1 (OC_{Ar} quat), 153.6 (C=O carbamate), 147.9 (C_{Ar}), 137.6 (C_{Ar} quat), 136.8 (C_{Ar} quat), 135.7 (C_{Ar}), 133.6 (C_{Ar} quat), 129.2 (C_{Ar} quat), 127.7 (2 × C_{Ar}), 127.2 (C_{Ar} quat), 127.1 (C_{Ar}), 126.8 (2 × C_{Ar}), 126.51 (C_{Ar}), 126.47 (C_{Ar} quat), 126.1 (C_{Ar}), 123.6 (C_{Ar}), 121.2 (C_{Ar}), 121.1 (C_{Ar}), 115.9 (C_{Ar}), 107.8 (C_{Ar}), 70.0 (CH_2CH_2O), 65.5 (OCH_2Ph), 49.7 (NCH_2CHAr), 49.3 (*C*HCO), 47.6 (NCH_2CHCO), 45.3 (CHAr), 28.4 (CH_2CH_2O); HRMS (ESI$^+$) *m*/*z* Calculated for $C_{30}H_{28}N_3O_4$ [M+H] 494.2080; Found 494.2079.

tert-Butyl _cis_-(±)-3-(4-(methylthio)phenyl)-4-(quinolin-8-ylcarbamoyl)pyrrolidine-1-carboxylate (3l)



Prepared according to **General Procedure A** using amide **2** (171 mg) and 4-iodophenyl methyl sulfide (375 mg). Purification by flash column chromatography (20% acetone/hexane) afforded arylated pyrrolidine **3l** as a pale yellow solid (127 mg, 55%). R_f 0.19 (20% acetone/hexane); mp = 61–67 °C (from Et_2O/pentane); ν_{max} (film)/cm^{-1} 3341 (NH br), 2974, 1682 (C=O), 1524, 1486, 1392, 1324, 1256, 1163, 1117, 875, 825, 791, 758; ^{1}H NMR (400 MHz, DMSO-d_6, 373 K) δ 9.72 (br s, 1 H, NH), 8.84 (dd, *J* = 4.2, 1.7 Hz, 1 H, HC_{Ar}), 8.36–8.28 (m, 2 H, HC_{Ar}), 7.62–7.54 (m, 2 H, HC_{Ar}), 7.47 (t, *J* = 8.0 Hz, 1 H, HC_{Ar}), 7.20–7.15 (m, 2 H, HC_{Ar}), 7.06–7.00 (m, 2 H, HC_{Ar}), 3.88–3.78 (m, 3 H, CHCO, CHAr, NC*H*HCHCO), 3.78–3.72 (m, 2 H, NCH_2CHAr), 3.70–3.62 (m, 1 H, NCH*H*CHCO), 2.25 (s, 3 H, SCH_3), 1.49 (s, 9 H, $C(CH_3)_3$); ^{13}C NMR (101 MHz, DMSO-d_6, 373 K) δ 169.3 (C=O amide), 153.2 (C=O carbamate), 148.0 (C_{Ar}), 137.7 (C_{Ar} quat), 135.8 (SC_{Ar} quat), 135.7 (C_{Ar}), 135.1 (C_{Ar} quat), 133.6 (C_{Ar} quat), 127.6 (2 × C_{Ar}), 127.2 (C_{Ar} quat), 126.12 (C_{Ar}), 126.09 (2 × C_{Ar}), 121.3 (C_{Ar}), 121.2 (C_{Ar}), 116.1 (C_{Ar}), 78.1 ($C(CH_3)_3$), 49.5 (NCH_2CHAr), 49.0 (*C*HCO), 47.5 (NCH_2CHCO), 45.0 (CHAr), 27.8 ($C(CH_3)_3$), 14.7 (SCH_3); HRMS (ESI$^+$) *m*/*z* Calculated for $C_{26}H_{30}N_3O_3S$ [M+H] 464.2008; Found 464.2001.

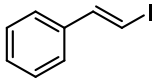
tert-Butyl _cis_-(±)-3-(4-(hydroxymethyl)phenyl)-4-(quinolin-8-ylcarbamoyl)pyrrolidine-1-carboxylate (3m)



Prepared according to **General Procedure A** using amide **2** (171 mg) and 4-iodobenzyl alcohol (351 mg). Purification by flash column chromatography (10% to 20% MeCN/CH_2Cl_2) afforded arylated pyrrolidine **3m** as a white solid (78.2 mg, 35%). R_f 0.23 (20% MeCN/CH_2Cl_2); mp = 82–86 °C (from Et_2O/pentane); ν_{max} (film)/cm^{-1} 3346 (OH, NH br), 2973, 1671 (C=O), 1525, 1486, 1404, 1324, 1163, 1117, 826,

791, 758; ^{1}H NMR (400 MHz, DMSO-d_6, 373 K) δ 9.78 (br s, 1 H, NH), 8.85 (dd, J = 4.2, 1.7 Hz, 1 H, HC_{Ar}), 8.35–8.30 (m, 2 H, HC_{Ar}), 7.60–7.55 (m, 2 H, HC_{Ar}), 7.47 (t, J = 8.0 Hz, 1 H, HC_{Ar}), 7.21–7.17 (m, 2 H, HC_{Ar}), 7.10–7.07 (m, 2 H, HC_{Ar}), 4.64–4.57 (m, 1 H, OH), 4.33–4.28 (m, 2 H, CH_2OH), 3.90–3.75 (m, 5 H, CHCO, CHAr, NCHHCHCO, NCH_2CHAr), 3.69–3.63 (m, 1 H, NCHHCHCO), 1.49 (s, 9 H, C(CH_3)$_3$); ^{13}C NMR (101 MHz, DMSO-d_6, 373 K) δ 169.3 (C=O amide), 153.2 (C=O carbamate), 148.0 (C_{Ar}), 140.4 (C_{Ar} quat), 137.7 (C_{Ar} quat), 136.5 (C_{Ar} quat), 135.7 (C_{Ar}), 133.6 (C_{Ar} quat), 127.2 (C_{Ar} quat), 126.7 (2 × C_{Ar}), 126.1 (C_{Ar}), 125.7 (2 × C_{Ar}), 121.3 (C_{Ar}), 121.1 (C_{Ar}), 116.1 (C_{Ar}), 78.0 (C(CH_3)$_3$), 62.1 (CH$_2$OH) 49.9 (NCH$_2$CHAr), 49.0 (CHCO), 47.5 (NCH$_2$CHCO), 45.2 (CHAr), 27.8 (C(CH$_3$)$_3$); HRMS (ESI$^+$) m/z Calculated for $C_{26}H_{30}N_3O_4$ [M+H] 448.2236; Found 448.2243.

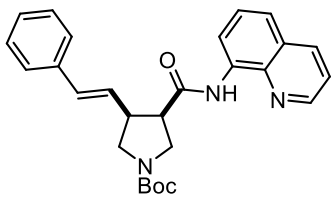
[(*E*)–2–Iodoethenyl]benzene (S1)



According to the procedure reported by Charette,[288] a solution of CH_2I_2 (967 μL, 12.0 mmol) in THF (3 mL) was added dropwise to a solution of NaHMDS (24.0 mL, 24.0 mmol, 1.0 M solution in THF) in anhydrous Et_2O (16 mL) at –78 ºC in the dark. After 20 min, a solution of benzyl bromide (951 μL, 8.0 mmol) in anhydrous THF (6 mL) was added dropwise. The reaction mixture was stirred for 2 h, then allowed to warm to rt. After 30 min, DBU (1.2 mL, 8.0 mmol) was added dropwise and the solution stirred for 2 h, before Et_2O (100 mL) was added. The mixture was filtered through a plug of Celite/silica and the solvent was removed under reduced pressure. The crude material was purified by flash column chromatography (100% hexane), affording vinyl iodide **S1** (1.54 g, 84%, 98:2 *E*/*Z*) as a yellow oil. R_f 0.67 (100% hexane); νmax (film)/cm^{-1} 3697, 3681, 3057, 3022, 2973, 2923, 2865, 2845, 1595, 1569, 1494, 1444, 1278, 1210, 1169, 1055, 1032, 1012, 944, 792, 726, 688; ^{1}H NMR (400 MHz, $CDCl_3$, 298 K) δ 7.45 (d, J = 14.9 Hz, 1 H, PhCH=CHI), 7.38–7.25 (m, 5 H, HC_{Ar}), 6.85 (d, J = 14.9 Hz, 1 H, CHI); ^{13}C NMR (101 MHz, $CDCl_3$, 298 K) δ 144.9 (PhCH=CHI), 137.6 (C_{Ar} quat), 128.7 (2 × C_{Ph}), 128.3 (C_{Ph}), 126.0 (2 × C_{Ph}), 76.7 (CHI).

Spectroscopic data (^{1}H and ^{13}C NMR) is consistent with what described in the literature.[288]

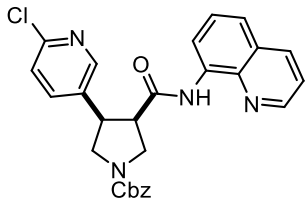
***tert*-Butyl *cis*-(±)-3-(quinolin-8-ylcarbamoyl)-4-((*E*)-styryl)pyrrolidine-1-carboxylate (3n)**



Prepared according to **General Procedure A** using amide **2** (171 mg) and ((*E*)-2-iodoethenyl)benzene **S1** (460 mg, 2.0 mmol). The reaction was stirred at 110 °C for 48 h. Purification by flash column chromatography (10% MeCN/CH_2Cl_2) afforded arylated pyrrolidine **3n** as a yellow solid (45.0 mg, 20%). R_f 0.34 (10% MeCN/CH_2Cl_2); mp = 63–69 °C (from Et_2O/pentane); ν_{max} (film)/cm^{-1} 3337 (NH br), 2973, 1683 (C=O), 1524, 1485, 1391, 1324, 1257, 1163, 1115, 966, 876, 826, 791, 750, 693; ^{1}H NMR

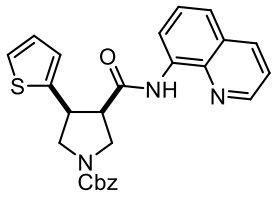
(400 MHz, DMSO-d_6, 373 K) δ 10.00 (br s, 1 H, NH), 8.81 (dd, *J* = 4.2, 1.7 Hz, 1 H, HC_{Ar}), 8.52 (dd, *J* = 7.6, 1.4 Hz, 1 H, HC_{Ar}), 8.33 (dd, *J* = 8.3, 1.7 Hz, 1 H, HC_{Ar}), 7.62 (dd, *J* = 8.3, 1.4 Hz, 1 H, HC_{Ar}), 7.56 (dd, *J* = 8.3, 4.2 Hz, 1 H, HC_{Ar}), 7.52 (t, *J* = 7.9 Hz, 1 H, HC_{Ar}), 7.18–7.09 (m, 5 H, HC_{Ar}), 6.56 (dd, *J* = 16.0, 0.9 Hz, 1 H, CH=C*H*Ph), 6.23 (dd, *J* = 15.9, 7.8 Hz, 1 H, C*H*=CHPh), 3.78 (dd, *J* = 10.7, 4.6 Hz, 1 H, NC*H*HCHCO), 3.69 (ddd, *J* = 6.8, 6.8, 4.6 Hz, 1 H, CHCO), 3.65–3.56 (m, 2 H, NC*H*HCHCH=CH, NCH*H*CHCO), 3.50–3.41 (m, 2 H, NCH*H*CHCH=CH, C*H*CH=CH), 1.47 (s, 9 H, $C(CH_3)_3$); ^{13}C NMR (101 MHz, DMSO-d_6, 373 K) δ 169.6 (C=O amide), 153.2 (C=O carbamate), 148.1 (C_{Ar}), 137.9 (C_{Ar} quat), 136.4 (C_{Ar} quat), 135.8 (C_{Ar}), 133.7 (C_{Ar} quat), 131.3 (CH=*C*HPh), 127.7 (2 × C_{Ar}), 127.3 (C_{Ar} quat), 126.64 (*C*H=CHPh), 126.58 (C_{Ar}), 126.2 (C_{Ar}), 125.4 (2 × C_{Ar}), 121.4 (C_{Ar}), 121.3 (C_{Ar}), 116.4 (C_{Ar}), 78.0 (*C*$(CH_3)_3$), 49.8 (N*C*H_2CHCH=CH), 48.4 (*C*HCO), 47.2 (N*C*H_2CHCO), 43.5 (*C*HCH=CH), 27.8 (C(*C*$H_3)_3$); HRMS (ESI$^+$) *m*/*z* Calculated for $C_{27}H_{30}N_3O_3$ [M+H] 444.2287; Found 444.2282.

Benzyl *cis*-(±)-3-(6-chloropyridin-3-yl)-4-(quinolin-8-ylcarbamoyl)pyrrolidine-1-carboxylate (13i)



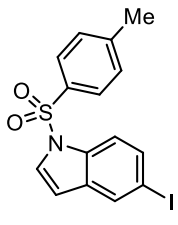
Prepared according to **General Procedure A** using amide **9** (187 mg) and 2-chloro-5-iodopyridine (359 mg). Purification by flash column chromatography (20% MeCN/CH_2Cl_2) afforded arylated pyrrolidine **13i** as a pale orange solid (54.9 mg, 23%). R_f 0.33 (20% MeCN/CH_2Cl_2); mp = 63–67 °C (from Et_2O/pentane); ν_{max} (film)/cm^{-1} 3330 (NH br), 2887, 1685 (C=O), 1525, 1486, 1459, 1420, 1359, 1324, 1106, 826, 791, 756, 697; ^{1}H NMR (400 MHz, DMSO-d_6, 373 K): δ 9.87 (br s, 1 H, NH), 8.85 (dd, *J* = 4.2, 1.7 Hz, 1 H, HC_{Ar}), 8.33 (dd, *J* = 8.3, 1.7 Hz, 1 H, HC_{Ar}), 8.31–8.28 (m, 2 H, HC_{Ar}, NHC_{Pyr}), 7.67 (dd, *J* = 8.3, 2.6 Hz, 1 H, HC_{Ar}), 7.62 (dd, *J* = 8.3, 1.3 Hz, 1 H, HC_{Pyr}), 7.58 (dd, *J* = 8.3, 4.2 Hz, 1 H, HC_{Ar}), 7.48 (t, *J* = 8.0 Hz, 1 H, HC_{Ar}), 7.44–7.35 (m, 4 H, HC_{Ar}), 7.35–7.29 (m, 1 H, HC_{Ar}), 7.21 (dd, *J* = 8.3, 0.7 Hz, 1 H, Cl-*o*-HC_{pyr}), 5.18 (s, 2 H, OCH_2Ph), 4.03–3.95 (m, 2 H, CHAr, CHCO), 3.95–3.82 (m, 3 H, NC*H*HCHCO, NC*H*$_2$CHAr), 3.78 (m, 1 H, NCH*H*CHCO);^{13}C NMR (101 MHz, DMSO-d_6, 373 K) δ 169.0 (C=O amide), 153.5 (C=O carbamate), 148.6 (N*C*H_{Pyr}), 148.3 (ClC_{Pyr} quat), 148.1 (C_{Ar}), 138.0 (C_{Pyr}), 137.9 (C_{Ar} quat), 136.6 (C_{Ar} quat), 135.8 (C_{Ar}), 133.3 (C_{Ar} quat), 133.2 (C_{Pyr} quat), 127.8 (2 × C_{Ar}), 127.3 (C_{Ar} quat), 127.1 (C_{Ar}), 126.8 (2 × C_{Ar}), 126.1 (C_{Ar}), 123.0 (Cl-*o*-C_{Pyr}), 121.6 (C_{Ar}), 121.3 (C_{Ar}), 116.7 (C_{Ar}), 65.6 (OCH_2Ph), 49.3 (N*C*H_2CHAr), 48.5 (*C*HCO), 47.7 (N*C*H_2CHCO), 42.4 (CHAr); HRMS (ESI$^+$) *m*/*z* Calculated for $C_{27}H_{24}N_4O_3{}^{35}Cl$ [M+H] 487.1537; Found 487.1526.

Benzyl *cis*-(±)-3-(quinolin-8-ylcarbamoyl)-4-(thiophen-2-yl)pyrrolidine-1-carboxylate (13j)



Prepared according to **General Procedure A** using amide **9** (187 mg) and 2-iodothiophene (315 mg). Purification by flash column chromatography (10% MeCN/CH_2Cl_2) afforded arylated pyrrolidine **13j** as a white solid (128 mg, 56%). R_f 0.41 (10% MeCN/CH_2Cl_2); mp = 48–51 °C (from Et_2O/pentane); ν_{max} (film)/cm^{-1} 3328 (NH br), 3031, 2883, 1682 (C=O), 1524, 1485, 1415, 1358, 1323, 1167, 1112, 825, 791, 755, 695; ^{1}H NMR (400 MHz, DMSO-d_6, 373 K): δ 9.90 (br s, 1 H, NH), 8.87 (dd, J = 4.2, 1.7 Hz, 1 H, HC_{Ar}), 8.41 (dd, J = 7.7, 1.4 Hz, 1 H, HC_{Ar}), 8.33 (dd, J = 8.3, 1.7 Hz, 1 H, HC_{Ar}), 7.62–7.56 (m, 2 H, HC_{Ar}), 7.49 (t, J = 7.9 Hz, 1 H, HC_{Ar}), 7.45–7.33 (m, 4 H, HC_{Ar}), 7.36–7.27 (m, 1 H, HC_{Ar}), 7.17 (dd, J = 5.1, 1.2 Hz, 1 H, SCH), 6.93 (ddd, J = 3.5, 1.2, 0.8 Hz, 1 H, SCHCHC*H*), 6.78 (dd, J = 5.1, 3.5 Hz, 1 H, SCHC*H*), 5.18 (s, 2 H, OCH_2Ph), 4.23 (m, 1 H, CHAr), 3.95–3.85 (m, 3 H, NC*H*HCHCO, NC*H*HCHAr, CHCO), 3.81 (dd, J = 10.3, 6.9 Hz, 1 H, NCH*H*CHAr), 3.77–3.71 (m, 1 H, NCH*H*CHCO); ^{13}C NMR (101 MHz, DMSO-d_6, 373 K) δ 168.7 (C=O amide), 153.5 (C=O carbamate), 148.1 (C_{Ar}), 140.2 (SC_{Ar} quat), 137.7 (C_{Ar} quat), 136.7 (C_{Ar} quat), 135.8 (C_{Ar}), 133.7 (C_{Ar} quat), 127.7 (2 × C_{Ar}), 127.2 (C_{Ar} quat), 127.1 (SCH*C*H$_{Ar}$), 126.8 (2 × C_{Ar}), 126.2 (C_{Ar}), 125.9 (SCHCH*C*H$_{Ar}$), 124.8 (S*C*H$_{Ar}$), 123.8 (C_{Ar}), 121.3 (C_{Ar}), 121.2 (C_{Ar}), 116.2 (C_{Ar}), 65.5 (OCH_2Ph), 51.4 (N*C*H$_2$CHAr), 49.2 (*C*HCO), 47.1 (N*C*H$_2$CHCO), 41.3 (CHAr); HRMS (ESI$^+$) *m*/*z* Calculated for $C_{26}H_{24}N_3O_3S$ [M+H] 458.1538; Found 458.1550.

5-Iodo-1-tosyl-1*H*-indole (S2)

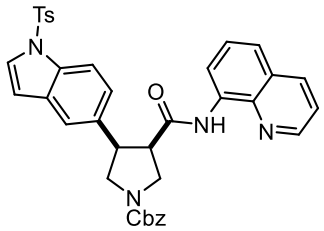


NaH (247 mg, 6.17 mmol, 60% dispersion in mineral oil) was added to a solution of 5-iodo-1*H*-indole (1.00 g, 4.11 mmol) in DMF (4.0 mL) at 0 °C. The resulting suspension was stirred at 0 °C for 30 min, then a solution of tosyl chloride (1.20 g, 6.17 mmol) in DMF (2.0 mL) was then added dropwise. The reaction was allowed to warm up to rt and stirred for further 2 h. The reaction was quenched by addition of H_2O (5 mL) and the product was extracted with EtOAc (3 × 10 mL). The combined organic extracts were washed with sat. aq. $NaHCO_3$ (20 mL), dried over Na_2SO_4 and the solvent was removed under reduced pressure. Purification by flash column chromatography (0 to 10% Et_2O/pentane) afforded *N*-Ts indole **S2** (1.52 g, 93%) as a white solid. R_f 0.27 (10% Et_2O/pentane); mp = 134–137 °C (from Et_2O/pentane, lit = 136–138 °C);[289] ν_{max} (film)/cm^{-1} 1595, 1437, 1361, 1252, 1193, 1168, 1130, 1092; ^{1}H NMR (400 MHz, $CDCl_3$, 298 K) δ 7.87 (s, 1 H, HC_{Ar}), 7.77–7.73 (m, 3 H, HC_{Ar}), 7.58 (d, J = 8.7 Hz, 1 H, HC_{Ar}), 7.53 (d, J = 3.6 Hz, 1 H, HC_{Ar}), 7.24 (d, J = 8.3 Hz, 2 H, HC_{Ar}), 6.58 (d, J = 3.6 Hz, 1 H, HC_{Ar}), 2.36 (s, 3 H, CH_3). ^{13}C NMR (101 MHz, $CDCl_3$, 298 K) δ 145.2 (C_{Ar} quat), 135.0 (C_{Ar}

quat) 134.1 (C_{Ar} quat), 133.0 (C_{Ar}), 133.0 (C_{Ar}) 130.2 (C_{Ar}), 130.0 (2 × C_{Ar}), 127.2 (C_{Ar} quat), 126.8 (2 × C_{Ar}), 115.3 (C_{Ar}), 108.0 (C_{Ar}), 87.4 (C_{Ar} quat), 21.6 (CH_3).

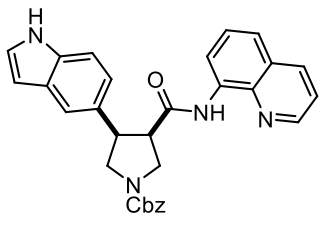
Spectroscopic data (^{1}H and ^{13}C NMR) is consistent with what described in the literature.[290]

Benzyl *cis*-(±)-3-(quinolin-8-ylcarbamoyl)-4-(1-tosyl-1*H*-indol-5-yl)pyrrolidine-1-carboxylate (13k)



Prepared according to **General Procedure A** using amide **9** (187 mg) and 5-iodo-1-tosyl-1*H*-indole **S2** (596 mg). Purification by flash column chromatography (30% acetone/hexane) afforded arylated pyrrolidine **13k** as a white solid (190 mg, 59%). R_f 0.20 (30% acetone/hexane); mp = 96–100 °C (from Et_2O/pentane); ν_{max} (film)/cm^{-1} 3331 (NH br), 2948, 1686 (C=O), 1524, 1486, 1416, 1360, 1324, 1169, 1120, 996, 825, 791, 765, 731, 673; ^{1}H NMR (400 MHz, DMSO-d_6, 373 K): δ 9.67 (br s, 1 H, NH), 8.70 (dd, *J* = 4.2, 1.7 Hz, 1 H, HC_{Ar}), 8.29 (dd, *J* = 8.3, 1.7 Hz, 1 H, HC_{Ar}), 8.22 (dd, *J* = 7.7, 1.3 Hz, 1 H, HC_{Ar}), 7.67–7.51 (m, 3 H, 2 × HC_{Ar}, NCHC*H*$_{Indole}$), 7.56 (dd, *J* = 8.3, 1.3 Hz, 1 H, HC_{Ar}), 7.53–7.49 (m, 2 H, HC_{Ar}), 7.47–7.45 (m, 1 H, HC_{Ar}), 7.44–7.35 (m, 5 H, HC_{Ar}), 7.35–7.29 (m, 1 H, HC_{Ar}), 7.26 (dd, *J* = 8.6, 1.8 Hz, 1 H, HC_{Ar}), 7.23–7.19 (m, 2 H, HC_{Ar}), 6.55 (dd, *J* = 3.7, 0.8 Hz, 1 H, NC*H*$_{Indole}$), 5.18 (s, 2 H, OCH_2Ph), 4.04–3.97 (m, 1 H, CHAr), 3.95–3.85 (m, 4 H, NC*H*HCHCO, NCH_2CHAr, CHCO), 3.78–3.72 (m, 1 H, NCH*H*CHCO), 2.28 (s, 3 H, CH_3); ^{13}C NMR (101 MHz, DMSO-d_6, 373 K) δ 169.3 (C=O amide), 153.6 (C=O carbamate), 147.8 (C_{Ar}), 144.5 (C_{Ar} quat), 137.7 (C_{Ar} quat), 136.7 (C_{Ar} quat), 135.6 (C_{Ar}), 134.3 (C_{Ar} quat), 133.4 (C_{Ar} quat), 132.95 (C_{Ar} quat), 132.90 (C_{Ar} quat), 130.0 (C_{Ar} quat), 129.4 (2 × C_{Ar}), 127.7 (2 × C_{Ar}), 127.12 (C_{Ar} quat), 127.07 (C_{Ar}), 126.8 (2 × C_{Ar}), 126.2 (C_{Ar}), 126.0 (C_{Ar}), 125.7 (2 × C_{Ar}), 124.0 (C_{Ar}), 121.21 (C_{Ar}), 121.16 (C_{Ar}), 119.8 (C_{Ar}), 116.2 (C_{Ar}), 112.2 (NCH*C*H$_{Indole}$), 108.5 (N*C*H$_{Indole}$), 65.5 (OCH_2Ph), 49.7 (N*C*H_2CHAr), 49.0 (*C*HCO), 47.8 (N*C*H_2CHCO), 45.4 (CHAr), 20.3 (CH_3); HRMS (ESI$^+$) *m*/*z* Calculated for $C_{37}H_{33}N_4O_5S$ [M+H] 645.2172; Found 645.2183.

Benzyl *cis*-(±)-3-(1*H*-indol-5-yl)-4-(quinolin-8-ylcarbamoyl)pyrrolidine-1–carboxylate (13l)

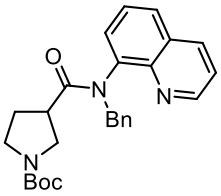


Prepared according to **General Procedure A** using amide **9** (187 mg) and 5-iodo-1*H*-indole (365 mg). The crude material was purified by flash column chromatography (30% to 40% acetone/hexane), the product containing fractions were combined and the solvent was removed under reduced pressure. CH_2Cl_2 (5 mL) and pentane (5 mL) were added and the solvent was removed under reduced pressure

to afford arylated pyrrolidine **13l** as a white solid (146 mg, 60%, containing <6% inseparable impurity). R_f 0.33 (40% acetone/hexane); mp = 87–93 °C (from CH_2Cl_2/pentane); ν_{max} (film)/cm^{-1} 3322 (NH br), 1678 (C=O), 1523, 1485, 1417, 1356, 1324, 1210, 1112, 825, 790, 763, 732, 696; ^{1}H NMR (400 MHz, DMSO-d_6, 373 K): δ 10.51 (br s, 1 H, HN_{Indole}), 9.70 (br s, 1 H, CONH), 8.71 (dd, J = 4.2, 1.7 Hz, 1 H, HC_{Ar}), 8.32 (dd, J = 7.7, 1.4 Hz, 1 H, HC_{Ar}), 8.26 (dd, J = 8.3, 1.7 Hz, 1 H, HC_{Ar}), 7.55–7.49 (m, 2 H, HC_{Ar}), 7.46–7.36 (m, 6 H, 5 × HC_{Ar}, HC_{Indole}), 7.35–7.30 (m, 1 H, HC_{Ar}), 7.15–7.10 (m, 2 H, HC_{Indole}), 7.00 (dd, J = 8.4, 1.8 Hz, 1 H, HC_{Indole}), 6.20 (ddd, J = 3.0, 1.9, 0.9 Hz, 1 H, NHCHCH_{Indole}), 5.20 (s, 2 H, OCH_2Ph), 4.04–3.90 (m, 4 H, CHAr, NC*H*HCHCO, NCH_2CHAr), 3.87 (ddd, J = 6.9, 6.9, 4.3 Hz, 1 H, CHCO), 3.76 (dd, J = 10.7, 7.0 Hz, 1 H, NCH*H*CHCO); ^{13}C NMR (101 MHz, DMSO-d_6, 373 K) δ 169.4 (C=O amide), 153.6 (C=O carbamate), 147.8 (C_{Ar}), 137.6 (C_{Ar} quat), 136.8 (C_{Ar} quat), 135.6 (C_{Ar}), 134.6 (C_{Indole} quat), 133.6 (C_{Ar} quat), 127.82 (C_{Indole} quat), 127.75 (2 × C_{Ar}), 127.3 (C_{Ar} quat), 127.11 (C_{Indole} quat), 127.05 (C_{Ar}), 126.8 (2 × C_{Ar}), 126.0 (C_{Ar}), 124.5 (NH*C*H$_{Indole}$), 121.1 (C_{Ar}), 121.0 (C_{Ar}), 120.3 (CH_{Indole}), 118.3 (CH_{Indole}), 115.9 (C_{Ar}), 110.4 (CH_{Indole}), 100.3 (NHCH*C*H$_{Indole}$), 66.5 (OCH_2Ph), 50.3 (N*C*H$_2$CHAr), 49.4 (*C*HCO), 47.8 (N*C*H$_2$CHCO), 45.8 (CHAr); HRMS (ESI$^+$) *m*/*z* Calculated for $C_{30}H_{27}N_4O_3$ [M+H] 491.2083; Found 491.2086.

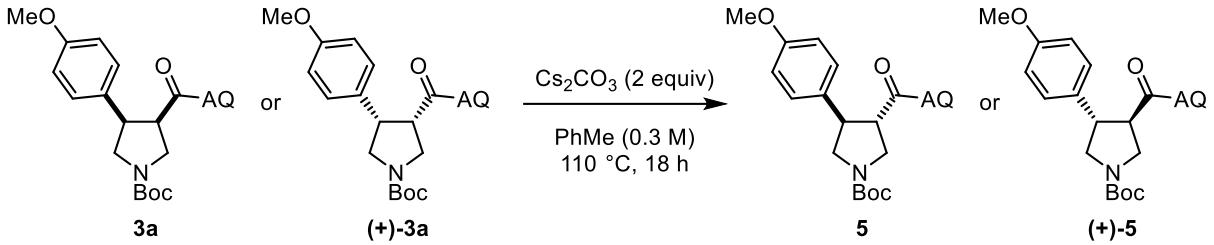
8.2.1.6 Reaction with Benzyl Bromide

tert–Butyl 3-(benzyl(quinoline-8-yl)carbamoyl)pyrrolidine-1-carboxylate (17)

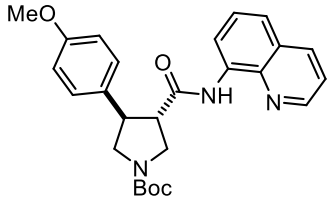


Prepared according to **General Procedure A** using amide **2** (171 mg) and benzyl bromide (178 μL). Purification by flash column chromatography (20% acetone/hexane) afforded amide **17** as a slightly yellow solid (62.2 mg, 29%). R_f 0.20 (20% acetone/hexane); mp = 52–56 °C; ν_{max} (film)/cm^{-1} 3681, 2973, 2844, 1689 (C=O), 1653, 1614, 1595, 1573, 1529, 1495, 1472, 1454, 1390, 1364, 1256, 1218, 1165, 1117, 1057, 1033, 1017, 988, 884, 834, 796, 763, 699, 673; ^{1}H NMR (400 MHz, $CDCl_3$, observed as mixture of rotamers) δ 8.99 (dd, *J* = 4.4, 1.9 Hz, 1 H, HC_{Ar}), 8.28–8.18 (m, 1 H, HC_{Ar}), 7.88–7.78 (m, 1 H, HC_{Ar}), 7.56–7.46 (m, 1 H, HC_{Ar}), 7.46–7.36 (m, 1 H, HC_{Ar}), 7.26–7.20 (m, 3 H, HC_{Ar}), 7.20–7.10 (m, 3 H, HC_{Ar}), 5.94–5.83 (m, 1 H, NC*H*HPh), 4.24–4.10 (m, 1 H, NCH*H*Ph), 3.59–3.39 (m, 2H, NC*H*HCH$_2$, NC*H*HCHCO), 3.39–2.85 (m, 2 H, NCH*H*CH$_2$, NCH*H*CHCO), 2.73–2.52 (m, 1 H, CHCO), 2.44–2.09 (m, 1 H, NCH$_2$C*H*H), 1.91–1.61 (m, 1 H, NCH$_2$CH*H*), 1.43–1.33 (m, 9 H, C(CH$_3$)$_3$); ^{13}C NMR (101 MHz, $CDCl_3$, observed as mixture of rotamers) δ 173.4 (C=O amide), 154.2 (C=O carbamate), 151.1 (C_{Ar}), 144.3 (C_{Ar} quat), 138.8 (C_{Ar} quat), 137.8 (C_{Ar} quat), 136.4 (C_{Ar}), 130.2–128.6 (m, 4 × C_{Ar}, C_{Ar} quat), 128.2 (2 × C_{Ar}), 127.2 (C_{Ar}), 126.3–125.9 (m, C_{Ar}), 122.2–122.0 (m, C_{Ar}), 79.1 and 78.9 (*C*(CH$_3$)$_3$), 52.8 (NCH$_2$Ph), 49.7–48.9 (m, N*C*H$_2$CHCO), 45.6 and 45.3 (N*C*H$_2$CH$_2$), 42.4–41.4 (m, *C*HCO), 30.5–29.1 (m, NCH$_2$*C*H$_2$), 28.4 (C(*C*H$_3$)$_3$); HRMS (ESI$^+$) *m*/*z* Calculated for $C_{26}H_{30}N_3O_3$ [M+H] 432.2287; Found 432.2278.

*8.2.1.7 Epimerisation of cis-3,4-Disubstituted Pyrrolidine **3a** and **(+)-3a**:*

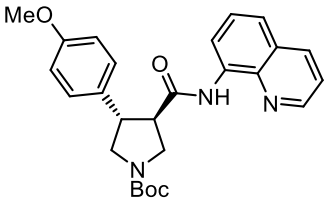


***tert*-Butyl *trans*-(±)-3-(4-methoxyphenyl)-4-(quinolin-8–ylcarbamoyl)pyrrolidine-1-carboxylate (5)**



A flame-dried reaction tube was charged with 3-aryl pyrrolidine **3a** (89.5 mg, 0.20 mmol) and Cs_2CO_3 (130 mg, 0.40 mmol). The reaction vessel was sealed and purged with argon, then toluene (667 μL, 0.3 M) was added by syringe. The reaction tube was then placed in a preheated oil bath and stirred at 110 ºC for 18 h. The reaction mixture was then allowed to cool to rt and EtOAc (5 mL) was added. The resulting mixture was filtered through a pad of Celite, eluting with further EtOAc (2 × 5 mL). The solvent was removed under reduced pressure and the crude material was purified by flash column chromatography (0% to 20% acetone/hexane). The product containing fractions were combined and the solvent was removed under reduced pressure. Et_2O (5 mL) and pentane (5 mL) were added and the solvent was removed under reduced pressure to afford arylated pyrrolidine **5** as a white solid (78.0 mg, 85%). R_f 0.20 (20% acetone/hexane); mp = 145–150 °C (from Et_2O/pentane); ν_{max} (film)/cm^{-1} 3341 (NH br), 2973, 1684 (C=O), 1526, 1485, 1387, 1325, 1246, 1161, 1125, 1033, 881, 826, 791, 770; ^{1}H NMR (400 MHz, DMSO-d_6, 373 K) δ 9.81 (br s, 1 H, NH), 8.77 (dd, *J* = 4.2, 1.7 Hz, 1 H, HC_{Ar}), 8.55 (dd, *J* = 7.6, 1.4 Hz, 1 H, HC_{Ar}), 8.32 (dd, *J* = 8.3, 1.7 Hz, 1 H, HC_{Ar}), 7.61 (dd, *J* = 8.3, 1.4 Hz, 1 H, HC_{Ar}), 7.58–7.49 (m, 2 H, HC_{Ar}), 7.37–7.30 (m, 2 H, HC_{Ar}), 6.91–6.86 (m, 2 H, HC_{Ar}), 3.92–3.87 (m, 1 H, NC*H*HCHCO), 3.87–3.82 (m, 1 H, NC*H*HCHAr), 3.72 (s, 3 H, OCH_3), 3.71–3.57 (m, 3 H, NCH*H*CHCO, CHCO, CHAr), 3.38–3.26 (m, 1 H, NCH*H*CHAr), 1.46 (s, 9 H, $C(CH_3)_3$); ^{13}C NMR (101 MHz, DMSO-d_6, 373 K) δ 169.4 (C=O amide), 158.2 (OC_{Ar} quat), 152.9 (C=O carbamate), 148.0 (C_{Ar}), 137.7 (C_{Ar} quat), 135.8 (C_{Ar}), 133.7 (C_{Ar} quat), 130.9 (C_{Ar} quat), 128.0 (2 × C_{Ar}), 127.3 (C_{Ar} quat), 126.2 (C_{Ar}), 121.44 (C_{Ar}), 121.37 (C_{Ar}), 116.2 (C_{Ar}), 113.9 (2 × C_{Ar}), 78.2 (*C*$(CH_3)_3$), 54.7 (OCH_3), 52.6 (N*C*H_2CHAr), 51.0 (*C*HCO), 48.6 (N*C*H_2CHCO), 46.2 (CHAr), 27.8 (C(*C*$H_3)_3$); HRMS (ESI$^+$) *m*/*z* Calculated for $C_{26}H_{30}N_3O_4$ [M+H] 448.2236; Found 448.2224.

***tert*-Butyl (+)-(3*S*,4*R*)-3-(4-methoxyphenyl)-4-(quinolin-8-ylcarbamoyl)pyrrolidine-1-carboxylate ((+)-5)**

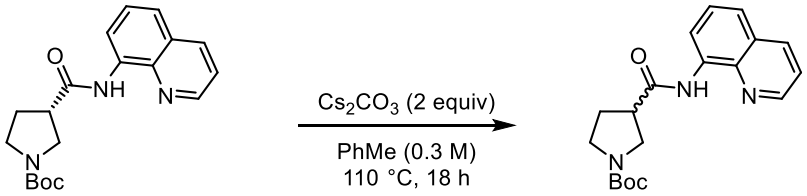


A flame-dried reaction tube was charged with 3-aryl pyrrolidine **(+)-3a** (89.5 mg, 0.20 mmol) and Cs_2CO_3 (130 mg, 0.40 mmol). The reaction vessel was sealed and purged with argon, then toluene (667 μL, 0.3 M) was added by syringe. The reaction tube was then placed in a preheated oil bath and stirred at 110 ºC for 18 h. The reaction mixture was then allowed to cool to rt and EtOAc (5 mL) was added. The resulting mixture was filtered through a pad of Celite, eluting with further EtOAc (2 × 5 mL). The solvent was removed under reduced pressure and the crude material was purified by flash column chromatography (20% acetone/hexane). The product containing fractions were combined and the solvent was removed under reduced pressure. Et_2O (5 mL) and pentane (5 mL) were added and the solvent was removed under reduced pressure to afford arylated pyrrolidine **(+)-5** as a white solid (61.1 mg, 68%, 97.4% *ee*). $[\alpha]_D^{25}$ +11.4 (*c* 0.90, $CHCl_3$).

Characterisation data identical to that reported for racemic pyrrolidine **5** (page 230).

HPLC Conditions: Chiralpak IF 3-column, 80:20 *n*-hexane:*i*-PrOH, flow rate: 1 mL·min^{-1}, 35 °C. UV detection wavelength: 210.4 nm. Retention times: 14.9 min (3*R,*4*S* enantiomer), 18.0 min (3*S,*4*R* enantiomer).

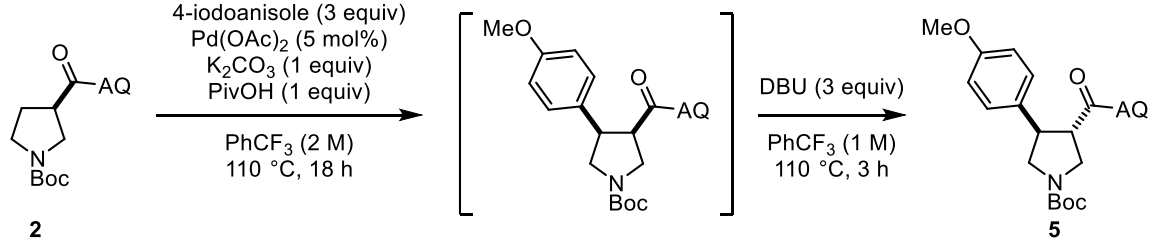
*8.2.1.8 Procedure for the Racemisation of Pyrrolidine (S)-**2** using Cs_2CO_3*



(*S*)-**2** (97% *ee*) (*S*)-**2** (78% *ee*)

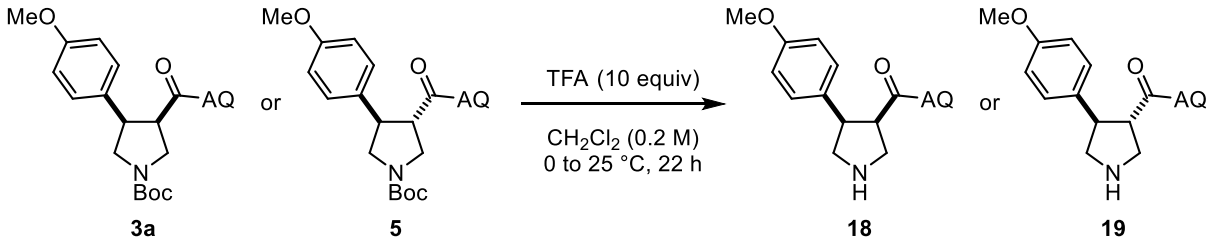
A flame-dried reaction tube was charged with enantioenriched amide (*S*)-**2** (68.3 mg, 0.20 mmol) and Cs_2CO_3 (130 mg, 0.40 mmol). The reaction vessel was sealed and purged with argon, then toluene (670 μL, 0.3 M) was added by syringe. The reaction tube was placed in a preheated oil bath and stirred at 110 ºC for 18 h. The reaction mixture was then allowed to cool to rt and EtOAc (5 mL) was added. The resulting mixture was filtered through a pad of Celite, eluting with further EtOAc (2 × 5 mL). The solvent was removed under reduced pressure and the crude material was purified by flash column chromatography (20% acetone/hexane). The product containing fractions were combined and the solvent was removed under reduced pressure. Et_2O (5 mL) and pentane (5 mL) were added and the solvent was removed under reduced pressure to afford amide (*S*)-**2** as a white solid (67.9 mg, quant., 78% *ee*). Characterisation data was identical to racemic pyrrolidine **2** (page 197).

*8.2.1.9 One-Pot C(4)–H Arylation/Epimerisation of Pyrrolidine **2**:*



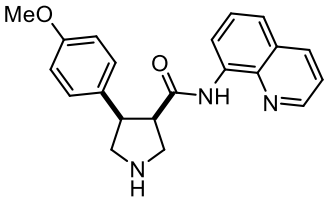
A large microwave vial (10–20 mL recommended volume) was charged with K_2CO_3 (420 mg, 3.00 mmol), flame-dried, and allowed to cool under argon. *tert*-Butyl 3-(quinolin-8-ylcarbamoyl)pyrrolidine-1-carboxylate **2** (1.02 g, 3.00 mmol), 4-iodoanisole (2.11 g, 9.00 mmol), $Pd(OAc)_2$ (33.8 mg, 0.15 mmol) and PivOH (310 mg, 3.00 mmol) were added sequentially. The reaction vessel was purged with argon, then $PhCF_3$ (1.5 mL, 2.0 M) was added by syringe. The reaction tube was placed in a preheated oil bath and stirred at 110 ºC for 18 h. The reaction mixture was then allowed to cool to rt and $PhCF_3$ (1.5 mL, 1.0 M) and DBU (1.3 mL, 9.00 mmol) were added by syringe. The reaction vessel was then stirred at 110 °C for additional 3 h. The reaction mixture was allowed to cool to rt and EtOAc (15 mL) was added. The resulting mixture was filtered through a pad of Celite, eluting with further EtOAc (2 × 40 mL). The solvent was removed under reduced pressure, and the crude material was purified by flash column chromatography (5% to 8% Et_2O/pentane) affording the *trans*-arylated pyrrolidine **5** as a pale yellow solid (720 mg, 53%). R_f 0.27 (5% Et_2O/pentane). Characterisation data identical to that reported for *trans*-pyrrolidine **5** obtained using Cs_2CO_3 (page 230).

*8.2.1.10 Boc-Deprotection of Pyrrolidine Derivatives **3a** and **5***



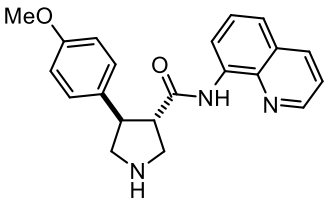
3a **5** **18** **19**

***cis*-(±)-4-(4–Methoxyphenyl)-*N*-(quinolin-8-yl)pyrrolidine-3-carboxamide (18)**



Freshly distilled trifluoroacetic acid (149 μL) was added dropwise to a solution of Boc-protected *cis*-pyrrolidine **3a** (89.5 mg, 0.20 mmol) in CH_2Cl_2 (1.0 mL) at 0 °C. The reaction was allowed to warm up and stirred at rt for 22 h. The reaction mixture was then diluted with H_2O (3 mL) and quenched with $NaHCO_3$ (250 mg). The organic layer was separated, and the aqueous layer was extracted with CH_2Cl_2 (4 × 5 mL). The combined organic layers were dried over Na_2SO_4 and the solvent was removed under reduced pressure. The resulting crude material was purified by flash column chromatography (98:2:1, CH_2Cl_2/MeOH/Et_3N), which afforded *cis*-pyrrolidine **18** as a yellow paste (62 mg, 89%). R_f 0.27 (95:5:1, CH_2Cl_2/MeOH/Et_3N); ν_{max} (film)/cm^{-1} 3344 (NH br), 2933, 1675 (C=O), 1526, 1487, 1425, 1379, 1324, 1249, 1181, 1036, 905, 826, 792, 727; ^{1}H NMR (400 MHz, $CDCl_3$, 298 K) δ 9.67 (br s, 1 H, CONH), 8.71 (dd, *J* = 4.3, 1.6 Hz, 1 H, HC_{Ar}), 8.51 (dd, *J* = 6.1, 2.9 Hz, 1 H, HC_{Ar}), 8.09 (d, *J* = 8.1 Hz, 1 H, HC_{Ar}), 7.46–7.38 (m, 3 H, HC_{Ar}), 7.23–7.18 (m, 2 H, HC_{Ar}), 7.61–7.56 (m, 2 H, HC_{Ar}), 3.77–3.65 (m, 2 H, CHAr, NC*H*HCHCO), 3.52 (s, 3 H, OCH_3), 3.44 (dd, 2 H, *J* = 8.4, 3.2 Hz, NCH_2CHAr), 3.38–3.29 (m, 2 H, CHCO, NCH*H*CHCO), 2.52 (br s, 1 H, NH); ^{13}C NMR (101 MHz, $CDCl_3$, 298 K) δ 171.6 (C=O amide), 158.2 (OC_{Ar} quat), 147.9 (C_{Ar}), 138.3 (C_{Ar} quat), 136.0 (C_{Ar}), 134.3 (C_{Ar} quat), 130.8 (C_{Ar} quat), 129.0 (2 × C_{Ar}), 127.7 (C_{Ar} quat), 127.1 (C_{Ar}), 121.3 (C_{Ar}), 121.2 (C_{Ar}), 116.3 (C_{Ar}), 113.6 (2 × C_{Ar}), 54.9 (OCH_3), 53.1 (*C*HCO), 52.0 (N*C*H_2CHAr), 50.7 (N*C*H_2CHCO), 49.2 (CHAr); HRMS (ESI$^+$) *m*/*z* Calculated for $C_{21}H_{22}N_3O_2$ [M+H] 348.1712; Found 348.1716.

***trans*-(±)-4-(4-Methoxyphenyl)-*N*-(quinolin-8-yl)pyrrolidine-3-carboxamide (19)**

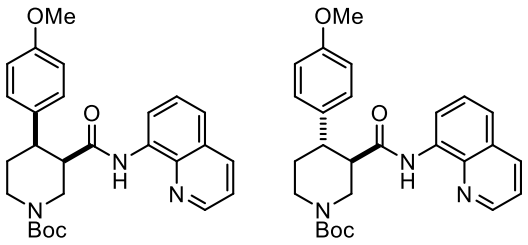


Freshly distilled trifluoroacetic acid (119 μL) was added dropwise to a solution of Boc-protected *trans*-pyrrolidine **5** (71.0 mg, 0.16 mmol) in CH_2Cl_2 (800 μL) at 0 °C. The reaction was allowed to warm up and stirred at rt for 22 h. The reaction mixture was then diluted with H_2O (3 mL) and quenched with $NaHCO_3$ (250 mg). The organic layer was separated, and the aqueous layer was extracted with CH_2Cl_2 (4 × 5 mL).

The combined organic layers were dried over Na_2SO_4 and the solvent was removed under reduced pressure, affording *trans*-pyrrolidine **19** as a pale orange oil (65.9 mg, 95%). R_f 0.27 (95:5:1, CH_2Cl_2/MeOH/Et_3N); ν_{max} (film)/cm^{-1} 3302 (NH br), 2929, 1676 (C=O), 1522, 1513, 1484, 1462, 1424, 1385, 1323, 1244, 1179, 1032, 824, 790; ^1H NMR (400 MHz, $CDCl_3$, 298 K) δ 9.78 (br s, 1 H, CONH), 8.76 (dd, *J* = 7.3, 1.7 Hz, 1 H, HC_{Ar}), 8.69 (dd, *J* = 4.3, 1.7 Hz, 1 H, HC_{Ar}), 8.13 (dd, *J* = 8.2, 1,7 Hz, 1 H, HC_{Ar}), 7.58–7.47 (m, 2 H, HC_{Ar}), 7.42 (dd, *J* = 8.3, 4.2 Hz, 1 H, HC_{Ar}), 7.27 (d, *J* = 8.7 Hz, 2 H, HC_{Ar}), 7.68 (d, *J* = 8.7 Hz, 2 H, HC_{Ar}), 3.79 (s, 3 H, OCH_3), 3.66–3.53 (m, 3 H, CHAr, NC*H*HCHCO, NC*H*HCHAr), 3.50–3.43 (m, 1 H, NCH*H*CHCO), 3.21–3.14 (m, 1 H, CHCO), 3.02–2.94 (m, 1 H, NCH*H*CHAr), 2.31 (br s, 1 H, NH); ^{13}C NMR (101 MHz, $CDCl_3$, 298 K) δ 173.0 (C=O amide), 158.4 (OC_{Ar} quat), 148.0 (C_{Ar}), 138.2 (C_{Ar} quat), 136.2 (C_{Ar}), 134.4 (C_{Ar} quat), 134.1 (C_{Ar} quat), 128.5 (2 × C_{Ar}), 127.8 (C_{Ar} quat), 127.3 (C_{Ar}), 121.5 (2 × C_{Ar}), 116.4 (C_{Ar}), 114.2 (2 × C_{Ar}), 56.7 (N*C*H_2CHAr), 56.5 (*C*HCO), 55.2 (OCH_3), 52.5 (N*C*H_2CHCO), 50.8 (CHAr); HRMS (ESI^+) *m*/*z* Calculated for $C_{21}H_{22}N_3O_2$ [M+H] 348.1712; Found 348.1708.

*8.2.1.11 Piperidine C–H Arylation: Scope of N-Protecting Groups and Aryl Iodides (**25a–g, 26a–g, 27a–c, 28a–c**)*

***tert*-Butyl *cis*-(±)-4-(4-methoxyphenyl)-3-(quinolin-8-ylcarbamoyl)piperidine-1-carboxylate (25a)** and ***tert*-butyl *trans*-(±)-4-(4-methoxyphenyl)-3-(quinolin-8-ylcarbamoyl)piperidine-1-carboxylate (26a):**



Prepared according to **General Procedure A** using amide **24** (178 mg) and 4-iodoanisole (351 mg). Purification by flash column chromatography (5% to 15% acetone/pentane) afforded the minor product *tert*-butyl *trans*-(±)-4-(4-methoxyphenyl)-3-(quinolin-8-ylcarbamoyl) piperidine-1-carboxylate **26a** as a white solid (46.2 mg, 20%) followed by the major product *tert*-butyl *cis*-(±)-4-(4-methoxyphenyl)-3-(quinolin-8-ylcarbamoyl)piperidine-1-carboxylate **25a** as a white solid (102 mg, 44%).

Major (**25a**): R_f 0.20 (15% acetone/pentane); mp = 68–72 °C (from Et_2O/pentane); ν_{max} (film)/cm^{-1} 3355 (NH), 2971, 1684 (C=O), 1522, 1485, 1424, 1324, 1246, 1162, 1120, 1035, 1004, 827, 792, 759; ^{1}H NMR (400 MHz, DMSO-d_6, 373 K) δ 9.71 (br s, 1 H, NH), 8.82 (dd, J = 4.2, 1.7 Hz, 1 H, HC_{Ar}), 8.47 (dd, J = 7.6, 1.4 Hz, 1 H, HC_{Ar}), 8.31 (dd, J = 8.3, 1.7 Hz, 1 H, HC_{Ar}), 7.58–7.54 (m, 2 H, HC_{Ar}), 7.48 (t, J = 7.9 Hz, 1 H, HC_{Ar}), 7.27–7.22 (m, 2 H, HC_{Ar}), 6.78–6.74 (m, 2 H, HC_{Ar}), 4.39 (ddd, J = 13.7, 2.5, 1.8 Hz, 1 H, NC*H*HCHCO), 4.24 (dddd, J = 13.1, 4.7, 2.8, 1.8 Hz, 1 H, NC*H*HCH$_2$), 3.63 (s, 3 H, OCH_3), 3.31 (dd, J = 13.7, 3.9 Hz, 1 H, NCH*H*CHCO), 3.26–3.21 (m, 1 H, CHCO), 3.12 (ddd, J = 12.3, 4.3, 4.3 Hz, 1 H, CHAr), 3.01–2.93 (m, 1 H, NCH*H*CH$_2$), 2.68 (dddd, J = 12.2, 12.2, 12.2, 4.7, 1 H, NCH$_2$C*H*H), 1.74–1.67 (m, 1 H, NCH$_2$CH*H*), 1.26 (s, 9 H, C(CH$_3$)$_3$); ^{13}C NMR (101 MHz, DMSO-d_6, 373 K) δ 170.1 (C=O amide), 157.3 (OC_{Ar} quat), 153.4 (C=O carbamate), 147.8 (C_{Ar}), 137.6 (C_{Ar} quat), 135.7 (C_{Ar}), 134.6 (C_{Ar} quat), 134.1 (C_{Ar} quat), 127.8 (2 × C_{Ar}), 127.2 (C_{Ar} quat), 126.2 (C_{Ar}), 121.2 (C_{Ar}), 120.7 (C_{Ar}), 115.6 (C_{Ar}), 113.2 (2 × C_{Ar}), 77.9 (*C*(CH$_3$)$_3$), 54.5 (OCH_3), 46.2 (N*C*H$_2$CHCO), 46.1 (*C*HCO), 43.1 (N*C*H$_2$CH$_2$), 41.6 (CHAr), 27.4 (C(*C*H$_3$)$_3$), 25.5 (NCH$_2$*C*H$_2$); HRMS (ESI$^+$) *m*/*z* Calculated for $C_{27}H_{32}N_3O_4$ [M+H] 462.2393; Found 462.2386.

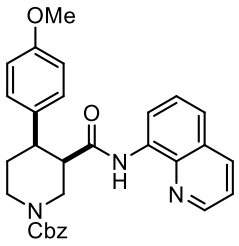
Minor (**26a**): R_f 0.27 (15% acetone/pentane); mp = 59–63 °C (from Et_2O/pentane); ν_{max} (film)/cm^{-1} 3348 (NH), 2931, 1681 (C=O), 1525, 1514, 1486, 1424, 1366, 1284, 1233, 1158, 1126, 1034, 826, 791, 762; ^{1}H NMR (500 MHz, DMSO-d_6, 373 K) δ 9.69 (br s, 1 H, NH), 8.84 (dd, J = 4.2, 1.7 Hz, 1 H, HC_{Ar}), 8.41 (dd, J = 7.7, 1.3 Hz, 1 H, HC_{Ar}), 8.31 (dd, J = 8.3, 1.7 Hz, 1 H, HC_{Ar}), 7.59–7.54 (m, 2 H, HC_{Ar}), 7.47 (t, J = 7.9 Hz, 1 H, HC_{Ar}), 7.26–7.23 (m, 2 H, HC_{Ar}), 6.76–6.63 (m, 2 H, HC_{Ar}), 4.37–4.30 (m, 1 H, NC*H*HCHCO), 4.12 (dddd, J = 13.2, 4.4, 2.2,

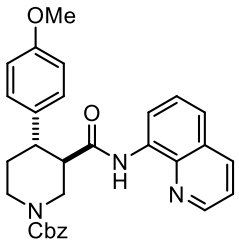
2.2 Hz, 1 H, NC*H*HCH$_2$), 3.59 (s, 3 H, OCH$_3$), 3.07–3.01 (m, 3 H, NCH*H*CHCO, CHCO, CHAr), 2.97–2.90 (m, 1 H, NCH*H*CH$_2$), 1.81–1.76 (m, 1 H, NCH$_2$C*H*H), 1.71–1.60 (m, 1 H, NCH$_2$CH*H*), 1.48 (s, 9 H, C(CH$_3$)$_3$); ^{13}C NMR (126 MHz, DMSO-d_6, 373 K) δ 170.0 (C=O amide), 157.5 (OC$_{Ar}$ quat), 153.4 (C=O carbamate), 148.0 (C$_{Ar}$), 137.6 (C$_{Ar}$ quat), 135.7 (C$_{Ar}$), 135.0 (C$_{Ar}$ quat), 133.6 (C$_{Ar}$ quat), 127.7 (2 × C$_{Ar}$), 127.2 (C$_{Ar}$ quat), 126.1 (C$_{Ar}$), 121.3 (C$_{Ar}$), 121.2 (C$_{Ar}$), 116.1 (C$_{Ar}$), 113.5 (2 × C$_{Ar}$), 78.5 (*C*(CH$_3$)$_3$), 54.5 (OCH$_3$), 49.8 (*C*HCO), 46.3 (N*C*H$_2$CHCO), 43.6 (CHAr), 43.5 (N*C*H$_2$CH$_2$), 32.4 (NCH$_2$*C*H$_2$), 27.7 (C(*C*H$_3$)$_3$); HRMS (ESI$^+$) *m*/*z* Calculated for C$_{27}$H$_{32}$N$_3$O$_4$ [M+H] 462.2393; Found 462.2403.

Larger scale C–H Arylation of Piperidine Amide 24:

A large microwave vial (10–20 mL recommended volume) was charged with K$_2$CO$_3$ (470 mg, 3.4 mmol), flame-dried, and allowed to cool under argon. Amide **24** (1.22 g, 3.4 mmol), 4-iodoanisole (2.41 g, 10.3 mmol), Pd(OAc)$_2$ (38.3 mg, 0.17 mmol) and PivOH (348 mg, 3.4 mmol) were added sequentially. The reaction vessel was sealed and purged with argon, then PhCF$_3$ (1.70 mL, 2.0 M) was added by syringe. The reaction tube was then placed in a preheated oil bath and stirred at 110 ºC for 18 h. The reaction mixture was then allowed to cool to rt and EtOAc (20 mL) was added. The resulting mixture was filtered through a pad of Celite, eluting with further EtOAc (2 × 50 mL). The solvent was removed under reduced pressure. The reaction mixture was purified by flash column chromatography (5% to 15% acetone/pentane). The product containing fractions were combined and the solvent was removed under reduced pressure. Et$_2$O (20 mL) and pentane (20 mL) were added and the solvent was removed under reduced pressure to afford the minor product *tert*-butyl *trans*-(±)-4-(4-methoxyphenyl)-3-(quinolin-8-ylcarbamoyl) piperidine-1-carboxylate **26a** as a white solid (253 mg, 16%) and the major product *tert*-butyl *cis*-(±)-4-(4-methoxyphenyl)-3-(quinolin-8-ylcarbamoyl)piperidine-1-carboxylate **25a** as a white solid (821 mg, 52%). Characterisation data identical to that reported on 0.5 mmol scale.

Benzyl *cis*-(±)-4-(4-methoxyphenyl)-3-(quinolin-8-ylcarbamoyl)piperidine-1-carboxylate (27a) and **benzyl *trans*-(±)-4-(4-methoxyphenyl)-3-(quinolin-8-ylcarbamoyl)piperidine-1-carboxylate (28a):**





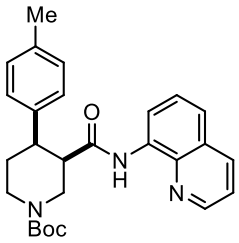
Prepared according to **General Procedure A** using amide **21** (195 mg) and 4-iodoanisole (351 mg). Purification by flash column chromatography (10% to 20% acetone/pentane) afforded the minor product *trans*-(±)-4-(4-methoxyphenyl)-3-(quinolin-8-ylcarbamoyl) piperidine-1-carboxylate **28a** as a

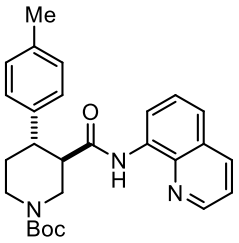
white solid (46.1 mg, 19%) followed by the major product benzyl *cis*-(±)-4-(4-methoxyphenyl)-3-(quinolin-8–ylcarbamoyl)piperidine-1-carboxylate **27a** as a white solid (125 mg, 50%).

Major (**27a**): R_f 0.21 (20% acetone/pentane); mp = 56–61 °C(from Et_2O/pentane); ν_{max} (film)/cm^{-1} 3339 (NH), 2912, 1684 (C=O), 1521, 1484, 1424, 1379, 1323, 1286, 1235, 1180, 1116, 1030, 1004, 826, 791, 758, 697; ^{1}H NMR (400 MHz, DMSO-d_6, 373 K) δ 9.68 (br s, 1 H, NH), 8.77 (dd, *J* = 4.2, 1.7 Hz, 1 H, HC_{Ar}), 8.45 (dd, *J* = 7.6, 1.4 Hz, 1 H, HC_{Ar}), 8.30 (dd, *J* = 8.3, 1.7 Hz, 1 H, HC_{Ar}), 7.60–7.50 (m, 2 H, HC_{Ar}), 7.48 (t, *J* = 7.9 Hz, 1 H, HC_{Ar}), 7.28–7.11 (m, 7 H, HC_{Ar}), 6.80-6.71 (m, 2 H, HC_{Ar}), 5.09–4.96 (m, 2 H, OCH_2Ph), 4.47 (ddd, *J* = 13.8, 2.5, 1.8 Hz, 1 H, NC*H*HCHCO), 4.32 (dddd, *J* = 13.0, 4.4, 2.7, 1.8 Hz, 1 H, NC*H*HCH$_2$), 3.61 (s, 3 H, OCH_3), 3.39 (dd, *J* = 13.8, 3.9 Hz, 1 H, NCH*H*CHCO), 3.26 (ddd, *J* = 4.0, 4.0, 4.0 Hz, 1 H, CHCO), 3.17 (ddd, *J* = 12.3, 4.3, 4.3 Hz, 1 H, CHAr), 3.08 (ddd, *J* = 12.7, 12.7, 3.3, 1 H, NCH*H*CH$_2$), 2.67 (dddd, *J* = 12.4, 12.4, 12.4, 4.6, 1 H, NCH$_2$C*H*H), 1.74 (dddd, *J* = 13.1, 3.2, 3.2, 3.2, 1 H, NCH$_2$CH*H*); ^{13}C NMR (101 MHz, DMSO-d_6, 373 K) δ 170.1 (C=O amide), 157.4 (OC_{Ar} quat), 154.2 (C=O carbamate), 147.8 (C_{Ar}), 137.5 (C_{Ar} quat), 136.5 (C_{Ar} quat), 135.7 (C_{Ar}), 134.4 (C_{Ar} quat), 133.9 (C_{Ar} quat), 127.7 (2 × C_{Ar}), 127.4 (2 × C_{Ar}), 127.2 (C_{Ar} quat), 126.8 (C_{Ar}), 126.6 (2 × C_{Ar}), 126.2 (C_{Ar}), 121.2 (C_{Ar}), 120.8 (C_{Ar}), 115.7 (C_{Ar}), 113.3 (2 × C_{Ar}), 65.6 (OCH_2Ph), 54.5 (OCH_3), 46.00 (N*C*H$_2$CHCO), 45.96 (*C*HCO), 43.4 (N*C*H$_2$CH$_2$), 41.6 (CHAr), 25.5 (NCH$_2$*C*H$_2$); HRMS (ESI$^+$) *m*/*z* Calculated for $C_{30}H_{30}N_3O_4$ [M+H] 496.2236; Found 496.2225.

Minor (**28a**): R_f 0.28 (20% acetone/pentane); mp = 56–62 °C (from Et_2O/pentane); ν_{max} (film)/cm^{-1} 3344 (NH), 2936, 1678 (C=O), 1524, 1514, 1486, 1466, 1424, 1325, 1281, 1220, 1124, 1032, 997, 950, 825, 791, 759, 697; ^{1}H NMR (400 MHz, DMSO-d_6, 373 K) δ 9.68 (br s, 1 H, NH), 8.83 (dd, *J* = 4.2, 1.7 Hz, 1 H, HC_{Ar}), 8.41 (dd, *J* = 7.6, 1.4 Hz, 1 H, HC_{Ar}), 8.29 (dd, *J* = 8.3, 1.7 Hz, 1 H, HC_{Ar}), 7.61–7.51 (m, 2 H, HC_{Ar}), 7.46 (t, *J* = 8.0 Hz, 1 H, HC_{Ar}), 7.46–7.29 (m, 5 H, HC_{Ar}), 7.28–7.20 (m, 2 H, HC_{Ar}), 6.78–6.70 (m, 2 H, HC_{Ar}), 5.18 (s, 2 H, OCH_2Ph), 4.45–4.38 (m, 1 H, NC*H*HCHCO), 4.20 (dddd, *J* = 13.3, 4.3, 2.1, 2.1 Hz, 1 H, NC*H*HCH$_2$), 3.59 (s, 3 H, OCH_3), 3.20–2.97 (m, 4 H, NCH*H*CHCO, CHCO, CHAr, NCH*H*CH$_2$), 1.85–1.77 (m, 1 H, NCH$_2$C*H*H), 1.76–1.64 (m, 1 H, NCH$_2$CH*H*); ^{13}C NMR (101 MHz, DMSO-d_6, 373 K) δ 169.9 (C=O amide), 157.5 (OC_{Ar} quat), 154.1 (C=O carbamate), 148.0 (C_{Ar}), 137.6 (C_{Ar} quat), 136.5 (C_{Ar} quat), 135.7 (C_{Ar}), 134.8 (C_{Ar} quat), 133.5 (C_{Ar} quat), 127.8 (2 × C_{Ar}), 127.7 (2 × C_{Ar}), 127.2 (C_{Ar}, C_{Ar} quat), 127.0 (2 × C_{Ar}), 126.1 (C_{Ar}), 121.27 (C_{Ar}), 121.25 (C_{Ar}), 116.1 (C_{Ar}), 113.5 (2 × C_{Ar}), 65.9 (OCH_2Ph), 54.5 (OCH_3), 49.8 (*C*HCO), 46.4 (N*C*H$_2$CHCO), 43.63 (N*C*H$_2$CH$_2$), 43.56 (CHAr), 32.3 (NCH$_2$*C*H$_2$); HRMS (ESI$^+$) *m*/*z* Calculated for $C_{30}H_{30}N_3O_4$ [M+H] 496.2236; Found 496.2253.

***tert*-Butyl *cis*-(±)-3-(quinolin-8-ylcarbamoyl)-4-(*p*-tolyl)piperidine-1-carboxylate (25b)** and ***tert*-butyl *trans*-(±)-3-(quinolin-8-ylcarbamoyl)-4-(*p*-tolyl)piperidine-1-carboxylate (26b):**





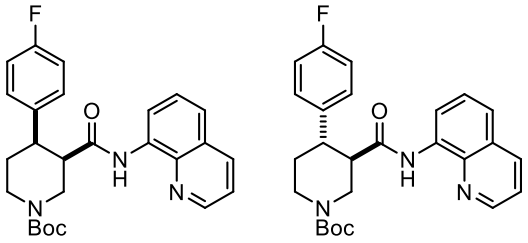
Prepared according to **General Procedure A** using amide **24** (178 mg) and 4-iodotoluene (327 mg). Purification by flash column chromatography (0% to 5% MeCN/CH_2Cl_2) afforded the minor product *tert*-butyl *trans*-(±)-3-(quinolin-8-ylcarbamoyl)-4-(*p*-tolyl) piperidine-1-carboxylate **26b** as a white solid (46.0 mg, 21%) followed by the major product *tert*–butyl *cis*-(±)-3-(quinolin-8-ylcarbamoyl)-4-(*p*-tolyl) piperidine-1-carboxylate **25b** as a white solid (79.3 mg, 35%).

Major (**25b**): R_f 0.42 (3% MeCN/CH_2Cl_2); mp = 60–66 °C (from Et_2O/pentane); ν_{max} (film)/cm^{-1} 3357 (NH), 2924, 1685 (C=O), 1522, 1484, 1424, 1365, 1324, 1243, 1160, 1121, 1006, 823, 791, 759; ^{1}H NMR (400 MHz, DMSO-d_6, 373 K) δ 9.72 (br s, 1 H, NH), 8.82 (dd, J = 4.2, 1.7 Hz, 1 H, HC_{Ar}), 8.46 (dd, J = 7.7, 1.4 Hz, 1 H, HC_{Ar}), 8.31 (dd, J = 8.3, 1.7 Hz, 1 H, HC_{Ar}), 7.59–7.53 (m, 2 H, HC_{Ar}), 7.48 (t, J = 7.9 Hz, 1 H, HC_{Ar}), 7.24–7.19 (m, 2 H, HC_{Ar}), 7.02–6.97 (m, 2 H, HC_{Ar}), 4.40 (ddd, J = 13.2, 2.2, 2.2 Hz, 1 H, NC*H*HCHCO), 4.24 (dddd, J = 13.1, 4.7, 2.6, 2.6 Hz, 1 H, NC*H*HCH$_2$), 3.32 (dd, J = 13.7, 3.9 Hz, 1 H, NCH*H*CHCO), 3.28–3.24 (m, 1 H, CHCO), 3.12 (ddd, J = 12.3, 4.3, 4.3 Hz, 1 H, CHAr), 3.02–2.93 (m, 1 H, NCH*H*CH$_2$), 2.70 (dddd, J = 12.3, 12.3, 12.3, 4.6, 1 H, NCH$_2$C*H*H), 2.15 (s, 3 H, CH_3), 1.75–1.68 (m, 1 H, NCH$_2$CH*H*), 1.26 (s, 9 H, C(CH_3)$_3$); ^{13}C NMR (101 MHz, DMSO-d_6, 373 K) δ 170.1 (C=O amide), 153.4 (C=O carbamate), 147.9 (C_{Ar}), 139.5 (C_{Ar} quat), 137.5 (C_{Ar} quat), 135.7 (C_{Ar}), 134.5 (C_{Ar} quat), 134.1 (C_{Ar} quat), 128.0 (2 × C_{Ar}), 127.2 (C_{Ar} quat), 126.7 (2 × C_{Ar}), 126.2 (C_{Ar}), 121.2 (C_{Ar}), 120.7 (C_{Ar}), 115.6 (C_{Ar}), 77.9 (*C*(CH_3)$_3$), 46.3 (N*C*H$_2$CHCO), 46.0 (*C*HCO), 43.1 (N*C*H$_2$CH$_2$), 41.9 (CHAr), 27.4 (C(*C*H$_3$)$_3$), 25.4 (NCH$_2$*C*H$_2$), 19.8 (CH_3); HRMS (ESI$^+$) *m*/*z* Calculated for $C_{27}H_{32}N_3O_3$ [M+H] 446.2444; Found 446.2466.

Minor (**26b**): R_f 0.53 (3% MeCN/CH_2Cl_2); mp = 57–63 °C (from Et_2O/pentane); ν_{max} (film)/cm^{-1} 3347 (NH), 2923, 1682 (C=O), 1524, 1486, 1423, 1365, 1324, 1234, 1155, 1126, 825, 790, 759; ^{1}H NMR (400 MHz, DMSO-d_6, 373 K) δ 9.71 (br s, 1 H, NH), 8.84 (dd, J = 4.2, 1.7 Hz, 1 H, HC_{Ar}), 8.41 (dd, J = 7.7, 1.4 Hz, 1 H, HC_{Ar}), 8.30 (dd, J = 8.3, 1.7 Hz, 1 H, HC_{Ar}), 7.59–7.54 (m, 2 H, HC_{Ar}), 7.46 (t, J = 8.0 Hz, 1 H, HC_{Ar}), 7.23-7.18 (m, 2 H, HC_{Ar}), 7.02-6.96 (m, 2 H, HC_{Ar}), 4.39-4.32 (m, 1 H, NC*H*HCHCO), 4.12 (ddt, J = 13.3, 4.3, 2.1 Hz, 1 H, NC*H*HCH$_2$), 3.10–3.03 (m, 3 H, NCH*H*CHCO, CHCO, CHAr), 2.99–2.89 (m, 1 H, NCH*H*CH$_2$), 2.12 (s, 3 H, CH_3), 1.79 (dddd, J = 13.3, 2.0, 2.0, 2.0 Hz, 1 H, NCH$_2$C*H*H), 1.72–1.63 (m, 1 H, NCH$_2$CH*H*), 1.49 (s, 9 H, C(CH_3)$_3$); ^{13}C NMR (101 MHz, DMSO-d_6, 373 K) δ 170.0 (C=O

amide), 153.4 (C=O carbamate), 148.0 (C_{Ar}), 139.9 (C_{Ar} quat), 137.6 (C_{Ar} quat), 135.7 (C_{Ar}), 134.7 (C_{Ar} quat), 133.6 (C_{Ar} quat), 128.3 (2 × C_{Ar}), 127.2 (C_{Ar} quat), 126.6 (2 × C_{Ar}), 126.1 (C_{Ar}), 121.3 (C_{Ar}), 121.2 (C_{Ar}), 116.0 (C_{Ar}), 78.5 (*C*$(CH_3)_3$), 49.6 (*C*HCO), 46.3 (N*C*H_2CHCO), 44.0 (CHAr), 43.5 (N*C*H_2CH_2), 32.4 (NCH$_2$*C*H_2), 27.7 (C(*C*$H_3)_3$), 19.8 (CH_3); HRMS (ESI$^+$) *m*/*z* Calculated for $C_{27}H_{32}N_3O_3$ [M+H] 446.2444; Found 446.2459.

***tert*-Butyl *cis*-(±)-4-(4-fluorophenyl)-3-(quinolin-8-ylcarbamoyl)piperidine-1-carboxylate (25c)** and ***tert*-butyl *trans*-(±)-4-(4-fluorophenyl)-3-(quinolin-8-ylcarbamoyl)piperidine-1-carboxylate (26c):**



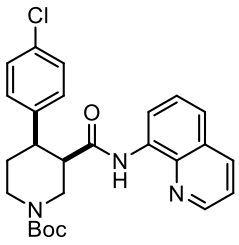
Prepared according to **General Procedure A** using amide **24** (178 mg) and 4-fluoroiodobenzene (333 mg). Purification by flash column chromatography (5% to 10% acetone/pentane) afforded the minor product *tert*-butyl *trans*-(±)-4-(4-fluorophenyl)-3-(quinolin-8-ylcarbamoyl) piperidine-1-carboxylate **26c** as a white solid (35.0 mg, 16%) followed by the major product *tert*-butyl *cis*-(±)-4-(4-fluorophenyl)-3-(quinolin-8-ylcarbamoyl)piperidine-1-carboxylate **25c** as a white solid (42.4 mg, 42%).

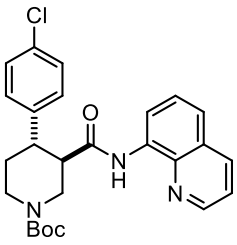
Major (**25c**): R_f 0.18 (10% acetone/pentane); mp = 66–72 °C (from Et_2O/pentane); ν_{max} (film)/cm^{-1} 3343 (NH), 2976, 1680 (C=O), 1522, 1485, 1424, 1365, 1324, 1223, 1158, 1122, 1005, 826, 791, 758, 671; ^{1}H NMR (400 MHz, DMSO-d_6, 373 K) δ 9.73 (br s, 1 H, NH), 8.82 (dd, *J* = 4.2, 1.7 Hz, 1 H, HC_{Ar}), 8.45 (dd, *J* = 7.7, 1.4 Hz, 1 H, HC_{Ar}), 8.31 (dd, *J* = 8.3, 1.6 Hz, 1 H, HC_{Ar}), 7.61–7.52 (m, 2 H, HC_{Ar}), 7.48 (t, *J* = 8.0 Hz, 1 H, HC_{Ar}), 7.41–7.32 (m, 2 H, HC_{Ar}), 7.01–6.93 (m, 2 H, HC_{Ar}), 4.41 (ddd, *J* = 13.3, 1.8, 1.8 Hz, 1 H, NC*H*HCHCO), 4.26 (dddd, *J* = 13.1, 4.6, 2.4, 2.4 Hz, 1 H, NC*H*HCH$_2$), 3.36–3.27 (m, 2 H, NCH*H*CHCO, CHCO), 3.18 (ddd, *J* = 12.4, 4.1, 4.1 Hz, 1 H, CHAr), 3.02–2.93 (m, 1 H, NCH*H*CH$_2$), 2.70 (dddd, *J* = 12.4, 12.4, 12.4, 4.6, 1 H, NCH$_2$C*H*H), 1.72 (dddd, *J* = 13.0, 3.4, 3.4, 3.4, 1 H, NCH$_2$CH*H*), 1.26 (s, 9 H, C$(CH_3)_3$); ^{13}C NMR (101 MHz, DMSO-d_6, 373 K) δ 169.9 (C=O amide), 160.3 (d, J_{CF} = 242.3 Hz, FC_{Ar} quat), 153.4 (C=O carbamate), 147.9 (C_{Ar}), 138.7 (d, J_{CF} = 3.4 Hz, F-*p*-C_{Ar} quat), 137.6 (C_{Ar} quat), 135.7 (C_{Ar}), 134.0 (C_{Ar} quat), 128.6 (d, J_{CF} = 7.9 Hz, 2 × F-*m*-C_{Ar}), 127.2 (C_{Ar} quat), 126.1 (C_{Ar}), 121.2 (C_{Ar}), 120.8 (C_{Ar}), 115.7 (C_{Ar}), 114.0 (d, J_{CF} = 20.9 Hz, 2 × F-*o*-C_{Ar}), 77.9 (*C*$(CH_3)_3$), 46.2 (N*C*H_2CHCO), 45.9 (*C*HCO), 43.0 (N*C*H_2CH_2), 41.6 (CHAr), 27.4 (C(*C*$H_3)_3$), 25.3 (NCH$_2$*C*H_2); ^{19}F NMR (376 MHz, DMSO-d_6, 373 K) δ –117.2 (ddd, J_{HF} = 14.6, 9.1, 5.5 Hz); HRMS (ESI$^+$) *m*/*z* Calculated for $C_{26}H_{29}N_3O_3F$ [M+H] 450.2193; Found 450.2207.

Minor (**26c**): R_f 0.24 (10% acetone/pentane); mp = 62–68 °C (from Et_2O/pentane); ν_{max} (film)/cm^{-1} 3345 (NH), 2976, 1681 (C=O), 1525, 1486, 1424, 1389, 1366, 1325, 1227, 1158,

1124, 826, 791, 760; ^{1}H NMR (400 MHz, DMSO-d_6, 373 K) δ 9.71 (br s, 1 H, NH), 8.84 (dd, J = 4.2, 1.7 Hz, 1 H, HC_{Ar}), 8.39 (dd, J = 7.6, 1.3 Hz, 1 H, HC_{Ar}), 8.31 (dd, J = 8.3, 1.7 Hz, 1 H, HC_{Ar}), 7.62–7.52 (m, 2 H, HC_{Ar}), 7.47 (t, J = 8.0 Hz, 1 H, HC_{Ar}), 7.43–7.32 (m, 2 H, HC_{Ar}), 7.02–6.91 (m, 2 H, HC_{Ar}), 4.40–4.31 (m, 1 H, NC*H*HCHCO), 4.13 (dddd, J = 13.3, 4.4, 2.2, 2.2 Hz, 1 H, NC*H*HCH$_2$), 3.15–2.99 (m, 3 H, NCH*H*CHCO, CHCO, CHAr), 2.99–2.90 (m, 1 H, NCH*H*CH$_2$), 1.81 (dddd, J = 13.8, 3.2, 3.2, 3.2 Hz, 1 H, NCH$_2$C*H*H), 1.73–1.61 (m, 1 H, NCH$_2$CH*H*), 1.49 (s, 9 H, C(CH$_3$)$_3$); ^{13}C NMR (101 MHz, DMSO-d_6, 373 K) δ 169.9 (C=O amide), 160.4 (d, J_{CF} = 242.2 Hz, FC_{Ar} quat), 153.4 (C=O carbamate), 148.0 (C_{Ar}), 139.0 (d, J_{CF} = 3.2 Hz, F-*p*-C_{Ar} quat), 137.7 (C_{Ar} quat), 135.7 (C_{Ar}), 133.5 (C_{Ar} quat), 128.6 (d, J_{CF} = 8.0 Hz, 2 × F-*m*-C_{Ar}), 127.2 (C_{Ar} quat), 126.1 (C_{Ar}), 121.4 (C_{Ar}), 121.3 (C_{Ar}), 116.3 (C_{Ar}), 114.3 (d, J_{CF} = 21.0 Hz, 2 × F-*o*-C_{Ar}), 78.6 (*C*(CH$_3$)$_3$), 49.6 (*C*HCO), 46.2 (N*C*H$_2$CHCO), 43.7 (CHAr), 43.4 (N*C*H$_2$CH$_2$), 32.2 (NCH$_2$*C*H$_2$), 27.7 (C(*C*H$_3$)$_3$); ^{19}F NMR (376 MHz, DMSO-d_6, 373 K) δ – 16.8 (ddd, J_{HF} = 14.1, 9.1, 5.2 Hz); HRMS (ESI$^+$) m/z Calculated for $C_{26}H_{29}N_3O_3F$ [M+H] 450.2193; Found 450.2216.

***tert*-Butyl *cis*-(±)-4-(4-chlorophenyl)-3-(quinolin-8-ylcarbamoyl)piperidine-1-carboxylate (25d)** and ***tert*-butyl *trans*-(±)-4-(4-chlorophenyl)-3-(quinolin-8-ylcarbamoyl)piperidine-1-carboxylate (26d):**





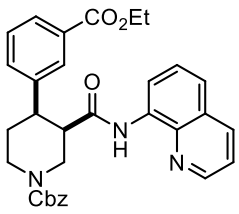
Prepared according to **General Procedure A** using amide **24** (178 mg) and 4-chloroiodobenzene (358 mg). Purification by flash column chromatography (0% to 5% MeCN/CH_2Cl_2) afforded the minor product *tert*–butyl *trans*-(±)-4-(4-chlorophenyl)-3-(quinolin-8-ylcarbamoyl) piperidine-1-carboxylate **26d** as a white solid (33.1 mg, 14%) followed by the major product *tert*-butyl *cis*-(±)-4-(4-chlorophenyl)-3-(quinolin-8-ylcarbamoyl)piperidine-1-carboxylate **25d** as a pale pink solid (71.0 mg, 30%).

Major (**25d**): R_f 0.34 (3% MeCN/CH_2Cl_2); mp = 64–70 °C (from Et_2O/pentane); ν_{max} (film)/cm^{-1} 3335 (NH), 2976, 1685 (C=O), 1522, 1485, 1424, 1365, 1324, 1244, 1161, 1121, 1092, 1005, 826, 791, 758; ^{1}H NMR (400 MHz, DMSO-d_6, 373 K) δ 9.75 (br s, 1 H, NH), 8.83 (dd, J = 4.2, 1.7 Hz, 1 H, HC_{Ar}), 8.45 (dd, J = 7.7, 1.4 Hz, 1 H, HC_{Ar}), 8.31 (dd, J = 8.3, 1.7 Hz, 1 H, HC_{Ar}), 7.61–7.52 (m, 2 H, HC_{Ar}), 7.48 (t, J = 7.9 Hz, 1 H, HC_{Ar}), 7.39–7.31 (m, 2 H, HC_{Ar}), 7.27–7.20 (m, 2 H, HC_{Ar}), 4.42 (ddd, J = 15.0, 3.5, 1.8 Hz, 1 H, NC*H*HCHCO), 4.25 (dddd, J = 13.2, 4.6, 2.4, 2.4 Hz, 1 H, NC*H*HCH$_2$), 3.37–3.27 (m, 2 H, NCH*H*CHCO, CHCO), 3.17 (ddd, J = 12.3, 4.1, 4.1 Hz, 1 H, CHAr), 3.03–2.91 (m, 1 H, NCH*H*CH$_2$), 2.69 (dddd, J = 12.3, 12.3, 12.3, 4.6 Hz, 1 H, NCH$_2$C*H*H), 1.76–1.69 (m, 1 H, NCH$_2$CH*H*), 1.25 (s, 9 H, C(CH$_3$)$_3$); ^{13}C NMR

(101 MHz, DMSO-d_6, 373 K) δ 169.9 (C=O amide), 153.4 (C=O carbamate), 147.9 (C_{Ar}), 141.6 (C_{Ar} quat), 137.6 (C_{Ar} quat), 135.7 (C_{Ar}), 133.9 (C_{Ar} quat), 130.4 (C_{Ar} quat), 128.7 (2 × C_{Ar}), 127.4 (2 × C_{Ar}), 127.2 (C_{Ar} quat), 126.1 (C_{Ar}), 121.2 (C_{Ar}), 120.8 (C_{Ar}), 115.7 (C_{Ar}), 77.9 ($C(CH_3)_3$), 46.2 (NCH_2CHCO), 45.7 ($CHCO$), 43.0 (NCH_2CH_2), 41.6 (CHAr), 27.4 ($C(CH_3)_3$), 25.1 (NCH_2CH_2); HRMS (ESI^+) *m*/*z* Calculated for $C_{26}H_{29}N_3O_3{}^{35}Cl$ [M+H] 466.1897; Found 466.1891.

Minor (**26d**): R_f 0.47 (3% MeCN/CH_2Cl_2); mp = 59–65 °C (from Et_2O/pentane); ν_{max} (film)/cm^{-1} 3348 (NH), 2930, 1678 (C=O), 1525, 1486, 1424, 1366, 1325, 1234, 1156, 1125, 1092, 825, 790, 759; ^1H NMR (400 MHz, DMSO-d_6, 373 K) δ 9.73 (br s, 1 H, NH), 8.85 (dd, *J* = 4.2, 1.7 Hz, 1 H, HC_{Ar}), 8.39 (dd, *J* = 7.7, 1.4 Hz, 1 H, HC_{Ar}), 8.31 (dd, *J* = 8.3, 1.7 Hz, 1 H, HC_{Ar}), 7.61–7.54 (m, 2 H, HC_{Ar}), 7.47 (t, *J* = 8.0 Hz, 1 H, HC_{Ar}), 7.40–7.34 (m, 2 H, HC_{Ar}), 7.24–7.19 (m, 2 H, HC_{Ar}), 4.36 (ddd, *J* = 12.6, 3.4, 1.7 Hz, 1 H, NC*H*HCHCO), 4.13 (dddd, *J* = 13.3, 4.5, 2.2, 2.2 Hz, 1 H, NC*H*HCH$_2$), 3.16–3.00 (m, 3 H, NCH*H*CHCO, CHCO, CHAr), 2.99–2.89 (m, 1 H, NCH*H*CH$_2$), 1.81 (dddd, *J* = 13.2, 2.9, 2.9, 2.9 Hz, 1 H, NCH$_2$C*H*H), 1.74–1.60 (m, 1 H, NCH$_2$CH*H*), 1.49 (s, 9 H, C(CH$_3$)$_3$); ^{13}C NMR (101 MHz, DMSO-d_6, 373 K) δ 169.8 (C=O amide), 153.4 (C=O carbamate), 148.0 (C_{Ar}), 141.9 (C_{Ar} quat), 137.7 (C_{Ar} quat), 135.7 (C_{Ar}), 133.5 (C_{Ar} quat), 130.6 (C_{Ar} quat), 128.7 (2 × C_{Ar}), 127.7 (2 × C_{Ar}), 127.2 (C_{Ar} quat), 126.1 (C_{Ar}), 121.4 (C_{Ar}), 121.3 (C_{Ar}), 116.3 (C_{Ar}), 78.6 ($C(CH_3)_3$), 49.3 ($CHCO$), 46.2 (NCH_2CHCO), 43.8 (CHAr), 43.3 (NCH_2CH_2), 32.0 (NCH_2CH_2), 27.7 ($C(CH_3)_3$); HRMS (ESI^+) *m*/*z* Calculated for $C_{26}H_{29}N_3O_3{}^{35}Cl$ [M+H] 466.1897; Found 466.1893.

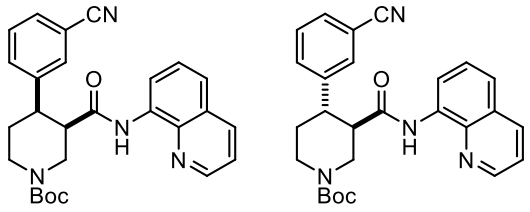
Benzyl *cis*-(±)-4-(3-(ethoxycarbonyl)phenyl)-3-(quinolin-8-ylcarbamoyl)piperidine-1-carboxylate (27b):



Prepared according to **General Procedure A** using amide **21** (195 mg) and ethyl 3-iodobenzoate (414 mg). Purification by flash column chromatography (40% EtOAc/hexane) afforded the *cis*-configured arylated product **27b** as a white solid (67.8 mg, 25%). R_f 0.27 (40% EtOAc/hexane); mp = 49–55 °C (from Et_2O/pentane); ν_{max} (film)/cm^{-1} 3345 (NH), 2924, 2855, 1682 (C=O), 1521, 1485, 1425, 1366, 1323, 1278, 1234, 1190, 1105, 1010, 826, 791, 753, 695; ^1H NMR (400 MHz, DMSO-d_6, 373 K) δ 9.72 (br s, 1 H, NH), 8.74 (dd, *J* = 4.2, 1.7 Hz, 1 H, HC_{Ar}), 8.41 (dd, *J* = 7.7, 1.4 Hz, 1 H, HC_{Ar}), 8.29 (dd, *J* = 8.3, 1.7 Hz, 1 H, HC_{Ar}), 7.98-7.92 (m, 1 H, HC_{Ar}), 7.67 (dt, *J* = 7.7, 1.4 Hz, 1 H, HC_{Ar}), 7.63–7.49 (m, 3 H, HC_{Ar}), 7.46 (t, *J* = 7.9 Hz, 1 H, HC_{Ar}), 7.33 (t, *J* = 7.7 Hz, 1 H, HC_{Ar}), 7.27–7.10 (m, 5 H, HC_{Ar}), 5.10-4.96 (m, 2 H, OCH_2Ph), 4.51 (ddd, *J* = 13.8, 2.2, 1.8 Hz, 1 H, NC*H*HCHCO), 4.36 (dddd, *J* = 13.1, 4.4, 2.7, 1.8 Hz, 1 H, NC*H*HCH$_2$), 4.23 (q, *J* = 7.1 Hz, 2 H, OC*H*$_2$CH$_3$), 3.42 (dd, *J* = 13.8, 3.7 Hz, 1 H, NCH*H*CHCO), 3.40–3.27 (m, 2 H, CHAr, CHCO), 3.10 (ddd, *J* = 12.7, 12.7, 3.2,

1 H, NCH*H*CH_2), 2.75 (dddd, *J* = 12.2, 12.2, 12.2, 4.6, 1 H, NCH_2CHH), 1.79 (dddd, *J* = 12.3, 3.2, 3.2, 3.2, 1 H, NCH_2CHH), 1.23 (t, *J* = 7.1 Hz, 3 H, OCH_2CH_3); ^{13}C NMR (101 MHz, DMSO-d_6, 373 K) δ 169.9 (C=O amide), 165.2 (C=O ester), 154.3 (C=O carbamate), 147.8 (C_{Ar}), 143.0 (C_{Ar} quat), 137.6 (C_{Ar} quat), 136.5 (C_{Ar} quat), 135.7 (C_{Ar}), 133.7 (C_{Ar} quat), 131.6 (C_{Ar}), 129.7 (C_{Ar} quat), 127.8 (C_{Ar}), 127.6 (C_{Ar}), 127.4 (2 × C_{Ar}), 127.2 (C_{Ar} quat), 126.8 (C_{Ar}), 126.6 (2 × C_{Ar}), 126.5 (C_{Ar}), 126.1 (C_{Ar}), 121.2 (C_{Ar}), 120.9 (C_{Ar}), 115.9 (C_{Ar}), 65.7 (OCH_2Ph), 59.8 (OCH_2CH_3), 46.0 (NCH_2CHCO), 45.5 (*C*HCO), 43.3 (NCH_2CH_2), 42.1 (CHAr), 25.1 (NCH_2CH_2), 13.4 (OCH_2CH_3); HRMS (ESI$^+$) *m*/*z* Calculated for $C_{32}H_{32}N_3O_5$ [M+H] 538.2342; Found 538.2357.

***tert*-Butyl *cis*-(±)-3-(quinolin-8-ylcarbamoyl)-4-(*p*-tolyl)piperidine-1-carboxylate (25e)** and ***tert*-butyl *trans*-(±)-4-(3-cyanophenyl)-3-(quinolin-8-ylcarbamoyl)piperidine-1-carboxylate (26e):**



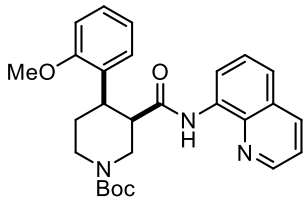
Prepared according to **General Procedure A** using amide **24** (178 mg) and 3-iodobenzonitrile (344 mg). Purification by flash column chromatography (20% acetone/pentane) afforded the minor product *tert*-butyl *trans*-(±)-4-(3-cyanophenyl)-3-(quinolin-8-ylcarbamoyl) piperidine-1-carboxylate **26e** as a white solid (29.0 mg, 13%) followed by the major product *tert*-butyl *cis*-(±)-3-(quinolin-8-ylcarbamoyl)-4-(*p*-tolyl)piperidine-1-carboxylate **25e** as a pale yellow solid (56.4 mg, 25%).

Major (**25e**): R_f 0.12 (20% acetone/pentane); mp = 77–85 °C (from Et_2O/pentane); ν_{max} (film)/cm^{-1} 3346 (NH), 2972, 2228 (CN), 1683 (C=O), 1522, 1484, 1424, 1380, 1365, 1323, 1244, 1161, 1122, 1013, 826, 792, 758, 690; ^{1}H NMR (400 MHz, DMSO-d_6, 373 K) δ 9.71 (br s, 1 H, NH), 8.83 (dd, *J* = 4.2, 1.7 Hz, 1 H, HC_{Ar}), 8.41 (dd, *J* = 7.6, 1.4 Hz, 1 H, HC_{Ar}), 8.30 (dd, *J* = 8.3, 1.7 Hz, 1 H, HC_{Ar}), 7.73 (t, *J* = 1.7 Hz, 1 H, HC_{Ar}), 7.67 (dddd, *J* = 7.9, 1.9, 1.3, 0.7 Hz, 1 H, HC_{Ar}), 7.60–7.52 (m, 2 H, HC_{Ar}), 7.51–7.44 (m, 2 H, HC_{Ar}), 7.40 (t, *J* = 7.9 Hz, 1 H, HC_{Ar}), 4.45 (ddd, *J* = 14.6, 3.7, 1.8 Hz, 1 H, NC*H*HCHCO), 4.27 (dddd, *J* = 13.2, 4.7, 2.6, 2.6 Hz, 1 H, NC*H*HCH_2), 3.40–3.32 (m, 2 H, NCH*H*CHCO, CHCO), 3.28 (ddd, *J* = 12.2, 4.2, 4.2 Hz, 1 H, CHAr), 3.01 (ddd, *J* = 13.1, 11.9, 3.3 Hz, 1 H, NCH*H*CH_2), 2.71 (dddd, *J* = 12.3, 12.3, 12.3, 4.6, 1 H, NCH_2CHH), 1.79 (dddd, *J* = 12.7, 3.2, 3.2, 3.2 Hz, 1 H, NCH_2CHH), 1.28 (s, 9 H, $C(CH_3)_3$); ^{13}C NMR (101 MHz, DMSO-d_6, 373 K) δ 169.5 (C=O amide), 153.3 (C=O carbamate), 147.7 (C_{Ar}), 144.1 (C_{Ar} quat), 137.6 (C_{Ar} quat), 135.5 (C_{Ar}), 133.7 (C_{Ar} quat), 131.6 (C_{Ar}), 130.5 (C_{Ar}), 129.1 (C_{Ar}), 128.4 (C_{Ar}), 127.1 (C_{Ar} quat), 125.9 (C_{Ar}), 121.0 (C_{Ar}), 120.8 (C_{Ar}), 117.9 (CN), 115.8 (C_{Ar}), 110.8 (C_{Ar}CN quat), 77.9 ($C(CH_3)_3$), 46.0 (NCH_2CHCO), 45.4 (*C*HCO),

42.8 (N*C*H$_2$CH$_2$), 41.6 (CHAr), 27.3 (C(*C*H$_3$)$_3$), 24.7 (NCH$_2$*C*H$_2$); HRMS (ESI$^+$) *m*/*z* Calculated for $C_{27}H_{29}N_4O_3$ [M+H] 457.2240; Found 457.2248.

Minor (**26e**): R_f 0.17 (20% acetone/pentane); mp = 182–185 °C (from Et$_2$O/pentane); ν_{max} (film)/cm^{-1} 3327 (NH), 2928, 2228 (CN), 1683 (C=O), 1531, 1487, 1423, 1363, 1238, 1161, 1127, 822, 785, 762, 694; ^{1}H NMR (500 MHz, DMSO-d_6, 373 K) δ 9.77 (br s, 1 H, NH), 8.86 (dd, *J* = 4.2, 1.7 Hz, 1 H, HC$_{Ar}$), 8.36 (dd, *J* = 7.7, 1.3 Hz, 1 H, HC$_{Ar}$), 8.31 (dd, *J* = 8.3, 1.7 Hz, 1 H, HC$_{Ar}$), 7.85 (t, *J* = 1.8 Hz, 1 H, HC$_{Ar}$), 7.66 (dt, *J* = 7.9, 1.5 Hz, 1 H, HC$_{Ar}$), 7.61–7.55 (m, 2 H, HC$_{Ar}$), 7.49–7.44 (m, 2 H, HC$_{Ar}$), 7.37 (t, *J* = 7.8 Hz, 1 H, HC$_{Ar}$), 4.37 (ddd, *J* = 13.1, 4.2, 1.7 Hz, 1 H, NC*H*HCHCO), 4.15 (dddd, *J* = 11.7, 4.5, 2.5, 1.7 Hz, 1 H, NC*H*HCH$_2$), 3.27 (td, *J* = 11.0, 4.1 Hz, 1 H, CHCO), 3.18 (td, *J* = 11.6, 3.8 Hz, 1 H, CHAr), 3.05 (dd, *J* = 13.1, 10.9 Hz, 1 H, NCH*H*CHCO), 3.01–2.91 (m, 1 H, NCH*H*CH$_2$), 1.83 (dddd, *J* = 13.3, 3.1, 3.1, 3.1 Hz, 1 H, NCH$_2$C*H*H), 1.70 (dddd, *J* = 12.6, 12.6, 12.6, 4.5, 1 H, NCH$_2$CH*H*), 1.49 (s, 9 H, C(CH$_3$)$_3$); ^{13}C NMR (126 MHz, DMSO-d_6, 373 K) δ 169.7 (C=O amide), 153.3 (C=O carbamate), 148.1 (C$_{Ar}$), 144.6 (C$_{Ar}$ quat), 137.8 (C$_{Ar}$ quat), 135.7 (C$_{Ar}$), 133.4 (C$_{Ar}$ quat), 132.0 (C$_{Ar}$), 130.4 (C$_{Ar}$), 129.6 (C$_{Ar}$), 128.8 (C$_{Ar}$), 127.2 (C$_{Ar}$ quat), 126.1 (C$_{Ar}$), 121.5 (C$_{Ar}$), 121.3 (C$_{Ar}$), 118.1 (CN), 116.5 (C$_{Ar}$), 111.2 (C$_{Ar}$CN quat), 78.6 (*C*(CH$_3$)$_3$), 48.8 (*C*HCO), 46.1 (N*C*H$_2$CHCO), 44.2 (CHAr), 43.2 (N*C*H$_2$CH$_2$), 31.8 (NCH$_2$*C*H$_2$), 27.7 (C(*C*H$_3$)$_3$); HRMS (ESI$^+$) *m*/*z* Calculated for $C_{27}H_{29}N_4O_3$ [M+H] 457.2240; Found 457.2242.

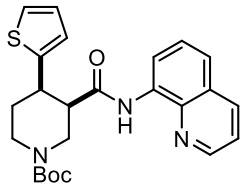
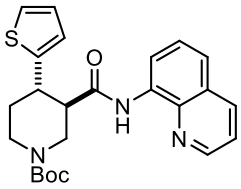
tert-Butyl _cis_-(±)-4-(2-methoxyphenyl)-3-(quinolin-8-ylcarbamoyl)piperidine-1-carboxylate (25f)



Prepared according to **General Procedure A** using amide **24** (178 mg) and 2-iodoanisole (351 mg). The crude material was purified by flash column chromatography (10% acetone/pentane), the product containing fractions were combined and the solvent was removed under reduced pressure. CH_2Cl_2 (5 mL) and pentane (5 mL) were added and the solvent was removed under reduced pressure to afford the *cis*-configured arylated product **25f** as a white solid (102 mg, 44%). R_f 0.18 (10% acetone/pentane); mp = 80–86 °C (from CH_2Cl_2/pentane); ν_{max} (film)/cm^{-1} 3350 (NH), 2928, 1685 (C=O), 1521, 1487, 1460, 1423, 1364, 1323, 1236, 1160, 1120, 1028, 1005, 826, 791, 751; ^{1}H NMR (400 MHz, DMSO-d_6, 373 K) δ 9.64 (br s, 1 H, NH), 8.81 (dd, *J* = 4.2, 1.7 Hz, 1 H, HC$_{Ar}$), 8.44 (dd, *J* = 7.6, 1.4 Hz, 1 H, HC$_{Ar}$), 8.29 (dd, *J* = 8.3, 16 Hz, 1 H, HC$_{Ar}$), 7.57–7.52 (m, 2 H, HC$_{Ar}$), 7.46 (t, *J* = 7.9 Hz, 1 H, HC$_{Ar}$), 7.19 (dd, *J* = 7.6, 1.7 Hz, 1 H, HC$_{Ar}$), 7.04 (ddd, *J* = 8.1, 7.3, 1.7 Hz, 1 H, HC$_{Ar}$), 6.92 (dd, *J* = 8.2, 1.2 Hz, 1 H, HC$_{Ar}$), 6.72 (td, *J* = 7.5, 1.2 Hz, 1 H, HC$_{Ar}$), 4.44–4.37 (m, 1 H, NC*H*HCHCO), 4.26 (dddd, *J* = 13.0, 4.2, 2.4, 1.8 Hz, 1 H, NC*H*HCH$_2$), 3.88 (s, 3 H, OCH$_3$), 3.47 (ddd, *J* = 12.5, 4.0, 4.0 Hz, 1 H, CHAr), 3.34–3.25 (m, 2 H, NCH*H*CHCO, CHCO), 3.04–

2.95 (m, 1 H, NCH*H*CH_2), 2.74 (dddd, *J* = 12.6, 12.6, 12.6, 4.6, 1 H, NCH_2CHH), 1.59 (dddd, *J* = 12.9, 3.2, 3.2, 3.2 Hz, 1 H, NCH_2CHH), 1.29 (s, 9 H, $C(CH_3)_3$); ^{13}C NMR (101 MHz, DMSO-d_6, 373 K) δ 170.1 (C=O amide), 156.4 (OC_{Ar} quat), 153.5 (C=O carbamate), 147.9 (C_{Ar}), 137.5 (C_{Ar} quat), 135.7 (C_{Ar}), 134.0 (C_{Ar} quat), 130.1 (C_{Ar} quat), 127.13 (C_{Ar} quat), 127.08 (C_{Ar}), 126.7 (C_{Ar}), 126.2 (C_{Ar}), 121.2 (C_{Ar}), 120.6 (C_{Ar}), 119.6 (C_{Ar}), 115.3 (C_{Ar}), 110.5 (C_{Ar}), 77.9 ($C(CH_3)_3$), 55.1 (OCH_3), 46.0 (NCH_2CHCO), 44.0 (*C*HCO), 43.3 (NCH_2CH_2), 36.1 (CHAr), 27.5 ($C(CH_3)_3$), 24.8 (NCH_2CH_2); HRMS (ESI^+) *m*/*z* Calculated for $C_{27}H_{32}N_3O_4$ [M+H] 462.2393; Found 462.2399.

***tert*-Butyl *cis*-(±)-3-(quinolin-8-ylcarbamoyl)-4-(thiophen-2-yl)piperidine-1-carboxylate (25g)** and ***tert*-butyl *trans*-(±)-3-(quinolin-8-ylcarbamoyl)-4-(thiophen-2-yl)piperidine-1-carboxylate (26g):**

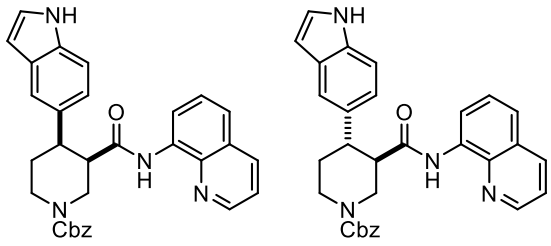



Prepared according to **General Procedure A** using amide **24** (178 mg) and 2-iodothiophene (315 mg). Purification by flash column chromatography (3% MeCN/CH_2Cl_2) afforded the minor product *tert*-butyl *trans*-(±)-3-(quinolin-8-ylcarbamoyl)-4-(thiophen-2-yl) piperidine-1-carboxylate **26g** as a pale yellow solid (52.8 mg, 24%) followed by the major product *tert*-butyl *cis*-(±)-3-(quinolin-8-ylcarbamoyl)-4-(thiophen-2-yl)piperidine-1-carboxylate **25g** as a pale pink solid (89.4 mg, 41%).

Major (**25g**): R_f 0.44 (3% MeCN/CH_2Cl_2); mp = 107–112 °C (from Et_2O/pentane); ν_{max} (film)/cm^{-1} 3344 (NH), 2976, 1685 (C=O), 1522, 1484, 1423, 1365, 1324, 1245, 1160, 1120, 1000, 825, 791, 760, 695; ^1H NMR (400 MHz, DMSO-d_6, 373 K) δ 9.88 (br s, 1 H, NH), 8.82 (dd, *J* = 4.2, 1.7 Hz, 1 H, HC_{Ar}), 8.44 (dd, *J* = 7.6, 1.4 Hz, 1 H, HC_{Ar}), 8.28 (dd, *J* = 8.3, 1.7 Hz, 1 H, HC_{Ar}), 7.57–7.50 (m, 2 H, HC_{Ar}), 7.45 (t, *J* = 7.9 Hz, 1 H, HC_{Ar}), 7.15 (dd, *J* = 5.1, 1.2 Hz, 1 H, SCH), 6.92 (m, 1 H, SCHCHC*H*), 6.81 (dd, *J* = 5.1, 3.5 Hz, 1 H, SCHC*H*), 4.21 (ddd, *J* = 13.8, 3.8, 1.6 Hz, 1 H, NC*H*HCHCO), 4.03 (dddd, *J* = 13.7, 10.9, 10.9, 4.5 Hz, 1 H, NC*H*HCH_2), 3.49 (ddd, *J* = 10.2, 4.5, 4.5 Hz, 1 H, CHAr), 3.38 (dd, *J* = 13.3, 4.3 Hz, 1 H, NCH*H*CHCO), 3.28 (ddd, *J* = 4.1, 4.1, 4.1 Hz, 1 H, CHCO), 3.06 (ddd, *J* = 13.7, 10.9, 4.5 Hz, 1 H, NCH*H*CH_2), 2.57 (dddd, *J* = 13.7, 10.9, 10.9, 4.5 Hz, 1 H, NCH_2CHH), 1.83 (dddd, *J* = 12.6, 4.0, 4.0, 4.0 Hz, 1 H, NCH_2CHH), 1.25 (s, 9 H, $C(CH_3)_3$); ^{13}C NMR (101 MHz, DMSO-d_6, 373 K) δ 169.8 (C=O amide), 153.4 (C=O carbamate), 148.0 (C_{Ar}), 145.9 (C_{Ar} quat), 137.7 (C_{Ar} quat), 135.8 (C_{Ar}), 134.1 (C_{Ar} quat), 127.2 (C_{Ar} quat), 126.2 (C_{Ar}), 125.8 ($SCHCH_{Ar}$), 123.5 ($SCHCHCH_{Ar}$), 122.9 (SCH_{Ar}), 121.3 (C_{Ar}), 120.8 (C_{Ar}), 115.9 (C_{Ar}), 78.0 ($C(CH_3)_3$), 46.0 (*C*HCO), 45.4 (NCH_2CHCO), 42.4 (NCH_2CH_2), 38.0 (CHAr), 27.8 (NCH_2CH_2), 27.4 ($C(CH_3)_3$); HRMS (ESI^+) *m*/*z* Calculated for $C_{24}H_{28}N_3O_3S$ [M+H] 438.1851; Found 438.1854.

Minor (**26g**): R_f 0.56 (3% MeCN/CH_2Cl_2); mp = 56–60 °C (from Et_2O/pentane); ν_{max} (film)/cm^{-1} 3335 (NH), 2974, 1682 (C=O), 1525, 1486, 1424, 1366, 1324, 1243, 1158, 950, 826, 791, 759, 695; ^{1}H NMR (400 MHz, DMSO-d_6, 373 K) δ 9.88 (br s, 1 H, NH), 8.87 (dd, J = 4.2, 1.7 Hz, 1 H, HC_{Ar}), 8.49 (dd, J = 7.7, 1.4 Hz, 1 H, HC_{Ar}), 8.33 (dd, J = 8.3, 1.7 Hz, 1 H, HC_{Ar}), 7.62 (dd, J = 8.3, 1.3 Hz, 1 H, HC_{Ar}), 7.58 (dd, J = 8.3, 4.2 Hz, 1 H, HC_{Ar}), 7.51 (t, J = 8.0 Hz, 1 H, HC_{Ar}), 7.18 (dd, J = 5.1, 1.2 Hz, 1 H, SCH), 6.99 (ddd, J = 3.5, 1.2, 0.7 Hz, 1 H, SCHCHC*H*), 6.82 (dd, J = 5.1, 3.5 Hz, 1 H, SCHC*H*), 4.36–4.27 (m, 1 H, NC*H*HCHCO), 4.10 (dddd, J = 13.4, 4.5, 2.5, 2.5 Hz, 1 H, NC*H*HCH_2), 3.52–3.40 (m, 1 H, CHAr), 3.11–2.92 (m, 3 H, CHCO, NCH*H*CH_2, NCH*H*CHCO), 2.01 (dddd, J = 13.3, 3.9, 2.8, 2.8 Hz, 1 H, NCH_2C*H*H), 1.76–1.64 (m, 1 H, NCH_2CH*H*), 1.47 (s, 9 H, $C(CH_3)_3$); ^{13}C NMR (101 MHz, DMSO-d_6, 373 K) δ 169.8 (C=O amide), 153.4 (C=O carbamate), 148.1 (C_{Ar}), 146.1 (C_{Ar} quat), 137.8 (C_{Ar} quat), 135.8 (C_{Ar}), 133.6 (C_{Ar} quat), 127.2 (C_{Ar} quat), 126.1 (C_{Ar}), 126.0 (SCH*C*H_{Ar}), 123.3 (SCHCH*C*H_{Ar}), 122.8 (S*C*H_{Ar}), 121.4 (C_{Ar}), 121.3 (C_{Ar}), 116.3 (C_{Ar}), 78.6 (*C*$(CH_3)_3$), 51.1 (*C*HCO), 46.2 (N*C*H_2CHCO), 43.2 (N*C*H_2CH_2), 38.9 (CHAr), 33.0 (NCH_2*C*H_2), 27.6 (C(*C*$H_3)_3$); HRMS (ESI^+) *m*/*z* Calculated for $C_{24}H_{28}N_3O_3S$ [M+H] 438.1851; Found 438.1834.

Benzyl *cis*-(±)-4-(1*H*-indol-5-yl)-3-(quinolin-8-ylcarbamoyl)piperidine-1-carboxylate (27c) and **benzyl *trans*-(±)-4-(1*H*-indol-5-yl)-3-(quinolin-8-ylcarbamoyl)piperidine-1-carboxylate (28c):**



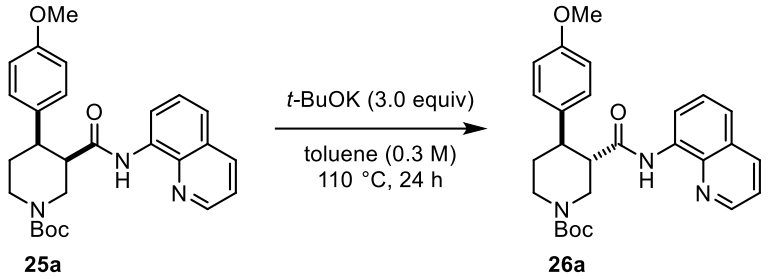
Prepared according to **General Procedure A** using amide **21** (195 mg) and 5-iodo-1*H*-indole (365 mg). The crude material was purified by flash column chromatography (40% EtOAc/hexane), the product containing fractions were combined and the solvent was removed under reduced pressure. CH_2Cl_2 (5 mL) and pentane (5 mL) were added and the solvent was removed under reduced pressure to afford the minor product benzyl *trans*-(±)-4-(1*H*-indol-5-yl)-3-(quinolin-8-ylcarbamoyl)piperidine-1-carboxylate **28c** as a white solid (49.2 mg, 19%) followed by the major product benzyl *cis*-(±)-4-(1*H*-indol-5-yl)-3-(quinolin-8-ylcarbamoyl)piperidine-1-carboxylate **27c** as a white solid (118 mg, 47%).

Major (**27c**): R_f 0.21 (40% EtOAc/hexane); mp = 94–98 °C (from CH_2Cl_2/pentane); ν_{max} (film)/cm^{-1} 3305 (NH), 1677 (C=O), 1523, 1485, 1420, 1357, 1324, 1114, 824, 790, 762, 729, 696; ^{1}H NMR (400 MHz, DMSO-d_6, 373 K) δ 10.54 (br s, 1 H, HN_{Indole}), 9.64 (s, 1 H, CONH), 8.62 (dd, J = 4.2, 1.7 Hz, 1 H, HC_{Ar}), 8.44 (dd, J = 7.6, 1.4 Hz, 1 H, HC_{Ar}), 8.25 (dd, J = 8.3, 1.7 Hz, 1 H, HC_{Ar}), 7.53 (dd, J = 8.3, 1.4 Hz, 1 H, HC_{Ar}), 7.51–7.42 (m, 3 H, HC_{Ar}), 7.28–7.19 (m, 3 H, HC_{Ar}), 7.19–7.12 (m, 4 H, HC_{Ar}), 7.09 (dd, J = 8.4, 1.8 Hz, 1 H, HC_{Indole}), 6.27 (ddd,

J = 3.0, 1.9, 0.9 Hz, 1 H, NHCHC*H*$_{Indole}$), 5.09–4.99 (m, 2 H, OCH_2Ph), 4.50 (ddd, *J* = 13.7, 2.3, 1.7 Hz, 1 H, NC*H*HCHCO), 4.36 (dddd, *J* = 13.1, 4.6, 2.8, 1.7 Hz, 1 H, NC*H*HCH_2), 3.43 (dd, *J* = 13.6, 3.5 Hz, 1 H, NCH*H*CHCO), 3.24–3.26 (m, 2 H, CHCO, CHAr), 3.12 (ddd, *J* = 13.1, 12.0, 3.3, 1 H, NCH*H*CH_2), 2.83–2.70 (m, 1 H, NCH_2C*H*H), 1.87–1.79 (m, 1 H, NCH_2CH*H*); ^{13}C NMR (101 MHz, DMSO-d_6, 373K) δ 170.3 (C=O amide), 154.3 (C=O carbamate), 147.7 (C_{Ar}), 137.5 (C_{Ar} quat), 136.6 (C_{Ar} quat), 135.6 (C_{Ar}), 134.4 (C_{Indole} quat), 133.9 (C_{Ar} quat), 132.6 (C_{Indole} quat), 127.5 (2 × C_{Ar}), 127.3 (C_{Ar} quat), 127.1 (C_{Indole} quat), 126.8 (C_{Ar}), 126.6 (2 × C_{Ar}), 126.1 (C_{Ar}), 124.4 (NH*C*H$_{Indole}$), 121.1 (C_{Ar}), 120.6 (C_{Ar}), 120.3 (CH$_{Indole}$), 117.9 (CH$_{Indole}$), 115.6 (C_{Ar}), 110.4 (CH$_{Indole}$), 100.4 (NHCH*C*H$_{Indole}$), 65.6 (O*C*H_2Ph), 46.6 (*C*HCO), 46.1 (N*C*H_2CHCO), 43.6 (N*C*H_2CH_2), 42.6 (CHAr), 25.9 (NCH_2*C*H_2); HRMS (ESI$^+$) *m*/*z* Calculated for $C_{31}H_{29}N_4O_3$ [M+H] 505.2240; Found 505.2240.

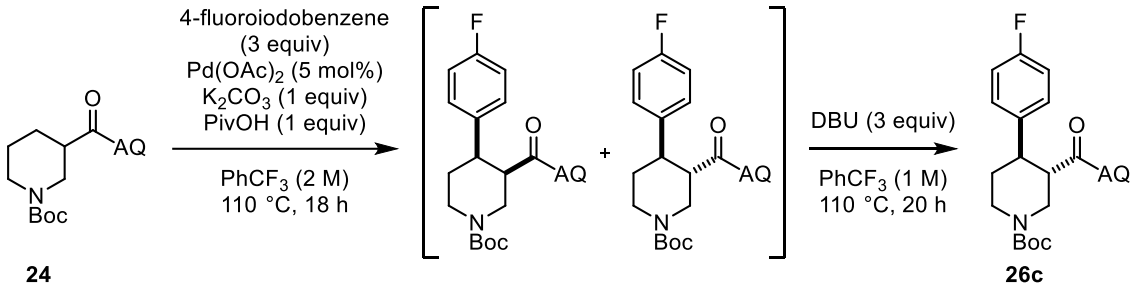
Minor (**28c**): R_f 0.26 (40% EtOAc/hexane); mp = 92–98 °C (from CH_2Cl_2/pentane); ν_{max} (film)/cm^{-1} 3323 (NH), 1676 (C=O), 1524, 1485, 1424, 1324, 1282, 1229, 1117, 825, 791, 762, 728, 697; ^{1}H NMR (400 MHz, DMSO-d_6, 373 K) δ 10.53 (br s, 1 H, HN$_{Indole}$), 9.66 (s, 1 H, CONH), 8.69 (dd, *J* = 4.2, 1.7 Hz, 1 H, HC$_{Ar}$), 8.39 (dd, *J* = 7.7, 1.4 Hz, 1 H, HC$_{Ar}$), 8.25 (dd, *J* = 8.3, 1.7 Hz, 1 H, HC$_{Ar}$), 7.56–7.47 (m, 3 H, HC$_{Ar}$), 7.45–7.36 (m, 5 H, HC$_{Ar}$), 7.36–7.30 (m, 1 H, HC$_{Ar}$), 7.21 (d, *J* = 8.4 Hz, 1 H, HC$_{Indole}$), 7.14 (t, *J* = 2.7 Hz, 1 H, NHC*H*$_{Indole}$), 7.06 (dd, *J* = 8.4, 1.7 Hz, 1 H, HC$_{Indole}$), 6.31–6.27 (m, 1 H, NHCHC*H*$_{Indole}$), 5.19 (s, 2 H, OCH_2Ph), 4.48–4.39 (m, 1 H, NC*H*HCHCO), 4.21 (dddd, *J* = 13.2, 4.3, 2.1, 2.1 Hz, 1 H, NC*H*HCH_2), 3.24–3.13 (m, 3 H, NCH*H*CHCO, CHCO, CHAr), 3.07 (ddd, *J* = 12.8, 12.8, 3.2 Hz, 1 H, NC*H*HCH_2), 1.91–1.84 (m, 1 H, NCH_2C*H*H), 1.84–1.72 (m, 1 H, NCH_2CH*H*); ^{13}C NMR (101 MHz, DMSO-d_6, 373 K) δ 170.1 (C=O amide), 154.1 (C=O carbamate), 147.8 (C_{Ar}), 137.5 (C_{Ar} quat), 136.6 (C_{Ar} quat), 135.6 (C_{Ar}), 134.5 (C_{Indole} quat), 133.5 (C_{Ar} quat), 133.1 (C_{Indole} quat), 127.8 (2 × C_{Ar}), 127.5 (C_{Ar} quat), 127.2 (C_{Ar}), 127.1 (C_{Indole} quat), 127.0 (2 × C_{Ar}), 126.0 (C_{Ar}), 124.5 (NH*C*H$_{Indole}$), 121.2 (C_{Ar}), 121.1 (C_{Ar}), 120.2 (CH$_{Indole}$), 117.8 (CH$_{Indole}$), 115.9 (C_{Ar}), 110.7 (CH$_{Indole}$), 100.4 (NHCH*C*H$_{Indole}$), 65.9 (O*C*H_2Ph), 50.1 (*C*HCO), 46.5 (N*C*H_2CHCO), 44.5 (CHAr), 43.8 (N*C*H_2CH_2), 33.1 (NCH_2*C*H_2); HRMS (ESI$^+$) *m*/*z* Calculated for $C_{31}H_{29}N_4O_3$ [M+H] 505.2240; Found 505.2238.

*8.2.1.12 Epimerisation of cis-3,4-Disubstituted Piperidine **25a***



A flame-dried reaction tube was charged with *cis*-3,4-disubstituted piperidine **25a** (92.3 mg, 0.20 mmol) and potassium *tert*-butoxide (67.3 mg, 0.60 mmol). The reaction vessel was sealed and purged with argon, then dry toluene (667 μL, 0.3 M) was added by syringe. The reaction tube was then placed in a preheated oil bath and stirred at 110 ºC for 18 h. The reaction mixture was then allowed to cool to rt and EtOAc (2 mL) and sat. aq. NH_4Cl (2 mL) were added. The phases were separated, and the aqueous layer was extracted with EtOAc (3 × 5 mL). The combined organic extracts were dried over Na_2SO_4 and filtered. The solvent was removed under reduced pressure. Et_2O (3 mL) and pentane (3 mL) were added and the solvent was removed under reduced pressure to afford pure *trans*-3,4-disubstituted piperidine **26a** as a white solid (89.9 mg, 97%). Characterisation data identical to that reported for *trans*-piperidine **26a** (page 236).

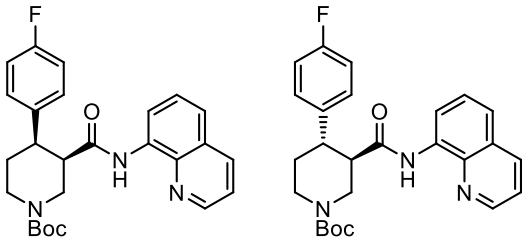
*8.2.1.13 One-Pot C(4)–H Arylation/Epimerisation of Piperidine **24***



A large microwave vial (10–20 mL recommended volume) was charged with K_2CO_3 (550 mg, 4.00 mmol), flame-dried, and allowed to cool under argon. *tert*-Butyl 3-(quinolin-8-ylcarbamoyl)piperidine-1-carboxylate **24** (1.42 g, 4.00 mmol), 4-fluoroiodobenzene (2.66 g, 12.0 mmol), $Pd(OAc)_2$ (45.0 mg, 0.20 mmol) and PivOH (410 mg, 4.00 mmol) were added sequentially. The reaction vessel purged with argon, then $PhCF_3$ (2.0 mL, 2.0 M) was added by syringe. The reaction tube was placed in a preheated oil bath and stirred at 110 ºC for 18 h. The reaction mixture was then allowed to cool to rt and $PhCF_3$ (2.0 mL, 1.0 M) and DBU (1.8 mL, 12.0 mmol, 3 equiv) were added by syringe. The reaction vessel was then stirred at 110 °C for additional 18 h. The reaction mixture was allowed to cool to rt and EtOAc (20 mL) was added. The resulting mixture was filtered through a pad of Celite, eluting with further EtOAc (2 × 50 mL). The solvent was removed under reduced pressure, and the crude material was purified by flash column chromatography (55:40:0.5 to 50:40:10, hexane:Et_2O:CH_2Cl_2). The product containing fractions were combined and the solvent was removed under reduced pressure. Et_2O (10 mL) and pentane (10 mL) were added and the solvent was removed under reduced pressure to afford the *trans*-arylated product **26c** as a pale yellow solid (954 mg, 53%). R_f 0.27 (50:40:10, hexane:Et_2O:CH_2Cl_2). Characterisation data identical to that reported for *trans*-piperidine **26c** (page 240).

8.2.1.14 C–H Arylation on Enantioenriched Piperidine Substrate ((+)25c, (–)26c, (+)26c)

***tert*-Butyl (+)-(*3R,4R*)-4-(4-fluorophenyl)-3-(quinolin-8-ylcarbamoyl)piperidine-1-carboxylate ((+)-25c)** and ***tert*-butyl (–)-(*3R,4S*)-4-(4-fluorophenyl)-3-(quinolin-8-ylcarbamoyl)piperidine-1-carboxylate ((–)-26c):**



A large microwave vial (10–20 mL recommended volume) was charged with K_2CO_3 (553 mg, 4.00 mmol), flame-dried, and allowed to cool under argon. *tert*-Butyl (*R*)-3-(quinolin-8-ylcarbamoyl)piperidine-1-carboxylate (*R*)-**24** (1.42 g, 4.00 mmol), 4-fluoroiodobenzene (2.66 g, 12.00 mmol), $Pd(OAc)_2$ (45.1 mg, 0.20 mmol) and PivOH (409 mg, 4.0 mmol) were added sequentially. The reaction vessel was sealed and purged with argon, then $PhCF_3$ (2.0 mL, 2.0 M) was added by syringe. The reaction tube was then placed in a preheated oil bath and stirred at 110 ºC for 18 h. The reaction mixture was then allowed to cool to rt and EtOAc (20 mL) was added. The resulting mixture was filtered through a pad of Celite, eluting with further EtOAc (2 × 50 mL). The solvent was removed under reduced pressure. The reaction mixture was purified by two consecutive flash column chromatographies: one (5% to 10% acetone/pentane) to isolate the major product *tert*-butyl (+)-(*3R,4R*)-4-(4-fluorophenyl)-3-(quinolin-8-ylcarbamoyl)piperidine-1-carboxylate **(+)-25c** followed by a second (50:40:10 hexane/Et_2O/CH_2Cl_2) to isolate the minor product *tert*-butyl (–)-(*3R,4S*)-4-(4-fluorophenyl)-3-(quinolin-8-ylcarbamoyl)piperidine-1-carboxylate **(–)-26c**. The product containing fractions were combined and the solvent was removed under reduced pressure. Et_2O (20 mL) and pentane (20 mL) were added and the solvent was removed under reduced pressure to afford the major product **(+)-25c** as a white solid (775 mg, 43%, 99.3% *ee*) and the minor product **(–)-26c** (216 mg, 12%, 99.2% *ee*).

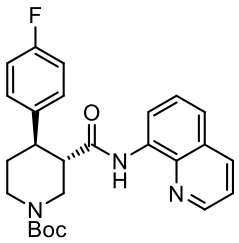
Major (**(+)-25c**): $[\alpha]_D^{21}$ +33.0 (*c* 1.21, $CHCl_3$). Characterisation data identical to that reported for racemic piperidine **25c** (page 240).

HPLC Conditions: Chiralpak IA 3-column, 85:15 *n*-hexane:*i*-PrOH, flow rate: 1 mL·min^{-1}, 35 ºC, UV detection wavelength: 210.4 nm. Retention times: 11.1 min (3*S,*4*S* enantiomer), 17.6 min (3*R,*4*R* enantiomer).

Minor (**(–)-26c**): $[\alpha]_D^{21}$ –22.2 (*c* 1.35, $CHCl_3$). Characterisation data identical to that reported for racemic piperidine **26c** (page 240).

HPLC Conditions: Chiralpak IA 3-column, 85:15 *n*-hexane:*i*-PrOH, flow rate: 1 mL·min^{-1}, 35 ºC, UV detection wavelength: 210.4 nm. Retention times: 8.4 min (3*R,*4*S* enantiomer), 10.2 min (3*S,*4*R* enantiomer).

***tert*-Butyl (+)-(*3S,4R*)-4-(4-fluorophenyl)-3-(quinolin-8-ylcarbamoyl)piperidine-1-carboxylate ((+)-26c)**

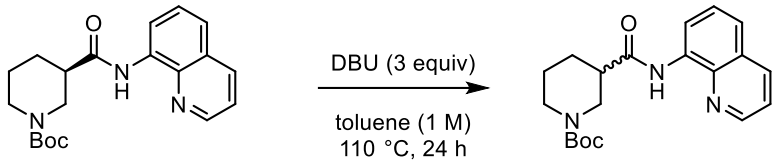


A flame-dried reaction tube was charged with *cis*-3,4-disubstituted piperidine **(+)-25c** (266 mg, 0.59 mmol) and DBU (268 μL, 1.77 mmol). The reaction vessel was sealed and purged with argon, then dry toluene (590 μL, 1.0 M) was added by syringe. The reaction tube was then placed in a preheated oil bath and stirred at 110 ºC for 18 h. The reaction mixture was then allowed to cool to rt and EtOAc (5 mL) and sat. aq. NH_4Cl (5 mL) were added. The phases were separated, and the aqueous layer was extracted with EtOAc (3 × 10 mL). The combined organic extracts were dried over Na_2SO_4 and filtered. The solvent was removed under reduced pressure. The reaction mixture was purified by flash column chromatography (10% acetone/pentane). The product containing fractions were combined and the solvent was removed under reduced pressure. Et_2O (10 mL) and pentane (10 mL) were added and the solvent was removed under reduced pressure to afford amide *tert*-butyl (+)-(*3S,4R*)-4-(4-fluorophenyl)-3-(quinolin-8-ylcarbamoyl) piperidine-1-carboxylate **(+)-26c** as a white solid (252 mg, 95%, 99.4% *ee*). $[\alpha]_D^{21}$ +29.4 (*c* 2.0, $CHCl_3$).

Characterisation data identical to that reported for racemic piperidine **26c** (page 240).

HPLC Conditions: Chiralpak IA 3-column, 85:15 *n*-hexane:*i*-PrOH, flow rate: 1 mL·min^{-1}, 35 ºC, UV detection wavelength: 210.4 nm. Retention times: 8.4 min (3*R,*4*S* enantiomer), 10.2 min (3*S,*4*R* enantiomer).

*8.2.1.15 Procedure for the Racemisation of Piperidine (R)-**24** using DBU:*

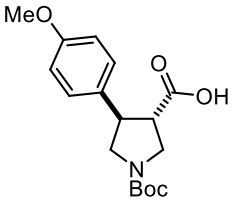


(*R*)-**24** (99% *ee*) **24** (3.3% *ee*)

A flame-dried reaction tube was charged with enantioenriched amide (*R*)-**24** (35.5 mg, 0.10 mmol) and DBU (45 μL, 0.30 mmol). The reaction vessel was sealed and purged with argon, then toluene (100 μL, 1.0 M) was added by syringe. The reaction tube was then placed in a preheated oil bath and stirred at 110 ºC for 24 h. The reaction mixture was then allowed to cool to rt and EtOAc (3 mL) and sat. aq. NH_4Cl (3 mL) were added. The phases were separated, and the aqueous layer was extracted with EtOAc (3 × 5 mL). The combined organic extracts were dried with Na_2SO_4 and filtered. The solvent was removed under reduced pressure. Et_2O (3 mL) and pentane (3 mL) were added and the solvent was removed under reduced pressure to afford amide **24** as a pale brown solid (35.9 mg, quant., 3.3% *ee*). Characterisation data was identical to racemic piperidine **24** (page 205).

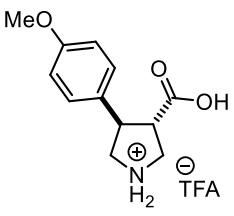
*8.2.1.15 Removal of AQ Directing Group (**30–45**)*

trans-(±)-1-(_tert_-Butoxycarbonyl)-4-(4-methoxyphenyl)pyrrolidine-3-carboxylic acid (30)



A reaction tube was charged with amide **3a** (89.5 mg, 0.20 mmol), followed by NaOH (80.0 mg, 2.00 mmol). The reaction vessel was sealed and EtOH (1.0 mL, 0.2 M) was added by syringe. The reaction tube was then placed in a preheated oil bath and stirred at 100 ºC for 30 min. The reaction mixture was then allowed to cool down to rt and diluted with EtOAc (1 mL) and 1 N NaOH (1 mL). The aqueous alkaline layer was collected, and the organic layer extracted with 1 N NaOH (3 × 5 mL). All the aqueous alkaline layers were combined, washed with EtOAc (10 mL), and acidified to pH ~ 1 with HCl, 37%. The acidic layer was extracted with EtOAc (5 × 20 mL). The combined organic extracts were dried over Na_2SO_4 and filtered. Solvent was removed under reduced pressure. Et_2O (5 mL) and pentane (5 mL) were added and the solvent was removed under reduced pressure to afford the pure *trans*-acid **30** as a pale orange solid (58.1 mg, 86%, single diastereoisomer). R_f 0.19 (80:20:0.5 acetone/pentane/TFA); mp = 144–148 °C (from Et_2O/pentane); ν_{max} (film)/cm^{-1} 3101 (OH br), 2979, 1727 (C=O), 1662 (C=O), 1517, 1435, 1408, 1369, 1253, 1165, 1136, 1030, 883, 817, 765, 666; ^{1}H NMR (400 MHz, $CDCl_3$, 298 K, observed as mixture of rotamers) δ 7.17 (d, J = 8.6 Hz, 2 H, HC_{Ar}), 6.86 (d, J = 8.5 Hz, 2 H, HC_{Ar}), 3.94–3.74 (m, 5 H, NC*H*HCHAr, NC*H*HCHCO, OCH_3), 3.66–3.53 (m, 2 H, NCH*H*CHCO, CHAr), 3.44–3.28 (m, 1 H, NCH*H*CHAr), 3.22–3.09 (m, 1 H, CHCO), 1.48 and 1.46 (2 × s, 9 H, $C(CH_3)_3$); ^{13}C NMR (101 MHz, $CDCl_3$, 298 K, observed as mixture of rotamers) δ 177.2 (COOH), 158.8 (OC_{Ar} quat), 154.1 (C=O carbamate), 130.8 and 130.7 (C_{Ar} quat), 128.3 (2 × C_{Ar}), 114.2 (2 × C_{Ar}), 80.0 ($C(CH_3)_3$), 55.2 (OCH_3), 52.9 and 52.2 (NCH_2CHAr), 50.4 and 49.4 (*C*HCO), 48.7 and 48.5 (NCH_2CHCO), 47.0 and 46.2 (CHAr), 28.4 ($C(CH_3)_3$); HRMS (ESI$^+$) *m*/*z* Calculated for $C_{17}H_{24}NO_5$ [M+H] 322.1654; Found 322.1642.

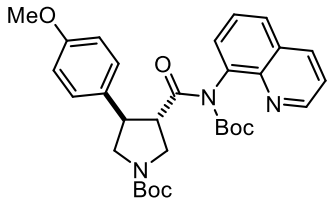
trans-(±)-4-(4-Methoxyphenyl)pyrrolidine-3-carboxylic acid trifluoroacetic acid salt (31)



Freshly distilled trifluoroacetic acid (74 μL, 1.00 mmol) was added to a solution of Boc-protected *trans*-acid **30** (33.5 mg, 0.10 mmol) in CH_2Cl_2 (1.0 mL, 0.1 M) at 0 °C. The reaction was allowed to warm up and stirred at 25 °C for 22 h. The solvent was removed under reduced pressure, affording *trans*-aminoacid **31** as the correspondent trifluoroacetate salt (brown paste, 32.9 mg, 98%, containing <7% of inseparable 2,3-disubstituted isomer). ν_{max} (film)/cm^{-1} 2920 (OH br), 1664 (C=O), 1516, 1427, 1250, 1177, 1130, 1031, 829, 796, 721; ^{1}H NMR (400 MHz, CD_3OD, 298 K) δ 7.29 (d, J = 8.7 Hz, 2 H, HC_{Ar}), 6.92 (d, J = 8.7 Hz, 2 H, HC_{Ar}), 3.78 (s, 3 H, OCH_3), 3.77–3.59 (m, 4 H, NC*H*HCHAr, NC*H*$_2$CHCO, CHAr), 3.37–3.28

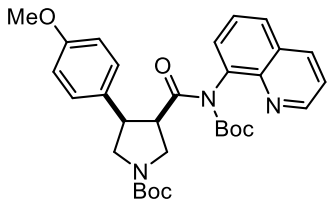
(m, 2 H, NCH*H*CHAr, CHCO); ^{13}C NMR (101 MHz, CD_3OD, 298 K) δ 174.1 (COOH), 160.9 (OC_{Ar} quat), 130.5 (C_{Ar} quat), 129.6 (2 × C_{Ar}), 115.4 (2 × C_{Ar}), 55.7 (OCH_3), 52.8 (N*C*H_2CHAr), 50.8 (*C*HCO), 49.1 (N*C*H_2CHCO), 48.5 (CHAr); ^{19}F NMR (377 MHz, CD_3OD, 298 K) δ –76.9 (s, CF_3); HRMS (ESI$^+$) *m*/*z* Calculated for $C_{12}H_{16}NO_3^+$ [M+H]$^+$ 222.1130; Found 222.1132.

tert-Butyl _trans_-(±)-3-((_tert_-butoxycarbonyl)(quinoline-8-yl)carbamoyl)-4-(4-methoxyphenyl)pyrrolidine-1-carboxylate (33)



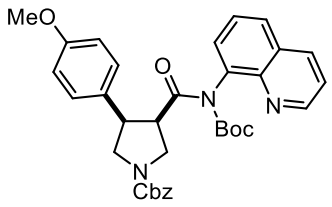
A flame-dried reaction tube was charged with amide **3a** (448 mg, 1.00 mmol), followed by Boc_2O (1.10 g, 5.00 mmol) and DMAP (366 mg, 3.00 mmol). The reaction vessel was sealed and purged with argon, then anhydrous MeCN (1.0 M, 1.0 mL) was added by syringe. The reaction tube was then placed in a preheated oil bath and stirred at 65 ºC for 24 h. The reaction mixture was then allowed to cool to rt and diluted with EtOAc (3 mL). The solvent was removed under reduced pressure. Purification by flash column chromatography (10% to 20% acetone/pentane) afforded product **33** as a white solid (136 mg, 25%, containing ~ 15% of *cis*-isomer **32**). R_f 0.39 (20% acetone/pentane); mp = 67–75 °C; ν_{max} (film)/cm^{-1} 2977, 2898, 1735 (C=O), 1691 (C=O), 1613, 1515, 1473, 1457, 1391, 1367, 1321, 1291, 1249, 1153, 1122, 1035, 879, 829, 791, 768; ^{1}H NMR (400 MHz, DMSO-d_6, 373 K) δ 8.83 (dd, *J* = 4.2, 1.7 Hz, 1 H, HC_{Ar}), 8.38 (dd, *J* = 8.4, 1.7 Hz, 1 H, HC_{Ar}), 7.96 (dd, *J* = 8.3, 1.4 Hz, 1 H, HC_{Ar}), 7.57 (dd, *J* = 8.2, 7.4 Hz, 1 H, HC_{Ar}), 7.54 (dd, *J* = 8.3, 4.2 Hz, 1 H, HC_{Ar}), 7.35 (dd, *J* = 7.3, 1.4 Hz, 1 H, HC_{Ar}), 7.25–7.21 (m, 2 H, HC_{Ar}), 6.93–6.89 (m, 2 H, HC_{Ar}), 4.27 (ddd, *J* = 7.7, 7.7, 7.7 Hz, 1 H, CHCO), 3.86 (dd, *J* = 10.9, 8.2 Hz, 1 H, NC*H*HCHCO), 3.78 (s, 3 H, OCH_3), 3.78–3.71 (m, 2 H, NCH*H*CHAr, CHAr),3.63 (dd, *J* = 10.9, 7.5 Hz, 1 H, NCH*H*CHCO), 3.40–3.31 (m, 1 H, NC*H*HCHAr), 1.44 (s, 9 H, $C(CH_3)_3$), 1.18 (s, 9 H, $C(CH_3)_3$); ^{13}C NMR (101 MHz, DMSO-d_6, 373 K) δ 174.2 (C=O amide), 158.0 (OC_{Ar} quat), 152.9 (C=O carbamate), 151.6 (C=O carbamate), 149.8 (C_{Ar}), 143.1 (C_{Ar} quat), 135.9 (C_{Ar} quat), 135.5 (C_{Ar}), 131.9 (C_{Ar} quat), 128.2 (C_{Ar}), 128.0 (C_{Ar} quat), 127.7 (2 × C_{Ar}), 127.6 (C_{Ar}), 125.4 (C_{Ar}), 121.1 (C_{Ar}), 113.7 (2 × C_{Ar}), 82.0 (*C*$(CH_3)_3$), 78.1 (*C*$(CH_3)_3$), 54.7 (OCH_3), 51.5 (N*C*H_2CHAr), 50.5 (*C*HCO), 48.6 (N*C*H_2CHCO), 45.9 (CHAr), 27.7 (C(*C*$H_3)_3$), 26.7 (C(*C*$H_3)_3$); HRMS (ESI$^+$) *m*/*z* Calculated for $C_{31}H_{38}N_3O_6$ [M+H] 548.2761; Found 548.2766.

***tert*-Butyl *cis*-(±)-3-((*tert*-butoxycarbonyl)(quinolin-8-yl)carbamoyl)-4-(4-methoxyphenyl)-pyrrolidine-1-carboxylate (32)**



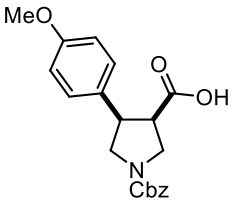
A flame-dried reaction tube was charged with amide **3a** (224 mg, 0.50 mmol), followed by Boc_2O (546 mg, 2.50 mmol) and DMAP (122 mg, 1.00 mmol). The reaction vessel was sealed and purged with argon, then anhydrous MeCN (1.0 mL, 0.5 M) was added by syringe. The reaction tube was then placed in a preheated oil bath and stirred at 55 ºC for 1 h. The reaction mixture was then allowed to cool to rt and sat. aq. NH_4Cl (2 mL) and CH_2Cl_2 (2 mL) were added. The phases were separated, and the aqueous layer was extracted with CH_2Cl_2 (3 × 10 mL). The combined organic extracts were dried over Na_2SO_4 and filtered. The solvent was removed under reduced pressure. The crude material was purified by flash column chromatography (20% acetone/pentane), the product containing fractions were combined and the solvent was removed under reduced pressure. Et_2O (5 mL) and pentane (5 mL) were added and the solvent was removed under reduced pressure to afford product **32** as a white solid (241 mg, 88%). R_f 0.37 (20% acetone/pentane); mp = 73–78 °C (from Et_2O/pentane); ν_{max} (film)/cm^{-1} 2974, 1735 (C=O), 1692 (C=O), 1515, 1392, 1367, 1293, 1250, 1155, 1122, 1031, 853, 830, 791, 767; ^{1}H NMR (400 MHz, DMSO-d_6, 373 K) δ 8.86 (dd, J = 4.2, 1.7 Hz, 1 H, HC_{Ar}), 8.34 (dd, J = 8.3, 1.7 Hz, 1 H, HC_{Ar}), 7.89 (dd, J = 8.3, 1.4 Hz, 1 H, HC_{Ar}), 7.52 (dd, J = 8.3, 4.2 Hz, 1 H, HC_{Ar}), 7.45 (dd, J = 8.3, 7.4 Hz, 1 H, HC_{Ar}), 7.22–7.17 (m, 2 H, HC_{Ar}), 6.96–6.90 (m, 2 H, HC_{Ar}), 6.74 (dd, J = 7.4, 1.3 Hz, 1 H, HC_{Ar}), 4.67 (ddd, J = 7.4, 7.4, 5.4 Hz, 1 H, CHCO), 3.91 (ddd, J = 7.2, 7.2, 7.2 Hz, 1 H, CHAr), 3.82 (dd, J = 11.3, 5.4 Hz, 1 H, NC*H*HCHCO), 3.79 (s, 3 H, OCH_3), 3.74 (dd, J = 10.5, 7.3 Hz, 1 H, NC*H*HCHAr), 3.69–3.61 (m, 2 H, NCH*H*CHAr, NCH*H*CHCO), 1.45 (s, 9 H, $C(CH_3)_3$), 1.17 (s, 9 H, $C(CH_3)_3$); ^{13}C NMR (101 MHz, DMSO-d_6, 373 K) δ 173.2 (C=O amide), 158.0 (OC_{Ar} quat), 153.1 (C=O carbamate), 151.6 (C=O carbamate), 149.7 (C_{Ar}), 143.2 (C_{Ar} quat), 135.9 (C_{Ar} quat), 135.4 (C_{Ar}), 130.7 (C_{Ar} quat), 128.3 (2 × C_{Ar}), 127.8 (C_{Ar}, C_{Ar} quat), 127.3 (C_{Ar}), 125.2 (C_{Ar}), 121.0 (C_{Ar}), 113.5 (2 × C_{Ar}), 81.8 ($C(CH_3)_3$), 78.0 ($C(CH_3)_3$), 54.8 (OCH_3), 50.3 (NCH_2CHAr), 47.9 (*C*HCO), 47.8 (NCH_2CHCO), 44.4 (CHAr), 27.7 (C(CH_3)$_3$), 26.7 (C(CH_3)$_3$); HRMS (ESI$^+$) *m*/*z* Calculated for $C_{31}H_{38}N_3O_6$ [M+H] 548.2761; Found 548.2740.

Benzyl *cis*-(±)-3-((*tert*-butoxycarbonyl)(quinolin-8-yl)carbamoyl)-4-(4-methoxyphenyl)-pyrrolidine-1-carboxylate (34)



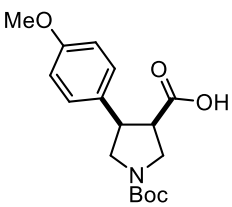
A flame-dried reaction tube was charged with amide **13a** (100 mg, 0.21 mmol), followed by Boc_2O (227 mg, 1.00 mmol) and DMAP (50.6 mg, 0.41 mmol). The reaction vessel was sealed and purged with argon, then anhydrous MeCN (450 μL, 0.5 M) was added by syringe. The reaction tube was then placed in a preheated oil bath and stirred at 55 ºC for 1 h. The reaction mixture was then allowed to cool to rt and sat. aq. NH_4Cl (1 mL) and CH_2Cl_2 (1 mL) were added. The phases were separated, and the aqueous layer was extracted with CH_2Cl_2 (3 × 5 mL). The combined organic extracts were dried over Na_2SO_4 and filtered. The solvent was removed under reduced pressure. The crude material was purified by flash column chromatography (20% acetone/pentane), the product containing fractions were combined and the solvent was removed under reduced pressure. Et_2O (5 mL) and pentane (5 mL) were added and the solvent was removed under reduced pressure to afford product **34** as a white solid (105 mg, 86%). R_f 0.19 (20% acetone/pentane); mp = 153–156 °C (from Et_2O/pentane); ν_{max} (film)/cm^{-1} 2976, 1735 (C=O), 1698 (C=O), 1514, 1416, 1367, 1292, 1249, 1153, 1122, 1030, 829, 791, 765, 697; ^{1}H NMR (400 MHz, DMSO-d_6, 373 K) δ 8.84 (dd, *J* = 4.2, 1.7 Hz, 1 H, HC_{Ar}), 8.34 (dd, *J* = 8.3, 1.7 Hz, 1 H, HC_{Ar}), 7.89 (dd, *J* = 8.3, 1.4 Hz, 1 H, HC_{Ar}), 7.51 (dd, *J* = 8.3, 4.2 Hz, 1 H, HC_{Ar}), 7.45 (dd, *J* = 8.2, 7.4 Hz, 1 H, HC_{Ar}), 7.40–7.28 (m, 5 H, HC_{Ar}), 7.23–7.18 (m, 2 H, HC_{Ar}), 6.95–6.90 (m, 2 H, HC_{Ar}), 6.75 (dd, *J* = 7.2, 1.3 Hz, 1 H, HC_{Ar}), 5.13 (s, 2 H, OCH_2Ph), 4.72 (ddd, *J* = 7.4, 7.4, 5.5 Hz, 1 H, CHCO), 4.01–3.87 (m, 2 H, CHAr, NC*H*HCHCO), 3.84 (dd, *J* = 10.4, 7.4 Hz, 1 H, NC*H*HCHAr), 3.79 (s, 3 H, OCH_3), 3.78–3.71 (m, 2 H, NCH*H*CHAr, NCH*H*CHCO), 1.17 (s, 9 H, $C(CH_3)_3$); ^{13}C NMR (101 MHz, DMSO-d_6, 373 K) δ 173.2 (C=O amide), 158.0 (OC_{Ar} quat), 153.5 (C=O Cbz), 151.6 (C=O Boc), 149.7 (C_{Ar}), 143.2 (C_{Ar} quat), 136.7 (C_{Ar} quat), 135.8 (C_{Ar} quat), 135.4 (C_{Ar}), 130.5 (C_{Ar} quat), 128.3 (2 × C_{Ar}), 127.8 (C_{Ar}, C_{Ar} quat), 127.7 (2 × C_{Ar}), 127.3 (C_{Ar}), 127.1 (C_{Ar}), 126.8 (2 × C_{Ar}), 125.2 (C_{Ar}), 121.0 (C_{Ar}), 113.5 (2 × C_{Ar}), 81.8 (*C*$(CH_3)_3$), 65.4 (OCH_2Ph), 54.8 (OCH_3), 50.4 (N*C*H_2CHAr), 48.0 (N*C*H_2CHCO), 47.8 (*C*HCO), 44.4 (CHAr), 26.7 (C(*C*$H_3)_3$); HRMS (ESI$^+$) *m*/*z* Calculated for $C_{34}H_{36}N_3O_6$ [M+H] 582.2604; Found 582.2614.

***cis*-(±)-1-((Benzyloxy)carbonyl)-4-(4-methoxyphenyl)pyrrolidine-3-carboxylic acid (35)**



A solution of H_2O_2 (30.6 μL, 0.30 mmol, 30 wt.% in H_2O) in THF (300 μL) was added to a solution of $LiOH·H_2O$ (8.4 mg, 0.20 mmol) in H_2O (300 μL) at 0 °C under argon. The resulting mixture was added dropwise to a solution of Boc-protected amide **34** (58.2 mg, 0.10 mmol) in THF (400 μL) at 0 °C under argon. The reaction was then stirred at 20 °C for 1 h. Sat. aq. $Na_2S_2O_3$ (1 mL) and EtOAc (1 mL) were then added and the reaction mixture was acidified to pH ~ 1 with 1 N HCl. The phases were separated, and the aqueous layer was extracted with EtOAc (3 × 5 mL). The combined organic extracts were dried over Na_2SO_4 and filtered. The solvent was removed under reduced pressure. The crude material was purified by flash column chromatography (5% MeOH/CH_2Cl_2), the product containing fractions were combined and the solvent was removed under reduced pressure. Et_2O (5 mL) and pentane (5 mL) were added and the solvent was removed under reduced pressure to afford acid **35** as a white solid (30.7 mg, 92%, single diastereoisomer). R_f 0.20 (5% MeOH/CH_2Cl_2); mp = 109–111 °C (from Et_2O/pentane); ν_{max} (film)/cm^{-1} 2953 (OH br), 1726, 1701 (C=O), 1660 (C=O), 1612, 1514, 1416, 1360, 1247, 1204, 1180, 1112, 1028, 830, 747, 696; ^{1}H NMR (400 MHz, $CDCl_3$, 298 K, observed as mixture of rotamers) δ 8.51 (br s, 1 H, OH), 7.48–7.29 (m, 5 H, HC_{Ar}), 7.09 (d, *J* = 8.2 Hz, 2 H, HC_{Ar}), 6.79 (d, *J* = 8.2 Hz, 2 H, HC_{Ar}), 5.27–5.08 (m, 2 H, OCH_2Ph), 3.88–3.77 (m, 3 H, N*C*H_2CHAr, N*CH*HCHCO), 3.75 (s, 3 H, OCH_3), 3.73–3.62 (m, 2 H, NCH*H*CHCO, CHAr), 3.36 (m, 1 H, CHCO); ^{13}C NMR (101 MHz, $CDCl_3$, 298 K, observed as mixture of rotamers) δ 176.2 and 175.9 (COOH), 158.7 (OC_{Ar} quat), 154.84 and 154.76 (C=O carbamate), 136.5 (C_{Ar} quat), 129.7 and 129.5 (C_{Ar} quat), 128.54 (2 × C_{Ar}), 128.46 (2 × C_{Ar}), 128.0 (C_{Ar}), 127.87 and 127.85 (2 × C_{Ar}), 113.9 (2 × C_{Ar}), 67.1 (OCH_2Ph), 55.1 (OCH_3), 51.0 and 50.3 (N*C*H_2CHAr), 48.6 and 47.7 (*C*HCO), 47.4 and 46.6 (N*C*H_2CHCO), 45.4 and 44.4 (CHAr); HRMS (ESI$^+$) *m*/*z* Calculated for $C_{20}H_{22}NO_5$ [M+H] 356.1498; Found 356.1515.

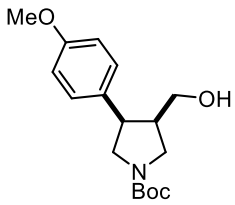
***cis*-(±)-1-(*tert*-Butoxycarbonyl)-4-(4-methoxyphenyl)pyrrolidine-3-carboxylic acid (36)**



A flame-dried reaction tube was charged with *cis*-arylated amide **3a** (327 mg, 0.75 mmol), followed by Boc_2O (818 mg, 3.75 mmol) and DMAP (183 mg, 1.50 mmol). The reaction vessel was sealed and purged with argon, then anhydrous MeCN (1.5 mL, 0.5 M) was added by syringe. The reaction tube was placed in an oil bath and gradually warmed up to 55 ºC. The reaction mixture was then stirred at 55 °C for 1 h. The reaction mixture was allowed to cool to rt and sat. aq. NH_4Cl (3 mL) and CH_2Cl_2 (3 mL) were added. The phases were separated, and the aqueous layer was extracted with CH_2Cl_2 (3 × 5 mL). The combined organic extracts were dried over Na_2SO_4 and filtered. The solvent was removed under reduced

pressure to afford the crude *N*-Boc protected pyrrolidine derivative **32**, which was used in the next step without further purification. A solution of H_2O_2 (30 wt.% in H_2O, 383 μL, 3.75 mmol) in THF (1.8 mL) was added to a solution of $LiOH·H_2O$ (63.0 mg, 1.50 mmol) in H_2O (1.9 mL) at 0 °C under argon. The resulting mixture was added dropwise to a solution of crude **32** in THF (3.8 mL) at 0 °C under argon. The reaction was then stirred at 20 °C for 1 h. Sat. aq. $Na_2S_2O_3$ (5 mL), EtOAc (5 mL) and 1 N NaOH (5 mL) were then added. The aqueous alkaline layer was collected, and the organic layer extracted with 1 N NaOH (3 × 15 mL). All the aqueous alkaline layers were combined, washed with EtOAc (40 mL), and acidified to pH ~ 1 with HCl, 37%. The acidic layer was extracted with EtOAc (5 × 50 mL). The combined organic extracts were dried over Na_2SO_4 and filtered. Solvent was removed under reduced pressure. Et_2O (5 mL) and pentane (5 mL) were added and the solvent was removed under reduced pressure to afford the pure *cis*-acid **36** as a white solid (214 mg, 89% over 2 steps). R_f 0.22 (30% acetone/pentane). mp = 137–141 °C (from Et_2O/pentane); ν_{max} (film)/cm^{-1} 2971 (OH br), 1730 (C=O), 1629 (C=O), 1513, 1431, 1405, 1245, 1163, 1126, 1021, 869, 835, 775; ^{1}H NMR (400 MHz, $CDCl_3$, 298 K, observed as mixture of rotamers) δ 7.15–7.07 (m, 2 H, HC_{Ar}), 6.85–6.79 (m, 2 H, HC_{Ar}), 3.84–3.71 (m, 6 H, NC*H*$_2$CHAr, NC*H*HCHCO, OCH_3), 3.71–3.59 (m, 2 H, NCH*H*CHCO, CHAr), 3.42–3.29 (m, 1 H, CHCO), 1.50 and 1.49 (2 × s, 9 H, $C(CH_3)_3$); ^{13}C NMR (101 MHz, $CDCl_3$, 298 K, observed as mixture of rotamers) δ 176.1 and 175.8 (COOH), 158.7 (OC_{Ar} quat), 154.53 and 154.47 (C=O carbamate), 130.2 and 129.9 (C_{Ar} quat), 128.6 (2 × C_{Ar}), 113.9 (2 × C_{Ar}), 79.9 (*C*$(CH_3)_3$), 55.1 (OCH_3), 50.64 and 50.57 (N*C*H_2CHAr), 48.6 and 47.8 (*C*HCO), 46.9 and 46.7 (N*C*H_2CHCO), 45.4 and 44.5 (CHAr), 28.5 (C(*C*$H_3)_3$); HRMS (ESI$^-$) *m*/*z* Calculated for $C_{17}H_{22}NO_5$ [M–H] 320.1498; Found 320.1500.

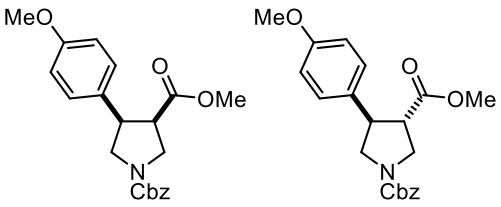
tert-Butyl _cis_-(±)-3-(hydroxymethyl)-4-(4-methoxyphenyl)pyrrolidine-1-carboxylate (37)



A solution of Boc-protected amide **32** (54.8 mg, 0.10 mmol) in dry THF (400 μL) was added dropwise to a suspension of $LiAlH_4$ (15.1 mg, 0.40 mmol) in dry THF (100 μL) at 0 °C under argon atmosphere. The mixture was then stirred at 20 °C for 30 min. The reaction mixture was then quenched by slow addition of sat. aq. NH_4Cl (2 mL) at 0 °C and stirred at rt for 30 min. The resulting suspension was filtered through a pad of Celite, eluting with EtOAc (3 × 5 mL). The phases were separated, and the aqueous layer was extracted with EtOAc (3 × 5 mL). The combined organic extracts were dried over Na_2SO_4 and filtered. The solvent was removed under reduced pressure. Purification by flash column chromatography (20% acetone/pentane) afforded primary alcohol **37** as a colourless paste (23.5 mg, 76%, single *cis*-diastereoisomer). R_f 0.28 (20% acetone/pentane); ν_{max} (film)/cm^{-1} 3407 (OH br), 2935, 1683 (C=O), 1513, 1401, 1365, 1246, 1162, 1124, 1027, 876, 826, 772; ^{1}H NMR (400 MHz,

DMSO-d_6, 373 K) δ 7.10–7.05 (m, 2 H, HC_{Ar}), 6.90–6.85 (m, 2 H, HC_{Ar}), 4.08 (t, *J* = 4.9 Hz, 1 H, OH), 3.75 (s, 3 H, OCH_3), 3.62 (dd, *J* = 10.7, 7.2 Hz, 1 H, NC*H*HCHAr), 3.51 (dd, *J* = 10.7, 5.8 Hz, 1 H, NCH*H*CHAr), 3.49–3.40 (m, 2 H, NC*H*HCHCH_2OH, CHAr), 3.25 (dd, *J* = 10.8, 6.6 Hz, 1 H, NCH*H*CHCH_2OH), 3.14 (dt, *J* = 10.2, 5.1 Hz, 1 H, C*H*HOH), 3.03–2.95 (m, 1 H, CH*H*OH), 2.57–2.47 (m, 1 H, C*H*CH_2OH), 1.46 (s, 9 H, $C(CH_3)_3$); ^{13}C NMR (101 MHz, DMSO-d_6, 373 K) δ 157.6 (OC_{Ar} quat), 153.3 (C=O carbamate), 131.2 (C_{Ar} quat), 128.1 (2 × C_{Ar}), 113.4 (2 × C_{Ar}), 77.8 (*C*$(CH_3)_3$), 59.6 (*C*H_2OH), 54.7 (OCH_3), 50.2 (N*C*H_2CHAr), 47.6 (N*C*H_2CHCH_2OH), 44.1 (*C*HCH$_2$OH), 43.2 (CHAr), 27.8 (C(*C*$H_3)_3$); HRMS (ESI$^+$) *m*/*z* Calculated for $C_{17}H_{26}NO_4$ [M+H] 308.1862; Found 308.1857.

1-Benzyl 3-methyl *cis*-(±)-4-(4-methoxyphenyl)pyrrolidine-1,3-dicarboxylate (38) and **1-benzyl 3-methyl *trans*-(±)-4-(4-methoxyphenyl)pyrrolidine-1,3-dicarboxylate (39)**



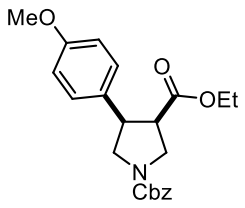
According to Chen's procedure,[210] a reaction tube was charged with K_2CO_3 (27.6 mg, 0.20 mmol), flame-dried, and allowed to cool under argon. Boc-protected amide **34** (58.2 mg, 0.10 mmol) was added and the reaction vessel sealed, purged with argon and cooled at 0 °C. Then anhydrous MeOH (2.0 mL, 0.05 M) was added by syringe. The reaction was then stirred at 25 °C for 22 h. The reaction mixture was diluted with EtOAc (2 mL). The resulting mixture was filtered through a pad of Celite, eluting with further EtOAc (2 × 5 mL). The solvent was removed under reduced pressure. The reaction mixture was purified by flash column chromatography (10% to 20% acetone/pentane). The product containing fractions were combined and the solvent was removed under reduced pressure. Et_2O (2 mL) and pentane (2 mL) were added and the solvent was removed under reduced pressure to afford the major product 1-benzyl 3-methyl *cis*-(±)-4-(4-methoxyphenyl)pyrrolidine-1,3-dicarboxylate **38** as a white solid (21.1 mg, 56%), followed by the minor product 1-benzyl 3-methyl *trans*-(±)-4-(4-methoxyphenyl)pyrrolidine-1,3-dicarboxylate **39** as a colourless oil (11.0 mg, 29%).

Major (**38**): R_f 0.34 (20% acetone/pentane); mp = 69–71 °C (from Et_2O/pentane); ν_{max} (film)/cm^{-1} 2960, 2880, 1732 (C=O ester), 1703 (C=O carbamate), 1515, 1414, 1353, 1327, 1305, 1251, 1194, 1135, 1028, 1001, 832, 816, 766, 733, 695; ^{1}H NMR (500 MHz, DMSO-d_6, 373 K) δ 7.42–7.35 (m, 4 H, HC_{Ar}), 7.34–7.28 (m, 1 H, HC_{Ar}), 7.25–7.19 (m, 2 H, HC_{Ar}), 6.92–6.86 (m, 2 H, HC_{Ar}), 5.11 (s, 2 H, OCH_2Ph), 3.88–3.80 (m, 2 H, NC*H*HCHAr, NC*H*HCHCO), 3.76 (s, 3 H, ArOCH_3), 3.62–3.54 (m, 5 H, CHAr, NCH*H*CHCO, CO_2CH_3), 3.36 (dd, *J* = 9.8, 9.8 Hz, 1 H, NCH*H*CHAr), 3.29 (ddd, *J* = 9.0, 9.0, 9.0 Hz, 1 H, CHCO); ^{13}C NMR (126 MHz, DMSO-d_6, 373 K) δ 171.6 (C=O ester), 158.0 (OC_{Ar} quat), 153.2 (C=O carbamate), 136.5 (C_{Ar} quat), 130.9 (C_{Ar} quat), 127.74 (2 × C_{Ar}), 127.67 (2 × C_{Ar}), 127.1 (C_{Ar}), 126.8 (2 × C_{Ar}), 113.7

(2 × C_{Ar}), 65.5 (OCH_2Ph), 54.7 ($ArOCH_3$), 51.9 (NCH_2CHAr), 51.0 (CO_2CH_3), 48.6 (*C*HCO), 48.0 (NCH_2CHCO), 45.7 (CHAr); HRMS (ESI^+) *m*/*z* Calculated for $C_{21}H_{24}NO_5$ [M+H] 370.1654; Found 370.1655.

Minor (**39**): R_f 0.29 (20% acetone/pentane); ν_{max} (film)/cm^{-1} 2958, 1717 (C=O ester), 1695 (C=O carbamate), 1517, 1419, 1356, 1329, 1252, 1208, 1179, 1132, 1026, 831, 767, 734, 697; ^1H NMR (500 MHz, DMSO-d_6, 373 K) δ 7.40–7.36 (m, 4 H, HC_{Ar}), 7.34–7.30 (m, 1 H, HC_{Ar}), 7.09–7.05 (m, 2 H, HC_{Ar}), 6.87–6.84 (m, 2 H, HC_{Ar}), 5.15 (s, 2 H, OCH_2Ph), 3.79 (dd, *J* = 9.4, 6.6 Hz, 1 H, NC*H*HCHAr), 3.75 (s, 3 H, $ArOCH_3$), 3.73–3.63 (m, 4 H, NCH_2CHCO, CHAr, NCH*H*CHAr), 3.49 (ddd, *J* = 7.1, 7.1, 5.7 Hz, 1 H, CHCO), 3.38 (s, 3 H, CO_2CH_3); ^{13}C NMR (126 MHz, DMSO-d_6, 373 K) δ 170.9 (C=O ester), 157.9 (OC_{Ar} quat), 153.5 (C=O carbamate), 136.7 (C_{Ar} quat), 130.0 (C_{Ar} quat), 127.8 (2 × C_{Ar}), 127.7 (2 × C_{Ar}), 127.1 (C_{Ar}), 126.8 (2 × C_{Ar}), 113.4 (2 × C_{Ar}), 65.5 (OCH_2Ph), 54.6 ($ArOCH_3$), 50.4 (CO_2CH_3), 49.8 (NCH_2CHAr), 47.2 (*C*HCO), 46.9 (NCH_2CHCO), 44.0 (CHAr); HRMS (ESI^+) *m*/*z* Calculated for $C_{21}H_{24}NO_5$ [M+H] 370.1654; Found 370.1653.

1-Benzyl 3-ethyl *cis*-(±)-4-(4-methoxyphenyl)pyrrolidine-1,3-dicarboxylate (40)

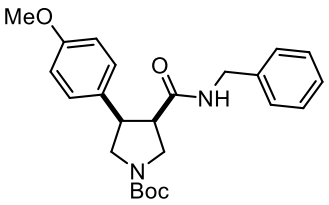


A reaction tube was charged with K_2CO_3 (27.6 mg, 0.20 mmol), flame-dried, and allowed to cool under argon. Boc-protected amide **34** (58.2 mg, 0.10 mmol) was added and the reaction vessel sealed, purged with argon and cooled at 0 °C. Then anhydrous MeOH (0.05 M, 2.0 mL) was added by syringe. The reaction was then stirred at 25 °C for 22 h. The reaction mixture was diluted with EtOAc (2 mL). The resulting mixture was filtered through a pad of Celite, eluting with further EtOAc (2 × 5 mL). The solvent was removed under reduced pressure. The reaction mixture was purified by flash column chromatography (10% to 20% acetone/pentane). The product containing fractions were combined and the solvent was removed under reduced pressure. Et_2O (2 mL) was added and the solvent was removed under reduced pressure to afford ethyl ester **40** as a colourless oil (10.0 mg, 27%). R_f 0.44 (20% acetone/pentane); ν_{max} (film)/cm^{-1} 2957, 2895, 2836, 1729 (C=O ester), 1701 (C=O carbamate), 1612, 1585, 1515, 1417, 1358, 1327, 1307, 1284, 1245, 1179, 1110, 1030, 955, 914, 829, 767, 737, 699; ^1H NMR (500 MHz, DMSO-d_6, 373 K) δ 7.39–7.34 (m, 4 H, HC_{Ar}), 7.34–7.29 (m, 1 H, HC_{Ar}), 7.24–7.20 (m, 2 H, HC_{Ar}), 6.90–6.87 (m, 2 H, HC_{Ar}), 5.12 (s, 2H, OCH_2Ph), 4.05 (qd, *J* = 7.1, 2.3 Hz, 2 H, OCH_2CH_3), 3.87–3.80 (m, 2 H, NC*H*HCHAr, NC*H*HCHCO), 3.76 (s, 3 H, OCH_3), 3.60–3.52 (m, 2 H, C*H*Ar, NCH*H*CHCO), 3.37 (dd, *J* = 10.5, 9.3 Hz, 1 H, NCH*H*CHAr), 3.26 (dt, *J* = 9.7, 8.4 Hz, 1 H, C*H*CO), 1.11 (t, *J* = 7.1 Hz, 3 H, OCH_2CH_3); ^{13}C NMR (126 MHz, DMSO-d_6, 373 K) δ 171.0 (C=O ester), 158.0 (OC_{Ar} quat), 153.2 (C=O carbamate), 136.6 (C_{Ar} quat), 130.9 (C_{Ar} quat), 127.7 (4 × C_{Ar}), 127.1 (C_{Ar}), 126.8

(2 × C_{Ar}), 113.7 (2 × C_{Ar}), 65.5 (OCH_2Ph), 59.7 (OCH_2CH_3), 54.7 (OCH_3), 51.9 (NCH_2CHAr), 48.8 (*C*HCO), 48.0 (NCH_2CHCO), 45.8 (CHAr), 13.3 (OCH_2CH_3); HRMS (ESI^+) *m*/*z* Calculated for $C_{22}H_{26}NO_5$ [M+H] 384.1811; Found 384.1819.

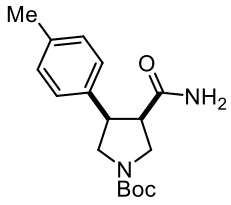
Note: Formation of ethyl ester **40** under the conditions outlined above was likely due to EtOH contamination in the MeOH solvent. The same product could be formed by treating Boc-protected amide **34** with K_2CO_3 in a 3:1 mixture of THF:EtOH at rt (23% conversion), but was not isolated.

***tert*-Butyl *cis*-(±)-3-(benzylcarbamoyl)-4-(4–methoxyphenyl)pyrrolidine-1-carboxylate (42)**



A flame-dried reaction tube was charged with Boc-protected amide **32** (54.7 mg, 0.10 mmol) and anhydrous toluene (200 μL, 0.5 M). The reaction vessel was cooled down to 0 °C and benzylamine (16.0 μL, 0.15 mmol) was added. The microwave vial was sealed, purged with argon and stirred at 60 ºC for 24 h. The reaction mixture was then allowed to cool down to rt and sat. aq. NH_4Cl (1 mL) and CH_2Cl_2 (1 mL) were added. The phases were separated, and the aqueous layer was extracted with CH_2Cl_2 (3 × 5 mL). The combined organic extracts were dried over Na_2SO_4 and filtered. The solvent was removed under reduced pressure. The reaction mixture was purified by flash column chromatography (20% acetone/pentane). The product containing fractions were combined and the solvent was removed under reduced pressure. Et_2O (5 mL) and pentane (5 mL) were added and the solvent was removed under reduced pressure to afford amide **42** as a white solid (28.5 mg, 69%, single diastereoisomer). R_f 0.20 (20% acetone/pentane); mp = 55–60 °C (from Et_2O/pentane); ν_{max} (film)/cm^{-1} 3297 (NH br), 2973, 1690 (C=O), 1647 (C=O), 1515, 1401, 1364, 1247, 1165, 1113, 1031, 877, 831, 730, 698; ^{1}H NMR (400 MHz, DMSO-d_6, 373 K) δ 7.83 (br t, *J* = 5.1 Hz, 1 H, NH), 7.25–7.14 (m, 3 H, HC_{Ar}), 7.16–7.07 (m, 2 H, HC_{Ar}), 6.94 (dd, *J* = 7.2, 2.2 Hz, 2 H, HC_{Ar}), 6.85–6.76 (m, 2 H, HC_{Ar}), 4.14 (dd, *J* = 15.1, 6.2 Hz, 1 H, NHC*H*H), 4.03 (dd, *J* = 15.1, 5.5 Hz, 1 H, NHCH*H*), 3.75 (s, 3 H, OCH_3), 3.73–3.66 (m, 1 H, NC*H*HCHAr), 3.66–3.58 (m, 3 H, NCH*H*CHAr, CHAr, NC*H*HCHCO), 3.52 (dd, *J* = 11.0, 7.3 Hz, 1 H, NCH*H*CHCO), 3.29 (ddd, *J* = 7.0, 4.4, 4.4 Hz, 1 H, CHCO), 1.46 (s, 9 H, $C(CH_3)_3$); ^{13}C NMR (101 MHz, DMSO-d_6, 373 K) δ 170.3 (C=O amide), 157.7 (OC_{Ar} quat), 153.2 (C=O carbamate), 138.5 (C_{Ar} quat), 130.3 (C_{Ar} quat), 128.3 (2 × C_{Ar}), 127.3 (2 × C_{Ar}), 126.7 (2 × C_{Ar}), 125.9 (C_{Ar}), 113.2 (2 × C_{Ar}), 77.8 ($C(CH_3)_3$), 54.6 (OCH_3), 49.9 (NCH_2CHAr), 47.8 (NCH_2CHCO), 47.4 (*C*HCO), 44.5 (CHAr), 41.6 ($NHCH_2$), 27.8 ($C(CH_3)_3$); HRMS (ESI^+) *m*/*z* Calculated for $C_{24}H_{31}N_2O_4$ [M+H] 411.2284; Found 411.2296.

***tert*-Butyl *cis*-(±)-3-carbamoyl-4-(*p*-tolyl)pyrrolidine-1-carboxylate (45)**



Using conditions reported by Maulide,[144b] arylated amide **3c** (86.3 mg, 0.20 mmol) was dissolved in anhydrous CH_2Cl_2 (13.0 mL) in a flame-dried round-bottom flask, and cooled to –78 °C. A stream of ozone was passed through until the characteristic blue colour appeared after 10 min minutes. A stream of oxygen was passed through until decolorization and the mixture was quenched with DMS (50.0 μL). After stirring at 20 °C for 2 h, the mixture was concentrated under reduced pressure. The residue was dissolved in NH_4OH (aq, 28%):THF (2.60 mL, 1:1) and stirred for 20 h at 25 °C. The mixture was diluted with CH_2Cl_2 (10 mL) and H_2O (5 mL). The organic layer was separated, and the aqueous layer was extracted with CH_2Cl_2 (4 × 15 mL). The combined organic layers were dried over Na_2SO_4 and the solvent was removed under reduced pressure. The crude material was purified by flash column chromatography (0% to 5% MeOH/CH_2Cl_2), the product containing fractions were combined and the solvent was removed under reduced pressure. Et_2O (5 mL) and pentane (5 mL) were added and the solvent was removed under reduced pressure to afford the free amide **45** as a white solid (33 mg, 49%). R_f 0.35 (5% MeOH/CH_2Cl_2); mp = 63–67 °C (from Et_2O/pentane); ν_{max} (film)/cm^{-1} 3331 (NH_2 br), 2976, 1663 (C=O), 1400, 1365, 1163, 1116, 876, 821, 771; ^{1}H NMR (500 MHz, DMSO-d_6, 373 K) δ 7.12–7.09 (m, 2 H, HC_{Ar}), 7.09–7.05 (m, 2 H, HC_{Ar}), 6.57 (br s, 2 H, NH_2), 3.69–3.62 (m, 2 H, NCH_2CHAr), 3.62–3.56 (m, 2 H, CHAr, NC*H*HCHCO), 3.48 (dd, *J* = 11.0, 7.5 Hz, 1 H, NCH*H*CHCO), 3.27–3.23 (m, 1 H, CHCO), 2.27 (s, 3 H, CH_3), 1.45 (s, 9 H, C(CH_3)$_3$); ^{13}C NMR (126 MHz, DMSO-d_6, 373 K) δ 172.0 (C=O amide), 153.2 (C=O carbamate), 135.8 (C_{Ar} quat), 134.9 (C_{Ar} quat), 128.0 (2 × C_{Ar}), 127.1 (2 × C_{Ar}), 77.8 (*C*(CH_3)$_3$), 50.2 (NCH_2CHAr), 47.5 (NCH_2CHCO), 47.0 (*C*HCO), 44.5 (CHAr), 27.8 (C(*C*H_3)$_3$), 19.9 (CH_3); HRMS (ESI$^+$) *m*/*z* Calculated for $C_{17}H_{24}N_2O_3Na$ [M+Na] 327.1685; Found 327.1692.

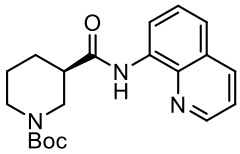
Procedure for the synthesis of amide 45 using IBX:

A reaction tube was charged with arylated amide **3c** (43.1 mg, 0.1 mmol) and IBX (45 wt.%, 137 mg, 0.22 mmol). The reaction vessel was stirred and HFIP (670 μL) and H_2O (330 μL) were added by syringe. After vigorous stirring at room temperature for 25 h, the mixture was diluted with EtOAc (3 mL). The resulting mixture was filtered through a pad of Celite, eluting with further EtOAc (3 × 5 mL). The solvent was removed under reduced pressure. The reaction mixture was purified by flash column chromatography (dry loading, 30% acetone/pentane) affording the desired free amide **45** as a white solid (20.2 mg, 66%). Characterisation data identical to that reported above for the reaction with O_3.

8.2.2 Compounds for Chapter 4: Synthesis of (–)-Paroxetine, Br-(–)-Paroxetine and I-(–)-Paroxetine

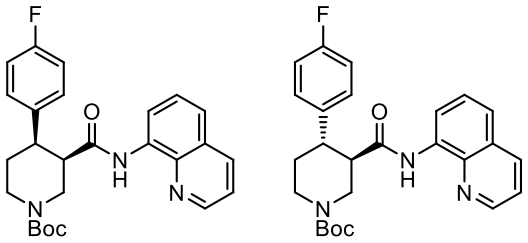
*8.2.2.1 Formal synthesis of (–)-paroxetine (**(–)-48**, **(+)-48**)*

tert-Butyl (–)-(*R*)-3-(quinolin-8-ylcarbamoyl)piperidine-1-carboxylate ((*R*)-24)



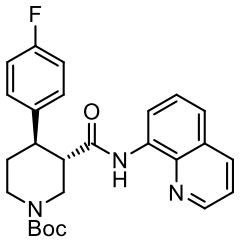
See procedure at page 206.

tert-Butyl (+)-(*3R,4R*)-4-(4-fluorophenyl)-3-(quinolin-8-ylcarbamoyl)piperidine-1-carboxylate ((+)-25c) and **_tert_-butyl (–)-(*3R,4S*)-4-(4-fluorophenyl)-3-(quinolin-8-ylcarbamoyl)piperidine-1-carboxylate ((–)-26c)**



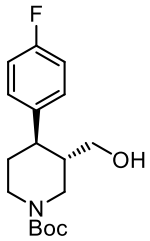
See procedure at page 250.

tert-Butyl (+)-(*3S,4R*)-4-(4-fluorophenyl)-3-(quinolin-8-ylcarbamoyl)piperidine-1-carboxylate ((+)-26c)



See procedure at page 251.

***tert*-Butyl (–)-(*3S,4R*)-4-(4-fluorophenyl)-3-(hydroxymethyl)piperidine-1-carboxylate ((–)-48)**

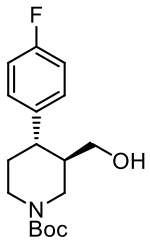


A flame-dried reaction tube was charged with amide **(+)-26c** (66.0 mg, 0.15 mmol), followed by Boc_2O (128 mg, 0.59 mmol) and DMAP (4.1 mg, 0.03 mmol). The reaction vessel was sealed and purged with argon, then MeCN (300 μL, 0.5 M) was added by syringe. The reaction tube was then placed in a preheated oil bath and stirred at 35 ºC for 24 h. The reaction mixture was then allowed to cool to rt and sat. aq. NH_4Cl (1 mL) and CH_2Cl_2 (1 mL) were added. The phases were separated, and the aqueous layer was extracted with CH_2Cl_2 (3 × 5 mL). The combined organic extracts were dried over Na_2SO_4 and filtered. The solvent was removed under reduced pressure to afford the crude *N*-Boc protected piperidine derivative. This was solubilised in dry THF (600 μL) and the resulting solution was added dropwise to a suspension of $LiAlH_4$ (22.8 mg, 0.60 mmol) in dry THF (100 μL) at 0 °C under argon atmosphere. The mixture was then stirred at 25 °C for 30 min. The reaction mixture was then quenched by slow addition of sat. aq. NH_4Cl (2 mL) at 0 °C and stirred at rt for 30 min. The resulting suspension was filtered through a pad of Celite, eluting with EtOAc (3 × 5 mL). The phases were separated, and the aqueous layer was extracted with EtOAc (3 × 10 mL). The combined organic extracts were dried over Na_2SO_4 and filtered. The solvent was removed under reduced pressure. Purification by flash column chromatography (10% acetone/pentane) afforded primary alcohol **(–)-48** as a colourless paste (36.5 mg, 79% over 2 steps, 99.1% *ee*). $[\alpha]_D^{22}$ –5.1 (*c* 1.56, MeOH). R_f 0.18 (10% acetone/pentane); ν_{max} (film)/cm^{-1} 3407 (OH), 2920, 1664 (C=O), 1509, 1425, 1365, 1280, 1223, 1158, 1128, 1059, 1015, 830, 769; ^{1}H NMR (400 MHz, $CDCl_3$, 298 K) δ 7.19–7.12 (m, 2 H, HC_{Ar}), 7.03–6.97 (m, 2 H, HC_{Ar}), 4.37 (br d, *J* = 13.4 Hz, 1 H, NC*H*HCHCH$_2$OH), 4.20 (br s, 1 H, NC*H*HCH$_2$), 3.44 (dd, *J* = 11.0, 3.2 Hz, 1 H, C*H*HOH), 3.26 (dd, *J* = 11.0, 6.4 Hz, 1 H, CH*H*OH), 2.86–2.65 (m, 2 H, NCH*H*CHCH$_2$OH, NCH*H*CH$_2$), 2.54 (td, *J* = 11.9, 3.9 Hz, 1 H, CHAr), 1.86–1.73 (m, 2 H, C*H*CH$_2$OH, NCH$_2$C*H*H), 1.73–1.60 (m, 2 H, NCH$_2$CH*H*, OH), 1.49 (s, 9 H, C(CH$_3$)$_3$); ^{13}C NMR (101 MHz, $CDCl_3$, 298 K) δ 161.6 (d, J_{CF} = 244.6 Hz, FC_{Ar} quat), 154.9 (C=O), 139.5 (d, J_{CF} = 2.7 Hz, F-*p*-C_{Ar} quat), 128.7 (d, J_{CF} = 7.8 Hz, 2 × F-*m*-C_{Ar}), 115.5 (d, J_{CF} = 21.1 Hz, 2 × F-*o*-C_{Ar}), 79.6 (*C*(CH$_3$)$_3$), 63.1 (CH$_2$OH), 46.9 (N*C*H$_2$CHCH$_2$OH), 44.4 (N*C*H$_2$CH$_2$), 44.1 (CHAr), 43.9 (*C*HCH$_2$OH), 34.1 (NCH$_2$*C*H$_2$), 28.5 (C(*C*H$_3$)$_3$); ^{19}F NMR (377 MHz, $CDCl_3$, 298 K) δ –116.4 (br s).

HPLC Conditions: Chiralpak IA 3-column, 90:10 *n*-hexane:*i*-PrOH, flow rate: 1 mL·min^{-1}, 35 ºC, UV detection wavelength: 210.4 nm. Retention times: 7.3 min (3*R,*4*S* enantiomer), 8.7 min (3*S,*4*R* enantiomer).

The observed characterisation data (IR, ^{1}H NMR, ^{13}C NMR) and the specific rotation ($[\alpha]_D^{22}$) were consistent with those previously reported in the literature.[227]

***tert*-Butyl (+)-(*3R,4S*)-4-(4-fluorophenyl)-3-(hydroxymethyl)piperidine-1-carboxylate ((+)-48)**



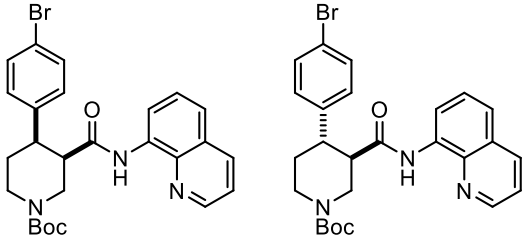
A flame-dried reaction tube was charged with amide **(–)-26c** (71.0 mg, 0.16 mmol), followed by Boc_2O (138 mg, 0.63 mmol) and DMAP (3.9 mg, 0.03 mmol). The reaction vessel was sealed and purged with argon, then MeCN (300 μL, 0.5 M) was added by syringe. The reaction tube was then placed in a preheated oil bath and stirred at 35 ºC for 24 h. The reaction mixture was then allowed to cool to rt and sat. aq. NH_4Cl (1 mL) and CH_2Cl_2 (1 mL) were added. The phases were separated, and the aqueous layer was extracted with CH_2Cl_2 (3 × 5 mL). The combined organic extracts were dried over Na_2SO_4 and filtered. The solvent was removed under reduced pressure to afford the crude *N*-Boc protected piperidine derivative. This was solubilised in dry THF (700 μL) and the resulting solution was added dropwise to a suspension of $LiAlH_4$ (24.2 mg, 0.64 mmol) in dry THF (200 μL) at 0 °C under argon atmosphere. The mixture was then stirred at 25 °C for 30 min. The reaction mixture was then quenched by slow addition of sat. aq. NH_4Cl (2 mL) at 0 °C and stirred at rt for 30 min. The resulting suspension was filtered through a pad of Celite, eluting with EtOAc (3 × 5 mL). The phases were separated, and the aqueous layer was extracted with EtOAc (3 × 10 mL). The combined organic extracts were dried over Na_2SO_4 and filtered. The solvent was removed under reduced pressure. Purification by flash column chromatography (10% acetone/pentane) afforded primary alcohol **(+)-48** as a colourless paste (38.6 mg, 78% over 2 steps, 98.6% *ee*). $[\alpha]_D^{22}$ +5.8 (*c* 0.92, MeOH).

HPLC Conditions: Chiralpak IA 3-column, 90:10 *n*-hexane:*i*-PrOH, flow rate: 1 mL·min^{-1}, 35 ºC, UV detection wavelength: 210.4 nm. Retention times: 7.3 min (3*R,*4*S* enantiomer), 8.7 min (3*S,*4*R* enantiomer).

Characterisation data identical to that reported for alcohol **(–)-48** (page 263). The specific rotation ($[\alpha]_D^{22}$) was consistent with that previously reported in the literature.[227]

*8.2.2.2 Synthesis of Br-(–)-paroxetine analogue (**49**, **51**, **52**, **(+)-51**, **(–)-52**, **(+)-52**, **(+)-55**, **(–)-55**, **(–)-57**)*

tert-Butyl _cis_-(±)-4-(4-bromophenyl)-3-(quinolin-8-ylcarbamoyl)piperidine-1-carboxylate (51) and **_tert_-butyl _trans_-(±)-4-(4-bromophenyl)-3-(quinolin-8-ylcarbamoyl)piperidine-1-carboxylate (52)**



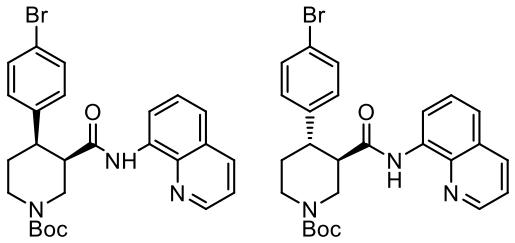
Prepared according to **General Procedure A** using amide **24** (178 mg) and 4-bromoiodobenzene (424 mg). Purification by flash column chromatography (0% to 5% CH_3CN/CH_2Cl_2) afforded the minor product *tert*–butyl *trans*-(±)-4-(4-bromophenyl)-3-(quinolin-8-ylcarbamoyl) piperidine-1-carboxylate **52** as a pale yellow solid (34.5 mg, 14%) followed by the major product *tert*-butyl *cis*-(±)-4-(4-bromophenyl)-3-(quinolin-8-ylcarbamoyl)piperidine-1-carboxylate **51** as an off-white solid (87.2 mg, 34%).

Major (**51**): R_f 0.31 (5% CH_3CN/CH_2Cl_2); mp = 81–86 °C (from Et_2O/pentane); ν_{max} (film)/cm^{-1} 3343 (NH), 2859, 1684 (C=O), 1521, 1484, 1423, 1364, 1323, 1245, 1163, 1006, 827, 790, 757; ^{1}H NMR (500 MHz, DMSO-d_6, 373 K) δ 9.75 (br s, 1 H, NH), 8.83 (dd, J = 4.2, 1.7 Hz, 1 H, HC_{Ar}), 8.45 (dd, J = 7.7, 1.4 Hz, 1 H, HC_{Ar}), 8.31 (dd, J = 8.3, 1.7 Hz, 1 H, HC_{Ar}), 7.60–7.53 (m, 2 H, HC_{Ar}), 7.48 (t, J = 7.9 Hz, 1 H, HC_{Ar}), 7.40–7.34 (m, 2 H, HC_{Ar}), 7.33–7.26 (m, 2 H, HC_{Ar}), 4.42 (ddd, J = 14.8, 3.6, 1.7 Hz, 1 H, NC*H*HCHCO), 4.25 (dddd, J = 13.1, 4.6, 2.3, 2.3 Hz, 1 H, NC*H*HCH$_2$), 3.36–3.28 (m, 2 H, NCH*H*CHCO, CHCO), 3.16 (ddd, J = 12.2, 4.0, 4.0 Hz, 1 H, CHAr), 3.02–2.92 (m, 1 H, NCH*H*CH$_2$), 2.68 (dddd, J = 12.4, 12.4, 12.4, 4.7 Hz, 1 H, NCH$_2$C*H*H), 1.72 (dddd, J = 12.9, 3.2, 3.2, 3.2 Hz, 1 H, NCH$_2$CH*H*), 1.25 (s, 9 H, C(CH$_3$)$_3$); ^{13}C NMR (126 MHz, DMSO-d_6, 373 K) δ 169.8 (C=O amide), 153.4 (C=O carbamate), 147.9 (C_{Ar}), 142.0 (C_{Ar} quat), 137.6 (C_{Ar} quat), 135.7 (C_{Ar}), 133.9 (C_{Ar} quat), 130.3 (2 × C_{Ar}), 129.1 (2 × C_{Ar}), 127.2 (C_{Ar} quat), 126.1 (C_{Ar}), 121.2 (C_{Ar}), 120.8 (C_{Ar}), 118.7 (BrC_{Ar} quat), 115.7 (C_{Ar}), 77.9 (*C*(CH$_3$)$_3$), 46.2 (N*C*H$_2$CHCO), 45.6 (*C*HCO), 42.9 (N*C*H$_2$CH$_2$), 41.7 (CHAr), 27.4 (C(*C*H$_3$)$_3$), 25.0 (NCH$_2$*C*H$_2$); HRMS (ESI$^+$) *m*/*z* Calculated for $C_{26}H_{29}N_3O_3{}^{79}Br$ [M+H] 510.1392; Found 510.1386.

Minor (**52**): R_f 0.41 (5% CH_3CN/CH_2Cl_2); mp = 77–83 °C (from Et_2O/pentane); ν_{max} (film)/cm^{-1} 3340 (NH), 2926, 1677 (C=O), 1521, 1484, 1424, 1323, 1230, 1156, 1126, 999, 824, 757; ^{1}H NMR (500 MHz, DMSO-d_6, 373 K) δ 9.73 (br s, 1 H, NH), 8.85 (dd, J = 4.2, 1.7 Hz, 1 H, HC_{Ar}), 8.39 (dd, J = 7.7, 1.4 Hz, 1 H, HC_{Ar}), 8.31 (dd, J = 8.3, 1.7 Hz, 1 H, HC_{Ar}), 7.61–7.54 (m, 2 H, HC_{Ar}), 7.47 (t, J = 8.0 Hz, 1 H, HC_{Ar}), 7.39–7.32 (m, 2 H, HC_{Ar}), 7.34–7.28 (m, 2 H, HC_{Ar}), 4.36 (ddd, J = 12.9, 3.7, 1.8 Hz, 1 H, NC*H*HCHCO), 4.13 (dddd, J = 13.3, 4.3, 2.2, 2.2 Hz, 1 H, NC*H*HCH$_2$), 3.18–3.00 (m, 3 H, NCH*H*CHCO, CHCO, CHAr), 2.99–2.90 (m, 1 H, NCH*H*CH$_2$),

1.81 (dddd, *J* = 12.9, 2.8, 2.8, 2.8 Hz, 1 H, NCH_2CHH), 1.66 (dddd, *J* = 12.8, 12.8, 12.8, 4.6 Hz, 1 H, NCH_2CHH), 1.49 (s, 9 H, $C(CH_3)_3$); ^{13}C NMR (126 MHz, DMSO-d_6, 373 K) δ 169.8 (C=O amide), 153.4 (C=O carbamate), 148.0 (C_{Ar}), 142.4 (C_{Ar} quat), 137.7 (C_{Ar} quat), 135.7 (C_{Ar}), 133.5 (C_{Ar} quat), 130.6 (2 × C_{Ar}), 129.1 (2 × C_{Ar}), 127.2 (C_{Ar} quat), 126.1 (C_{Ar}), 121.4 (C_{Ar}), 121.3 (C_{Ar}), 118.9 (BrC_{Ar} quat), 116.3 (C_{Ar}), 78.6 ($C(CH_3)_3$), 49.2 (*C*HCO), 46.2 (NCH_2CHCO), 43.9 (CHAr), 43.3 (NCH_2CH_2), 32.0 (NCH_2CH_2), 27.7 ($C(CH_3)_3$); HRMS (ESI^+) *m*/*z* Calculated for $C_{26}H_{29}N_3O_3{}^{79}Br$ [M+H] 510.1392; Found 510.1382.

***tert*-Butyl (+)-(*3R,4R*)-4-(4-bromophenyl)-3-(quinolin-8-ylcarbamoyl)piperidine-1-carboxylate ((+)-51)** and ***tert*-butyl (–)-(*3R,4S*)-4-(4-bromophenyl)-3-(quinolin-8-ylcarbamoyl)piperidine-1-carboxylate ((–)-52)**



A large microwave vial (10–20 mL recommended volume) was charged with K_2CO_3 (553 mg, 4.00 mmol), flame-dried, and allowed to cool under argon. Amide (*R*)-**24** (1.42 g, 4.00 mmol), 4-bromoiodobenzene (3.40 g, 12.0 mmol), $Pd(OAc)_2$ (45.1 mg, 0.20 mmol) and PivOH (409 mg, 4.00 mmol) were added sequentially. The reaction vessel was sealed and purged with argon, then anhydrous $PhCF_3$ (2.0 mL, 2.0 M) was added by syringe. The reaction tube was then placed in a preheated oil bath and stirred at 110 ºC for 18 h. The reaction mixture was then allowed to cool to rt and EtOAc (20 mL) was added. The resulting mixture was filtered through a pad of Celite, eluting with further EtOAc (2 × 50 mL). The solvent was removed under reduced pressure. The reaction mixture was purified by two consecutive chromatographic separations: one (0% to 5% CH_3CN/CH_2Cl_2) to isolate the minor *trans*-product *tert*-butyl (–)-(*3R,4S*)-4-(4-bromophenyl)-3-(quinolin-8-ylcarbamoyl)piperidine-1-carboxylate **(–)-52** followed by a second (10% to 15% acetone/pentane) to isolate the major *cis*-product *tert*-butyl (+)-(*3R,4R*)-4-(4-bromophenyl)-3-(quinolin-8-ylcarbamoyl)piperidine-1-carboxylate **(+)-51**. The product containing fractions were combined and the solvent was removed under reduced pressure. Et_2O (20 mL) and pentane (20 mL) were added and the solvent was removed under reduced pressure to afford the minor *trans*-product **(–)-52** as a pale yellow solid (371 mg, 18%, 98.0% *ee*) and the major *cis*-product **(+)-51** as a white solid (730 mg, 36%, 98.2% *ee*).

Major (**(+)-51**): $[\alpha]_D^{23}$ + 15.4 (*c* 1.3, $CHCl_3$).

Characterization data identical to that reported for racemic *cis*-piperidine **51** (page 266).

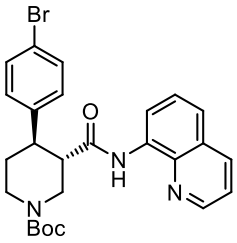
HPLC Conditions: Chiralpak IA 3-column, 85:15 *n*-hexane:*i*-PrOH, flow rate: 1 mL·min^{-1}, 35 ºC, UV detection wavelength: 210.4 nm. Retention times: 11.9 min (3*S,*4*S* enantiomer), 17.3 min (3*R,*4*R* enantiomer).

Minor (**(–)-52**): $[\alpha]_D^{23}$ – 35.4 (*c* 1.3, $CHCl_3$).

Characterization data identical to that reported for racemic *trans*-piperidine **52** (page 266).

HPLC Conditions: Chiralpak IA 3-column, 85:15 *n*-hexane:*i*-PrOH, flow rate: 1 mL·min^{-1}, 35 ºC, UV detection wavelength: 254.1 nm. Retention times: 9.1 min (3*R,*4*S* enantiomer), 12.2 min (3*S,*4*R* enantiomer).

***tert*-Butyl (+)-(*3S,4R*)-4-(4-bromophenyl)-3-(quinolin-8-ylcarbamoyl)piperidine-1-carboxylate ((+)-52)**



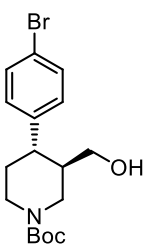
A flame-dried reaction tube was charged with *cis*-3,4-disubstituted piperidine **(+)-51** (662 mg, 1.30 mmol) and DBU (600 μL, 3.90 mmol). The reaction vessel was sealed and purged with argon, then anhydrous toluene (1.30 mL, 1.0 M) was added by syringe. The reaction tube was then placed in a preheated oil bath and stirred at 110 ºC for 24 h. The reaction mixture was then allowed to cool to rt and CH_2Cl_2 (5 mL) and sat. aq. NH_4Cl (5 mL) were added. The phases were separated, and the aqueous layer was extracted with CH_2Cl_2 (3 × 10 mL). The combined organic extracts were dried over Na_2SO_4 and filtered. The solvent was removed under reduced pressure. The reaction mixture was purified by flash column chromatography (15% acetone/pentane). The product containing fractions were combined and the solvent was removed under reduced pressure. Et_2O (10 mL) and pentane (10 mL) were added and the solvent was removed under reduced pressure to afford amide *tert*-butyl (+)-(*3S,4R*)-4-(4-bromophenyl)-3-(quinolin-8-ylcarbamoyl) piperidine-1-carboxylate **(+)-52** as a white solid (621 mg, 94%, 98.4% *ee*).

$[\alpha]_D^{23}$ + 52.0 (*c* 1.0, $CHCl_3$).

Characterization data identical to that reported for racemic *trans*-piperidine **52** (page 266).

HPLC Conditions: Chiralpak IA 3-column, 85:15 *n*-hexane:*i*-PrOH, flow rate: 1 mL·min^{-1}, 35 ºC, UV detection wavelength: 254.1 nm. Retention times: 9.1 min (3*R,*4*S* enantiomer), 12.2 min (3*S,*4*R* enantiomer).

***tert*-Butyl (+)-(*3R,4S*)-4-(4-bromophenyl)-3-(hydroxymethyl)piperidine-1-carboxylate ((+)-55)**

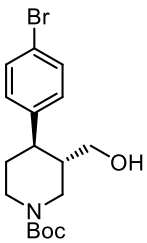


A flame-dried reaction tube was charged with amide **(–)-52** (102 mg, 0.20 mmol), followed by Boc_2O (175 mg, 0.80 mmol) and DMAP (4.9 mg, 0.04 mmol). The reaction vessel was sealed and purged with argon, then anhydrous MeCN (400 μL, 0.5 M) was added by syringe. The mixture was then stirred at 35 ºC for 22 h. The reaction mixture was then allowed to cool to rt and sat. aq. NH_4Cl (1 mL)

and CH_2Cl_2 (1 mL) were added. The phases were separated, and the aqueous layer was extracted with CH_2Cl_2 (3 × 5 mL). The combined organic extracts were dried over Na_2SO_4 and filtered. The solvent was removed under reduced pressure to afford the crude *N*-Boc protected piperidine derivative. This was solubilised in anhydrous THF (800 μL, 0.2 M) and the resulting solution was added dropwise to a suspension of $LiAlH_4$ (15.2 mg, 0.40 mmol) in anhydrous THF (200 μL, 2.0 M) at 0 °C under argon atmosphere. The mixture was then stirred at 20 °C for 30 min. The reaction mixture was then quenched by slow addition of sat. aq. NH_4Cl (2 mL) at 0 °C and stirred at rt for 30 min. The resulting suspension was filtered through a pad of Celite, eluting with EtOAc (3 × 5 mL). The phases were separated, and the aqueous layer was extracted with EtOAc (3 × 5 mL). The combined organic extracts were dried over Na_2SO_4 and filtered. The solvent was removed under reduced pressure. Purification by flash column chromatography (10% to 20% acetone/hexane) afforded primary alcohol **(+)-55** as a yellow solid (52.0 mg, 70% over 2 steps, 98.1% *ee*). $[\alpha]_D^{23}$ + 5.0 (*c* 0.8, $CHCl_3$); R_f 0.21 (20% acetone/hexane); mp = 49–54 °C; ν_{max} (film)/cm^{-1} 3407 (OH), 2922, 1662 (C=O), 1476, 1424, 1230, 1159, 1129, 1059, 1006, 816, 769; ^{1}H NMR (400 MHz, $CDCl_3$, 298 K) δ 7.47–7.40 (m, 2 H, HC_{Ar}), 7.11–7.05 (m, 2 H, HC_{Ar}), 4.36 (br d, *J* = 13.2 Hz, 1 H, NC*H*HCHCH$_2$OH), 4.20 (br s, 1 H, NC*H*HCH$_2$), 3.43 (dd, *J* = 11.0, 3.1 Hz, 1 H, C*H*HOH), 3.26 (dd, *J* = 11.0, 6.4 Hz, 1 H, CH*H*OH), 2.87–2.62 (m, 2 H, NCH*H*CHCH$_2$OH, NCH*H*CH$_2$), 2.59–2.47 (m, 1 H, CHAr), 1.88–1.59 (m, 4 H, C*H*CH$_2$OH, NCH$_2$C*H*$_2$, OH), 1.49 (s, 9 H, C(CH$_3$)$_3$); ^{13}C NMR (101 MHz, $CDCl_3$, 298 K, observed as a mixture of rotamers) δ 154.8 (C=O), 142.8 (C_{Ar} quat), 131.8 (2 × C_{Ar}), 129.1 (2 × C_{Ar}), 120.3 (BrC_{Ar} quat), 79.7 (*C*(CH$_3$)$_3$), 62.9 (CH$_2$OH), 46.5 (br m, N*C*H$_2$CHCH$_2$OH), 44.2 and 43.6 (N*C*H$_2$CH$_2$, CHAr, *C*HCH$_2$OH), 33.8 (NCH$_2$*C*H$_2$), 28.5 (C(*C*H$_3$)$_3$); HRMS (ESI$^+$) *m*/*z* Calculated for $C_{19}H_{27}N_2O_3Na^{79}Br$ [M+CH$_3$CN+Na] 433.1103; Found 433.1110.

HPLC Conditions: Chiralpak ID 3-column, 90:10 *n*-hexane:*i*-PrOH, flow rate: 1 mL·min^{-1}, 35 ºC, UV detection wavelength: 210.4 nm. Retention times: 8.0 min (3*R*,4*S* enantiomer), 8.6 min (3*S*,4*R* enantiomer).

tert-Butyl (–)-(3*S*,4*R*)-4-(4-bromophenyl)-3-(hydroxymethyl)piperidine-1-carboxylate ((–)-55)



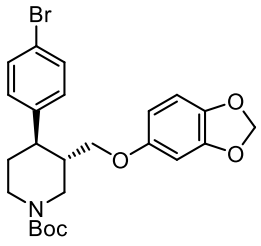
A flame-dried round-bottom flask was charged with amide **(+)-52** (565 mg, 1.11 mmol), followed by Boc_2O (969 mg, 4.44 mmol) and DMAP (26.9 mg, 0.22 mmol). The reaction vessel was sealed and purged with argon, then anhydrous MeCN (3.7 mL) and anhydrous CH_2Cl_2 (0.5 mL) were added by syringe. The mixture (0.3 M) was then stirred at 35 ºC for 22 h. The reaction mixture was then allowed to cool to rt and sat. aq. NH_4Cl (5 mL) and CH_2Cl_2 (5 mL) were added.

The phases were separated, and the aqueous layer was extracted with CH_2Cl_2 (3 × 10 mL). The combined organic extracts were dried over Na_2SO_4 and filtered. The solvent was removed under reduced pressure to afford the crude *N*-Boc protected piperidine derivative. This was solubilised in anhydrous THF (3.5 mL, 0.3 M) and the resulting solution was added dropwise to a suspension of $LiAlH_4$ (84.2 mg, 2.22 mmol) in anhydrous THF (2.0 mL, 1.0 M) at 0 °C under argon atmosphere. The mixture was then stirred at 20 °C for 30 min. The reaction mixture was then quenched by slow addition of sat. aq. NH_4Cl (5 mL) at 0 °C and stirred at rt for 30 min. The resulting suspension was filtered through a pad of Celite, eluting with EtOAc (3 × 10 mL). The phases were separated, and the aqueous layer was extracted with EtOAc (3 × 10 mL). The combined organic extracts were dried over Na_2SO_4 and filtered. The solvent was removed under reduced pressure. Purification by flash column chromatography (10% to 20% acetone/hexane) afforded primary alcohol **(–)-55** as a white solid (316 mg, 77% over 2 steps, 98.1% *ee*). $[\alpha]_D^{23}$ – 8.0 (*c* 1.0, $CHCl_3$).

Characterization data identical to that reported for enantiomeric alcohol **(+)-55** (page 268).

HPLC Conditions: Chiralpak ID 3-column, 90:10 *n*-hexane:*i*-PrOH, flow rate: 1 mL·min^{-1}, 35 ºC, UV detection wavelength: 210.4 nm. Retention times: 8.0 min (3*R,*4*S* enantiomer), 8.6 min (3*S,*4*R* enantiomer).

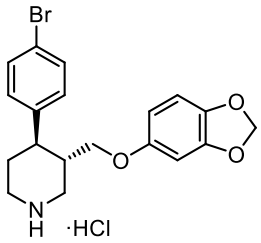
tert-Butyl (3*S*,4*R*)-3-((benzo[*d*][1,3]dioxol-5-yloxy)methyl)-4-(4-bromophenyl)piperidine-1-carboxylate ((–)-57)



Alcohol **(–)-55** (280 mg, 0.76 mmol) and triethylamine (147 μL, 1.10 mmol) were added to a flame-dried round-bottom flask, dissolved in anhydrous CH_2Cl_2 (4.0 mL, 0.2 M) and cooled down to 0 °C. Methanesulfonyl chloride (75 μL, 0.97 mmol) was then added by Gilson pipette. After stirring 5 min at 0 °C, the reaction mixture was stirred at 25 °C for 2 h, then diluted with CH_2Cl_2 (5 mL) and sat. aq. $NaHCO_3$ (5 mL). The phases were separated, and the aqueous layer was extracted with CH_2Cl_2 (3 × 10 mL). The combined organic extracts were dried over Na_2SO_4 and filtered. The solvent was removed under reduced pressure to afford the crude mesylated alcohol derivative. NaH (60% dispersion in mineral oil, 51.8 mg, 1.30 mmol) was added to a solution of sesamol (168 mg, 1.20 mmol) in anhydrous THF (4.0 mL, 0.3 M) at 0 °C. The mixture was then stirred at 25 °C for 1 h. A solution of the crude mesylated alcohol in anhydrous THF (5.0 mL, 0.1 M) was then added dropwise to this suspension. The resulting mixture was stirred at 70 °C for 18 h. The reaction mixture was then quenched by addition of H_2O (5 mL) and diluted with EtOAc (5 mL). The phases were separated, and the aqueous layer was extracted with EtOAc (4 × 10 mL). The combined organic extracts were dried over Na_2SO_4 and filtered. The solvent was removed under reduced

pressure. Purification by flash column chromatography (5% acetone/pentane) afforded piperidine **(–)-57** as a white solid (225 mg, 60% over 2 steps). $[\alpha]_D^{23}$ – 36.0 (*c* 1.0, $CHCl_3$); R_f 0.20 (5% acetone/pentane); mp = 53–58 °C; ν_{max} (film)/cm^{-1} 2915, 1685 (C=O), 1483, 1424, 1230, 1163, 1129, 1036, 928, 816, 769; ^{1}H NMR (400 MHz, $CDCl_3$, 298 K) δ 7.45–7.38 (m, 2 H, HC_{Ar}), 7.10–7.03 (m, 2 H, HC_{Ar}), 6.64 (d, *J* = 8.5 Hz, 1 H, HC_{Ar}), 6.36 (d, *J* = 2.5 Hz, 1 H, HC_{Ar}), 6.14 (dd, *J* = 8.5, 2.5 Hz, 1 H, HC_{Ar}), 5.89 (s, 2 H, OCH_2O), 4.44 (br s, 1 H, NC*H*HCHCH$_2$OAr), 4.25 (br s, 1 H, NC*H*HCH$_2$), 3.61 (dd, *J* = 9.4, 2.8 Hz, 1 H, C*H*HOAr), 3.45 (dd, *J* = 9.4, 6.4 Hz, 1 H, CH*H*OAr), 2.92–2.73 (br m, 2 H, NCH*H*CHCH$_2$OAr, NCH*H*CH$_2$), 2.67 (ddd, *J* = 11.7, 11.7, 3.9 Hz, 1 H, CHAr), 2.08–1.97 (br m, 1 H, C*H*CH$_2$OAr), 1.85–1.77 (br m, 1 H, NCH$_2$C*H*H), 1.76–1.67 (m, 1 H, NCH$_2$CH*H*), 1.50 (s, 9 H, C(CH$_3$)$_3$); ^{13}C NMR (101 MHz, $CDCl_3$, 298 K) δ 154.7 (C=O), 154.2 (OC_{Ar} quat), 148.1 (OC_{Ar} quat), 142.4 (C_{Ar} quat), 141.7 (OC_{Ar} quat), 131.8 (2 × C_{Ar}), 129.1 (2 × C_{Ar}), 120.4 (BrC_{Ar} quat), 107.8 (C_{Ar}), 105.5 (C_{Ar}), 101.1 (OCH_2O), 98.0 (C_{Ar}), 79.7 (*C*(CH$_3$)$_3$), 68.7 (CH_2OAr), 47.3 (br m, N*C*H$_2$CHCH$_2$OAr), 44.2 (N*C*H$_2$CH$_2$, CHAr), 41.7 (*C*HCH$_2$OAr), 33.7 (NCH$_2$*C*H$_2$), 28.4 (C(*C*H$_3$)$_3$); HRMS (ESI$^+$) *m*/*z* Calculated for $C_{24}H_{29}NO_5{}^{79}Br$ [M+H] 490.1229; Found 490.1240.

(3*S*,4*R*)-3-((Benzo[*d*][1,3]dioxol-5-yloxy)methyl)-4-(4-bromophenyl)piperidine-1-ium chloride (49)

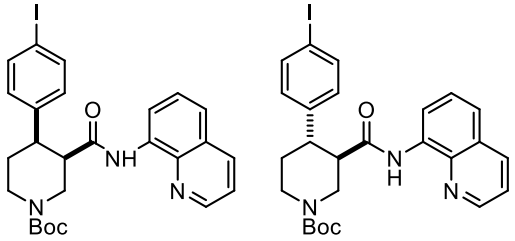


4 N HCl in 1,4-dioxane (500 μL, 2.00 mmol) was added to a solution of *N*-Boc protected piperidine **(–)-57** (98.1 mg, 0.20 mmol) in 1,4-dioxane (500 μL, 0.4 M) at 0 °C under air. The solution was stirred at 25 ºC for 18 h, then an ice-cold 1:1 mixture of Et_2O/pentane (1 mL) was added and formation of a solid precipitate was observed. This was filtered and washed with further ice-cold Et_2O/pentane mixture (2 × 5 mL). The solid precipitate was dried under reduced pressure to afford (3*S*,4*R*)-3-((benzo[*d*][1,3]dioxol-5-yloxy)methyl)-4-(4-bromophenyl) piperidine-1-ium chloride **49** as an off-white solid (73.5 mg, 86%). $[\alpha]_D^{23}$ – 82.0 (*c* 1.0, MeOH); mp = 206–209 ºC; ν_{max} (film)/cm^{-1} 3317 (NH), 2926, 2687, 1484, 1182, 1103, 1033, 932, 846, 813, 787; ^{1}H NMR (400 MHz, CD_3OD, 298 K) δ 7.50–7.44 (m, 2 H, HC_{Ar}), 7.24–7.18 (m, 2 H, HC_{Ar}), 6.63 (d, *J* = 8.4 Hz, 1 H, HC_{Ar}), 6.39 (d, *J* = 2.5 Hz, 1 H, HC_{Ar}), 6.18 (dd, *J* = 8.5, 2.5 Hz, 1 H, HC_{Ar}), 5.87–5.84 (m, 2 H, OCH_2O), 3.71–3.62 (m, 2 H, C*H*HOAr, NC*H*HCHCH$_2$OAr), 3.59–3.49 (m, 2 H, CH*H*OAr, NC*H*HCH$_2$), 2.21–2.11 (m, 2 H, NCH*H*CHCH$_2$OAr, NCH*H*CH$_2$), 3.03–2.91 (m, 1 H, CHAr), 2.49–2.37 (m, 1 H, C*H*CH$_2$OAr), 2.10–2.01 (m, 2 H, NCH$_2$C*H*$_2$); ^{13}C NMR (101 MHz, CD_3OD, 298 K) δ 155.3 (OC_{Ar} quat), 149.7 (OC_{Ar} quat), 143.5 (C_{Ar} quat), 142.4 (OC_{Ar} quat), 133.0 (2 × C_{Ar}), 130.5 (2 × C_{Ar}), 122.0 (BrC_{Ar} quat), 108.8 (C_{Ar}), 106.7 (C_{Ar}), 102.5 (OCH_2O), 98.9 (C_{Ar}), 69.0 (CH_2OAr), 47.7

(NCH_2CHCH_2OAr), 45.5 (NCH_2CH_2), 42.9 (CHAr), 40.6 (*C*HCH_2OAr), 31.4 (NCH_2CH_2); HRMS (ESI$^+$) *m*/*z* Calculated for $C_{19}H_{21}NO_3{}^{79}Br$ [M–Cl] 390.0705; Found 390.0698.

*8.2.2.3 Synthesis of l-(–)-paroxetine analogue (**50**, **53**, **54**, **(+)-53**, **(–)-54**, **(+)-54**, **(+)-56**, **(–)-56**, **(–)-58**)*

***tert*-Butyl *cis*-(±)-4-(4-iodophenyl)-3-(quinolin-8-ylcarbamoyl)piperidine-1-carboxylate (53)** and ***tert*-butyl *trans*-(±)-4-(4-iodophenyl)-3-(quinolin-8-ylcarbamoyl)piperidine-1-carboxylate (54)**



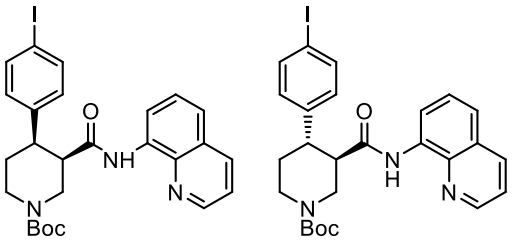
Prepared according to **General Procedure A** using amide **24** (178 mg) and 1,4-diiodobenzene (660 mg). Purification by flash column chromatography (0% to 5% CH_3CN/CH_2Cl_2) afforded the minor product *tert*–butyl *trans*-(±)-4-(4-iodophenyl)-3-(quinolin-8-ylcarbamoyl)piperidine-1-carboxylate **54** as a pale yellow solid (52.2 mg, 19%) followed by the major product *tert*-butyl *cis*-(±)-4-(4-iodophenyl)-3-(quinolin-8-ylcarbamoyl)piperidine-1-carboxylate **53** as a pale yellow solid (97.9 mg, 35%).

Major (**53**): R_f 0.30 (5% CH_3CN/CH_2Cl_2); mp = 91–95 °C (from Et_2O/pentane); ν_{max} (film)/cm^{-1} 3343 (NH), 2926, 1685 (C=O), 1521, 1483, 1424, 1364, 1323, 1245, 1159, 1118, 1003, 824, 790, 757; ^{1}H NMR (500 MHz, DMSO-d_6, 373 K) δ 9.75 (br s, 1 H, NH), 8.83 (dd, J = 4.2, 1.7 Hz, 1 H, HC_{Ar}), 8.45 (dd, J = 7.6, 1.4 Hz, 1 H, HC_{Ar}), 8.31 (dd, J = 8.3, 1.7 Hz, 1 H, HC_{Ar}), 7.60–7.53 (m, 4 H, HC_{Ar}), 7.48 (t, J = 8.0 Hz, 1 H, HC_{Ar}), 7.19–7.12 (m, 2 H, HC_{Ar}), 4.42 (ddd, J = 14.9, 3.7, 1.8 Hz, 1 H, NC*H*HCHCO), 4.25 (dddd, J = 13.2, 4.7, 2.4, 2.4 Hz, 1 H, NC*H*HCH_2), 3.35–3.28 (m, 2 H, NCH*H*CHCO, CHCO), 3.14 (ddd, J = 12.4, 4.2, 4.2 Hz, 1 H, CHAr), 3.01–2.92 (m, 1 H, NCH*H*CH_2), 2.67 (dddd, J = 12.4, 12.4, 12.4, 4.6 Hz, 1 H, NCH_2C*H*H), 1.71 (dddd, J = 13.0, 3.4, 3.4, 3.4 Hz, 1 H, NCH_2CH*H*), 1.25 (s, 9 H, $C(CH_3)_3$); ^{13}C NMR (126 MHz, DMSO-d_6, 373 K) δ 169.8 (C=O amide), 153.4 (C=O carbamate), 147.9 (C_{Ar}), 142.5 (C_{Ar} quat), 137.6 (C_{Ar} quat), 136.3 (2 × C_{Ar}), 135.7 (C_{Ar}), 133.9 (C_{Ar} quat), 129.3 (2 × C_{Ar}), 127.2 (C_{Ar} quat), 126.1 (C_{Ar}), 121.2 (C_{Ar}), 120.8 (C_{Ar}), 115.7 (C_{Ar}), 90.9 (IC_{Ar} quat), 77.9 (*C*$(CH_3)_3$), 46.2 (N*C*H_2CHCO), 45.6 (*C*HCO), 42.9 (N*C*H_2CH_2), 41.8 (CHAr), 27.4 (C(*C*$H_3)_3$), 25.0 (NCH_2*C*H_2); HRMS (ESI$^+$) *m*/*z* Calculated for $C_{26}H_{29}N_3O_3{}^{127}I$ [M+H] 558.1254; Found 558.1260.

Minor (**54**): R_f 0.41 (5% CH_3CN/CH_2Cl_2); mp = 93–96 °C (from Et_2O/pentane); ν_{max} (film)/cm^{-1} 3336 (NH), 2922, 1677 (C=O), 1521, 1483, 1424, 1323, 1230, 1156, 1062, 1003, 824, 757; ^{1}H NMR (500 MHz, DMSO-d_6, 373 K) δ 9.73 (br s, 1 H, NH), 8.85 (dd, J = 4.2, 1.7 Hz, 1 H, HC_{Ar}), 8.39 (dd, J = 7.7, 1.3 Hz, 1 H, HC_{Ar}), 8.31 (dd, J = 8.3, 1.7 Hz, 1 H, HC_{Ar}), 7.62–7.55 (m, 2 H, HC_{Ar}), 7.55–7.51 (m, 2 H, HC_{Ar}), 7.47 (t, J = 8.0 Hz, 1 H, HC_{Ar}), 7.19–7.14 (m, 2 H, HC_{Ar}), 4.35 (ddd, J = 12.8, 3.8, 1.8 Hz, 1 H, NC*H*HCHCO), 4.12 (dddd, J = 13.3, 4.4, 2.1, 2.1 Hz, 1 H, NC*H*HCH_2), 3.17–2.99 (m, 3 H, NCH*H*CHCO, CHCO, CHAr), 2.98–2.90 (m, 1 H, NCH*H*CH_2), 1.80 (dddd, J = 13.3, 3.0, 3.0, 3.0 Hz, 1 H, NCH_2C*H*H), 1.65 (dddd, J = 12.7, 4.6, 4.6, 4.6 Hz,

1 H, $NCH_2CH\mathit{H}$), 1.48 (s, 9 H, $C(CH_3)_3$); ^{13}C NMR (126 MHz, DMSO-d_6, 373 K) δ 169.8 (C=O amide), 153.4 (C=O carbamate), 148.1 (C_{Ar}), 142.8 (C_{Ar} quat), 137.7 (C_{Ar} quat), 136.6 (2 × C_{Ar}), 135.7 (C_{Ar}), 133.5 (C_{Ar} quat), 129.3 (2 × C_{Ar}), 127.2 (C_{Ar} quat), 126.1 (C_{Ar}), 121.4 (C_{Ar}), 121.3 (C_{Ar}), 116.3 (C_{Ar}), 91.1 (IC_{Ar} quat), 78.6 ($\mathit{C}(CH_3)_3$), 49.1 ($\mathit{C}HCO$), 46.2 (NCH_2CHCO), 44.0 (CHAr), 43.3 ($N\mathit{C}H_2CH_2$), 32.0 ($NCH_2\mathit{C}H_2$), 27.7 ($C(\mathit{C}H_3)_3$); HRMS (ESI^+) *m*/*z* Calculated for $C_{26}H_{29}N_3O_3{}^{127}I$ [M+H] 558.1254; Found 558.1247.

***tert*-Butyl (+)-(*3R,4R*)-4-(4-iodophenyl)-3-(quinolin-8-ylcarbamoyl)piperidine-1-carboxylate ((+)-53)** and ***tert*-butyl (–)-(*3R,4S*)-4-(4-iodophenyl)-3-(quinolin-8-ylcarbamoyl)piperidine-1-carboxylate ((–)-54)**



A large microwave vial (10–20 mL recommended volume) was charged with K_2CO_3 (553 mg, 4.00 mmol), flame-dried, and allowed to cool under argon. Amide (*R*)-**24** (1.42 g, 4.00 mmol), 1,4-diiodobenzene (5.28 g, 16.0 mmol), $Pd(OAc)_2$ (45.1 mg, 0.20 mmol) and PivOH (409 mg, 4.00 mmol) were added sequentially. The reaction vessel was sealed and purged with argon, then anhydrous $PhCF_3$ (2.0 mL, 2.0 M) was added by syringe. The reaction tube was then placed in a preheated oil bath and stirred at 110 ºC for 18 h. The reaction mixture was then allowed to cool to rt and EtOAc (20 mL) was added. The resulting mixture was filtered through a pad of Celite, eluting with further EtOAc (2 × 50 mL). The solvent was removed under reduced pressure. The reaction mixture was purified by two consecutive chromatographic separations: one (0% to 5% CH_3CN/CH_2Cl_2) to isolate the minor *trans*-product *tert*-butyl (–)-(*3R,4S*)-4-(4-iodophenyl)-3-(quinolin-8-ylcarbamoyl)piperidine-1-carboxylate **(–)-54** followed by a second (10% to 15% acetone/pentane) to isolate the major *cis*-product *tert*-butyl (+)-(*3R,4R*)-4-(4-iodophenyl)-3-(quinolin-8-ylcarbamoyl)piperidine-1-carboxylate **(+)-53**. The product containing fractions were combined and the solvent was removed under reduced pressure. Et_2O (20 mL) and pentane (20 mL) were added and the solvent was removed under reduced pressure to afford the minor *trans*-product **(–)-54** as a pale orange solid (441 mg, 20%, 98.1% *ee*) and the major *cis*-product **(+)-53** (775 mg, 35%, 98.2% *ee*).

Major (**(+)-53**): $[\alpha]_D^{23}$ + 9.1 (*c* 1.1, $CHCl_3$).

Characterisation data identical to that reported for racemic *cis*-piperidine **53** (page 273).

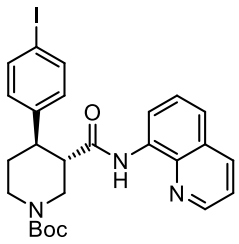
HPLC Conditions: Chiralpak IA 3-column, 85:15 *n*-hexane:*i*-PrOH, flow rate: 1 mL·min^{-1}, 35 ºC, UV detection wavelength: 210.4 nm. Retention times: 12.2 min (3*S,*4*S* enantiomer), 17.7 min (3*R,*4*R* enantiomer).

Minor (**(–)-54**): $[\alpha]_D^{23}$ – 45.5 (*c* 1.1, $CHCl_3$).

Characterisation data identical to that reported for racemic *trans*-piperidine **54** (page 273).

HPLC Conditions: Chiralpak IA 3-column, 85:15 *n*-hexane:*i*-PrOH, flow rate: 1 mL·min^{-1}, 35 ºC, UV detection wavelength: 254.1 nm. Retention times: 9.4 min (3*R,*4*S* enantiomer), 13.3 min (3*S,*4*R* enantiomer).

***tert*-Butyl (+)-(*3S,4R*)-4-(4-iodophenyl)-3-(quinolin-8-ylcarbamoyl)piperidine-1-carboxylate ((+)-54)**

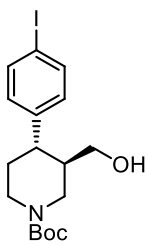


A flame-dried reaction tube was charged with *cis*-3,4-disubstituted piperidine **(+)-53** (687 mg, 1.23 mmol) and DBU (550 μL, 3.70 mmol). The reaction vessel was sealed and purged with argon, then anhydrous toluene (1.20 mL, 1.0 M) was added by syringe. The reaction tube was then placed in a preheated oil bath and stirred at 110 ºC for 24 h. The reaction mixture was then allowed to cool to rt and CH_2Cl_2 (5 mL) and sat. aq. NH_4Cl (5 mL) were added. The phases were separated, and the aqueous layer was extracted with CH_2Cl_2 (3 × 10 mL). The combined organic extracts were dried over Na_2SO_4 and filtered. The solvent was removed under reduced pressure. The reaction mixture was purified by flash column chromatography (10% acetone/pentane). The product containing fractions were combined and the solvent was removed under reduced pressure. Et_2O (10 mL) and pentane (10 mL) were added and the solvent was removed under reduced pressure to afford amide *tert*-butyl (+)-(*3S,4R*)-4-(4-iodophenyl)-3-(quinolin-8-ylcarbamoyl) piperidine-1-carboxylate **(+)-54** as a white solid (626 mg, 91%, 98.0% *ee*). $[\alpha]_D^{23}$ + 48.0 (*c* 1.0, $CHCl_3$).

Characterisation data identical to that reported for racemic *trans*-piperidine **54** (page 273).

HPLC Conditions: Chiralpak IA 3-column, 85:15 *n*-hexane:*i*-PrOH, flow rate: 1 mL·min^{-1}, 35 ºC, UV detection wavelength: 254.1 nm. Retention times: 9.4 min (3*R,*4*S* enantiomer), 13.3 min (3*S,*4*R* enantiomer).

***tert*-Butyl (+)-(*3R,4S*)-4-(4-iodophenyl)-3-(hydroxymethyl)piperidine-1-carboxylate ((+)-56)**

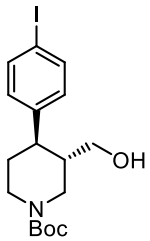


A flame-dried reaction tube was charged with amide **(–)-54** (111 mg, 0.20 mmol), followed by Boc_2O (175 mg, 0.80 mmol) and DMAP (4.9 mg, 0.04 mmol). The reaction vessel was sealed and purged with argon, then anhydrous MeCN (400 μL, 0.5 M) was added by syringe. The mixture was then stirred at 40 ºC for 22 h. The reaction mixture was then allowed to cool to rt and sat. aq. NH_4Cl (1 mL)

and CH_2Cl_2 (1 mL) were added. The phases were separated, and the aqueous layer was extracted with CH_2Cl_2 (3 × 5 mL). The combined organic extracts were dried over Na_2SO_4 and filtered. The solvent was removed under reduced pressure to afford the crude *N*-Boc protected piperidine derivative. This was solubilised in anhydrous THF (800 μL, 0.2 M) and the resulting solution was added dropwise to a suspension of $LiAlH_4$ (15.2 mg, 0.40 mmol) in anhydrous THF (200 μL, 2.0 M) at 0 °C under argon atmosphere. The mixture was then stirred at 20 °C for 30 min. The reaction mixture was then quenched by slow addition of sat. aq. NH_4Cl (2 mL) at 0 °C and stirred at rt for 30 min. The resulting suspension was filtered through a pad of Celite, eluting with EtOAc (3 × 5 mL). The phases were separated, and the aqueous layer was extracted with EtOAc (3 × 5 mL). The combined organic extracts were dried over Na_2SO_4 and filtered. The solvent was removed under reduced pressure. Purification by flash column chromatography (10% to 15% acetone/pentane) afforded primary alcohol **(+)-56** as a white solid (52.3 mg, 63% over 2 steps, 98.1% *ee*, containing approx. 10% deiodinated derivative). $[\alpha]_D^{23}$ + 2.0 (*c* 1.0, $CHCl_3$); R_f 0.24 (15% acetone/pentane); mp = 53–59 °C; ν_{max} (film)/cm^{-1} 3422 (OH), 2922, 1662 (C=O), 1479, 1424, 1364, 1234, 1163, 1129, 1059, 1006, 816, 764; ^{1}H NMR (400 MHz, $CDCl_3$, 298 K) δ 7.66–7.61 (m, 2 H, HC_{Ar}), 6.99–6.93 (m, 2 H, HC_{Ar}), 4.36 (br d, *J* = 13.2 Hz, 1 H, NC*H*HCHCH$_2$OH), 4.20 (br s, 1 H, NC*H*HCH$_2$), 3.44 (dt, *J* = 11.0, 3.5 Hz, 1 H, C*H*HOH), 3.26 (dt, *J* = 11.3, 5.8 Hz, 1 H, CH*H*OH), 2.87–2.63 (m, 2 H, NCH*H*CHCH$_2$OH, NCH*H*CH$_2$), 2.51 (ddd, *J* = 10.2, 5.2, 5.2, 5.2 Hz, 1 H, CHAr), 1.87–1.72 (m, 2 H, C*H*CH$_2$OH, NCH$_2$C*H*H), 1.71–1.58 (m, 2 H, NCH$_2$CH*H*, OH), 1.49 (s, 9 H, C(CH$_3$)$_3$); ^{13}C NMR (101 MHz, $CDCl_3$, 298 K, observed as a mixture of rotamers) δ 154.8 (C=O), 143.5 (C_{Ar} quat), 137.7 (2 × C_{Ar}), 129.5 (2 × C_{Ar}), 91.7 (IC_{Ar} quat), 79.7 (*C*(CH$_3$)$_3$), 63.0 (CH_2OH), 46.4 (br m, NCH_2CHCH$_2$OH), 44.4 and 43.5 (N*C*H$_2$CH$_2$, CHAr, *C*HCH$_2$OH), 33.8 (NCH$_2$*C*H$_2$), 28.5 (C(*C*H$_3$)$_3$); HRMS (ESI$^+$) *m*/*z* Calculated for $C_{17}H_{25}NO_3{}^{127}I$ [M+H] 418.0879; Found 418.0886.

HPLC Conditions: Chiralpak ID 3-column, 90:10 *n*-hexane:*i*-PrOH, flow rate: 1 mL·min^{-1}, 35 ºC, UV detection wavelength: 230.1 nm. Retention times: 6.7 min (3*R,*4*S* enantiomer), 7.4 min (3*S,*4*R* enantiomer).

tert-Butyl (–)-(*3S,4R*)-4-(4-iodophenyl)-3-(hydroxymethyl)piperidine-1-carboxylate ((–)-56)



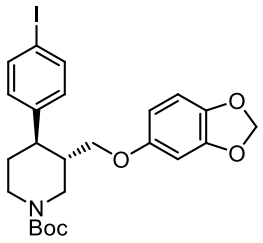
A flame-dried round-bottom flask was charged with amide **(+)-54** (558 mg, 1.00 mmol), followed by Boc_2O (873 mg, 4.00 mmol) and DMAP (24.4 mg, 0.20 mmol). The reaction vessel was sealed and purged with argon, then anhydrous MeCN (3.3 mL) and anhydrous CH_2Cl_2 (0.5 mL) were added by syringe. The mixture (0.3 M) was then stirred at 40 ºC for 22 h. The reaction mixture was then allowed to cool to rt and sat. aq. NH_4Cl (5 mL) and CH_2Cl_2 (5 mL) were added.

The phases were separated, and the aqueous layer was extracted with CH_2Cl_2 (3 × 10 mL). The combined organic extracts were dried over Na_2SO_4 and filtered. The solvent was removed under reduced pressure to afford the crude *N*-Boc protected piperidine derivative. This solubilised in anhydrous THF (3.5 mL, 0.3 M) and the resulting solution was added dropwise to a suspension of $LiAlH_4$ (75.9 mg, 2.00 mmol) in anhydrous THF (1.5 mL, 1.0 M) at 0 °C under argon atmosphere. The mixture was then stirred at 20 °C for 30 min. The reaction mixture was then quenched by slow addition of sat. aq. NH_4Cl (5 mL) at 0 °C and stirred at rt for 30 min. The resulting suspension was filtered through a pad of Celite, eluting with EtOAc (3 × 10 mL). The phases were separated, and the aqueous layer was extracted with EtOAc (3 × 10 mL). The combined organic extracts were dried over Na_2SO_4 and filtered. The solvent was removed under reduced pressure. Purification by flash column chromatography (10% to 15% acetone/pentane) afforded primary alcohol **(–)-56** as a white solid (315 mg, 75% over 2 steps, 98.0% *ee*, containing approx. 15% deiodinated derivative). $[\alpha]_D^{23}$ – 8.0 (*c* 1.0, $CHCl_3$).

Characterisation data identical to that reported for enantiomeric alcohol **(+)-56** (page 275).

HPLC Conditions: Chiralpak ID 3-column, 90:10 *n*-hexane:*i*-PrOH, flow rate: 1 mL·min^{-1}, 35 ºC, UV detection wavelength: 230.1 nm. Retention times: 6.7 min (3*R,*4*S* enantiomer), 7.4 min (3*S,*4*R* enantiomer).

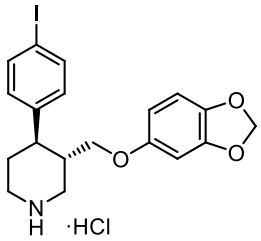
tert-Butyl (3*S*,4*R*)-3-((benzo[*d*][1,3]dioxol-5-yloxy)methyl)-4-(4-iodophenyl)piperidine-1-carboxylate ((–)-58)



Alcohol **(–)-56** (203 mg, 0.49 mmol) and triethylamine (96 μL, 0.69 mmol) were added to a flame-dried round-bottom flask, dissolved in anhydrous CH_2Cl_2 (2.5 mL, 0.2 M) and cooled down to 0 °C. Methanesulfonyl chloride (49 μL, 0.64 mmol) was then added by Gilson pipette. After stirring 5 min at 0 °C, the reaction mixture was stirred at 25 °C for 2 h, then diluted with CH_2Cl_2 (5 mL) and sat. aq. $NaHCO_3$ (5 mL). The phases were separated, and the aqueous layer was extracted with CH_2Cl_2 (3 × 10 mL). The combined organic extracts were dried over Na_2SO_4 and filtered. The solvent was removed under reduced pressure to afford the crude mesylated alcohol derivative. NaH (60% dispersion in mineral oil, 45.2 mg, 1.10 mmol) was added to a solution of sesamol (135 mg, 0.98 mmol) in anhydrous DMF (3.0 mL, 0.3 M) at 0 °C. The mixture was then stirred at 25 °C for 1 h. A solution of the crude mesylated alcohol in dry DMF (2.0 mL, 0.2 M) was then added dropwise to this suspension. The resulting mixture was stirred at 90 °C for 20 h. The reaction mixture was quenched by addition of H_2O (5 mL) and aq NaOH 1 N (5 mL) and EtOAc (10 mL) were then added. The phases were separated, and the aqueous layer was extracted with EtOAc (4 × 20 mL). The combined organic extracts were washed with brine (2 × 50 mL), dried over

Na_2SO_4 and filtered. The solvent was removed under reduced pressure. Purification by flash column chromatography (5% acetone/pentane) afforded piperidine **(–)-58** as a white solid (188 mg, 71% over 2 steps). $[\alpha]_D^{23}$ – 43.3 (*c* 1.2, $CHCl_3$). R_f 0.15 (5% acetone/pentane); mp = 51–54 °C; ν_{max} (film)/cm^{-1} 2919, 1685 (C=O), 1483, 1424, 1230, 1163, 1129, 1036, 1106, 928, 813, 764; ^{1}H NMR (400 MHz, $CDCl_3$, 298 K) δ 7.65–7.59 (m, 2 H, HC_{Ar}), 6.67–6.91 (m, 2 H, HC_{Ar}), 6.64 (d, *J* = 8.4 Hz, 1 H, HC_{Ar}), 6.36 (d, *J* = 2.5 Hz, 1 H, HC_{Ar}), 6.14 (dd, *J* = 8.5, 2.5 Hz, 1 H, HC_{Ar}), 5.89 (s, 2 H, OCH_2O), 4.43 (br s, 1 H, NC*H*HCHCH$_2$OAr), 4.25 (br s, 1 H, NC*H*HCH$_2$), 3.61 (dd, *J* = 9.4, 2.9 Hz, 1 H, C*H*HOAr), 3.45 (dd, *J* = 9.4, 6.4 Hz, 1 H, CH*H*OAr), 2.91–2.71 (br m, 2 H, NCH*H*CHCH$_2$OAr, NCH*H*CH$_2$), 2.65 (ddd, *J* = 11.8, 11.8, 3.8 Hz, 1 H, CHAr), 2.08–1.96 (br m, 1 H, C*H*CH$_2$OAr), 1.86–1.76 (br m, 1 H, NCH$_2$C*H*H), 1.76–1.63 (m, 1 H, NCH$_2$CH*H*), 1.50 (s, 9 H, C(CH$_3$)$_3$); ^{13}C NMR (101 MHz, $CDCl_3$, 298 K) δ 154.7 (C=O), 154.2 (OC_{Ar} quat), 148.1 (OC_{Ar} quat), 143.1 (C_{Ar} quat), 141.7 (OC_{Ar} quat), 137.7 (2 × C_{Ar}), 129.4 (2 × C_{Ar}), 107.8 (C_{Ar}), 105.5 (C_{Ar}), 101.1 (OCH_2O), 98.0 (C_{Ar}), 91.8 (IC_{Ar} quat), 79.7 (*C*(CH$_3$)$_3$), 68.7 (CH$_2$OAr), 47.0 (br m, N*C*H$_2$CHCH$_2$OAr), 44.3 (N*C*H$_2$CH$_2$, CHAr), 41.6 (*C*HCH$_2$OAr), 33.6 (NCH$_2$*C*H$_2$), 28.4 (C(*C*H$_3$)$_3$); HRMS (ESI$^+$) *m*/*z* Calculated for $C_{24}H_{29}NO_5{}^{127}I$ [M+H] 538.1090; Found 538.1104.

(3*S*,4*R*)-3-((Benzo[*d*][1,3]dioxol-5-yloxy)methyl)-4-(4-iodophenyl)piperidine-1-ium chloride (50)



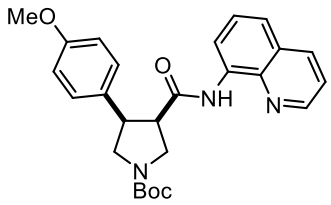
4 N HCl in 1,4-dioxane (250 μL, 1.00 mmol) was added to a solution of *N*-Boc protected piperidine **(–)-58** (56.9 mg, 0.10 mmol) in 1,4-dioxane (250 μL, 0.4 M) at 0 °C under air. The solution was stirred at 25 ºC for 18 h, then an ice-cold 1:1 mixture of Et_2O/pentane (1 mL) was added and formation of a solid precipitate was observed. This was filtered and washed with further ice-cold Et_2O/pentane mixture (2 × 5 mL). The solid precipitate was dried under reduced pressure to afford (3*S*,4*R*)-3-((benzo[*d*][1,3]dioxol-5-yloxy)methyl)-4-(4-iodophenyl)piperidine-1-ium chloride **50** (38.5 mg, 81%) as an off-white solid. $[\alpha]_D^{23}$ – 86.0 (*c* 0.9, MeOH); mp = 203–205 ºC; ν_{max} (film)/cm^{-1} 3321 (NH), 2926, 2807, 1618, 1484, 1185, 1103, 1033, 1003, 932, 846, 813, 787; ^{1}H NMR (400 MHz, CD_3OD, 298 K) δ 7.71–7.64 (m, 2 H, HC_{Ar}), 7.11–7.04 (m, 2 H, HC_{Ar}), 6.63 (d, *J* = 8.5 Hz, 1 H, HC_{Ar}), 6.39 (d, *J* = 2.5 Hz, 1 H, HC_{Ar}), 6.18 (dd, *J* = 8.5, 2.5 Hz, 1 H, HC_{Ar}), 5.89–5.82 (m, 2 H, OCH_2O), 3.71–3.62 (m, 2 H, C*H*HOAr, NC*H*HCHCH$_2$OAr), 3.60–3.48 (m, 2 H, CH*H*OAr, NC*H*HCH$_2$), 2.21–2.11 (m, 2 H, NCH*H*CHCH$_2$OAr, NCH*H*CH$_2$), 3.00–2.90 (m, 1 H, CHAr), 2.49–2.37 (m, 1 H, C*H*CH$_2$OAr), 2.09–2.00 (m, 2 H, NCH$_2$C*H*$_2$); ^{13}C NMR (101 MHz, CD_3OD, 298 K) δ 155.2 (OC_{Ar} quat), 149.7 (OC_{Ar} quat), 143.5 (C_{Ar} quat), 143.0 (OC_{Ar} quat), 139.1 (2 × C_{Ar}), 130.7 (2 × C_{Ar}), 108.8 (C_{Ar}), 106.6 (C_{Ar}), 102.5 (OCH_2O), 98.9 (C_{Ar}), 93.1 (IC_{Ar} quat), 68.9 (CH$_2$OAr), 47.7

(NCH_2CHCH_2OAr), 45.4 (NCH_2CH_2), 43.0 (CHAr), 40.5 (CHCH_2OAr), 31.3 (NCH$_2C$H$_2$); HRMS (ESI$^+$) *m*/*z* Calculated for $C_{19}H_{21}NO_3{}^{127}I$ [M–Cl] 438.0566; Found 438.0571.

8.2.3 Compounds for Chapter 4: Fragment Library Synthesis

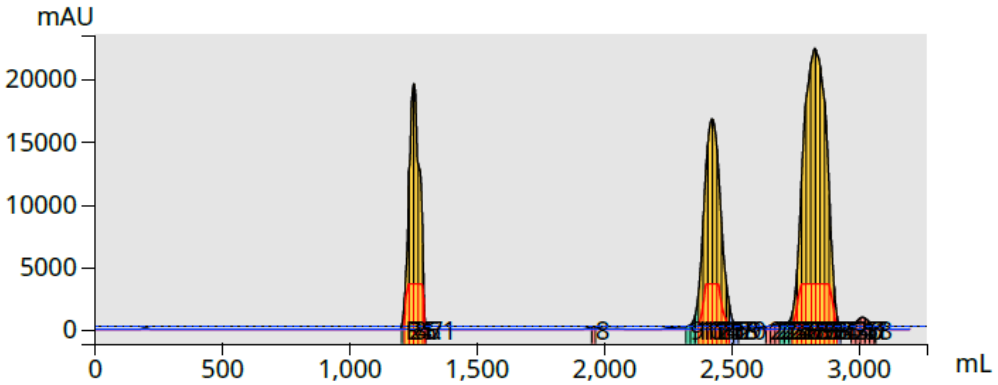
*8.2.3.1 Pyrrolidine and piperidine C(4)–H arylation (**3a**, **3d**, **5**, **25a**, **26a**, **26c**, **59**)*

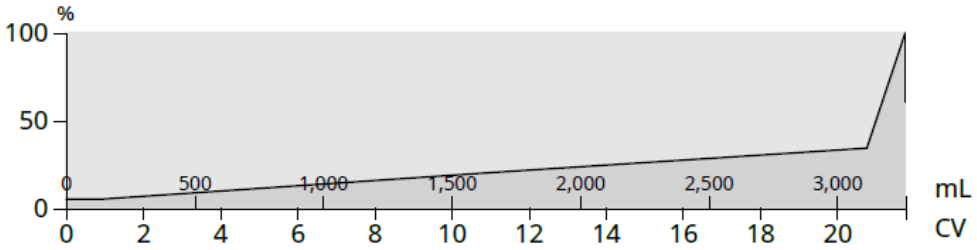
tert-Butyl _cis_-(±)-3-(4-methoxyphenyl)-4-(quinolin-8-ylcarbamoyl)pyrrolidine-1-carboxylate (3a)



A large microwave vial (10–20 mL recommended volume) was charged with K_2CO_3 (550 mg, 4.00 mmol), flame-dried, and allowed to cool under argon. Amide **2** (1.37 g, 4.00 mmol), 4-iodoanisole (2.81 g, 12.0 mmol), $Pd(OAc)_2$ (45.0 mg, 0.20 mmol) and PivOH (410 mg, 4.00 mmol) were added sequentially. The reaction vessel was sealed and purged with argon, then $PhCF_3$ (2.0 mL, 2.0 M) was added by syringe. The reaction tube was then placed in a preheated oil bath and stirred at 110 ºC for 18 h. The reaction mixture was then allowed to cool to rt and EtOAc (20 mL) was added. The resulting mixture was filtered through a pad of silica, eluting with further EtOAc (2 × 50 mL). The solvent was removed under reduced pressure, and the crude material was purified by automated flash column chromatography (silica, 0–100% acetone/pentane). The product containing fractions were combined and the solvent was removed under reduced pressure. Et_2O (10 mL) and pentane (10 mL) were added and the solvent was removed under reduced pressure to afford the *cis*-arylated product **3a** as a pale yellow solid (1.02 g, 56%).

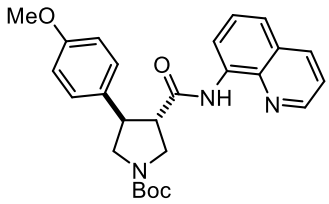
Automated Column Conditions: Run on Biotage® Selekt. Column Type: Biotage® Sfär HC 100 g. Flow Rate: 120 mL/min. Sample Mass: 5000 mg. Solvent A: Pentane, Solvent B: acetone. UV wavelength detection: λ 200–400 nm. See trace and gradient below. From the left: 1st peak: unreacted aryl iodide. 2nd peak: Unreacted starting material. 3rd peak: *cis*-arylated product **3a**.





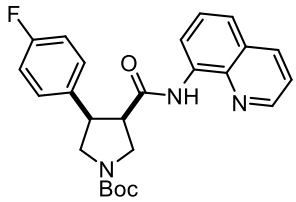
The observed characterisation data was identical to what previously reported for pyrrolidine **3a** (page 208).

***tert*-Butyl *trans*-(±)-3-(4-methoxyphenyl)-4-(quinolin-8-ylcarbamoyl)pyrrolidine-1-carboxylate (5)**



See procedure at page 233.

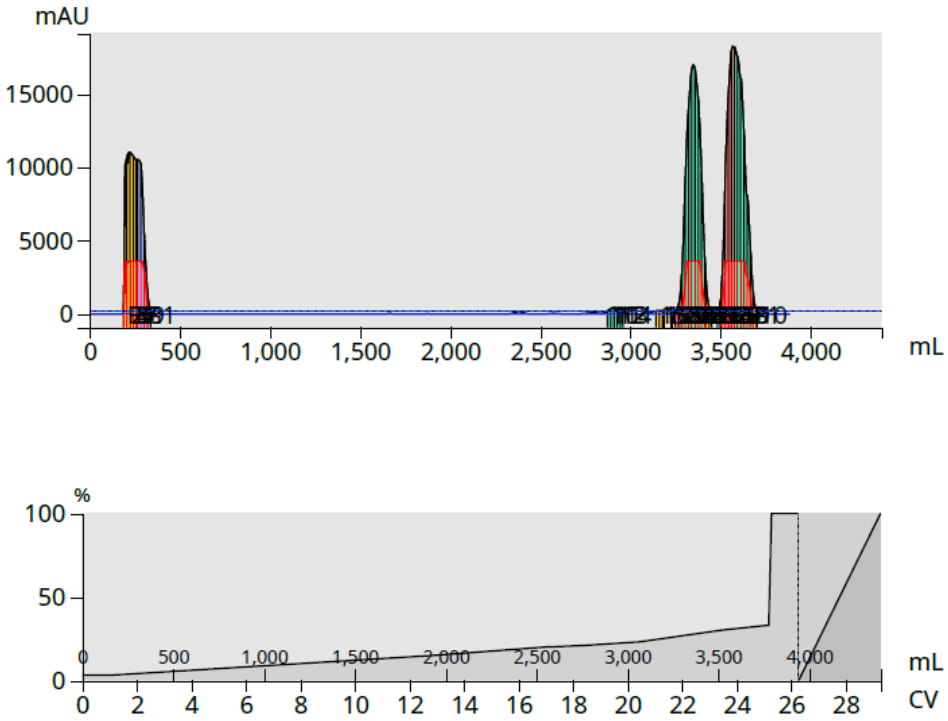
***tert*-Butyl *cis*-(±)-3-(4-fluorophenyl)-4-(quinolin-8-ylcarbamoyl)pyrrolidine-1-carboxylate (3d)**



A large microwave vial (10–20 mL recommended volume) was charged with K_2CO_3 (550 mg, 4.00 mmol), flame-dried, and allowed to cool under argon. Amide **2** (1.37 g, 4.00 mmol), 4-fluoroiodobenzene (3.55 g, 16.0 mmol), $Pd(OAc)_2$ (45.0 mg, 0.20 mmol) and PivOH (410 mg, 4.00 mmol) were added sequentially. The reaction vessel was sealed and purged with argon, then $PhCF_3$ (2.0 mL, 2.0 M) was added by syringe. The reaction tube was then placed in a preheated oil bath and stirred at 110 ºC for 18 h. The reaction mixture was then allowed to cool to rt and EtOAc (20 mL) was added. The resulting mixture was filtered through a pad of silica, eluting with further EtOAc (2 × 50 mL). The solvent was removed under reduced pressure, and the crude material was purified by automated flash column chromatography (silica, 0–100% acetone/pentane). The product containing fractions were combined and the solvent was removed under reduced pressure. Et_2O (10 mL) and pentane (10 mL) were added and the solvent was removed under reduced pressure to afford the *cis*-arylated product **3d** as an off-white solid (810 mg, 46%).

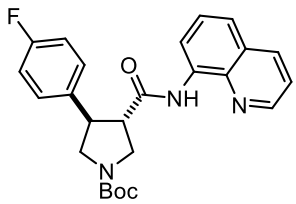
The same procedure was repeated on a second batch of amide **2** (1.00 g, 3.00 mmol), using K_2CO_3 (415 mg, 3.00 mmol), 4-fluoroiodobenzene (2.67 g, 12.0 mmol), $Pd(OAc)_2$ (33.8 mg, 0.15 mmol), PivOH (307 mg, 3.00 mmol) and $PhCF_3$ (1.5 mL, 2.0 M). Purification by automated flash column chromatography (silica, 0–100% acetone/pentane) afforded the *cis*-arylated product **3d** as an off-white solid (573 mg, 44%).

Automated Column Conditions: Run on Biotage® Selekt. Column Type: Biotage® Sfär HC 100 g. Flow Rate: 120 mL/min. Sample Mass: 5000 mg. Solvent A: Pentane, Solvent B: acetone. Solvent C: MeOH. UV wavelength detection: λ 200–400 nm. See trace and gradient below. From the left: 1st peak: unreacted aryl iodide. 2nd peak: Unreacted starting material. 3rd peak: *cis*-arylated product **3d**.



The observed characterisation data was identical to what previously reported for pyrrolidine **3d** (page 215).

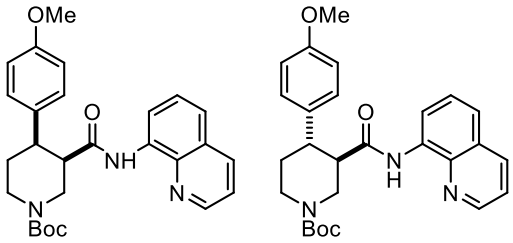
***tert*-Butyl *trans*-(±)-3-(4-fluorophenyl)-4-(quinolin-8-ylcarbamoyl)pyrrolidine-1-carboxylate (59)**



A large microwave vial (10–20 mL recommended volume) was charged with K_2CO_3 (550 mg, 4.00 mmol), flame-dried, and allowed to cool under argon. Amide **2** (1.37 g, 4.00 mmol), 4-fluoroiodobenzene (3.55 g, 16.0 mmol), $Pd(OAc)_2$ (45.0 mg, 0.20 mmol) and PivOH (410 mg, 4.00 mmol) were added sequentially.

The reaction vessel was sealed and purged with argon, then $PhCF_3$ (2.0 mL, 2.0 M) was added by syringe. The reaction tube was placed in a preheated oil bath and stirred at 110 ºC for 18 h. The reaction mixture was then allowed to cool to rt and $PhCF_3$ (2.0 mL, 1.0 M) and DBU (1.8 mL, 12.0 mmol) were added by syringe. The reaction vessel was then stirred at 110 °C for additional 3 h. The reaction mixture was allowed to cool to rt and EtOAc (20 mL) was added. The resulting mixture was filtered through a pad of Celite, eluting with further EtOAc (2 × 50 mL). The solvent was removed under reduced pressure, and the crude material was purified by flash column chromatography (5% Et_2O/CH_2Cl_2). The product containing fractions were combined and the solvent was removed under reduced pressure. Et_2O (10 mL) and pentane (10 mL) were added and the solvent was removed under reduced pressure to afford the *cis*-arylated product **59** as a pale yellow solid (620 mg, 36%). R_f 0.23 (5% Et_2O/CH_2Cl_2). mp = 70–74 °C (from Et_2O/pentane); ν_{max} (film)/cm^{-1} 3332 (NH br), 2974, 1685 (C=O), 1528, 1486, 1387, 1327, 1159, 1126, 828, 790; ^{1}H NMR (500 MHz, DMSO-d_6, 373 K) δ 9.82 (br s, 1 H, NH), 8.78 (dd, J = 4.2, 1.7 Hz, 1 H, HC_{Ar}), 8.54 (dd, J = 7.7, 1.3 Hz, 1 H, HC_{Ar}), 8.32 (dd, J = 8.3, 1.7 Hz, 1 H, HC_{Ar}), 7.62 (dd, J = 8.3, 1.3 Hz, 1 H, HC_{Ar}), 7.57 (dd, J = 8.3, 4.2 Hz, 1 H, HC_{Ar}), 7.53 (t, J = 7.9 Hz, 1 H, HC_{Ar}), 7.49–7.44 (m, 2 H, HC_{Ar}), 7.14–7.08 (m, 2 H, HC_{Ar}), 3.93–3.86 (m, 2 H, NC*H*HCHAr, NC*H*HCHCO), 3.78–3.69 (m, 2 H, CHCO, CHAr), 3.65–3.58 (m, 1 H, NCH*H*CHCO), 3.38–3.32 (m, 1 H, NCH*H*CHAr), 1.46 (s, 9 H, $C(CH_3)_3$); ^{13}C NMR (126 MHz, DMSO-d_6, 373 K) δ 169.2 (C=O amide), 161.0 (d, J_{CF} = 243.5 Hz, FC_{Ar} quat), 152.9 (C=O carbamate), 148.0 (C_{Ar}), 137.7 (C_{Ar} quat), 135.8 (C_{Ar}), 135.1 (d, J_{CF} = 2.9 Hz, F-*p*-C_{Ar} quat), 133.6 (C_{Ar} quat), 129.0 (d, J_{CF} = 8.1 Hz, 2 × F-*m*-C_{Ar}), 127.3 (C_{Ar} quat), 126.2 (C_{Ar}), 121.5 (C_{Ar}), 121.4 (C_{Ar}), 116.3 (C_{Ar}), 114.8 (d, J_{CF} = 21.3 Hz, 2 × F-*o*-C_{Ar}), 78.2 (*C*$(CH_3)_3$), 52.4 (N*C*H_2CHAr), 50.9 (*C*HCO), 48.5 (N*C*H_2CHCO), 46.0 (CHAr), 27.7 (C(*C*$H_3)_3$); ^{19}F NMR (471 MHz, DMSO-d_6, 373 K) δ –115.9 (tt, J_{HF} = 9.7, 5.6 Hz); HRMS (ESI$^+$) *m*/*z* Calculated for $C_{25}H_{27}N_3O_3F$ [M+H] 436.2036; Found 436.2030.

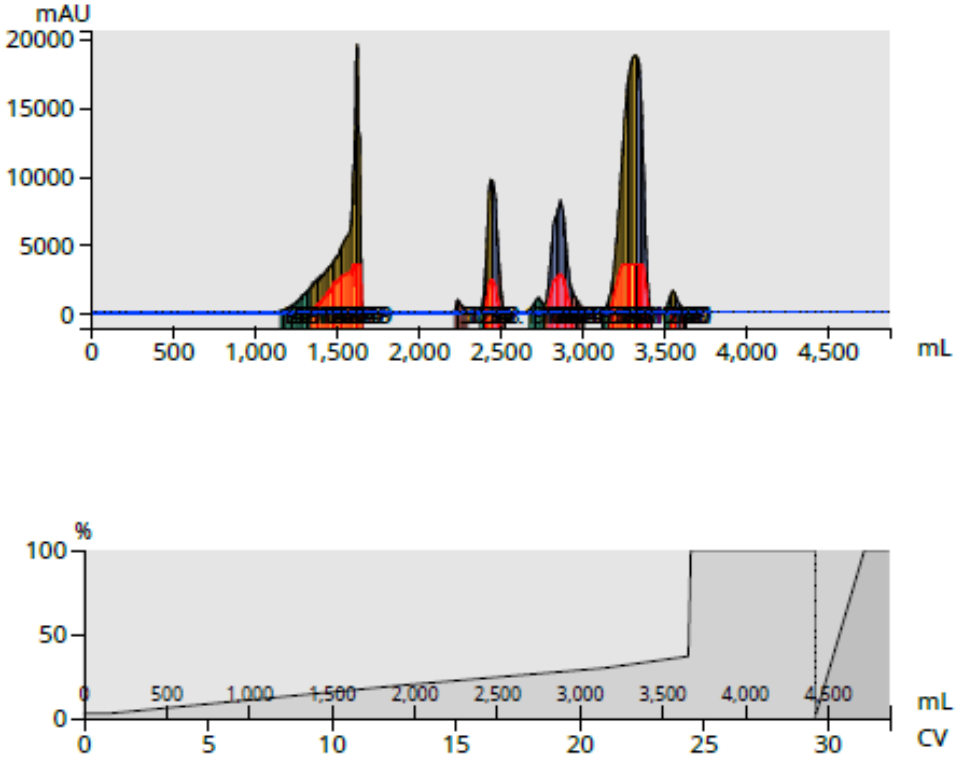
tert-Butyl _cis_-(±)-4-(4-methoxyphenyl)-3-(quinolin-8-ylcarbamoyl)piperidine-1-carboxylate (25a) and **_tert_-butyl _trans_-(±)-4-(4-methoxyphenyl)-3-(quinolin-8-ylcarbamoyl)piperidine-1-carboxylate (26a)**



A large microwave vial (10–20 mL recommended volume) was charged with K_2CO_3 (550 mg, 4.00 mmol), flame-dried, and allowed to cool under argon. Amide **24** (1.42 g, 4.00 mmol), 4-iodoanisole (2.81 g, 12 mmol), $Pd(OAc)_2$ (45.0 mg, 0.20 mmol) and PivOH (410 mg, 4.00 mmol) were added sequentially. The reaction vessel was sealed and purged with argon, then $PhCF_3$ (2.0 mL, 2.0 M) was added by syringe. The reaction tube was then placed in a preheated oil bath and

stirred at 110 ºC for 18 h. The reaction mixture was then allowed to cool to rt and EtOAc (20 mL) was added. The resulting mixture was filtered through a pad of silica, eluting with further EtOAc (2 × 50 mL). The solvent was removed under reduced pressure, and the crude material was purified by automated flash column chromatography (silica, 0–100% acetone/pentane). The product containing fractions were combined and the solvent was removed under reduced pressure. Et_2O (10 mL) and pentane (10 mL) were added and the solvent was removed under reduced pressure to afford the minor product *tert*-butyl *trans*-(±)-4-(4-methoxyphenyl)-3-(quinolin-8-ylcarbamoyl) piperidine-1-carboxylate **26a** as a white solid (286 mg, 15%) and the major product *tert*-butyl *cis*-(±)-4-(4-methoxyphenyl)-3-(quinolin-8-ylcarbamoyl)piperidine-1-carboxylate **25a** as a white solid (852 mg, 46%).

Automated Column Conditions: Run on Biotage® Selekt. Column Type: Biotage® Sfär HC 100 g. Flow Rate: 120 mL/min. Sample Mass: 5000 mg. Solvent A: Pentane, Solvent B: acetone. Solvent C: MeOH. UV wavelength detection: λ 200–400 nm. See trace and gradient below. From the left: 1st peak: unreacted aryl iodide. 2nd peak: Unreacted starting material. 3rd peak: *trans*-arylated product **26a**. 4th peak: *cis*-arylated product **25a**.



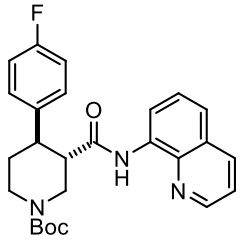
The same procedure was repeated on a second batch of amide **24** (1.22 g, 3.40 mmol), using K_2CO_3 (470 mg, 3.40 mmol), 4-iodoanisole (2.41 g, 10.3 mmol), $Pd(OAc)_2$ (38.3 mg, 0.17 mmol), PivOH (348 mg, 3.40 mmol) and $PhCF_3$ (1.7 mL, 2.0 M). Manual purification by flash column chromatography (5% to 15% acetone/pentane) afforded the minor product *tert*-

butyl *trans*-(±)-4-(4-methoxyphenyl)-3-(quinolin-8-ylcarbamoyl) piperidine-1-carboxylate **26a** as a white solid (253 mg, 16%) and the major product *tert*-butyl *cis*-(±)-4-(4-methoxyphenyl)-3-(quinolin-8-ylcarbamoyl)piperidine-1-carboxylate **25a** as a white solid (821 mg, 52%).

Major (**25a**): The observed characterisation data was identical to what previously reported for pyrrolidine **25a** (page 236).

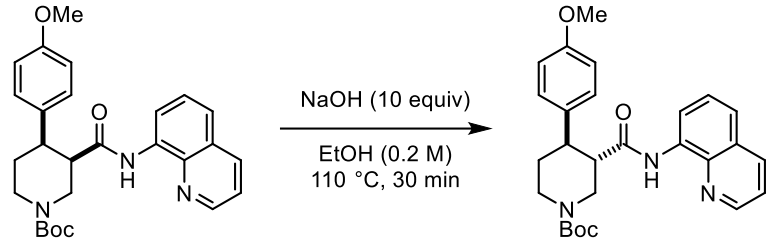
Minor (**26a**): The observed characterisation data was identical to what previously reported for pyrrolidine **26a** (page 236).

***tert*-Butyl *trans*-(±)-3-(4-fluorophenyl)-4-(quinolin-8-ylcarbamoyl)piperidine-1-carboxylate (26c)**



See procedure at page 249.

*8.2.3.2 Epimerisation of cis-3,4-disubstituted piperidine **25a***

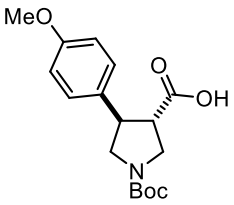


25a **26a**

A flame-dried round-bottom-flask was charged with *cis*-arylated amide **25a** (224 mg, 0.49 mmol) and EtOH (2.5 mL, 0.2 M). NaOH (powder, 199 mg, 4.90 mmol) was then added and the resulting mixture was stirred at 100 ºC for 30 min. The reaction crude was allowed to cool down to rt and diluted with EtOAc (5 mL) and H_2O (5 mL). The phases were separated, and the aqueous layer was extracted with EtOAc (3 × 10 mL). The combined organic extracts were dried over Na_2SO_4 and filtered. The solvent was removed under reduced pressure. Et_2O (5 mL) and pentane (5 mL) were added and the solvent was removed under reduced pressure to afford pure *trans*-3,4-disubstituted piperidine **26a** as a white solid (220 mg, 97%). Characterisation data identical to that reported for *trans*-piperidine **26a** (page 236).

8.2.3.3 Directing group removal: carboxylic acid derivatives (**30–64**)

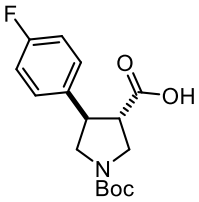
***trans*-(±)-1-(*tert*-Butoxycarbonyl)-4-(4-methoxyphenyl)pyrrolidine-3-carboxylic acid (30)**



A round-bottom-flask was charged with *cis*-arylated amide **3a** (290 mg, 0.65 mmol) and EtOH (3.3 mL, 0.2 M). NaOH (powder, 263 mg, 6.50 mmol) was then added and the resulting mixture was stirred at 100 ºC for 30 min. The reaction crude was allowed to cool down to rt and diluted with EtOAc (5 mL) and 1 N NaOH (5 mL). The aqueous alkaline layer was collected, and the organic layer extracted with 1 N NaOH (3 × 10 mL). All the aqueous alkaline layers were combined, washed with EtOAc (30 mL), and acidified to pH ~ 1 with HCl, 37%. The acidic layer was extracted with EtOAc (5 × 40 mL). The combined organic extracts were dried over Na_2SO_4 and filtered. Solvent was removed under reduced pressure. Et_2O (5 mL) and pentane (5 mL) were added and the solvent was removed under reduced pressure to afford the pure *trans*-acid **30** as a pale orange solid (172 mg, 82%).

The observed characterisation data was identical to what previously reported for pyrrolidine **30** (page 253).

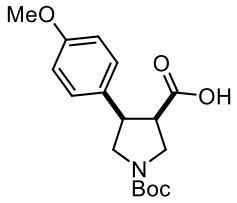
***trans*-(±)-1-(*tert*-Butoxycarbonyl)-4-(4-fluorophenyl)pyrrolidine-3-carboxylic acid (60)**



A round-bottom-flask was charged with *cis*-arylated amide **3d** (310 mg, 0.71 mmol) and EtOH (3.5 mL, 0.2 M). NaOH (powder, 288 mg, 7.10 mmol) was then added and the resulting mixture was stirred at 100 ºC for 30 min. The reaction crude was allowed to cool down to rt and diluted with EtOAc (5 mL) and 1 N NaOH (5 mL). The aqueous alkaline layer was collected, and the organic layer extracted with 1 N NaOH (3 × 10 mL). All the aqueous alkaline layers were combined, washed with EtOAc (30 mL), and acidified to pH ~ 1 with HCl, 37%. The acidic layer was extracted with EtOAc (5 × 40 mL). The combined organic extracts were dried over Na_2SO_4 and filtered. Solvent was removed under reduced pressure. Et_2O (5 mL) and pentane (5 mL) were added and the solvent was removed under reduced pressure to afford the pure *trans*-acid **60** as a pale yellow solid (210 mg, 96%). R_f 0.12 (5% MeOH/CH_2Cl_2). mp = decomposed at T >120 °C; ν_{max} (film)/cm^{-1} 2978 (OH br), 1726 (C=O), 1655 (C=O), 1513, 1420, 1226, 1141, 835; ^{1}H NMR (500 MHz, DMSO-d_6, 373 K) δ 7.38–7.33 (m, 2 H, HC_{Ar}), 7.14–7.08 (m, 2 H, HC_{Ar}), 3.78 (dd, J = 10.5, 7.8 Hz, 1 H, NC*H*HCHAr), 3.74 (dd, J = 10.6, 8.2 Hz, 1 H, NC*H*HCHCO), 3.58 (ddd, J = 9.3, 9.3, 7.7 Hz, 1 H, CHAr), 3.48 (dd, J = 10.8, 8.5 Hz, 1 H, NCH*H*CHCO), 3.26 (dd, J = 10.6, 9.2 Hz, 1 H, NCH*H*CHAr), 3.19 (ddd, J = 9.6, 8.4, 8.4 Hz, 1 H, CHCO), 1.44 (s, 9 H, $C(CH_3)_3$); ^{13}C NMR (126 MHz, DMSO-d_6, 373 K) δ 172.4 (COOH), 160.8 (d, J_{CF} = 243.1 Hz, FC_{Ar} quat), 152.8 (C=O carbamate), 135.7 (d, J_{CF} = 3.1 Hz, F-*p*-C_{Ar}

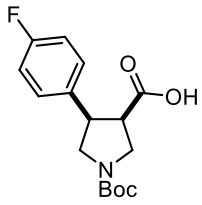
quat), 128.6 (d, J_{CF} = 8.1 Hz, 2 × F-*m*-C_{Ar}), 114.5 (d, J_{CF} = 21.3 Hz, 2 × F-*o*-C_{Ar}), 78.2 (*C*$(CH_3)_3$), 52.0 (N*C*H_2CHAr), 48.7 (*C*HCO), 48.0 (N*C*H_2CHCO), 45.6 (CHAr), 27.7 (C(*C*$H_3)_3$); ^{19}F NMR (471 MHz, DMSO-d_6, 373 K) δ –116.2 (tt, J_{HF} = 9.3, 5.5 Hz); HRMS (FTMS – pAPCI) *m*/*z* Calculated for $C_{16}H_{19}NO_4F^-$ $[M–H]^-$ 308.1293; Found 308.1301.

cis-(±)-1-(_tert_-Butoxycarbonyl)-4-(4-methoxyphenyl)pyrrolidine-3-carboxylic acid (36)



See procedure at page 257.

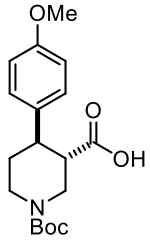
cis-(±)-1-(_tert_-Butoxycarbonyl)-4-(4-fluorophenyl)pyrrolidine-3-carboxylic acid (61)



A flame-dried reaction tube was charged with *cis*-arylated amide **3d** (283 mg, 0.65 mmol), followed by Boc_2O (709 mg, 3.25 mmol) and DMAP (159 mg, 1.30 mmol). The reaction vessel was sealed and purged with argon, then anhydrous MeCN (1.3 mL, 0.5 M) was added by syringe. The reaction tube was placed in an oil bath and gradually warmed up to 55 ºC. The reaction mixture was then stirred at 55 °C for 1 h. The reaction mixture was allowed to cool to rt and sat. aq. NH_4Cl (3 mL) and CH_2Cl_2 (3 mL) were added. The phases were separated, and the aqueous layer was extracted with CH_2Cl_2 (3 × 5 mL). The combined organic extracts were dried over Na_2SO_4 and filtered. The solvent was removed under reduced pressure to afford the crude *N*-Boc protected pyrrolidine derivative. A solution of H_2O_2 (30 wt.% in H_2O, 332 μL, 3.25 mmol) in THF (1.5 mL) was added to a solution of $LiOH·H_2O$ (55.0 mg, 1.30 mmol) in H_2O (1.6 mL) at 0 °C under argon. The resulting mixture was added dropwise to a solution of crude *N*-Boc protected pyrrolidine in THF (3.4 mL) at 0 °C under argon. The reaction was then stirred at 20 °C for 1 h. Sat. aq. $Na_2S_2O_3$ (5 mL), EtOAc (5 mL) and 1 N NaOH (5 mL) were then added. The aqueous alkaline layer was collected, and the organic layer extracted with 1 N NaOH (3 × 15 mL). All the aqueous alkaline layers were combined, washed with EtOAc (40 mL), and acidified to pH ~ 1 with HCl, 37%. The acidic layer was extracted with EtOAc (5 × 50 mL). The combined organic extracts were dried over Na_2SO_4 and filtered. Solvent was removed under reduced pressure. Et_2O (5 mL) and pentane (5 mL) were added and the solvent was removed under reduced pressure to afford the pure *cis*-acid **61** as a white solid (192 mg, 95% over 2 steps). R_f 0.28 (20% acetone/pentane). mp = 125–128 °C (from Et_2O/pentane); ν_{max} (film)/cm^{-1} 2974 (OH br), 1730 (C=O), 1633 (C=O), 1510, 1428, 1204, 1129, 1156, 872; ^{1}H NMR (400 MHz, $CDCl_3$, 298 K, observed as a mixture of rotamers) δ 7.18–7.07 (m, 2 H,

HC_{Ar}), 7.00–6.90 (m, 2 H, HC_{Ar}), 3.80–3.58 (m, 5 H, NCH_2CHAr, NCH_2CHCO, CHAr), 3.36 (m, 1 H, CHCO), 1.49 and 1.48 (2 × s, 9 H, $C(CH_3)_3$); ^{13}C NMR (101 MHz, $CDCl_3$, 298 K, observed as a mixture of rotamers) δ 175.9 and 175.7 (COOH), 161.9 (d, J_{CF} = 245.9 Hz, FC_{Ar} quat), 154.5 (C=O carbamate), 134.0 and 133.8 (F-*p*-C_{Ar} quat, observed as singlets), 129.1 (d, J_{CF} = 8.0 Hz, 2 × F-*m*-C_{Ar}), 115.4 (d, J_{CF} = 21.3 Hz, 2 × F-*o*-C_{Ar}), 80.2 ($C(CH_3)_3$), 50.62 and 50.55 (NCH_2CHAr), 48.4 and 47.6 (*C*HCO), 46.7 and 46.6 (NCH_2CHCO), 45.3 and 44.4 (CHAr), 28.4 ($C(CH_3)_3$); ^{19}F NMR (377 MHz, $CDCl_3$, 298 K, observed as a mixture of rotamers) δ –115.0 (m); HRMS (ESI$^-$) *m*/*z* Calculated for $C_{16}H_{19}NO_4F$ [M–H] 308.1298; Found 308.1304.

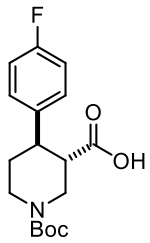
trans-(±)-1-(_tert_-Butoxycarbonyl)-4-(4-methoxyphenyl)piperidine-3-carboxylic acid (62)



A flame-dried reaction tube was charged with *trans*-arylated amide **26a** (280 mg, 0.61 mmol), followed by Boc_2O (533 mg, 2.40 mmol) and DMAP (14.9 mg, 0.12 mmol). The reaction vessel was sealed and purged with argon, then MeCN (2.0 mL, 0.3 M) was added by syringe. The reaction tube was then placed in an oil bath and gradually warmed up to 40 ºC. The reaction was then stirred at 40 °C for 20 h. The reaction mixture was allowed to cool to rt and sat. aq. NH_4Cl (3 mL) and CH_2Cl_2 (3 mL) were added. The phases were separated, and the aqueous layer was extracted with CH_2Cl_2 (3 × 5 mL). The combined organic extracts were dried over Na_2SO_4 and filtered. The solvent was removed under reduced pressure to afford the crude *N*-Boc protected piperidine derivative. A solution of H_2O_2 (30 wt.% in H_2O, 313 μL, 3.05 mmol) in THF (2.0 mL) was added to a solution of $LiOH{\cdot}H_2O$ (51.2 mg, 1.22 mmol) in H_2O (1.5 mL) at 0 °C under argon. The resulting mixture was added dropwise to a solution of crude *N*-Boc protected piperidine in THF (2.5 mL) at 0 °C under argon. The reaction was then stirred at 20 °C for 24 h. The reaction mixture was then allowed to cool down to rt and sat. aq. $Na_2S_2O_3$ (5 mL), EtOAc (5 mL) and 1 N NaOH (5 mL) were added. The aqueous alkaline layer was collected, and the organic layer extracted with 1 N NaOH (3 × 15 mL). All the aqueous alkaline layers were combined, washed with EtOAc (40 mL), and acidified to pH ~ 1 with HCl, 37%. The acidic layer was extracted with EtOAc (5 × 50 mL). The combined organic extracts were dried over Na_2SO_4 and filtered. Solvent was removed under reduced pressure. The crude material was purified by flash column chromatography (5% MeOH/CH_2Cl_2), the product containing fractions were combined and the solvent was removed under reduced pressure. Et_2O (5 mL) and pentane (5 mL) were added and the solvent was removed under reduced pressure to afford the pure *trans*-acid **62** as a white solid (183 mg, 89% over 2 steps). R_f 0.33 (5% MeOH/CH_2Cl_2). mp = 57–62 °C; ν_{max} (film)/cm^{-1} 2933 (OH br), 1692 (C=O), 1655 (C=O), 1513, 1428, 1286, 1238, 1156, 1126, 1033, 828, 764; ^{1}H NMR (400 MHz, $CDCl_3$, 298 K, observed as a mixture of rotamers) δ 7.09 (d, *J* = 8.3 Hz, 2 H, HC_{Ar}), 6.81 (d, *J* = 8.6 Hz, 2 H, HC_{Ar}), 4.37 (br s, 1 H, NC*H*HCHCO), 4.21 (br s, 1 H, NC*H*HCH_2), 3.78 (s, 3 H, OCH_3), 2.99–2.71 (m, 3 H, NCH*H*CHCO, NCH*H*CH_2, CHAr),

2.71–2.57 (m, 1 H, CHCO), 1.83–1.70 (m, 1 H, NCH_2CHH), 1.68–1.54 (m, 1 H, NCH_2CHH), 1.48 (s, 9 H, $C(CH_3)_3$); ^{13}C NMR (101 MHz, $CDCl_3$, 298 K, observed as a mixture of rotamers) δ 177.5 (br, COOH), 158.3 (OC_{Ar} quat), 154.5 (C=O carbamate), 134.6 (C_{Ar} quat), 128.2 (2 × C_{Ar}), 113.9 (2 × C_{Ar}), 80.2 ($C(CH_3)_3$), 55.1 (OCH_3), 48.8 (br, *C*HCO), 46.5 (br, NCH_2CHCO), 44.2 (CHAr), 43.7 (br, NCH_2CH_2), 32.8 (br, NCH_2CH_2), 28.4 ($C(CH_3)_3$); HRMS (ESI^+) *m*/*z* Calculated for $C_{18}H_{26}NO_5$ [M+H] 336.1811; Found 336.1824.

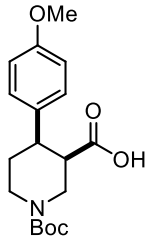
trans-(±)-1-(_tert_-Butoxycarbonyl)-4-(4-fluorophenyl)piperidine-3-carboxylic acid (63)



A flame-dried reaction tube was charged with *trans*-arylated amide **26c** (360 mg, 0.80 mmol), followed by Boc_2O (698 mg, 3.20 mmol) and DMAP (19.5 mg, 0.16 mmol). The reaction vessel was sealed and purged with argon, then anhydrous MeCN (2.7 mL, 0.3 M) was added by syringe. The reaction tube was placed in an oil bath and gradually warmed up to 40 ºC. The reaction mixture was then stirred at 40 °C for 20 h. The reaction mixture was allowed to cool to rt and sat. aq. NH_4Cl (3 mL) and CH_2Cl_2 (3 mL) were added. The phases were separated, and the aqueous layer was extracted with CH_2Cl_2 (3 × 5 mL). The combined organic extracts were dried over Na_2SO_4 and filtered. The solvent was removed under reduced pressure to afford the crude *N*-Boc protected piperidine derivative. A solution of H_2O_2 (30 wt.% in H_2O, 410 μL, 4.00 mmol) in THF (2.5 mL) was added to a solution of $LiOH{\cdot}H_2O$ (67.1 mg, 1.60 mmol) in H_2O (2.0 mL) at 0 °C under argon. The resulting mixture was added dropwise to a solution of crude *N*-Boc protected piperidine in THF (3.5 mL) at 0 °C under argon. The reaction was then stirred at 20 °C for 24 h. Sat. aq. $Na_2S_2O_3$ (5 mL), EtOAc (5 mL) and 1 N NaOH (5 mL) were then added. The aqueous alkaline layer was collected, and the organic layer extracted with 1 N NaOH (3 × 15 mL). All the aqueous alkaline layers were combined, washed with EtOAc (40 mL), and acidified to pH ~ 1 with HCl, 37%. The acidic layer was extracted with EtOAc (5 × 50 mL). The combined organic extracts were dried over Na_2SO_4 and filtered. Solvent was removed under reduced pressure. Et_2O (5 mL) and pentane (5 mL) were added and the solvent was removed under reduced pressure to afford the pure *trans*-acid **63** as a pale yellow solid (240 mg, 93% over 2 steps). R_f 0.23 (20% acetone/pentane). mp = 137–139 °C (from Et_2O/pentane); ν_{max} (film)/cm^{-1} 2974 (OH br), 1692 (C=O), 1655 (C=O), 1510, 1424, 1282, 1226, 1156, 1126, 831, 775; ^1H NMR (400 MHz, $CDCl_3$, 298 K, observed as a mixture of rotamers) δ 7.17–7.09 (m, 2 H, HC_{Ar}), 7.00–6.92 (m, 2 H, HC_{Ar}), 4.39 (br s, 1 H, NC*H*HCHCO), 4.22 (br s, 1 H, NC*H*HCH_2), 2.97–2.71 (m, 3 H, NCH*H*CHCO, CHAr, NCH*H*CH_2), 2.71–2.59 (m, 1 H, CHCO), 1.78 (dddd, *J* = 13.4, 2.8, 2.8, 2.8 Hz, 1 H, NCH_2CHH), 1.60 (dddd, *J* = 13.6, 13.6, 13.6, 4.1 Hz, 1 H, NCH_2CHH), 1.48 (s, 9 H, $C(CH_3)_3$); ^{13}C NMR (101 MHz, $CDCl_3$, 298 K, observed as a mixture of rotamers) δ 177.1 (COOH), 161.7 (d, J_{CF} = 245.0 Hz, FC_{Ar} quat), 154.4 (C=O carbamate), 138.1 (d, J_{CF} = 2.6 Hz, F-*p*-C_{Ar} quat), 128.7 (d, J_{CF} = 7.8 Hz, 2 × F-*m*-C_{Ar}), 115.4 (d, J_{CF} =

21.2 Hz, 2 × F-*o*-C_{Ar}), 80.4 (*C*$(CH_3)_3$), 48.7 (br, *C*HCO), 46.4 (br, N*C*H_2CHCO), 44.4 (CHAr), 43.6 (br, N*C*$H_2C H_2$), 32.7 (br, NCH_2*C*H_2), 28.4 (C(*C*$H_3)_3$); ^{19}F NMR (377 MHz, $CDCl_3$, 298 K) δ –115.6 (br s); HRMS (ESI$^+$) *m*/*z* Calculated for $C_{17}H_{23}NO_4F$ [M+H] 324.1611; Found 324.1625.

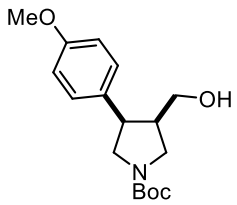
cis-(±)-1-(_tert_-Butoxycarbonyl)-4-(4-methoxyphenyl)piperidine-3-carboxylic acid (64)



A flame-dried round-bottom flask was charged with *cis*-arylated amide **25a** (346 mg, 0.75 mmol), followed by Boc_2O (982 mg, 4.50 mmol) and DMAP (18.3 mg, 0.15 mmol). The reaction vessel was sealed and purged with argon, then MeCN (1.25 mL, 0.6 M) was added by syringe. The reaction mixture was then placed in an oil bath and gradually warmed up to 70 ºC. The reaction was then stirred at 70 °C for 48 h. The reaction mixture was allowed to cool to rt and sat. aq. NH_4Cl (3 mL) and CH_2Cl_2 (3 mL) were added. The phases were separated, and the aqueous layer was extracted with CH_2Cl_2 (3 × 5 mL). The combined organic extracts were dried over Na_2SO_4 and filtered. The solvent was removed under reduced pressure to afford the crude *N*-Boc protected piperidine derivative. A solution of H_2O_2 (30 wt.% in H_2O, 0.90 mL, 9.00 mmol) in THF (2.4 mL) was added to a solution of $LiOH·H_2O$ (252 mg, 6.00 mmol,) in H_2O (1.9 mL) at 0 °C under argon. The resulting mixture was added dropwise to a solution of crude *N*-Boc protected piperidine in THF (3.2 mL) at 0 °C under argon. The reaction was then stirred at 45 °C for 24 h. The reaction mixture was then allowed to cool down to rt and sat. aq. $Na_2S_2O_3$ (8 mL), EtOAc (5 mL) and 1 N NaOH (5 mL) were added. The aqueous alkaline layer was collected, and the organic layer extracted with 1 N NaOH (3 × 15 mL). All the aqueous alkaline layers were combined, washed with EtOAc (40 mL), and acidified to pH ~ 1 with HCl, 37%. The acidic layer was extracted with EtOAc (5 × 50 mL). The combined organic extracts were dried over Na_2SO_4 and filtered. Solvent was removed under reduced pressure. Et_2O (5 mL) and pentane (5 mL) were added and the solvent was removed under reduced pressure to afford the pure *cis*-acid **64** as an off-white solid (223 mg, 89% over 2 steps). R_f 0.17 (3% MeOH/CH_2Cl_2); mp = 186–191 °C (from Et_2O/pentane); ν_{max} (film)/cm^{-1} 2933 (OH br), 1706 (C=O), 1681 (C=O), 1514, 1465, 1418, 1366, 1244, 1178, 1118, 1040, 1006, 830, 769; ^{1}H NMR (400 MHz, $CDCl_3$, 298 K) δ 7.20–7.11 (m, 2 H, HC_{Ar}), 6.85–6.80 (m, 2 H, HC_{Ar}), 4.44 (br d, *J* = 13.6, 1 H, NC*H*HCHCO), 4.27 (br d, *J* = 12.5, 1 H, NC*H*HCH_2), 3.78 (s, 3 H, OCH_3), 3.18 (dd, *J* = 13.9, 3.8 Hz, 1 H, NCH*H*CHCO), 2.99–2.81 (m, 3 H, CHCO, CHAr, NCH*H*CH_2), 2.54 (dddd, *J* = 12.3, 12.3, 12.3, 4.5 Hz, 1 H, NCH_2C*H*H), 1.67 (dddd, *J* = 13.0, 3.3, 3.3, 3.3 Hz, 1 H, NCH_2CH*H*), 1.39 (s, 9 H, C$(CH_3)_3$); ^{13}C NMR (101 MHz, DMSO-d_6, 373 K) δ 176.6 (COOH), 158.3 (OC_{Ar} quat), 154.6 (C=O carbamate), 134.2 (C_{Ar} quat), 128.4 (2 × C_{Ar}), 113.8 (2 × C_{Ar}), 79.8 (*C*$(CH_3)_3$), 55.2 (OCH_3), 46.1 (N*C*H_2CHCO), 45.4 (*C*HCO), 43.9 (N*C*$H_2C H_2$), 42.3 (CHAr), 28.3 (C(*C*$H_3)_3$), 25.9 (NCH_2*C*H_2); HRMS (ESI$^+$) *m*/*z* Calculated for $C_{18}H_{26}NO_5$ [M+H] 336.1811; Found 336.1819.

*8.2.3.4 Directing group removal: primary alcohol derivatives (**37**, **65–69**)*

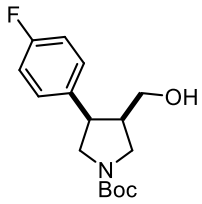
tert-Butyl _cis_-(±)-3-(hydroxymethyl)-4-(4-methoxyphenyl)pyrrolidine-1-carboxylate (37)



A flame-dried reaction tube was charged with *cis*-arylated amide **3a** (340 mg, 0.76 mmol), followed by Boc_2O (829 mg, 3.80 mmol) and DMAP (186 mg, 1.52 mmol). The reaction vessel was sealed and purged with argon, then anhydrous MeCN (1.5 mL, 0.5 M) was added by syringe. The reaction tube was placed in an oil bath and gradually warmed up to 55 ºC. The reaction mixture was then stirred at 55 °C for 1 h. The reaction mixture was allowed to cool to rt and sat. aq. NH_4Cl (3 mL) and CH_2Cl_2 (3 mL) were added. The phases were separated, and the aqueous layer was extracted with CH_2Cl_2 (3 × 5 mL). The combined organic extracts were dried over Na_2SO_4 and filtered. The solvent was removed under reduced pressure to afford the crude *N*-Boc protected pyrrolidine derivative. A solution of the crude *N*-Boc protected pyrrolidine derivative in dry THF (2.5 mL) was added dropwise to a suspension of $LiAlH_4$ (115 mg, 3.04 mmol) in dry THF (1.5 mL) at 0 °C under argon atmosphere. The mixture was then stirred at 20 °C for 30 min. The reaction mixture was quenched by slow addition of sat. aq. NH_4Cl (2 mL) at 0 °C and stirred at rt for 30 min. The resulting suspension was filtered through a pad of Celite, eluting with EtOAc (3 × 5 mL). The phases were separated, and the aqueous layer was extracted with EtOAc (3 × 5 mL). The combined organic extracts were dried over Na_2SO_4 and filtered. The solvent was removed under reduced pressure. The crude material was purified by flash column chromatography (20% acetone/pentane). The product containing fractions were combined and the solvent was removed under reduced pressure. Et_2O (5 mL) and pentane (5 mL) were added and the solvent was removed under reduced pressure to afford the *cis*-alcohol derivative **37** as a colourless paste (192 mg, 82% over 2 steps).

The observed characterisation data was identical to what previously reported for pyrrolidine **37** (page 258).

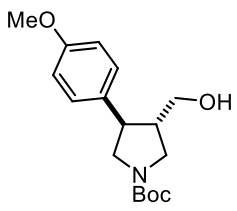
tert-Butyl _cis_-(±)-3-(hydroxymethyl)-4-(4-fluorophenyl)pyrrolidine-1-carboxylate (65)



A flame-dried reaction tube was charged with *cis*-arylated amide **3d** (261 mg, 0.60 mmol), followed by Boc_2O (655 mg, 3.00 mmol) and DMAP (147 mg, 1.20 mmol). The reaction vessel was sealed and purged with argon, then anhydrous MeCN (1.2 mL, 0.5 M) was added by syringe. The reaction tube was placed in an oil bath and gradually warmed up to 55 ºC. The reaction mixture was then stirred at 55 °C for 1 h. The reaction mixture was allowed to cool to rt and sat. aq. NH_4Cl (3 mL) and CH_2Cl_2 (3 mL) were added. The phases were separated, and the aqueous layer was extracted with CH_2Cl_2 (3 × 5 mL). The combined organic extracts were

dried over Na_2SO_4 and filtered. The solvent was removed under reduced pressure to afford the crude *N*-Boc protected pyrrolidine derivative. A solution of the crude *N*-Boc protected pyrrolidine derivative in dry THF (2.0 mL) was added dropwise to a suspension of $LiAlH_4$ (91.0 mg, 2.40 mmol) in dry THF (1.0 mL) at 0 °C under argon atmosphere. The mixture was then stirred at 20 °C for 30 min. The reaction mixture was quenched by slow addition of sat. aq. NH_4Cl (2 mL) at 0 °C and stirred at rt for 30 min. The resulting suspension was filtered through a pad of Celite, eluting with EtOAc (3 × 5 mL). The phases were separated, and the aqueous layer was extracted with EtOAc (3 × 5 mL). The combined organic extracts were dried over Na_2SO_4 and filtered. The solvent was removed under reduced pressure. The crude material was purified by flash column chromatography (15% to 20% acetone/pentane). The product containing fractions were combined and the solvent was removed under reduced pressure. Et_2O (5 mL) and pentane (5 mL) were added and the solvent was removed under reduced pressure to afford the *cis*-alcohol derivative **65** as a colourless paste (145 mg, 82% over 2 steps). R_f 0.12 (15% acetone/pentane). ν_{max} (film)/cm^{-1} 3407 (OH br), 2933, 1670 (C=O), 1510, 1394, 1226, 1156, 1126, 1047, 835; ^{1}H NMR (400 MHz, $CDCl_3$, 298 K, observed as a mixture of rotamers) δ 7.18–7.10 (m, 2 H, HC_{Ar}), 7.05–6.97 (m, 2 H, HC_{Ar}), 3.80–3.56 (m, 3 H, NCH_2CHAr, NC*H*HCHCH$_2$OH), 3.51 (ddd, J = 6.9, 6.9, 3.4 Hz, 1 H, CHAr), 3.38–3.21 (m, 3 H, CH_2OH, NCH*H*CHCH$_2$OH), 2.73–2.58 (m, 1 H, C*H*CH$_2$OH), 1.50 and 1.49 (2 × s, 9 H, C(CH$_3$)$_3$); ^{13}C NMR (101 MHz, $CDCl_3$, 298 K, observed as a mixture of rotamers) δ 161.7 (d, J_{CF} = 245.1 Hz, FC_{Ar} quat), 154.6 (C=O carbamate), 135.2 (F-*p*-C_{Ar} quat, observed as broad singlet), 129.3 and 129.2 (2 × d, J_{CF} = 7.4 Hz, 2 × F-*m*-C_{Ar}), 115.4 (d, J_{CF} = 21.1 Hz, 2 × F-*o*-C_{Ar}), 79.6 (*C*(CH$_3$)$_3$), 61.6 and 61.4 (CH$_2$OH), 51.5 and 50.9 (N*C*H$_2$CHAr), 47.6 and 47.2 (N*C*H$_2$CHCH$_2$OH), 45.2 and 44.5 (*C*HCH$_2$OH), 44.4 and 43.6 (CHAr), 28.5 (C(*C*H$_3$)$_3$); ^{19}F NMR (377 MHz, $CDCl_3$, 298 K, observed as a mixture of rotamers) δ –115.9 (m); HRMS (ESI$^+$) *m*/*z* Calculated for $C_{16}H_{23}NO_3F$ [M+H] 296.1662; Found 296.1663.

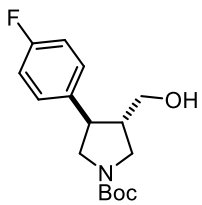
tert-Butyl _trans_-(±)-3-(hydroxymethyl)-4-(4-methoxyphenyl)pyrrolidine-1-carboxylate (66)



A flame-dried reaction tube was charged with *trans*-arylated amide **5** (323 mg, 0.72 mmol), followed Boc_2O (786 mg, 3.60 mmol) and DMAP (176 mg, 1.44 mmol). The reaction vessel was sealed and purged with argon, then anhydrous MeCN (1.4 mL, 0.5 M) was added by syringe. The reaction tube was placed in an oil bath and gradually warmed up to 55 ºC. The reaction mixture was then stirred at 55 °C for 1 h. The reaction mixture was allowed to cool to rt and sat. aq. NH_4Cl (3 mL) and CH_2Cl_2 (3 mL) were added. The phases were separated, and the aqueous layer was extracted with CH_2Cl_2 (3 × 5 mL). The combined organic extracts were dried over Na_2SO_4 and filtered. The solvent was removed under reduced

pressure to afford the crude *N*-Boc protected pyrrolidine derivative. A solution of the crude *N*-Boc protected pyrrolidine derivative in dry THF (2.3 mL) was added dropwise to a suspension of $LiAlH_4$ (109 mg, 2.88 mmol) in dry THF (1.3 mL) at 0 °C under argon atmosphere. The mixture was then stirred at 20 °C for 30 min. The reaction mixture was quenched by slow addition of sat. aq. NH_4Cl (2 mL) at 0 °C and stirred at rt for 30 min. The resulting suspension was filtered through a pad of Celite, eluting with EtOAc (3 × 5 mL). The phases were separated, and the aqueous layer was extracted with EtOAc (3 × 5 mL). The combined organic extracts were dried over Na_2SO_4 and filtered. The solvent was removed under reduced pressure. The crude material was purified by flash column chromatography (15% to 20% acetone/pentane). The product containing fractions were combined and the solvent was removed under reduced pressure. Et_2O (5 mL) and pentane (5 mL) were added and the solvent was removed under reduced pressure to afford the *trans*-alcohol derivative **66** as a colourless paste (198 mg, 89% over 2 steps). R_f 0.28 (20% acetone/pentane); ν_{max} (film)/cm^{-1} 3470 (OH br), 2930, 1685 (C=O), 1513, 1416, 1245, 1170, 1133, 1033, 826, 768; ^1H NMR (400 MHz, $CDCl_3$, 298 K, observed as a mixture of rotamers) δ 7.20–7.13 (m, 2 H, HC_{Ar}), 6.90–6.83 (m, 2 H, HC_{Ar}), 3.88–3.69 (m, 5 H, OCH_3, NC*H*HCHAr, NC*H*HCH$_2$OH), 3.69–3.61 (br m, 1 H, C*H*HOH), 3.57–3.45 (br m, 1 H, CH*H*OH), 3.40–3.20 (m, 2 H, NCH*H*CHCH$_2$OH, NCH*H*CHAr), 3.15–2.98 (m, 1 H, CHAr), 2.51–2.38 (br m, 1 H, C*H*CH$_2$OH), 1.87 (br s, 1 H, OH), 1.48 and 1.45 (2 × s, 9 H, C(CH_3)$_3$); ^{13}C NMR (101 MHz, $CDCl_3$, 298 K, observed as a mixture of rotamers) δ 158.6 (OC_{Ar} quat), 154.5 (C=O carbamate), 131.9 and 131.8 (C_{Ar} quat), 128.5 (2 × C_{Ar}), 114.1 (2 × C_{Ar}), 79.3 (*C*(CH_3)$_3$), 62.8 and 62.6 (CH_2OH), 55.2 (OCH_3), 53.6 and 52.9 (N*C*H$_2$CHAr), 49.3 and 48.7 (N*C*H$_2$CHCH$_2$OH), 48.3 and 47.4 (*C*HCH$_2$OH), 45.8 and 45.1 (CHAr), 28.5 (C(*C*H$_3$)$_3$); HRMS (ESI$^+$) *m*/*z* Calculated for $C_{17}H_{26}NO_4$ [M+H] 308.1862; Found 308.1854.

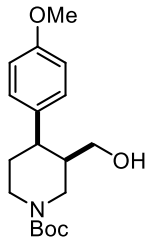
tert-Butyl _trans_-(±)-3-(hydroxymethyl)-4-(4-fluorophenyl)pyrrolidine-1-carboxylate (67)



A flame-dried reaction tube was charged with *trans*-arylated amide **59** (280 mg, 0.64 mmol), followed by Boc_2O (701 mg, 3.21 mmol) and DMAP (156 mg, 1.30 mmol). The reaction vessel was sealed and purged with argon, then anhydrous MeCN (1.3 mL, 0.5 M) was added by syringe. The reaction tube was placed in an oil bath and gradually warmed up to 55 ºC. The reaction mixture was then stirred at 55 °C for 1 h. The reaction mixture was allowed to cool to rt and sat. aq. NH_4Cl (3 mL) and CH_2Cl_2 (3 mL) were added. The phases were separated, and the aqueous layer was extracted with CH_2Cl_2 (3 × 5 mL). The combined organic extracts were dried over Na_2SO_4 and filtered. The solvent was removed under reduced pressure to afford the crude *N*-Boc protected pyrrolidine derivative. A solution of the crude *N*-Boc protected pyrrolidine derivative in dry THF (2.1 mL) was added dropwise to a suspension of $LiAlH_4$

(97.2 mg, 2.56 mmol) in dry THF (1.1 mL) at 0 °C under argon atmosphere. The mixture was then stirred at 20 °C for 30 min. The reaction mixture was quenched by slow addition of sat. aq. NH_4Cl (2 mL) at 0 °C and stirred at rt for 30 min. The resulting suspension was filtered through a pad of Celite, eluting with EtOAc (3 × 5 mL). The phases were separated, and the aqueous layer was extracted with EtOAc (3 × 5 mL). The combined organic extracts were dried over Na_2SO_4 and filtered. The solvent was removed under reduced pressure. The crude material was purified by flash column chromatography (15% to 20% acetone/pentane). The product containing fractions were combined and the solvent was removed under reduced pressure. Et_2O (5 mL) and pentane (5 mL) were added and the solvent was removed under reduced pressure to afford the *trans*-alcohol derivative **67** as a white solid (167 mg, 88% over 2 steps). R_f 0.11 (15% acetone/pentane). mp = 101–104 °C (from Et_2O/pentane); ν_{max} (film)/cm^{-1} 3466 (OH br), 2978, 1677 (C=O), 1513, 1416, 1226, 1133, 1074, 880, 831, 768; ^1H NMR (400 MHz, $CDCl_3$, 298 K, observed as a mixture of rotamers) δ 7.25–7.18 (m, 2 H, HC_{Ar}), 7.07–6.99 (m, 2 H, HC_{Ar}), 3.92–3.72 (m, 2 H, NC*H*HCHAr, NC*H*HCHCH$_2$OH), 3.68 (dt, J = 10.7, 4.6 Hz, 1 H, C*H*HOH), 3.60–3.49 (br m, 1 H, CH*H*OH), 3.42–3.24 (m, 2 H, NCH*H*CHCH$_2$OH, NCH*H*CHAr), 3.22–2.05 (m, 1 H, CHAr), 2.52–2.40 (m, 1 H, C*H*CH$_2$OH), 1.49 and 1.47 (2 × s, 9 H, C(CH$_3$)$_3$), 1.33 (br m, 1 H, OH); ^{13}C NMR (101 MHz, $CDCl_3$, 298 K, observed as a mixture of rotamers) δ 161.9 (d, J_{CF} = 245.5 Hz, FC_{Ar} quat), 154.4 (C=O carbamate), 135.8 (F-*p*-C_{Ar} quat, observed as broad singlet), 129.0 (d, J_{CF} = 7.9 Hz, 2 × F-*m*-C_{Ar}), 115.6 (d, J_{CF} = 21.2 Hz, 2 × F-*o*-C_{Ar}), 79.5 (*C*(CH$_3$)$_3$), 62.6 and 62.4 (CH$_2$OH), 53.5 and 52.8 (NCH$_2$CHAr), 49.2 and 48.6 (NCH$_2$CHCH$_2$OH), 48.4 and 47.5 (*C*HCH$_2$OH), 45.8 and 45.1 (CHAr), 28.5 (C(*C*H$_3$)$_3$); ^{19}F NMR (377 MHz, $CDCl_3$, 298 K) δ –115.6 (tt, J_{HF} = 8.6, 5.5 Hz); HRMS (ESI$^+$) *m*/*z* Calculated $C_{16}H_{23}NO_3F$ [M+H] 296.1662; Found 296.1673.

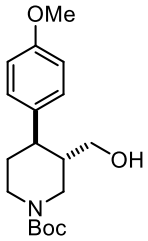
tert-Butyl _cis_-(±)-3-(hydroxymethyl)-4-(4-methoxyphenyl)piperidine-1-carboxylate (68)



A flame-dried round-bottom flask was charged with *cis*-arylated amide **25a** (346 mg, 0.75 mmol), followed by Boc_2O (982 mg, 4.50 mmol) and DMAP (18.3 mg, 0.15 mmol). The reaction vessel was sealed and purged with argon, then MeCN (1.2 mL, 0.6 M) was added by syringe. The reaction mixture was placed in an oil bath and gradually warmed up to 70 ºC. The reaction was then stirred at 70 °C for 48 h. The reaction mixture was allowed to cool to rt and sat. aq. NH_4Cl (3 mL) and CH_2Cl_2 (3 mL) were added. The phases were separated, and the aqueous layer was extracted with CH_2Cl_2 (3 × 5 mL). The combined organic extracts were dried over Na_2SO_4 and filtered. The solvent was removed under reduced pressure to afford the crude *N*-Boc protected piperidine derivative. A solution of the crude *N*-Boc protected derivative in dry THF (3.0 mL) was added dropwise to a suspension of $LiAlH_4$ (114 mg, 3.00 mmol) in dry THF (2.0 mL) at 0 °C under argon atmosphere. The mixture was then stirred at 20 °C for 30 min.

The resulting suspension was filtered through a pad of Celite, eluting with EtOAc (3 × 5 mL). The phases were separated, and the aqueous layer was extracted with EtOAc (3 × 5 mL). The combined organic extracts were dried over Na_2SO_4 and filtered. The solvent was removed under reduced pressure. The crude material was purified by flash column chromatography (15% acetone/pentane). The product containing fractions were combined and the solvent was removed under reduced pressure. Et_2O (5 mL) and pentane (5 mL) were added and the solvent was removed under reduced pressure to afford the *cis*-alcohol **68** as a white paste (160 mg, 66% over 2 steps). R_f 0.24 (15% acetone/pentane); ν_{max} (film)/cm^{-1} 3452 (OH br), 2930, 1659 (C=O), 1513, 1428, 1238, 1163, 1126, 1033, 999, 838,772; ^{1}H NMR (400 MHz, $CDCl_3$, 298 K, observed as a mixture of rotamers) δ 7.10–7.04 (m, 2 H, HC_{Ar}), 6.89–6.82 (m, 2 H, HC_{Ar}), 4.49–4.15 (br m, 2 H, NC*H*HCHCH$_2$OH, NC*H*HCH$_2$), 3.80 (s, 3 H, OCH_3), 3.59–3.28 (br m, 1 H, C*H*HOH), 3.15 (br s, 1 H, CH*H*OH), 3.03 (m, 1 H, CHAr), 2.92 (br s, 2 H, NCH*H*CHCH$_2$OH, NCH*H*CH$_2$), 2.13 (br s, 1 H, C*H*CH$_2$OH), 1.94 (dddd, *J* = 13.0, 13.0, 13.0, 4.7 Hz, 1 H, NCH$_2$CH*H*), 1.84 (br s, 0.4 H, OH), 1.71–1.60 (m, 1 H, NCH$_2$CH*H*), 1.50 and 1.48 (2 × s, 9 H, C(CH$_3$)$_3$); ^{13}C NMR (101 MHz, $CDCl_3$, 298 K, observed as a mixture of rotamers) δ 158.1 (OC_{Ar} quat), 134.6 (C_{Ar} quat), 127.9 (2 × C_{Ar}), 113.8 (2 × C_{Ar}), 80.1 (*C*(CH$_3$)$_3$), 57.8 (br, CH_2OH), 55.2 (OCH_3), 45.7 (br, N*C*H$_2$CHCH$_2$OH), 45.3 (br, N*C*H$_2$CH$_2$), 42.6 (CHAr), 42.1 (br, *C*HCH$_2$OH), 28.4 (C(*C*H$_3$)$_3$), 25.3 (NCH$_2$*C*H$_2$); the quaternary signal from the C=O (carbamate) was not observed; HRMS (ESI$^+$) *m*/*z* Calculated for $C_{18}H_{28}NO_4$ [M+H] 322.2018; Found 322.2020.

tert-Butyl _trans_-(±)-3-(hydroxymethyl)-4-(4-methoxyphenyl)piperidine-1-carboxylate (69)

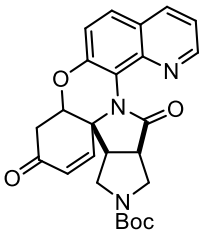


A flame-dried reaction tube was charged with *trans*-arylated amide **26a** (323 mg, 0.70 mmol), followed by Boc_2O (611 mg, 2.80 mmol) and DMAP (17.1 mg, 0.14 mmol). The reaction vessel was sealed and purged with argon, then MeCN (2.3 mL, 0.3 M) was added by syringe. The reaction tube was placed in an oil bath and gradually warmed up to 40 ºC. The reaction mixture was then stirred at 40 °C for 24 h. The reaction mixture was allowed to cool to rt and sat. aq. NH_4Cl (3 mL) and CH_2Cl_2 (3 mL) were added. The phases were separated, and the aqueous layer was extracted with CH_2Cl_2 (3 × 5 mL). The combined organic extracts were dried over Na_2SO_4 and filtered. The solvent was removed under reduced pressure to afford the crude *N*-Boc protected piperidine derivative. A solution of the crude *N*-Boc protected derivative in dry THF (2.3 mL) was added dropwise to a suspension of $LiAlH_4$ (53.1 mg, 1.40 mmol) in dry THF (1.2 mL) at 0 °C under argon atmosphere. The mixture was then stirred at 20 °C for 30 min. The resulting suspension was filtered through a pad of Celite, eluting with EtOAc (3 × 5 mL). The phases were separated, and the aqueous layer was extracted with EtOAc (3 × 5 mL). The

combined organic extracts were dried over Na_2SO_4 and filtered. The solvent was removed under reduced pressure. The crude material was purified by flash column chromatography (15% acetone/pentane). The product containing fractions were combined and the solvent was removed under reduced pressure. Et_2O (5 mL) and pentane (5 mL) were added and the solvent was removed under reduced pressure to afford the *trans*-alcohol **69** as a colourless paste (188 mg, 84% over 2 steps). R_f 0.19 (15% acetone/pentane); ν_{max} (film)/cm^{-1} 3422 (OH br), 2930, 1662 (C=O), 1513, 1424, 1364, 1230, 1159, 1126, 1033, 826,760; ^{1}H NMR (400 MHz, $CDCl_3$, 298 K, observed as a mixture of rotamers) δ 7.14–7.08 (m, 2 H, HC_{Ar}), 6.89–6.83 (m, 2 H, HC_{Ar}), 4.36 (br d, *J* = 13.4 Hz, 1 H, NC*H*HCHCH$_2$OH), 4.21 (br s, 1 H, NC*H*HCH$_2$), 3.80 (s, 3 H, OCH_3), 3.46 (dd, *J* = 11.0, 3.4 Hz, 1 H, C*H*HOH), 3.29 (dd, *J* = 11.0, 6.4 Hz, 1 H, CH*H*OH), 2.84–2.73 (m, 1 H, NCH*H*CH$_2$), 2.69 (dd, *J* = 13.3, 11.3 Hz, 1 H, NCH*H*CHCH$_2$OH), 2.48 (br ddd, *J* = 11.7, 11.7, 3.9 Hz, 1 H, CHAr), 1.88–1.73 (m, 2 H, C*H*CH$_2$OH, NCH$_2$C*H*H), 1.73–1.61 (m, 2 H, NCH$_2$CH*H*, OH), 1.50 (s, 9 H, C(CH$_3$)$_3$); ^{13}C NMR (101 MHz, $CDCl_3$, 298 K, observed as a mixture of rotamers) δ 158.2 (OC_{Ar} quat), 154.9 (C=O carbamate), 135.8 (C_{Ar} quat), 128.2 (2 × C_{Ar}), 114.0 (2 × C_{Ar}), 79.6 (*C*(CH$_3$)$_3$), 63.3 (CH$_2$OH), 55.2 (OCH_3), 47.2 (br, N*C*H$_2$CHCH$_2$OH), 44.6 (br, N*C*H$_2$CH$_2$), 44.1 (CHAr), 43.9 (*C*HCH$_2$OH), 34.1 (NCH$_2$*C*H$_2$), 28.4 (C(*C*H$_3$)$_3$); HRMS (ESI$^+$) *m*/*z* Calculated for $C_{18}H_{28}NO_4$ [M+H] 322.2018; Found 322.2018.

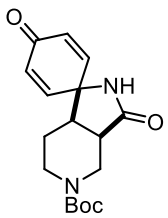
*8.2.3.5 IBX-Mediated cyclisation: spirocyclic derivatives (**70**, **76**, **78**, **79**)*

tert-Butyl (±)-6,16-dioxo-3,3a,7,7a,16,16a-hexahydro-6*H*-pyrido[2,3-a]pyrrolo[3',4':3,4] pyrrolo [2,1-l]phenoxazine-2(1*H*)-carboxylate (70)



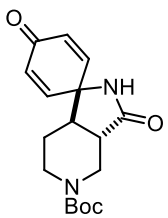
A reaction tube was charged with *cis*-arylated pyrrolidine **3a** (89.4 mg, 0.20 mmol) and IBX (45 wt. %, 249 mg, 0.40 mmol) under air. H_2O (700 μL) and HFIP (700 μL) were then added, the vial was sealed, and the solution was stirred at 60 °C for 1.5 h. The reaction mixture was then allowed to cool to rt and sat. aq. $NaHCO_3$ (3 mL) was added. The aqueous layer was extracted with CH_2Cl_2 (3 × 5 mL). The combined organic extracts were dried over Na_2SO_4 and filtered. The solvent was removed under reduced pressure. The crude material was purified by flash column chromatography (40% acetone/pentane). The product containing fractions were combined and the solvent was removed under reduced pressure. Et_2O (2 mL) and pentane (2 mL) were added and the solvent was removed under reduced pressure to afford product **70** as a white solid (15.7 mg, 16%). R_f 0.36 (40% acetone/pentane); mp = 154–158 °C (from Et_2O/pentane); ν_{max} (film)/cm^{-1} 3358, 2974, 1685 (C=O), 1618, 1394, 1226, 1163, 1122, 1029, 831, 790; ^{1}H NMR (400 MHz, DMSO-d_6, 373 K) δ 8.84 (dd, *J* = 4.2, 1.6 Hz, 1 H, $HC_{Ar}N$), 8.22 (dd, *J* = 8.2, 1.6 Hz, 1 H, HC_{Ar}), 7.75 (d, *J* = 9.0 Hz, 1 H, HC_{Ar}), 7.38 (dd, *J* = 8.2, 4.2 Hz, 1 H, HC_{Ar}), 7.19 (d, *J* = 8.9 Hz, 1 H, HC_{Ar}), 6.57 (dd, *J* = 10.4, 2.7 Hz, 1 H, C*H*=CHCO), 5.99 (dd, *J* = 10.4, 1.2 Hz, 1 H, CH=C*H*CO), 4.97–4.93 (m, 1 H, OCH), 3.84 (dd, *J* = 11.4, 2.9 Hz, 1 H, NC*H*HCHCO$_{amide}$), 3.76–3.66 (m, 2 H, NCH*H*CHCO$_{amide}$, NC*H*HCH), 3.61 (dd, *J* = 11.8, 8.1 Hz, 1 H, NCH*H*CH), 3.50 (ddd, *J* = 8.3, 8.3, 5.8 Hz, 1 H, NCH_2CH), 3.45–3.34 (m, 2 H, $CHCO_{amide}$, C*H*HCO$_{ketone}$), 2.93–2.82 (m, 1 H, CH*H*CO$_{ketone}$), 1.48 (s, 9 H, $C(CH_3)_3$); ^{13}C NMR (101 MHz, DMSO-d_6, 373 K) δ 192.9 (C=O ketone), 171.6 (C=O amide), 152.7 (C=O carbamate), 149.3 (NC_{Ar}), 147.9 (OC_{Ar} quat), 145.0 (*C*H=CHCO), 143.0 (C_{Ar} quat), 134.9 (C_{Ar}), 131.8 (CH=*C*HCO), 126.4 (C_{Ar}), 122.9 (C_{Ar} quat), 118.9 (C_{Ar}), 117.0 (C_{Ar}), 116.1 (C_{Ar} quat), 78.6 (*C*$(CH_3)_3$), 77.9 (OCH), 58.0 (N*C*CH_2=CH_2), 47.7 (N*C*H_2CHCO$_{amide}$), 46.2 (N*C*H_2CH), 44.5 (*C*HCO$_{amide}$), 41.2 (NCH_2*C*H), 39.5 (*C*H_2CO$_{ketone}$), 27.6 (C(*C*$H_3)_3$); HRMS (ESI$^+$) *m*/*z* Calculated for $C_{25}H_{26}N_3O_5$ [M+H] 448.1867; Found 448.1878.

***tert*-Butyl *cis*-(±)-3',4-dioxo-2',3',3a',6',7',7a'-hexahydrospiro[cyclohexane-1,1'-pyrrolo [3,4-c]pyridine]-2,5-diene-5'(4'*H*)-carboxylate (76)**



A reaction tube was charged with *cis*-arylated piperidine **25a** (46.2 mg, 0.10 mmol) and IBX (30 wt.%, 187 mg, 0.20 mmol) under air. H_2O (350 μL) and HFIP (250 μL) were then added, the vial was sealed and the solution (0.15 M) was stirred at 60 °C for 1.5 h. The reaction mixture was then allowed to cool to rt and sat. aq. $NaHCO_3$ (3 mL) was added. The aqueous layer was extracted with CH_2Cl_2 (3 × 5 mL). The combined organic extracts were dried over Na_2SO_4 and filtered. The solvent was removed under reduced pressure. The crude material was purified by flash column chromatography (40% acetone/pentane). The product containing fractions were combined and the solvent was removed under reduced pressure. Et_2O (2 mL) and pentane (2 mL) were added and the solvent was removed under reduced pressure to afford the product **76** as a pale yellow paste (12.5 mg, 39%). R_f 0.26 (40% acetone/pentane); ν_{max} (film)/cm^{-1} 3250 (NH br), 2974, 1666 (C=O), 1625 (C=O), 1405, 1245, 1159, 1118, 865, 746; ^{1}H NMR (400 MHz, $CDCl_3$, 298 K, observed as a mixture of rotamers) δ 6.92 (dd, *J* = 10.1, 3.0 Hz, 1 H, (C*H*=CH)CO(CH=CH)), 6.87 (dd, *J* = 10.3, 3.1 Hz, 1 H, (CH=CH)CO(CH=C*H*)), 6.37 (dd, *J* = 10.3, 1.9 Hz, 1 H, (CH=CH)CO(C*H*=CH)), 6.30 (br s, 1 H, NH), 6.25 (dd, *J* = 10.0, 2.0 Hz, 1 H, (CH=C*H*)CO(CH=CH)), 4.16 (br s, 1 H, NC*H*HCHCO), 3.85 (br s, 1 H, NC*H*HCH$_2$), 3.49–3.28 (br m, 1 H, NCH*H*CHCO), 2.97–2.73 (br m, 2 H, NCH*H*CH$_2$, CHCO), 2.66–2.55 (m, 1 H, NCH$_2$CH$_2$C*H*), 1.81–1.66 (br m, 2 H, NCH$_2$C*H*$_2$), 1.46 (s, 9 H, C(CH$_3$)$_3$); ^{13}C NMR (101 MHz, $CDCl_3$, 298 K, observed as a mixture of rotamers) δ 184.0 (C=O ketone), 175.6 (C=O amide), 154.6 (C=O carbamate), 148.8 ((*C*H=CH)CO(CH=CH)), 146.7 ((CH=CH)CO(CH=*C*H)), 131.5 ((CH=CH)CO(*C*H=CH)), 128.6 ((CH=*C*H)CO(CH=CH)), 80.2 (*C*(CH$_3$)$_3$), 58.5 (CNH quat), 44.0 (NCH$_2$CH$_2$*C*H), 41.4 (br, N*C*H$_2$CH$_2$), 40.5 (br, N*C*H$_2$CHCO), 40.3 (*C*HCO), 28.3 (C(*C*H$_3$)$_3$), 24.5 (NCH$_2$*C*H$_2$); HRMS (ESI$^-$) *m*/*z* Calculated for $C_{17}H_{21}N_2O_4$ [M–H] 317.1501; Found 317.1504.

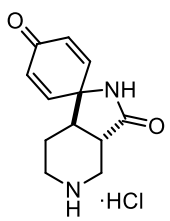
***tert*-Butyl *trans*-(±)-3',4-dioxo-2',3',3a',6',7',7a'-hexahydrospiro[cyclohexane-1,1'-pyrrolo [3,4-c]pyridine]-2,5-diene-5'(4'*H*)-carboxylate (78)**



A round bottom flask was charged with *trans*-arylated piperidine **26a** (360 mg, 0.78 mmol) and IBX (30 wt.%, 1.46 g, 1.56 mmol) under air. H_2O (2.6 mL) and HFIP (2.6 mL) were then added, and the resulting solution (0.15 M) was stirred at 60 °C for 1.5 h. The reaction mixture was then allowed to cool to rt and sat. aq. $NaHCO_3$ (3 mL) was added. The aqueous layer was extracted with CH_2Cl_2 (3 × 5 mL). The combined organic extracts were dried over Na_2SO_4 and filtered. The solvent was removed under reduced pressure. The crude material was purified by flash column chromatography (30% to 40% acetone/pentane). The product containing fractions were

combined and the solvent was removed under reduced pressure. Et_2O (5 mL) and pentane (5 mL) were added and the solvent was removed under reduced pressure to afford the product **78** as an off-white solid (153 mg, 62%). R_f 0.23 (30% acetone/pentane); mp = 200–204 °C (from Et_2O/pentane); ν_{max} (film)/cm^{-1} 3191 (NH br), 2974, 1700 (C=O), 1670 (C=O), 1629, 1413, 1238, 1129, 865, 768; ^{1}H NMR (400 MHz, $CDCl_3$, 298 K, observed as a mixture of rotamers) δ 6.86 (dd, *J* = 10.1, 3.1 Hz, 1 H, (C*H*=CH)CO(CH=CH)), 6.69 (dd, *J* = 9.9, 3.0 Hz, 1 H, (CH=CH)CO(CH=C*H*)), 6.41–6.29 (m, 3 H, CO(C*H*=CH)$_2$, NH), 4.62 (br s, 1 H, NC*H*HCHCO), 4.35 (br s, 1 H, NC*H*HCH$_2$), 2.71 (br s, 1 H, NCH*H*CHCO), 2.64–2.51 (br m, 1 H, NCH*H*CH$_2$), 2.33 (ddd, *J* = 14.5, 10.9, 4.0 Hz, 1 H, CHCO), 2.13 (ddd, *J* = 12.9, 12.9, 3.2 Hz, 1 H, NCH$_2$CH$_2$C*H*), 1.62–1.50 (br m, 1 H, NCH$_2$C*H*H), 1.45 (s, 9 H, C(CH$_3$)$_3$), 1.36–1.26 (br m, 1 H, NCH$_2$CH*H*); ^{13}C NMR (101 MHz, $CDCl_3$, 298 K, observed as a mixture of rotamers) δ 184.4 (C=O ketone), 174.7 (C=O amide), 154.6 (C=O carbamate), 148.4 ((*C*H=CH)CO(CH=CH)), 145.0 ((CH=CH)CO(CH=*C*H)), 131.4 ((CH=CH)CO(*C*H=CH)), 130.8 ((CH=*C*H)CO(CH=CH)), 80.5 (*C*(CH$_3$)$_3$), 59.4 (CNH quat), 52.0 (NCH$_2$CH$_2$*C*H), 44.9 (br, N*C*H$_2$CHCO), 43.5 (*C*HCO), 43.2 (br, N*C*H$_2$CH$_2$), 28.3 (C(*C*H$_3$)$_3$), 25.1 (NCH$_2$*C*H$_2$); HRMS (ESI$^-$) *m*/*z* Calculated for $C_{17}H_{21}N_2O_4$ [M–H] 317.1501; Found 317.1508.

trans-(±)-3',4-Dioxo-2',3',3a',4',5',6',7',7a'-octahydrospiro[cyclohexane-1,1'-pyrrolo[3,4-c]pyridine]-2,5-dien-5'-ium chloride (79)



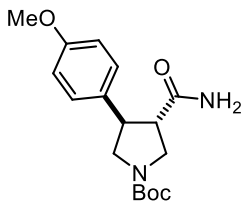
4 N HCl in 1,4-dioxane (0.9 mL, 3.60 mmol) was added to *N*-Boc protected derivative **78** (120 mg, 0.38 mmol) at 0 °C. The resulting solution was warmed up to 20 ºC and the product began to crush out of solution. The reaction mixture was stirred at 20 °C for 1 h and then ice-cold Et_2O (2 mL) was added. The reaction mixture was filtered and the precipate was washed with further ice-cold Et_2O (2 × 5 mL). The solid precipitate was found to be hygroscopic and turned quickly into a paste. This was then solubilised in MeOH and the resulting solution was concentrated under reduced pressure. Et_2O (3 mL) and pentane (3 mL) were added and the solvent was removed under reduced pressure to afford to afford the deprotected product as the corresponding hydrochloride salt **79** as a pale yellow solid (92.8 mg, 96%). mp = 270–274 °C (from Et_2O/pentane); ν_{max} (film)/cm^{-1} 2769 (br NH), 1666 (C=O), 1625 (C=O), 1394, 1290, 1059, 861; ^{1}H NMR (400 MHz, CD_3OD, 298 K) δ 7.17 (dd, *J* = 10.3, 2.7 Hz, 1 H, (C*H*=CH)CO(CH=CH)), 6.88 (dd, *J* = 10.2, 2.8 Hz, 1 H, (CH=CH)CO(CH=C*H*)), 6.37 (d, *J* = 10.2 Hz, 2 H, CO(C*H*=CH)$_2$), 3.78 (dd, *J* = 11.6, 3.2 Hz, 1 H, NC*H*HCHCO), 3.52 (br dd, *J* = 12.7, 3.6 Hz, 1 H, NC*H*HCH$_2$), 3.16 (dd, *J* = 11.9, 11.9 Hz, 1 H, NCH*H*CHCO), 3.00 (ddd, *J* = 12.7, 12.7, 3.5 Hz, 1 H, NCH*H*CH$_2$), 2.89 (ddd, *J* = 12.9, 12.9, 3.5 Hz, 1 H, CHCO), 2.56 (ddd, *J* = 12.8, 12.8, 3.0 Hz, 1 H, NCH$_2$CH$_2$C*H*), 1.81 (br d, *J* = 13.1 Hz, 1 H, NCH$_2$C*H*H), 1.66 (dddd, *J* = 13.2, 13.2, 13.2, 4.0 Hz, 1 H, NCH$_2$CH*H*); ^{13}C NMR (101 MHz, CD_3OD, 298 K) δ 186.4 (C=O ketone),

175.0 (C=O amide), 150.0 ((*C*H=CH)CO(CH=CH)), 147.2 ((CH=CH)CO(CH=*C*H)), 131.7 ((CH=CH)CO(*C*H=CH)), 131.5 ((CH=*C*H)CO(CH=CH)), 60.6 (CNH quat), 49.0 (NCH_2CH_2CH), 45.9 (NCH_2CHCO), 45.3 (NCH_2CH_2), 42.2 (*C*HCO), 23.7 (NCH_2CH_2); HRMS (ESI^+) *m*/*z* Calculated for $C_{12}H_{15}N_2O_2$ [M–Cl] 219.1134; Found 219.1141.

Note: Hygroscopic solid.

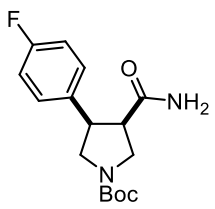
*8.2.3.6 Directing group removal: primary amide derivatives (**72–74**, **80**)*

tert-Butyl _trans_-(±)-3-carbamoyl-4-(4-methoxyphenyl)pyrrolidine-1-carboxylate (72)



According to the procedure reported by Zhang and Chen,[144a] a round-bottom flask was charged with *trans*-arylated pyrrolidine **5** (356 mg, 0.80 mmol) and IBX (30 wt.%, 1.50 g, 1.60 mmol) under air. H_2O (2.7 mL) and HFIP (2.7 mL) were then added, and the resulting solution (0.15 M) was stirred at 60 °C for 1.5 h. The reaction mixture was then allowed to cool to rt and sat. aq. $NaHCO_3$ (10 mL) and CH_2Cl_2 (10 ml) were added. The phases were separated, and the aqueous layer was extracted with CH_2Cl_2 (3 × 15 mL). The combined organic extracts were dried over Na_2SO_4 and filtered. The solvent was removed under reduced pressure. The crude material was purified by flash column chromatography (40% acetone/pentane). The product containing fractions were combined and the solvent was removed under reduced pressure. Et_2O (5 mL) and pentane (5 mL) were added and the solvent was removed under reduced pressure to afford the primary amide **72** as a pale yellow solid (203 mg, 79%). R_f 0.28 (40% acetone/pentane); mp = 147–150 °C (from Et_2O/pentane); ν_{max} (film)/cm^{-1} 3403 (NH br), 3168 (NH br), 2967, 1692 (C=O), 1655 (C=O), 1405, 1179, 1129, 828; ^{1}H NMR (400 MHz, $CDCl_3$, 298 K, observed as a mixture of rotamers) δ 7.20 (d, *J* = 8.3 Hz, 2 H, HC_{Ar}), 6.88 (d, *J* = 8.4 Hz, 2 H, HC_{Ar}), 5.60 (br s, 1 H, N*H*H), 5.33 and 5.20 (2 × br s, 1 H, NH*H*), 3.96–3.73 (m, 5 H, NC*H*HCHAr, NC*H*HCHCO, OCH_3), 3.72–3.60 (m, 1 H, NCH*H*CHCO), 3.59–3.30 (m, 2 H, CHAr, NCH*H*CHAr), 3.04–2.88 (m, 1 H, CHCO), 1.47 and 1.45 (2 × s, 9 H, $C(CH_3)_3$); ^{13}C NMR (101 MHz, $CDCl_3$, 298 K, observed as a mixture of rotamers) δ 173.1 (C=O amide), 159.0 and 158.9 (OC_{Ar} quat), 154.2 and 154.1 (C=O carbamate), 130.9 and 130.6 (C_{Ar} quat), 128.5 and 128.4 (2 × C_{Ar}), 114.5 and 114.4 (2 × C_{Ar}), 79.6 ($C(CH_3)_3$), 55.3 (OCH_3), 53.2 and 52.8 (NCH_2CHAr), 51.9 and 51.1 (*C*HCO), 48.7 and 48.6 (NCH_2CHCO), 47.6 and 47.1 (CHAr), 28.4 ($C(CH_3)_3$); HRMS (ESI$^+$) *m*/*z* Calculated for $C_{17}H_{24}N_2O_4Na$ [M+Na] 343.1634; Found 343.1625.

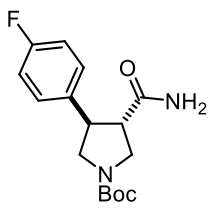
tert-Butyl _cis_-(±)-3-carbamoyl-4-(4-fluorophenyl)pyrrolidine-1-carboxylate (73)



According to the procedure reported by Zhang and Chen,[144a] a round-bottom flask was charged with *cis*-arylated pyrrolidine **3d** (327 mg, 0.75 mmol) and IBX (30 wt.%, 1.40 g, 1.50 mmol) under air. H_2O (2.5 mL) and HFIP (2.5 mL) were then added, and the resulting solution (0.15 M) was stirred at 60 °C for 1.5 h. The reaction mixture was then allowed to cool to rt and sat. aq. $NaHCO_3$ (10 mL) and CH_2Cl_2 (10 ml) were added. The phases were separated, and the aqueous layer was extracted with CH_2Cl_2 (3 × 15 mL). The combined organic extracts were dried over Na_2SO_4 and filtered. The solvent was removed under reduced pressure. The crude

material was purified by flash column chromatography (35% acetone/pentane). The product containing fractions were combined and the solvent was removed under reduced pressure. Et_2O (5 mL) and pentane (5 mL) were added and the solvent was removed under reduced pressure to afford the primary amide **73** as a pale yellow solid (179 mg, 77%). R_f 0.33 (40% acetone/pentane); mp = 73–76 °C (from Et_2O/pentane); ν_{max} (film)/cm^{-1} 3317 (NH br), 3194 (NH br), 2974, 1659 (C=O), 1513, 1394, 1223, 1159, 1118, 835; ^{1}H NMR (400 MHz, $CDCl_3$, 298 K, observed as a mixture of rotamers) δ 7.25–7.14 (m, 2 H, HC_{Ar}), 7.03–6.94 (m, 2 H, HC_{Ar}), 5.53–5.32 (br m, 2 H, NH_2), 3.83–3.70 (m, 3 H, NC*H*$_2$CHAr, NC*H*HCHCO), 3.67–3.56 (m, 2 H, NCH*H*CHCO, CHAr), 3.21–3.09 (m, 1 H, CHCO), 1.48 (s, 9 H, $C(CH_3)_3$); ^{13}C NMR (101 MHz, $CDCl_3$, 298 K, observed as a mixture of rotamers) δ 172.2 and 173.0 (C=O amide), 161.7 (d, J_{CF} = 245.9 Hz, FC_{Ar} quat), 154.39 and 154.37 (C=O carbamate), 133.6 and 133.3 (F-*p*-C_{Ar} quat, observed as singlets), 129.4–129.2 (2 × F-*m*-C_{Ar}, observed as triplet), 115.4 (d, J_{CF} = 21.3 Hz, 2 × F-*o*-C_{Ar}), 79.8 (*C*$(CH_3)_3$), 50.0 (N*C*H_2CHAr), 49.5 and 48.7 (*C*HCO), 47.8 and 47.7 (N*C*H_2CHCO), 46.1 and 45.3 (CHAr), 28.5 (C(*C*$H_3)_3$); ^{19}F NMR (377 MHz, $CDCl_3$, 298 K) δ –115.0 (tt, J_{HF} = 8.5, 4.3 Hz); HRMS (ESI$^+$) *m*/*z* Calculated for $C_{16}H_{21}N_2O_3FNa$ [M+Na] 331.1434; Found 331.1436.

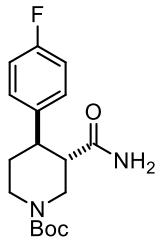
tert-Butyl _trans_-(±)-3-carbamoyl-4-(4-fluorophenyl)pyrrolidine-1-carboxylate (74)



According to the procedure reported by Zhang and Chen,[144a] a round-bottom flask was charged with *trans*-arylated pyrrolidine **59** (220 mg, 0.50 mmol) and IBX (30 wt.%, 940 mg, 1.00 mmol) under air. H_2O (1.7 mL) and HFIP (1.7 mL) were then added, and the resulting solution (0.15 M) was stirred at 60 °C for 1.5 h. The reaction mixture was then allowed to cool to rt and sat. aq. $NaHCO_3$ (10 mL) and CH_2Cl_2 (10 ml) were added. The phases were separated, and the aqueous layer was extracted with CH_2Cl_2 (3 × 15 mL). The combined organic extracts were dried over Na_2SO_4 and filtered. The solvent was removed under reduced pressure. The crude material was purified by flash column chromatography (35% acetone/pentane). The product containing fractions were combined and the solvent was removed under reduced pressure. Et_2O (5 mL) and pentane (5 mL) were added and the solvent was removed under reduced pressure to afford the primary amide **74** as a white solid (114 mg, 74%). R_f 0.35 (40% acetone/pentane); mp = 162–165 °C (from Et_2O/pentane); ν_{max} (film)/cm^{-1} 3388 (NH br), 3198 (NH br), 2967, 1662 (C=O), 1513, 1402, 1219, 1174, 1126, 831; ^{1}H NMR (400 MHz, $CDCl_3$, 298 K, observed as a mixture of rotamers) δ 7.28–7.22 (m, 2 H, HC_{Ar}), 7.07–7.00 (m, 2 H, HC_{Ar}), 5.59 (br s, 1 H, N*H*H), 3.59 and 5.24 (2 × br s, 1 H, NH*H*), 3.99–3.75 (m, 2 H, NC*H*HCHAr, NC*H*HCHCO), 3.71–3.49 (m, 2 H, NCH*H*CHCO, CHAr), 3.44–3.31 (m, 1 H, NCH*H*CHAr), 3.02–2.87 (m, 1 H, CHCO), 1.47 and 1.46 (2 × s, 9 H, $C(CH_3)_3$); ^{13}C NMR

(101 MHz, $CDCl_3$, 298 K, observed as a mixture of rotamers) δ 172.8 (C=O amide), 162.1 (d, J_{CF} = 244.5 Hz, FC_{Ar} quat), 154.1 (C=O carbamate), 134.8 and 134.6 (F-*p*-C_{Ar} quat, observed as singlets), 129.0 (d, J_{CF} = 6.9 Hz, 2 × F-*m*-C_{Ar}), 115.94 and 115.85 (2 × d, J_{CF} = 21.6 Hz, 2 × F-*o*-C_{Ar}), 79.8 ($C(CH_3)_3$), 52.9 and 52.5 (NCH_2CHAr), 52.1 and 51.2 (*C*HCO), 49.0 and 48.9 (NCH_2CHCO), 47.4 and 46.9 (CHAr), 28.4 ($C(CH_3)_3$); ^{19}F NMR (377 MHz, $CDCl_3$, 298 K, observed as a mixture of rotamers) δ –114.2 and –114.7 (2 × m); HRMS (ESI^+) *m*/*z* Calculated for $C_{18}H_{24}N_3O_3FNa$ [M+MeCN+Na] 372.1699; Found 372.1699.

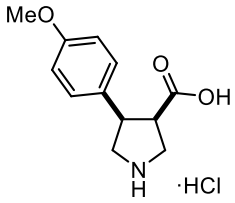
tert-Butyl _trans_-(±)-3-carbamoyl-4-(4-fluorophenyl)piperidine-1-carboxylate (80)



According to the procedure reported by Zhang and Chen,[144a] a round-bottom flask was charged with *trans*-arylated piperidine **26c** (360 mg, 0.80 mmol) and IBX (30 wt.%, 1.50 g, 1.60 mmol) under air. H_2O (2.7 mL) and HFIP (2.7 mL) were then added, and the resulting solution (0.15 M) was stirred at 60 °C for 1.5 h. The reaction mixture was then allowed to cool to rt and sat. aq. $NaHCO_3$ (10 mL) and CH_2Cl_2 (10 ml) were added. The phases were separated, and the aqueous layer was extracted with CH_2Cl_2 (3 × 15 mL). The combined organic extracts were dried over Na_2SO_4 and filtered. The solvent was removed under reduced pressure. The crude material was purified by flash column chromatography (30% acetone/pentane). The product containing fractions were combined and the solvent was removed under reduced pressure. Et_2O (5 mL) and pentane (5 mL) were added and the solvent was removed under reduced pressure to afford the primary amide **80** as a white solid (211 mg, 65%). R_f 0.30 (35% acetone/pentane); mp = 180–183 °C (from Et_2O/pentane); ν_{max} (film)/cm^{-1} 3422 (NH br), 3329 (NH br), 2978, 1685 (C=O), 1614 (C=O), 1510, 1428, 1364, 1219, 1159, 1129, 876, 828, 772; ^1H NMR (400 MHz, $CDCl_3$, 298 K, observed as a mixture of rotamers) δ 7.22–7.12 (m, 2 H, HC_{Ar}), 7.04–6.91 (m, 2 H, HC_{Ar}), 5.72–4.87 (br m, 2 H, NH_2), 4.57–4.95 (br m, 2 H, NC*H*HCHCO, NC*H*HCH_2), 3.16–2.71 (br m, 3 H, NCH*H*CHCO, CHAr, NCH*H*CH_2), 2.53–2.25 (br s, 1 H, CHCO), 1.86–1.75 (br m, 1 H, NCH_2CHH), 1.74–1.58 (br m, 1 H, NCH_2CHH), 1.49 (s, 9 H, $C(CH_3)_3$); ^{13}C NMR (101 MHz, $CDCl_3$, 298 K, observed as a mixture of rotamers) δ 174.0 (C=O amide), 161.7 (d, J_{CF} = 245.0 Hz, FC_{Ar} quat), 154.6 (C=O carbamate), 138.7 (d, J_{CF} = 3.3 Hz, F-*p*-C_{Ar} quat), 128.7 (d, J_{CF} = 7.8 Hz, 2 × F-*m*-C_{Ar}), 115.5 (d, J_{CF} = 21.1 Hz, 2 × F-*o*-C_{Ar}), 80.1 ($C(CH_3)_3$), 50.1 (br, *C*HCO), 46.5 (br, NCH_2CHCO), 44.4 (br, CHAr, NCH_2CH_2), 32.4 (br, NCH_2CH_2), 28.4 ($C(CH_3)_3$); ^{19}F NMR (377 MHz, $CDCl_3$, 298 K, observed as a mixture of rotamers) δ –115.9 (br s); HRMS (ESI^+) *m*/*z* Calculated for $C_{17}H_{24}N_2O_3F$ [M+H] 323.1771; Found 323.1772.

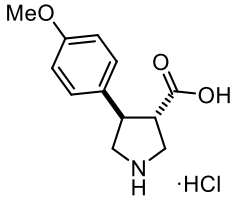
*8.2.3.7 N-Boc Deprotection: pyrrolidine fragments (**81–91**)*

cis-(±)-3-Carboxy-4-(4-methoxyphenyl)pyrrolidin-1-ium chloride (81)



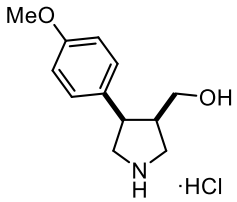
4 N HCl in 1,4-dioxane (1.1 mL, 4.50 mmol) was added to *N*-Boc protected pyrrolidine **36** (145 mg, 0.45 mmol) at 0 °C. The resulting solution was warmed up to 20 ºC and the product began to crush out of solution. The reaction mixture was stirred at 20 °C for 1 h and then ice-cold Et_2O (2 mL) was added. The reaction mixture was filtered and the precipate was washed with further ice-cold Et_2O (2 × 5 mL). The solid precipitate was dried under reduced pressure to afford the deprotected pyrrolidine product as the corresponding hydrochloride salt **81** as an off-white solid (97.4 mg, 84%). mp = 214–218 °C (from dioxane/Et_2O); ν_{max} (film)/cm^{-1} 2911 (NH, OH br), 1703 (C=O), 1517, 1387, 1252, 1200, 1170, 1029, 839, 779; ^{1}H NMR (400 MHz, CD_3OD, 298 K) δ 7.26–7.20 (m, 2 H, HC_{Ar}), 6.93–6.87 (m, 2 H, HC_{Ar}), 3.91 (ddd, *J* = 9.5, 9.5, 7.5 Hz, 1 H, CHAr), 3.77 (s, 3 H, OCH_3), 3.75–3.68 (m, 3 H, NC*H*HCHCO, NCH_2CHAr), 3.59 (dd, *J* = 12.2, 6.8 Hz, 1 H, NCH*H*CHCO), 3.49 (ddd, *J* = 7.6, 6.8, 3.4 Hz, 1 H, CHCO); ^{13}C NMR (101 MHz, CD_3OD, 298 K) δ 174.7 (COOH), 160.8 (OC_{Ar} quat), 130.0 (2 × C_{Ar}), 128.0 (C_{Ar} quat), 115.1 (2 × C_{Ar}), 55.7 (OCH_3), 49.4 (*C*HCO), 49.25 (N*C*H$_2$CHAr), 49.23 (N*C*H$_2$CHCO), 46.9 (CHAr); HRMS (ESI$^+$) *m*/*z* Calculated for $C_{12}H_{16}NO_3$ [M–Cl] 222.1130; Found 222.1135.

trans-(±)-3-Carboxy-4-(4-methoxyphenyl)pyrrolidin-1-ium chloride (83)



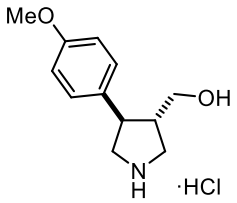
4 N HCl in 1,4-dioxane (1.0 mL, 4.00 mmol) was added to *N*-Boc protected pyrrolidine **30** (130 mg, 0.40 mmol) at 0 °C. The resulting solution was warmed up to 20 ºC and the product began to crush out of solution. The reaction mixture was stirred at 20 °C for 1 h and then ice-cold Et_2O (2 mL) was added. The reaction mixture was filtered and the precipate was washed with further ice-cold Et_2O (2 × 5 mL). The solid precipitate was dried under reduced pressure to afford the deprotected pyrrolidine product as the corresponding hydrochloride salt **83** as an off-white solid (93.7 mg, 91%). mp = 209–213 °C (from dioxane/Et_2O); ν_{max} (film)/cm^{-1} 2915 (NH, OH br), 1730 (C=O), 1513, 1383, 1256, 1163, 1029, 850, 678; ^{1}H NMR (400 MHz, CD_3OD, 298 K) δ 7.33–7.28 (m, 2 H, HC_{Ar}), 6.96–6.90 (m, 2 H, HC_{Ar}), 3.83–3.70 (m, 5 H, NC*H*HCHAr, NC*H*HCHCO, OCH_3), 3.70–3.59 (m, 2 H, NCH*H*CHCO, CHAr), 3.40–3.32 (m, 2 H, NCH*H*CHAr, CHCO); ^{13}C NMR (101 MHz, CD_3OD, 298 K) δ 173.9 (COOH), 160.9 (OC_{Ar} quat), 130.0 (C_{Ar} quat), 129.7 (2 × C_{Ar}), 115.4 (2 × C_{Ar}), 55.2 (OCH_3), 55.7 (N*C*H$_2$CHAr), 52.8 (*C*HCO), 50.7 (N*C*H$_2$CHCO), 48.5 (CHAr); HRMS (ESI$^+$) *m*/*z* Calculated for $C_{12}H_{16}NO_3$ [M–Cl] 222.1130; Found 222.1126.

***cis*-(±)-3-(Hydroxymethyl)-4-(4-methoxyphenyl)pyrrolidin-1-ium chloride (85)**



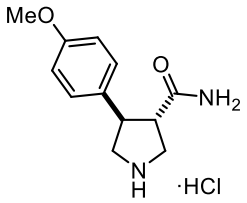
4 N HCl in 1,4-dioxane (1.2 mL, 4.90 mmol) was added to *N*-Boc protected pyrrolidine **37** (150 mg, 0.49 mmol) at 0 °C. The reaction mixture was stirred at 20 °C for 18 h until the product completely crushed out of solution. Ice-cold Et_2O (3 mL) was then added. The reaction mixture was filtered and the precipate was washed with further ice-cold Et_2O (2 × 5 mL). The solid precipitate was dried under reduced pressure to afford the deprotected pyrrolidine product as the corresponding hydrochloride salt **85** as an off-white solid (113.1 mg, 95%). mp = 138–142 °C (from dioxane/Et_2O); ν_{max} (film)/cm^{-1} 3355 (OH br), 2967 (NH br), 2766, 1517, 1305, 1252, 1185, 1029, 828; ^{1}H NMR (400 MHz, CD_3OD, 298 K) δ 7.28–7.22 (m, 2 H, HC_{Ar}), 6.95–6.90 (m, 2 H, HC_{Ar}), 3.79 (s, 3 H, OCH_3), 3.76–3.57 (m, 3 H, NC*H*$_2$CHAr, CHAr), 3.56–3.50 (m, 2 H, NC*H*$_2$CHCH$_2$OH), 3.39 (dd, *J* = 10.6, 4.2 Hz, 1 H, C*H*HOH), 3.27 (dd, *J* = 10.6, 5.7 Hz, 1 H, CH*H*OH), 3.68–3.58 (m, 1 H, C*H*CH$_2$OH); ^{13}C NMR (101 MHz, CD_3OD, 298 K) δ 160.5 (OC_{Ar} quat), 130.3 (2 × C_{Ar}), 128.9 (C_{Ar} quat), 115.1 (2 × C_{Ar}), 61.3 (CH_2OH), 55.7 (OCH_3), 50.1 (N*C*H$_2$CHAr), 49.6 (N*C*H$_2$CHCH$_2$OH), 46.3 (CHAr), 45.0 (*C*HCH$_2$OH); HRMS (ESI$^+$) *m*/*z* Calculated for $C_{12}H_{18}NO_2$ [M–Cl] 208.1338; Found 208.1342.

***trans*-(±)-3-(Hydroxymethyl)-4-(4-methoxyphenyl)pyrrolidin-1-ium chloride (87)**



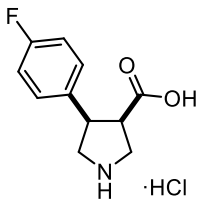
4 N HCl in 1,4-dioxane (1.0 mL, 4.00 mmol) was added to *N*-Boc protected pyrrolidine **66** (123 mg, 0.40 mmol) at 0 °C. The resulting solution was warmed up to 20 ºC and the product began to crush out of solution. The reaction mixture was stirred at 20 °C for 3 h and then ice-cold Et_2O (2 mL) was added. The reaction mixture was filtered and the precipate was washed with further ice-cold Et_2O (2 × 5 mL). The solid precipitate was dried under reduced pressure to afford the deprotected pyrrolidine product as the corresponding hydrochloride salt **87** as an off-white solid (83.3 mg, 85%). mp = 193–195 °C (from dioxane/Et_2O); ν_{max} (film)/cm^{-1} 3355 (OH br), 2952 (NH br), 1517, 1398, 1252, 1182, 1074, 1029, 813; ^{1}H NMR (400 MHz, CD_3OD, 298 K) δ 7.31–7.24 (m, 2 H, HC_{Ar}), 6.96–6.89 (m, 2 H, HC_{Ar}), 3.78 (s, 3 H, OCH_3), 3.70–3.58 (m, 3 H, NC*H*HCHAr, NC*H*HCHCH$_2$OH, C*H*HOH), 3.47 (dd, *J* = 11.2, 6.0 Hz, 1 H, CH*H*OH), 3.37–3.21 (m, 3 H, NCH*H*CHCH$_2$OH, NCH*H*CHAr, CHAr), 3.60–3.46 (m, 1 H, C*H*CH$_2$OH); ^{13}C NMR (101 MHz, CD_3OD, 298 K) δ 160.7 (OC_{Ar} quat), 130.6 (C_{Ar} quat), 129.8 (2 × C_{Ar}), 115.5 (2 × C_{Ar}), 60.7 (*C*H$_2$OH), 55.7 (OCH_3), 52.9 (N*C*H$_2$CHAr), 49.3 (N*C*H$_2$CHCH$_2$OH), 48.9 (*C*HCH$_2$OH), 45.8 (CHAr); HRMS (ESI$^+$) *m*/*z* Calculated for $C_{12}H_{18}NO_2$ [M–Cl] 208.1338; Found 208.1335.

***trans*-(±)-3-Carbamoyl-4-(4-methoxyphenyl)pyrrolidin-1-ium chloride (89)**



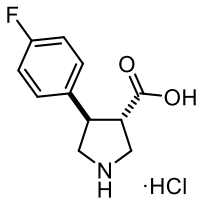
4 N HCl in 1,4-dioxane (1.0 mL, 4.00 mmol) was added to *N*-Boc protected pyrrolidine **72** (128 mg, 0.40 mmol) at 0 °C. The resulting solution was warmed up to 20 ºC and the product began to crush out of solution. The reaction mixture was stirred at 20 °C for 3 h and then ice-cold Et_2O (2 mL) was added. The reaction mixture was filtered and the precipate was washed with further ice-cold Et_2O (2 × 5 mL). The solid precipitate was dried under reduced pressure to afford the deprotected pyrrolidine product as the corresponding hydrochloride salt **89** as a white solid (94.4 mg, 92%). mp = 275–278 °C (from dioxane/Et_2O); ν_{max} (film)/cm^{-1} 3362 (CONH br), 3175 (CONH br), 2952 (NH br), 1689 (C=O), 1521, 1413, 1252, 1182, 1029, 828; ^{1}H NMR (400 MHz, DMSO-*d*$_6$, 298 K) δ 10.04–9.80 (br m, 1 H, N*H*H$^+$), 9.70–9.48 (br m, 1 H, NH*H*$^+$), 7.59 (s, 1 H, CON*H*H), 7.30–7.20 (m, 2 H, HC_{Ar}), 7.09 (s, 1 H, CONH*H*), 6.94–6.83 (m, 2 H, HC_{Ar}), 3.73 (s, 3 H, OCH_3), 3.65–3.56 (m, 3 H, NC*H*HCHAr, NC*H*HCHCO, CHAr), 3.26–3.02 (m, 3 H, NCH*H*CHAr, NCH*H*CHCO, CHCO); ^{13}C NMR (101 MHz, DMSO-*d*$_6$, 298 K) δ 171.3 ($CONH_2$), 158.5 (OC_{Ar} quat), 129.5 (C_{Ar} quat), 128.7 (2 × C_{Ar}), 114.0 (2 × C_{Ar}), 55.1 (OCH_3), 50.2 (N*C*H$_2$CHAr), 49.7 (*C*HCO), 47.7 (N*C*H$_2$CHCO), 46.4 (CHAr); HRMS (ESI$^+$) *m*/*z* Calculated for $C_{12}H_{17}N_2O_2$ [M–Cl] 221.1290; Found 221.1288.

***cis*-(±)-3-Carboxy-4-(4-fluorophenyl)pyrrolidin-1-ium chloride (82)**



4 N HCl in 1,4-dioxane (1.0 mL, 4.00 mmol) was added to *N*-Boc protected pyrrolidine **61** (124 mg, 0.40 mmol) at 0 °C. The resulting solution was warmed up to 20 ºC and the product began to crush out of solution. The reaction mixture was stirred at 20 °C for 2 h and then ice-cold Et_2O (2 mL) was added. The reaction mixture was filtered and the precipate was washed with further ice-cold Et_2O (2 × 5 mL). The solid precipitate was dried under reduced pressure to afford the deprotected pyrrolidine product as the corresponding hydrochloride salt **82** as a white solid (74.0 mg, 75%). mp = 210–213 °C (from dioxane/Et_2O); ν_{max} (film)/cm^{-1} 2807 (NH, OH br), 1730 (C=O), 1551, 1513, 1401, 1208, 835, 693; ^{1}H NMR (400 MHz, CD_3OD, 298 K) δ 7.37–7.30 (m, 2 H, HC_{Ar}), 7.13–7.05 (m, 2 H, HC_{Ar}), 3.96 (ddd, *J* = 9.5, 9.5, 7.3 Hz, 1 H, CHAr), 3.77–3.70 (m, 3 H, NC*H*HCHAr, NC*H*$_2$CHCO), 3.59 (dd, *J* = 12.0, 6.8 Hz, 1 H, NCH*H*CHAr), 3.52 (ddd, *J* = 7.1, 7.1, 3.0 Hz, 1 H, CHCO); ^{13}C NMR (101 MHz, CD_3OD, 298 K) δ 174.6 (COOH), 163.8 (d, J_{CF} = 245.4 Hz, FC_{Ar} quat), 132.3 (d, J_{CF} = 3.4 Hz, F-*p*-C_{Ar} quat), 130.9 (d, J_{CF} = 8.2 Hz, 2 × F-*m*-C_{Ar}), 116.4 (d, J_{CF} = 21.7 Hz, 2 × F-*o*-C_{Ar}), 49.4 (*C*HCO), 49.3 (N*C*H$_2$CHAr), 49.1 (N*C*H$_2$CHCO), 46.8 (CHAr); ^{19}F NMR (377 MHz, CD_3OD, 298 K) δ –116.6 (tt, J_{HF} = 8.7, 5.2 Hz); HRMS (ESI$^+$) *m*/*z* Calculated for $C_{11}H_{13}NO_2F$ [M–Cl] 210.0930; Found 210.0936.

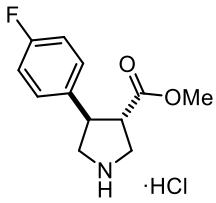
***trans*-(±)-3-Carboxy-4-(4-fluorophenyl)pyrrolidin-1-ium chloride (84)**



4 N HCl in 1,4-dioxane (1.0 mL, 4.00 mmol) was added to *N*-Boc protected pyrrolidine **60** (124 mg, 0.40 mmol) at 0 °C. The reaction mixture was stirred at 20 °C for 2 h. Ice-cold Et_2O (3 mL) was then added and the product crushed out of solution. The reaction mixture was filtered and the precipate was washed with further ice-cold Et_2O (2 × 5 mL). The solid precipitate was found to be hygroscopic and turned quickly into a paste. This was solubilised in a 1:1 mixture of deionized H_2O and acetone. The resulting solution was concentrated under reduced pressure. Et_2O (3 mL) and pentane (3 mL) were added and the solvent was removed under reduced pressure to afford the caroxylic acid product as the corresponding hydrochloride salt **84** as a dark orange solid (95.6 mg, 97%). mp = 71–74 °C (from Et_2O/pentane); ν_{max} (film)/cm^{-1} 2896 (NH, OH br), 2747 (NH br), 1718 (C=O), 1513, 1398, 1223, 1163, 831; ^{1}H NMR (400 MHz, CD_3OD, 298 K) δ 7.45–7.38 (m, 2 H, HC_{Ar}), 7.16–7.08 (m, 2 H, HC_{Ar}), 3.83–3.62 (m, 4 H, CHAr, NC*H*HCHAr, NCH_2CHCO), 3.43–3.32 (m, 2 H, CHCO, NCH*H*CHAr); ^{13}C NMR (101 MHz, CD_3OD, 298 K) δ 173.6 (COOH), 163.8 (d, J_{CF} = 245.1 Hz, FC_{Ar} quat), 134.4 (d, J_{CF} = 2.9 Hz, F-*p*-C_{Ar} quat), 130.6 (d, J_{CF} = 8.2 Hz, 2 × F-*m*-C_{Ar}), 116.7 (d, J_{CF} = 21.8 Hz, 2 × F-*o*-C_{Ar}), 52.8 (N*C*H_2CHAr), 50.6 (*C*HCO), 48.9 (N*C*H_2CHCO), 48.2 (CHAr); ^{19}F NMR (377 MHz, CD_3OD, 298 K) δ –116.7 (tt, J_{HF} = 9.0, 5.4 Hz); HRMS (ESI$^+$) *m*/*z* Calculated for $C_{11}H_{13}NO_2F$ [M–Cl] 210.0930; Found 210.0936.

Note: Hygroscopic solid. Avoid concentration from MeOH solution, as this could led to partial or complete esterification to the corresponding methyl ester **S3**.

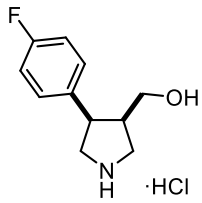
***trans*-(±)-3-(4-Fluorophenyl)-4-(methoxycarbonyl)pyrrolidin-1-ium chloride (S3)**



4 N HCl in 1,4-dioxane (1.0 mL, 4.00 mmol) was added to *N*-Boc protected pyrrolidine **60** (124 mg, 0.40 mmol) at 0 °C. The reaction mixture was stirred at 20 °C for 18 h. Ice-cold Et_2O (3 mL) was then added and the product crushed out of solution. The reaction mixture was filtered and the precipate was washed with further ice-cold Et_2O (2 × 5 mL). The solid precipitate was found to be hygroscopic and turned quickly into a paste. This was solubilised in MeOH and the resulting solution was concentrated under reduced pressure. The reaction was performed a second time on the crude mixture under the same conditions. Following an identical work-up procedure, Et_2O (3 mL) and pentane (3 mL) were added and the solvent was removed under reduced pressure to afford the methyl ester product as the corresponding hydrochloride salt **S3** as an off-white solid (86.3 mg, 83%). mp = 152–155 °C (from Et_2O/pentane); ν_{max} (film)/cm^{-1} 2848 (NH br), 2751 (NH br), 1718 (C=O), 1513, 1439, 1349, 1226, 1159, 1096, 816; ^{1}H NMR (400 MHz, CD_3OD, 298 K) δ 7.47–7.37 (m, 2 H, HC_{Ar}), 7.16–7.07 (m, 2 H, HC_{Ar}),

3.89–3.60 (m, 7 H, CHAr, NC*H*HCHAr, NC*H*$_2$CHCO, OCH$_3$), 3.46 (ddd, *J* = 9.0, 9.0, 9.0 Hz, 1 H, CHCO), 3.37 (dd, *J* = 10.1, 10.1 Hz, 1 H, NCH*H*CHAr); ^{13}C NMR (101 MHz, CD$_3$OD, 298 K) δ 172.6 (*C*OOCH$_3$), 163.8 (d, J_{CF} = 245.3 Hz, FC$_{Ar}$ quat), 134.1 (d, J_{CF} = 2.7 Hz, F-*p*-C$_{Ar}$ quat), 130.6 (d, J_{CF} = 8.4 Hz, 2 × F-*m*-C$_{Ar}$), 116.8 (d, J_{CF} = 21.7 Hz, 2 × F-*o*-C$_{Ar}$), 53.0 (OCH$_3$), 52.7 (N*C*H$_2$CHAr), 50.5 (*C*HCO), 48.8 (N*C*H$_2$CHCO), 48.3 (CHAr); ^{19}F NMR (377 MHz, CD$_3$OD, 298 K) δ –116.5 (tt, J_{HF} = 9.2, 5.1 Hz); HRMS (ESI$^+$) *m*/*z* Calculated for C$_{12}$H$_{15}$NO$_2$F [M–Cl] 224.1087; Found 224.1088.

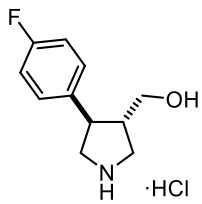
***cis*-(±)-3-(4-Fluorophenyl)-4-(hydroxymethyl)pyrrolidin-1-ium chloride (86)**



4 N HCl in 1,4-dioxane (0.9 mL, 3.70 mmol) was added to *N*-Boc protected pyrrolidine **65** (110 mg, 0.37 mmol) at 0 °C. The reaction mixture was stirred at 20 °C for 18 h. Ice-cold Et$_2$O (3 mL) was then added and the product crushed out of solution. The reaction mixture was filtered and the precipate was washed with further ice-cold Et$_2$O (2 × 5 mL). The solid precipitate was found to be hygroscopic and turned quickly into a paste. This was then solubilised in MeOH and the resulting solution was concentrated under reduced pressure to afford the deprotected pyrrolidine product as the corresponding hydrochloride salt **86** as a bright orange paste (81.9 mg, 96%). ν_{max} (film)/cm^{-1} 3343 (OH br), 2904 (NH br), 2725 (NH br), 1603, 1513, 1402, 1223, 1163, 1045, 835; ^{1}H NMR (400 MHz, CD$_3$OD, 298 K) δ 7.41–7.34 (m, 2 H, HC$_{Ar}$), 7.15–7.06 (m, 2 H, HC$_{Ar}$), 3.84–3.59 (m, 3 H, NC*H*HCHAr, NC*H*HCHCH$_2$OH, CHAr), 3.59–3.52 (m, 2 H, NCH*H*CHCH$_2$OH, NCH*H*CHAr), 3.40 (dd, *J* = 10.6, 4.1 Hz, 1 H, C*H*HOH), 3.27 (dd, *J* = 10.7, 5.1 Hz, 1 H, CH*H*OH), 2.71–2.62 (m, 1 H, C*H*CH$_2$OH); ^{13}C NMR (101 MHz, CD$_3$OD, 298 K) δ 163.5 (d, J_{CF} = 244.7 Hz, FC$_{Ar}$ quat), 133.2 (d, J_{CF} = 3.3 Hz, F-*p*-C$_{Ar}$ quat), 131.2 (d, J_{CF} = 8.0 Hz, 2 × F-*m*-C$_{Ar}$), 116.4 (d, J_{CF} = 21.6 Hz, 2 × F-*o*-C$_{Ar}$), 61.2 (CH$_2$OH), 50.1 (N*C*H$_2$CHAr), 49.6 (N*C*H$_2$CHCH$_2$OH), 46.4 (CHAr), 44.9 (*C*HCH$_2$OH); ^{19}F NMR (377 MHz, CD$_3$OD, 298 K) δ –117.3 (tt, J_{HF} = 9.1, 5.5 Hz); HRMS (ESI$^+$) *m*/*z* Calculated for C$_{11}$H$_{15}$NOF [M–Cl] 196.1138; Found 196.1143.

Note: Highly hygroscopic solid.

***trans*-(±)-3-(4-Fluorophenyl)-4-(hydroxymethyl)pyrrolidin-1-ium chloride (88)**

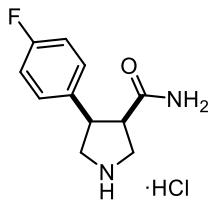


4 N HCl in 1,4-dioxane (1.2 mL, 4.00 mmol) was added to *N*-Boc protected pyrrolidine **67** (118 mg, 0.40 mmol) at 0 °C. The reaction mixture was stirred at 20 °C for 18 h. Ice-cold Et$_2$O (3 mL) was then added and the product crushed out of solution. The reaction mixture was filtered and the precipate was washed with further ice-cold Et$_2$O (2 × 5 mL). The solid precipitate was found to be hygroscopic and turned quickly into a paste. This was then solubilised in MeOH

and the resulting solution was concentrated under reduced pressure. Et_2O (3 mL) and pentane (3 mL) were added and the solvent was removed under reduced pressure to afford the deprotected pyrrolidine product as the corresponding hydrochloride salt **88** as a bright orange solid (87.1 mg, 94%). mp = 120–123 °C (from Et_2O/pentane); ν_{max} (film)/cm^{-1} 3347 (OH br), 2956 (NH br), 2740 (NH br), 1513, 1398, 1227, 1096, 826; ^{1}H NMR (400 MHz, CD_3OD, 298 K) δ 7.43–7.36 (m, 2 H, HC_{Ar}), 7.14–7.07 (m, 2 H, HC_{Ar}), 3.74–3.64 (m, 2 H, NC*H*HCHAr, NC*H*HCHCH$_2$OH), 3.62 (dd, *J* = 11.3, 3.5 Hz, 1 H, C*H*HOH), 3.47 (dd, *J* = 11.3, 5.8 Hz, 1 H, CH*H*OH), 3.40–3.28 (m, 3 H, NCH*H*CHCH$_2$OH, NCH*H*CHAr, CHAr), 2.62–2.51 (m, 1 H, C*H*CH$_2$OH); ^{13}C NMR (101 MHz, CD_3OD, 298 K) δ 163.7 (d, J_{CF} = 244.9 Hz, FC_{Ar} quat), 135.1 (d, J_{CF} = 3.1 Hz, F-*p*-C_{Ar} quat), 130.7 (d, J_{CF} = 8.1 Hz, 2 × F-*m*-C_{Ar}), 116.8 (d, J_{CF} = 21.7 Hz, 2 × F-*o*-C_{Ar}), 60.5 (CH_2OH), 52.9 (N*C*H$_2$CHAr), 49.2 (N*C*H$_2$CHCH$_2$OH), 49.0 (*C*HCH$_2$OH), 45.8 (CHAr); ^{19}F NMR (377 MHz, CD_3OD, 298 K) δ –117.0 (tt, J_{HF} = 9.0, 5.4 Hz); HRMS (ESI$^+$) *m*/*z* Calculated for $C_{11}H_{15}NOF$ [M–Cl] 196.1138; Found 196.1145.

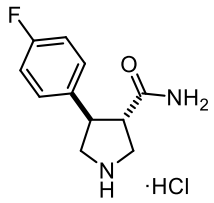
Note: Hygroscopic solid.

***cis*-(±)-3-Carbamoyl-4-(4-fluorophenyl)pyrrolidin-1-ium chloride (90)**



4 N HCl in 1,4-dioxane (1.0 mL, 4.00 mmol) was added to *N*-Boc protected pyrrolidine **73** (123 mg, 0.40 mmol) at 0 °C. The resulting solution was warmed up to 20 ºC and the product began to crush out of solution. The reaction mixture was stirred at 20 °C for 2 h and then ice-cold Et_2O (2 mL) was added. The reaction mixture was filtered and the precipate was washed with further ice-cold Et_2O (2 × 5 mL). The solid precipitate was dried under reduced pressure to afford the deprotected pyrrolidine product as the corresponding hydrochloride salt **90** as an off-white solid (91.8 mg, 94%). mp = 237–240 °C (from dioxane/Et_2O); ν_{max} (film)/cm^{-1} 3373 (CONH br), 3194 (CONH br), 2937 (NH br), 1685 (C=O), 1513, 1394, 1223, 1159, 835; ^{1}H NMR (400 MHz, CD_3OD, 298 K) δ 7.39–7.32 (m, 2 H, HC_{Ar}), 7.12–7.02 (m, 2 H, HC_{Ar}), 3.92 (ddd, *J* = 11.8, 7.6, 7.6 Hz, 1 H, CHAr), 3.80 (dd, *J* = 11.4, 11.4 Hz, 1 H, NC*H*HCHCO), 3.72–3.64 (m, 2 H, NCH*H*CHCO, NC*H*HCHAr), 3.57 (dd, *J* = 12.0, 6.6 Hz, 1 H, NCH*H*CHAr), 3.43 (ddd, *J* = 6.9, 6.9, 2.3 Hz, 1 H, CHCO); ^{13}C NMR (101 MHz, CD_3OD, 298 K) δ 175.8 ($CONH_2$), 163.8 (d, J_{CF} = 245.3 Hz, FC_{Ar} quat), 132.1 (d, J_{CF} = 3.4 Hz, F-*p*-C_{Ar} quat), 131.1 (d, J_{CF} = 8.1 Hz, 2 × F-*m*-C_{Ar}), 116.4 (d, J_{CF} = 21.8 Hz, 2 × F-*o*-C_{Ar}), 49.7 (N*C*H$_2$CHAr), 49.3 (*C*HCO), 49.1 (N*C*H$_2$CHCO), 47.2 (CHAr); ^{19}F NMR (377 MHz, CD_3OD, 298 K) δ –116.7 (tt, J_{HF} = 9.0, 5.5 Hz); HRMS (ESI$^+$) *m*/*z* Calculated for $C_{11}H_{14}N_2OF$ [M–Cl] 209.1090; Found 209.1087.

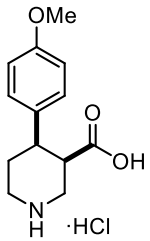
***trans*-(±)-3-Carbamoyl-4-(4-fluorophenyl)pyrrolidin-1-ium chloride (91)**



4 N HCl in 1,4-dioxane (0.8 mL, 3.20 mmol) was added to *N*-Boc protected pyrrolidine **74** (100 mg, 0.32 mmol) at 0 °C. The resulting solution was warmed up to 20 ºC and the product began to crush out of solution. The reaction mixture was stirred at 20 °C for 3 h and then ice-cold Et_2O (2 mL) was added. The reaction mixture was filtered and the precipate was washed with further ice-cold Et_2O (2 × 5 mL). The solid precipitate was dried under reduced pressure to afford the deprotected pyrrolidine product as the corresponding hydrochloride salt **91** as a white solid (64.0 mg, 82%). mp = 252–255 °C (from dioxane/Et_2O); ν_{max} (film)/cm^{-1} 3362 (CONH br), 3183 (CONH br), 2907 (NH br), 2766 (NH br), 1681 (C=O), 1513, 1416, 1223, 831; ^{1}H NMR (400 MHz, CD_3OD, 298 K) δ 7.45–7.37 (m, 2 H, HC_{Ar}), 7.16–7.08 (m, 2 H, HC_{Ar}), 3.81–3.73 (m, 2 H, NC*H*HCHCO, NC*H*HCHAr), 3.69 (ddd, *J* = 10.2, 10.2, 7.9 Hz, 1 H, CHAr), 3.52 (dd, *J* = 11.8, 9.2 Hz, 1 H, NCH*H*CHCO), 3.39 (dd, *J* = 10.9, 10.9 Hz, 1 H, NCH*H*CHAr), 3.33–3.24 (m, 1 H, CHCO); ^{13}C NMR (101 MHz, CD_3OD, 298 K) δ 174.3 ($CONH_2$), 163.9 (d, J_{CF} = 245.5 Hz, FC_{Ar} quat), 133.8 (d, J_{CF} = 3.1 Hz, F-*p*-C_{Ar} quat), 130.7 (d, J_{CF} = 8.2 Hz, 2 × F-*m*-C_{Ar}), 116.8 (d, J_{CF} = 21.8 Hz, 2 × F-*o*-C_{Ar}), 52.3 (N*C*H_2CHAr), 51.6 (*C*HCO), 49.6 (N*C*H_2CHCO), 48.9 (CHAr); ^{19}F NMR (377 MHz, CD_3OD, 298 K) δ –116.5 (tt, J_{HF} = 8.5, 5.1 Hz); HRMS (ESI$^+$) *m*/*z* Calculated for $C_{11}H_{14}N_2OF$ [M–Cl] 209.1090; Found 209.1092.

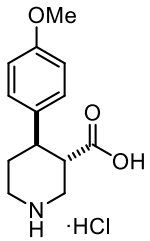
*8.2.3.8 N-Boc Deprotection: piperidine fragments (**92–95**)*

cis-(±)-3-Carboxy-4-(4-methoxyphenyl)piperidin-1-ium chloride (92)



4 N HCl in 1,4-dioxane (1.1 mL, 4.50 mmol) was added to *N*-Boc protected piperidine **64** (151 mg, 0.45 mmol) at 0 °C. The resulting solution was warmed up to 20 ºC and the product began to crush out of solution. The reaction mixture was stirred at 20 °C for 1 h and then ice-cold Et_2O (2 mL) was added. The reaction mixture was filtered and the precipate was washed with further ice-cold Et_2O (2 × 5 mL). The solid precipitate was dried under reduced pressure to afford the deprotected piperidine product as the corresponding hydrochloride salt **92** as a white solid (106 mg, 87%). mp = 253–256 °C (from dioxane/Et_2O); ν_{max} (film)/cm^{-1} 3064 (NH br), 2837 (OH br), 1685 (C=O), 1554, 1513, 1416, 1249, 1111, 1033, 876, 813, 705; ^{1}H NMR (400 MHz, CD_3OD, 298 K) δ 7.22–7.15 (m, 2 H, HC_{Ar}), 6.91–6.84 (m, 2 H, HC_{Ar}), 3.77 (s, 3 H, OCH_3), 3.64 (ddd, *J* = 13.0, 1.8, 1.8 Hz, 1 H, NC*H*HCHCO), 3.58–3.51 (ddd, *J* = 12.6, 4.1, 4.1 Hz, 1 H, NC*H*HCH$_2$), 3.35–3.26 (m, 2 H, CHAr, NCH*H*CHCO), 3.17 (ddd, *J* = 12.7, 12.7, 3.3 Hz, 1 H, NCH*H*CH$_2$), 3.13–3.09 (m, 1 H, CHCO), 2.54 (dddd, *J* = 14.2, 12.8, 12.8, 4.2 Hz, 1 H, NCH$_2$C*H*H), 1.98 (dddd, *J* = 14.4, 2.9, 2.9, 2.9 Hz, 1 H, NCH$_2$CH*H*); ^{13}C NMR (101 MHz, CD_3OD, 298 K) δ 176.1 (COOH), 160.3 (OC_{Ar} quat), 134.1 (C_{Ar} quat), 129.3 (2 × C_{Ar}), 114.9 (2 × C_{Ar}), 55.6 (OCH_3), 46.5 (N*C*H$_2$CHCO), 45.3 (N*C*H$_2$CH$_2$), 44.1 (*C*HCO), 41.0 (CHAr), 24.7 (NCH$_2$*C*H$_2$); HRMS (ESI$^+$) *m*/*z* Calculated for $C_{13}H_{18}NO_3$ [M–Cl] 236.1287; Found 236.1284.

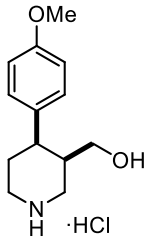
trans-(±)-3-Carboxy-4-(4-methoxyphenyl)piperidin-1-ium chloride (94)



4 N HCl in 1,4-dioxane (1.0 mL, 4.00 mmol) was added to *N*-Boc protected piperidine **62** (134 mg, 0.40 mmol) at 0 °C. The resulting solution was warmed up to 20 ºC and the product began to crush out of solution. The reaction mixture was stirred at 20 °C for 1 h and then ice-cold Et_2O (2 mL) was added. The reaction mixture was filtered and the precipate was washed with further ice-cold Et_2O (2 × 5 mL). The solid precipitate was dried under reduced pressure to afford the deprotected piperidine product as the corresponding hydrochloride salt **94** as a white solid (87.3 mg, 80%). mp = 269–272 °C (from dioxane/Et_2O); ν_{max} (film)/cm^{-1} 3101 (NH br), 2792 (OH br), 1722 (C=O), 1513, 1409, 1230, 1182, 1033, 828, 678; ^{1}H NMR (400 MHz, CD_3OD, 298 K) δ 7.22–7.17 (m, 2 H, HC_{Ar}), 6.90–6.84 (m, 2 H, HC_{Ar}), 3.76 (s, 3 H, OCH_3), 3.68–3.61 (m, 1 H, NC*H*HCHCO), 3.50 (dddd, *J* = 12.8, 3.3, 3.3, 1.6 Hz, 1 H, NC*H*HCH$_2$), 3.23–3.13 (m, 2 H, NCH*H*CHCO, NCH*H*CH$_2$), 3.08–2.97 (m, 2 H, CHAr, CHCO), 2.08–1.91 (m, 2 H, NCH$_2$C*H*$_2$); ^{13}C NMR (101 MHz, CD_3OD, 298 K) δ 173.7 (COOH), 160.4 (OC_{Ar} quat), 134.8 (C_{Ar} quat), 129.4 (2 × C_{Ar}), 115.0 (2 × C_{Ar}), 55.7 (OCH_3), 47.6 (*C*HCO), 46.8 (N*C*H$_2$CHCO),

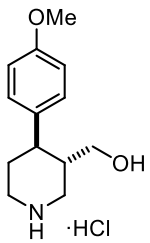
45.4 (N*C*H$_2$CH$_2$), 43.8 (CHAr), 31.1 (NCH$_2$*C*H$_2$); HRMS (ESI$^+$) *m*/*z* Calculated for $C_{13}H_{18}NO_3$ [M–Cl] 236.1287; Found 236.1296.

cis-(±)-3-(Hydroxymethyl)-4-(4-methoxyphenyl)piperidin-1-ium chloride (96)



4 N HCl in 1,4-dioxane (1.0 mL, 4.00 mmol) was added to *N*-Boc protected piperidine **68** (131 mg, 0.41 mmol) at 0 °C. The resulting solution was warmed up to 20 ºC and the product began to crush out of solution. The reaction mixture was stirred at 20 °C for 2 h and then ice-cold Et$_2$O (2 mL) was added. The reaction mixture was filtered and the precipate was washed with further ice-cold Et$_2$O (2 × 5 mL). The solid precipitate was dried under reduced pressure to afford the deprotected piperidine product as the corresponding hydrochloride salt **96** as a bright orange solid (74.8 mg, 71%). mp = 174–177 °C (from dioxane/Et$_2$O); ν_{max} (film)/cm^{-1} 3377 (OH br), 2945 (NH br), 2803 (NH br), 1595, 1513, 1457, 1271, 1245, 1178, 1021, 980, 828; ^{1}H NMR (400 MHz, CD$_3$OD, 298 K) δ 7.24–7.17 (m, 2 H, HC$_{Ar}$), 6.94–6.88 (m, 2 H, HC$_{Ar}$), 3.78 (s, 3 H, OCH$_3$), 3.68 (ddd, *J* = 13.1, 1.9, 1.9 Hz, 1 H, NC*H*HCHCH$_2$OH), 3.59 (dd, *J* = 10.8, 5.8 Hz, 1 H, C*H*HOH), 3.56–3.50 (m, 1 H, NC*H*HCH$_2$), 3.47 (dd, *J* = 10.8, 4.2 Hz, 1 H, CH*H*OH), 3.37–3.30 (m, 1 H, NCH*H*CHCH$_2$OH), 3.26–3.11 (m, 2 H, NCH*H*CH$_2$, CHAr), 2.49 (dddd, *J* = 13.2, 13.2, 13.2, 4.3 Hz, 1 H NCH$_2$C*H*H), 2.20–2.12 (m, 1 H, C*H*CH$_2$OH), 1.93 (dddd, *J* = 14.1, 3.4, 3.4, 3.4 Hz, 1 H, NCH$_2$CH*H*); ^{13}C NMR (101 MHz, CD$_3$OD, 298 K) δ 160.0 (OC$_{Ar}$ quat), 135.0 (C$_{Ar}$ quat), 129.4 (2 × C$_{Ar}$), 115.0 (2 × C$_{Ar}$), 60.9 (CH$_2$OH), 55.7 (OCH$_3$), 48.0 (N*C*H$_2$CHCH$_2$OH), 45.7 (N*C*H$_2$CH$_2$), 41.8 (CHAr), 39.7 (*C*HCH$_2$OH), 25.1 (NCH$_2$*C*H$_2$); HRMS (ESI$^+$) *m*/*z* Calculated for $C_{13}H_{20}NO_2$ [M–Cl] 222.1494; Found 222.1496.

trans-(±)-3-(Hydroxymethyl)-4-(4-methoxyphenyl)piperidin-1-ium chloride (97)

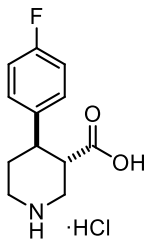


4 N HCl in 1,4-dioxane (1.0 mL, 4.00 mmol) was added to *N*-Boc protected piperidine **69** (130 mg, 0.40 mmol) at 0 °C. The reaction mixture was stirred at 20 °C for 18 h. Ice-cold Et$_2$O (3 mL) was then added and the product crushed out of solution. The reaction mixture was filtered and the precipate was washed with further ice-cold Et$_2$O (2 × 5 mL). The solid precipitate was found to be hygroscopic and turned quickly into a paste. This was then solubilised in MeOH and the resulting solution was concentrated under reduced pressure. Et$_2$O (3 mL) and pentane (3 mL) were added and the solvent was removed under reduced pressure to afford the deprotected piperidine product as the corresponding hydrochloride salt **97** as a bright orange solid (99.8 mg, 97%). mp = 56–60 °C (from Et$_2$O/pentane); ν_{max} (film)/cm^{-1} 3343 (OH br), 2930 (NH br), 2796 (NH br), 1610, 1513, 1461, 1241, 1178, 1029, 828; ^{1}H NMR (400 MHz, CD$_3$OD, 298 K) δ 7.21–7.14 (m, 2 H, HC$_{Ar}$), 6.92–6.86 (m, 2 H, HC$_{Ar}$), 3.77 (s, 3 H, OCH$_3$), 3.61 (ddd, *J* = 12.7, 4.1, 1.5 Hz, 1 H, NC*H*HCHCH$_2$OH), 3.47 (dddd, *J* = 12.0, 3.1, 3.1, 1.4 Hz, 1 H,

NC*H*HCH$_2$), 3.36 (dd, *J* = 11.1, 3.2 Hz, 1 H, C*H*HOH), 3.20 (dd, *J* = 11.1, 7.1 Hz, 1 H, CH*H*OH), 3.08 (ddd, *J* = 12.9, 9.8, 7.8 Hz, 1 H, NCH*H*CH$_2$), 2.96 (dd, *J* = 12.4, 12.4 Hz, 1 H, NCH*H*CHCH$_2$OH), 2.67 (ddd, *J* = 11.4, 9.3, 6.8 Hz, 1 H, CHAr), 2.20–2.08 (m, 1 H, C*H*CH$_2$OH), 2.01–1.93 (m, 2 H, NCH$_2$C*H*$_2$); ^{13}C NMR (101 MHz, CD_3OD, 298 K) δ 160.2 (OC_{Ar} quat), 135.5 (C_{Ar} quat), 129.4 (2 × C_{Ar}), 115.2 (2 × C_{Ar}), 62.2 (CH_2OH), 55.7 (OCH_3), 48.2 (N*C*H$_2$CHCH$_2$OH), 45.8 (N*C*H$_2$CH$_2$), 42.8 (CHAr), 42.7 (*C*HCH$_2$OH), 32.0 (NCH$_2$*C*H$_2$); HRMS (ESI$^+$) *m*/*z* Calculated for $C_{13}H_{20}NO_2$ [M–Cl] 222.1494; Found 222.1503.

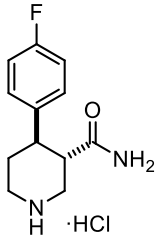
Note: Hygroscopic solid.

***trans*-(±)-3-Carboxy-4-(4-fluorophenyl)piperidin-1-ium chloride (93)**



4 N HCl in 1,4-dioxane (1.0 mL, 4.00 mmol) was added to *N*-Boc protected piperidine **63** (134 mg, 0.40 mmol) at 0 °C. The resulting solution was warmed up to 20 ºC and the product began to crush out of solution. The reaction mixture was stirred at 20 °C for 1 h and then ice-cold Et_2O (2 mL) was added. The reaction mixture was filtered and the precipate was washed with further ice-cold Et_2O (2 × 5 mL). The solid precipitate was dried under reduced pressure to afford the deprotected piperidine product as the corresponding hydrochloride salt **93** as a white solid (81.3 mg, 78%). mp = 269–271 °C (from dioxane/Et_2O); ν_{max} (film)/cm^{-1} 2926 (OH br), 2281, 1733 (C=O), 1510, 1394, 1215, 1185, 1111, 794; ^{1}H NMR (400 MHz, CD_3OD, 298 K) δ 7.34–7.27 (m, 2 H, HC_{Ar}), 7.09–7.01 (m, 2 H, HC_{Ar}), 3.66 (ddd, *J* = 12.2, 3.2, 1.4 Hz, 1 H, NC*H*HCHCO), 3.51 (dddd, *J* = 12.8, 3.3, 3.3, 1.5 Hz, 1 H, NC*H*HCH$_2$), 3.25–3.15 (m, 2 H, NCH*H*CHCO, NCH*H*CH$_2$), 3.15–3.03 (m, 2 H, CHAr, CHCO), 2.09–1.95 (m, 2 H, NCH$_2$C*H*$_2$); ^{13}C NMR (101 MHz, CD_3OD, 298 K) δ 173.5 (COOH), 163.4 (d, J_{CF} = 244.0 Hz, FC_{Ar} quat), 139.0 (d, J_{CF} = 3.1 Hz, F-*p*-C_{Ar} quat), 130.3 (d, J_{CF} = 7.9 Hz, 2 × F-*m*-C_{Ar}), 116.3 (d, J_{CF} = 21.5 Hz, 2 × F-*o*-C_{Ar}), 47.3 (*C*HCO), 46.7 (N*C*H$_2$CHCO), 45.3 (N*C*H$_2$CH$_2$), 43.8 (CHAr), 31.0 (NCH$_2$*C*H$_2$); ^{19}F NMR (377 MHz, $CDCl_3$, 298 K) δ –117.6 (tt, J_{HF} = 8.8, 5.3 Hz); HRMS (ESI$^+$) *m*/*z* Calculated for $C_{12}H_{15}NO_2F$ [M–Cl] 224.1087; Found 224.1082.

***trans*-(±)-3-Carbamoyl-4-(4-fluorophenyl)piperidin-1-ium chloride (95)**



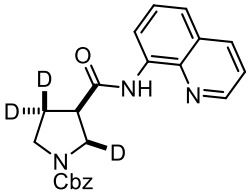
4 N HCl in 1,4-dioxane (1.0 mL, 4.00 mmol) was added to *N*-Boc protected piperidine **80** (130 mg, 0.40 mmol) at 0 °C. The resulting solution was warmed up to 20 ºC and the product began to crush out of solution. The reaction mixture was stirred at 20 °C for 1 h and then ice-cold Et_2O (2 mL) was added. The reaction mixture was filtered and the precipate was washed with further ice-cold Et_2O (2 × 5 mL). The solid precipitate was dried under reduced pressure to afford the deprotected piperidine product as the corresponding hydrochloride salt **95** as an off-white

solid (93.8 mg, 91%). mp > 300 °C (from dioxane/Et_2O); ν_{max} (film)/cm^{-1} 3247 (CONH br), 3124 (CONH br), 3019 (NH br), 1670 (C=O), 1510, 1431, 1219, 828; ^1H NMR (400 MHz, DMSO-d_6, 298 K) δ 9.64–9.12 (br m, 1 H, NH_2^+), 7.46 (s, 1 H, CON*H*H), 7.29–7.18 (m, 2 H, HC_{Ar}), 7.18–7.06 (m, 2 H, HC_{Ar}), 6.82 (s, 1 H, CONH*H*), 3.46–3.33 (m, 1 H, NC*H*HCHCO), 3.29 (br d, J = 12.9 Hz, 1 H, NC*H*HCH_2), 3.08–2.86 (m, 4 H, NCH*H*CHCO, NCH*H*CH_2, CHAr, CHCO), 2.02–1.87 (br m, 1 H, NCH_2C*H*H), 1.87–1.76 (br m, 1 H, NCH_2CH*H*); ^{13}C NMR (101 MHz, DMSO-d_6, 298 K) δ 171.5 ($CONH_2$), 161.0 (d, J_{CF} = 242.2 Hz, FC_{Ar} quat), 138.7 (F-*p*-C_{Ar} quat, observed as singlet), 129.2 (d, J_{CF} = 8.0 Hz, 2 × F-*m*-C_{Ar}), 115.0 (d, J_{CF} = 21.0 Hz, 2 × F-*o*-C_{Ar}), 45.3 (*C*HCO), 45.1 (br, N*C*H_2CHCO), 43.1 (N*C*H_2CH_2), 41.6 (CHAr), 29.4 (NCH_2*C*H_2); ^{19}F NMR (377 MHz, $CDCl_3$, 298 K) δ –116.3 (br s); HRMS (ESI^+) *m*/*z* Calculated for $C_{12}H_{16}N_2OF$ [M–Cl] 223.1247; Found 223.1240.

8.2.4 Compounds for Chapter 5

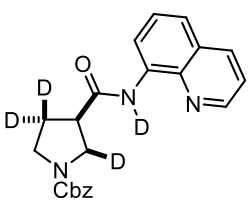
*8.2.4.1 Deuterated Substrates for KIE Determination (**9-d_3** and **9-d_4**)*

Benzyl (±)-3-(quinolin-8-ylcarbamoyl)pyrrolidine-1-carboxylate-2,4,4-d_3 (9-d_3)



A large microwave vial (10–20 mL recommended volume) was flame-dried and allowed to cool under argon. This was then charged with amide **9** (500 mg, 1.30 mmol), $Pd(OAc)_2$ (14.7 mg, 65.0 μmol), AcOD-d_4 (2.3 mL) and toluene-d_8 (6.7 mL). The reaction vessel was sealed and purged with argon, then placed in a preheated oil bath and stirred at 110 ºC for 24 h. The reaction mixture was then allowed to cool to rt and EtOAc (10 mL) was added. The resulting mixture was filtered through a pad of Celite, eluting with further EtOAc (3 × 20 mL). The solvent was removed under reduced pressure. ^{1}H NMR at 298 K of the crude mixture showed approximately 85–88% *cis*-C(4) and *trans*-C(4) deuteration and 50–55% *cis*-C(2) deuteration. The reaction was launched a second time on the crude and in the same conditions to achieve full deuteration. Following an identical work-up procedure, the crude material was purified by flash column chromatography (80% Et_2O/pentane). The product containing fractions were combined and the solvent was removed under reduced pressure to afford amide **9-d_3** as a pale yellow solid (410 mg, 83%, 94% D *cis*-C(4), 94% D *trans*-C(4) and 88% D *cis*-C(2)). R_f 0.30 (80% Et_2O/hexane); mp = 123–126 °C (from Et_2O/pentane); ν_{max} (film)/cm^{-1} 3343 (NH), 2889, 1685 (C=O), 1525, 1424, 1327, 1137, 824, 787, 727, 686; ^{1}H NMR (500 MHz, DMSO-d_6, d_1 = 70 s, 373 K) δ 10.06 (br s, 1 H, NH), 8.91 (dd, *J* = 4.2, 1.7 Hz, 1 H, HC_{Ar}), 8.59 (dd, *J* = 7.6, 1.4 Hz, 1 H, HC_{Ar}), 8.37 (dd, *J* = 8.3, 1.7 Hz, 1 H, HC_{Ar}), 7.66 (dd, *J* = 8.3, 1.3 Hz, 1 H, HC_{Ar}), 7.60 (dd, *J* = 8.3, 4.2 Hz, 1 H, HC_{Ar}), 7.57 (t, *J* = 7.9 Hz, 1 H, HC_{Ar}), 7.40–7.33 (m, 4 H, HC_{Ar}), 7.32–7.28 (m, 1 H, HC_{Ar}), 5.12 (s, 2 H, OCH_2Ph), 3.71 (d, *J* = 7.8 Hz, 1 H, NC$H_{(trans)}$DCHCO), 3.63 (dd, *J* = 10.7, 6.6 Hz, 0.12 H, residual NCH$H_{(cis)}$CHCO), 3.56 (d, 1 H, *J* = 10.5 Hz, NC$H_{(cis)}HCD_2$), 3.52 (d, 1 H, *J* = 7.8 Hz, CHCO), 3.43 (d, *J* = 10.5 Hz, 1 H, NCH$H_{(trans)}CD_2$), 2.25 (ddd, *J* = 7.0, 7.0, 7.0 Hz, 0.06 H, residual $NCH_2CH_{(trans)}D$), 2.17 (ddd, *J* = 7.5, 7.5, 7.5 Hz, 0.06 H, residual $NCH_2CDH_{(cis)}$); ^{13}C NMR (101 MHz, DMSO-d_6, 373 K) δ 170.8 (C=O amide), 153.5 (C=O carbamate), 148.3 (C_{Ar}), 137.9 (C_{Ar} quat), 136.7 (C_{Ar} quat), 135.9 (C_{Ar}), 133.9 (C_{Ar} quat), 127.7 (2 × C_{Ar}), 127.4 (C_{Ar} quat), 127.1 (C_{Ar}), 126.8 (2 × C_{Ar}), 126.3 (C_{Ar}), 121.45 (C_{Ar}), 121.41 (C_{Ar}), 116.5 (C_{Ar}), 65.4 (OCH_2Ph), 47.8 (t, $J_{C\text{-}D}$ = 22.0 Hz, N*C*HDCHCO), 44.9 (NCH_2CD_2), 43.7 (*C*HCO); the signal for the NCH_2CD_2 carbon (expected as a 1:2:3:2:1 quintet at approx. δ 28.4 ppm) was not observed due to low intensity; FTMS (+ pNSI) *m*/*z* Calculated for $C_{22}H_{20}D_2N_3O_3^+$ $[M\text{-}D+2H]^+$ 378.1781; Found 378.1785 (22.5% relative abundance); *m*/*z* Calculated for $C_{22}H_{19}D_3N_3O_3^+$ $[M+H]^+$ 379.1844; Found 379.1842 (100% relative abundance). Isotopic prolife corresponding to *bis*- (18.4%) and *tris*-deuteration (81.6%).

Benzyl (±)-3-(quinolin-8-ylcarbamoyl-*d*)pyrrolidine-1-carboxylate-2,4,4-d_3 (9-d_4)



Deuterated amide **9-d_3** (251 mg, 0.66 mmol) was solubilised in $CDCl_3$ (1 mL) and CD_3OD-d_4 (3.8 mL). The reaction mixture was stirred at 50 °C for 3 h, then allowed to cool to rt. The solvent was removed under reduced pressure to afford amide **9-d_4** as a pale yellow solid (250 mg, 99.8%, ≥ 86% deuterium incorporation at COND, 95% D *cis*-C(4), 94% D *trans*-C(4) and 90% D *cis*-C(2)).[§§§] ν_{max} (film)/cm^{-1} 3042, 2960, 2889, 2482 (ND), 1681 (C=O), 1498, 1472, 1416, 1323, 1137, 824, 787, 753, 727, 693; ^{1}H NMR (400 MHz, $CDCl_3$, 298 K, observed as a mixture of rotamers) δ 9.97 (br s, 0.14 H, residual NH), 8.80 (dd, *J* = 4.2, 1.7 Hz, 1 H, HC_{Ar}), 8.75 (dd, *J* = 6.1, 2.9 Hz, 1 H, HC_{Ar}), 8.19 (dd, *J* = 8.3, 1.7 Hz, 1 H, HC_{Ar}), 7.59–7.51 (m, 2 H, HC_{Ar}), 7.48 (dd, *J* = 8.3, 4.2 Hz, 1 H, HC_{Ar}), 7.43–7.20 (m, 5 H, HC_{Ar}), 5.22–5.12 (m, 2 H, OCH_2Ph), 3.91 and 3.85 (2 × d, *J* = 7.9 Hz, 1 H, NC$H_{(trans)}$DCHCO), 3.76 and 3.71 (2 × d, 1 H, *J* = 10.9 Hz, NC*H*HCD_2), 3.53 and 3.52 (2 × d, *J* = 10.8 Hz, 1 H, NCH*H*CD_2), 3.33–3.25 (m, 1 H, CHCO); HRMS (ESI$^+$) *m*/*z* Calculated for $C_{22}H_{19}D_3N_3O_3$ [M–D+2H] 379.1849; Found 379.1832. A similar isotopic profile to **9-d_3** was observed, likely because of fast D/H exchange at the most acidic position prior to ionization.[291]

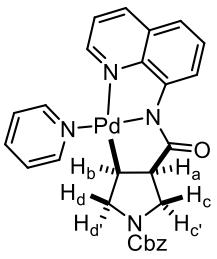
^{13}C NMR identical to that reported for deuterated amide **9-d_3** (page 316).

[§§§] Deuterium incorporation on the pyrrolidine ring was quantified by ^{1}H NMR in DMSO-d_6 at 373 K (with d_1 = 70 s). However, due to fast proton-deuterium exchange in DMSO-d_6 at high temperature, % D at the COND position was estimated by ^{1}H NMR in $CDCl_3$ at 298 K.

In addition, the absence of absorption at 3343 cm^{-1} (N–H stretch) in the FT-IR spectrum and the appearance of a new signal at 2482 cm^{-1} (N–D stretch), is consistent with full deuteration of this position.

*8.2.4.2 Palladacycle complexes (**98-Py**, **99-PPh$_3$** and **100-PCy$_3$**)*

Mononuclear 5-membered *cis*-(±)-palladacycle-pyridine complex (98-Py)



A reaction vial was flame-dried and allowed to cool under argon. Pyrrolidine-3-carboxamide **9** (113 mg, 0.30 mmol), $Pd(OAc)_2$ (74.0 mg, 0.33 mmol) and pyridine (53 μL, 0.66 mmol) were then added sequentially. The reaction vessel was sealed and purged with argon and CH_3CN (6.0 mL, 0.05 M) was added by syringe. The reaction tube was then placed in a preheated oil bath and stirred at 60 ºC for 5 h. The reaction mixture was then allowed to cool to rt and was diluted with $CHCl_3$ (3 mL). The resulting mixture was filtered through a pad of Celite, eluting with further $CHCl_3$ (3 × 5 mL), then the solvent was removed under reduced pressure. Purification by flash column chromatography (70% EtOAc/CH_2Cl_2) afforded *cis*-(±)-palladacycle-pyridine complex **98-Py** as a bright yellow solid (110 mg, 66%). R_f 0.38 (70% EtOAc/CH_2Cl_2); mp = 64–66 °C (from EtOAc/CH_2Cl_2); ν_{max} (film)/cm^{-1} 2878, 1685 (C=O), 1599, 1461, 1387, 1345, 1163, 1107, 1074, 824, 753, 693;

Characterisation in $CDCl_3$:[****] ^{1}H NMR (400 MHz, $CDCl_3$, 298 K, observed as a mixture of rotamers) δ 9.10 (dd, *J* = 7.9, 1.1 Hz, 1 H, HC_{Ar}), 8.88–8.79 (m, 2 H, $N_{Py}HC_{Ar}$), 8.20–8.12 (m, 1 H, HC_{Ar}), 7.94–7.85 (m, 1 H, HC_{Ar}), 7.79–7.70 (m, 1 H, HC_{Ar}), 7.54–7.42 (m, 3 H, HC_{Ar}), 7.40–7.20 (m, 7 H, HC_{Ar}), 5.15–5.00 (m, 2 H, OCH_2Ph), 3.96–3.85 (m, 1 H, NCH_cHCHCO), 3.71–3.61 (m, 1 H, NCH$H_{c'}$CHCO), 3.52–3.39 (m, 2 H, CH_aCO, NCH_dHCHPd), 3.35–3.20 (m, 1 H, NCH$H_{d'}$CHPd), 2.34–2.23 (m, 1 H, CH_bPd); ^{13}C NMR (101 MHz, $CDCl_3$, 298 K, observed as a mixture of rotamers) δ 184.8 and 184.5 (C=O amide), 164.0 and 163.3 (C_{Ar} quat), 154.6 (C=O carbamate), 152.1 (2 × $N_{Py}CH$), 146.5 (C_{Ar} quat), 145.2 (C_{Ar}), 138.2 (C_{Ar}), 137.8 (C_{Ar}), 137.2 (C_{Ar} quat), 129.8 (C_{Ar} quat), 129.3 (C_{Ar}), 128.3 (2 × C_{Ar}), 127.9 and 127.6 (C_{Ar}), 127.5 (2 × C_{Ar}), 125.9 (2 × C_{Ar}), 120.9 (C_{Ar}), 120.5 (C_{Ar}), 118.6–118.5 (m, C_{Ar}), 66.3 (m, OCH_2Ph), 56.8 and 56.0 (*C*HCO), 51.5 and 51.0 (N*C*H_2CHPd), 49.9 and 49.5 (N*C*H_2CHCO), 23.6 (CHPd);

^{1}H NMR in toluene-d_8:[††††] ^{1}H NMR (500 MHz, toluene-d_8, 298 K, observed as a 7:3 mixture of 2 rotamers) δ 9.63 (d, *J* = 7.9 Hz, 0.7 H, HC_{Ar}), 9.57 (d, *J* = 7.9 Hz, 0.3 H, HC_{Ar}), 8.19 (br s, 2 H, $N_{Py}HC_{Ar}$), 7.41 (d, *J* = 8.3 Hz, 0.7 H, HC_{Ar}), 7.36 (d, *J* = 8.2 Hz, 0.3 H, HC_{Ar}), 7.33–7.14 (m, 4 H, HC_{Ar}), 7.07–7.02 (m, 1 H, HC_{Ar}), 6.88 (t, *J* = 6.7 Hz, 1 H, HC_{Ar}), 6.78 (d, *J* = 7.9 Hz,

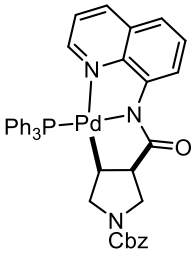
[****] Most signals were observed as multiplets deriving from the partial overlap of at least 2 rotameric species. Assignments are based on COSY, NOESY, DEPT-135 and HSQC experiments.

[††††] In toluene-d_8, fully resolved signals were often observed for the 2 rotameric species and, when possible, these are reported separately. This enabled stereochemical assignment based on NOESY experiments.

0.7 H, HC_{Ar}), 6.72 (d, *J* = 7.6 Hz, 0.3 H, HC_{Ar}), 6.64–6.45 (m, 3 H, HC_{Ar}), 6.15–6.11 (m, 1 H, HC_{Ar}), 5.19–5.02 (m, 2 H, OCH_2Ph), 4.43 (dd, *J* = 10.7, 3.1 Hz, 0.3 H, NC*H*$_c$HCHCO), 4.32 (dd, *J* = 10.7, 3.7 Hz, 0.7 H, NC*H*$_c$HCHCO), 3.79 (dd, *J* = 9.7, 9.7 Hz, 0.3 H, NCH*H*$_c$CHCO), 3.67 (dd, *J* = 9.6, 9.6 Hz, 0.7 H, NCH*H*$_c$CHCO), 3.59 (dd, *J* = 11.7, 7.6 Hz, 0.7 H, NC*H*$_d$HCHPd), 3.53 (dd, *J* = 11.1, 8.6 Hz, 0.3 H, NC*H*$_d$HCHPd), 3.50–3.40 (m, 1 H, CH_aCO), 3.32–3.18 (m, 1 H, NCH*H*$_d$CHPd), 2.02 (ddd, *J* = 8.1, 8.1, 8.1 Hz, 1 H, CH_bPd);

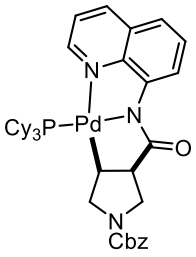
FTMS (+pNSI) *m*/*z* Calculated for $C_{24}H_{22}N_4O_3{}^{106}PdNa^+$ $[M–Py+CH_3CN+Na]^+$ 543.0619; Found 543.0614.

Mononuclear 5-membered *cis*-(±)-palladacycle-triphenylphosphine complex (99-PPh$_3$)



A round-bottom flask was charged with palladacycle **98-Py** (88.1 mg, 0.16 mmol), triphenylphosphine (83.9 mg, 0.32 mmol) and $CHCl_3$ (800 μL, 0.2 M), then purged with argon. The reaction mixture was stirred at 25 °C for 1 h and then diluted with $CHCl_3$ (3 mL). The resulting mixture was filtered through a pad of Celite, eluting with further $CHCl_3$ (3 × 5 mL), then the solvent was removed under reduced pressure. Purification by flash column chromatography (40% EtOAc/CH_2Cl_2) afforded *cis*-(±)-palladacycle-triphenylphospine complex **99-PPh$_3$** as a bright yellow solid (90.5 mg, 76%). R_f 0.28 (40% EtOAc/CH_2Cl_2); mp = 108–110 °C (from EtOAc/CH_2Cl_2); ν_{max} (film)/cm^{-1} 3056, 2870, 1692 (C=O), 1614, 1498, 1390, 1349, 1163, 1096, 828, 746, 693; ^{1}H NMR (400 MHz, $CDCl_3$, 298 K, observed as a mixture of rotamers) δ 9.20 (d, *J* = 7.9 Hz, 1 H, HC_{Ar}), 8.12 (d, *J* = 8.2 Hz, 1 H, HC_{Ar}), 7.79–7.70 (m, 6 H, HC_{Ar}), 7.58 (t, *J* = 8.1 Hz, 1 H, HC_{Ar}), 7.55–7.38 (m, 11 H, HC_{Ar}), 7.38–7.30 (m, 5 H, HC_{Ar}), 6.91 (dd, *J* = 7.9, 5.2 Hz, 1 H, HC_{Ar}), 5.11–4.92 (m, 2 H, OCH_2Ph), 3.95 (dd, *J* = 11.0 Hz, 0.7 H, NC*H*HCHCO), 3.88 (dd, *J* = 11.2 Hz, 0.3 H, NC*H*HCHCO), 3.74–3.47 (m, 2 H, CHCO, NC*H*HCHPd), 3.33 (dd, *J* = 11.1, 8.3 Hz, 0.3 H, NCH*H*CHCO), 3.24 (dd, *J* = 10.4, 7.9 Hz, 0.7 H, NCH*H*CHCO), 2.92 (dd, *J* = 11.1, 8.7 Hz, 0.7 H, NCH*H*CHPd), 2.68 (dd, *J* = 11.1, 8.6 Hz, 0.3 H, NCH*H*CHPd), 1.88–1.75 (m, 1 H, CHPd); ^{13}C NMR (101 MHz, $CDCl_3$, 298 K, observed as a mixture of rotamers) δ 183.5 (C=O amide), 160.3 and 159.6 (C_{Ar} quat), 154.4 (C=O carbamate), 148.9 (C_{Ar}), 146.7 (C_{Ar} quat), 138.3 (C_{Ar}), 136.9 (C_{Ar} quat), 134.5 and 134.4 (6 × C_{Ar}), 132.1–131.9 (3 × PC_{Ar} quat), 131.3–130.9 (m, 3 × C_{Ar}), 130.0 (C_{Ar} quat), 129.4 (C_{Ar}), 128.9-128.8 (m, 6 × C_{Ar}), 128.5 and 128.4 (C_{Ar}), 128.3 (2 × C_{Ar}), 127.7 and 127.5 (2 × C_{Ar}), 120.8 and 120.7 (C_{Ar}), 120.3–120.2 (m, C_{Ar}), 118.9 and 118.8 (C_{Ar}), 66.3 (OCH_2Ph), 56.9 and 55.9 (*C*HCO), 50.5 (N*C*H$_2$CHPd), 49.2 and 49.0 (N*C*H$_2$CHCO), 30.3 and 30.2 (CHPd); ^{31}P{^{1}H} NMR (162 MHz, $CDCl_3$, 298 K, observed as a mixture of 2 rotamers) δ 33.5 and 33.4; HRMS (ESI$^+$) *m*/*z* Calculated for $C_{40}H_{35}N_3O_3P^{106}Pd$ [M+H] 742.1451; Found 742.1444.

Mononuclear 5-membered *cis*-(±)-palladacycle-tricyclohexylphosphine complex (100-PCy_3)



A reaction vial was flame-dried and allowed to cool under argon. Palladacycle **98-Py** (84.2 mg, 0.15 mmol) and tricyclohexylphosphine (PCy_3, 84.1 mg, 0.30 mmol) were added sequentially. The reaction vessel was sealed and purged with argon and $CHCl_3$ (750 μL, 0.2 M) was added by syringe. The reaction tube was then stirred at 23 ºC for 1 h. The reaction mixture was diluted with $CHCl_3$ (3 mL) and filtered through a pad of Celite, eluting with further $CHCl_3$ (3 × 5 mL). The solvent was removed under reduced pressure. Purification by flash column chromatography (20% to 40% EtOAc/pentane) afforded *cis*-(±)-palladacycle-tricyclohexylphosphine complex **100-PCy_3** as a bright yellow solid (58.3 mg, 51%). R_f 0.24 (30% EtOAc/pentane); mp = decomposes at T > 160 °C (from EtOAc/pentane); ν_{max} (film)/cm^{-1} 2926, 2848, 1696 (C=O), 1614, 1461, 1387, 1353, 1323, 1163, 1107, 1003, 824, 738, 697; ^{1}H NMR (400 MHz, $CDCl_3$, 298 K, observed as a mixture of rotamers)‡‡‡‡ δ 9.21–9.15 (m, 1 H, HC_{Ar}), 8.50–8.40 (m, 1 H, HC_{Ar}), 8.28–8.16 (m, 1 H, HC_{Ar}), 7.59–7.52 (m, 1 H, HC_{Ar}), 7.45–7.28 (m, 7 H, HC_{Ar}), 5.24–5.02 (m, 2 H, OCH_2Ph), 4.05–3.97 (m, 1 H, NC*H*HCHCO), 3.71–3.61 (m, 2 H, NC*H*$_2$CHPd), 3.61–3.55 (m, 1 H, CHCO), 3.44–3.30 (m, 1 H, NCH*H*CHCO), 2.14–1.93 (br m, 9 H, 3 × CH, 3 × CH_2), 1.92–1.79 (br s, 7 H, CHPd, 3 × CH_2), 1.79–1.68 (br m, 6 H, 3 × CH_2), 1.68–1.53 (br m, 6 H, 3 × CH_2), 1.37–1.18 (br s, 6 H, 3 × CH_2); ^{13}C NMR (101 MHz, $CDCl_3$, 298 K, observed as a mixture of rotamers) δ 182.4 and 182.3 (C=O amide), 154.5 and 154.3 (C=O carbamate), 149.0 and 148.9 (C_{Ar}), 146.8 (C_{Ar} quat), 146.4 and 146.3 (C_{Ar} quat), 138.6 (C_{Ar}), 137.4 and 137.3 (C_{Ar} quat), 130.2 (C_{Ar} quat), 129.33 and 129.29 (br, C_{Ar}), 128.3 and 128.2 (2 × C_{Ar}), 127.7 and 127.55 (2 × C_{Ar}), 127.49 and 127.46 (C_{Ar}), 120.8 (C_{Ar}), 120.1 (C_{Ar}), 118.9 and 118.8 (C_{Ar}), 66.3 and 66.2 (OCH_2Ph), 56.9 and 56.0 (*C*HCO), 51.6 and 51.2 (N*C*H_2CHPd), 49.0 and 48.8 (N*C*H_2CHCO), 32.9 and 32.8 (d, $^2J_{CP}$ = 20.2 Hz, 3 × PCH), 30.2–29.7 (m, 6 × PCH*C*H_2), 28.3 and 28.2 (weak, CHPd), 27.6 (d, $^4J_{CP}$ = 10.4 Hz, 6 × PCHCH$_2$*C*H$_2$), 26.2 (3 × PCHCH$_2$CH$_2$*C*H$_2$);§§§§ ^{31}P{^{1}H} NMR (162 MHz, $CDCl_3$, 298 K, observed as a mixture of 2 rotamers) δ 33.1 and 33.0; FTMS (+p APCI) *m*/*z* Calculated for $C_{40}H_{53}N_3O_3P^{106}Pd^+$ $[M+H]^+$ 760.2854; Found 760.2844.

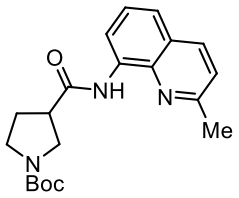
‡‡‡‡ Most signals were observed as multiplets deriving from the partial overlap of at least 2 rotameric species. Assignments are based on DEPT-90 and HMQC experiments.

§§§§ The signals at δ 28.3 and 28.2 ppm (assigned as CHPd), had very low intensity in the ^{13}C NMR spectrum, but could be observed more clearly by DEPT-90 spectroscopy.

8.2.5 Compounds for Chapter 6

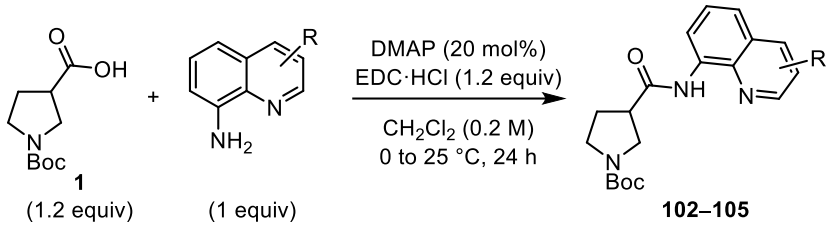
*8.2.5.1 Synthesis of pyrrolidine amide **101***

tert-Butyl (±)-3-((2-methylquinolin-8-yl)carbamoyl)pyrrolidine-1-carboxylate (101)



HOBt hydrate (422 mg, 2.80 mmol) was added to a solution of *N*-Boc-pyrrolidine-3-carboxylic acid **1** (500 mg, 2.30 mmol) and 2-methyl-8-aminoquinoline (437 mg, 2.80 mmol) in dry CH_2Cl_2 (7.5 mL) at rt, and was stirred for 5 min. EDC·HCl (529 mg, 2.80 mmol) was then added and the solution was stirred for 3 days. The reaction was diluted with CH_2Cl_2 (10 mL), then a solution of sat. aq. $NaHCO_3$ (10 mL) was added and the aqueous layer was extracted with CH_2Cl_2 (3 × 15 mL). The combined organic extracts were dried over Na_2SO_4 and filtered. The solvent was removed under reduced pressure. Purification by flash column chromatography (55% Et_2O/pentane) afforded amide **101** as a yellow paste (725 mg, 89%). R_f 0.28 (60% Et_2O/pentane); ν_{max} (film)/cm^{-1} 3340 (NH), 2974, 2878, 1681 (C=O), 1525, 1491, 1387, 1334, 1163, 1118, 880, 835, 757; ^{1}H NMR (400 MHz, $CDCl_3$, 298 K, observed as a mixture of rotamers) δ 10.13–9.89 (br m, 1 H, NH), 8.72 (dd, J = 5.8, 3.3 Hz, 1 H, HC_{Ar}), 8.03 (d, J = 8.4 Hz, 1 H, HC_{Ar}), 7.50–7.41 (m, 2 H, HC_{Ar}), 7.32 (dd, J = 8.4 Hz, 1 H, HC_{Ar}), 3.93–3.74 (m, 1 H, NC*H*HCHCO), 3.74–3.56 (m, 2 H, NCH*H*CHCO, NC*H*HCH_2), 3.52–3.38 (m, 1 H, NCH*H*CH_2), 3.35–3.20 (m, 1 H, CHCO), 2.75 (s, 3 H, CH_3), 2.42–2.21 (m, 2 H, NCH_2CH_2), 1.49 (s, 9 H, $C(CH_3)_3$); ^{13}C NMR (101 MHz, $CDCl_3$, 298 K, observed as a mixture of rotamers) δ 170.7 (C=O amide), 157.3 (CH_3C_{Ar} quat), 154.3 (C=O carbamate), 137.6 (C_{Ar} quat), 136.4 (C_{Ar}), 133.5 (C_{Ar} quat), 126.2 (C_{Ar}), 126.0 (C_{Ar} quat), 122.5 (C_{Ar}), 121.5 (C_{Ar}), 116.5 (C_{Ar}), 79.4 ($C(CH_3)_3$), 48.8 and 48.7 (NCH_2CHCO), 46.4 (*C*HCO), 45.6 and 45.4 (NCH_2CH_2), 29.5 and 29.1 (NCH_2CH_2), 28.5 ($C(CH_3)_3$), 25.2 (CH_3); HRMS (ESI$^+$) *m*/*z* Calculated for $C_{20}H_{26}N_3O_3$ [M+H] 356.1974; Found 356.1979.

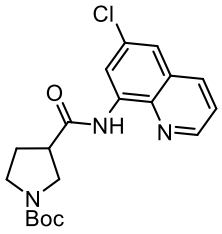
8.2.5.2 ***General Procedure B*** *for the synthesis of amides* ***102–105***



EDC·HCl (659 mg, 3.40 mmol) was added to a solution of *N*-Boc-pyrrolidine-3-carboxylic acid **1** (738 mg, 3.40 mmol) and the requisite 8-aminoquinoline derivative (2.90 mmol) in anhydrous CH_2Cl_2 (15 mL, 0.2 M) at 0 °C. DMAP (70.1 mg, 0.60 mmol) was then added and the solution was stirred at 25 °C for 24 h. The reaction was diluted with CH_2Cl_2 (15 mL), then a solution of sat. aq. $NaHCO_3$ (15 mL) was added and the aqueous layer was extracted with CH_2Cl_2 (3 × 20 mL). The combined organic extracts were dried over Na_2SO_4 and filtered. The solvent was removed under reduced pressure. The crude material was purified by flash column chromatography under the specified conditions to afford the amide product.

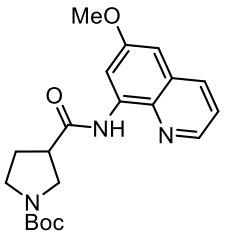
*8.2.5.3 Synthesis of amides **102–110***

tert-Butyl (±)-3-((6-chloroquinolin-8-yl)carbamoyl)pyrrolidine-1-carboxylate (102)



Prepared according to **General procedure B** (adapted to 1.30 mmol scale), using EDC·HCl (255 mg, 1.30 mmol), *N*-Boc-pyrrolidine-3-carboxylic acid **1** (300 mg, 1.30 mmol), 6-chloroquinolin-8-amine (200 mg, 1.10 mmol) and DMAP (48.9 mg, 0.20 mmol) in CH_2Cl_2 (5.5 mL, 0.2 M). At the end of the reaction, CH_2Cl_2 (5 mL) and sat. aq. $NaHCO_3$ solution (5 mL) were added and the aqueous layer was extracted with CH_2Cl_2 (3 × 10 mL). Purification by flash column chromatography (70% Et_2O/pentane) afforded amide **102** as a white solid (346 mg, 84%). R_f 0.28 (70% Et_2O/pentane); mp = 134–136 °C (from Et_2O/pentane); ν_{max} (film)/cm^{-1} 3329 (NH), 2974, 2889, 1685 (C=O), 1532, 1402, 1167, 1126, 861, 779, 701; ^{1}H NMR (400 MHz, DMSO-d_6, 373 K) δ 10.13 (br s, 1 H, NH), 8.92 (dd, J = 4.2, 1.7 Hz, 1 H, HC_{Ar}), 8.62 (d, J = 2.3 Hz, 1 H, HC_{Ar}), 8.35 (dd, J = 8.3, 1.7 Hz, 1 H, HC_{Ar}), 7.75 (d, J = 2.3 Hz, 1 H, HC_{Ar}), 7.66 (dd, J = 8.3, 4.2 Hz, 1 H, HC_{Ar}), 3.67–3.60 (m, 1 H, NC*H*HCHCO), 3.57–3.50 (m, 2 H, NCH*H*CHCO, CHCO), 3.47 (ddd, J = 10.5, 8.0, 5.2 Hz, 1 H, NC*H*HCH_2), 3.34 (ddd, J = 10.6, 7.4, 7.4 Hz, 1 H, NCH*H*CH_2), 2.27–2.19 (m, 1 H, NCH_2C*H*H), 2.17–2.09 (m, 1 H, NCH_2CH*H*), 1.44 (s, 9 H, C(CH_3)$_3$); ^{13}C NMR (101 MHz, DMSO-d_6, 373 K) δ 171.4 (C=O amide), 153.0 (C=O carbamate), 148.6 (C_{Ar}), 136.4 (C_{Ar} quat), 135.31 (C_{Ar}), 135.29 (C_{Ar} quat), 130.9 (C_{Ar} quat), 127.9 (C_{Ar} quat), 122.5 (C_{Ar}), 119.8 (C_{Ar}), 116.5 (C_{Ar}), 77.9 (*C*(CH_3)$_3$), 47.9 (NCH_2CHCO), 44.8 (NCH_2CH_2), 43.9 (*C*HCO), 28.3 (NCH_2CH_2), 27.7 (C(*C*H_3)$_3$); HRMS (FTMS pAPCI$^+$) *m*/*z* Calculated for $C_{19}H_{23}N_3O_3{}^{35}Cl^+$ $[M+H]^+$ 376.1422; Found 376.1433.

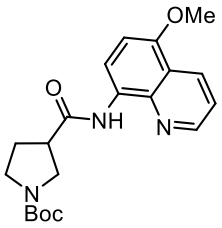
tert-Butyl (±)-3-((6-methoxyquinolin-8-yl)carbamoyl)pyrrolidine-1-carboxylate (103)



Prepared according to **General procedure B**, using 6-methoxyquinolin-8-amine (500 mg). Purification by flash column chromatography (60% to 80% Et_2O/pentane) afforded amide **103** as a white solid (968 mg, 91%). R_f 0.28 (60% Et_2O/pentane); mp = 53–57 °C (from Et_2O/pentane); ν_{max} (film)/cm^{-1} 3337 (NH), 2971, 2879, 1677 (C=O), 1523, 1450, 1385, 1364, 1212, 1156, 1117, 876, 830, 791; ^{1}H NMR (400 MHz, DMSO-d_6, 373 K) δ 10.01 (br s, 1 H, NH), 8.73 (dd, J = 4.2, 1.6 Hz, 1 H, HC_{Ar}), 8.31 (d, J = 2.8 Hz, 1 H, HC_{Ar}), 8.24 (dd, J = 8.2, 1.6 Hz, 1 H, HC_{Ar}), 7.54 (dd, J = 8.3, 4.2 Hz, 1 H, HC_{Ar}), 7.06 (d, J = 2.7 Hz, 1 H, HC_{Ar}), 3.91 (s, 3 H, OCH_3), 3.66–3.59 (m, 1 H, NC*H*HCHCO), 3.54–3.43 (m, 3 H, NCH*H*CHCO, CHCO, NC*H*HCH_2), 3.34 (ddd, J = 10.5, 7.5, 7.5 Hz, 1 H, NCH*H*CH_2), 2.26–2.18 (m, 1 H, NCH_2C*H*H), 2.17–2.10 (m, 1 H, NCH_2CH*H*), 1.44 (s, 9 H, C(CH_3)$_3$); ^{13}C NMR (101 MHz, DMSO-d_6, 373 K) 171.0 (C=O amide), 157.2 (OC_{Ar} quat), 153.0 (C=O carbamate), 145.6 (C_{Ar}), 134.8 (C_{Ar} quat), 134.7 (C_{Ar}), 134.3 (C_{Ar} quat), 128.4 (C_{Ar} quat), 121.8 (C_{Ar}), 108.7 (C_{Ar}), 100.0 (C_{Ar}), 77.9 (*C*(CH_3)$_3$), 55.1 (OCH_3),

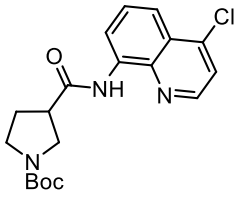
47.9 (N*C*H$_2$CHCO), 44.8 (N*C*H$_2$CH$_2$), 44.0 (*C*HCO), 28.4 (NCH$_2$*C*H$_2$), 27.7 (C(*C*H$_3$)$_3$); HRMS (ESI$^+$) *m*/*z* Calculated for $C_{20}H_{26}N_3O_4$ [M+H] 372.1923; Found 372.1924.

***tert*-Butyl (±)-3-((5-methoxyquinolin-8-yl)carbamoyl)pyrrolidine-1-carboxylate (104)**



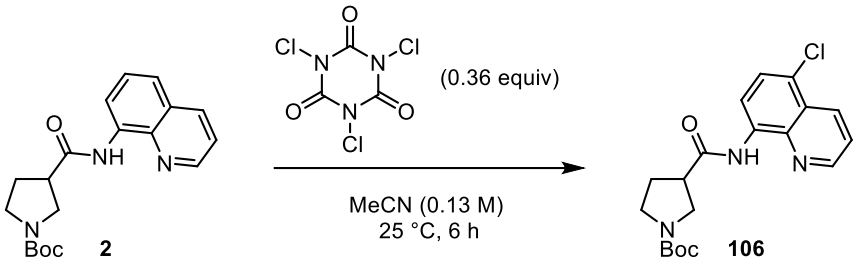
Prepared according to **General procedure B**, using 5-methoxyquinolin-8-amine (500 mg). Purification by flash column chromatography (80% Et$_2$O/pentane) afforded amide **104** as a pale yellow solid (1.01 g, 95%). R_f 0.30 (80% Et$_2$O/pentane); mp = 130–132 °C (from Et$_2$O/pentane); ν_{max} (film)/cm^{-1} 3340 (NH), 2982, 1681 (C=O), 1528, 1491, 1394, 1267, 1156, 1111, 872, 835, 787; ^{1}H NMR (400 MHz, DMSO-d_6, 373 K) δ 9.77 (br s, 1 H, NH), 8.93 (dd, *J* = 4.2, 1.7 Hz, 1 H, HC$_{Ar}$), 8.57 (dd, *J* = 8.4, 1.7 Hz, 1 H, HC$_{Ar}$), 8.48 (d, *J* = 8.5 Hz, 1 H, HC$_{Ar}$), 7.59 (dd, *J* = 8.5, 4.2 Hz, 1 H, HC$_{Ar}$), 7.03 (d, *J* = 8.6 Hz, 1 H, HC$_{Ar}$), 4.00 (s, 3 H, OCH$_3$), 3.62 (dd, *J* = 10.4, 7.7 Hz, 1 H, NC*H*HCHCO), 3.54–3.40 (m, 3 H, NCH*H*CHCO, CHCO, NC*H*HCH$_2$), 3.33 (ddd, *J* = 10.5, 7.5, 7.5 Hz, 1 H, NCH*H*CH$_2$), 2.26–2.07 (m, 2 H, NCH$_2$C*H*$_2$), 1.44 (s, 9 H, C(CH$_3$)$_3$); ^{13}C NMR (101 MHz, DMSO-d_6, 373 K) δ 170.4 (C=O amide), 153.1 (C=O carbamate), 149.8 (OC$_{Ar}$ quat), 148.6 (C$_{Ar}$), 138.8 (C$_{Ar}$ quat), 130.2 (C$_{Ar}$), 127.3 (C$_{Ar}$ quat), 120.6 (C$_{Ar}$), 119.6 (C$_{Ar}$ quat), 117.3 (C$_{Ar}$), 104.6 (C$_{Ar}$), 77.8 (*C*(CH$_3$)$_3$), 55.6 (OCH$_3$), 48.0 (N*C*H$_2$CHCO), 44.9 (N*C*H$_2$CH$_2$), 43.9 (*C*HCO), 28.4 (NCH$_2$*C*H$_2$), 27.7 (C(*C*H$_3$)$_3$); HRMS (ESI$^+$) *m*/*z* Calculated for $C_{20}H_{26}N_3O_4$ [M+H] 372.1923; Found 372.1924.

***tert*-Butyl (±)-3-((4-chloroquinolin-8-yl)carbamoyl)pyrrolidine-1-carboxylate (105)**



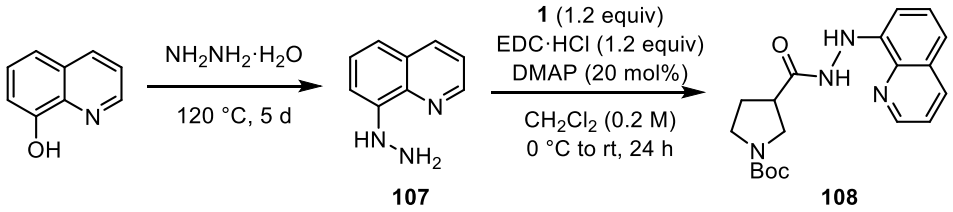
Prepared according to **General procedure B**, using 4-chloroquinolin-8-amine (513 mg). Purification by flash column chromatography (50% to 60% Et$_2$O/pentane) afforded amide **105** as a yellow solid (966 mg, 90%). R_f 0.19 (50% Et$_2$O/pentane); mp = 166–168 °C (from Et$_2$O/pentane); ν_{max} (film)/cm^{-1} 3347 (NH), 2967, 2892, 1681 (C=O), 1528, 1480, 1398, 1364, 1312, 1163, 1126, 872, 772, 664; ^{1}H NMR (400 MHz, DMSO-d_6, 373 K) δ 10.07 (br s, 1 H, NH), 8.85 (d, *J* = 4.7 Hz, 1 H, HC$_{Ar}$), 8.68 (dd, *J* = 7.7, 1.3 Hz, 1 H, HC$_{Ar}$), 7.90 (d, *J* = 8.5 Hz, 1 H, HC$_{Ar}$), 7.82 (d, *J* = 4.7 Hz, 1 H, HC$_{Ar}$), 7.72 (t, *J* = 8.1 Hz, 1 H, HC$_{Ar}$), 3.67–3.59 (m, 1 H, NC*H*HCHCO), 3.56–3.44 (m, 3 H, NCH*H*CHCO, CHCO, NC*H*HCH$_2$), 3.34 (ddd, *J* = 10.5, 7.5, 7.5 Hz, 1 H, NCH*H*CH$_2$), 2.28–2.18 (m, 1 H, NCH$_2$C*H*H), 2.18–2.10 (m, 1 H, NCH$_2$CH*H*), 1.44 (s, 9 H, C(CH$_3$)$_3$); ^{13}C NMR (101 MHz, DMSO-d_6, 373 K) δ 171.1 (C=O amide), 153.1 (C=O carbamate), 148.0 (C$_{Ar}$), 141.3 (C$_{Ar}$ quat), 138.8 (C$_{Ar}$ quat), 134.5 (C$_{Ar}$ quat), 127.8 (C$_{Ar}$), 125.2 (C$_{Ar}$ quat), 121.7 (C$_{Ar}$), 117.5 (C$_{Ar}$), 116.9 (C$_{Ar}$), 77.9 (*C*(CH$_3$)$_3$), 48.0 (N*C*H$_2$CHCO), 44.8 (N*C*H$_2$CH$_2$), 44.0 (*C*HCO), 28.4 (NCH$_2$*C*H$_2$), 27.7 (C(*C*H$_3$)$_3$); HRMS (ESI$^+$) *m*/*z* Calculated for $C_{19}H_{23}N_3O_3{}^{35}Cl$ [M+H] 376.1428; Found 376.1420.

***tert*-Butyl (±)-3-((5-chloroquinolin-8-yl)carbamoyl)pyrrolidine-1-carboxylate (106)**



Adapting conditions reported by Uredi and Watkins,[276] trichloroisocyanuric acid (84.1 mg, 0.40 mmol) was added to a solution of amide **2** (341 mg, 1.0 mmol) in CH_3CN (7.7 mL, 0.15 M) under air. The solution was then stirred at 25 °C for 6 h. The reaction mixture was concentrated under reduced pressure and purified by flash column chromatography (5% to 10% CH_3CN/CH_2Cl_2). The product containing fractions were combined and the solvent was removed under reduced pressure. Et_2O (3 mL) and pentane (3 mL) were added and the solvent was removed under reduced pressure to afford amide **106** as a white solid (171 mg, 45%). R_f 0.37 (10% CH_3CN/CH_2Cl_2); mp = 122–124 °C (from Et_2O/pentane); ν_{max} (film)/cm^{-1} 3347 (NH), 2974, 1677 (C=O), 1528, 1484, 1416, 1170, 1122, 932, 880, 779; ^{1}H NMR (400 MHz, DMSO-d_6, 373 K) δ 10.08 (br s, 1 H, NH), 9.01 (dd, J = 4.2, 1.6 Hz, 1 H, HC_{Ar}), 8.65–6.54 (m, 2 H, HC_{Ar}), 7.78 (dd, J = 8.5, 4.2 Hz, 1 H, HC_{Ar}), 7.72 (d, J = 8.4 Hz, 1 H, HC_{Ar}), 3.68–3.58 (m, 1 H, NC*H*HCHCO), 3.57–3.43 (m, 3 H, NCH*H*CHCO, CHCO, NC*H*HCH_2), 3.34 (ddd, J = 10.5, 7.5, 7.5 Hz, 1 H, NCH*H*CH_2), 2.29–2.18 (m, 1 H, NCH_2CHH), 2.18–2.08 (m, 1 H, NCH_2CHH), 1.44 (s, 9 H, $C(CH_3)_3$); ^{13}C NMR (101 MHz, DMSO-d_6, 373 K) δ 171.1 (C=O amide), 153.1 (C=O carbamate), 149.0 (C_{Ar}), 138.5 (C_{Ar} quat), 133.6 (C_{Ar} quat), 132.2 (C_{Ar}), 126.4 (C_{Ar}), 125.0 (C_{Ar} quat), 122.9 (C_{Ar} quat), 122.6 (C_{Ar}), 116.5 (C_{Ar}), 77.9 ($C(CH_3)_3$), 48.0 (NCH_2CHCO), 44.8 (NCH_2CH_2), 44.9 (*C*HCO), 28.4 (NCH_2CH_2), 27.7 ($C(CH_3)_3$); HRMS (ESI$^+$) *m*/*z* Calculated for $C_{19}H_{23}N_3O_3{}^{35}Cl$ [M+H] 376.1428; Found 376.1430.

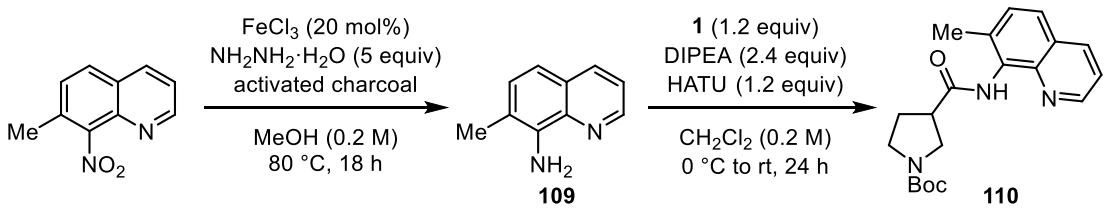
***tert*-Butyl (±)-3-(2-(quinolin-8-yl)hydrazine-1-carbonyl)pyrrolidine-1-carboxylate (108)**



Adapting Lemaire's procedure,[277] a flame-dried round bottom flask was charged with 8-hydroxyquinoline (1.00 g, 6.90 mmol) and hydrazine monohydrate (7.8 mL). The resulting mixture was stirred at 120 °C for 5 days. The mixture was allowed to cool down to rt and deionised H_2O was added (20 mL). The solvent was removed under reduced pressure to afford

the crude 8-hydrazinoquinoline product **107**, which was used in the next step without any further purification. EDC·HCl (1.59 g, 8.30 mmol) was added to a solution of crude 8-hydrazinoquinoline **107** and *N*-Boc-pyrrolidine-3-carboxylic acid **1** (1.78 g, 8.30 mmol) in dry CH_2Cl_2 (34 mL, 0.2 M) at 0 °C. 4-Dimethylaminopyridine (306 mg, 1.40 mmol) was then added and the solution was stirred at 25 °C for 24 h. The reaction mixture was then diluted with CH_2Cl_2 (40 mL). A solution of sat. aq. $NaHCO_3$ (40 mL) was added and the aqueous layer was extracted with CH_2Cl_2 (3 × 50 mL). The combined organic extracts were dried over Na_2SO_4 and filtered. The solvent was removed under reduced pressure. The crude material was purified by flash column chromatography (20% MeCN/CH_2Cl_2), the product containing fractions were combined and the solvent was removed under reduced pressure. Et_2O (10 mL) and pentane (10 mL) were added and the solvent was removed under reduced pressure to afford amide **108** as an orange solid (794 mg, 32% over 2 steps). R_f 0.19 (20% MeCN/CH_2Cl_2); mp = 78–82 °C (from Et_2O/pentane); ν_{max} (film)/cm^{-1} 3343 (NH), 2974, 1689 (C=O carbamate), 1662 (C=O amide), 1506, 1364, 1163, 1118, 876, 824, 790, 824; ^{1}H NMR (500 MHz, DMSO-d_6, 373 K) δ 9.86 (br s, 1 H, CON*H*NH), 8.80 (dd, *J* = 4.1, 1.7 Hz, 1 H, HC_{Ar}), 8.25 (dd, *J* = 8.3, 1.7 Hz, 1 H, HC_{Ar}), 8.09 (br s, 1 H, CONHN*H*), 7.52 (dd, *J* = 8.3, 4.2 Hz, 1 H, HC_{Ar}), 7.42 (t, *J* = 7.9 Hz, 1 H, HC_{Ar}), 7.30 (dd, *J* = 8.2, 1.3 Hz, 1 H, HC_{Ar}), 6.91 (dd, *J* = 7.5, 1.3 Hz, 1 H, HC_{Ar}), 3.56 (br dd, *J* = 8.8, 8.8 Hz, 1 H, NC*H*HCHCO), 3.45–3.37 (m, 2 H, NCH*H*CHCO, NC*H*HCH$_2$), 3.29 (br ddd, *J* = 8.0, 8.0, 8.0 Hz, 1 H, NCH*H*CH$_2$), 3.18–3.06 (br m, 1 H, CHCO), 2.20–2.02 (m, 2 H, NCH$_2$C*H*$_2$), 1.43 (s, 9 H, C(CH$_3$)$_3$); ^{13}C NMR (126 MHz, DMSO-d_6, 373 K) δ 171.2 (C=O amide), 153.0 (C=O carbamate), 147.1 (C_{Ar}), 144.1 (NHNHC_{Ar} quat), 136.8 (C_{Ar} quat), 135.3 (C_{Ar}), 127.6 (C_{Ar} quat), 126.5 (C_{Ar}), 121.1 (C_{Ar}), 116.5 (C_{Ar}), 106.9 (C_{Ar}), 77.8 (*C*(CH$_3$)$_3$), 47.8 (N*C*H$_2$CHCO), 44.8 (N*C*H$_2$CH$_2$), 40.9 (*C*HCO), 28.0 (NCH$_2$*C*H$_2$), 27.7 (C(*C*H$_3$)$_3$); HRMS (ESI$^+$) *m*/*z* Calculated for $C_{19}H_{25}N_4O_3$ [M+H] 357.1927; Found 357.1926.

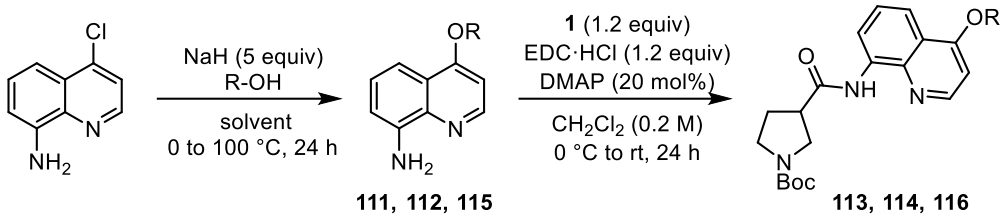
***tert*-Butyl (±)-3-((7-methylquinolin-8-yl)carbamoyl)pyrrolidine-1-carboxylate (110)**



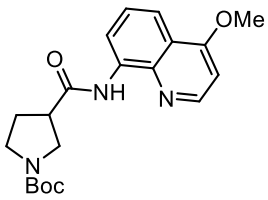
According to the procedure reported by Kuninobu and Kanai,[278] a flame-dried round bottom flask was sequentially charged with iron chloride (86.2 mg, 0.50 mmol), 7-methyl-8-nitroquinoline (500 mg, 2.70 mmol), activated charcoal (266 mg), hydrazine monohydrate (645 μL, 13.0 mmol) and anhydrous MeOH (13 mL, 0.2 M). The resulting solution was stirred at 80 °C for 18 h. The reaction mixture was then allowed to cool to rt and CH_2Cl_2 (10 mL) was added. The resulting mixture was filtered through a pad of Celite, eluting with further CH_2Cl_2

(3 × 10 mL). The solvent was removed under reduced pressure to afford the crude 7-methyl-8-aminoquinoline product **109**, which was used in the next step without any further purification. DIPEA (1.0 mL, 6.00 mmol) was added to a solution of *N*-Boc-pyrrolidine-3-carboxylic acid **1** (673 mg, 3.00 mmol) and HATU (1.14 g, 3.00 mmol) in anhydrous CH_2Cl_2 (13 mL, 0.2 M) at 0 °C, and was stirred for 5 min. The crude 7-methyl-8-aminoquinoline **109** was then added and the solution was stirred for 24 h at 25 °C. The reaction was diluted with CH_2Cl_2 (10 mL), then a solution of sat. aq. $NaHCO_3$ (10 mL) was added and the aqueous layer was extracted with CH_2Cl_2 (3 × 15 mL). The combined organic extracts were dried over Na_2SO_4 and filtered. The solvent was removed under reduced pressure. The crude material was purified by flash column chromatography (3% to 5% MeOH/CH_2Cl_2), the product containing fractions were combined and the solvent was removed under reduced pressure. Et_2O (6 mL) and pentane (6 mL) were added and the solvent was removed under reduced pressure to afford amide **110** as a white solid (493 mg, 52% over 2 steps). R_f 0.20 (4% MeOH/CH_2Cl_2); mp = 123–125 °C (from Et_2O/pentane); ν_{max} (film)/cm^{-1} 3265 (NH), 2971, 1692 (C=O carbamate), 1662 (C=O amide), 1525, 1409, 1364, 1174, 1126, 872, 835, 768; ^{1}H NMR (500 MHz, DMSO-d_6, 373 K) δ 9.48 (br s, 1 H, NH), 8.88 (dd, *J* = 4.2, 1.7 Hz, 1 H, HC_{Ar}), 8.30 (dd, *J* = 8.2, 1.7 Hz, 1 H, HC_{Ar}), 7.77 (d, *J* = 8.4 Hz, 1 H, HC_{Ar}), 7.51–7.45 (m, 2 H, HC_{Ar}), 3.65–3.54 (m, 2 H, NC*H*$_2$CHCO), 3.46 (ddd, *J* = 10.4, 6.6, 6.6 Hz, 1 H, NC*H*HCH_2), 3.39 (ddddd, *J* = 7.4, 7.4, 7.4, 7.4, 7.4 Hz, 1 H, CHCO), 3.32 (ddd, *J* = 10.5, 7.4, 7.4 Hz, 1 H, NCH*H*CH_2), 2.37 (s, 3 H, CH_3), 2.23–2.17 (m, 2 H, NCH_2CH_2), 1.44 (s, 9 H, $C(CH_3)_3$); ^{13}C NMR (126 MHz, DMSO-d_6, 373 K) δ 170.8 (C=O amide), 153.1 (C=O carbamate), 149.2 (C_{Ar}), 143.4 (C_{Ar} quat), 135.2 (C_{Ar}), 134.9 (C_{Ar} quat), 131.9 (C_{Ar} quat), 128.8 (C_{Ar}), 126.2 (C_{Ar} quat), 124.9 (C_{Ar}), 120.2 (C_{Ar}), 77.7 (*C*$(CH_3)_3$), 48.1 (N*C*H_2CHCO), 44.9 (N*C*H_2CH_2), 42.8 (*C*HCO), 28.3 (NCH_2CH_2), 27.8 (C(*C*$H_3)_3$), 18.1 (CH_3); HRMS (ESI^+) *m*/*z* Calculated for $C_{20}H_{26}N_3O_3$ [M+H] 356.1974; Found 356.1978.

*8.2.5.4 Synthesis of amides **113**, **114** and **116***



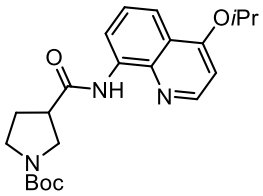
tert-Butyl (±)-3-((4-methoxyquinolin-8-yl)carbamoyl)pyrrolidine-1-carboxylate (113)



A flame-dried round bottom flask was charged with NaH (60% dispersion in mineral oil, 440 mg, 11.0 mmol) and anhydrous MeOH (11 mL, 0.2 M) was added dropwise at 0 °C. The resulting suspension was stirred at 25 °C for 30 min. 4-Chloroquinolin-8-amine (400 mg, 2.20 mmol) was added in a single portion and the solution was stirred at 100 °C for 24 h. The reaction was then allowed to cool down to rt. The reaction was quenched by slow addition of sat. aq. NH_4Cl (5 mL), then diluted with EtOAc (10 ml). The phases were separated, and the aqueous layer was extracted with EtOAc (4 × 10 mL). The combined organic extracts were dried over Na_2SO_4 and filtered. The solvent was removed under reduced pressure and the crude material was purified by flash column chromatography (5% MeCN/CH_2Cl_2) to afford the 4-methoxyquinolin-8-amine intermediate **111** (372 mg, 2.10 mmol), which was directly used in the next step. EDC·HCl (506 mg, 2.60 mmol) was added to a solution of *N*-Boc-pyrrolidine-3-carboxylic acid **1** (592 mg, 2.60 mmol) and 4-methoxyquinolin-8-amine **111** (372 mg, 2.10 mmol) in anhydrous CH_2Cl_2 (11 mL, 0.2 M) at 0 °C. DMAP (97.8 mg, 0.40 mmol) was then added and the solution was stirred at 25 °C for 24 h. The reaction was diluted with CH_2Cl_2 (10 mL), then a solution of sat. aq. $NaHCO_3$ (10 mL) was added and the aqueous layer was extracted with CH_2Cl_2 (3 × 15 mL). The combined organic extracts were dried over Na_2SO_4 and filtered. The solvent was removed under reduced pressure. Purification by flash column chromatography (90% to 100% Et_2O/pentane) afforded amide **113** as a white solid (644 mg, 79% over 2 steps). R_f 0.21 (90% Et_2O/pentane); mp = 132–134 °C (from Et_2O/pentane); ν_{max} (film)/cm^{-1} 3329 (NH), 2974, 1677 (C=O), 1536, 1398, 1320, 1163, 1118, 869, 805, 682; ^{1}H NMR (500 MHz, DMSO-d_6, 373 K) δ 10.01 (br s, 1 H, NH), 8.75 (d, J = 5.2 Hz, 1 H, HC_{Ar}), 8.58 (dd, J = 7.7, 1.3 Hz, 1 H, HC_{Ar}), 7.82 (dd, J = 8.4, 1.3 Hz, 1 H, HC_{Ar}), 7.50 (t, J = 8.0 Hz, 1 H, HC_{Ar}), 7.10 (d, J = 5.2 Hz, 1 H, HC_{Ar}), 4.09 (s, 3 H, OCH_3), 3.63 (dd, J = 10.5, 7.5 Hz, 1 H, NC*H*HCHCO), 3.54–3.42 (m, 3 H, NCH*H*CHCO, CHCO, NC*H*HCH_2), 3.34 (ddd, J = 10.5, 7.5, 7.5 Hz, 1 H, NCH*H*CH_2), 2.22 (dddd, J = 12.2, 7.1, 7.1, 4.9 Hz, 1 H, NCH_2C*H*H), 2.13 (dddd, J = 12.4, 7.7, 7.7, 7.7 Hz, 1 H, NCH_2CH*H*), 1.44 (s, 9 H, $C(CH_3)_3$); ^{13}C NMR (126 MHz, DMSO-d_6, 373 K) δ 170.7 (C=O amide), 161.7 (OC_{Ar} quat), 153.0 (C=O carbamate), 149.4 (C_{Ar}), 138.8 (C_{Ar} quat), 133.7 (C_{Ar} quat), 125.2 (C_{Ar}), 120.2 (C_{Ar}

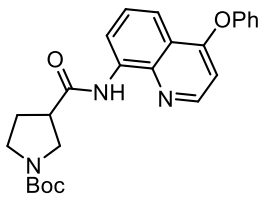
quat), 116.5 (C_{Ar}), 114.9 (C_{Ar}), 101.2 (C_{Ar}), 77.9 ($C(CH_3)_3$), 55.7 (OCH_3), 47.9 (NCH_2CHCO), 44.8 (NCH_2CH_2), 44.1 ($CHCO$), 28.4 (NCH_2CH_2), 27.7 ($C(CH_3)_3$); HRMS (ESI$^+$) *m*/*z* Calculated for $C_{20}H_{26}N_3O_4$ [M+H] 372.1923; Found 372.1922.

***tert*-Butyl (±)-3-((4-isopropoxyquinolin-8-yl)carbamoyl)pyrrolidine-1-carboxylate (114)**



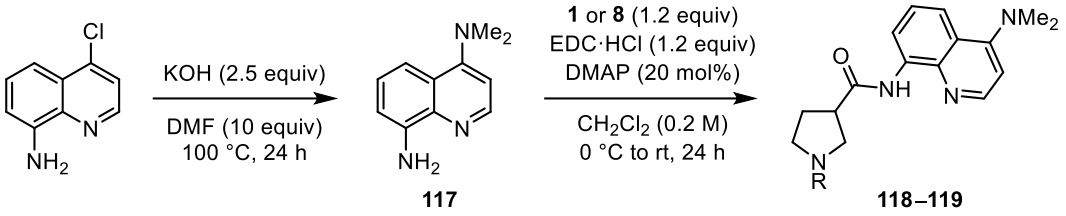
A flame-dried round bottom flask was charged with NaH (60% dispersion in mineral oil, 168 mg, 4.20 mmol) and anhydrous *i*PrOH (4.2 mL, 0.2 M) was added dropwise at 0 °C. The resulting suspension was stirred at 25 °C for 30 min. 4-Chloroquinolin-8-amine (150 mg, 0.80 mmol) was added in a single portion and the solution was stirred at 100 °C for 24 h. The reaction was then allowed to cool down to rt. The reaction was quenched by slow addition of sat. aq. NH_4Cl (2 mL), then diluted with EtOAc (5 ml). The phases were separated, and the aqueous layer was extracted with EtOAc (4 × 5 mL). The combined organic extracts were dried over Na_2SO_4 and filtered. The solvent was removed under reduced pressure and the crude material was purified by flash column chromatography (10% MeCN/CH_2Cl_2) to afford the 4-isoproxyquinolin-8-amine intermediate **112** (97.7 mg, 0.50 mmol), which was directly used in the next step. EDC·HCl (110 mg, 0.60 mmol) was added to a solution of *N*-Boc-pyrrolidine-3-carboxylic acid **1** (125 mg, 0.60 mmol) and 4-isoproxyquinolin-8-amine **112** (97.7 mg, 0.50 mmol) in anhydrous CH_2Cl_2 (2.4 mL, 0.2 M) at 0 °C. DMAP (25.8 mg, 0.10 mmol) was then added and the solution was stirred at 25 °C for 24 h. The reaction was diluted with CH_2Cl_2 (5 mL), then a solution of sat. aq. $NaHCO_3$ (5 mL) was added and the aqueous layer was extracted with CH_2Cl_2 (3 × 10 mL). The combined organic extracts were dried over Na_2SO_4 and filtered. The solvent was removed under reduced pressure. Purification by flash column chromatography (90% Et_2O/pentane) afforded amide **114** as a pale yellow solid (171 mg, 51% over 2 steps). R_f 0.24 (90% Et_2O/pentane); mp = 54–58 °C (from Et_2O/pentane); ν_{max} (film)/cm^{-1} 3336 (NH), 2974, 1685 (C=O), 1521, 1387, 1308, 1163, 1111, 965, 813, 760; ^{1}H NMR (500 MHz, DMSO-d_6, 373 K) δ 10.00 (br s, 1 H, NH), 8.72 (d, *J* = 5.2 Hz, 1 H, HC_{Ar}), 8.56 (d, *J* = 7.6 Hz, 1 H, HC_{Ar}), 7.83 (d, *J* = 8.4 Hz, 1 H, HC_{Ar}), 7.48 (t, *J* = 8.1 Hz, 1 H, HC_{Ar}), 7.09 (d, *J* = 5.3 Hz, 1 H, HC_{Ar}), 4.98 (hept, *J* = 6.0 Hz, 1 H, $OCH(CH_3)_2$), 3.63 (dd, *J* = 10.6, 7.8 Hz, 1 H, $NCHHCHCO$), 3.56–3.41 (m, 3 H, $NCHHCHCO$, $CHCO$, $NCHHCH_2$), 3.34 (ddd, *J* = 10.5, 7.5, 7.5 Hz, 1 H, $NCHHCH_2$), 2.26–2.18 (m, 1 H, NCH_2CHH), 2.13 (dddd, *J* = 12.2, 7.7, 7.7, 7.7 Hz, 1 H, NCH_2CHH), 1.50–1.41 (m, 15 H, $OCH(CH_3)_2$, $C(CH_3)_3$); ^{13}C NMR (126 MHz, DMSO-d_6, 373 K) δ 170.7 (C=O amide), 159.9 (OC_{Ar} quat), 153.0 (C=O carbamate), 149.3 (C_{Ar}), 139.1 (C_{Ar} quat), 133.7 (C_{Ar} quat), 124.9 (C_{Ar}), 120.9 (C_{Ar} quat), 116.4 (C_{Ar}), 115.2 (C_{Ar}), 102.5 (C_{Ar}), 77.8 ($C(CH_3)_3$), 70.7 ($OCH(CH_3)_2$), 47.9 (NCH_2CHCO), 44.8 (NCH_2CH_2), 44.1 ($CHCO$), 28.4 (NCH_2CH_2), 27.7 ($C(CH_3)_3$), 21.0 ($OCH(CH_3)_2$); HRMS (ESI$^+$) *m*/*z* Calculated for $C_{22}H_{30}N_3O_4$ [M+H] 400.2236; Found 400.2243.

***tert*-Butyl (±)-3-((4-phenoxyquinolin-8-yl)carbamoyl)pyrrolidine-1-carboxylate (116)**

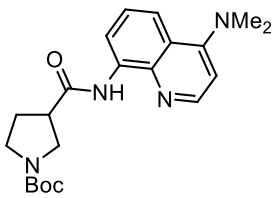


Phenol (411 mg, 4.40 mmol) was added in a single portion to a suspension of NaH (60% dispersion in mineral oil, 168 mg, 4.20 mmol) in anhydrous DMF (4.2 mL, 0.2 M) at 0 °C. The mixture was stirred at 25 °C for 30 min. 4-Chloroquinolin-8-amine (150 mg, 0.80 mmol) was added in a single portion and the solution was stirred at 100 °C for 24 h. The reaction was then allowed to cool down to rt, quenched by slow addition of sat. aq. NH_4Cl (2 mL) and diluted with EtOAc (5 ml). The phases were separated, and the aqueous layer was extracted with EtOAc (4 × 5 mL). The combined organic extracts were washed with 1 N NaOH (2 × 10 mL), dried over Na_2SO_4 and filtered. The solvent was removed under reduced pressure and the crude material was purified by flash column chromatography (5% MeCN/CH_2Cl_2) to afford the 4-phenoxy-quinoline-8-amine intermediate **115** (148 mg, 0.20 mmol), which was directly used in the next step. EDC·HCl (145 mg, 0.80 mmol) was added to a solution of *N*-Boc-pyrrolidine-3-carboxylic acid **1** (145 mg, 0.80 mmol) and 4-phenoxyquinolin-8-amine **115** (148 mg, 0.20 mmol) in anhydrous CH_2Cl_2 (3.2 mL, 0.2 M) at 0 °C. DMAP (28.0 mg, 0.10 mmol) was then added and the solution was stirred at 25 °C for 24 h. The reaction was diluted with CH_2Cl_2 (5 mL), then a solution of sat. aq. $NaHCO_3$ (5 mL) was added and the aqueous layer was extracted with CH_2Cl_2 (3 × 10 mL). The combined organic extracts were dried over Na_2SO_4 and filtered. The solvent was removed under reduced pressure. Purification by flash column chromatography (60% Et_2O/pentane) afforded amide **116** as a white solid (272 mg, 75% over 2 steps). R_f 0.18 (60% Et_2O/pentane); mp = 112–115 °C (from Et_2O/pentane); ν_{max} (film)/cm^{-1} 3321 (NH), 2982, 1685 (C=O), 1543, 1394, 1316, 1167, 1123, 809, 772; ^{1}H NMR (500 MHz, DMSO-d_6, 373 K) δ 10.05 (br s, 1 H, NH), 8.73 (d, J = 5.1 Hz, 1 H, HC_{Ar}), 8.65 (d, J = 7.7, 1.3 Hz, 1 H, HC_{Ar}), 7.97 (dd, J = 8.4, 1.3 Hz, 1 H, HC_{Ar}), 7.60 (t, J = 8.1 Hz, 1 H, HC_{Ar}), 7.55–7.51 (m, 2 H, HC_{Ph}), 7.36–7.32 (m, 1 H, HC_{Ph}), 7.28–7.25 (m, 2 H, HC_{Ph}), 6.78 (d, J = 5.1 Hz, 1 H, HC_{Ar}), 3.64 (dd, J = 10.5, 7.7 Hz, 1 H, NC*H*HCHCO), 3.55–3.45 (m, 3 H, NCH*H*CHCO, CHCO, NC*H*HCH$_2$), 3.34 (ddd, J = 10.6, 7.5, 7.5 Hz, 1 H, NCH*H*CH$_2$), 2.27–2.20 (m, 1 H, NCH$_2$C*H*H), 2.14 (dddd, J = 12.7, 7.8, 7.8, 7.8 Hz, 1 H, NCH$_2$CH*H*), 1.44 (s, 9 H, C(CH$_3$)$_3$); ^{13}C NMR (126 MHz, DMSO-d_6, 373 K) δ 170.9 (C=O amide), 160.6 (OC_{Ar} quat), 153.9 (OC_{Ph} quat), 153.0 (C=O carbamate), 149.2 (C_{Ar}), 139.5 (C_{Ar} quat), 134.0 (C_{Ar} quat), 129.8 (2 × C_{Ph}), 126.0 (C_{Ar}), 125.0 (C_{Ph}), 120.5 (C_{Ar} quat), 119.9 (2 × C_{Ph}), 117.0 (C_{Ar}), 114.9 (C_{Ar}), 105.4 (C_{Ar}), 77.9 (*C*(CH$_3$)$_3$), 48.0 (N*C*H$_2$CHCO), 44.8 (N*C*H$_2$CH$_2$), 44.0 (*C*HCO), 28.4 (NCH$_2$*C*H$_2$), 27.7 (C(*C*H$_3$)$_3$); HRMS (ESI$^+$) m/z Calculated for $C_{25}H_{28}N_3O_4$ [M+H] 434.2080; Found 434.2080.

*8.2.5.5 Synthesis of amides **118** and **119** via intermediate **117***



tert-Butyl (±)-3-((4-dimethylamino-8-yl)carbamoyl)pyrrolidine-1-carboxylate (118)

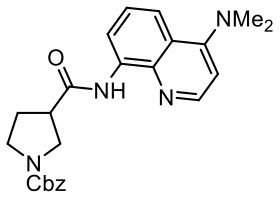


A flame-dried microwave vial (10–20 mL recommended volume) was charged with 4-chloroquinoline-8-amine (1.14 g, 6.40 mmol), KOH (powder, 895 mg, 16.0 mmol) and anhydrous DMF (4.9 mL, 64.0 mmol). The reaction vessel was sealed, placed in a preheated oil bath and stirred at 100 ºC for 24 h under air atmosphere. The reaction was then allowed to cool down and was then diluted with EtOAc (10 mL) and H_2O (10 mL). The phases were separated, and the aqueous layer was extracted with EtOAc (4 × 15 mL). The combined organic extracts were dried over Na_2SO_4 and filtered. The solvent was removed under reduced pressure to afford the crude N^4,N^4-dimethylquinoline-4,8-diamine **117**, which was used in the next step without any further purification. For full characterisation of N^4,N^4-dimethylquinoline-4,8-diamine **117**, see page 358.

EDC·HCl (1.50 g, 7.70 mmol) was added to a solution of *N*-Boc-pyrrolidine-3-carboxylic acid **1** (1.70 g, 4.40 mmol), and the crude **117** in anhydrous CH_2Cl_2 (32 mL, 0.2 M) at 0 °C. DMAP (284 mg, 1.30 mmol) was then added and the solution was stirred at 25 °C for 24 h. The reaction was diluted with CH_2Cl_2 (30 mL), then a solution of sat. aq. $NaHCO_3$ (30 mL) was added and the aqueous layer was extracted with CH_2Cl_2 (3 × 40 mL). The combined organic extracts were dried over Na_2SO_4 and filtered. The solvent was removed under reduced pressure. The crude reaction was purified by flash column chromatography (15% MeCN/CH_2Cl_2), the product containing fractions were combined and the solvent was removed under reduced pressure. Et_2O (15 mL) and pentane (15 mL) were added and the solvent was removed under reduced pressure to afford amide **118** as a white solid (1.63 g, 66% over 2 steps). R_f 0.23 (15% MeCN/CH_2Cl_2); mp = 109–111 °C (from Et_2O/pentane); ν_{max} (film)/cm^{-1} 3288 (NH), 2971, 2881, 1670 (C=O), 1536, 1398, 1361, 1312, 1163, 1122, 872, 805; ^{1}H NMR (500 MHz, DMSO-d_6, 373 K) δ 10.09 (br s, 1 H, NH), 8.59 (d, J = 5.2 Hz, 1 H, HC_{Ar}), 8.51 (dd, J = 7.6, 1.3 Hz, 1 H, HC_{Ar}), 7.77 (dd, J = 8.6, 1.2 Hz, 1 H, HC_{Ar}), 7.43 (dd, J = 8.6, 7.6 Hz, 1 H, HC_{Ar}), 6.93 (d, J = 5.2 Hz, 1 H, HC_{Ar}), 3.62 (dd, J = 10.7, 7.9 Hz, 1 H, NC*H*HCHCO), 3.52 (dd, J = 10.7, 6.8 Hz, 1 H, NCH*H*CHCO), 3.50–3.40 (m, 2 H, CHCO, NC*H*HCH$_2$), 3.34 (ddd, J = 10.5, 7.5, 7.5 Hz, 1 H, NCH*H*CH$_2$), 3.05 (s, 6 H, N(CH$_3$)$_2$), 2.22 (dddd, J = 12.3, 7.3, 7.3,

5.0 Hz, 1 H, NCH_2CHH), 2.13 (dddd, *J* = 12.4, 7.7, 7.7, 7.7 Hz, 1 H, NCH_2CHH), 1.44 (s, 9 H, $C(CH_3)_3$); ^{13}C NMR (126 MHz, DMSO-d_6, 373 K) δ 170.5 (C=O amide), 156.8 ($N(CH_3)_2C_{Ar}$ quat), 153.0 (C=O carbamate), 148.0 (C_{Ar}), 139.4 (C_{Ar} quat), 134.1 (C_{Ar} quat), 123.7 (C_{Ar}), 121.5 (C_{Ar} quat), 118.1 (C_{Ar}), 115.5 (C_{Ar}), 107.1 (C_{Ar}), 77.8 ($C(CH_3)_3$), 47.9 (NCH_2CHCO), 44.8 (NCH_2CH_2), 44.2 (*C*HCO), 43.0 ($N(CH_3)_2$) 28.4 (NCH_2CH_2), 27.7 ($C(CH_3)_3$); HRMS (ESI^+) *m*/*z* Calculated for $C_{21}H_{29}N_4O_3$ [M+H] 385.2240; Found 385.2242.

Benzyl (±)-3-((4-(dimethylamino)quinolin-8-yl)carbamoyl)pyrrolidine-1-carboxylate (119)



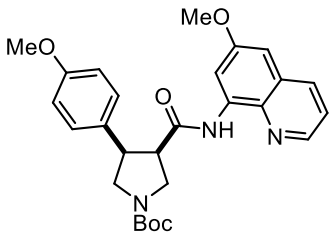
A flame-dried microwave vial (10–20 mL recommended volume) was charged with 4-chloroquinoline-8-amine (652 mg, 3.70 mmol), KOH (powder, 512 mg, 9.10 mmol) and anhydrous DMF (2.8 mL, 37.0 mmol). The reaction vessel was sealed, placed in a preheated oil bath and stirred at 100 ºC for 24 h under air atmosphere. The reaction was then allowed to cool down and then was diluted with EtOAc (5 mL) and H_2O (5 mL). The phases were separated, and the aqueous layer was extracted with EtOAc (4 × 10 mL). The combined organic extracts were dried over Na_2SO_4 and filtered. The solvent was removed under reduced pressure to afford the crude N^4,N^4-dimethylquinoline-4,8-diamine **117**, which was used in the next step without any further purification. For full characterisation of N^4,N^4-dimethylquinoline-4,8-diamine **117**, see page 358.

EDC·HCl (840 mg, 4.40 mmol) was added to a solution of *N*-Cbz-pyrrolidine-3-carboxylic acid **8** (1.10 g, 4.40 mmol), and the crude **117** in anhydrous CH_2Cl_2 (18 mL, 0.2 M) at 0 °C. DMAP (162 mg, 0.70 mmol) was then added and the solution was stirred at 25 °C for 24 h. The reaction was diluted with CH_2Cl_2 (20 mL), then a solution of sat. aq. $NaHCO_3$ (20 mL) was added and the aqueous layer was extracted with CH_2Cl_2 (3 × 30 mL). The combined organic extracts were dried over Na_2SO_4 and filtered. The solvent was removed under reduced pressure. The crude reaction was purified by flash column chromatography (15% MeCN/CH_2Cl_2) affording amide **119** as a pale yellow paste (959 mg, 63% over 2 steps). R_f 0.31 (15% MeCN/CH_2Cl_2); ν_{max} (film)/cm^{-1} 3325 (NH), 2948, 2878, 1677 (C=O), 1521, 1409, 1312, 1170, 1111, 962, 813, 760; ^1H NMR (500 MHz, DMSO-d_6, 373 K) δ 10.11 (br s, 1 H, NH), 8.58 (d, *J* = 5.2 Hz, 1 H, HC_{Ar}), 8.52 (dd, *J* = 7.7, 1.3 Hz, 1 H, HC_{Ar}), 7.77 (dd, *J* = 8.6, 1.3 Hz, 1 H, HC_{Ar}), 7.43 (dd, *J* = 8.5, 7.7 Hz, 1 H, HC_{Ar}), 7.40–7.33 (m, 4 H, HC_{Ar}), 7.32–7.27 (m, 1 H, HC_{Ar}), 6.92 (d, *J* = 5.2 Hz, 1 H, HC_{Ar}), 5.12 (s, 2 H, OCH_2Ph), 3.72 (dd, *J* =10.7, 7.9 Hz, 1 H, NC*H*HCHCO), 3.63 (dd, *J* = 10.7, 6.6 Hz, 1 H, NCH*H*CHCO), 3.57 (ddd, *J* = 10.5, 8.0, 5.1 Hz, 1 H, NC*H*HCH_2), 3.52–3.39 (m, 2 H, CHCO, NCH*H*CH_2), 3.05 (s, 6 H, $N(CH_3)_2$), 2.26 (dddd, *J* = 12.5, 7.4, 7.4, 5.2 Hz, 1 H, NCH_2CHH), 2.17 (dddd, *J* = 12.5, 7.6, 7.6, 7.6 Hz, 1 H,

$NCH_2CH\mathit{H}$); ^{13}C NMR (126 MHz, DMSO-d_6, 373 K) δ 170.4 (C=O amide), 156.8 ($N(CH_3)_2\mathit{C}_{Ar}$ quat), 153.4 (C=O carbamate), 148.0 (C_{Ar}), 139.4 (C_{Ar} quat), 136.7 (C_{Ar} quat), 134.1 (C_{Ar} quat), 127.7 (2 × C_{Ar}), 127.0 (C_{Ar}), 126.8 (2 × C_{Ar}), 123.7 (C_{Ar}), 121.4 (C_{Ar} quat), 118.1 (C_{Ar}), 115.5 (C_{Ar}), 107.1 (C_{Ar}), 65.4 (OCH_2Ph), 48.1 (NCH_2CHCO), 45.0 (NCH_2CH_2), 44.1 ($\mathit{C}HCO$), 43.0 ($N(CH_3)_2$), 28.4 ($NCH_2\mathit{C}H_2$); HRMS (ESI^+) *m*/*z* Calculated for $C_{24}H_{27}N_4O_3$ [M+H] 419.2083; Found 419.2079.

*8.2.5.6 Directing group screening: arylated pyrrolidines **124a**, **125a** and **128a**.*[*****]

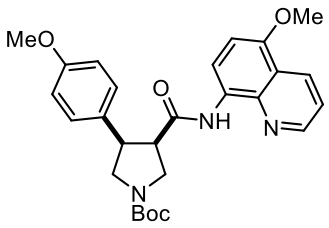
tert-Butyl _cis_-(±)-3-(4-methoxyphenyl)-4-((6-methoxyquinolin-8-yl)carbamoyl) pyrrolidine-1-carboxylate (124a)



A reaction vial was charged with K_2CO_3 (27.7 mg, 0.20 mmol), flame-dried, and allowed to cool under argon. Carboxamide **103** (74.3 mg, 0.20 mmol), 4-iodoanisole (140 mg, 0.60 mmol), $Pd(OAc)_2$ (2.2 mg, 10.0 μmol) and PivOH (20.5 mg, 0.20 mmol) were added sequentially. The reaction vessel was sealed and purged with argon, then $PhCF_3$ (200 μL, 1.0 M) was added by syringe. The reaction tube was placed in a preheated oil bath and stirred at 110 ºC for 18 h. The reaction mixture was then allowed to cool to rt and EtOAc (5 mL) was added. The resulting mixture was filtered through a pad of Celite, eluting with further EtOAc (3 × 5 mL). The solvent was removed under reduced pressure, and the crude material was purified by flash column chromatography (20% acetone/pentane). The product containing fractions were combined and the solvent was removed under reduced pressure. Et_2O (3 mL) and pentane (3 mL) were added and the solvent was removed under reduced pressure to afford arylated pyrrolidine **124a** as a pale yellow solid (63.2 mg, 66%). R_f 0.19 (20% acetone/pentane); mp = 75–79 °C (from Et_2O/pentane); ν_{max} (film)/cm^{-1} 3340 (NH br), 2971, 1685 (C=O), 1525, 1454, 1387, 1249, 1159, 1115, 1029, 876, 831; ^{1}H NMR (400 MHz, DMSO-d_6, 373 K) δ 9.66 (br s, 1 H, NH), 8.65 (dd, *J* = 4.2, 1.7 Hz, 1 H, HC_{Ar}), 8.19 (dd, *J* = 8.2, 1.5 Hz, 1 H, HC_{Ar}), 8.06 (d, *J* = 2.7 Hz, 1 H, HC_{Ar}), 7.50 (dd, *J* = 8.3, 4.2 Hz, 1 H, HC_{Ar}), 7.17–7.10 (m, 2 H, HC_{Ar}), 6.98 (d, *J* = 2.7 Hz, 1 H, HC_{Ar}), 6.70–6.64 (m, 2 H, HC_{Ar}), 3.87 (s, 3 H, OCH_3), 3.84–3.76 (m, 3 H, CHAr, NC*H*HCHCO, CHCO), 3.75–3.70 (m, 2 H, NC*H*$_2$CHAr), 3.67–3.59 (m, 1 H, NCH*H*CHCO), 3.56 (s, 3 H, OCH_3), 1.49 (s, 9 H, $C(CH_3)_3$); ^{13}C NMR (101 MHz, DMSO-d_6, 373 K) δ 169.6 (C=O amide), 157.7 (OC_{Ar} quat), 157.1 (OC_{Ar} quat), 153.2 (C=O carbamate), 145.3 (C_{Ar}), 134.5 (C_{Ar}), 134.4 (C_{Ar} quat), 134.2 (C_{Ar} quat), 129.9 (C_{Ar} quat), 128.2 (C_{Ar} quat), 128.0 (2 × C_{Ar}), 121.7 (C_{Ar}), 113.3 (2 × C_{Ar}), 108.3 (C_{Ar}), 99.7 (C_{Ar}), 78.0 (*C*$(CH_3)_3$), 55.0 (OCH_3), 54.4 (OCH_3), 49.8 (N*C*H$_2$CHAr), 49.2 (br and weak, *C*HCO), 47.4 (N*C*H$_2$CHCO), 44.8 (br and weak, CHAr), 27.8 (C(*C*H$_3$)$_3$); HRMS (ESI$^+$) *m*/*z* Calculated for $C_{27}H_{32}N_3O_5$ [M+H] 478.2342; Found 478.2327.

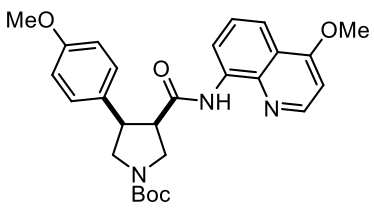
[*****] These were isolated as representative examples for 3,4-disubstituted pyrrolidine derivatives bearing a 6-, 5- or 4-substituted AQ ring, respectively. The ^{1}H NMR yields of other derivatives reported in Tables 6.5 and 6.6 (pp 172 and 173) were determined by analogy of proton signals with pyrrolidine **124a**, **125a** or **128a**, as appropriate.

***tert*-Butyl *cis*-(±)-3-(4-methoxyphenyl)-4-((5-methoxyquinolin-8-yl)carbamoyl) pyrrolidine-1-carboxylate (125a)**



A reaction vial was charged with K_2CO_3 (27.7 mg, 0.20 mmol), flame-dried, and allowed to cool under argon. Carboxamide **104** (74.3 mg, 0.20 mmol), 4-iodoanisole (140 mg, 0.60 mmol), $Pd(OAc)_2$ (2.2 mg, 10.0 μmol) and PivOH (20.5 mg, 0.20 mmol) were added sequentially. The reaction vessel was sealed and purged with argon, then $PhCF_3$ (200 μL, 1.0 M) was added by syringe. The reaction tube was placed in a preheated oil bath and stirred at 110 ºC for 18 h. The reaction mixture was then allowed to cool to rt and EtOAc (5 mL) was added. The resulting mixture was filtered through a pad of Celite, eluting with further EtOAc (3 × 5 mL). The solvent was removed under reduced pressure, and the crude material was purified by flash column chromatography (15% acetone/pentane). The product containing fractions were combined and the solvent was removed under reduced pressure. Et_2O (3 mL) and pentane (3 mL) were added and the solvent was removed under reduced pressure to afford arylated pyrrolidine **125a** as a pale yellow solid (60.6 mg, 63%). R_f 0.22 (20% acetone/pentane); mp = 127–131 °C (from Et_2O/pentane); ν_{max} (film)/cm^{-1} 3347 (NH br), 2971, 1685 (C=O), 1536, 1394, 1271, 1163, 1118, 1033, 828, 783; ^{1}H NMR (400 MHz, DMSO-d_6, 373 K) δ 9.44 (br s, 1 H, NH), 8.84 (dd, *J* = 4.2, 1.7 Hz, 1 H, HC_{Ar}), 8.51 (dd, *J* = 8.4, 1.7 Hz, 1 H, HC_{Ar}), 8.24 (d, *J* = 8.5 Hz, 1 H, HC_{Ar}), 7.55 (dd, *J* = 8.4, 4.2 Hz, 1 H, HC_{Ar}), 7.18–7.12 (m, 2 H, HC_{Ar}), 6.94 (d, *J* = 8.6 Hz, 1 H, HC_{Ar}), 6.71–6.65 (m, 2 H, HC_{Ar}), 3.96 (s, 3 H, OCH_3), 3.84–3.69 (m, 5 H, CHAr, NC*H*HCHCO, CHCO, NCH_2CHAr), 3.62 (dd, *J* = 10.1, 6.3 Hz, 1 H, NCH*H*CHCO), 3.57 (s, 3 H, OCH_3), 1.48 (s, 9 H, $C(CH_3)_3$); ^{13}C NMR (101 MHz, DMSO-d_6, 373 K) δ 168.9 (C=O amide), 157.7 (OC_{Ar} quat), 153.2 (C=O carbamate), 149.5 (OC_{Ar} quat), 148.4 (C_{Ar}), 138.6 (C_{Ar} quat), 130.04 (C_{Ar} quat), 130.00 (C_{Ar}), 128.1 (2 × C_{Ar}), 127.1 (C_{Ar} quat), 120.4 (C_{Ar}), 119.4 (C_{Ar} quat), 116.8 (C_{Ar}), 113.3 (2 × C_{Ar}), 104.5 (C_{Ar}), 78.0 ($C(CH_3)_3$), 55.6 (OCH_3), 54.5 (OCH_3), 49.8 (NCH_2CHAr), 49.0 (br and weak, *C*HCO), 47.5 (NCH_2CHCO), 44.8 (br and weak, CHAr), 27.8 (C(CH_3)$_3$); HRMS (ESI$^+$) *m*/*z* Calculated for $C_{27}H_{32}N_3O_5$ [M+H] 478.2342; Found 478.2342.

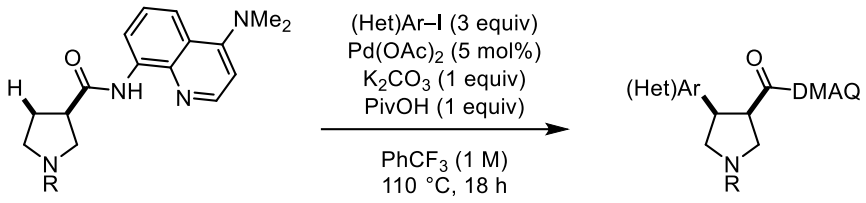
***tert*-Butyl *cis*-(±)-3-(4-methoxyphenyl)-4-((4-methoxyquinolin-8-yl)carbamoyl)pyrrolidine-1-carboxylate (128a)**



A reaction vial was charged with K_2CO_3 (27.7 mg, 0.20 mmol), flame-dried, and allowed to cool under argon. Carboxamide **113** (74.3 mg, 0.20 mmol), 4-iodoanisole (140 mg, 0.60 mmol), $Pd(OAc)_2$ (2.2 mg, 10.0 μmol) and PivOH (20.5 mg, 0.20 mmol) were added sequentially. The reaction vessel was sealed and

purged with argon, then $PhCF_3$ (200 μL, 1.0 M) was added by syringe. The reaction tube was placed in a preheated oil bath and stirred at 110 ºC for 18 h. The reaction mixture was then allowed to cool to rt and EtOAc (5 mL) was added. The resulting mixture was filtered through a pad of Celite, eluting with further EtOAc (3 × 5 mL). The solvent was removed under reduced pressure, and the crude material was purified by flash column chromatography (20% acetone/pentane). The product containing fractions were combined and the solvent was removed under reduced pressure. Et_2O (3 mL) and pentane (3 mL) were added and the solvent was removed under reduced pressure to afford arylated pyrrolidine **128a** as a white solid (74.0 mg, 77%). R_f 0.18 (20% acetone/pentane); mp = 81–85 °C (from Et_2O/pentane); ν_{max} (film)/cm^{-1} 3336 (NH br), 2971, 1685 (C=O), 1525, 1409, 1312, 1249, 1163, 1111, 1036, 760; ^1H NMR (500 MHz, DMSO-d_6, 373 K) δ 9.68 (br s, 1 H, NH), 8.67 (d, *J* = 5.2 Hz, 1 H, HC_{Ar}), 8.34 (dd, *J* = 7.7, 1.3 Hz, 1 H, HC_{Ar}), 7.75 (dd, *J* = 8.4, 1.3 Hz, 1 H, HC_{Ar}), 7.40 (t, *J* = 8.1 Hz, 1 H, HC_{Ar}), 7.16–7.12 (m, 2 H, HC_{Ar}), 7.06 (d, *J* = 5.3 Hz, 1 H, HC_{Ar}), 6.69–6.64 (m, 2 H, HC_{Ar}), 4.06 (s, 3 H, OCH_3), 3.84–3.71 (m, 5 H, CHAr, NC*H*HCHCO, CHCO, NCH_2CHAr), 3.63 (dd, *J* = 10.5, 6.5 Hz, 1 H, NCH*H*CHCO), 3.57 (s, 3 H, OCH_3), 1.48 (s, 9 H, $C(CH_3)_3$); ^{13}C NMR (126 MHz, DMSO-d_6, 373 K) δ 169.3 (C=O amide), 161.6 (OC_{Ar} quat), 157.7 (OC_{Ar} quat), 153.2 (C=O carbamate), 149.1 (C_{Ar}), 138.6 (C_{Ar} quat), 133.5 (C_{Ar} quat), 130.0 (C_{Ar} quat), 128.0 (2 × C_{Ar}), 125.1 (C_{Ar}), 120.0 (C_{Ar} quat), 116.1 (C_{Ar}), 114.6 (C_{Ar}), 113.3 (2 × C_{Ar}), 101.1 (C_{Ar}), 78.0 (*C*$(CH_3)_3$), 55.7 (OCH_3), 54.5 (OCH_3), 49.8 (N*C*H_2CHAr), 49.2 (br and weak, *C*HCO), 47.4 (N*C*H_2CHCO), 44.8 (br and weak, CHAr), 27.8 (C(*C*$H_3)_3$); HRMS (ESI^+) *m*/*z* Calculated for $C_{27}H_{32}N_3O_5$ [M+H] 478.2342; Found 478.2339.

8.2.5.7 ***General procedure C*** *for C–H arylation of N-protected pyrrolidines with DMAQ directing group.*



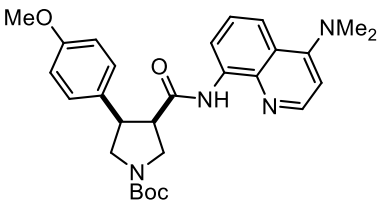
R = Boc **118**
R = Cbz **119**

R = Boc **131a–l**
R = Cbz **132a–g**

A reaction vial was charged with K_2CO_3 (27.7 mg, 0.20 mmol), flame-dried, and allowed to cool under argon. The starting carboxamide (0.20 mmol), the requisite aryl iodide (0.60 mmol), $Pd(OAc)_2$ (2.2 mg, 10.0 μmol) and PivOH (20.5 mg, 0.20 mmol) were added sequentially. The reaction vessel was sealed and purged with argon, then $PhCF_3$ (200 μL, 1.0 M) was added by syringe. The reaction tube was placed in a preheated oil bath and stirred at 110 ºC for 18 h. The reaction mixture was then allowed to cool to rt and EtOAc (5 mL) was added. The resulting mixture was filtered through a pad of Celite, eluting with further EtOAc (3 × 5 mL). The solvent was removed under reduced pressure, and the crude material was purified by flash column chromatography under the specified conditions. The product containing fractions were combined and the solvent was removed under reduced pressure. Et_2O (3 mL) and pentane (3 mL) were added and the solvent was removed under reduced pressure to afford the arylated derivative.

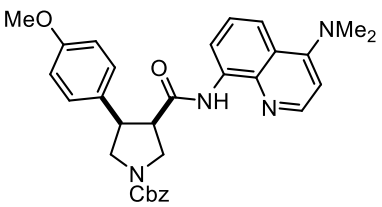
*8.2.5.8 Synthesis of pyrrolidine amides **131a–l** and **132a–g** with DMAQ directing group*

tert-Butyl _cis_-(±)-3-((4-(dimethylamino)quinolin-8-yl)carbamoyl)-4-(4-methoxyphenyl) pyrrolidine-1-carboxylate (131a)



Prepared according to **General Procedure C** using amide **118** (76.9 mg) and 4-iodoanisole (140 mg). Purification by flash column chromatography (20% acetone/pentane) afforded arylated pyrrolidine **131a** as a white solid (76.5 mg, 78%). R_f 0.32 (20% acetone/pentane); mp = 80–84 °C (from Et_2O/pentane); ν_{max} (film)/cm^{-1} 3325 (NH br), 2937, 1685 (C=O), 1521, 1402, 1305, 1249, 1163, 1111, 1033, 965, 813, 764; ^{1}H NMR (500 MHz, DMSO-d_6, 373 K) δ 9.78 (br s, 1 H, NH), 8.52 (d, J = 5.2 Hz, 1 H, HC_{Ar}), 8.28 (dd, J = 7.7, 1.3 Hz, 1 H, HC_{Ar}), 7.69 (dd, J = 8.6, 1.3 Hz, 1 H, HC_{Ar}), 7.34 (dd, J = 8.6, 7.7 Hz, 1 H, HC_{Ar}), 7.17–7.12 (m, 2 H, HC_{Ar}), 6.90 (d, J = 5.2 Hz, 1 H, HC_{Ar}), 6.70–6.65 (m, 2 H, HC_{Ar}), 3.83–3.76 (m, 2 H, CHAr, NC*H*HCHCO), 3.76–3.69 (m, 3 H, CHCO, NCH_2CHAr), 3.63 (dd, J = 10.8, 6.9 Hz, 1 H, NCH*H*CHCO), 3.57 (s, 3 H, OCH_3), 3.03 (s, 6 H, $N(CH_3)_2$), 1.48 (s, 9 H, $C(CH_3)_3$); ^{13}C NMR (126 MHz, DMSO-d_6, 373 K) δ 169.1 (C=O amide), 157.7 (OC_{Ar} quat), 156.7 ($N(CH_3)_2C_{Ar}$ quat), 153.2 (C=O carbamate), 147.7 (C_{Ar}), 139.2 (C_{Ar} quat), 133.9 (C_{Ar} quat), 130.0 (C_{Ar} quat), 128.0 (2 × C_{Ar}), 123.6 (C_{Ar}), 121.3 (C_{Ar} quat), 117.8 (C_{Ar}), 115.1 (C_{Ar}), 113.3 (2 × C_{Ar}), 107.0 (C_{Ar}), 78.0 ($C(CH_3)_3$), 54.5 (OCH_3), 49.9 (NCH_2CHAr), 49.3 (br and weak, *C*HCO), 47.4 (NCH_2CHCO), 44.8 (br and weak, CHAr), 42.9 ($N(CH_3)_2$), 27.8 ($C(CH_3)_3$); HRMS (ESI$^+$) *m*/*z* Calculated for $C_{28}H_{35}N_4O_4$ [M+H] 491.2658; Found 491.2668.

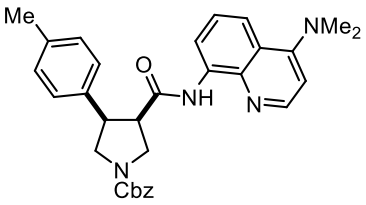
Benzyl _cis_-(±)-3-((4-(dimethylamino)quinolin-8-yl)carbamoyl)-4-(4-methoxyphenyl) pyrrolidine-1-carboxylate (132a)



Prepared according to **General Procedure C** using amide **119** (83.7 mg) and 4-iodoanisole (140 mg). Purification by flash column chromatography (20% acetone/pentane) afforded arylated pyrrolidine **132a** as a pale yellow solid (83.6 mg, 80%). R_f 0.23 (25% acetone/pentane); mp = 64–68 °C (from Et_2O/pentane); ν_{max} (film)/cm^{-1} 3325 (NH br), 2948, 1700 (C=O), 1521, 1409, 1305, 1249, 1107, 1029, 813, 764, 697; ^{1}H NMR (400 MHz, DMSO-d_6, 373 K) δ 9.79 (br s, 1 H, NH), 8.50 (d, J = 5.2 Hz, 1 H, HC_{Ar}), 8.27 (dd, J = 7.7, 1.3 Hz, 1 H, HC_{Ar}), 7.70 (dd, J = 8.6, 1.3 Hz, 1 H, HC_{Ar}), 7.44–7.28 (m, 6 H, HC_{Ar}), 7.18–7.12 (m, 2 H, HC_{Ar}), 6.89 (d, J = 5.2 Hz, 1 H, HC_{Ar}), 6.70–6.64 (m, 2 H, HC_{Ar}), 5.18 (s, 2 H, OCH_2Ph), 3.91–3.80 (m, 4 H, NCH_2CHAr, CHAr, NC*H*HCHCO), 3.80–3.69 (m, 2 H, CHCO, NCH*H*CHCO), 3.57 (s, 3 H, OCH_3), 3.03 (s, 6 H, $N(CH_3)_2$); ^{13}C NMR (101 MHz, DMSO-d_6, 373 K) δ 169.1 (C=O amide), 157.7 (OC_{Ar} quat),

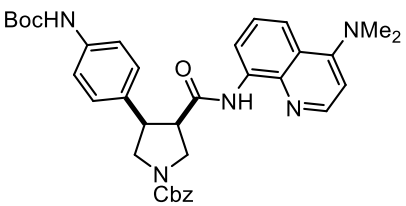
156.7 ($N(CH_3)_2C_{Ar}$ quat), 153.6 (C=O carbamate), 147.7 (C_{Ar}), 139.1 (C_{Ar} quat), 136.8 (C_{Ar} quat), 133.9 (C_{Ar} quat), 129.7 (C_{Ar} quat), 128.0 (2 × C_{Ar}), 127.8 (2 × C_{Ar}), 127.1 (C_{Ar}), 126.8 (2 × C_{Ar}), 123.6 (C_{Ar}), 121.3 (C_{Ar} quat), 117.9 (C_{Ar}), 115.3 (C_{Ar}), 113.3 (2 × C_{Ar}), 107.0 (C_{Ar}), 65.5 (OCH_2Ph), 54.5 (OCH_3), 49.9 (NCH_2CHAr), 49.2 (br and weak, *C*HCO), 47.7 (NCH_2CHCO), 44.8 (br and weak, CHAr), 43.0 ($N(CH_3)_2$); HRMS (ESI$^+$) *m*/*z* Calculated for $C_{31}H_{33}N_4O_4$ [M+H] 525.2502; Found 525.2516.

Benzyl *cis*-(±)-3-((4-(dimethylamino)quinolin-8-yl)carbamoyl)-4-(p-tolyl)pyrrolidine-1-carboxylate (132b)



Prepared according to **General Procedure C** using amide **119** (83.7 mg) and 4-iodotoluene (131 mg). Purification by flash column chromatography (70% EtOAc/hexane) afforded arylated pyrrolidine **132b** as a white solid (69.6 mg, 68%). R_f 0.42 (70% EtOAc/hexane); mp = 65–69 °C (from Et_2O/pentane); ν_{max} (film)/cm^{-1} 3325 (NH br), 2945, 1700 (C=O), 1521, 1413, 1305, 1111, 965, 813, 764, 697; ^{1}H NMR (400 MHz, DMSO-d_6, 373 K) δ 9.81 (br s, 1 H, NH), 8.51 (d, *J* = 5.2 Hz, 1 H, HC_{Ar}), 8.27 (dd, *J* = 7.7, 1.3 Hz, 1 H, HC_{Ar}), 7.70 (dd, *J* = 8.6, 1.3 Hz, 1 H, HC_{Ar}), 7.44–7.28 (m, 6 H, HC_{Ar}), 7.14–7.09 (m, 2 H, HC_{Ar}), 6.94–6.91 (m, 2 H, HC_{Ar}), 6.90 (d, *J* = 5.2 Hz, 1 H, HC_{Ar}), 5.18 (s, 2 H, OCH_2Ph), 3.90–3.83 (m, 4 H, NCH_2CHAr, CHAr, NC*H*HCHCO), 3.83–3.79 (m, 1 H, CHCO), 3.73 (dd, *J* = 10.4, 6.7 Hz, 1 H, NCH*H*CHCO), 3.03 (s, 6 H, $N(CH_3)_2$), 2.10 (s, 3 H, CH_3); ^{13}C NMR (101 MHz, DMSO-d_6, 373 K) δ 169.0 (C=O amide), 156.7 ($N(CH_3)_2C_{Ar}$ quat), 153.6 (C=O carbamate), 147.7 (C_{Ar}), 139.2 (C_{Ar} quat), 136.8 (C_{Ar} quat), 135.2 (C_{Ar} quat), 134.8 (C_{Ar} quat), 133.9 (C_{Ar} quat), 128.1 (2 × C_{Ar}), 127.7 (2 × C_{Ar}), 127.1 (C_{Ar}), 126.84 (2 × C_{Ar}), 126.79 (2 × C_{Ar}), 123.6 (C_{Ar}), 121.3 (C_{Ar} quat), 117.9 (C_{Ar}), 115.2 (C_{Ar}), 107.0 (C_{Ar}), 65.5 (OCH_2Ph), 49.8 (weak, NCH_2CHAr), 49.0 (br and weak, *C*HCO), 47.7 (weak, NCH_2CHCO), 45.1 (br and weak, CHAr), 42.9 ($N(CH_3)_2$), 19.8 (CH_3); HRMS (FTMS pAPCI$^+$) *m*/*z* Calculated for $C_{31}H_{33}N_4O_3^+$ $[M+H]^+$ 509.2547; Found 509.2525.

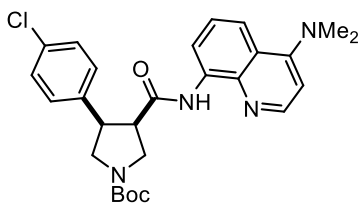
Benzyl *cis*-(±)-3-(4-((*tert*-butoxycarbonyl)amino)phenyl)-4-((4-(dimethylamino)quinolin-8-yl)carbamoyl)pyrrolidine-1-carboxylate (132c)



Prepared according to **General Procedure C** using amide **119** (83.7 mg) and *N*-Boc-4-iodoaniline (191 mg). Purification by flash column chromatography (25% acetone/pentane) afforded arylated pyrrolidine **132c** as a pale yellow solid (66.5 mg, 55%). R_f 0.22 (30% acetone/pentane); mp = 104–108 °C (from Et_2O/pentane); ν_{max} (film)/cm^{-1} 3321 (NH br), 2945, 1685 (C=O), 1525, 1413, 1305, 1159, 1111, 764, 697; ^{1}H NMR (400 MHz, DMSO-d_6, 373 K) δ

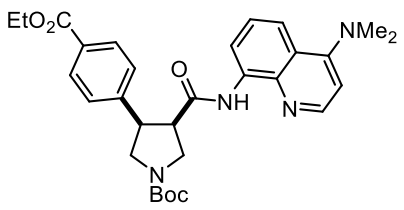
9.83 (br s, 1 H, CONH), 8.70 (br s, 1 H, NHBoc), 8.51 (d, *J* = 5.2 Hz, 1 H, HC_{Ar}), 8.27 (dd, *J* = 7.7, 1.3 Hz, 1 H, HC_{Ar}), 7.70 (dd, *J* = 8.6, 1.3 Hz, 1 H, HC_{Ar}), 7.44–7.28 (m, 6 H, HC_{Ar}), 7.23–7.18 (m, 2 H, HC_{Ar}), 7.14–7.08 (m, 2 H, HC_{Ar}), 6.88 (d, *J* = 5.2 Hz, 1 H, HC_{Ar}), 5.18 (s, 2 H, OCH_2Ph), 3.91–3.75 (m, 5 H, NCH_2CHAr, CHAr, CHCO, NCHHCHCO), 3.72 (dd, *J* = 10.3, 6.7 Hz, 1 H, NCHHCHCO), 3.03 (s, 6 H, $N(CH_3)_2$), 1.48 (s, 9 H, $C(CH_3)_3$); ^{13}C NMR (101 MHz, DMSO-d_6, 373 K) δ 169.0 (C=O amide), 156.7 ($N(CH_3)_2C_{Ar}$ quat), 153.6 (C=O Cbz), 152.1 (C=O Boc), 147.8 (C_{Ar}), 139.2 (C_{Ar} quat), 137.7 ($BocNHC_{Ar}$ quat), 136.8 (C_{Ar} quat), 133.9 (C_{Ar} quat), 131.4 (C_{Ar} quat), 127.8 (2 × C_{Ar}), 127.12 (2 × C_{Ar}), 127.07 (C_{Ar}), 126.8 (2 × C_{Ar}), 123.6 (C_{Ar}), 121.3 (C_{Ar} quat), 117.9 (C_{Ar}), 117.7 (2 × C_{Ar}), 115.3 (C_{Ar}), 107.0 (C_{Ar}), 78.3 ($C(CH_3)_3$), 65.5 (OCH_2Ph), 49.9 (br and weak, NCH_2CHAr), 49.0 (br and weak, CHCO), 47.7 (br and weak, NCH_2CHCO), 44.9 (br and weak, CHAr), 43.0 ($N(CH_3)_2$), 27.6 ($C(CH_3)_3$); HRMS (FTMS ESI$^+$) *m*/*z* Calculated for $C_{35}H_{40}N_5O_5^+$ $[M+H]^+$ 610.3024; Found 610.3026.

tert-Butyl _cis_-(±)-3-(4-chlorophenyl)-4-((4-(dimethylamino)quinolin-8-yl)carbamoyl) pyrrolidine-1-carboxylate (131b)



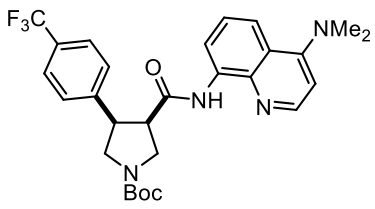
Prepared according to **General Procedure C** using amide **118** (76.9 mg) and 1-chloro-4-iodobenzene (143 mg). Purification by flash column chromatography (10% to 20% acetone/pentane) afforded arylated pyrrolidine **131b** as a white solid (69.8 mg, 71%). R_f 0.24 (20% acetone/pentane); mp = 80–84 °C (from Et_2O/pentane); ν_{max} (film)/cm^{-1} 3321 (NH br), 2974, 1685 (C=O), 1521, 1394, 1305, 1163, 1111, 813, 760; ^1H NMR (500 MHz, DMSO-d_6, 373 K) δ 9.82 (br s, 1 H, NH), 8.53 (d, *J* = 5.1 Hz, 1 H, HC_{Ar}), 8.25 (dd, *J* = 7.7, 1.3 Hz, 1 H, HC_{Ar}), 7.71 (dd, *J* = 8.6, 1.3 Hz, 1 H, HC_{Ar}), 7.34 (dd, *J* = 8.6, 7.6 Hz, 1 H, HC_{Ar}), 7.27–7.22 (m, 2 H, HC_{Ar}), 7.18–7.13 (m, 2 H, HC_{Ar}), 6.90 (d, *J* = 5.2 Hz, 1 H, HC_{Ar}), 3.89–3.71 (m, 5 H, CHAr, CHCO, NCHHCHCO, NCH_2CHAr), 3.68–3.63 (m, 1 H, NCHHCHCO), 3.03 (s, 6 H, $N(CH_3)_2$), 1.48 (s, 9 H, $C(CH_3)_3$); ^{13}C NMR (126 MHz, DMSO-d_6, 373 K) δ 169.9 (C=O amide), 156.7 ($N(CH_3)_2C_{Ar}$ quat), 153.1 (C=O carbamate), 147.8 (C_{Ar}), 139.2 (C_{Ar} quat), 137.2 (C_{Ar} quat), 133.8 (C_{Ar} quat), 130.9 (C_{Ar} quat), 128.8 (2 × C_{Ar}), 127.4 (2 × C_{Ar}), 123.6 (C_{Ar}), 121.4 (C_{Ar} quat), 118.0 (C_{Ar}), 115.3 (C_{Ar}), 107.0 (C_{Ar}), 78.1 ($C(CH_3)_3$), 49.5 (NCH_2CHAr), 49.0 (br and weak, CHCO), 47.5 (NCH_2CHCO), 44.8 (br and weak, CHAr), 42.9 ($N(CH_3)_2$), 27.8 ($C(CH_3)_3$); HRMS (ESI$^+$) *m*/*z* Calculated for $C_{27}H_{32}N_4O_3{}^{35}Cl$ [M+H] 495.2163; Found 495.2159.

***tert*-Butyl *cis*-(±)-3-((4-(dimethylamino)quinolin-8-yl)carbamoyl)-4-(4-(ethoxycarbonyl) phenyl)pyrrolidine-1-carboxylate (131c)**



Prepared according to **General Procedure C** using amide **118** (76.9 mg) and ethyl 4-iodobenzoate (167 mg). Purification by flash column chromatography (25% acetone/pentane) afforded arylated pyrrolidine **131c** as a pale yellow solid (67.7 mg, 60%). R_f 0.10 (20% acetone/pentane); mp = 75–79 °C (from Et_2O/pentane); ν_{max} (film)/cm^{-1} 3321 (NH br), 2975, 1689 (C=O), 1525, 1402, 1305, 1275, 1163, 1103, 813, 760; ^{1}H NMR (500 MHz, DMSO-d_6, 373 K) δ 9.81 (br s, 1 H, NH), 8.50 (d, J = 5.1 Hz, 1 H, HC_{Ar}), 8.22 (dd, J = 7.6, 1.3 Hz, 1 H, HC_{Ar}), 7.74–7.66 (m, 3 H, HC_{Ar}), 7.38–7.34 (m, 2 H, HC_{Ar}), 7.32 (dd, J = 8.6, 7.6 Hz, 1 H, HC_{Ar}), 6.88 (d, J = 5.2 Hz, 1 H, HC_{Ar}), 4.23 (q, J = 7.1 Hz, 2 H, OCH_2CH_3), 3.94 (ddd, J = 7.3, 7.3, 7.3 Hz, 1 H, CHAr), 3.86 (ddd, J = 7.2, 7.2, 4.5 Hz, 1 H, CHCO), 3.83–3.78 (m, 3 H, $NCHHCHCO$, NCH_2CHAr), 3.67 (dd, J = 11.1, 7.3 Hz, 1 H, $NCHHCHCO$), 3.02 (s, 6 H, $N(CH_3)_2$), 1.49 (s, 9 H, $C(CH_3)_3$), 1.26 (t, J = 7.1 Hz, 3 H, OCH_2CH_3); ^{13}C NMR (126 MHz, DMSO-d_6, 373 K) δ 168.7 (C=O amide), 164.8 (C=O ester), 156.6 ($N(CH_3)_2C_{Ar}$ quat), 153.1 (C=O carbamate), 147.7 (C_{Ar}), 143.6 (C_{Ar} quat), 139.2 (C_{Ar} quat), 133.7 (C_{Ar} quat), 128.3 (2 × C_{Ar}), 128.1 (C_{Ar} quat), 127.2 (2 × C_{Ar}), 123.5 (C_{Ar}), 121.3 (C_{Ar} quat), 117.9 (C_{Ar}), 115.3 (C_{Ar}), 106.9 (C_{Ar}), 78.1 ($C(CH_3)_3$), 59.7 (OCH_2CH_3), 49.3 (NCH_2CHAr), 49.1 (br and weak, $CHCO$), 47.5 (NCH_2CHCO), 45.3 (br and weak, CHAr), 42.9 ($N(CH_3)_2$), 27.7 ($C(CH_3)_3$), 13.4 (OCH_2CH_3); HRMS (ESI$^+$) m/z Calculated for $C_{30}H_{37}N_4O_5$ [M+H] 533.2764; Found 533.2761.

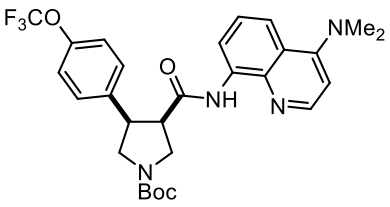
***tert*-Butyl *cis*-(±)-3-((4-(dimethylamino)quinolin-8-yl)carbamoyl)-4-(4-(trifluoromethyl) phenyl)pyrrolidine-1-carboxylate (131d)**



Prepared according to **General Procedure C** using amide **118** (76.9 mg) and 4-iodobenzotrifluoride (163 mg). Purification by flash column chromatography (10% to 15% acetone/pentane) afforded arylated pyrrolidine **131d** as a white solid (60.5 mg, 57%). R_f 0.06 (10% acetone/pentane); mp = 73–77 °C (from Et_2O/pentane); ν_{max} (film)/cm^{-1} 3317 (NH br), 2974, 1685 (C=O), 1525, 1409, 1327, 1163, 1115, 1070, 764; ^{1}H NMR (500 MHz, DMSO-d_6, 373 K) δ 9.82 (br s, 1 H, NH), 8.51 (d, J = 5.2 Hz, 1 H, HC_{Ar}), 8.21 (dd, J = 7.7, 1.3 Hz, 1 H, HC_{Ar}), 7.70 (dd, J = 8.6, 1.3 Hz, 1 H, HC_{Ar}), 7.47–7.42 (m, 4 H, HC_{Ar}), 7.32 (dd, J = 8.6, 7.7 Hz, 1 H, HC_{Ar}), 6.89 (d, J = 5.2 Hz, 1 H, HC_{Ar}), 3.97 (ddd, J = 7.4, 7.4, 7.4 Hz, 1 H, CHAr), 3.88 (ddd, J = 7.2, 7.2, 4.4 Hz, 1 H, CHCO), 3.85–3.77 (m, 3 H, $NCHHCHCO$, NCH_2CHAr), 3.68 (dd, J = 11.1, 7.3 Hz, 1 H, $NCHHCHCO$), 3.02 (s, 6 H, $N(CH_3)_2$), 1.49 (s, 9 H, $C(CH_3)_3$); ^{13}C NMR (126 MHz, DMSO-d_6, 373 K) δ 168.8 (C=O

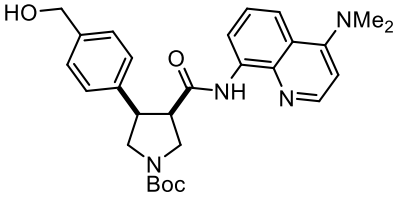
amide), 156.7 ($N(CH_3)_2C_{Ar}$ quat), 153.1 (C=O carbamate), 147.7 (C_{Ar}), 143.0 (C_{Ar} quat), 139.2 (C_{Ar} quat), 133.7 (C_{Ar} quat), 127.8 (2 × C_{Ar}), 127.0 (q, J_{CF} = 31.6 Hz, F_3CC_{Ar} quat), 124.3 (q, J_{CF} = 4.2 Hz, 2 × C_{Ar}), 123.6 (q, J_{CF} = 271.8 Hz, CF_3 quat), 123.5 (C_{Ar}), 121.3 (C_{Ar} quat), 118.0 (C_{Ar}), 115.4 (C_{Ar}), 107.0 (C_{Ar}), 78.2 ($C(CH_3)_3$), 49.3 (NCH_2CHAr), 49.0 (br and weak, $CHCO$), 47.6 (NCH_2CHCO), 45.2 (br and weak, CHAr), 42.9 ($N(CH_3)_2$), 27.8 ($C(CH_3)_3$); ^{19}F NMR (471 MHz, DMSO-d_6, 373 K) δ –61.2; HRMS (ESI$^+$) *m*/*z* Calculated for $C_{28}H_{32}N_4O_3F_3$ [M+H] 529.2427; Found 529.2418.

tert-Butyl _cis_-(±)-3-((4-(dimethylamino)quinolin-8-yl)carbamoyl)-4-(4-(trifluoromethoxy) phenyl)pyrrolidine-1-carboxylate (131e)



Prepared according to **General Procedure C** using amide **118** (76.9 mg) and 4-(trifluoromethoxy)iodobenzene (173 mg). Purification by flash column chromatography (10% acetone/pentane) afforded arylated pyrrolidine **131e** as a white solid (66.1 mg, 61%). R_f 0.24 (20% acetone/pentane); mp = 68–72 °C (from Et_2O/pentane); ν_{max} (film)/cm^{-1} 3317 (NH br), 2974, 1685 (C=O), 1521, 1402, 1252, 1219, 1159, 1111, 965, 760; ^1H NMR (400 MHz, DMSO-d_6, 373 K) δ 9.80 (br s, 1 H, NH), 8.52 (d, *J* = 5.2 Hz, 1 H, HC_{Ar}), 8.21 (dd, *J* = 7.6, 1.3 Hz, 1 H, HC_{Ar}), 7.70 (dd, *J* = 8.6, 1.3 Hz, 1 H, HC_{Ar}), 7.38–7.29 (m, 3 H, HC_{Ar}), 7.09–7.04 (m, 2 H, HC_{Ar}), 6.90 (d, *J* = 5.2 Hz, 1 H, HC_{Ar}), 3.91 (ddd, *J* = 7.2, 7.2, 7.2 Hz, 1 H, CHAr), 3.86–3.72 (m, 4 H, CHCO, NC*H*HCHCO, NCH_2CHAr), 3.70–3.62 (m, 1 H, NCH*H*CHCO), 3.02 (s, 6 H, $N(CH_3)_2$), 1.49 (s, 9 H, $C(CH_3)_3$); ^{13}C NMR (101 MHz, DMSO-d_6, 373 K) δ 168.9 (C=O amide), 156.7 ($N(CH_3)_2C_{Ar}$ quat), 153.1 (C=O carbamate), 147.7 (C_{Ar}), 146.8 (C_{Ar} quat), 139.2 (C_{Ar} quat), 137.4 (C_{Ar} quat), 133.7 (C_{Ar} quat), 128.8 (2 × C_{Ar}), 123.6 (C_{Ar}), 121.3 (C_{Ar} quat), 119.7 (2 × C_{Ar}), 118.0 (C_{Ar}), 115.4 (C_{Ar}), 107.0 (C_{Ar}), 78.1 ($C(CH_3)_3$), 49.5 (NCH_2CHAr), 49.0 (br and weak, $CHCO$), 47.5 (NCH_2CHCO), 44.8 (br and weak, CHAr), 42.9 ($N(CH_3)_2$), 27.8 ($C(CH_3)_3$); the signal for the quaternary OCF_3 (expected as a quartet at approx. δ 120 ppm) could not be observed in the ^{13}C NMR spectrum due to low intensity; ^{19}F NMR (376 MHz, DMSO-d_6, 373 K) δ –56.9; HRMS (FTMS pAPCI$^+$) *m*/*z* Calculated for $C_{28}H_{32}N_4O_4F_3^+$ $[M+H]^+$ 545.2370; Found 545.2366.

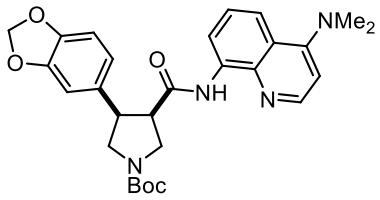
tert-Butyl _cis_-(±)-3-((4-(dimethylamino)quinolin-8-yl)carbamoyl)-4-(4-(hydroxymethyl) phenyl)pyrrolidine-1-carboxylate (131f)



Prepared according to **General Procedure C** using amide **118** (76.9 mg) and 4-iodobenzyl alcohol (140 mg). Purification by flash column chromatography (35% acetone/pentane) afforded arylated pyrrolidine **131f** as a yellow solid (65.8 mg, 67%). R_f 0.15 (30% acetone/pentane);

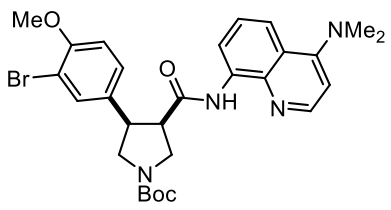
mp = 94–98 °C (from Et_2O/pentane); ν_{max} (film)/cm^{-1} 3375 (OH, NH br), 2973, 1676 (C=O), 1523, 1409, 1305, 1163, 1114, 1053, 965, 813, 762; ^{1}H NMR (400 MHz, DMSO-d_6, 373 K) δ 9.86 (br s, 1 H, NH), 8.55 (d, J = 5.2 Hz, 1 H, HC_{Ar}), 8.27 (dd, J = 7.7, 1.3 Hz, 1 H, HC_{Ar}), 7.70 (dd, J = 8.6, 1.3 Hz, 1 H, HC_{Ar}), 7.33 (dd, J = 8.6, 7.6 Hz, 1 H, HC_{Ar}), 7.22–7.16 (m, 2 H, HC_{Ar}), 7.13–7.06 (m, 2 H, HC_{Ar}), 6.90 (d, J = 5.2 Hz, 1 H, HC_{Ar}), 4.62 (t, J = 5.7 Hz, 1 H, OH), 4.33 (d, J = 5.5 Hz, 2 H, CH_2OH), 3.88–3.74 (m, 5 H, CHAr, NCHHCHCO, CHCO, NCH_2CHAr), 3.66 (dd, J = 12.6, 8.5 Hz, 1 H, NCHHCHCO), 3.03 (s, 6 H, N$(CH_3)_2$), 1.49 (s, 9 H, C$(CH_3)_3$); ^{13}C NMR (101 MHz, DMSO-d_6, 373 K) δ 169.0 (C=O amide), 156.7 (N$(CH_3)_2C_{Ar}$ quat), 153.2 (C=O carbamate), 147.8 (C_{Ar}), 140.4 (C_{Ar} quat), 139.2 (C_{Ar} quat), 136.5 (C_{Ar} quat), 133.9 (C_{Ar} quat), 126.7 (2 × C_{Ar}), 125.7 (2 × C_{Ar}), 123.6 (C_{Ar}), 121.4 (C_{Ar} quat), 117.9 (C_{Ar}), 115.2 (C_{Ar}), 107.0 (C_{Ar}), 78.0 (C(CH$_3$)$_3$), 62.2 (CH$_2$OH), 50.0 (NCH$_2$CHAr), 49.1 (br and weak, CHCO), 47.5 (NCH$_2$CHCO), 45.2 (br and weak, CHAr), 43.0 (N$(CH_3)_2$), 27.8 (C(CH$_3$)$_3$); HRMS (ESI$^+$) m/z Calculated for $C_{28}H_{35}N_4O_4$ [M+H] 491.2658; Found 491.2665.

tert-Butyl _cis_-(±)-3-(benzo[d][1,3]dioxol-5-yl)-4-((4-(dimethylamino)quinolin-8-yl)carbamoyl)pyrrolidine-1-carboxylate (131g)



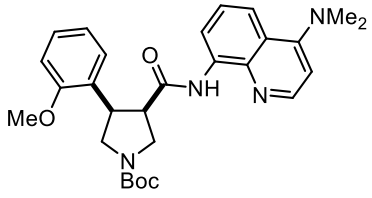
Prepared according to **General Procedure C** using amide **118** (76.9 mg) and 5-iodo-1,3-benzodioxole (149 mg). Purification by flash column chromatography (20% acetone/pentane) afforded arylated pyrrolidine **131g** as a white solid (78.9 mg, 78%). R_f 0.30 (25% acetone/pentane); mp = 85–89 °C (from Et_2O/pentane); ν_{max} (film)/cm^{-1} 3321 (NH br), 2881, 1684 (C=O), 1525, 1405, 1305, 1238, 1167, 1118, 1036, 932, 813, 764; ^{1}H NMR (400 MHz, DMSO-d_6, 373 K) δ 9.78 (br s, 1 H, NH), 8.52 (d, J = 5.2 Hz, 1 H, HC_{Ar}), 8.29 (dd, J = 7.7, 1.3 Hz, 1 H, HC_{Ar}), 7.70 (dd, J = 8.6, 1.3 Hz, 1 H, HC_{Ar}), 7.35 (dd, J = 8.6, 7.7 Hz, 1 H, HC_{Ar}), 6.90 (d, J = 5.2 Hz, 1 H, HC_{Ar}), 6.76 (d, J = 1.8 Hz, 1 H, HC_{Ar}), 6.69 (dd, J = 8.1, 1.6 Hz, 1 H, HC_{Ar}), 6.61 (d, J = 7.9 Hz, 1 H, HC_{Ar}), 5.77 (d, J = 1.0 Hz, 1 H, OCHHO), 5.74 (d, J = 1.0 Hz, 1 H, OCHHO), 3.82–3.67 (m, 5 H, CHAr, NCHHCHCO, CHCO, NCH_2CHAr), 3.61 (dd, J = 10.6, 6.5 Hz, 1 H, NCHHCHCO), 3.03 (s, 6 H, N$(CH_3)_2$), 1.48 (s, 9 H, C$(CH_3)_3$); ^{13}C NMR (101 MHz, DMSO-d_6, 373 K) δ 169.1 (C=O amide), 156.7 (N$(CH_3)_2C_{Ar}$ quat), 153.2 (C=O carbamate), 147.7 (C_{Ar}), 146.7 (OC_{Ar} quat), 145.4 (OC_{Ar} quat), 139.2 (C_{Ar} quat), 133.9 (C_{Ar} quat), 131.7 (C_{Ar} quat), 123.6 (C_{Ar}), 121.3 (C_{Ar} quat), 120.1 (C_{Ar}), 117.9 (C_{Ar}), 115.2 (C_{Ar}), 107.4 (C_{Ar}), 107.2 (C_{Ar}), 107.0 (C_{Ar}), 100.0 (OCH_2O), 78.0 (C(CH$_3$)$_3$), 49.7 (NCH$_2$CHAr), 49.3 (br and weak, CHCO), 47.4 (NCH$_2$CHCO), 45.3 (br and weak, CHAr), 43.0 (N$(CH_3)_2$), 27.8 (C(CH$_3$)$_3$); HRMS (ESI$^+$) m/z Calculated for $C_{28}H_{33}N_4O_5$ [M+H] 505.2451; Found 505.2446.

***tert*-Butyl *cis*-(±)-3-(3-bromo-4-methoxyphenyl)-4-((4-(dimethylamino)quinolin-8-yl) carbamoyl)pyrrolidine-1-carboxylate (131h)**



Prepared according to **General Procedure C** using amide **118** (76.9 mg) and 2-bromo-4-iodoanisole (188 mg). Purification by flash column chromatography (15% to 20% acetone/pentane) afforded arylated pyrrolidine **131h** as a white solid (79.4 mg, 70%). R_f 0.33 (20% acetone/pentane); mp = 95–99 °C (from Et_2O/pentane); ν_{max} (film)/cm^{-1} 3317 (NH br), 2945, 1685 (C=O), 1521, 1402, 1305, 1256, 1163, 1118, 1055, 965, 876, 813, 764, 678; ^{1}H NMR (400 MHz, DMSO-d_6, 373 K) δ 9.78 (br s, 1 H, NH), 8.52 (d, J = 5.2 Hz, 1 H, HC_{Ar}), 8.27 (dd, J = 7.6, 1.3 Hz, 1 H, HC_{Ar}), 7.71 (dd, J = 8.6, 1.3 Hz, 1 H, HC_{Ar}), 7.42 (d, J = 2.2 Hz, 1 H, HC_{Ar}), 7.34 (dd, J = 8.6, 7.6 Hz, 1 H, HC_{Ar}), 7.15 (dd, J = 8.5, 2.2 Hz, 1 H, HC_{Ar}), 6.90 (d, J = 5.2 Hz, 1 H, HC_{Ar}), 6.81 (d, J = 8.5 Hz, 1 H, HC_{Ar}), 3.85–3.74 (m, 3 H, CHAr, NC*H*HCHCO, CHCO), 3.74–3.66 (m, 2 H, NCH_2CHAr), 3.65–3.58 (m, 4 H, NCH*H*CHCO, OCH_3), 3.03 (s, 6 H, $N(CH_3)_2$), 1.49 (s, 9 H, $C(CH_3)_3$); ^{13}C NMR (101 MHz, DMSO-d_6, 373 K) δ 169.0 (C=O amide), 156.7 ($N(CH_3)_2C_{Ar}$ quat), 154.0 (OC_{Ar} quat), 153.1 (C=O carbamate), 147.8 (C_{Ar}), 139.3 (C_{Ar} quat), 133.8 (C_{Ar} quat), 131.9 (C_{Ar} quat), 131.7 (C_{Ar}), 127.3 (C_{Ar}), 123.6 (C_{Ar}), 121.4 (C_{Ar} quat), 118.0 (C_{Ar}), 115.4 (C_{Ar}), 112.3 (C_{Ar}), 110.3 (BrC_{Ar} quat), 107.0 (C_{Ar}), 78.1 ($C(CH_3)_3$), 55.7 (OCH_3), 49.6 (NCH_2CHAr), 49.2 (br and weak, *C*HCO), 47.3 (NCH_2CHCO), 44.4 (br and weak, CHAr), 43.0 ($N(CH_3)_2$), 27.8 (C(CH_3)$_3$); HRMS (ESI$^+$) *m*/*z* Calculated for $C_{28}H_{34}N_4O_4{}^{79}Br$ [M+H] 569.1763; Found 569.1756.

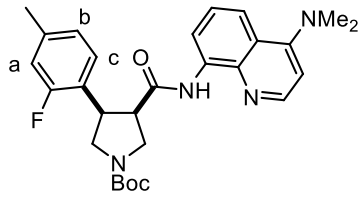
***tert*-Butyl *cis*-(±)-3-((4-(dimethylamino)quinolin-8-yl)carbamoyl)-4-(2-methoxyphenyl) pyrrolidine-1-carboxylate (131i)**



Prepared according to **General Procedure C** using amide **118** (76.9 mg) and 2-iodoanisole (140 mg). Purification by flash column chromatography (15% MeCN/CH_2Cl_2) afforded arylated pyrrolidine **131i** as an off-white solid (44.1 mg, 45%). R_f 0.48 (20% MeCN/CH_2Cl_2); mp = 82–86 °C (from Et_2O/pentane); ν_{max} (film)/cm^{-1} 3332 (NH br), 2971, 1684 (C=O), 1525, 1409, 1305, 1238, 1167, 1115, 969, 753; ^{1}H NMR (500 MHz, DMSO-d_6, 373 K) δ 9.73 (br s, 1 H, NH), 8.53 (d, J = 5.2 Hz, 1 H, HC_{Ar}), 8.27 (dd, J = 7.7, 1.3 Hz, 1 H, HC_{Ar}), 7.65 (dd, J = 8.6, 1.3 Hz, 1 H, HC_{Ar}), 7.29 (dd, J = 8.6, 7.7 Hz, 1 H, HC_{Ar}), 7.06 (dd, J = 7.6, 1.1 Hz, 1 H, HC_{Ar}), 7.00 (td, J = 8.0, 1.6 Hz, 1 H, HC_{Ar}), 6.89 (d, J = 5.2 Hz, 1 H, HC_{Ar}), 6.81 (dd, J = 8.2, 0.9 Hz, 1 H, HC_{Ar}), 6.71 (td, J = 7.5, 0.9 Hz, 1 H, HC_{Ar}), 4.01 (ddd, J = 7.4, 7.4, 7.4 Hz, 1 H, CHAr), 3.86–3.76 (m, 6 H, NC*H*HCHCO, CHCO, NC*H*HCHAr, OCH_3), 3.73 (dd, J = 10.3, 7.4 Hz, 1 H, NCH*H*CHAr), 3.64 (dd, J = 10.7,

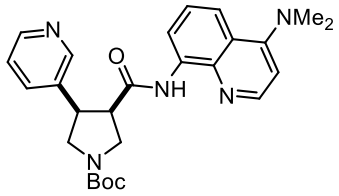
6.9 Hz, 1 H, NCH*H*CHCO), 3.02 (s, 6 H, $N(CH_3)_2$), 1.49 (s, 9 H, $C(CH_3)_3$); ^{13}C NMR (126 MHz, DMSO-d_6, 373 K) δ 169.3 (C=O amide), 156.7 ($N(CH_3)_2C_{Ar}$ quat), 156.6 (OC_{Ar} quat), 153.2 (C=O carbamate), 147.6 (C_{Ar}), 138.9 (C_{Ar} quat), 133.9 (C_{Ar} quat), 127.3 (C_{Ar}), 126.3 (C_{Ar}), 125.7 (C_{Ar} quat), 123.6 (C_{Ar}), 121.2 (C_{Ar} quat), 119.6 (C_{Ar}), 117.6 (C_{Ar}), 114.5 (C_{Ar}), 110.3 (C_{Ar}), 107.0 (C_{Ar}), 77.9 ($C(CH_3)_3$), 54.9 (OCH_3), 48.3 (NCH_2CHAr), 47.7 (NCH_2CHCO), 47.6 (br and weak, *C*HCO), 42.9 ($N(CH_3)_2$), 39.7 (br and weak, CHAr), 27.8 ($C(CH_3)_3$); HRMS (ESI^+) *m*/*z* Calculated for $C_{28}H_{35}N_4O_4$ [M+H] 491.2658; Found 491.2642.

tert-Butyl _cis_-(±)-3-((4-(dimethylamino)quinolin-8-yl)carbamoyl)-4-(2-fluoro-4-methylphenyl)pyrrolidine-1-carboxylate (131j)



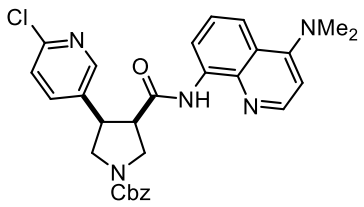
Prepared according to **General Procedure C** using amide **118** (76.9 mg) and 2-fluoro-4-iodotoluene (142 mg). Purification by flash column chromatography (15% acetone/pentane) afforded arylated pyrrolidine **131j** as a white solid (40.7 mg, 41%). R_f 0.46 (20% acetone/pentane); mp = 75–79 °C (from Et_2O/pentane); ν_{max} (film)/cm^{-1} 3325 (NH br), 2971, 1685 (C=O), 1525, 1409, 1305, 1167, 1115, 813, 764; ^1H NMR (400 MHz, DMSO-d_6, 373 K) δ 9.83 (br s, 1 H, NH), 8.52 (d, *J* = 5.2 Hz, 1 H, HC_{Ar}), 8.27 (dd, *J* = 7.7, 1.3 Hz, 1 H, HC_{Ar}), 7.69 (dd, *J* = 8.6, 1.2 Hz, 1 H, HC_{Ar}), 7.33 (dd, *J* = 8.6, 7.6 Hz, 1 H, HC_{Ar}), 7.08 (dd, J_{HH} = 8.0 Hz, J_{HF} = 8.0 Hz, 1 H, H_c), 6.90 (d, *J* = 5.2 Hz, 1 H, HC_{Ar}), 6.80 (br d, J_{HF} = 11.7 Hz, 1 H, H_a), 6.76 (br d, J_{HH} = 8.0 Hz, 1 H, H_b), 4.00 (ddd, *J* = 7.5, 7.5, 7.5 Hz, 1 H, CHAr), 3.84–3.72 (m, 4 H, NC*H*HCHCO, CHCO, NCH_2CHAr), 3.71–7.63 (m, 1 H, NCH*H*CHCO), 3.02 (s, 6 H, $N(CH_3)_2$), 2.11 (s, 3 H, CH_3), 1.48 (s, 9 H, $C(CH_3)_3$); ^{13}C NMR (101 MHz, DMSO-d_6, 373 K) δ 168.9 (C=O amide), 159.8 (d, J_{CF} = 244 Hz, FC_{Ar} quat), 156.7 ($N(CH_3)_2C_{Ar}$ quat), 153.2 (C=O carbamate), 147.7 (C_{Ar}), 139.1 (C_{Ar} quat), 138.0 (d, J_{CF} = 8.5 Hz, F-*m*-C_{Ar} quat), 133.9 (C_{Ar} quat), 127.5 (d, J_{CF} = 5.1 Hz, F-*m*-C_c), 124.1 (d, J_{CF} = 2.4 Hz, F-*p*-C_b), 123.6 (C_{Ar}), 121.6 (d, J_{CF} = 14.6 Hz, F-*o*-C_{Ar} quat), 121.3 (C_{Ar} quat), 117.9 (C_{Ar}), 115.1 (C_{Ar}), 115.0 (d, J_{CF} = 22.8 Hz, F-*o*-C_a), 107.0 (C_{Ar}), 78.1 ($C(CH_3)_3$), 48.8 (NCH_2CHAr), 48.2 (br and weak, *C*HCO), 47.7 (NCH_2CHCO), 43.0 ($N(CH_3)_2$), 38.5 (br and weak, CHAr), 27.8 ($C(CH_3)_3$), 19.6 (CH_3); ^{19}F NMR (376 MHz, DMSO-d_6, 373 K) δ –117.2 (dd, J_{HF} = 11.6, 8.2 Hz); HRMS (ESI^+) *m*/*z* Calculated for $C_{28}H_{34}N_4O_3F$ [M+H] 493.2615; Found 493.2624.

***tert*-Butyl *cis*-(±)-3-((4-(dimethylamino)quinolin-8-yl)carbamoyl)-4-(pyridin-3-yl)pyrrolidine-1-carboxylate (131k)**



Prepared according to **General Procedure C** using amide **118** (76.9 mg) and 3-iodopyridine (123 mg). Purification by flash column chromatography (40% acetone/pentane) afforded arylated pyrrolidine **131k** as a white solid (28.8 mg, 31%). R_f = 0.15 (40% acetone/pentane); mp = 78–81 °C (from Et_2O/pentane); ν_{max} (film)/cm^{-1} 3325 (NH br), 2974, 1685 (C=O), 1525, 1405, 1305, 1163, 1118, 813, 764, 712; ^{1}H NMR (500 MHz, DMSO-d_6, 373 K) δ 9.91 (br s, 1 H, NH), 8.53 (d, J = 5.2 Hz, 1 H, HC_{Ar}), 8.46 (d, J = 2.0 Hz, 1 H, HC_{Ar}), 8.27 (dd, J = 4.7, 1.6 Hz, 1 H, HC_{Ar}), 8.22 (dd, J = 7.7, 1.3 Hz, 1 H, HC_{Ar}), 7.71 (dd, J = 8.6, 1.3 Hz, 1 H, HC_{Ar}), 7.61–7.57 (m, 1 H, HC_{Ar}), 7.33 (dd, J = 8.6, 7.6 Hz, 1 H, HC_{Ar}), 7.14 (ddd, J = 8.0, 4.7, 0.9 Hz, 1 H, HC_{Ar}), 6.90 (d, J = 5.2 Hz, 1 H, HC_{Ar}), 3.93–3.85 (m, 2 H, CHAr, CHCO), 3.84–3.76 (m, 3 H, NC*H*HCHCO, NCH_2CHAr), 3.68 (dd, J = 11.1, 7.2 Hz, 1 H, NCH*H*CHCO), 3.03 (s, 6 H, N$(CH_3)_2$), 1.49 (s, 9 H, C$(CH_3)_3$); ^{13}C NMR (126 MHz, DMSO-d_6, 373 K) δ 168.8 (C=O amide), 156.7 (N$(CH_3)_2C_{Ar}$ quat), 153.1 (C=O carbamate), 148.5 (C_{Ar}), 147.8 (C_{Ar}), 147.3 (C_{Ar}), 139.3 (C_{Ar} quat), 134.2 (C_{Ar}), 133.8 (C_{Ar} quat), 133.7 (C_{Ar} quat), 123.6 (C_{Ar}), 122.4 (C_{Ar}), 121.4 (C_{Ar} quat), 118.1 (C_{Ar}), 115.5 (C_{Ar}), 107.0 (C_{Ar}), 78.2 (*C*$(CH_3)_3$), 49.6 (N*C*H_2CHAr), 48.8 (br and weak, *C*HCO), 47.4 (N*C*H_2CHCO), 43.1 (br and weak, CHAr), 42.9 (N$(CH_3)_2$), 27.8 (C(*C*$H_3)_3$); HRMS (ESI$^+$) m/z Calculated for $C_{26}H_{32}N_5O_3$ [M+H] 462.2505; Found 462.2492.

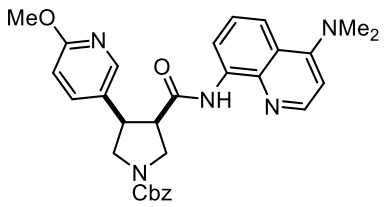
Benzyl *cis*-(±)-3-(6-chloropyridin-3-yl)-4-((4-(dimethylamino)quinolin-8-yl)carbamoyl) pyrrolidine-1-carboxylate (132d)



Prepared according to **General Procedure C** using amide **119** (83.7 mg) and 2-chloro-4-iodopyridine (144 mg). Purification by flash column chromatography (35% acetone/pentane) afforded arylated pyrrolidine **132d** as a pale yellow solid (37.4 mg, 35%). R_f 0.15 (30% acetone/pentane); mp = 69–73 °C (from Et_2O/pentane); ν_{max} (film)/cm^{-1} 3314 (NH br), 2881, 1677 (C=O), 1521, 1409, 1103, 969, 813, 764, 697; ^{1}H NMR (400 MHz, DMSO-d_6, 373 K) δ 9.92 (br s, 1 H, NH), 8.52 (d, J = 5.2 Hz, 1 H, HC_{Ar}), 8.28 (br d, J = 2.6 Hz, 1 H, HC_{Ar}), 8.22 (dd, J = 7.7, 1.3 Hz, 1 H, HC_{Ar}), 7.73 (dd, J = 8.6, 1.3 Hz, 1 H, HC_{Ar}), 7.67 (dd, J = 8.6, 2.6 Hz, 1 H, HC_{Ar}), 7.45–7.29 (m, 6 H, HC_{Ar}), 7.23 (dd, J = 8.3, 0.7 Hz, 1 H, HC_{Ar}), 6.91 (d, J = 5.2 Hz, 1 H, HC_{Ar}), 5.18 (s, 2 H, OCH_2Ph), 4.00–3.81 (m, 5 H, NCH_2CHAr, CHAr, CHCO, NC*H*HCHCO), 3.77 (dd, J = 10.9, 6.7 Hz 1 H, NCH*H*CHCO), 3.04 (s, 6 H, N$(CH_3)_2$); ^{13}C NMR (101 MHz, DMSO-d_6, 373 K) δ 168.7 (C=O amide), 156.7 (N$(CH_3)_2C_{Ar}$ quat), 153.5 (C=O carbamate), 148.5 (C_{Ar}), 148.3 (ClC_{Ar} quat),

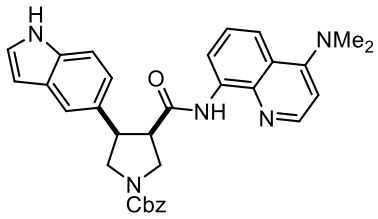
147.9 (C_{Ar}), 139.4 (C_{Ar} quat), 138.0 (C_{Ar}), 136.6 (C_{Ar} quat), 133.6 (C_{Ar} quat), 133.2 (C_{Ar} quat), 127.8 (2 × C_{Ar}), 127.1 (C_{Ar}), 126.8 (2 × C_{Ar}), 123.6 (C_{Ar}), 123.0 (C_{Ar}), 121.4 (C_{Ar} quat), 118.3 (C_{Ar}), 115.7 (C_{Ar}), 107.0 (C_{Ar}), 65.6 (OCH_2Ph), 49.3 (br and weak, N*C*H_2CHAr), 48.6 (br and weak, *C*HCO), 47.7 (br and weak, N*C*H_2CHCO), 43.0 ($N(CH_3)_2$), 42.4 (br and weak, CHAr); HRMS (ESI$^+$) *m*/*z* Calculated for $C_{29}H_{29}N_5O_3{}^{35}Cl$ [M+H] 530.1959; Found 530.1961.

Benzyl *cis*-(±)-3-((4-(dimethylamino)quinolin-8-yl)carbamoyl)-4-(6-methoxypyridin-3-yl) pyrrolidine-1-carboxylate (132e)



Prepared according to **General Procedure C** using amide **119** (83.7 mg) and 2-methoxy-4-iodopyridine (141 mg). Purification by flash column chromatography (30% acetone/pentane) afforded arylated pyrrolidine **132e** as a pale yellow solid (45.9 mg, 44%). R_f 0.20 (30% acetone/pentane); mp = 63–67 °C (from Et_2O/pentane); ν_{max} (film)/cm^{-1} 3317 (NH br), 2945, 1681 (C=O), 1521, 1495, 1409, 1111, 1025, 813, 764, 697; ^{1}H NMR (400 MHz, DMSO-d_6, 373 K) δ 9.86 (br s, 1 H, NH), 8.50 (d, *J* = 5.2 Hz, 1 H, HC_{Ar}), 8.26 (dd, *J* = 7.7, 1.3 Hz, 1 H, HC_{Ar}), 8.02 (dd, *J* = 2.6, 0.7 Hz, 1 H, HC_{Ar}), 7.71 (dd, *J* = 8.6, 1.3 Hz, 1 H, HC_{Ar}), 7.52 (dd, *J* = 8.6, 2.6 Hz, 1 H, HC_{Ar}), 7.44–7.28 (m, 6 H, HC_{Ar}), 6.89 (d, *J* = 5.2 Hz, 1 H, HC_{Ar}), 6.53 (dd, *J* = 8.6, 0.7 Hz, 1 H, HC_{Ar}), 5.18 (s, 2 H, OCH_2Ph), 3.92–3.79 (m, 5 H, N*C*H_2CHAr, CHAr, CHCO, N*CH*HCHCO), 3.74 (dd, *J* = 10.3, 6.5 Hz, 1 H, NCH*H*CHCO), 3.69 (s, 3 H, OCH_3), 3.03 (s, 6 H, $N(CH_3)_2$); ^{13}C NMR (101 MHz, DMSO-d_6, 373 K) δ 168.9 (C=O amide), 162.2 (OC_{Ar} quat), 156.7 ($N(CH_3)_2C_{Ar}$ quat), 153.6 (C=O carbamate), 147.8 (C_{Ar}), 145.3 (C_{Ar}), 139.3 (C_{Ar} quat), 137.6 (C_{Ar}), 136.7 (C_{Ar} quat), 133.7 (C_{Ar} quat), 127.8 (2 × C_{Ar}), 127.1 (C_{Ar}), 126.8 (2 × C_{Ar}), 126.3 (C_{Ar} quat), 123.6 (C_{Ar}), 121.4 (C_{Ar} quat), 118.1 (C_{Ar}), 115.5 (C_{Ar}), 109.2 (C_{Ar}), 107.0 (C_{Ar}), 65.5 (OCH_2Ph), 52.2 (OCH_3), 49.6 (br and weak, N*C*H_2CHAr), 48.9 (br and weak, *C*HCO), 47.6 (br and weak, N*C*H_2CHCO), 43.0 ($N(CH_3)_2$), 42.6 (br and weak, CHAr); HRMS (FTMS ESI$^+$) *m*/*z* Calculated for $C_{30}H_{32}N_5O_4{}^+$ $[M+H]^+$ 526.2449; Found 526.2437.

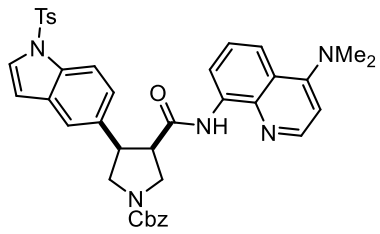
Benzyl *cis*-(±)-3-((4-(dimethylamino)quinolin-8-yl)carbamoyl)-4-(1*H*-indol-5-yl)pyrrolidine-1-carboxylate (132f)



Prepared according to **General Procedure C** using amide **119** (83.7 mg) and 5-iodo-1*H*-indole (146 mg). Purification by flash column chromatography (35% acetone/pentane) afforded arylated pyrrolidine **132f** as a pale yellow solid (37.6 mg, 35%). R_f 0.15 (30% acetone/pentane); mp = 89–93 °C (from $CHCl_3$); ν_{max} (film)/cm^{-1} 3302 (NH br), 2904, 1677 (C=O), 1521, 1409, 1305, 1107, 965, 813, 760, 727, 697; ^{1}H NMR (400 MHz, DMSO-d_6, 373 K) δ 10.46 (br s, 1 H, NH indole), 9.77 (br s, 1 H,

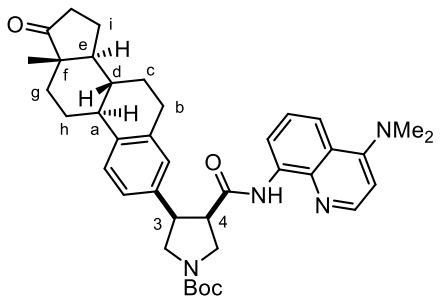
CONH), 8.41 (d, *J* = 5.2 Hz, 1 H, HC_{Ar}), 8.22 (d, *J* = 7.8 Hz, 1 H, HC_{Ar}), 7.67 (dd, *J* = 8.6, 1.3 Hz, 1 H, HC_{Ar}), 7.46–7.35 (m, 5 H, HC_{Ar}), 7.35–7.25 (m, 2 H, HC_{Ar}), 7.17–7.10 (m, 2 H, HC_{Ar}), 7.00 (dd, *J* = 8.4, 1.8 Hz, 1 H, HC_{Ar}), 6.84 (d, *J* = 5.2 Hz, 1 H, HC_{Ar}), 6.21 (ddd, *J* = 3.0, 1.9, 0.9 Hz, 1 H, HC_{Ar}), 5.20 (s, 2 H, OCH_2Ph), 4.02–3.86 (m, 4 H, CHAr, NC*H*$_2$CHAr, NC*H*HCHCO), 3.83–3.72 (m, 2 H, NCH*H*CHCO, CHCO), 3.02 (s, 6 H, $N(CH_3)_2$); ^{13}C NMR (101 MHz, DMSO-d_6, 373 K) δ 169.1 (C=O amide), 156.6 ($N(CH_3)_2C_{Ar}$ quat), 153.6 (C=O carbamate), 147.4 (C_{Ar}), 139.0 (C_{Ar} quat), 136.8 (C_{Ar} quat), 134.6 (C_{Ar} quat), 133.8 (C_{Ar} quat), 127.8 (C_{Ar} quat), 127.7 (2 × C_{Ar}), 127.3 (C_{Ar} quat), 127.0 (C_{Ar}), 126.7 (2 × C_{Ar}), 124.5 (C_{Ar}), 123.5 (C_{Ar}), 121.2 (C_{Ar} quat), 120.3 (C_{Ar}), 118.2 (C_{Ar}), 117.8 (C_{Ar}), 115.3 (C_{Ar}), 110.4 (C_{Ar}), 106.8 (C_{Ar}), 100.3 (C_{Ar}), 65.4 (OCH_2Ph), 50.4 (N*C*H$_2$CHAr), 49.5 (br and weak, *C*HCO), 47.8 (N*C*H$_2$CHCO), 45.7 (br and weak, CHAr), 42.9 ($N(CH_3)_2$); HRMS (ESI$^+$) *m*/*z* Calculated for $C_{32}H_{32}N_5O_3$ [M+H] 534.2505; Found 534.2515.

Benzyl *cis*-(±)-3-((4-(dimethylamino)quinolin-8-yl)carbamoyl)-4-(1-tosyl-1*H*-indol-5-yl)pyrrolidine-1-carboxylate (132g)



Prepared according to **General Procedure C** using amide **119** (83.7 mg) and 5-iodo-1-tosyl-1*H*-indole **S2** (238 mg). Purification by flash column chromatography (30% acetone/pentane) afforded arylated pyrrolidine **132g** as a pale yellow solid (87.5 mg, 64%). R_f 0.18 (30% acetone/pentane); mp = 106–110 °C (from Et_2O/pentane); ν_{max} (film)/cm^{-1} 3317 (NH br), 2885, 1700 (C=O), 1521, 1413, 1361, 1170, 1118, 813, 764, 693; ^{1}H NMR (400 MHz, DMSO-d_6, 373 K) δ 9.75 (br s, 1 H, NH), 8.40 (d, *J* = 5.2 Hz, 1 H, HC_{Ar}), 8.16 (dd, *J* = 7.7, 1.3 Hz, 1 H, HC_{Ar}), 7.70–7.62 (m, 4 H, HC_{Ar}), 7.51 (d, *J* = 3.6 Hz, 1 H, HC_{Ar}), 7.46–7.29 (m, 6 H, HC_{Ar}), 7.29–7.23 (m, 2 H, HC_{Ar}), 7.23–7.19 (m, 2 H, HC_{Ar}), 6.84 (d, *J* = 5.2 Hz, 1 H, HC_{Ar}), 6.55 (dd, *J* = 3.7, 0.8 Hz, 1 H, HC_{Ar}), 5.18 (s, 2 H, OCH_2Ph), 4.01–3.93 (m, 1 H, CHAr), 3.93–3.81 (m, 4 H, NC*H*$_2$CHAr, NC*H*HCHCO, CHCO), 3.74 (dd, *J* = 10.6, 6.9 Hz, 1 H, NCH*H*CHCO), 3.02 (s, 6 H, $N(CH_3)_2$), 1.27 (s, 3 H, CH_3); ^{13}C NMR (101 MHz, DMSO-d_6, 373 K) δ 169.0 (C=O amide), 156.6 ($N(CH_3)_2C_{Ar}$ quat), 153.6 (C=O carbamate), 147.6 (C_{Ar}), 144.5 (C_{Ar} quat), 139.2 (C_{Ar} quat), 136.7 (C_{Ar} quat), 134.3 (C_{Ar} quat), 133.7 (C_{Ar} quat), 133.0 (C_{Ar} quat), 132.9 (C_{Ar} quat), 130.0 (C_{Ar} quat), 129.4 (2 × C_{Ar}), 127.7 (2 × C_{Ar}), 127.1 (C_{Ar}), 126.8 (2 × C_{Ar}), 126.2 (C_{Ar}), 125.8 (2 × C_{Ar}), 124.0 (C_{Ar}), 123.5 (C_{Ar}), 121.3 (C_{Ar} quat), 119.7 (C_{Ar}), 117.9 (C_{Ar}), 115.4 (C_{Ar}), 112.2 (C_{Ar}), 108.5 (C_{Ar}), 106.9 (C_{Ar}), 65.5 (OCH_2Ph), 49.8 (br and weak, N*C*H$_2$CHAr), 49.1 (br and weak, *C*HCO), 47.8 (br and weak, N*C*H$_2$CHCO), 45.4 (br and weak, CHAr), 42.9 ($N(CH_3)_2$), 20.3 (CH_3); HRMS (FTMS ESI$^+$) *m*/*z* Calculated for $C_{39}H_{38}N_5O_5S^+$ [M+H]$^+$ 688.2588; Found 688.2590.

***tert*-Butyl *3,4-cis*-3-((4-(dimethylamino)quinolin-8-yl)carbamoyl)-4-((8*R*,9*S*,13*S*,14*S*)-13-methyl-17-oxo-7,8,9,11,12,13,14,15,16,17-decahydro-6*H*-cyclopenta[*a*]phenanthren-3-yl)pyrrolidine-1-carboxylate (131l)**

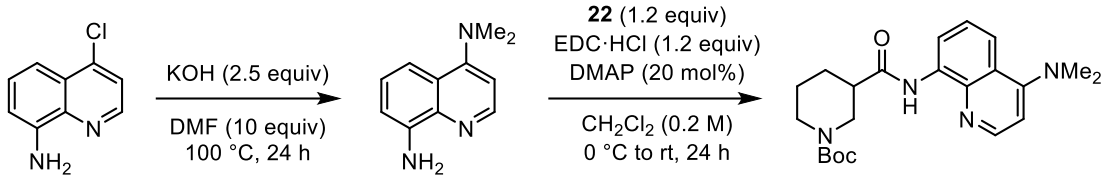


A reaction vial was charged with K_2CO_3 (23.5 mg, 0.17 mmol), flame-dried, and allowed to cool under argon. Amide **118** (65.4 mg, 0.17 mmol), (8*R*,9*S*,13*S*,14*S*)-3-iodo-13-methyl-6,7,8,9,11,12,13,14,15,16-decahydro-17*H*-cyclopenta[*a*] phenanthren-17-one[47c] (65.0 mg, 0.17 mmol), $Pd(OAc)_2$ (1.9 mg, 8.50 μmol) and PivOH (17.4 mg, 0.17 mmol) were added sequentially. The reaction vessel was sealed and purged with argon, then $PhCF_3$ (170 μL, 1.0 M) was added by syringe. The reaction tube was placed in a preheated oil bath and stirred at 110 ºC for 18 h. The reaction mixture was then allowed to cool to rt and EtOAc (5 mL) was added. The resulting mixture was filtered through a pad of Celite, eluting with further EtOAc (3 × 5 mL). The solvent was removed under reduced pressure, and the crude material was purified by flash column chromatography (20% acetone/pentane). The product containing fractions were combined and the solvent was removed under reduced pressure. Et_2O (3 mL) and pentane (3 mL) were added and the solvent was removed under reduced pressure to afford arylated pyrrolidine **131l** as a white solid (46.1 mg, 43%, 1:1 mixture of *3,4-cis*-diastereomers). R_f 0.21 (20% acetone/pentane); mp = 131–135 °C (from Et_2O/pentane); ν_{max} (film)/cm^{-1} 3329 (NH br), 2930, 1737 (C=O), 1689 (C=O), 1525, 1405, 1305, 1238, 1167, 1115, 813, 764; ^{1}H NMR (500 MHz, DMSO-d_6, 373 K) δ 9.62 and 9.59 (2 × br s, 1 H, NH), 8.49–8.45 (m, 1 H, HC_{Ar}), 8.32–8.28 (m, 1 H, HC_{Ar}), 7.70–7.65 (m, 1 H, HC_{Ar}), 7.36–7.31 (m, 1 H, HC_{Ar}), 6.98–6.94 (m, 2 H HC_{Ar}), 6.90–6.85 (m, 2 H HC_{Ar}), 3.82–3.73 (m, 2 H, C_3HAr, NC*H*HCHCO), 3.73–3.65 (m, 3 H, C_4HCO, NCH_2CHAr), 3.63–3.57 (m, 1 H, NCH*H*CHCO), 3.02 and 3.01 (2 × s, 6 H, $N(CH_3)_2$), 2.59–2.43 (m, 1 H, C_b*H*H), 2.43–2.34 (m, 2 H, C_bH*H*, C*H*HCO), 2.18–2.09 (m, 1 H, C_h*H*H), 2.06–1.96 (m, 1 H, CH*H*CO), 1.96–1.85 (m, 2 H, C_aH, C_i*H*H), 1.76–1.65 (m, 2 H, C_g*H*H, C_c*H*H), 1.54–1.43 (m, 10 H, C_iH*H*, $C(CH_3)_3$), 1.38–1.24 (m, 2 H, C_gH*H*, C_eH), 1.24–0.99 (m, 3 H, C_dH, C_hH*H*, C_cH*H*), 0.74 and 0.73 (2 × s, 3 H, CH_3); ^{13}C NMR (126 MHz, DMSO-d_6, 373 K) δ 218.2 (C=O ketone), 169.3 (C=O amide), 156.6 ($N(CH_3)_2C_{Ar}$ quat), 153.2 (C=O carbamate), 147.6 (C_{Ar}), 139.10 and 139.08 (C_{Ar} quat), 137.6 (C_{Ar} quat), 135.4 and 135.3 (C_{Ar} quat), 134.69 and 134.67 (C_{Ar} quat), 133.98 and 133.96 (C_{Ar} quat), 127.3 and 127.2 (C_{Ar}), 124.5 and 124.21 (C_{Ar}), 124.16 (C_{Ar}), 123.6 (C_{Ar}), 121.2 (C_{Ar} quat), 117.71 and 117.67 (C_{Ar}), 114.9 and 114.8 (C_{Ar}), 106.93 and 106.88 (C_{Ar}), 78.0 ($C(CH_3)_3$), 49.6 (br and weak, *C*HCO), 49.52 and 49.48 (C_eH), 49.3 and 49.1 (N*C*H_2CHAr), 47.42 and 47.39 (N*C*H_2CHCO), 46.6 (C_f quat), 45.4 (br and weak, CHAr), 43.00 (C_aH), 42.96 ($N(CH_3)_2$), 37.1 (C_dH), 34.7 (*C*H_2CO), 30.9 (C_gH_2), 27.94 and 27.88 (C_bH_2), 27.8

($C(CH_3)_3$), 25.2 (C_cH_2), 24.5 (C_hH_2), 20.51 and 20.49 (C_iH_2), 13.13 and 13.10 (CH_3); HRMS (FTMS pAPCI$^+$) *m*/*z* Calculated for $C_{39}H_{49}N_4O_4^+$ $[M+H]^+$ 637.3748; Found 637.3738.

*8.2.5.9 Synthesis of amide **133** via intermediate **117***

tert-Butyl (±)-3-((4-dimethylamino-8-yl)carbamoyl)piperidine-1-carboxylate (133)



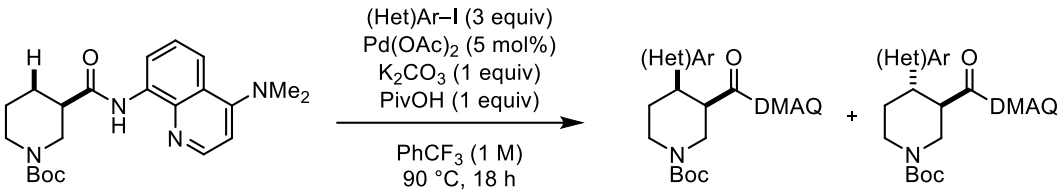
117 **133**

A flame-dried microwave vial (10–20 mL recommended volume) was charged with 4-chloroquinoline-8-amine (1.00 g, 5.60 mmol), KOH (powder, 785 mg, 14.0 mmol) and anhydrous DMF (4.3 mL, 56.0 mmol). The reaction vessel was sealed, placed in a preheated oil bath and stirred at 100 ºC for 24 h under air atmosphere. The reaction was then allowed to cool down and then was diluted with EtOAc (10 mL) and H_2O (10 mL). The phases were separated, and the aqueous layer was extracted with EtOAc (4 × 15 mL). The combined organic extracts were dried over Na_2SO_4 and filtered. The solvent was removed under reduced pressure to afford the crude N^4,N^4-dimethylquinoline-4,8-diamine **117**, which was used in the next step without any further purification. For full characterisation of N^4,N^4-dimethylquinoline-4,8-diamine **117**, see page 358.

EDC·HCl (1.30 g, 6.70 mmol) was added to a solution of *N*-Boc-piperidine-3-carboxylic acid **22** (1.50 g, 6.70 mmol), and the crude **117** in anhydrous CH_2Cl_2 (28 mL, 0.2 M) at 0 °C. DMAP (249 mg, 1.10 mmol) was then added and the solution was stirred at 25 °C for 24 h. The reaction was diluted with CH_2Cl_2 (30 mL), then a solution of sat. aq. $NaHCO_3$ (30 mL) was added and the aqueous layer was extracted with CH_2Cl_2 (3 × 40 mL). The combined organic extracts were dried over Na_2SO_4 and filtered. The solvent was removed under reduced pressure. The crude reaction was purified by flash column chromatography (5% to 10% MeCN/CH_2Cl_2), the product containing fractions were combined and the solvent was removed under reduced pressure. Et_2O (15 mL) and pentane (15 mL) were added and the solvent was removed under reduced pressure to afford amide **133** as a white solid (1.45 g, 65% over 2 steps). R_f 0.51 (15% MeCN/CH_2Cl_2); mp = 106–109 °C (from Et_2O/pentane); ν_{max} (film)/cm^{-1} 3295 (NH), 2937, 2855, 1677 (C=O), 1525, 1413, 1241, 1137, 947, 764; ^{1}H NMR (500 MHz, DMSO-d_6, 373 K) δ 10.07 (br s, 1 H, NH), 8.58 (d, J = 5.1 Hz, 1 H, HC_{Ar}), 8.52 (d, J = 7.6 Hz, 1 H, HC_{Ar}), 7.76 (d, J = 8.6 Hz, 1 H, HC_{Ar}), 7.42 (t, J = 8.1 Hz, 1 H, HC_{Ar}), 6.93 (d, J = 5.2 Hz, 1 H, HC_{Ar}), 4.10 (dd, J = 13.1, 3.9 Hz, 1 H, NC*H*HCHCO), 3.84 (ddd, J = 13.3, 3.5, 3.5 Hz, 1 H, NC*H*HCH$_2$), 3.11–3.06 (m, 1 H, NCH*H*CHCO), 3.05 (s, 6 H, N(CH$_3$)$_2$), 2.89 (ddd, J = 13.5, 11.4, 2.9 Hz, 1 H, NCH*H*CH$_2$), 2.72 (dddd, J = 10.2, 10.2, 4.0, 4.0 Hz, 1 H, CHCO), 2.11–2.03 (m, 1 H, N(CH$_2$)$_2$C*H*H), 1.80–1.70 (m, 2 H, N(CH$_2$)$_2$CH*H*, NCH$_2$C*H*H), 1.57–1.45 (m, 1 H,

$NCH_2CH\mathit{H}$), 1.43 (s, 9 H, $C(CH_3)_3$); ^{13}C NMR (126 MHz, DMSO-d_6, 373 K) δ 170.8 (C=O amide), 156.8 ($N(CH_3)_2\mathit{C}_{Ar}$ quat), 153.5 (C=O carbamate), 147.9 (C_{Ar}), 139.3 (C_{Ar} quat), 134.1 (C_{Ar} quat), 123.7 (C_{Ar}), 121.4 (C_{Ar} quat), 118.0 (C_{Ar}), 115.3 (C_{Ar}), 107.1 (C_{Ar}), 78.2 ($\mathit{C}(CH_3)_3$), 45.7 ($N\mathit{C}H_2CHCO$), 43.2 ($N\mathit{C}H_2CH_2$), 43.0 ($N(CH_3)_2$), 42.9 ($\mathit{C}HCO$), 27.6 ($C(\mathit{C}H_3)_3$), 26.8 ($N(CH_2)_2\mathit{C}H_2$), 23.3 ($NCH_2\mathit{C}H_2$); HRMS (ESI^+) *m*/*z* Calculated for $C_{22}H_{31}N_4O_3$ [M+H] 399.2396; Found 399.2389.

8.2.5.10 ***General procedure D*** *for C–H arylation of N-protected piperidines with DMAQ directing group.*

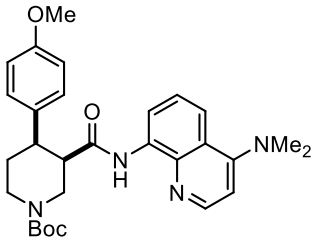


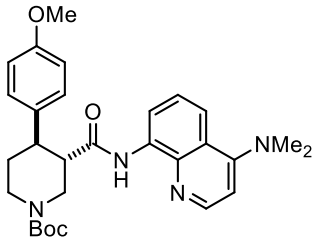
133 **134a–d** **135**

A reaction vial was charged with K_2CO_3 (27.7 mg, 0.20 mmol), flame-dried, and allowed to cool under argon. *tert*-Butyl (±)-3-((4-dimethylamino-8-yl)carbamoyl)piperidine-1-carboxylate **133** (79.7 mg, 0.20 mmol), the requisite aryl iodide (0.60 mmol), $Pd(OAc)_2$ (2.2 mg, 10.0 μmol) and PivOH (20.5 mg, 0.20 mmol) were added sequentially. The reaction vessel was sealed and purged with argon, then $PhCF_3$ (200 μL, 1.0 M) was added by syringe. The reaction tube was placed in a preheated oil bath and stirred at 90 ºC for 18 h. The reaction mixture was then allowed to cool to rt and EtOAc (5 mL) was added. The resulting mixture was filtered through a pad of Celite, eluting with further EtOAc (3 × 5 mL). The solvent was removed under reduced pressure, and the crude material was purified by flash column chromatography under the specified conditions, separating the 2 diastereomeric products. The products containing fractions were combined and the solvent was removed under reduced pressure. Et_2O (3 mL) and pentane (3 mL) were added and the solvent was removed under reduced pressure to afford the arylated derivatives.

*8.2.5.11 Synthesis of piperidine amides **134a–d** and **135** with DMAQ directing group*

tert-Butyl _cis_-(±)-3-((4-(dimethylamino)quinolin-8-yl)carbamoyl)-4-(4-methoxyphenyl) piperidine-1-carboxylate (134a) and **_tert_-butyl _trans_-(±)-3-((4-(dimethylamino)quinolin-8-yl)carbamoyl)-4-(4-methoxyphenyl)piperidine-1-carboxylate (135)**





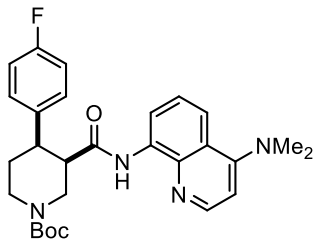
Prepared according to **General Procedure D** using 4-iodoanisole (140 mg). Purification by flash column chromatography (10% to 15% acetone/pentane) afforded the minor product *tert*-butyl *trans*-(±)-3-((4-(dimethylamino)quinolin-8-yl)carbamoyl)-4-(4-methoxyphenyl)piperidine-1-carboxylate **135** as a white solid (13.4 mg, 13%) followed by the major product *tert*-butyl *cis*-(±)-3-((4-(dimethylamino)quinolin-8-yl)carbamoyl)-4-(4-methoxyphenyl)piperidine-1-carboxylate **134a** as a white solid (71.5 mg, 71%).

Major (**134a**): R_f 0.39 (20% acetone/pentane); mp = 87–91 °C (from Et_2O/pentane); ν_{max} (film)/cm^{-1} 3336 (NH), 2926, 1685 (C=O), 1521, 1413, 1305, 1245, 1163, 1118, 813, 764; ^{1}H NMR (400 MHz, DMSO-d_6, 373 K) δ 9.80 (br s, 1 H, NH), 8.50 (d, J = 5.2 Hz, 1 H, HC_{Ar}), 8.38 (d, J = 7.6 Hz, 1 H, HC_{Ar}), 7.68 (dd, J = 8.6, 1.3 Hz, 1 H, HC_{Ar}), 7.35 (dd, J = 8.6, 7.7 Hz, 1 H, HC_{Ar}), 7.27–7.20 (m, 2 H, HC_{Ar}), 6.89 (d, J = 5.2 Hz, 1 H, HC_{Ar}), 6.79–6.73 (m, 2 H, HC_{Ar}), 4.37 (ddd, J = 13.8, 2.1, 2.1 Hz, 1 H, NC*H*HCHCO), 4.23 (dddd, J = 13.1, 4.6, 2.6, 2.6 Hz, 1 H, NC*H*HCH$_2$), 3.64 (s, 3 H, OCH_3), 3.31 (dd, J = 13.7, 3.8 Hz, 1 H, NCH*H*CHCO), 3.16 (ddd, J = 3.8, 3.8, 3.8 Hz, 1 H, CHCO), 3.10 (ddd, J = 12.5, 4.5, 4.5 Hz, 1 H, CHAr), 3.06–2.90 (m, 7 H, N(CH_3)$_2$, NCH*H*CH$_2$), 2.68 (dddd, J = 12.3, 12.3, 12.3, 4.6 Hz, 1 H, NCH$_2$C*H*H), 1.69 (dddd, J = 12.6, 3.0, 3.0, 3.0 Hz, 1 H, NCH$_2$CH*H*), 1.27 (s, 9 H, C(CH_3)$_3$); ^{13}C NMR (101 MHz, DMSO-d_6, 373 K) δ 169.9 (C=O amide), 157.3 (OC_{Ar} quat), 156.8 (N(CH_3)$_2$*C*$_{Ar}$ quat), 153.4 (C=O carbamate), 147.5 (weak, C_{Ar}), 139.0 (C_{Ar} quat), 134.6 (C_{Ar} quat), 134.3 (C_{Ar} quat), 127.8 (2 × C_{Ar}), 123.7 (C_{Ar}), 121.3 (C_{Ar} quat), 117.5 (C_{Ar}), 114.9 (weak, C_{Ar}), 113.2 (2 × C_{Ar}), 106.9 (C_{Ar}), 77.9 (*C*(CH_3)$_3$), 54.5 (OCH_3), 46.24 (*C*HCO), 46.19 (br and weak, N*C*H$_2$CHCO), 43.1 (br and weak, N*C*H$_2$CH$_2$), 43.0 (N(CH_3)$_2$), 41.6 (CHAr), 27.4 (C(*C*H$_3$)$_3$), 25.6 (NCH$_2$*C*H$_2$); HRMS (ESI$^+$) m/z Calculated for $C_{29}H_{37}N_4O_4$ [M+H] 505.2815; Found 505.2813.

Minor (**135**): R_f 0.51 (20% acetone/pentane); mp = 80–84 °C (from Et_2O/pentane); ν_{max} (film)/cm^{-1} 3325 (NH), 2933, 1685 (C=O), 1525, 1413, 1230, 1159, 1036, 813, 764; ^{1}H NMR (400 MHz, DMSO-d_6, 373 K) δ 9.77 (br s, 1 H, NH), 8.51 (d, J = 5.2 Hz, 1 H, HC_{Ar}), 8.32 (dd, J = 7.7, 1.3 Hz, 1 H, HC_{Ar}), 7.69 (dd, J = 8.6, 1.3 Hz, 1 H, HC_{Ar}), 7.33 (dd, J = 8.6, 7.7 Hz, 1 H, HC_{Ar}), 7.25–7.20 (m, 2 H, HC_{Ar}), 6.89 (d, J = 5.2 Hz, 1 H, HC_{Ar}), 6.77–6.71 (m, 2 H, HC_{Ar}), 4.31

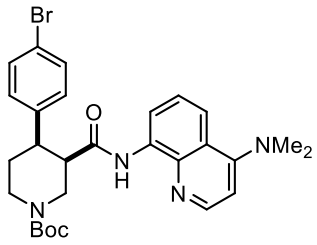
(ddd, *J* = 12.5, 3.5, 1.7 Hz, 1 H, NC*H*HCHCO), 4.10 (dddd, *J* = 13.3, 4.1, 1.9, 1.9 Hz, 1 H, NC*H*HCH$_2$), 3.60 (s, 3 H, OCH$_3$), 3.08–2.87 (m, 10 H, N(CH$_3$)$_2$, NCH*H*CHCO, CHCO, CHAr, NCH*H*CH$_2$), 1.77 (dddd, *J* = 13.5, 3.0, 3.0, 3.0 Hz, 1 H, NCH$_2$C*H*H), 1.64 (dddd, *J* = 12.6, 12.6, 12.6, 4.4 Hz, 1 H, NCH$_2$CH*H*), 1.47 (s, 9 H, C(CH$_3$)$_3$); ^{13}C NMR (101 MHz, DMSO-d_6, 373 K) δ 169.7 (C=O amide), 157.5 (OC$_{Ar}$ quat), 156.7 (N(CH$_3$)$_2$*C*$_{Ar}$ quat), 153.4 (C=O carbamate), 147.8 (C$_{Ar}$), 139.1 (C$_{Ar}$ quat), 135.0 (C$_{Ar}$ quat), 133.8 (C$_{Ar}$ quat), 127.7 (2 × C$_{Ar}$), 123.6 (C$_{Ar}$), 121.3 (C$_{Ar}$ quat), 118.0 (C$_{Ar}$), 115.2 (C$_{Ar}$), 113.5 (2 × C$_{Ar}$), 107.0 (C$_{Ar}$), 78.5 (*C*(CH$_3$)$_3$), 54.5 (OCH$_3$), 50.1 (*C*HCO), 46.4 (N*C*H$_2$CHCO), 43.5 (N*C*H$_2$CH$_2$, CHAr), 42.9 (N(CH$_3$)$_2$), 32.4 (NCH$_2$*C*H$_2$), 27.7 (C(*C*H$_3$)$_3$); HRMS (ESI$^+$) *m*/*z* Calculated for C$_{29}$H$_{37}$N$_4$O$_4$ [M+H] 505.2815; Found 505.2805.

tert-Butyl _cis_-(±)-3-((4-(dimethylamino)quinolin-8-yl)carbamoyl)-4-(4-fluorophenyl) piperidine-1-carboxylate (134b)



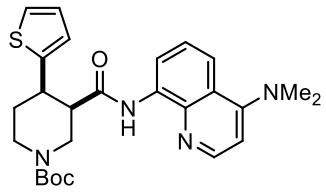
Prepared according to **General Procedure D** using 1-fluoro-4-iodobenzene (133 mg). Purification by flash column chromatography (15% acetone/pentane) afforded *tert*-butyl *cis*-(±)-3-((4-(dimethylamino)quinolin-8-yl)carbamoyl)-4-(4-fluorophenyl)piperidine-1-carboxylate **134b** as a white solid (63.2 mg, 64%). R_f 0.29 (20% acetone/pentane); mp = 79–83 °C (from Et$_2$O/pentane); ν_{max} (film)/cm^{-1} 3332 (NH), 2922, 1685 (C=O), 1521, 1413, 1305, 1223, 1163, 1010, 835, 760; ^{1}H NMR (500 MHz, DMSO-d_6, 373 K) δ 9.81 (br s, 1 H, NH), 8.50 (d, *J* = 5.1 Hz, 1 H, HC$_{Ar}$), 8.37 (dd, *J* = 7.7, 1.3 Hz, 1 H, HC$_{Ar}$), 7.68 (dd, *J* = 8.6, 1.3 Hz, 1 H, HC$_{Ar}$), 7.39–7.31 (m, 3 H, HC$_{Ar}$), 7.02–6.94 (m, 2 H, HC$_{Ar}$), 6.89 (d, *J* = 5.2 Hz, 1 H, HC$_{Ar}$), 4.39 (ddd, *J* = 13.8, 2.1, 2.1 Hz, 1 H, NC*H*HCHCO), 4.25 (dddd, *J* = 13.1, 4.5, 2.3, 2.3 Hz, 1 H, NC*H*HCH$_2$), 3.31 (dd, *J* = 13.8, 3.9 Hz, 1 H, NCH*H*CHCO), 3.22 (ddd, *J* = 3.9, 3.9, 3.9 Hz, 1 H, CHCO), 3.16 (ddd, *J* = 12.3, 4.3, 4.3 Hz, 1 H, CHAr), 3.02 (s, 6 H, N(CH$_3$)$_2$), 3.00–2.92 (m, 1 H, NCH*H*CH$_2$), 2.70 (dddd, *J* = 12.3, 12.3, 12.3, 4.7, 1 H, NCH$_2$C*H*H), 1.71 (dddd, *J* = 12.8, 3.1, 3.1, 3.1 Hz, 1 H, NCH$_2$CH*H*), 1.27 (s, 9 H, C(CH$_3$)$_3$); ^{13}C NMR (126 MHz, DMSO-d_6, 373 K) δ 169.7 (C=O amide), 160.3 (d, J_{CF} = 243 Hz, FC$_{Ar}$ quat), 156.7 (N(CH$_3$)$_2$*C*$_{Ar}$ quat), 153.4 (C=O carbamate), 147.7 (C$_{Ar}$), 139.1 (C$_{Ar}$ quat), 138.7 (d, J_{CF} = 3.2 Hz, F-*p*-C$_{Ar}$ quat), 134.3 (C$_{Ar}$ quat), 128.6 (d, J_{CF} = 7.8 Hz, 2 × F-*m*-C$_{Ar}$), 123.6 (C$_{Ar}$), 121.3 (C$_{Ar}$ quat), 117.5 (C$_{Ar}$), 114.9 (C$_{Ar}$), 114.0 (d, J_{CF} = 20.8 Hz, 2 × F-*o*-C$_{Ar}$), 107.0 (C$_{Ar}$), 77.9 (*C*(CH$_3$)$_3$), 46.2 (br and weak, N*C*H$_2$CHCO), 46.0 (*C*HCO), 43.0 (br and weak, N*C*H$_2$CH$_2$), 42.9 (N(CH$_3$)$_2$), 41.6 (CHAr), 27.4 (C(*C*H$_3$)$_3$), 25.4 (NCH$_2$*C*H$_2$); ^{19}F NMR (471 MHz, DMSO-d_6, 373 K) δ –117.2 (ddd, J_{HF} = 14.5, 9.2, 5.5 Hz); HRMS (ESI$^+$) *m*/*z* Calculated for C$_{28}$H$_{34}$N$_4$O$_3$F [M+H] 493.2615; Found 493.2606.

***tert*-Butyl *cis*-(±)-4-(4-bromophenyl)-3-((4-(dimethylamino)quinolin-8-yl)carbamoyl) piperidine-1-carboxylate (134c)**



Prepared according to **General Procedure D** using 1-bromo-4-iodobenzene (170 mg). Purification by flash column chromatography (10% acetone/pentane) afforded *tert*-butyl *cis*-(±)-4-(4-bromophenyl)-3-((4-(dimethylamino)quinolin-8-yl)carbamoyl)piperidine-1-carboxylate **134c** as a white solid (64.6 mg, 58%). R_f 0.16 (10% acetone/pentane); mp = 96–100 °C (from Et_2O/pentane); ν_{max} (film)/cm^{-1} 3325 (NH), 2855, 1685 (C=O), 1521, 1413, 1305, 1241, 1163, 1118, 1006, 813, 760; ^{1}H NMR (500 MHz, DMSO-d_6, 373 K) δ 9.83 (br s, 1 H, NH), 8.51 (d, J = 5.1 Hz, 1 H, HC_{Ar}), 8.36 (dd, J = 7.6, 1.3 Hz, 1 H, HC_{Ar}), 7.69 (dd, J = 8.6, 1.3 Hz, 1 H, HC_{Ar}), 7.39–7.31 (m, 3 H, HC_{Ar}), 7.31–7.27 (m, 2 H, HC_{Ar}), 6.90 (d, J = 5.2 Hz, 1 H, HC_{Ar}), 4.39 (ddd, J = 13.8, 2.5, 1.8 Hz, 1 H, NC*H*HCHCO), 4.24 (dddd, J = 12.9, 4.3, 2.3, 2.3 Hz, 1 H, NC*H*HCH$_2$), 3.32 (dd, J = 13.8, 3.9 Hz, 1 H, NCH*H*CHCO), 3.24 (ddd, J = 4.0, 4.0, 4.0 Hz, 1 H, CHCO), 3.14 (ddd, J = 12.3, 4.3, 4.3 Hz, 1 H, CHAr), 3.03 (s, 6 H, N(CH$_3$)$_2$), 3.00–2.92 (m, 1 H, NCH*H*CH$_2$), 2.69 (dddd, J = 12.4, 12.4, 12.4, 4.7, 1 H, NCH$_2$C*H*H), 1.71 (dddd, J = 13.1, 3.4, 3.4, 3.4 Hz, 1 H, NCH$_2$CH*H*), 1.26 (s, 9 H, C(CH$_3$)$_3$); ^{13}C NMR (126 MHz, DMSO-d_6, 373 K) δ 169.6 (C=O amide), 156.7 (N(CH$_3$)$_2$*C*$_{Ar}$ quat), 153.4 (C=O carbamate), 147.7 (C_{Ar}), 142.0 (C_{Ar} quat), 139.1 (C_{Ar} quat), 134.2 (C_{Ar} quat), 130.3 (2 × C_{Ar}), 129.1 (2 × C_{Ar}), 123.6 (C_{Ar}), 121.3 (C_{Ar} quat), 118.7 (BrC_{Ar} quat), 117.6 (C_{Ar}), 115.0 (C_{Ar}), 107.0 (C_{Ar}), 77.9 (*C*(CH$_3$)$_3$), 46.2 (br and weak, N*C*H$_2$CHCO), 45.8 (*C*HCO), 42.9 (N*C*H$_2$CH$_2$ and N(CH$_3$)$_2$), 41.7 (CHAr), 27.4 (C(*C*H$_3$)$_3$), 25.1 (NCH$_2$*C*H$_2$); HRMS (ESI$^+$) *m*/*z* Calculated for $C_{28}H_{34}N_4O_3{}^{79}Br$ [M+H] 553.1814; Found 553.1794.

***tert*-Butyl *cis*-(±)-3-((4-(dimethylamino)quinolin-8-yl)carbamoyl)-4-(thiophen-2-yl) piperidine-1-carboxylate (134d)**

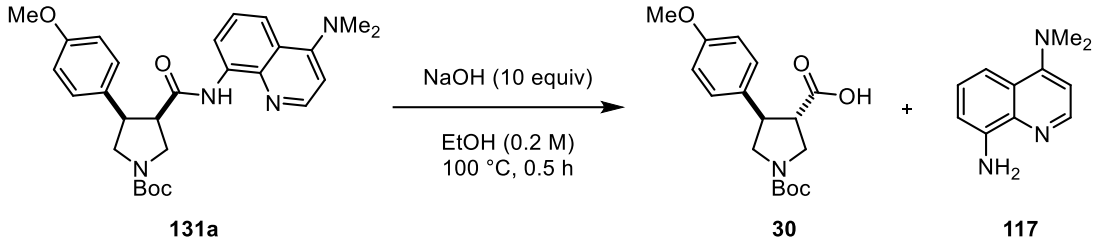


Prepared according to **General Procedure D** using 2-iodothiophene (126 mg). Purification by flash column chromatography (10% acetone/pentane) afforded *tert*-butyl *cis*-(±)-3-((4-(dimethylamino)quinolin-8-yl)carbamoyl)-4-(thiophen-2-yl)piperidine-1-carboxylate **134d** as a white solid (50.5 mg, 53%). R_f 0.14 (10% acetone/pentane); mp = 86–90 °C (from Et_2O/pentane); ν_{max} (film)/cm^{-1} 3332 (NH), 2974, 1685 (C=O), 1521, 1413, 1305, 1245, 1163, 813, 760, 693; ^{1}H NMR (400 MHz, DMSO-d_6, 373 K) δ 10.00 (br s, 1 H, NH), 8.55 (d, J = 5.1 Hz, 1 H, HC_{Ar}), 8.42 (dd, J = 7.7, 1.3 Hz, 1 H, HC_{Ar}), 7.70 (dd, J = 8.6, 1.3 Hz, 1 H, HC_{Ar}), 7.36 (dd, J = 8.6, 7.7 Hz, 1 H, HC_{Ar}), 7.21 (dd, J = 5.1, 1.2 Hz, 1 H, SCH), 6.97–6.94 (m, 1 H, SCHCHC*H*), 6.91 (d, J = 5.2 Hz, 1 H,

HC_{Ar}), 6.86 (dd, *J* = 5.1, 3.5 Hz, 1 H, SCHC*H*), 4.23 (ddd, *J* = 13.8, 3.8, 1.5 Hz, 1 H, NC*H*HCHCO), 4.06 (dddd, *J* = 13.4, 4.2, 4.2, 1.3 Hz, 1 H, NC*H*HCH_2), 3.53 (ddd, *J* = 11.0, 4.3, 4.3 Hz, 1 H, CHAr), 3.43 (dd, *J* = 13.8, 3.9 Hz, 1 H, NCH*H*CHCO), 3.26 (ddd, *J* = 4.1, 4.1, 4.1 Hz, 1 H, CHCO), 3.11 (ddd, *J* = 13.7, 10.8, 3.5 Hz, 1 H, NCH*H*CH_2), 3.03 (s, 6 H, $N(CH_3)_2$), 2.61 (dddd, *J* = 13.0, 10.8, 10.8, 4.5, 1 H, NCH_2C*H*H), 1.87 (dddd, *J* = 12.5, 3.9, 3.9, 3.9 Hz, 1 H, NCH_2CH*H*), 1.27 (s, 9 H, $C(CH_3)_3$); ^{13}C NMR (101 MHz, DMSO-d_6, 373 K) δ 169.5 (C=O amide), 156.8 ($N(CH_3)_2C_{Ar}$ quat), 153.4 (C=O carbamate), 147.8 (C_{Ar}), 145.8 (SC_{Ar} quat), 139.2 (C_{Ar} quat), 134.4 (C_{Ar} quat), 125.9 (SCH*C*H_{Ar}), 123.7 (C_{Ar}), 123.5 (SCHCH*C*H_{Ar}), 122.9 (SCH_{Ar}), 121.4 (C_{Ar} quat), 117.6 (C_{Ar}), 115.1 (C_{Ar}), 107.0 (C_{Ar}), 78.0 (*C*$(CH_3)_3$), 46.2 (*C*HCO), 45.3 (br and weak, N*C*H_2CHCO), 43.0 ($N(CH_3)_2$), 42.3 (N*C*H_2CH_2), 38.0 (CHAr), 27.8 (NCH_2*C*H_2), 27.4 (C(*C*$H_3)_3$); HRMS (ESI$^+$) *m*/*z* Calculated for $C_{26}H_{33}N_4O_3S$ [M+H] 481.2273; Found 481.2267.

*8.2.5.12 Removal of DMAQ directing group (**117**, **136**)*

***N*⁴,*N*⁴-dimethylquinoline-4,8-diamine (117)** and ***trans*-(±)-1-(*tert*-Butoxycarbonyl)-4-(4-methoxyphenyl)pyrrolidine-3-carboxylic acid (30)**



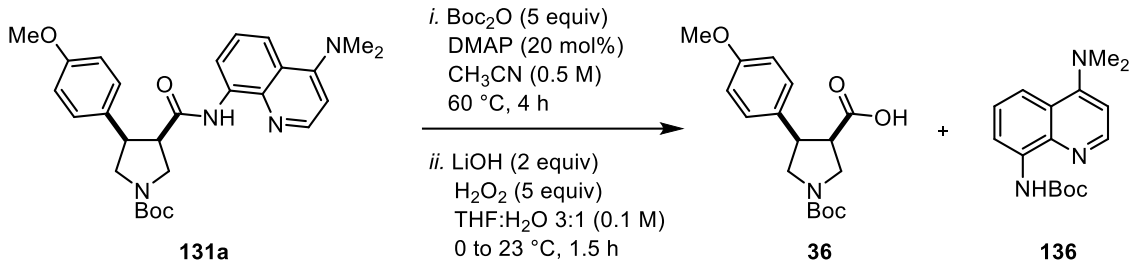
131a **30** **117**

A reaction tube was charged with amide **131a** (50.2 mg, 0.10 mmol), followed by NaOH (41.0 mg, 1.00 mmol). The reaction vessel was sealed and EtOH (500 μL, 0.2 M) was added by syringe. The reaction tube was then placed in a preheated oil bath and stirred at 100 ºC for 30 min. The reaction mixture was then allowed to cool down to rt and diluted with EtOAc (1 mL) and 1 N NaOH (1 mL). The aqueous alkaline layer was collected, and the organic layer extracted with 1 N NaOH (3 × 3 mL). The aqueous alkaline layers were combined, washed with EtOAc (5 mL), and acidified to pH ~1 with HCl, 37%. The organic portions were combined, dried over Na_2SO_4 and filtered. The solvent was removed under reduced pressure. Purification by flash column chromatography (3% MeOH/CH_2Cl_2) afforded *N*⁴,*N*⁴-dimethylquinoline-4,8-diamine **117** as a brown oil (15.2 mg, 81%). In parallel, the acidic layer was extracted with EtOAc (5 × 10 mL). The combined organic extracts were dried over Na_2SO_4 and filtered. Solvent was removed under reduced pressure. Et_2O (3 mL) and pentane (3 mL) were added and the solvent was removed under reduced pressure to afford the pure *trans*-acid **30** as a white solid (27.3 mg, 85%).

*N*⁴,*N*⁴-Dimethylquinoline-4,8-diamine (**117**): R_f 0.14 (4% MeOH/CH_2Cl_2); ν_{max} (film)/cm^{-1} 3452 (NH), 3325 (NH), 2840, 1569, 1513, 1398, 1312, 1137, 1051, 969, 809, 753; ^{1}H NMR (400 MHz, $CDCl_3$, 298 K) δ 8.58 (d, *J* = 5.1 Hz, 1 H, HC_{Ar}), 7.41 (dd, *J* = 8.5, 1.3 Hz, 1 H, HC_{Ar}), 7.30 (dd, *J* = 7.2, 1.3 Hz, 1 H, HC_{Ar}), 6.92 (dd, *J* = 7.4, 1.3 Hz, 1 H, HC_{Ar}), 6.80 (d, *J* = 5.1 Hz, 1 H, HC_{Ar}), 4.89 (br s, 2 H, NH_2), 3.06 (s, 6 H, $N(CH_3)_2$);^{13}C NMR (101 MHz, $CDCl_3$, 298 K) δ 157.6 ($N(CH_3)_2C_{Ar}$ quat), 147.4 (C_{Ar}), 144.3 (NH_2C_{Ar} quat), 139.6 (C_{Ar} quat), 125.3 (C_{Ar}), 123.4 (C_{Ar} quat), 112.9 (C_{Ar}), 109.8 (C_{Ar}), 107.7 (C_{Ar}), 43.8 ($N(CH_3)_2$); HRMS (ESI$^+$) *m*/*z* Calculated for $C_{11}H_{14}N_3$ [M+H] 188.1188; Found 188.1183.

trans-Acid (**30**): The observed characterisation data was identical to what previously reported for pyrrolidine **30** (page 253).

***tert*-Butyl (4-(dimethylamino)quinolin-8-yl)carbamate (136)** and ***cis*-(±)-1-(*tert*-Butoxycarbonyl)-4-(4-methoxyphenyl)pyrrolidine-3-carboxylic acid (36)**



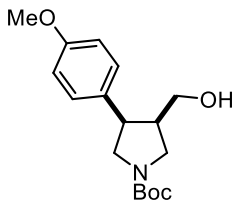
A flame-dried reaction tube was charged with amide **131a** (86.2 mg, 0.18 mmol), followed by Boc_2O (218 mg, 1.00 mmol) and DMAP (5.1 mg, 40.0 μmol). The reaction vessel was sealed and purged with argon, then MeCN (400 μL, 0.5 M) was added by syringe. The reaction tube was then placed in an oil bath and gradually warm up to 60 ºC. The reaction mixture was then stirred at 60 °C for 4 h. The reaction mixture was then allowed to cool to rt and sat. aq. NH_4Cl (1 mL) and CH_2Cl_2 (1 mL) were added. The phases were separated, and the aqueous layer was extracted with CH_2Cl_2 (3 × 5 mL). The combined organic extracts were dried over Na_2SO_4 and filtered. The solvent was removed under reduced pressure to afford the crude *N*-Boc protected pyrrolidine derivative, which was used in the next step without further purification. A solution of H_2O_2 (102 μL, 1.00 mmol, 30 wt.% in H_2O) in THF (500 μL) was added to a solution of $LiOH·H_2O$ (16.8 mg, 0.40 mmol) in H_2O (500 μL) at 0 °C under argon. The resulting mixture was added dropwise to a solution of crude *N*-Boc protected pyrrolidine in THF (1.0 mL) at 0 °C under argon. The reaction was then stirred at 25 °C for 1.5 h. Sat. aq. $Na_2S_2O_3$ (3 mL), EtOAc (5 mL) and 1 N NaOH (5 mL) were then added. The aqueous alkaline layer was collected, and the organic layer extracted with 1 N NaOH (3 × 5 mL). The aqueous alkaline layers were combined, washed with EtOAc (15 mL), and acidified to pH ~1 with HCl, 37%. The organic portions were combined, dried over Na_2SO_4 and filtered. The solvent was removed under reduced pressure. Purification by flash column chromatography (5% Et_2O/pentane) afforded *tert*-butyl (4-(dimethylamino)quinolin-8-yl)carbamate **136** as a white solid (35.8 mg, 71% over 2 steps). In parallel, the acidic layer was extracted with EtOAc (5 × 20 mL). The combined organic extracts were dried over Na_2SO_4 and filtered. Solvent was removed under reduced pressure. Et_2O (5 mL) and pentane (5 mL) were added and the solvent was removed under reduced pressure to afford the pure *cis*-acid **36** as a white solid (45.6 mg, 81% over 2 steps).

tert-Butyl (4-(dimethylamino)quinolin-8-yl)carbamate (**136**): R_f 0.28 (10% Et_2O/pentane); ν_{max} (film)/cm^{-1} 3325 (NH), 2978, 1715 (C=O), 1528, 1416, 1148, 1051, 965, 797, 760, 686; ^1H NMR (400 MHz, $CDCl_3$, 298 K) δ 9.13 (br s, 1 H, NH), 8.54 (d, *J* = 5.1 Hz, 1 H, HC_{Ar}), 8.35 (d, *J* = 7.7 Hz, 1 H, HC_{Ar}), 7.64 (dd, *J* = 8.6, 1.3 Hz, 1 H, HC_{Ar}), 7.41 (t, *J* = 8.1 Hz, 1 H, HC_{Ar}),

6.78 (d, *J* = 5.1 Hz, 1 H, HC_{Ar}), 3.04 (s, 6 H, $N(CH_3)_2$), 1.58 (s, 9 H, $C(CH_3)_3$); ^{13}C NMR (101 MHz, $CDCl_3$, 298 K) δ 157.7 ($N(CH_3)_2C_{Ar}$ quat), 153.0 (C=O), 148.0 (C_{Ar}), 139.6 (C_{Ar} quat), 135.5 (NHC_{Ar} quat), 125.0 (C_{Ar}), 122.5 (C_{Ar} quat), 117.0 (C_{Ar}), 113.9 (C_{Ar}), 107.7 (C_{Ar}), 80.1 ($C(CH_3)_3$), 43.9 ($N(CH_3)_2$), 28.4 ($C(CH_3)_3$); HRMS (ESI^+) *m*/*z* Calculated for $C_{16}H_{22}N_3O_2$ [M+H] 288.1712; Found 288.1709.

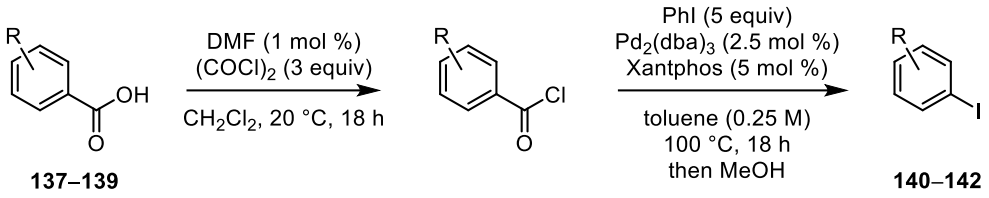
cis-acid **36**: The observed characterisation data was identical to what previously reported for pyrrolidine **36** (page 257).

***tert*-Butyl *cis*-(±)-3-(hydroxymethyl)-4-(4-methoxyphenyl)pyrrolidine-1-carboxylate (37)**



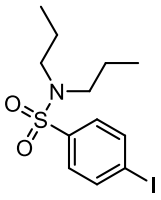
A flame-dried reaction tube was charged with amide **131a** (98.1 mg, 0.20 mmol), followed by Boc_2O (218 mg, 1.00 mmol) and DMAP (48.9 mg, 0.40 mmol). The reaction vessel was sealed and purged with argon, then MeCN (400 μL, 0.5 M) was added by syringe. The reaction tube was then placed in an oil bath and gradually warm up to 55 ºC. The reaction mixture was then stirred at 55 °C for 1 h. The reaction mixture was then allowed to cool to rt and sat. aq. NH_4Cl (1 mL) and CH_2Cl_2 (1 mL) were added. The phases were separated, and the aqueous layer was extracted with CH_2Cl_2 (3 × 5 mL). The combined organic extracts were dried over Na_2SO_4 and filtered. The solvent was removed under reduced pressure to afford the crude *N*-Boc protected pyrrolidine derivative, which was used in the next step without further purification. This was solubilised in dry THF (700 μL) and the resulting solution was added dropwise to a suspension of $LiAlH_4$ (40.4 mg, 0.80 mmol) in dry THF (600 μL) at 0 °C under argon atmosphere. The mixture was then stirred at 20 °C for 30 min. The reaction mixture was quenched by slow addition of sat. aq. NH_4Cl (1 mL) at 0 °C and stirred at rt for 30 min. The resulting suspension was filtered through a pad of Celite, eluting with EtOAc (3 × 3 mL). The phases were separated, and the aqueous layer was extracted with EtOAc (3 × 3 mL). The combined organic extracts were dried over Na_2SO_4 and filtered. The solvent was removed under reduced pressure. Purification by flash column chromatography (20% acetone/pentane) afforded primary alcohol **37** as a colourless paste (42.7 mg, 69%, single diastereoisomer). The observed characterisation data was identical to what previously reported for pyrrolidine **37** (page 258).

*8.2.5.13 Late-stage functionalisation of acid-containing drugs: aryl iodides **140–142***



137–139 **140–142**

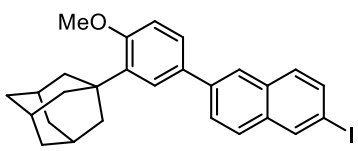
4-Iodo-*N*,*N*-dipropylbenzenesulfonamide (140)



Adapting Morandi's procedure,[282] a flame-dried round bottom flask was charged with Probenecid **137** (571 mg, 2.00 mmol), anhydrous CH_2Cl_2 (6.0 mL, 0.3 M) and DMF (2 μL, 0.03 mmol). The flask was sealed and purged with argon. Oxalyl chloride (500 μL, 6.00 mmol) was added dropwise using a syringe. The resulting mixture was stirred at 20 °C for 18 h. The reaction was then concentrated under reduced pressure to afford the corresponding benzoyl chloride (607 mg, quant.), which was used in the next step without further purification. A flame-dried microwave vial (10–20 mL recommended volume) was charged with $Pd_2(dba)_3$ (31.4 mg, 34.3 μmol), Xantphos (39.6 mg, 68.4 μmol) and Probenecid benzoyl chloride (417 mg, 1.37 mmol). The reaction vessel was sealed, and then evacuated and refilled with nitrogen three times. A solution of iodobenzene (1.40 g, 6.85 mmol) in anhydrous toluene (6.8 mL, 1.0 M) was degassed bubbling a stream of nitrogen for 5 min, then added to the reaction vessel by syringe. The reaction tube was placed in a preheated oil bath and stirred at 100 ºC for 18 h. The reaction mixture was then allowed to cool to rt and transferred to a round-bottom flask. CH_2Cl_2 (10 mL) and MeOH (5 mL) were added and the reaction stirred at 45 °C for 30 min. The mixture was allowed to cool to rt and filtered through a pad of silica, eluting with further CH_2Cl_2 (3 × 5 mL). The solvent was removed under reduced pressure. Purification by flash column chromatography (5% Et_2O/pentane) afforded aryl iodide **140** as a white solid (395 mg, 79% over 2 steps). R_f 0.27 (5% Et_2O/pentane); mp = 77–79 °C (from Et_2O/pentane); ν_{max} (film)/cm^{-1} 3803, 2960, 1874, 1469, 1379, 1327, 1163, 1088, 988, 865, 775, 716; ^{1}H NMR (400 MHz, $CDCl_3$, 298 K) δ 7.88–7.83 (m, 2 H, HC_{Ar}), 7.55–7.49 (m, 2 H, HC_{Ar}), 3.11–3.03 (m, 4 H, 2 × NCH_2), 1.61–1.50 (m, 4 H, 2 × NCH_2CH_2), 0.88 (t, *J* = 7.4 Hz, 6 H, 2 × CH_3); ^{13}C NMR (101 MHz, $CDCl_3$, 298 K) δ 139.9 (SC_{Ar} quat), 138.2 (2 × C_{Ar}), 128.4 (2 × C_{Ar}), 99.4 (IC_{Ar} quat), 50.0 (2 × NCH_2), 22.0 (2 × NCH_2CH_2), 11.2 (2 × CH_3).

Spectroscopic data (^{1}H and ^{13}C NMR) is consistent with what described in the literature.[282]

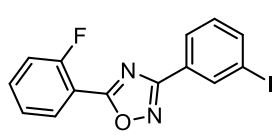
(3r,5r,7r)-1-(5-(6-Iodonaphthalen-2-yl)-2-methoxyphenyl)adamantane (141)



Adapting Morandi's procedure,[282] a flame-dried round bottom flask was charged with Adapalene **138** (618 mg, 1.50 mmol), anhydrous CH_2Cl_2 (5.0 mL, 0.3 M) and DMF (2 μL, 0.03 mmol). The flask was sealed and purged with argon. Oxalyl chloride (386 μL, 4.50 mmol) was added dropwise using a syringe. The resulting mixture was stirred at 20 °C for 18 h. The reaction was then concentrated under reduced pressure to afford the corresponding benzoyl chloride (645 mg, quant.), which was used in the next step without further purification. A flame-dried microwave vial (10–20 mL recommended volume) was charged with $Pd_2(dba)_3$ (18.3 mg, 20.0 μmol), Xantphos (23.1 mg, 40.0 μmol) and Adapalene benzoyl chloride (345 mg, 0.80 mmol). The reaction vessel was sealed, and then evacuated and refilled with nitrogen three times. A solution of iodobenzene (816 mg, 4.00 mmol) in anhydrous toluene (4.0 mL, 1.0 M) was degassed bubbling a stream of nitrogen for 5 min, then added to the reaction vessel by syringe. The reaction tube was placed in a preheated oil bath and stirred at 100 ºC for 18 h. The reaction mixture was then allowed to cool to rt and transferred to a round-bottom flask. CH_2Cl_2 (5 mL) and MeOH (3 mL) were added and the reaction stirred at 45 °C for 30 min. The mixture was allowed to cool to rt and filtered through a pad of silica, eluting with further CH_2Cl_2 (3 × 5 mL). The solvent was removed under reduced pressure. Purification by flash column chromatography (0 to 1% Et_2O/pentane) afforded aryl iodide **141** as a white solid (262 mg, 66% over 2 steps). R_f 0.63 (4% Et_2O/pentane); mp = 226–228 °C (from Et_2O/pentane); ν_{max} (film)/cm^{-1} 2891, 2846, 1485, 1443, 1234, 1142, 1025, 878, 809; ^{1}H NMR (400 MHz, $CDCl_3$, 298 K) δ 8.25 (d, *J* = 1.8 Hz, 1 H, HC_{Ar}), 7.94 (br s, 1 H, HC_{Ar}), 7.79–7.75 (m, 2 H, HC_{Ar}), 7.73 (dd, *J* = 8.7, 1.7 Hz, 1 H, HC_{Ar}), 7.63 (d, *J* = 8.7 Hz, 1 H, HC_{Ar}), 7.59 (d, *J* = 2.3 Hz, 1 H, HC_{Ar}), 7.53 (dd, *J* = 8.4, 2.3 Hz, 1 H, HC_{Ar}), 7.00 (d, *J* = 8.4 Hz, 1 H, HC_{Ar}), 3.91 (s, 3 H, OCH_3), 2.20 (br d, *J* = 3.2 Hz, 6 H, 3 × CH_2), 2.16–2.09 (br m, 3 H, 3 × CH), 1.83 (br t, *J* = 3.0 Hz, 6 H, 3 × CH_2); ^{13}C NMR (101 MHz, $CDCl_3$, 298 K) δ 158.7 (OC_{Ar} quat), 139.6 (C_{Ar} quat), 138.9 (C_{Ar} quat), 136.3 (C_{Ar}), 134.6 (C_{Ar}), 133.7 (C_{Ar} quat), 132.6 (C_{Ar} quat), 132.4 (C_{Ar} quat), 129.6 (C_{Ar}), 127.1 (C_{Ar}), 126.5 (C_{Ar}), 125.8 (C_{Ar}), 125.5 (C_{Ar}), 124.8 (C_{Ar}), 112.0 (C_{Ar}), 90.8 (IC_{Ar} quat), 55.1 (OCH_3), 40.6 (3 × CH_2), 37.2 (C_{Ad} quat), 37.1 (3 × CH_2), 29.1 (3 × CH).

Spectroscopic data (^{1}H and ^{13}C NMR) is consistent with what described in the literature.[282]

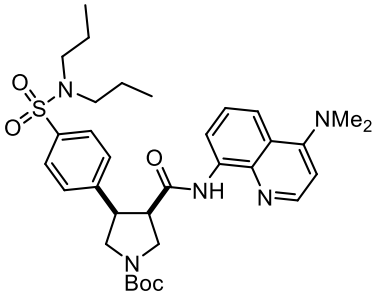
5-(2-Fluorophenyl)-3-(3-iodophenyl)-1,2,4-oxadiazole (142)



Adapting Morandi's procedure,[282] a flame-dried round bottom flask was charged with Ataluren **139** (568 mg, 2.00 mmol), anhydrous CH_2Cl_2 (6.0 mL, 0.3 M) and DMF (2 μL, 0.03 mmol). The flask was sealed and purged with argon. Oxalyl chloride (500 μL, 6.00 mmol) was added dropwise using a syringe. The resulting mixture was stirred at 20 °C for 18 h. The reaction was then concentrated under reduced pressure to afford the corresponding benzoyl chloride (604 mg, quant.), which was used in the next step without further purification. A flame-dried microwave vial (10–20 mL recommended volume) was charged with $Pd_2(dba)_3$ (22.9 mg, 25.0 μmol), Xantphos (28.9 mg, 50.0 μmol) and Ataluren benzoyl chloride (303 mg, 1.00 mmol). The reaction vessel was sealed, and then evacuated and refilled with nitrogen three times. A solution of iodobenzene (1.02 g, 5.00 mmol) in anhydrous toluene (5.0 mL, 1.0 M) was degassed bubbling a stream of nitrogen for 5 min, then added to the reaction vessel by syringe. The reaction tube was placed in a preheated oil bath and stirred at 125 ºC for 18 h. The reaction mixture was then allowed to cool to rt and transferred to a round-bottom flask. CH_2Cl_2 (5 mL) and MeOH (3 mL) were added and the reaction stirred at 45 °C for 30 min. The mixture was allowed to cool to rt and filtered through a pad of silica, eluting with further CH_2Cl_2 (3 × 5 mL). The solvent was removed under reduced pressure. Purification by flash column chromatography (2% Et_2O/pentane) afforded aryl iodide **142** as a white solid (300 mg, 82% over 2 steps). R_f 0.56 (3% Et_2O/pentane); mp = 90–92 °C (from Et_2O/pentane); ν_{max} (film)/cm^{-1} 3064, 1618, 1428, 1338, 1223, 828, 798, 746, 675; ^{1}H NMR (400 MHz, $CDCl_3$, 298 K) δ 8.55 (t, *J* = 1.7 Hz, 1 H, HC_{Ar}), 8.23 (ddd, *J* = 7.8, 7.0, 1.8 Hz, 1 H, HC_{Ar}), 8.17 (dt, *J* = 7.8, 1.3 Hz, 1 H, HC_{Ar}), 7.87 (ddd, *J* = 7.9, 1.8, 1.1 Hz, 1 H, HC_{Ar}), 7.67–7.59 (m, 1 H, HC_{Ar}), 7.37 (td, *J* = 7.6, 1.1 Hz, 1 H, HC_{Ar}), 7.31 (ddd, *J* = 10.5, 8.4, 1.1 Hz, 1 H, HC_{Ar}), 7.29–7.24 (m, 1 H, HC_{Ar}); ^{13}C NMR (101 MHz, $CDCl_3$, 298 K) δ 173.0 (d, J_{CF} = 4.0 Hz, OCN quat), 167.4 (NCN quat), 160.7 (d, J_{CF} = 260.5 Hz, FC_{Ar} quat), 140.1 (C_{Ar}), 136.3 (C_{Ar}), 134.8 (d, J_{CF} = 8.8 Hz, F-*m*-C_{Ar}), 130.9 (C_{Ar}), 130.5 (C_{Ar}), 128.6 (C_{Ar} quat), 126.6 (C_{Ar}), 124.7 (d, J_{CF} = 3.9 Hz, F-*m*-C_{Ar}), 117.2 (d, J_{CF} = 20.9 Hz, F-*o*-C_{Ar}), 112.6 (d, J_{CF} = 11.5 Hz, F-*o*-C_{Ar} quat), 94.4 (IC_{Ar} quat); ^{19}F NMR (377 MHz, $CDCl_3$, 298 K) δ –108.2 (m); FTMS (+p APCI) *m*/*z* Calculated for $C_{14}H_9N_2OFI^+$ $[M+H]^+$ 366.9738; Found 366.9735.

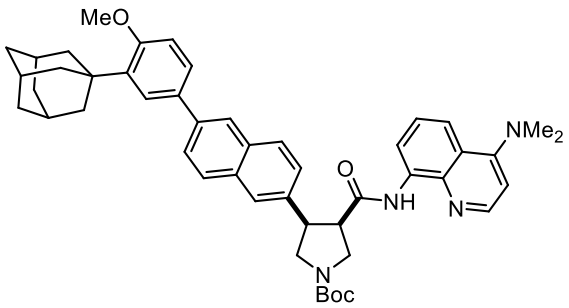
*8.2.5.14 Late-stage functionalisation of acid-containing drugs: arylated pyrrolidines **143–145***

tert-Butyl _cis_-(±)-3-((4-(dimethylamino)quinolin-8-yl)carbamoyl)-4-(4-(_N_,_N_-dipropylsulfamoyl)phenyl)pyrrolidine-1-carboxylate (143)



A reaction vial was charged with K_2CO_3 (138 mg, 1.00 mmol), flame-dried, and allowed to cool under argon. Amide **118** (367 mg, 1.00 mmol), Probenecid iodide **140** (384 mg, 1.00 mmol), $Pd(OAc)_2$ (11.3 mg, 50.0 μmol) and PivOH (102 mg, 1.00 mmol) were added sequentially. The reaction vessel was sealed and purged with argon, then $PhCF_3$ (0.5 mL, 2.0 M) was added by syringe. The reaction tube was placed in a preheated oil bath and stirred at 110 ºC for 18 h. The reaction mixture was then allowed to cool to rt and EtOAc (5 mL) was added. The resulting mixture was filtered through a pad of Celite, eluting with further EtOAc (2 × 10 mL). The solvent was removed under reduced pressure, and the crude material was purified by flash column chromatography (20% acetone/pentane). The product containing fractions were combined and the solvent was removed under reduced pressure. Et_2O (5 mL) and pentane (5 mL) were added and the solvent was removed under reduced pressure to afford the *cis*-arylated product **143** as a pale yellow solid (247 mg, 40%). R_f 0.28 (20% acetone/pentane); mp = 81–85 °C (from Et_2O/pentane); ν_{max} (film)/cm^{-1} 3324 (NH br), 2963, 1685 (C=O), 1525, 1402, 1334, 1305, 1156, 1115, 988, 764; ^{1}H NMR (400 MHz, DMSO-d_6, 373 K) δ 9.78 (br s, 1 H, NH), 8.53 (d, J = 5.2 Hz, 1 H, HC_{Ar}), 8.22 (dd, J = 7.7, 1.3 Hz, 1 H, HC_{Ar}), 7.69 (dd, J = 8.6, 1.3 Hz, 1 H, HC_{Ar}), 7.56–7.50 (m, 2 H, HC_{Ar}), 7.49–7.44 (m, 2 H, HC_{Ar}), 7.31 (dd, J = 8.6, 7.7 Hz, 1 H, HC_{Ar}), 6.89 (d, J = 5.2 Hz, 1 H, HC_{Ar}), 3.98 (ddd, J = 7.5, 7.5, 7.5 Hz, 1 H, CHAr), 3.87 (ddd, J = 7.3, 7.3, 4.2 Hz, 1 H, CHCO), 3.84–3.77 (m, 3 H, NC*H*HCHCO, NCH_2CHAr), 3.67 (dd, J = 11.1, 7.3 Hz, 1 H, NCH*H*CHCO), 3.02 (s, 6 H, $N(CH_3)_2$), 2.68–2.61 (m, 4 H, 2 × SO_2NCH_2), 1.49 (s, 9 H, $C(CH_3)_3$), 1.26 (h, J = 7.4 Hz, 4 H, 2 × $SO_2NCH_2CH_2$), 0.67 (t, J = 7.4 Hz, 6 H, 2 × CH_3); ^{13}C NMR (101 MHz, DMSO-d_6, 373 K) δ 168.9 (C=O amide), 156.7 ($N(CH_3)_2C_{Ar}$ quat), 153.1 (C=O carbamate), 147.8 (C_{Ar}), 143.0 (C_{Ar} quat), 139.2 (C_{Ar} quat), 137.5 (C_{Ar} quat), 133.7 (C_{Ar} quat), 127.8 (2 × C_{Ar}), 126.0 (2 × C_{Ar}), 123.5 (C_{Ar}), 121.3 (C_{Ar} quat), 118.0 (C_{Ar}), 115.3 (C_{Ar}), 107.0 (C_{Ar}), 78.2 ($C(CH_3)_3$), 49.1 (br and weak, *C*HCO), 49.04 (NCH_2CHAr), 48.99 (2 × SO_2NCH_2), 47.6 (NCH_2CHCO), 45.3 (br and weak, CHAr), 42.9 ($N(CH_3)_2$), 27.8 ($C(CH_3)_3$), 20.7 (2 × $SO_2NCH_2CH_2$), 10.2 (2 × CH_3); HRMS (ESI$^+$) m/z Calculated for $C_{33}H_{46}N_5O_5S$ [M+H] 624.3220; Found 624.3222.

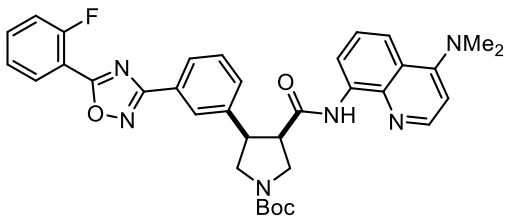
***tert*-Butyl *cis*-(±)-3-(6-(3-((3r,5r,7r)-adamantan-1-yl)-4-methoxyphenyl)naphthalen-2-yl)-4-((4-(dimethylamino)quinolin-8-yl)carbamoyl)pyrrolidine-1-carboxylate (144)**



A reaction vial was charged with K_2CO_3 (27.7 mg, 0.20 mmol), flame-dried, and allowed to cool under argon. Amide **118** (76.9 mg, 0.20 mmol), $Pd(OAc)_2$ (2.2 mg, 10.0 μmol) and PivOH (20.5 mg, 0.20 mmol) were added sequentially, followed by Adapalene iodide **141** (98.9 mg, 0.20 mmol). The reaction vessel was sealed and purged with argon, then $PhCF_3$ (270 μL, 0.75 M) was added by syringe. The reaction tube was placed in a preheated oil bath and stirred at 110 ºC for 18 h. The reaction mixture was then allowed to cool to rt and EtOAc (3 mL) was added. The resulting mixture was filtered through a pad of Celite, eluting with further EtOAc (2 × 5 mL). The solvent was removed under reduced pressure, and the crude material was purified by flash column chromatography (13% acetone/pentane). The product containing fractions were combined and the solvent was removed under reduced pressure. Et_2O (3 mL) and pentane (3 mL) were added and the solvent was removed under reduced pressure to afford the *cis*-arylated product **144** as a pale yellow solid (60.7 mg, 54%). R_f 0.18 (15% acetone/pentane); mp = 138–142 °C (from Et_2O/pentane); ν_{max} (film)/cm^{-1} 3675, 3332, (NH br), 2971, 2900, 1692 (C=O), 1525, 1409, 1308, 1238, 1170, 1115, 1059, 880, 813, 764; ^{1}H NMR (400 MHz, DMSO-d_6, 373 K) δ 9.86 (br s, 1 H, NH), 8.44 (d, J = 5.2 Hz, 1 H, HC_{Ar}), 8.21 (dd, J = 7.7, 1.3 Hz, 1 H, HC_{Ar}), 7.84–7.81 (m, 1 H, HC_{Ar}), 7.73–7.67 (m, 2 H, HC_{Ar}), 7.65 (d, J = 8.6 Hz, 1 H, HC_{Ar}), 7.63–7.58 (m, 2 H, HC_{Ar}), 7.51–7.46 (m, 2 H, HC_{Ar}), 7.39 (dd, J = 8.5, 1.9 Hz, 1 H, HC_{Ar}), 7.26 (dd, J = 8.6, 7.7 Hz, 1 H, HC_{Ar}), 7.08–7.03 (m, 1 H, HC_{Ar}), 6.77 (d, J = 5.2 Hz, 1 H, HC_{Ar}), 4.04 (ddd, J = 7.3, 7.3, 7.3 Hz, 1 H, CHAr), 3.96–3.83 (m, 7 H, CHCO, NC*H*HCHCO, NC*H*$_2$CHAr, OCH_3), 3.70 (dd, J = 12.2, 8.5 Hz, 1 H, NCH*H*CHCO), 2.94 (s, 6 H, $N(CH_3)_2$), 2.14 (br d, J = 3.0 Hz, 6 H, 3 × CH_2), 2.07 (br t, J = 3.2 Hz, 3 H, 3 × CH), 1.78 (br t, J = 3.1 Hz, 6 H, 3 × CH_2) 1.52 (s, 9 H, $C(CH_3)_3$); ^{13}C NMR (101 MHz, DMSO-d_6, 373 K) δ 169.1 (C=O amide), 157.9 (OC_{Ar} quat), 156.5 ($N(CH_3)_2C_{Ar}$ quat), 153.2 (C=O carbamate), 147.6 (C_{Ar}), 139.1 (C_{Ar} quat), 137.8 (C_{Ar} quat), 137.2 (C_{Ar} quat), 135.3 (C_{Ar} quat), 133.8 (C_{Ar} quat), 131.9 (C_{Ar} quat), 131.8 (C_{Ar} quat), 131.2 (C_{Ar} quat), 127.3 (2 × C_{Ar}), 125.8 (C_{Ar}), 125.2 (C_{Ar}), 124.7 (C_{Ar}), 124.5 (C_{Ar}), 124.3 (C_{Ar}), 123.5 (C_{Ar}), 123.3 (C_{Ar}), 121.2 (C_{Ar} quat), 117.8 (C_{Ar}), 115.1 (C_{Ar}), 112.6 (C_{Ar}), 106.9 (C_{Ar}), 78.1 ($C(CH_3)_3$), 54.9 (OCH_3), 49.5 (N*C*H$_2$CHAr), 49.4 (br and weak, *C*HCO), 47.6 (N*C*H$_2$CHCO), 45.7 (br and weak, CHAr), 42.8 ($N(CH_3)_2$), 39.9 (3 × CH_2), 36.3 (C_{Ad} quat), 36.2 (3 × CH_2), 28.1 (3 × CH), 27.8 (C(*C*H$_3$)$_3$); FTMS (+p APCI) *m*/*z* Calculated for $C_{48}H_{55}N_4O_4^+$ $[M+H]^+$ 751.4218; Found 751.4203.

Note: the order of addition (ArI addedd last) was crucial to obtain optimal reactivity, due to the low solubility of iodide **141**.

***tert*-Butyl *cis*-(±)-3-((4-(dimethylamino)quinolin-8-yl)carbamoyl)-4-(3-(5-(2-fluorophenyl)-1,2,4-oxadiazol-3-yl)phenyl)pyrrolidine-1-carboxylate (145)**

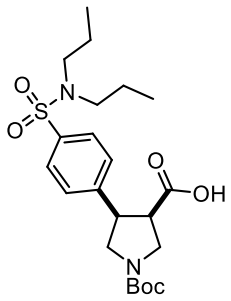


A reaction vial was charged with K_2CO_3 (27.7 mg, 0.20 mmol), flame-dried, and allowed to cool under argon. Amide **118** (76.9 mg, 0.20 mmol), Ataluren iodide **142** (73.2 mg, 0.20 mmol), $Pd(OAc)_2$ (2.2 mg, 10.0 μmol) and PivOH (20.5 mg, 0.20 mmol) were added sequentially. The reaction vessel was sealed and purged with argon, then $PhCF_3$ (200 μL, 1.0 M) was added by syringe. The reaction tube was placed in a preheated oil bath and stirred at 110 ºC for 18 h. The reaction mixture was then allowed to cool to rt and EtOAc (5 mL) was added. The resulting mixture was filtered through a pad of Celite, eluting with further EtOAc (2 × 10 mL). The solvent was removed under reduced pressure, and the crude material was purified by flash column chromatography (20% acetone/pentane). The product containing fractions were combined and the solvent was removed under reduced pressure. Et_2O (5 mL) and pentane (5 mL) were added and the solvent was removed under reduced pressure to afford the *cis*-arylated product **145** as a white solid (66.4 mg, 53%). R_f 0.18 (20% acetone/pentane); mp = 95–99 °C (from Et_2O/pentane); ν_{max} (film)/cm^{-1} 3310 (NH br), 2974, 1685 (C=O), 1525, 1405, 1305, 1163, 1115, 813, 753; ^{1}H NMR (400 MHz, DMSO-d_6, 373 K) δ 9.86 (br s, 1 H, NH), 8.44 (d, J = 5.2 Hz, 1 H, HC_{Ar}), 8.21 (dd, J = 7.7, 1.3 Hz, 1 H, HC_{Ar}), 8.08 (ddd, J = 7.9, 7.2, 1.8 Hz, 1 H, HC_{Ar}), 7.99 (t, J = 1.7 Hz, 1 H, HC_{Ar}), 7.81–7.73 (m, 2 H, HC_{Ar}), 7.60 (dd, J = 8.6, 1.3 Hz, 1 H, HC_{Ar}), 7.52–7.43 (m, 3 H, HC_{Ar}), 7.34 (td, J = 7.8, 0.5 Hz, 1 H, HC_{Ar}), 7.23 (dd, J = 8.6, 7.7 Hz, 1 H, HC_{Ar}), 6.81 (d, J = 5.2 Hz, 1 H, HC_{Ar}), 4.01 (ddd, J = 7.2, 7.2, 7.2 Hz, 1 H, CHAr), 3.90 (ddd, J = 7.1, 7.1, 4.7 Hz, 1 H, CHCO), 3.88–3.81 (m, 3 H, NC*H*HCHCO, NC*H*$_2$CHAr), 3.69 (dd, J = 10.9, 7.1 Hz, 1 H, NCH*H*CHCO), 2.96 (s, 6 H, $N(CH_3)_2$), 1.50 (s, 9 H, $C(CH_3)_3$); ^{13}C NMR (101 MHz, DMSO-d_6, 373 K) δ 171.7 (d, J_{CF} = 3.7 Hz, OCN quat), 168.9 (C=O amide), 167.4 (NCN quat), 159.5 (d, J_{CF} = 257.9 Hz, FC_{Ar} quat), 156.6 ($N(CH_3)_2C_{Ar}$ quat), 153.2 (C=O carbamate), 147.7 (C_{Ar}), 139.4 (C_{Ar} quat), 139.2 (C_{Ar} quat), 134.8 (d, J_{CF} = 8.7 Hz, F-*m*-C_{Ar}), 133.7 (C_{Ar} quat), 130.3 (C_{Ar}), 130.2 (C_{Ar}), 128.4 (C_{Ar}), 126.1 (C_{Ar}), 125.6 (C_{Ar} quat), 125.0 (C_{Ar}), 124.7 (d, J_{CF} = 3.5 Hz, F-*m*-C_{Ar}), 123.4 (C_{Ar}), 121.2 (C_{Ar} quat), 117.9 (C_{Ar}), 116.6 (d, J_{CF} = 20.8 Hz, F-*o*-C_{Ar}), 115.3 (C_{Ar}), 111.5 (d, J_{CF} = 11.9 Hz, F-*o*-C_{Ar} quat), 106.9 (C_{Ar}), 78.1 ($C(CH_3)_3$), 49.6 (N*C*H$_2$CHAr), 49.2 (br and weak, *C*HCO), 47.3 (N*C*H$_2$CHCO), 45.4 (br and weak, CHAr), 42.8 ($N(CH_3)_2$), 27.8 ($C(CH_3)_3$);

^{19}F NMR (377 MHz, DMSO-d_6, 373 K) δ –109.7 (m); FTMS (+p APCI) *m*/*z* Calculated for $C_{35}H_{36}N_6O_4F^+$ $[M+H]^+$ 623.2777; Found 623.2765.

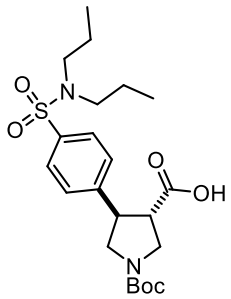
*8.2.5.15 Late-stage functionalisation of acid-containing drugs: DG removal (**146**, **147**)*

cis-(±)-1-(_tert_-Butoxycarbonyl)-4-(4-(_N_,_N_-dipropylsulfamoyl)phenyl)pyrrolidine-3-carboxylic acid (146)



A flame-dried reaction tube was charged with amide 1**43** (62.4 mg, 0.10 mmol), followed by Boc_2O (109 mg, 0.50 mmol) and DMAP (2.4 mg, 20.0 μmol). The reaction vessel was sealed and purged with argon, then MeCN (200 μL, 0.5 M) was added by syringe. The reaction tube was then placed in an oil bath and gradually warm up to 60 ºC. The reaction mixture was then stirred at 60 °C for 4 h. The reaction mixture was then allowed to cool to rt and sat. aq. NH_4Cl (1 mL) and CH_2Cl_2 (1 mL) were added. The phases were separated, and the aqueous layer was extracted with CH_2Cl_2 (3 × 3 mL). The combined organic extracts were dried over Na_2SO_4 and filtered. The solvent was removed under reduced pressure to afford the crude *N*-Boc protected pyrrolidine derivative, which was used in the next step without further purification. A solution of H_2O_2 (51 μL, 0.50 mmol, 30 wt.% in H_2O) in THF (250 μL) was added to a solution of $LiOH·H_2O$ (8.4 mg, 0.20 mmol) in H_2O (250 μL) at 0 °C under argon. The resulting mixture was added dropwise to a solution of crude *N*-Boc protected pyrrolidine in THF (500 μL) at 0 °C under argon. The reaction was then stirred at 25 °C for 3 h. Sat. aq. $Na_2S_2O_3$ (1 mL), EtOAc (3 mL) and 1 N NaOH (3 mL) were then added. The aqueous alkaline layer was collected, and the organic layer extracted with 1 N NaOH (3 × 3 mL). The aqueous alkaline layers were combined, washed with EtOAc (10 mL), and acidified to pH ~1 with HCl, 37%. The acidic layer was extracted with EtOAc (5 × 15 mL). The combined organic extracts were dried over Na_2SO_4 and filtered. Solvent was removed under reduced pressure. Et_2O (3 mL) and pentane (3 mL) were added and the solvent was removed under reduced pressure to afford the pure *cis*-acid **146** as a white solid (45.0 mg, 97% over 2 steps). mp = 51–55 °C (from Et_2O/pentane); ν_{max} (film)/cm^{-1} 3217 (OH br), 2967, 1733 (C=O), 1696 (C=O), 1655, 1394, 1334, 1152, 992, 872, 772, 738; ^1H NMR (400 MHz, $CDCl_3$, 298 K, observed as mixture of rotamers) δ 7.75–7.67 (m, 2 H, HC_{Ar}), 7.34–7.27 (m, 2 H, HC_{Ar}), 6.61 (br s, 1 H, OH), 3.83–3.59 (m, 5 H, NCH_2CHAr, NCH_2CHCO, CHAr), 3.51–3.38 (m, 1 H, CHCO), 3.10–3.00 (m, 4 H, 2 × NCH_2), 1.59–1.42 (m, 13 H, 2 × NCH_2CH_2, $C(CH_3)_3$), 0.85 (t, *J* = 7.4 Hz, 6 H, 2 × CH_3); ^{13}C NMR (101 MHz, $CDCl_3$, 298 K, observed as mixture of rotamers) δ 174.5 and 174.3 (COOH), 154.4 (C=O carbamate), 143.4 and 143.0 (SC_{Ar} quat), 139.1 and 139.0 (C_{Ar} quat), 128.3 (2 × C_{Ar}), 127.2 (2 × C_{Ar}), 80.3 ($C(CH_3)_3$), 50.5 and 50.2 (NCH_2CHAr), 49.9 (2 × NCH_2), 48.3 and 47.4 (*C*HCO), 47.0 and 46.6 (NCH_2CHCO), 45.7 and 44.8 (CHAr), 28.5 ($C(CH_3)_3$), 21.9 (2 × NCH_2CH_2), 11.1 (2 × CH_3); FTMS (–p APCI) *m*/*z* Calculated for $C_{22}H_{33}N_2O_6S^-$ $[M+H]^-$ 453.2065; Found 453.2060.

trans-(±)-1-(_tert_-Butoxycarbonyl)-4-(4-(_N_,_N_-dipropylsulfamoyl)phenyl)pyrrolidine-3-carboxylic acid (147)



A reaction tube was charged with amide **143** (62.4 mg, 0.10 mmol), followed by NaOH (41.0 mg, 1.00 mmol). The reaction vessel was sealed and EtOH (500 μL, 0.2 M) was added by syringe. The reaction tube was then placed in a preheated oil bath and stirred at 100 ºC for 30 min. The reaction mixture was then allowed to cool down to rt and diluted with EtOAc (1 mL) and 1 N NaOH (1 mL). The aqueous alkaline layer was collected, and the organic layer extracted with 1 N NaOH (3 × 3 mL). The aqueous alkaline layers were combined, washed with EtOAc (5 mL), and acidified to pH ~1 with HCl, 37%. The acidic layer was extracted with EtOAc (5 × 10 mL). The combined organic extracts were dried over Na_2SO_4 and filtered. Solvent was removed under reduced pressure. Et_2O (3 mL) and pentane (3 mL) were added and the solvent was removed under reduced pressure to afford the pure *trans*-acid **147** as a pale yellow solid (42.3 mg, 95%). mp = 47–51 °C (from Et_2O/pentane); ν_{max} (film)/cm^{-1} 3183 (OH br), 2967, 1733 (C=O), 1692 (C=O), 1394, 1331, 1152, 992, 772, 738; ^{1}H NMR (400 MHz, $CDCl_3$, 298 K, observed as mixture of rotamers) δ 7.76 (d, *J* = 8.3 Hz, 2 H, HC_{Ar}), 7.38 (d, *J* = 8.2 Hz, 2 H, HC_{Ar}), 6.32 (br s, 1 H, OH), 3.99–3.79 (m, 2 H, NC*H*HCHAr, NC*H*HCHCO), 3.78–3.66 (m, 1 H, CHAr), 3.66–3.56 (m, 1 H, NCH*H*CHCO), 3.51–3.34 (m, 1 H, NCH*H*CHAr), 3.27–3.14 (m, 1 H, CHCO), 3.11–3.02 (m, 4 H, 2 × NCH_2), 1.56 (h, *J* = 7.4 Hz, 4 H, 2 × NCH_2CH_2), 1.47 and 1.46 (2 × s, 9 H, $C(CH_3)_3$), 0.87 (t, *J* = 7.4 Hz, 6 H, 2 × CH_3); ^{13}C NMR (101 MHz, $CDCl_3$, 298 K, observed as mixture of rotamers) δ 175.7 (COOH), 154.1 (C=O carbamate), 143.9 (SC_{Ar} quat), 139.3 (C_{Ar} quat), 128.0 (2 × C_{Ar}), 127.6 (2 × C_{Ar}), 80.4 ($C(CH_3)_3$), 52.4 and 51.9 (NCH_2CHAr), 50.1 (2 × NCH_2), 49.9 (br and weak, *C*HCO), 48.5 (br m, NCH_2CHCO), 47.1 and 46.4 (CHAr), 28.4 ($C(CH_3)_3$), 22.1 (2 × NCH_2CH_2), 11.1 (2 × CH_3); FTMS (–p APCI) *m*/*z* Calculated for $C_{22}H_{33}N_2O_6S^-$ $[M+H]^-$ 453.2065; Found 453.2061.

8.2.6 General Procedures and Raw Data for Mechanistic and Kinetic Experiments

8.2.6.1 Mechanistic Experiments

*Deuteration of amides **9**, **10**, **13b** and **21** (Schemes 3.16, 5.3 and 5.12)*

A flame-dried reaction vial was charged with the required substrate (0.20 mmol), $Pd(OAc)_2$ (2.3 mg, 10.0 μmol), AcOD-d_4 (350 μL, 6.00 mmol) and toluene-d_8 (1.0 mL, 0.2 M). The reaction vessel was sealed and purged with argon, then placed in a preheated oil bath and stirred at 110 ºC for 18 h. The reaction mixture was allowed to cool to rt and EtOAc (2 mL) was added. The resulting mixture was filtered through a pad of Celite, eluting with further EtOAc (3 × 5 mL). The solvent was removed under reduced pressure and the crude was analysed by ^{1}H NMR in DMSO-d_6 at 373 K to determine the % D.

Deuteration of pyrrolidine **13b** and piperidine **21** was performed adapting the same procedure to smaller 0.06 and 0.1 mmol scale, respectively.

For *N*-Cbz pyrrolidines **9** and **13b**, as well as for piperidine **21**, a delay time d_1 = 70 s was used to account for the longest relaxation time T_1 ~ 13 s of an aromatic Cbz proton resonating at δ 7.30 ppm.

*Deuteration of palladacycle **98-Py** (Table 5.1)*

A flame-dried reaction vial was charged with palladacycle **98-Py** (28.0 mg, 50.0 μmol), toluene-d_8 (170 μL, 0.3 M) and either AcOD-d_4 (6.0 μL, 0.10 mmol) or HFIP-d_2 (53 μL, 0.50 mmol).The reaction vessel was sealed and purged with argon, then placed in a preheated oil bath and stirred at 110 °C for 18 h. The reaction mixture was allowed to cool to rt and EtOAc (1 mL) was added. The resulting mixture was filtered through a pad of Celite, eluting with further EtOAc (3 × 2 mL). The solvent was removed under reduced pressure and derivative **9-d_x** was purified by flash column chromatography (80% Et_2O/pentane). The % D was determined on the isolated material by ^{1}H NMR in DMSO-d_6 at 373 K.

*Use of palladacycle **98-Py** as pre-catalyst in the C–H arylation of pyrrolidine **9** (Scheme 5.7a)*

A reaction vial was charged with K_2CO_3 (13.8 mg, 0.10 mmol), flame-dried, and allowed to cool under argon. Carboxamide **9** (37.5 mg, 0.10 mmol), 4-iodoanisole (70.2 mg, 0.30 mmol), **98-Py** (2.6 mg, 5.00 μmol) and PivOH (10.2 mg, 0.10 mmol) were added sequentially. The reaction vessel was sealed and purged with argon, then $PhCF_3$ (100 μL, 1.0 M) was added by syringe. The reaction tube was placed in a preheated oil bath and stirred at 110 ºC for 18 h. The reaction mixture was allowed to cool to rt and EtOAc (1 mL) was added. The resulting mixture was filtered through a pad of Celite, eluting with further EtOAc (3 × 3 mL). The solvent was removed under reduced pressure, and accurately weighed 1,3,5-trimethoxybenzene (4.2 mg,

25.0 μmol) was added. The resulting mixture was dissolved in $CDCl_3$ and a sample of this solution was analysed by ^1H NMR spectroscopy. The yield of the arylated product (**13a**) was calculated by ^1H NMR by comparison to the internal standard.

*Stoichiometric arylation of Pd-cycle **98-Py** with 4-iodoanisole (Scheme 5.7b)*

A reaction vial was charged with K_2CO_3 (11.0 mg, 80.0 μmol), flame-dried, and allowed to cool under argon. Palladacycle **98-Py** (44.0 mg, 80.0 μmol), 4-iodoanisole (56.2 mg, 0.20 mmol) and PivOH (8.2 mg, 80.0 μmol) were added sequentially. The reaction vessel was sealed and purged with argon, then $PhCF_3$ (80 μL, 1.0 M) was added by syringe. The reaction tube was placed in a preheated oil bath and stirred at 110 ºC for 18 h. The reaction mixture was allowed to cool to rt and EtOAc (1 mL) was added. The resulting mixture was filtered through a pad of Celite, eluting with further EtOAc (3 × 3 mL). The solvent was removed under reduced pressure, and accurately weighed 1,3,5-trimethoxybenzene (3.5 mg, 21.0 μmol) was added. The resulting mixture was dissolved in $CDCl_3$ and a sample of this solution was analysed by ^1H NMR spectroscopy. The yield of the arylated product (**13a**) was calculated by ^1H NMR by comparison to the internal standard.

H/D Scrambling experiments (Table 5.2)

A flame-dried reaction vial was charged with deuterated pyrrolidine **9-d_3** (37.8 mg, 0.10 mmol), $Pd(OAc)_2$ (1.1 mg, 5.00 μmol), and the base and additives specified in Table 5.2. The reaction vessel was sealed and purged with argon, then either $PhCF_3$ or toluene-d_8 (100 μL, 1.0 M) was added by syringe. The reaction vial was placed in a preheated oil bath and stirred at 110 ºC for specified time. The reaction mixture was allowed to cool to rt and EtOAc (1 mL) was added. The resulting mixture was filtered through a pad of Celite, eluting with further EtOAc (3 × 3 mL). The solvent was removed under reduced pressure and the crude was analysed by ^1H NMR under the specified conditions.

8.2.6.2 Deuteration Kinetics

*Deuteration profile for pyrrolidine amide **9** (Scheme 5.4 and Figure 5.1)*

A flame-dried vial was charged with *N*-Cbz pyrrolidine **9** (19 mg, 50.0 μmol), $Pd(OAc)_2$ (0.6 mg, 2.50 μmol), AcOD-d_4 (86 μL, 1.50 mmol) and toluene-d_8 (600 μL). The resulting solution was transferred to an over-dried J-Young NMR tube by syringe. The tube was purged with argon and sealed. The NMR tube was placed in a pre-heated Brucker 400 MHz Spectrometer and the reaction was followed by collection of consecutive ^{1}H NMR spectra (6 scans, d_1 = 1 s) at 373 K. The spectra were recorded every 5 min for the 1st h, and every 15 min over the following 20 h. Raw kinetic data is given in Appendix II.

*Deuteration profile for 3,4-disubstituted pyrrolidine **13b** (Scheme 5.13 and Figure 5.20)*

A flame-dried vial was charged with *N*-Cbz 4-aryl-pyrrolidine **13b** (23.2 mg, 50.0 μmol), $Pd(OAc)_2$ (1.1 mg, 5.00 μmol), AcOD-d_4 (86 μL, 1.50 mmol) and toluene-d_8 (600 μL). The resulting solution was transferred to an over-dried J-Young NMR tube by syringe. The tube was purged with argon and sealed. The NMR tube was placed in a pre-heated Brucker 400 MHz Spectrometer and the reaction was followed by collection of consecutive ^{1}H NMR spectra (1 scans, d_1 = 70 s) at 373 K. The spectra were recorded every 5 min over 12 h. Raw kinetic data is given in Appendix II.

*Deuteration profile for a mixture of pyrrolidine derivatives **9** and **13b** (Scheme 5.14 and Figure 5.21)*

A flame-dried vial was charged with pyrrolidine amide **9** (9.4 mg, 25.0 μmol), 4-aryl-pyrrolidine **13b** (14.0 mg, 30.0 μmol), $Pd(OAc)_2$ (1.1 mg, 5.00 μmol), AcOD-d_4 (86 μL, 1.50 mmol) and toluene-d_8 (600 μL). The resulting solution was transferred to an over-dried J-Young NMR tube by syringe. The tube was purged with argon and sealed. The NMR tube was placed in a pre-heated Brucker 500 MHz Spectrometer and the reaction was followed by collection of consecutive ^{1}H NMR spectra (8 scans, d_1 = 1 s) at 373 K. The spectra were recorded every 5 min over 12 h. Raw kinetic data is given in Appendix II.

8.2.6.3 Evaluation of Kinetic Isotope Effect

Intermolecular KIE determined by parallel experiments (Table 5.3 and Figure 5.2)

Discrete reactions were stopped and worked-up at different time points (0–45 min) following the procedure outlined below.

A reaction vial was charged with K_2CO_3 (13.8 mg, 0.10 mmol), flame-dried, and allowed to cool under argon. Either the protic substrate **9** (37.5 mg, 0.10 mmol) or the deuterated carboxamide **9-*d*$_4$** (37.9 mg, 0.10 mmol) was added, followed by 4-iodoanisole (70.2 mg, 0.30 mmol), $Pd(OAc)_2$ (1.1 mg, 5.00 μmol) and PivOH (10.2 mg, 0.10 mmol). The reaction vessel was sealed and purged with argon, then $PhCF_3$ (100 μL) was added by syringe. The reaction tube was then placed in a preheated oil bath and stirred at 110 ºC for the specified time. The mixture was removed from the heat source and cold EtOAc (1 mL) was immediately added to stop the reaction. The resulting mixture was filtered through a pad of Celite, eluting with further EtOAc (3 × 3 mL). The solvent was removed under reduced pressure, and accurately weighed 1,3,5-trimethoxybenzene (2.5–5.0 mg, 15–30 μmol) was added. The resulting crude mixture was dissolved in $CDCl_3$ and a sample of this solution was analysed by ^{1}H NMR spectroscopy. The yield of the arylated product (**13a**) and the % of remaining starting material (**9** or **9-*d*$_4$**) were calculated by ^{1}H NMR by comparison to the internal standard. A corrected volume of 228 μL, accounting for both the solvent (100 μL) and the volume occupied by the reagents as measured with a volumetric flask, was used to derive concentration values. Changes in this value between experiments were assumed negligible. For raw data see Table 5.3, page 128.

Intermolecular KIE determined by one pot competition (Scheme 5.10)

A reaction vial was charged with K_2CO_3 (27.7 mg, 0.20 mmol), flame-dried, and allowed to cool under argon. The protic substrate **9** (37.5 mg, 0.10 mmol), the deuterated amide **9-*d*$_4$** (37.9 mg, 0.10 mmol), 4-iodoanisole (11.7 mg, 50.0 μmol), $Pd(OAc)_2$ (2.2 mg, 10.0 μmol) and PivOH (20.5 mg, 0.10 mmol) were then added sequentially. The reaction vessel was sealed and purged with argon, then $PhCF_3$ (200 μL) was added by syringe. The reaction tube was placed in a preheated oil bath and stirred at 110 ºC for 7 h. The mixture was removed from the heat source and cold EtOAc (2 mL) was immediately added to stop the reaction. The resulting mixture was filtered through a pad of Celite, eluting with further EtOAc (3 × 5 mL). The solvent was removed under reduced pressure, and accurately weighed 1,3,5-trimethoxybenzene (6.9 mg, 41.0 μmol) was added. The resulting crude mixture was dissolved in $CDCl_3$ and a sample of this solution was analysed by ^{1}H NMR spectroscopy. This showed the formation of 4-arylated products in 7% overall NMR yield (0.014 mmol).

8.2.6.4 Electronic Effect of the Aryl Iodides on the Reaction Rate

Competition experiments (Scheme 5.11)

In each experiment, two different aryl iodides **A** and **B** had to compete for a limiting amount of pyrrolidine **2**, where **A** and **B** can be 4-iodoanisole, iodobenzene or 4-iodobenzotrifluoride.

A reaction vial was charged with K_2CO_3 (27.7 mg, 0.20 mmol), flame-dried, and allowed to cool under argon. *N*-Boc pyrrolidine amide **2** (68.3 mg, 0.20 mmol), the required aryl iodide **A** (0.60 mmol), the required aryl iodide **B** (0.60 mmol), $Pd(OAc)_2$ (2.2 mg, 10.0 μmol) and PivOH (20.5 mg, 0.20 mmol) were added sequentially. The reaction vessel was sealed and purged with argon, then $PhCF_3$ (200 μL) was added by syringe. The reaction tube was placed in a preheated oil bath and stirred at 110 ºC for 0.5–1 h. The mixture was removed from the heat source and cold EtOAc (2 mL) was immediately added to stop the reaction. The resulting mixture was filtered through a pad of Celite, eluting with further EtOAc (3 × 5 mL). The solvent was removed under reduced pressure, and accurately weighed 1,3,5-trimethoxybenzene (5.0–7.5 mg, 30–45 μmol) was added. The resulting crude mixture was dissolved in $CDCl_3$ and a sample of this solution was analysed by ^{1}H NMR spectroscopy. The yield of the corresponding arylated products (**3a**, **3b** or **3g**) was calculated by ^{1}H NMR by comparison to the internal standard.

Intermolecular KIE determined by parallel experiments (Table 5.5 and Figure 5.9)

Discrete reactions were stopped and worked-up at different time points (0–60 min) following the procedure outlined below.

Six different aryl iodides were evaluated: 4-iodoanisole, 4-iodotoluene, iodobenzene, 4-chloro-iodobenzene, ethyl 4-iodobenzoate and 4-iodobenzotrifluoride.

A reaction vial was charged with K_2CO_3 (13.8 mg, 0.10 mmol), flame-dried, and allowed to cool under argon. *N*-Boc pyrrolidine amide **2** (34.1 mg, 0.10 mmol), the required aryl iodide (0.30 mmol), $Pd(OAc)_2$ (1.1 mg, 5.00 μmol) and PivOH (10.2 mg, 0.10 mmol). The reaction vessel was sealed and purged with argon, then $PhCF_3$ (100 μL) was added by syringe. The reaction tube was then placed in a preheated oil bath and stirred at 110 ºC for the specified time. The mixture was removed from the heat source and cold EtOAc (1 mL) was immediately added to stop the reaction. The resulting mixture was filtered through a pad of Celite, eluting with further EtOAc (3 × 3 mL). The solvent was removed under reduced pressure, and accurately weighed 1,3,5-trimethoxybenzene (2.5–5.0 mg, 15–30 μmol) was added. The resulting crude mixture was dissolved in $CDCl_3$ and a sample of this solution was analysed by ^{1}H NMR spectroscopy. The yield of the arylated product (**3a**, **3b**, **3c**, **3e**, **3h** and **3g**) and the % of remaining starting material (**2**) were calculated by ^{1}H NMR by comparison to the internal

standard. A corrected volume of 228 μL, accounting for both the solvent (100 μL) and the volume occupied by the reagents as measured with a volumetric flask, was used to derive concentration values. Changes in this value between experiments were assumed negligible. For raw data see Table 5.5, page 138.

8.2.6.5 VTNA and RPKA Studies

General procedure E *for the construction of reaction profiles*

Discrete reactions were stopped and worked-up at different time points following the general procedure outlined below.

A reaction vial was charged with K_2CO_3 (27.7 mg, 0.20 mmol), flame-dried, and allowed to cool under argon. *N*-Boc pyrrolidine amide **2** (68.3 mg, 0.20 mmol), 4-iodoanisole (140 mg, 0.60 mmol), $Pd(OAc)_2$ (2.2 mg, 10.0 μmol) and PivOH (20.5 mg, 0.20 mmol). The reaction vessel was sealed and purged with argon, then $PhCF_3$ (200 μL) was added by syringe. The reaction tube was then placed in a preheated oil bath and stirred at 110 ºC for the specified time. The mixture was removed from the heat source and cold EtOAc (1 mL) was immediately added to stop the reaction. The resulting mixture was filtered through a pad of Celite, eluting with further EtOAc (3 × 5 mL). The solvent was removed under reduced pressure, and accurately weighed 1,3,5-trimethoxybenzene (5.0–7.5 mg, 30–45 μmol) was added. The resulting crude mixture was dissolved in $CDCl_3$ and a sample of this solution was analysed by ^{1}H NMR spectroscopy. The yield of the arylated product (**3a**) and the % of remaining starting material (**2**) were calculated by ^{1}H NMR by comparison to the internal standard. A corrected volume of 455 μL, accounting for both the solvent (200 μL) and the volume occupied by the reagents as measured with a volumetric flask, was used to derive concentration values. Changes in this value between experiments were assumed negligible.

Standard reaction profile with AQ directing group (Figure 5.4)

Constructed following **General Procedure E**. For raw data see Table 5.4 (page 131) and Table 8.1 below.

entry	time (h)	3a (%)	[3a] (M)
1	0.08	8	0.035
2	0.25	13	0.057
3	0.5	20	0.088
4	1	27	0.119
5	2	34	0.150

Table 8.1 Time points repetition to ensure reproducibility of kinetic data, following **General Procedure E**.

Order in $Pd(OAc)_2$ (Figure 5.5)

Different profiles were constructed following **General Procedure E**, differing only by the initial loading of $Pd(OAc)_2$ (Tables 8.2 and 8.3).

	[3a] (mM)			
time (min)	**cat = 3.5 mol%**	**cat = 5.0 mol%**	**cat = 7.5 mol%**	**cat = 10 mol%**
0	0	0	0	0
5	26	35	44	48
10	35	48	53	62
15	48	53	66	79
30	57	79	101	110
45	62	97	119	132

Table 8.2 Raw data obtained following **General Procedure E** for different catalyst concentrations.

	$\Delta t \cdot [cat]^X$											
	X = 0.5				**X = 1.0**				**X = 2.0**			
time (min)	**3.5 mol%**	**5.0 mol%**	**7.5 mol%**	**10 mol%**	**3.5 mol%**	**5.0 mol%**	**7.5 mol%**	**10 mol%**	**3.5 mol%**	**5.0 mol%**	**7.5 mol%**	**10 mol%**
0	0	0	0	0	0	0	0	0	0	0	0	0
5	0.612	0.742	0.908	1.049	0.075	0.11	0.165	0.22	0.001	0.002	0.005	0.010
10	1.225	1.483	1.817	2.098	0.15	0.22	0.33	0.44	0.002	0.005	0.011	0.019
15	1.837	2.225	2.725	3.146	0.225	0.33	0.495	0.66	0.003	0.007	0.016	0.029
30	3.674	4.450	5.450	6.293	0.45	0.66	0.99	1.32	0.007	0.015	0.033	0.058
45	5.511	6.675	8.175	9.439	0.675	0.99	1.485	1.98	0.010	0.022	0.049	0.087

Table 8.3 Normalised time data for different catalyst concentrations at orders of 0.5, 1.0 and 2.0.

Order in aryl iodide (Figure 5.6)

Different profiles were constructed following **General Procedure E**, differing only by the initial loading of 4-iodoanisole (Tables 8.4 and 8.5).

	ArI = 2.25 equiv		**ArI = 3.00 equiv**		**ArI = 3.75 equiv**		**ArI = 4.50 equiv**	
time (h)	**[3a] (mM)**	**[ArI] (M)**	**[3a] (mM)**	**[ArI] (M)**	**[3a] (mM)**	**[ArI] (M)**	**[3a] (mM)**	**[ArI] (M)**
0	0	0.99	0	1.32	0	1.65	0	2.02
0.08	26	1.02	31	1.31	35	1.65	54	1.84
0.25	48	0.95	53	1.28	62	1.58	90	1.84
0.5	66	0.91	84	1.27	92	1.57	121	1.78
1	110	0.88	114	1.20	149	1.55	171	1.78
2	158	0.83	167	1.16	198	1.43	207	1.64
3	171	0.8	-	-	-	-	-	-
4	-	-	229	1.08	237	1.42	243	1.60
5	193	0.71	-	-	-	-	-	-
6	-	-	246	0.99	268	1.27	267	1.66

Table 8.4 Raw data obtained following **General Procedure E** for different concentrations of 4-iodoanisole.

	Σ [ArI]$^{X}\cdot\Delta$t							
	X = 1.0				**X = 2.0**			
time (h)	**2.25 equiv**	**3.00 equiv**	**3.75 equiv**	**4.50 equiv**	**2.25 equiv**	**3.00 equiv**	**3.75 equiv**	**4.50 equiv**
0	0	0	0	0	0	0	0	0
0.08	0.101	0.131	0.165	0.193	0.101	0.172	0.272	0.372
0.25	0.298	0.390	0.489	0.561	0.295	0.506	0.793	1.050
0.5	0.484	0.644	0.803	0.923	0.468	0.830	1.289	1.705
1	0.931	1.261	1.581	1.813	0.869	1.590	2.502	3.289
2	1.786	2.441	3.073	3.522	1.600	2.982	4.726	6.210
3	2.601	-	-	-	2.264	-	-	-
4	-	4.682	5.925	6.758	-	5.493	8.793	11.45
5	4.111	-	-	-	3.404	-	-	-
6	-	6.752	8.612	10.01	-	7.636	12.40	16.75

Table 8.5 Normalised time data for different ArI concentrations at orders of 1.0 and 2.0.

Order in pyrrolidine substrate (Figure 5.7)

Different profiles were constructed following **General Procedure E**, differing only by the initial loading of pyrrolidine **2** (Tables 8.6 and 8.7).

	2 (0.15 mmol)		**2** (0.20 mmol)	
time (h)	**[3a] (mM)**	**[2] (mM)**	**[3a] (mM)**	**[2] (mM)**
0	0	-	0	-
0.08	30	0.307	31	418
0.25	56	0.287	53	404
0.5	82	0.254	84	378
1	125	0.181	114	330
2	171	0.152	167	264
4	211	0.122	229	193
6	214	0.076	246	185

Table 8.6 Raw data obtained following **General Procedure E** for different initial loadings of pyrrolidine **2**.

	Σ **[2]$^1\cdot\Delta$t**	
time (h)	**2** (0.15 mmol)	**2** (0.20 mmol)
0	0	0
0.08	0.032	0.043
0.25	0.091	0.125
0.5	0.145	0.203
1	0.254	0.380
2	0.421	0.677
4	0.695	1.134
6	0.893	1.512

Table 8.7 Normalised time data for different initial loadings of pyrrolidine **2** at order = 1.0.

Order in K_2CO_3/PivOH (Figure 5.8)

Different profiles were constructed following **General Procedure E**, differing only by the initial loading of K_2CO_3 and PivOH (Tables 8.8).

	[3a] (mM)	
time (h)	**K_2CO_3/PivOH = 0.5 equiv**	**K_2CO_3/PivOH = 1.0 equiv**
0	0	0
0.08	22	13
0.25	40	48
0.5	62	79
1	105	110
2	171	176
4	189	229
6	207	246

Table 8.8 Raw data obtained following **General Procedure E** for different initial concentrations of pyrrolidine **2**.

“Same excess” RPKA experiments (Figure 5.22)

“Same excess” profiles were constructed following **General Procedure E**, using a lower initial loading of pyrrolidine **2** (44.4 mg, 0.13 mmol), 4-iodoanisole (124 mg, 0.53 mmol) and K_2CO_3 (18.0 mg, 0.13 mmol), while adding $KHCO_3$ (7.0 mg, 0.07 mmol), in order to match their concentrations in the standard reaction at t = 1 h (see Table 5.7, page 155).

To evaluate the presence of product inhibition, additional “same excess” profiles were built adding to the above conditions either 4-aryl-pyrrolidine **3a** (31.3 mg, 0.07 mmol) or KI (11.6 mg, 0.07 mmol).

Raw data for substrate consumption is given below (Table 8.9)

		[2] (mM)			
time (h)	**adjusted time (h)[a]**	**standard profile**	**“same excess”**	**“same excess” + 3a**	**“same excess” + KI**
0	1	-	-	-	-
0.08	1.08	418	260	254	223
0.25	1.25	404	226	231	-
0.5	1.5	378	197	225	197
1	2	330	183	194	157
2	3	264	137	168	117
3	4	-	134	134	-
4	5	193	-	-	-
5	6	-	-	126	-
7	8	185	-	-	-

Table 8.9 Raw data obtained following **General Procedure E** for “same excess” RPKA experiments. [a] Adjusted time scale to enable comparison of the profiles after t = 1 h.

Estimation of Catalyst Deactivation Profile with AQ Directing Group (Figure 5.23)

The concentration of [active cat.] at different time points was estimated through mathematic linearisation of the VTNA profile, using Microsoft Excel's add-in Solver and imposing as the only constraint that the catalyst concentration cannot increase over time.[268]

The normalised time scale for $\Sigma\,[ArI]^1\cdot[cat]_t^1\cdot\Delta t$ and the Solution found by Solver is given below (Table 8.10).

time (h)	[3a] (mM)	$\Sigma\,[ArI]^1\cdot[cat]_t^1\cdot\Delta t$ (for $[cat]_t = [cat]_0$ = constant)[a]	$\Sigma\,[ArI]^1\cdot[cat]_t^1\cdot\Delta t$ (for $[cat]_t$ = variable)[b]	$[cat]_t$ (mM)	% [cat]
0	0	0	0	21.0	100
0.1	31	0.0028	0.00207	10.6	50.6
0.3	53	0.00818	0.00476	10.2	48.4
0.5	84	0.01353	0.00676	5.49	26.2
1	114	0.02647	0.00959	3.71	17.7
1.5	141	0.03873	0.01176	3.71	17.7
2	167	0.05077	0.01388	3.71	17.7
3	207	0.07361	0.01727	2.51	12.0
4	229	0.09562	0.01895	0.70	3.33
5	233	0.11749	0.01967	0.70	3.33
6	246	0.13839	0.02037	0.70	3.33

Table 8.10 Estimation of catalyst deactivation profile with AQ directing group by calculation of variable catalyst concentration values that allow linearisation of the VTNA plot. [a] Non-linear correlation for [**3a**] *vs* $\Sigma\,[ArI]^1\cdot[cat]_t^1\cdot\Delta t$ observed. [b] Linear correlation for [**3a**] *vs* $\Sigma\,[ArI]^1\cdot[cat]_t^1\cdot\Delta t$ with $R^2 = 0.999$.

Standard reaction profile with DMAQ directing group (Scheme 6.5)

Constructed following **General Procedure E**, using pyrrolidine amide **118** (76.9 mg, 0.20 mmol) in place of pyrrolidine **2**.

time (h)	118 (%)	131a (%)	tot (%)	[118] (mM)	[131a] (mM)	[ArI] (M)
0.08	87	10	97	382	44	1.21
0.25	69	23	92	303	101	1.20
0.5	53	43	96	233	189	1.10
1	38	53	91	167	233	0.98
1.5	29	61	90	127	268	0.95
2	22	67	89	97	295	0.94
3	19	71	90	84	312	0.91
4	14	73	87	62	321	0.87
5	12	75	86	53	330	0.86
6	6	80	86	26	352	0.80

Table 8.11 Raw kinetic data for the C(4)–H arylation of pyrrolidine **118** over time.

*Order in pyrrolidine-3-DMAQ amide **118***

In addition to the data collected above, another concentration profile was constructed following **General Procedure E**, using a lower initial loading of pyrrolidine **118** (50.0 mg, 0.13 mmol).

Raw and normalised time data are given in Tables 8.12 and 8.13.

time (h)	[131a] (mM)	[118] (mM)
0	0	-
0.08	63	220
0.25	111	166
0.5	177	74
1	203	49
2	223	40
3	229	29

Table 8.12 Raw data obtained following **General Procedure E** with a lower initial concentration of pyrrolidine **118** (50.0 mg, 0.13 mmol).

	Σ [118]^1·Δt	
time (h)	**118** (0.13 mmol)	**118** (0.20 mmol)
0	0	0
0.08	0.025	0.041
0.25	0.064	0.110
0.5	0.088	0.163
1	0.119	0.263
2	0.163	0.395
4	0.198	0.486

Table 8.13 Normalised time data for different initial concentrations of pyrrolidine **118** at order = 1.0.

Comparison of the reaction profiles obtained at a different initial loading of amide **118** showed a zero-order dependency in pyrrolidine substrate (Figure 8.1).

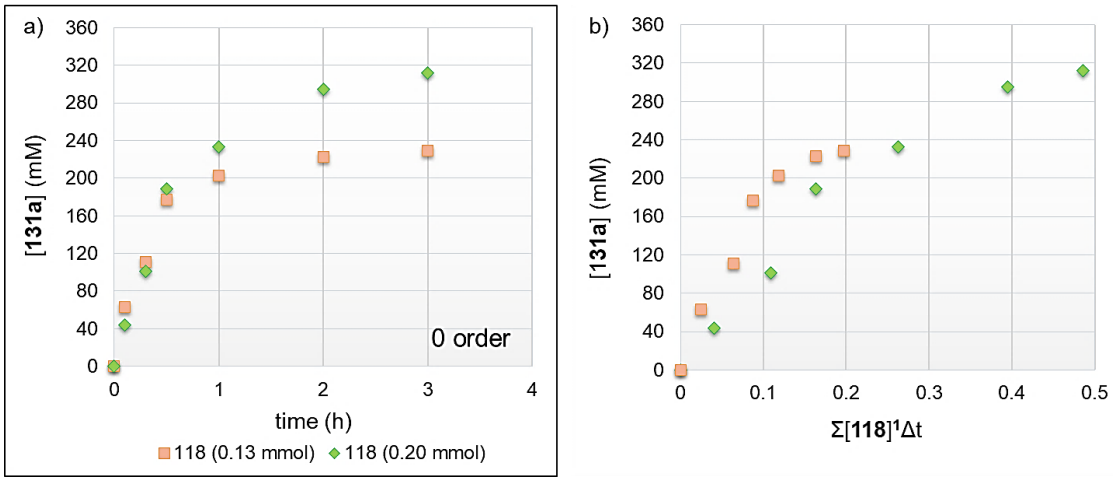


Figure 8.1 Use of VTNA to determine the kinetic order in pyrrolidine amide **118**. The profile obtained under standard arylation conditions is represented by green diamonds.

Estimation of Catalyst Deactivation Profile with DMAQ Directing Group (Figure 6.1)

The concentration of [active cat.] at different time points was estimated through mathematic linearisation of the VTNA profile, using Microsoft Excel's add-in Solver and imposing as the only constraint that the catalyst concentration cannot increase over time.[268]

The normalised time scale for $\Sigma\,[Arl]^1\cdot[cat]_t^1\cdot\Delta t$ and the Solution found by Solver is given below (Table 8.14).

time (h)	[131a] (mM)	$\Sigma\,[Arl]^1\cdot[cat]_t^1\cdot\Delta t$ (for $[cat]_t = [cat]_0$ = constant)[a]	$\Sigma\,[Arl]^1\cdot[cat]_t^1\cdot\Delta t$ (for $[cat]_t$ = variable)[b]	$[cat]_t$ (mM)	% [cat]
0	0	0	0	21.0	100
0.1	44	0.00270	0.00264	20.7	98.5
0.3	101	0.00794	0.00763	20.7	98.5
0.5	189	0.01293	0.011457	12.7	60.3
1	233	0.02417	0.015867	4.4	20.8
1.5	268	0.03463	0.017966	4.4	20.8
2	295	0.04487	0.019419	1.8	8.57
3	312	0.06491	0.020690	1.0	4.55
4	321	0.08424	0.021540	1.0	4.55
5	330	0.10300	0.022364	1.0	4.55
6	352	0.12104	0.023157	1.0	4.55

Table 8.14 Estimation of catalyst deactivation profile with AQ directing group by calculation of variable catalyst concentration values that allow linearisation of the VTNA plot. [a] Non-linear correlation for [**131a**] *vs* $\Sigma\,[Arl]^1\cdot[cat]_t^1\cdot\Delta t$ observed. [b] Linear correlation for [**131a**] *vs* $\Sigma\,[Arl]^1\cdot[cat]_t^1\cdot\Delta t$ with $R^2 = 0.997$.

8.2.6.6 Kinetic Effect of 4-Substituents on the Directing Group

Competition experiments (Table 6.8)

In each experiment, two pyrrolidine-3-carboxamides had to compete for a limiting amount of 4-iodoanisole. In particular, competition experiments were carried out between unsubstituted substrate **2** and another pyrrolidine-3-carboxamide **X**, bearing a substituent at the quinoline 4-position, following the procedure outline below.

4-NMe_2 (**118**), 4-OMe (**113**), 4-OPh (**116**) and 4-Cl (**105**) substituents were evaluated.

A reaction vial was charged with K_2CO_3 (27.7 mg, 0.20 mmol), flame-dried, and allowed to cool under argon. *N*-Boc pyrrolidine amide **2** (34.1 mg, 0.10 mmol), the required 4-substituted pyrrolidine amide **X** (0.10 mmol), 4-iodoanisole (11.7 mg, 0.05 mmol), $Pd(OAc)_2$ (2.2 mg, 10.0 μmol) and PivOH (20.5 mg, 0.20 mmol) were added sequentially. The reaction vessel was sealed and purged with argon, then $PhCF_3$ (200 μL) was added by syringe. The reaction tube was placed in a preheated oil bath and stirred at 110 ºC for 18 h. The mixture was removed from the heat source and cold EtOAc (2 mL) was immediately added to stop the reaction. The resulting mixture was filtered through a pad of Celite, eluting with further EtOAc (3 × 5 mL). The solvent was removed under reduced pressure, and accurately weighed 1,3,5-trimethoxybenzene (5.0–7.5 mg, 30–45 μmol) was added. The resulting crude mixture was dissolved in $CDCl_3$ and a sample of this solution was analysed by ^{1}H NMR spectroscopy. The yield of the corresponding arylated products (**3a** and one of **127a**, **128a**, **130a**, or **131a**) was calculated by ^{1}H NMR by comparison to the internal standard.

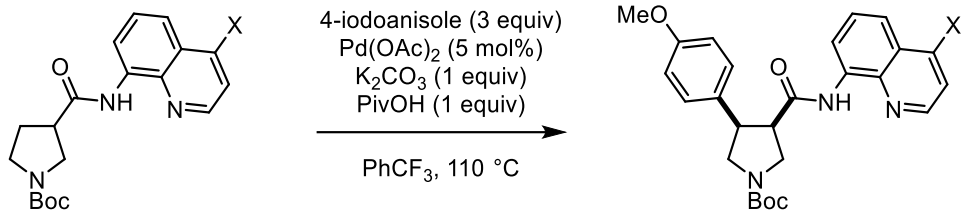
Individual arylation rates with different 4-substituted directing groups (Table 6.9 and Figure 6.3)

Discrete reactions were stopped and worked-up at different time points (0–30 min) following the procedure outlined below.

Four different substituents at the quinoline 4-position were evaluated, including 4-Cl (**105**), 4-H (**2**), 4-OMe (**113**) and 4-NMe_2 (**118**).

A reaction vial was charged with K_2CO_3 (27.7 mg, 0.20 mmol), flame-dried, and allowed to cool under argon. The required pyrrolidine substrate (0.20 mmol), 4-iodoanisole (140 mg, 0.60 mmol), $Pd(OAc)_2$ (2.2 mg, 10.0 μmol) and PivOH (20.5 mg, 0.20 mmol) were added sequentially. The reaction vessel was sealed and purged with argon, then $PhCF_3$ (200 μL) was added by syringe. The reaction tube was then placed in a preheated oil bath and stirred at 110 ºC for the specified time. The mixture was removed from the heat source and cold EtOAc (2 mL) was immediately added to stop the reaction. The resulting mixture was filtered through

a pad of Celite, eluting with further EtOAc (3 × 5 mL). The solvent was removed under reduced pressure, and accurately weighed 1,3,5-trimethoxybenzene (5.0–7.5 mg, 30–45 μmol) was added. The resulting crude mixture was dissolved in $CDCl_3$ and a sample of this solution was analysed by ^{1}H NMR spectroscopy. The yield of the arylated product (**3a**, **127a**, **128a** or **131a**) and the % of remaining starting material (**2**, **105**, **113** or **118**) were calculated by ^{1}H NMR by comparison to the internal standard. A corrected volume of 455 μL, accounting for both the solvent (200 μL) and the volume occupied by the reagents as measured with a volumetric flask, was used to derive concentration values. Changes in this value between experiments were assumed negligible.



2, 105, 113, 118 **3a, 127a, 128a, 131a**

X	time (min)	SM	[SM] (mM)	P	[P] (mM)
Cl	0	**105**	-	**127a**	0
	5		409		18
	15		400		35
	30		396		62
	45		387		70
H	0	**2**	-	**3a**	0
	5		404		26
	10		390		39
	15		377		53
	20		368		61
OMe	0	**113**	-	**128a**	0
	5		382		44
	10		374		62
	20		330		105
	30		312		136
NMe_2	0	**118**	-	**131a**	0
	5		382		44
	10		330		84
	15		303		101
	20		303		136
	45		233		189

Table 8.15 Raw kinetic data for the C(4)–arylation using different 4-substituted DGs.

9. References

(1) Maehr, H. *J. Chem. Educ.* **1985**, *62*, 114–120.

(2) Gormely, G.; Salazar, D. E. Modern Drug Discovery and Development. In *Clinical and Translational Science: Principles of Human Research*, 2nd Edition; Robertson, D., Williams, G. H., Eds.; Elsevier – Academic Press: Cambridge, MA, 2017; pp 719–743.

(3) (a) Holenz, J.; Stoy, P. *Bioorg. Med. Chem. Lett.* **2019**, *29*, 517–524. (b) Hughes, J. P.; Rees, S.; Kalindjian, S. B.; Philpott, K. L. *Br. J. Pharmacol.* **2011**, *162*, 1239–1249.

(4) (a) Wouters O. J.; McKee M.; Luyten J. *JAMA* **2020**, *323*, 844–853. (b) DiMasi, J. A.; Grabowski, H. G.; Hansen, R. W. *J. Health Econ.* **2016**, *47*, 20–33. (c) Mullard, A. *Nat. Rev. Drug Discov.* **2014**, *13*, 877.

(5) Mullard, A. *Nat. Rev. Drug Discov.* **2019**, *18*, 85–89.

(6) (a) Hay, M.; Thomas, D. W.; Craighead, J. L.; Economides, C.; Rosenthal, J. *Nat. Biotechnol.* **2014**, *32*, 40–51. (b) Bunnage, M. E. *Nat. Chem. Biol.* **2011**, *7*, 335–339. (c) Paul, S. M.; Mytelka, D. S.; Dunwiddie, C. T.; Persinger, C. C.; Munos, C. H.; Lindborg, S. R.; Schacht, A. L. *Nat. Rev. Drug Discov.* **2010**, *9*, 203–214.

(7) Dowden, H.; Munro, J. *Nat. Rev. Drug Discov.* **2019**, *18*, 495–496.

(8) (a) Harrison, R. K. *Nat. Rev. Drug Discov.* **2016**, *15*, 817–818. (b) Kola, I.; Landis, J. *Nat. Rev. Drug Discov.* **2004**, *3*, 711–716.

(9) (a) Morgan, P.; Brown, D.; Lennard, S.; Anderton, M. J.; Barrett, J. C.; Eriksson, U.; Fidock, M.; Hamrén, B.; Johnson, A.; March, R. E.; Matcham, J.; Mettetal, J.; Nicholls, D. J.; Platz, S.; Rees, S.; Snowden, M. A.; Pangalos, M. N. *Nat. Rev. Drug Discov.* **2018**, *17*, 167–181. (b) Waring, M. J.; Arrowsmith, J.; Leach, A. R.; Leeson, P. D.; Mandrell, S.; Owen, R. M.; Pairaudeau, G.; Pennie, W. D.; Pickett, S. D.; Wang, J.; Wallace, O.; Weir, A. *Nat. Rev. Drug Discov.* **2015**, *14*, 475–486. (c) Leeson, P.; Springthorpe, B. *Nat. Rev. Drug Discov.* **2007**, *6*, 881–890.

(10) Kerns, E. H.; Di, L. *Drug-like properties: concepts, structure design and methods: from ADME to toxicity optimization*; Elsevier – Academic Press: Cambridge, MA, 2008; pp 6–16.

(11) Van de Waterbeemd, H.; Smith, D. A.; Beaumont, K.; Walker, D. K. *J. Med. Chem.* **2001**, *44*, 1313–1333.

(12) Gleeson, M. P. *J. Med. Chem.* **2008**, *51*, 817–834.

(13) Waring, M. J. *Expert Opin. Drug Discov.* **2010**, *5*, 235–248.

(14) Waring, M. J. *Bioorg. Med. Chem. Lett*. **2009**, *19*, 2844–2851.

(15) Hann, M. M. *Med. Chem. Commun.* **2011**, *2*, 349–355.

(16) Mannhold, R.; Poda, G. I.; Ostermann, C.; Tetko, I. V. *J. Pharm. Sci.* **2009**, *98*, 861–893.

(17) Ran, Y.; Jain, N.; Yalkowsky, S. H. *J. Chem. Inf. Comp. Sci.* **2001**, *41*, 1208–1217.

(18) Johnson, T. W.; Dress, K. R.; Edwards, M. *Bioorg. Med. Chem. Lett.* **2009**, *19*, 5560–5564.

(19) Veber, D. F.; Johnson, S. R.; Cheng, H.; Smith, B. R.; Ward, K. W.; Kopple, K. D. *J. Med. Chem*. **2002**, *45*, 2615–2623.

(20) Nassar, A.-E. F.; Kamel, A. M.; Clarimont, C. *Drug Discov. Today* **2004**, *9*, 1020–1028.

(21) Waring, M. J.; Johnstone, C. *Bioorg. Med. Chem. Lett.* **2007**, *17*, 1759–1764.
(22) C. A. Lipinski, C. A.; Lombardo, F.; Dominy, B. W.; Feeney, P. J. *Adv. Drug Deliv. Rev.* **1997**, *23*, 3–25.
(23) (a) Bergström, C. A. S.; Strafford, M.; Lazorova, L.; Avdeef, A.; Luthman, K.; Artursson, P. *J. Med. Chem.* **2003**, *46*, 558–570. (b) Ertl, P.; Rohde, B.; Selzer, P. *J. Med. Chem.* **2000**, *43*, 3714–3717. (c) Palm, K.; Luthman, K.; Ungell, A.-L.; Strandlund, G.; Artursson, P. *J. Pharm. Sci.* **1996**, *85*, 32–39.
(24) Hughes, J. D.; Blagg, J.; Price, D. A.; Bailey, S.; DeCrescenzo, G. A.; Devraj, R. V.; Ellsworth, E.; Fobian, Y. M.; Gibbs, M. E.; Gilles, R. W.; Greene, N.; Huang, E.; Krieger-Burke, T.; Loesel, J.; Wager,T.; Whiteley, L.; Zhang, Y. *Bioorg. Med. Chem. Lett.* **2008**, *18*, 4872–4875.
(25) Lovering, F.; Bikker, J.; Humblet, C. *J. Med. Chem.* **2009**, *52*, 6752–6756.
(26) Arya, P.; Joseph, R.; Gan, Z.; Rakic, B. *Chem. Biol.* **2005**, *12*, 163–180.
(27) (a) Osolodkin, D. I.; Radchenko, E. W.; Orlov, A. A.; Voronkov, A. E.; Palyulin, V. A.; Zefirov, N. S. *Expert Opin. Drug Discov.* **2015**, *10*, 959–973. (b) Lipinski, C.; Hopkins, A. *Nature* **2004**, *432*, 855–861.
(28) Lovering, F. *Med. Chem. Commun.* **2013**, *4*, 515–519.
(29) Ritchie, T. J.; Macdonald, S. J. F. *Drug Discov. Today* **2009**, *14*, 1011–1020.
(30) Ritchie, T. J.; Macdonald, S. J. F.; Young, R. J.; Pickett, S. D. *Drug Discov. Today* **2011**, *16*, 164–171.
(31) Nadin, A.; Hattotuwagama, C.; Churcher, I. *Angew. Chem. Int. Ed.* **2012**, *51*, 1114–1122.
(32) Carr, R. A. E.; Congreve, M.; Murray, C. W.; Rees, D. C. *Drug Discov. Today* **2005**, *10*, 987–992.
(33) Congreve, M.; Carr, R.; Murray, C.; Jhoti, H. *Drug Discov. Today* **2003**, *8*, 876–877.
(34) Köster, H.; Craan, T.; Brass, S.; Herhaus, C.; Zentgraf, M.; Neumann, L.; Heine, A.; Klebe, G. *J. Med. Chem.* **2011**, *54*, 7784–7796.
(35) Murray, C. W.; Rees, D. C. *Angew. Chem. Int. Ed.* **2016**, *55*, 488–492.
(36) (a) Grygorenko, O. O.; Volochnyuk, D. M.; Ryabukhin, S. V.; Judd, D. B. *Chem. Eur. J.* **2020**, *26*, 1196–1237. (b) Campos, K. R.; Coleman, P. J.; Alvarez, J. C.; Dreher, S. D.; Garbaccio, R. M.; Terrett, N. K.; Tillyer, R. D.; Truppo, M. D.; Parmee, E. R. *Science* **2019**, *363*, eaat0805.
(37) Blakemore, D. C.; Castro, L.; Churcher, I.; Rees, D. C.; Thomas, A. W.; Wilson, D. M.; Wood, A. *Nat. Chem.* **2018**, *10*, 383–394.
(38) Brown, D. G.; Boström, J. *J. Med. Chem.* **2016**, *59*, 4443–4458.
(39) (a) Prosser, K. E.; Stokes, R. W.; Cohen, S. M. *ACS Med. Chem. Lett.*, **2020**, *11*, 1292–1298. (b) Morley, A. D.; Pugliese, A.; Birchall, K.; Bower, J.; Brennan, P.; Brown, N.; Chapman, T.; Drysdale, M.; Gilbert, I. H.; Hoelder, S.; Jordan, A.; Ley, S. V; Merritt, A.; Miller, D.; Swarbrick, M. E.; Wyatt, P. G. *Drug Discov. Today* **2013**, *18*, 1221–1227.
(40) Clemons, P. A.; Bodycombe, N. E.; Carrinski, H. A.; Wilson, J. A.; Shamji, A. F.; Wagner, B. K.; Koehler, A. N.; Schreiber, S. L. *Proc. Natl. Acad. Sci.* **2010**, *107*, 18787–18792.
(41) (a) Joule, J. A. Natural Products Containing Nitrogen Heterocycles - Some Highlights 1990–2015. In *Advances in Heterocyclic Chemistry: Heterocyclic Chemistry in the 21st Century: A Tribute to Alan Katritzky,* 1st Edition; Scriven, E. F. V., Ramsden, C. A., Eds.; Elsevier – Academic Press: Cambridge,

MA, 2016; Vol. 119, pp 81–106. (b) Galliford, C. V.; Scheidt, K. A. *Angew. Chem. Int. Ed.* **2007**, *46*, 8748–8758. (c) O'Hagan, D. *Nat. Prod. Rep.* **2000**, *17*, 435–446.

(42) (a) Taylor, R. D.; MacCoss, M.; Lawson, A. D. G. *J. Med. Chem.* **2014**, *57*, 5845–5859. (b) Aldeghi, M.; Malhotra, S.; Selwood, D. L.; Chan, A. W. E. *Chem. Biol. Drug Des.* **2014**, *83*, 450–461. (c) Vitaku, E.; Smith, D. T.; Njardarson, J. T. *J. Med. Chem.* **2014**, *57*, 10257–10274.

(43) Structures retrieved from www.drugbank.ca, as for August 2020. Wishart, D. S.; Feunang, Y. D.; Guo, A. C.; Lo, E. J.; Marcu, A.; Grant, J. R.; Sajed, T.; Johnson, D.; Li, C.; Sayeeda, Z.; Assempour, N.; Iynkkaran, I.; Liu, Y.; Maciejewski, A.; Gale, N.; Wilson, A.; Chin, L.; Cummings, R.; Le, D.; Pon, A.; Knox, C.; Wilson, M. *Nucleic Acids Res.* **2017**, *46*, D1074–D1082.

(44) Vardanyan, R.; *Piperidine-Based Drug Discovery*; Elsevier: Amsterdam; 2017.

(45) For selected reviews, see: (a) Katritzky, A. R.; Ramsden, C. A.; Joule, J. A.; Zhdankin, V. V. Synthesis of Monocyclic Rings with One Heteroatom. In *Handbook of Heterocyclic Chemistry*, 3rd Edition; Katritzky, A. R., Ramsden, C. A., Joule, J. A., Zhdankin, V. V., Eds.; Elsevier: Amsterdam, 2010; pp 652–703. (b) Deiters, A.; Martin, S. F. *Chem. Rev.* **2004**, *104*, 2199–2238. (c) Nakamura, I.; Yamamoto, Y. *Chem. Rev.* **2004**, *104*, 2127–2198. (d) Royer, J.; Bonin, M.; Micouin, L. *Chem. Rev.* **2004**, *104*, 2311–2352.

(46) For selected reviews focusing on piperidine synthesis, see: (a) Nebe, M. M.; Opatz, T. Synthesis of Piperidines and Dehydropiperidines: Construction of the Six-Membered Ring. In *Advances in Heterocyclic Chemistry*, 1st Edition; Scriven, E. F. V, Ramsden, C., Eds.; Elsevier – Academic Press: Cambridge, MA, 2017; Vol. 122, pp 191–244. (b) Buffat, M. G. P. *Tetrahedron*, **2004**, *60*, 1701–1729.

(47) For selected recent examples of cyclisation strategies towards pyrrolidines and piperidines, see: (a) Chamberlain, A. E. R.; Paterson, K. J.; Armstrong, R. J.; Twin, H. C.; Donohoe, T. J. *Chem. Commun.* **2020**, *56*, 3563–3566. (b) Ma, X.; Hazelden, I. R.; Langer, T.; Munday, R. H.; Bower, J. F. *J. Am. Chem. Soc.* **2019**, *141*, 3356–3360. (c) Boddy, A. J.; Affron, D. P.; Cordier, C. J.; Rivers, E. L.; Spivey, A. C.; Bull, J. A. *Angew. Chem. Int. Ed*. **2019**, *58*, 1458–1462. (d) Dai, X.-J.; Engl, O. D.; León, T.; Buchwald, S. L. *Angew. Chem. Int. Ed.* **2019**, *58*, 3407–3411. (e) Wang, Y.; Wen, X.; Cui, X.; Zhang, X. P. *J. Am. Chem. Soc.* **2018**, *140*, 4792–4796. (f) Barber, D. M.; Ďuriš, A.; Thompson, A. L.; Sanganee, H. J.; Dixon, D. J. *ACS Catal.* **2014**, *4*, 634.

(48) (a) Kumar, G.; Pradhan, S.; Chatterjee, I. *Chem. Asian J.* **2020**, *15*, 651–672. (b) Zhang, M.; Wang, Q.; Peng, Y.; Chen, Z.; Wan, C.; Chen, J.; Zhao, Y.; Zhang, R.; Zhang, A. Q. *Chem. Commun.* **2019**, *55*, 13048–13065.

(49) For selected reviews on heteroarenes hydrogenation, see: (a) Wiesenfeldt, M. P.; Nairoukh, Z.; Dalton, T.; Glorius, F. *Angew. Chem. Int. Ed.* **2019**, *58*, 10460–10476. (b) Liu, G.-Q.; Opatz, T. Recent Advances in the Synthesis of Piperidines: Functionalization of Preexisting Ring Systems. In *Advances in Heterocyclic Chemistry*, 1st Edition; Scriven, E. F. V, Ramsden, C., Eds.; Elsevier – Academic Press: Cambridge, MA, 2018; Vol. 125, pp 107–234. (c) Wang, D.-S.; Chen, Q.-A.; Lu, S.-M.; Zhou, Y.-G. *Chem. Rev.* **2012**, *112*, 2557–2590.

(50) For selected reviews on cycloaddition strategies, see: (a) Adrio, J.; Carretero, J. C. *Chem. Commun.* **2019**, *55*, 11979–11991. (b) Arrastia, I.; Arrieta, A.; Cossio, F. P. *Eur. J. Org. Chem.* **2018**,

5889–5904.; (c) Girling, P. R.; Kiyoi, T.; Whiting, A. *Org. Biomol. Chem.* **2011**, *9*, 3105–3121. (d) Pandey, G.; Banerjee, P.; Gadre, S. R. *Chem. Rev.* **2006**, *106*, 4484–4517.
(51) González-Bobes, F.; Fu, G. C. *J. Am. Chem. Soc.* **2006**, *128*, 5360–5361.
(52) (a) Strotman, N. A.; Sommer, S.; Fu, G. C. *Angew. Chem. Int. Ed.* **2007**, *46*, 3556–3558. (b) Powell, D. A.; Fu, G. C. *J. Am. Chem. Soc.* **2004**, *126*, 7788–7789.
(53) For a metal-free arylation of sulfonylhydrazones with (hetero)aromatic boronic acids, see: Allwood, D. M.; Blakemore, D. C.; Brown, A. D.; Ley, S. V. *J. Org. Chem.* **2014**, *79*, 328–338.
(54) (a) Yang, Y.; Niedermann, K.; Han, C.; Buchwald, S. L. *Org. Lett.* **2014**, *16*, 4638–4641. (b) Pompeo, M.; Froese, R. D. J.; Hadei, N.; Organ, M. G. *Angew. Chem. Int. Ed.* **2012**, *51*, 11354–11357. (c) Han, C.; Buchwald, S. L. *J. Am. Chem. Soc.* **2009**, *131*, 7532–7533. (d) Corley, E. G.; Conrad, K.; Murry, J. A.; Savarin, C.; Holko, J.; Boice, G. *J. Org. Chem.* **2004**, *69*, 5120–5123.
(55) Bhonde, V. R.; O'Neill, B. T.; Buchwald, S. L. *Angew. Chem. Int. Ed.* **2016**, *55*, 1849–1853.
(56) Vechorkin, O.; Proust, V.; Hu, X. *J. Am. Chem. Soc.* **2009**, *131*, 9756–9766.
(57) (a) Gonnard, L.; Guérinot, A.; Cossy, J. *Chem. Eur. J.* **2015**, *21*, 12797–12803. (b) Barré, B.; Gonnard, L.; Campagne, R.; Reymond, S.; Marin, J.; Ciapetti, P.; Brellier, M.; Guérinot, A.; Cossy, J. *Org. Lett.* **2014**, *16*, 6160–6163. (c) Despiau, C. F.; Dominey, A. P.; Harrowven, D. C.; Linclau, B. *Eur. J. Org. Chem.* **2014**, *2014*, 4335–4341.
(58) For Co-catalysed coupling of alkyl halides with diarylmanganese reagents, see: Hofmayer, M. S.; Hammann, J. M.; Haas, D.; Knochel, P. *Org. Lett.* **2016**, *18*, 6456–6459.
(59) For Fe-catalysed couplings of alkyl sulfones with Grignard reagents, see: Denmark, S. E.; Cresswell, A. J. *J. Org. Chem.* **2013**, *78*, 12593–12628.
(60) (a) Cornella, J.; Edwards, J. T.; Qin, T.; Kawamura, S.; Wang, J.; Pan, C.-M.; Gianatassio, R.; Schmidt, M.; Eastgate, M. D.; Baran, P. S. *J. Am. Chem. Soc*. **2016**, *138*, 2174–2177. (b) Wang, J.; Qin, T.; Chen, T.-G.; Wimmer, L.; Edwards, J. T.; Cornella, J.; Vokits, B.; Shaw, S. A.; Baran, P. S. *Angew. Chem. Int. Ed.* **2016**, *55*, 9676–9679. (c) Toriyama, F.; Cornella, J.; Wimmer, L.; Chen, T.-G.; Dixon, D. D.; Creech, G.; Baran, P. S. *J. Am. Chem. Soc.* **2016**, *138*, 11132–11135.
(61) Sandfort, F.; O'Neill, M. J.; Cornella, J.; Wimmer, L.; Baran, P. S. *Angew. Chem. Int. Ed.* **2017**, *56*, 3319–3323.
(62) Chen, T.-G.; Zhang, H.; Mykhailiuk, P. K.; Merchant, R. R.; Smith, C. A.; Qin, T.; Baran, P. S. *Angew. Chem. Int. Ed*. **2019**, *58*, 2454–2458.
(63) Merchant, R. R.; Edwards, J. T.; Qin, T.; Kruszyk, M. M.; Bi, C.; Che, G.; Bao, D.-H.; Qiao, W.; Sun, L.; Collins, M. R.; Fadeyi, O. O.; Gallego, G. M.; Mousseau, J. J.; Nuhant, P.; Baran, P. S. *Science*, **2018**, *360*, 75–80.
(64) C. H.; Liao, J.; Xu, J.; Piane, J. J.; Watson, M. P. *J. Am. Chem. Soc.* **2017**, *139*, 5313–5316.
(65) (a) Mennie, K. M.; Vara, B. A.; Levi, S. M. *Org. Lett.* **2020**, *22*, 556–559. (b) Molander, G. A.; Traister, K. M.; O'Neill, B. T. *J. Org. Chem.* **2014**, *79*, 5771–5780. (c) Wang, S.; Qian, Q.; Gong, H. *Org. Lett.* **2012**, *14*, 3352–3355.
(66) Wang, X.; Ma, G.; Peng, Y.; Pitsch, C. E.; Moll, B. J.; Ly, T. D.; Wang, X.; Gong, H. *J. Am. Chem. Soc.* **2018**, *140*, 14490–14497.

(67) Molander, G. A.; Traister, K. M.; O' Neill, B.T. *J. Org. Chem.* **2015**, *80*, 2907–2911.
(68) Zhao, Y.; Weix, D. J. *J. Am. Chem. Soc.* **2015**, *137*, 3237–3240.
(69) Huihui, K. M. M.; Caputo, J. A.; Melchor, Z.; Olivares, A. M.; Spiewak, A. M.; Johnson, K. A.; DiBenedetto, T. A.; Kim, S.; Ackerman, L. K. G.; Weix, D. J. *J. Am. Chem. Soc.* **2016**, *138*, 5016–5019.
(70) (a) Liao, J.; Basch, C. H.; Hoerrner, M. E.; Talley, M. R.; Boscoe, B. P.; Tucker, J. W.; Garnsey, M. R.; Watson, M. P. *Org. Lett.* **2019**, *21*, 2941–2946. (b) Yue, H.; Zhu, C.; Shen, L.; Geng, Q.; Hock, K. J.; Yuan, T.; Cavallo, L.; Rueping, M. *Chem. Sci.* **2019**, *10*, 4430–4435.
(71) Hughes, J. M. E.; Fier, P. S. *Org. Lett.* **2019**, *21*, 5650–5654.
(72) (a) Truesdell, B. L.; Hamby, T. B.; Sevov, C. S. *J. Am. Chem. Soc.* **2020**, *142*, 5884–5893. (b) Perkins, R. J.; Hughes, A. J.; Weix, D. J.; Hansen, E. C. *Org. Process Res. Dev.* **2019**, *23*, 1746–1751.
(73) (a) Primer, D. N.; Karakaya, I.; Tellis, J. C.; Molander, G. A. *J. Am. Chem. Soc.* **2015**, *137*, 2195–2198. (b) Tellis, J. C.; Primer, D. N.; Molander, G. A. *Science*, **2014**, *345*, 433–436. (c) Zuo, Z.; Ahneman, D. T.; Chu, L.; Terrett, J. A.; Doyle, A. G.; MacMillan, D. W. C. *Science*, **2014**, *345*, 437–440.
(74) Zhang, X.; MacMillan, D. W. C. *J. Am. Chem. Soc*. **2016**, *138*, 13862–13865.
(75) (a) Sakai, H. A.; Liu, W.; Le, C. "C."; MacMillan, D. W. C. *J. Am. Chem. Soc.* **2020**, *142*, 11691–11697. (b) Zhang, P.; Le, C. "C."; MacMillan, D. W. C. *J. Am. Chem. Soc.* **2016**, *138*, 8084–8087.
(76) Yi, J.; Badir, S. O.; Kammer, L. M.; Ribagorda, M.; Molander, G. A. *Org. Lett.* **2019**, *21*, 3346–3351.
(77) For selected recent examples, see: (a) Sun, Z.; Zhao, J.; Deng, H.; Tian, L.; Tang, B.; Liu, K. K.-C.; Zhu, H. Y. *Adv. Synth. Catal.* **2020**, *362*, 1502–1508. (b) Chen, Y.; Lu, P.; Wang, Y. *Org. Lett.* **2019**, *21*, 2130–2133. (c) Zuo, Z.; MacMillan, D. W. C. *J. Am. Chem. Soc.* **2014**, *136*, 5257–5260.
(78) For selected recent examples, see: (a) Pitre, S. P.; Muuronen, M.; Fishman, D. A.; Overman, L. E. *ACS Catal.* **2019**, *9*, 3413–3418. (b) Sherwood, T. C.; Li, N.; Yazdani, A. N.; Dhar, T. G. M. *J. Org. Chem.* **2018**, *83*, 3000–3012. (c) Nuhant, P.; Oderinde, M. S.; Genovino, J.; Juneau, A.; Gagné, Y.; Allais, C.; Chinigo, G. M.; Choi, C.; Sach, N. W.; Bernier, L.; Fobian, Y. M.; Bundesmann, M. W.; Khunte, B.; Frenette, M.; Fadeyi, O. O. *Angew. Chem. Int. Ed.* **2017**, *56*, 15309–15313. (d) Matsui, J. K.; Primer, D. N.; Molander, G. A. *Chem. Sci.* **2017**, *8*, 3512–3522. (e) Cheng, W.-M.; Shang, R.; Fu, M.-C.; Fu, Y. *Chem. Eur. J.* **2017**, *23*, 2537–2541. (f) Klauck, F. J. R.; James, M. J.; Glorius, F. *Angew. Chem. Int. Ed.* **2017**, *56*, 12336–12339.
(79) (a) Vo, C.-V. T.; Bode, J. W. *J. Org. Chem.* **2014**, *79*, 2809–2815. (b) Mitchell, E. A.; Peschiulli, A.; Lefevre, N.; Meerpoel, L.; Maes, B. U. W. *Chem. Eur. J.* **2012**, *18*, 10092–10142. (c) Campos, K. R. *Chem. Soc. Rev.* **2007**, 36, 1069–1084.
(80) Luo, Y.-R.; *Comprehensive Handbook of Chemical Bond Energies*; CRC Press: Boca Raton; 2007.
(81) Protonation Calculator Plugin was used for pK_a calculation, Marvin 19.27.0, 2019, ChemAxon.
(82) (a) Beak, P.; Kerrick, S. T.; Wu, S.; Chu, J. *J. Am. Chem. Soc.* **1994**, *116*, 3231–3239. (b) Kerrick, S. T.; Beak, P. *J. Am. Chem. Soc*. **1991**, *113*, 9708–9710.
(83) Campos, K. R.; Klapars, A.; Waldman, J. H.; Dormer, P. G.; Chen, C.-Y. *J. Am. Chem. Soc.* **2006**, *128*, 3538–3539.

(84) (a) Barker, G.; McGrath, J. L.; Klapars, A.; Stead, D.; Zhou, G.; Campos, K. R.; O'Brien, P. *J. Org. Chem.* **2011**, *76*, 5936–5953. (b) Barker, G.; O'Brien, P.; Campos, K. R. *Org. Lett.* **2010**, *12*, 4176–4179.
(85) (a) Beng, T. K.; Gawley, R. E. *Org. Lett.* **2011**, *13*, 394–397. (b) Stead, D.; Carbone, G.; O'Brien, P.; Campos, K. R.; Coldham, I.; Sanderson, A. *J. Am. Chem. Soc.* **2010**, *132*, 7260–7261. (c) Coldham, I.; Leonori, D. Org. Lett. **2008**, *10*, 3923–3925.
(86) Seel, S.; Thaler, T.; Takatsu, K.; Zhang, C.; Zipse, H.; Straub, B. F.; Mayer, P.; Knochel, P. *J. Am. Chem. Soc.* **2011**, *133*, 4774–4777.
(87) For selected examples, see: (a) Alagiri, K.; Kumara, G. S. R.; Prabhu, K. R. *Chem. Commun.* **2011**, *47*, 11787–11789. (b) Ghobrial, M.; Schnürch, M.; Mihovilovic, M. D. *J. Org. Chem.* **2011**, *76*, 8781–8793. (c) Liu, P.; Zhou, C.-Y.; Xiang, S.; Che, C.-M. *Chem. Commun.* **2010**, *46*, 2739–2741. (d) Li, Z.; Bohle, D. S.; Li, C.-J. *Proc. Natl. Acad. Sci.* **2006**, *103*, 8928–8933. (e) Li, Z.; Li, C.-J. *J. Am. Chem. Soc.* **2005**, *127*, 6968–6969.
(88) For a 2-steps metal-free oxidative arylation, see: Schweitzer-Chaput, B.; Klussmann, M. *Eur. J. Org. Chem.* **2013**, *2013*, 666–671.
(89) For a 2-steps photochemical oxidataion/arylation process, see: Freeman, D. B.; Furst, L.; Condie, A. G.; Stephenson, C. R. J. *Org. Lett.* **2012**, *14*, 94–97.
(90) Baslé, O.; Li, C.-J. *Org. Lett.* **2008**, *10*, 3661–3663.
(91) (a) Seidel, D. *Acc. Chem. Res.* **2015**, *48*, 317–328. (b) Haibach, M. C.; Seidel, D. *Angew. Chem. Int. Ed.* **2014**, *53*, 5010–5036. (c) Peng, B.; Maulide, N. *Chem. Eur. J.* **2013**, *19*, 13274–13287.
(92) (a) Chen, W.; Wilde, R. G.; Seidel, D. *Org. Lett.* **2014**, *16*, 730–732. (b) Jurberg, I. D.; Peng, B.; Wöstefeld, E.; Wasserloos, M.; Maulide, N. *Angew. Chem. Int. Ed.* **2012**, *51*, 1950–1953.
(93) Chen, W.; Ma, L.; Paul, A.; Seidel, D. *Nat. Chem.* **2018**, *10*, 165–169.
(94) Chen, W.; Paul, A.; Abboud, K. A.; Seidel, D. *Nat. Chem.* **2020**, *12*, 545–550.
(95) Yoshikai, N.; Mieczkowski, A.; Matsumoto, A.; Ilies, L.; Nakamura, E. *J. Am. Chem. Soc.* **2010**, *132*, 5568–5569.
(96) McNally, A.; Prier, C. K.; MacMillan, D. W. C. *Science*, **2011**, *334*, 1114–1117.
(97) Walker, M. M.; Koronkiewicz, B.; Chen, S.; Houk, K. N.; Mayer, J. M.; Ellman, J. A. *J. Am. Chem. Soc*. **2020**, *142*, 8194–8202.
(98) Prier, C. K.; MacMillan, D. W. C. *Chem. Sci.* **2014**, *5*, 4173–4178.
(99) Ahneman, D. T.; Doyle, A. G. *Chem. Sci.* **2016**, *7*, 7002–7006.
(100) MacMillan, D. W. C.; Cuthbertson, J. D.; Terrett, J. A.; Shurtleff, V. W.; Shaw, M. H. *Science*, **2016**, *352*, 1304–1308.
(101) Grainger, R.; Heightman, T. D.; Ley, S. V.; Lima, F.; Johnson, C. N. *Chem. Sci.* **2019**, *10*, 2264–2271.
(102) (a) Zhou, L.; Shen, Y.-B.; An, X.-D.; Li, X.-J.; Li, S.-S.; Liu, Q.; Xiao, J. *Org. Lett.* **2019**, *21*, 8543–8547. (b) Sundararaju, B.; Achard, M.; Sharma, G. V. M.; Bruneau, C. *J. Am. Chem. Soc.* **2011**, *133*, 10340–10343.

(103) (a) Lee, M.; Sanford, M. S. *Org. Lett.* **2017**, *19*, 572–575. (b) Osorio-Nieto, U.; Chamorro-Arenas, D.; Quintero, L.; Höpfl, H.; Sartillo-Piscil, F. *J. Org. Chem.* **2016**, *81*, 8625–8632.
(104) Sarver, P. J.; Bacauanu, V.; Schultz, D. M.; DiRocco, D. A.; Lam, Y.; Sherer, E. C.; MacMillan, D. W. C. *Nat. Chem.* **2020**, *12*, 459–467.
(105) Oeschger, R.; Su, B.; Yu, I.; Ehinger, C.; Romero, E.; He, S.; Hartwig, J. *Science*, **2020**, *368*, 736–741.
(106) Millet, A.; Larini, P.; Clot, E.; Baudoin, O. *Chem. Sci.* **2013**, *4*, 2241–2247.
(107) Lin, W.; Zhang, K.-F.; Baudoin, O. *Nat. Catal.* **2019**, *2*, 882–888.
(108) Chen, M.; Liu, F.; Dong, G. *Angew. Chem. Int. Ed.* **2018**, *57*, 3815–888.
(109) (a) Wencel-Delord, J.; Glorius, F. *Nat. Chem.* **2013**, *5*, 369–375. (b) Yamaguchi, J.; Yamaguchi, A. D.; Itami, K. *Angew. Chem. Int. Ed.* **2012**, *51*, 8960–9009. (c) Godula, K.; Sames, D. *Science* **2006**, 312, 67–72.
(110) (a) Balcells, D.; Clot, E.; Eisenstein, O. *Chem. Rev.* **2010**, *110*, 749–823. (b) Boutadla, Y.; Davies, D. L.; Macgregor, S. A.; Poblador-Bahamonde, A. I. *Dalton Trans.* **2009**, *0*, 5820–5831.
(111) For selected reviews, see: (a) Davies, D. L.; Macgregor, S. A.; McMullin, C. L. *Chem. Rev.* **2017**, *117*, 8649–8709. (b) Ackermann, L. *Chem. Rev.* **2011**, *111*, 1315–1345. (c) Lapointe, D.; Fagnou, K. *Chem. Lett.* **2010**, *39*, 1118–1126.
(112) Liu, J.-B.; Tian, Y.-Y.; Zhang, X.; Wang, L.-L.; Chen, D.-Z. *Dalt. Trans.* **2018**, *47*, 4893–4901.
(113) Davies, D. L.; Donald, S. M. A.; Macgregor, S. A. *J. Am. Chem. Soc.* **2005**, *127*, 13754–13755.
(114) (a) Sambiagio, C.; Schönbauer, D.; Blieck, R.; Dao-Huy, T.; Pototschnig, G.; Schaaf, P.; Wiesinger, T.; Zia, M. F.; Wencel-Delord, J.; Besset, T.; Maes, B. U. W.; Shnürch, M. *Chem. Soc. Rev.* **2018**, *47*, 6603–6743. (b) Chen, Z.; Wang, B.; Zhang, J.; Yu, W.; Liu, Z.; Zhang, Y. *Org. Chem. Front.* **2015**, *2*, 1107–1295.
(115) Alberico, D.; Scott, M. E.; Lautens, M. *Chem. Rev.* **2007**, *107*, 174–238.
(116) (a) Sasmal, S.; Dutta, U.; Lahiri, G. K.; Maiti, D. *Chem. Lett.* **2020**, *49*, 1406–1420. (b) Yang, J. *Org. Biomol. Chem.* **2015**, *13*, 1930–1941.
(117) (a) He, J.; Wasa, M.; Chan, K. S. L.; Shao, Q.; Yu, J.-Q. *Chem. Rev.* **2017**, *117*, 8754–8786. (b) Baudoin, O. *Chem. Soc. Rev.* **2011**, *40*, 4902–4911.
(118) Baudoin, O. *Acc. Chem. Res.* **2017**, *50*, 1114–1123.
(119) Davies, H. M. L. *J. Org. Chem.* **2019**, *84*, 12722–12745.
(120) White, M. C. *Science*, **2012**, *335*, 807–809.
(121) St John-Campbell, S.; Bull, J. A. *Adv. Synth. Catal.* **2019**, *361*, 3662–3682.
(122) (a) Dangel, B. D.; Godula, K.; Youn, S. W.; Sezen, B.; Sames, D. *J. Am. Chem. Soc.* **2002**, *124*, 11856–11857. (b) Balavoine, G.; Clinet, J. C. *J. Organomet. Chem.* **1990**, *390*, c84–c88.
(123) (a) Shabashov, D.; Daugulis, O. *Org. Lett.* **2005**, *7*, 3657–3659. (b) Kalyani, D.; Deprez, N. R.; Desai, L. V; Sanford, M. S. *J. Am. Chem. Soc.* **2005**, *127*, 7330–7331.
(124) Zaitsev, V. G.; Shabashov, D.; Daugulis, O. *J. Am. Chem. Soc.* **2005**, *127*, 13154–13155.
(125) Shabashov, D.; Daugulis, O. *J. Am. Chem. Soc.* **2010**, *132*, 3965–3972.

(126) For a DFT study on the mechanism of a related Pd-catalysed, AQ-assisted C(sp^3)–H arylation, see: Wei, Y.; Tang, H.; Cong, X.; Rao, B.; Wu, C.; Zeng, X. *Org. Lett.* **2014**, *16*, 2248–2251.
(127) For the isolation of an aryl-Pd(IV) complex, see: Vicente, J.; Arcas, A.; Juliá-Hernández, F.; Bautista, D. *Angew. Chem. Int. Ed.* **2011**, *50*, 6896–6899.
(128) (a) Rej, S.; Ano, Y.; Chatani, N. *Chem. Rev.* **2020**, *120*, 1788–1887. (b) Rouquet, G.; Chatani, N. *Angew. Chem. Int. Ed.* **2013**, *52*, 11726–11743.
(129) For selected examples, see: (a) Kinsinger, T.; Kazmaier, U. *Org. Lett.* **2018**, *20*, 7726–7730. (b) Wang, B.; Nack, W. A.; He, G.; Zhang, S.-Y.; Chen, G. *Chem. Sci.* **2014**, *5*, 3952–3957. (c) Feng, Y.; Chen, G. *Angew. Chem. Int. Ed.* **2010**, *49*, 958− 961. (d) Reddy, B. V. S.; Reddy, L. R.; Corey, E. J. *Org. Lett.* **2006**, *8*, 3391–3394.
(130) For selected examples, see: (a) Parella, R.; Gopalakrishnan, B.; Babu, S. A. *Org. Lett.* **2013**, *15*, 3238–3241. (b) Hoshiya, N.; Kobayashi, T.; Arisawa, M.; Shuto, S. *Org. Lett.* **2013**, *15*, 6202–6205.
(131) For selected examples of cyclobutane C–H functionalisation, see: (a) Beck, J. C.; Lacker, C. R.; Chapman, L. M.; Reisman, S. E. *Chem. Sci.* **2019**, *10*, 2315–2319. (b) Chapman, L. M.; Beck, J. C.; Wu, L.; Reisman, S. E. *J. Am. Chem. Soc.* **2016**, *138*, 9803–9806. (c) Gutekunst, W. R.; Gianatassio, R.; Baran, P. S. *Angew. Chem. Int. Ed.* **2012**, *51*, 7507−7510.
(132) Nack, W. A.; Wang, B.; Wu, X.; Jiao, R.; He, G.; Chen, G. *Org. Chem. Front.* **2016**, *3*, 561−564.
(133) Zhang, X.; Lu, G.; Sun, M.; Mahankali, M.; Ma, Y.; Zhang, M.; Hua, W.; Hu, Y.; Wang, Q.; Chen, J.; He, G.; Qi, X.; Shen, W.; Liu, P.; Chen, G. *Nat. Chem*. **2018**, *10*, 540–548.
(134) Tong, H.-R.; Zheng, S.; Li, X.; Deng, Z.; Wang, H.; He, G.; Peng, Q.; Chen, G. *ACS Catal.* **2018**, *8*, 11502–11512.
(135) For selected examples, see: (a) Yan, S.-Y.; Han, Y.-Q.; Yao, Q.-J.; Nie, X.-L.; Liu, L.; Shi, B.-F. *Angew. Chem. Int. Ed.* **2018**, *57*, 9093–9097. (b) He, G.; Zhang, S.-Y.; Nack, W. A.; Pearson, R.; Rabb-Lynch, J.; Chen, G. *Org. Lett.* **2014**, *16*, 6488–6491. (c) Chen, F.-J.; Zhao, S.; Hu, F.; Chen, K.; Zhang, Q.; Zhang, S.-Q.; Shi, B.-F. *Chem. Sci.* **2013**, *4*, 4187–4192.
(136) For selected examples, see: (a) Bauer, M.; Wang, W.; Lorion, M. M.; Dong, C.; Ackermann, L. *Angew. Chem. Int. Ed.* **2018**, *57*, 203–207. (b) Gu, Q.; Al Mamari, H. H.; Graczyk, K.; Diers, E.; Ackermann, L. *Angew. Chem. Int. Ed.* **2014**, *53*, 3868–3871.
(137) Chen, K.; Li, Z.-W.; Shen, P.-X.; Zhao, H.-W.; Shi, Z.-J. *Chem. Eur. J.* **2015**, *21*, 7389–7393.
(138) For selected examples, see: (a) Ting, C. P.; Maimone, T. J. *Angew. Chem. Int. Ed.* **2014**, *53*, 3115–3119. (b) Gutekunst, W. R.; Baran, P. S. *J. Am. Chem. Soc.* **2011**, *133*, 19076–19079.
(139) For selected examples, see: (a) Mu, D.; Gao, F.; Chen, G.; He, G. *ACS Catal.* **2017**, *7*, 1880–1885. (b) Jerhaoui, S.; Chahdoura, F.; Rose, C.; Djukic, J.-P.; Wencel-Delord, J.; Colobert, F. *Chem. Eur. J.* **2016**, *22*, 17397−17406.
(140) Gong, W.; Zhang, G.; Liu, T.; Giri, R.; Yu, J.-Q. *J. Am. Chem. Soc.* **2014**, *136*, 16940–16946.
(141) (a) Zhang, S.-K.; Yang, X.-Y.; Zhao, X.-M.; Li, P.-X.; Niu, J.-L.; Song, M.-P. *Organometallics* **2015**, *34*, 4331–4339. (b) Liu, J.; Xie, Y.; Zeng, W.; Lin, D.; Deng, Y.; Lu, X. *J. Org. Chem.* **2015**, *80*, 4618–4626.

(142) For selected examples, see: (a) Fan, M.; Ma, D. *Angew. Chem. Int. Ed.* **2013**, *52*, 12152–12155. (b) Rodríguez, N.; Romero-Revilla, J. A.; Fernández-Ibáñez, M. Á.; Carretero, J. C. *Chem. Sci.* **2013**, *4*, 175–179. (c) He, G.; Chen, G. *Angew. Chem. Int. Ed.* **2011**, *50*, 5192–5196.
(143) (a) Xia, G.; Zhuang, Z.; Liu, L.-Y.; Schreiber, S. L.; Melillo, B.; Yu, J.-Q. *Angew. Chem. Int. Ed.* **2020**, *59*, 7783–7787. (b) Xia, G.; Weng, J.; Liu, L.; Verma, P.; Li, Z.; Yu, J.-Q. *Nat. Chem.* **2019**, *11*, 571–577.
(144) (a) Zhang, Z.; Li, X.; Song, M.; Wan, Y.; Zheng, D.; Zhang, G.; Chen, G. *J. Org. Chem.* **2019**, *84*, 12792–12799. (b) Berger, M.; Chauhan, R.; Rodrigues, C. A. B.; Maulide, N. *Chem. Eur. J.* **2016**, *22*, 16805–16808. (c) He, G.; Zhang, S.-Y.; Nack, W. A.; Li, Q.; Chen, G. *Angew. Chem. Int. Ed.* **2013**, *52*, 11124–11128.
(145) (a) Nicke, L.; Horx, P.; Harms, K.; Geyer, A. *Chem. Sci.* **2019**, *10*, 8634–8641. (b) Verho, O.; Pourghasemi Lati, M.; Oschmann, M. *J. Org. Chem.* **2018**, *83*, 4464–4476. (c) Deguchi, T.; Xin, H.-L.; Morimoto, H.; Ohshima, T. *ACS Catal.* **2017**, *7*, 3157–3161. (d) Nishii, Y.; Hirai, T.; Fernandez, S.; Knochel, P.; Mashima, K. *Eur. J. Org. Chem.* **2017**, *2017*, 5010–5014. (e) Liao, G.; Yin, X.-S.; Chen, K.; Zhang, Q.; Zhang, S.-Q.; Shi, B.-F. *Nat. Commun.* **2016**, *7*, 12901.
(146) For reviews, see: (a) Higham, J.; Bull, J. A. *Org. Biomol. Chem.* **2020**, *18*, 7291–7315. (b) St John-Campbell, S.; Bull, J. A., *Org. Biomol. Chem.* **2018**, *16*, 4582–4595.
(147) For reviews, see: (a) Shao, Q.; Wu, K.; Zhuang, Z.; Qian, S.; Yu, J.-Q. *Acc. Chem. Res.* **2020**, *53*, 833–851. (b) Engle, K. M.; Mei, T.-S.; Wasa, M.; Yu, J.-Q. *Acc. Chem. Res.* **2012**, *45*, 788–802.
(148) Saint-Denis, T. G.; Zhu, R.-Y.; Chen, G.; Wu, Q.-F.; Yu, J.-Q. *Science*, **2018**, *359*, eaao4798.
(149) Giri, R.; Maugel, N.; Li, J.; Wang, D.; Breazzano, S. P.; Saunders, L. B.; Yu, J. *J. Am. Chem. Soc.* **2007**, *129*, 3510.
(150) For selected recent examples see: (a) Wu, Q.; Shen, P.; He, J.; Wang, X.; Zhang, F.; Shao, Q.; Zhu, R.-Y.; Mapelli, C.; Qiao, J. X.; Poss, M. A.; Yu, J. *Science*, **2017**, *355*, 499–503. (b) Chen, G.; Gong, W.; Zhuang, Z.; Andrä, M. S.; Chen, Y.-Q.; Hong, X.; Yang, Y.-F.; Liu, T.; Houk, K. N.; Yu, J.-Q. *Science*, **2016**, *353*, 1023–1027. (c) Chan, K. S. L.; Fu, H. Y.; Yu, J. Q. *J. Am. Chem. Soc.* **2015**, *137*, 2042–2046. (d) He, J.; Li, S.; Deng, Y.; Fu, H.; Laforteza, B. N.; Spangler, J. E.; Homs, A.; Yu, J.-Q. *Science*, **2014**, *343*, 1216–1220. (e) Chan, K. S. L.; Wasa, M.; Chu, L.; Laforteza, B. N.; Miura, M.; Yu, J.-Q. *Nat. Chem.* **2014**, *6*, 146–150. (f) Xiao, K.-J.; Lin, D. W.; Miura, M.; Zhu, R.-Y.; Gong, W.; Wasa, M.; Yu, J.-Q. *J. Am. Chem. Soc.* **2014**, *136*, 8138–8142.
(151) (a) Hu, L.; Shen, P.-X.; Shao, Q.; Hong, K.; Qiao, J. X.; Yu, J.-Q. *Angew. Chem. Int. Ed.* **2019**, *58*, 2134–2138. (b) Chen, G.; Zhuang, Z.; Li, G.-C.; Saint-Denis, T. G.; Hsiao, Y.; Joe, C. L.; Yu, J.-Q. *Angew. Chem. Int. Ed.* **2017**, *56*, 1506–1509.
(152) (a) Rodrigalvarez, J.; Nappi, M.; Azuma, H.; Flodén, N. J.; Burns, M. E.; Gaunt, M. J. *Nat. Chem.* **2020**, *12*, 76–81. (b) Zhuang, Z.; Yu, J.-Q. *J. Am. Chem. Soc.* **2020**, *142*, 12015–12019. (c) He, C.; Whitehurst, W. G.; Gaunt, M. J. *Chem* **2019**, *5*, 1031–1058.
(153) Antermite, D.; Bull, J. A. *Synthesis* **2019**, *51*, 3171–3204.
(154) Pastine, S. J.; Gribkov, D. V.; Sames, D. *J. Am. Chem. Soc.* **2006**, *128*, 14220–14221.

(155) (a) Peschiulli, A.; Smout, V.; Storr, T. E.; Mitchell, E. A.; Eliáš, Z.; Herrebout, W.; Berthelot, D.; Meerpoel, L.; Maes, B. U. W. *Chem. Eur. J.* **2013**, *19*, 10378–10387. (b) Prokopcová, H.; Bergman, S. D.; Aelvoet, K.; Smout, V.; Herrebout, W.; Van der Veken, B.; Meerpoel, L.; Maes, B. U. W. *Chem. Eur. J.* **2010**, *16*, 13063–13067.

(156) Spangler, J. E.; Kobayashi, Y.; Verma, P.; Wang, D.-H.; Yu, J.-Q. *J. Am. Chem. Soc.* **2015**, *137*, 11876–11879.

(157) Jain, P.; Verma, P.; Xia, G.; Yu, J.-Q. *Nat. Chem.* **2017**, *9*, 140–144.

(158) Jiang, H.-J.; Zhong, X.-M.; Yu, J.; Zhang, Y.; Zhang, X.; Wu, Y.-D.; Gong, L.-Z. *Angew. Chem. Int. Ed.* **2019**, *58*, 1803–1807.

(159) Greβies, S.; Klauck, F. J. R.; Kim, J. H.; Daniliuc, C. G.; Glorius, F. *Angew. Chem. Int. Ed.* **2018**, *57*, 9950–9954.

(160) Topczewski, J. J.; Cabrera, P. J.; Saper, N. I.; Sanford, M. S. *Nature* **2016**, *531*, 220–224.

(161) (a) Aguilera, E. Y.; Sanford, M. S. *Organometallics* **2019**, *38*, 138–142. (b) Dewyer, A. L.; Zimmerman, P. M. *ACS Catal.* **2017**, *7*, 5466–5477.

(162) Cabrera, P. J.; Lee, M.; Sanford, M. S. *J. Am. Chem. Soc.* **2018**, *140*, 5599–5606.

(163) For an additional recent example, see: Li, Z.; Dechantsreiter, M.; Dandapani, S. *J. Org. Chem*. **2020**, *85*, 6747–6760.

(164) Lee, M.; Adams, A.; Cox, P. B.; Sanford, M. S. *Synlett* **2019**, *30*, 417–422.

(165) Affron, D. P.; Davis, O. A.; Bull, J. A. *Org. Lett.* **2014**, *16*, 4956–4959.

(166) Yang, X.; Sun, T.-Y.; Rao, Y. *Chem. Eur. J.* **2016**, 22, 3273–3277.

(167) Affron, D. P.; Bull, J. A. *Eur. J. Org. Chem.* **2016**, *2016*, 139–149.

(168) For the use of *N*-Pivaloyl group, see: Feng, R.; Wang, B.; Liu, Y.; Liu, Z.; Zhang, Y. *Eur. J. Org. Chem.* **2015**, *2015*, 142–151.

(169) Kayser, S.; Hansen, J. C.; Staudt, M.; Moroz, A.; Larsen, Y.; Temperini, P.; Yi, F.; Syrenne, J. T.; Krogsgaard-Larsen, N.; Iliadis, S.; Nielsen, B.; Hansen, K. B.; Pickering, D. S.; Bunch, L. *ACS Chem. Neurosci.* **2020**, *11*, 674–701.

(170) Probst, N. P.; Grelier, G.; Dahaoui, S.; Alami, M.; Gandon, V.; Messaoudi, S. *ACS Catal.* **2018**, *8*, 7781–7786.

(171) (a) Johnson, F. *Chem. Rev.* **1968**, *68*, 375–413. (b) Chow, Y. L.; Colón, C. J.; Tam, J. N. S. *Can. J. Chem.* **1968**, *46*, 2821–2825.

(172) (a) Yu, Q.-Y.; Zhong, H.-M.; Sun, W.-W.; Zhang, S.-J.; Cao, P.; Dong, X.-P.; Qin, H.-B.; Liu, J.-K.; Wu, B. *Asian J. Org. Chem.* **2016**, *5*, 608–612. (b) Zhang, S.-J.; Sun, W.-W.; Yu, Q.-Y.; Cao, P.; Dong, X.-P.; Wu, B. *Tetrahedron Lett.* **2017**, *58*, 606–609.

(173) Mondal, B.; Roy, B.; Kazmaier, U. *J. Org. Chem.* **2016**, *81*, 11646–11655.

(174) Verho, O.; Maetani, M.; Melillo, B.; Zoller, J.; Schreiber, S. L. *Org. Lett.* **2017**, *19*, 4424–4427.

(175) Maetani, M.; Zoller, J.; Melillo, B.; Verho, O.; Kato, N.; Pu, J.; Comer, E.; Schreiber, S. L. *J. Am. Chem. Soc.* **2017**, *139*, 11300–11306.

(176) Shang, M.; Feu, K. S.; Vantourout, J. C.; Barton, L. M.; Osswald, H. L.; Kato, N.; Gagaring, K.; McNamara, C. W.; Chen, G.; Hu, L.; Ni, S.; Fernández-Canelas, P.; Chen, M.; Merchant, R. R.; Qin, T.; Schreiber, S. L.; Melillo, B.; Yu, J.-Q.; Baran, P. S. *Proc. Natl. Acad. Sci.* **2019**, *116*, 8721–8727.
(177) Gerry, C. J.; Wawer, M. J.; Clemons, P. A.; Schreiber, S. L. *J. Am. Chem. Soc.* **2019**, *141*, 10225–10235.
(178) Hutskalova, V.; Mykhailiuk, P. K. *Org. Biomol. Chem.* **2019**, *17*, 4342–4349.
(179) Ye, S.; Yang, W.; Coon, T.; Fanning, D.; Neubert, T.; Stamos, D.; Yu, J.-Q. *Chem. Eur. J.* **2016**, *22*, 4748–4752.
(180) Van Steijvoort, B. F.; Kaval, N.; Kulago, A. A.; Maes, B. U. W. *ACS Catal.* **2016**, *6*, 4486–4490.
(181) For an additional recent example, see: Alemán-Ponce de León, D.; Sánchez-Chávez, A. C.; Polindara-García, L. A. *J. Org. Chem.* **2019**, *84*, 12809–12834.
(182) O' Donovan, D. H.; Aillard, P.; Berger, M.; de la Torre, A.; Petkova, D.; Knittl-Frank, C.; Geerdink, D.; Kaiser, M.; Maulide, N. *Angew. Chem. Int. Ed.* **2018**, *57*, 10737–10741.
(183) Antermite, D.; Affron, D. P.; Bull, J. A. *Org. Lett.* **2018**, *20*, 3948–3952.
(184) Fleischmann, R.; Pangan, A. L.; Song, I.-H.; Mysler, E.; Bessette, L.; Peterfy, C.; Durez, P.; Ostor, A. J.; Li, Y.; Zhou, Y.; *et al. Arthritis Rheumatol.* **2019**, *71*, 1788–1800.
(185) Bourin, M.; Chue, P.; Guillon, Y. *CNS Drug Rev.* **2001**, *7*, 25–47.
(186) Pipkorn, U.; Bende, M.; Hedner, J.; Hednerm, T. *Allergy* **1985**, *40*, 491–496.
(187) (a) Heerspink, H. J. L.; Parving, H.-H.; Andress, D. L.; Bakris, G.; Correa-Rotter, R.; Hou, F.-F.; Kitzman, D. W.; Kohan, D.; Makino, H.; McMurray, J. J. V; *et al. Lancet* **2019**, *393*, 1937–1947. (b) Chiappori, A. A.; Haura, E.; Rodriguez, F. A.; Boulware, D.; Kapoor, R.; Neuger, A. M.; Lush, R.; Padilla, B.; Burton, M.; Williams, C.; Simon, G.; Antonia, S.; Sullivan, D. M.; Bepler, G. *Clin. Cancer Res.* **2008**, 14, 1464–1469.
(188) Zeidner, J. F.; Karp, J. E. *Leuk. Res.* **2015**, *39*, 13121318.
(189) Charnigo, R. J.; Beidler, D.; Rybin, D.; Pittman, D. D.; Tan, B.; Howard, J.; Michelson, A. D.; Frelinger, A. L., III; Clarke, N. *Clin. Transl. Sci.* **2019**, *12*, 180–188.
(190) Lansdell, M. I.; Hepworth, D.; Calabrese, A.; Brown, A. D.; Blagg, J.; Burring, D. J.; Wilson, P.; Fradet, D.; Brown, T. B.; Quinton, F.; *et al. J. Med. Chem.* **2010**, *53*, 3183–3197.
(191) Weng, Q.; Che, J.; Zhang, Z.; Zheng, J.; Zhan, W.; Lin, S.; Tian, T.; Wang, J.; Gai, R.; Hu, Y.; *et al. J. Med. Chem.* **2019**, *62*, 3268–3285.
(192) (a) Meyers, M. J.; Liu, J.; Liu, Z.; Ma, H.; Dai, L.; Adah, D.; Zhao, S.; Li, X.; Liu, X.; Lu, Y.; *et al. ACS Med. Chem. Lett*. **2019**, *10*, 966–971. (b) Meyers, M. J.; Liu, J.; Xu, J.; Leng, F.; Guan, J.; Liu, Z.; McNitt, S. A.; Qin, L.; Dai, L.; Ma, H.; *et al. J. Med. Chem.* **2019**, *62*, 3503–3512.
(193) Wang, Y.; Zhao, H.; Brewer, J. T.; Li, H.; Lao, Y.; Amberg, W.; Behl, B.; Akritopoulou-Zanze, I.; Dietrich, J.; Lange, U. E. W. ; *et al. J. Med. Chem.* **2018**, *61*, 7486–7502.
(194) Dawadi, S.; Simmons, N.; Miklossy, G.; Bohren, K. M.; Faver, J. C.; Ucisik, M. N.; Nyshadham, P.; Yu, Z.; Matzuk, M. M. *Proc. Natl. Acad. Sci.* **2020**, *117*, 16782–16789.
(195) For a comparison with the chemical shifts of NC*H*Ar protons in *N*-Boc 2-aryl pyrrolidine-3-carboxylic acid derivatives, see: Buchholz, M.; Reiβig, H.-U. *Eur. J. Org. Chem*. **2003**, *2003*, 3524–3533.

(196) Chung, J. Y. L.; Wasicak, J. T.; Arnold, W. A.; May, C. S.; Nadzan, A. M.; Holladay, M. W. *J. Org. Chem.* **1990**, *55*, 270–275.
(197) Lafrance, M.; Fagnou, K. *J. Am. Chem. Soc.* **2006**, *128*, 16496–16497.
(198) For selected examples, see: (a) Nadres, E. T.; Santos, G. I. F.; Shabashov, D.; Daugulis, O. *J. Org. Chem.* **2013**, *78*, 9689–9714. (b) Roman, D. S.; Charette, A. B. *Org. Lett.* **2013**, *15*, 4394–4397.
(199) (a) Tanji, Y.; Hamaguchi, R.; Tsuji, Y.; Fujihara, T. *Chem. Commun.* **2020**, *56*, 3843–3846. (b) Tanji, Y.; Mitsutake, N.; Fujihara, T.; Tsuji, Y. *Angew. Chem. Int. Ed.* **2018**, *57*, 10314–10317.
(200) For a study on the conformational difference between *N*-trifluoroacetyl piperidine and *N*-piperidine amides, see: Shlykov, S. A.; Phien, T. D.; Trang, N. H. *Tetrahedron* **2017**, *73*, 5311–5320.
(201) Hirsch, J. A. Table of Conformational Energies–1967. In *Topics in Stereochemistry*; Allinger, N. L., Eliel, E. L. Eds.; John Wiley & Sons, Inc.: New York, 1967; Vol. 1; pp 199–222.
(202) (a) Lambert, J. B.; Goldstein, J. E. *J. Am. Chem. Soc.* **1977**, *99*, 5689–5693. (b) Lambert, J. B.; Featherman, S. I. *Chem. Rev.* **1975**, *75*, 611–626.
(203) Abraham, R. J.; Mobli, M.; Smith, R. J. *Magn. Reson. Chem.* **2003**, *41*, 26–36.
(204) For a recent example, see: Andrä, M. S.; Schifferer, L.; Pollok, C. H.; Merten, C.; Gooßen, L. J.; Yu, J.-Q. *Chem. A Eur. J.* **2019**, *25*, 8503–8507.
(205) Gopalakrishnan, B.; Babu, S. A.; Padmavathi, R. *Tetrahedron* **2015**, *71*, 8333–8349.
(206) Roane, J.; Daugulis, O. *J. Am. Chem. Soc.* **2016**, *138*, 4601–4607.
(207) (a) Evans, D. A.; Carter, P. H.; Dinsmore, C. J.; Barrow, J. C.; Katz, J. L.; Kung, D. W. *Tetrahedron Lett.* **1997**, *38*, 4535–4538. (b) Flynn, D. L.; Zelle, R. E.; Grieco, P. A. *J. Org. Chem.* **1983**, *48*, 2424–2426.
(208) Affron, D. P. *Functionalisation of Saturated Heterocycles at Unactivated Positions by Palladium-Catalysed Directed C(sp^3)–H Arylation*. PhD Thesis. Imperial College London, London, **2016**.
(209) Ragnarsson, U.; Grehna, L.; Monteirob, L. S.; Maiab, H. L. S. *Synlett* **2003**, *15*, 2386–2388.
(210) Feng, Y.; Wang, Y.; Landgraf, B.; Liu, S.; Chen, G. *Org. Lett.* **2010**, *12*, 3414–3417.
(211) Liu, Y.; Shi, S.; Achtenhagen, M.; Liu, R.; Szostak, M. *Org. Lett.* **2017**, *19*, 1614–1617.
(212) Zhang, Z.; Zheng, D.; Wan, Y.; Zhang, G.; Bi, J.; Liu, Q.; Liu, T.; Shi, L. *J. Org. Chem.* **2018**, *83*, 1369–1376.
(213) Berger, M.; Gray, J. A.; Roth, B. L. *Annu. Rev. Med.* **2009**, *60*, 355–366.
(214) Kristensen, A. S.; Andersen, J.; Jørgensen, T. N.; Sørensen, L.; Eriksen, J.; Loland, C. J.; Strømgaard, K.; Gether, U. *Pharmacol. Rev.* **2011**, *63*, 585–640.
(215) Coleman, J. A.; Green, E. M.; Gouaux, E. *Nature* **2016**, *532*, 334–339.
(216) Prescription data source: Medical Expenditure Panel Survey (MEPS) 2007-2017. Agency for Healthcare Research and Quality (AHRQ), Rockville, MD. ClinCalc DrugStats Database version 20.1. Retrieved from https://clincalc.com/DrugStats/Top300Drugs.aspx, September 2020.
(217) For detailed reviews, see: (a) Jana, S.; Sarkar, S.; Morris, S. A. *Tetrahedron* **2020**, *76*, 131215. (b) De Risi, C.; Fanton, G.; Pollini, G. P.; Trapella, C.; Valente, F.; Zanirato, V. *Tetrahedron Asymmetry* **2008**, *19*, 131–155.

(218) Brandau, S.; Landa, A.; Franzén, J.; Marigo, M.; Jørgensen, K. A. *Angew. Chem. Int. Ed*. **2006**, *45*, 4305–4309.
(219) For a recent enantioselective formal synthesis of (–)-paroxetine in continuous flow process, see: Ötvös, S. B.; Pericàs, M. A.; Kappe, C. O. *Chem. Sci.* **2019**, *10*, 11141–11146.
(220) For selected examples, see: (a) Porey, A.; Santra, S.; Guin, J. *J. Org. Chem.* **2019**, *84*, 5313–5327. (b) Zhang, Y.; Liao, Y.; Liu, X.; Yao, Q.; Zhou, Y.; Lin, L.; Feng, X. *Chem. Eur. J.* **2016**, *22*, 15119–15124. (c) Jensen, K. L.; Poulsen, P. H.; Donslund, B. S.; Morana, F.; Jørgensen, K. A. *Org. Lett.* **2012**, *14*, 1516–1519. (d) Valero, G.; Schimer, J.; Cisarova, I.; Vesely, J.; Moyano, A.; Rios, R. *Tetrahedron Lett.* **2009**, *50*, 1943–1946. (e) Hynes, P. S.; Stupple, P. A.; Dixon, D. J. *Org. Lett.* **2008**, *10*, 1389–1391.
(221) (a) White, N. A.; Ozboya, K. E.; Flanigan, D. M.; Rovis, T. *Asian J. Org. Chem.* **2014**, *3*, 442–444. (b) White, N. A.; DiRocco, D. A.; Rovis, T. *J. Am. Chem. Soc.* **2013**, *135*, 8504–8507.
(222) Kim, M.; Park, Y.; Jeong, B.-S.; Park, H.; Jew, S. *Org. Lett.* **2010**, *12*, 2826–2829.
(223) Wang, X.; Wang, X.; Han, Z.; Wang, Z.; Ding, K. *Angew. Chem. Int. Ed.* **2017**, *56*, 1116–1119.
(224) Krautwald, S.; Schafroth, M. A.; Sarlah, D.; Carreira, E. M. *J. Am. Chem. Soc.* **2014**, *136*, 3020–3023.
(225) Wang, Y.-M.; Bruno, N. C.; Placeres, Á. L.; Zhu, S.; Buchwald, S. L. *J. Am. Chem. Soc.* **2015**, *137*, 10524–10527.
(226) Kubota, K.; Watanabe, Y.; Hayama, K.; Ito, H. *J. Am. Chem. Soc.* **2016**, *138*, 4338–4341.
(227) Amat, M.; Bosch, J.; Hidalgo, J.; Cantó, M.; Pérez, M.; Llor, N.; Molins, E.; Miravitlles, C.; Orozco, M.; Luque, J. *J. Org. Chem.* **2000**, *65*, 3074–3084.
(228) Coleman, J. A.; Navratna, V.; Antermite, D.; Yang, D.; Bull, J. A.; Gouaux, E. *eLife* **2020**; 9:e56427.
(229) Karabatsos, G. J.; Shone, R. L. *J. Org. Chem.* **1968**, *33*, 619–621.
(230) Slack, R. D.; Abramyan, A. M.; Tang, H.; Meena, S.; Davis, B. A.; Bonifazi, A.; Giancola, J. B.; Deschamps, J. R.; Naing, S.; Yano, H.; Singh, S. K.; Newman, A. H.; Shi, L. *ACS Chem. Neurosci.* **2019**, *10*, 3946–3952.
(231) For reviews, see: (a) Scott, D. E.; Coyne, A. G.; Hudson, S. A.; Abell, C. *Biochemistry* **2012**, *51*, 4990–5003. (b) Murray, C. W.; Rees, D. C. *Nat. Chem.* **2009**, *1*, 187–192. (c) Rees, D. C.; Congreve, M.; Murray, C. W.; Carr, R. *Nat. Rev. Drug Discov.* **2004**, *3*, 660–672.
(232) Bancet, A.; Raingeval, C.; Lomberget, T.; Le Borgne, M.; Guichou, J.-F.; Krimm, I. *J. Med. Chem.* **2020**, *63*, 11420–11435.
(233) Tsai, J.; Lee, J. T.; Wang, W.; Zhang, J.; Cho, H.; Mamo, S.; Bremer, R.; Gillette, S.; Kong, J.; Haass, N. K.; *et al. Proc. Natl. Acad. Sci.* **2008**, *105*, 3041–3046.
(234) Bollag, G.; Hirth, P.; Tsai, J.; Zhang, J.; Ibrahim, P. N.; Cho, H.; Spevak, W.; Zhang, C.; Zhang, Y.; Habets, G.; *et al. Nature* **2010**, *467*, 596–599.
(235) Petros, A. M.; Dinges, J.; Augeri, D. J.; Baumeister, S. A.; Betebenner, D. A.; Bures, M. G.; Elmore, S. W.; Hajduk, P. J.; Joseph, M. K.; Landis, S. K.; Nettesheim, D. G.; Rosenberg, S. H.; Shen, W.; Thomas, S.; Wang, X.; Zanze, I.; Zhang, H.; Fesik, S. W. *J. Med. Chem.* **2006**, *49*, 656–663.
(236) (a) Park, C.-M.; Bruncko, M.; Adickes, J.; Bauch, J.; Ding, H.; Kunzer, A.; Marsh, K. C.; Nimmer, P.; Shoemaker, A. R.; Song, X.; *et al. J. Med. Chem.* **2008**, *51*, 6902–6915. (b) Bruncko, M.; Oost, T.

K.; Belli, B. A.; Ding, H.; Joseph, M. K.; Kunzer, A.; Martineau, D.; McClellan, W. J.; Mitten, M.; Ng, S.-C.; *et al. J. Med. Chem.* **2007**, *50*, 641–662. (c) Wendt, M. D.; Shen, W.; Kunzer, A.; McClellan, W. J.; Bruncko, M.; Oost, T. K.; Ding, H.; Joseph, M. K.; Zhang, H.; Nimmer, P. M.; *et al. J. Med. Chem.* **2006**, *49*, 1165–1181.

(237) Souers, A. J.; Leverson, J. D.; Boghaert, E. R.; Ackler, S. L.; Catron, N. D.; Chen, J.; Dayton, B. D.; Ding, H.; Enschede, S. H.; Fairbrother, W. J.; *et al. Nat. Med.* **2013**, *19*, 202–208.

(238) Murray, C. W.; Newell, D. R.; Angibaud, P. *Med. Chem. Comm.* **2019**, *10*, 1509–1511.

(239) (a) Page, M. I.; Jencks, W. P. *Proc. Natl. Acad. Sci.* **1971**, *68*, 1678–1683. (b) Jencks, W. P. *Proc. Natl. Acad. Sci.* **1981**, *78*, 4046–4050.

(240) Murray, C. W.; Verdonk, M. L. *J. Comput. Aided Mol. Des.* **2002**, *16*, 741–753.

(241) Hall, R. J.; Mortenson, P. N.; Murray, C. W. *Prog. Biophys. Mol. Biol.* **2014**, *116*, 82–91.

(242) Fink, T.; Reymond, J.-L. *J. Chem. Inf. Model.* **2007**, *47*, 342–353.

(243) Ruddigkeit, L.; van Deursen, R.; Blum, L. C.; Reymond, J.-L. *J. Chem. Inf. Model.* **2012**, *52*, 2864–2875.

(244) For a review, see: Kidd, S. L.; Osberger, T. J.; Mateu, N.; Sore, H. F.; Spring, D. R. *Front. Chem.* **2018**, *6*, 460.

(245) For recent examples of 3D fragment-oriented synthesis, see: (a) Downes, T. D.; Jones, S. P.; Klein, H. F.; Wheldon, M. C.; Atobe, M.; Bond, P. S.; Firth, J. D.; Chan, N. S.; Waddelove, L.; Hubbard, R. E.; Blakemore, D. C.; De Fusco, C.; Roughley, S. D.; Vidler, L. R.; Whatton, M. A.; Woolford, A. J.-A.; Wrigley, G. L.; O'Brien, P. *Chem. Eur. J.* **2020**, *26*, 8969–8975. (b) Cox, B.; Zdorichenko, V.; Cox, P. B.; Booker-Milburn, K. I.; Paumier, R.; Elliott, L. D.; Robertson-Ralph, M.; Bloomfield, G. *ACS Med. Chem. Lett.* **2020**, *11*, 1185–1190.

(246) Osberger, T. J.; Kidd, S. L.; King, T. A.; Spring, D. R. *Chem. Commun.* **2020**, *56*, 7423–7426.

(247) Nicolaou, K. C.; Baran, P. S.; Zhong, Y.-L.; Sugita, K. *J. Am. Chem. Soc.* **2002**, *124*, 2212–2220.

(248) Dohi, T.; Maruyama, A.; Minamitsuji, Y.; Takenaga, N.; Kita, Y. *Chem. Commun.* **2007**, 1224–1226.

(249) Colomer, I.; Empson, C. J.; Craven, P.; Owen, Z.; Doveston, R. G.; Churcher, I.; Marsden, S. P.; Nelson, A. *Chem. Commun.* **2016**, *52*, 7209–7212.

(250) Available free of charge at https://llama.leeds.ac.uk.

(251) Sauer, W. H. B.; Schwarz, M. K. *J. Chem. Inf. Comput. Sci*. **2003**, *43*, 987–1003.

(252) Firth, N. C.; Brown, N.; Blagg, J. *J. Chem. Inf. Model.* **2012**, *52*, 2516–2525.

(253) For selected mechanistic studies on C–C and C–heteroatom bond-forming reductive elimination from Pd(IV) complexes, see: (a) Hývl, J.; Roithová, J. *Org. Lett.* **2014**, *16*, 200–203. (b) Ball, N. D.; Kampf, J. W.; Sanford, M. S. *J. Am. Chem. Soc.* **2010**, *132*, 2878–2879. (c) Furuya, T.; Benitez, D.; Tkatchouk, E.; Strom, A. E.; Tang, P.; Goddard, W. A.; Ritter, T. *J. Am. Chem. Soc.* **2010**, *132*, 3793–3807. (d) Racowski, J. M.; Dick, A. R.; Sanford, M. S. *J. Am. Chem. Soc.* **2009**, *131*, 10974–10983.

(254) (a) Powers, D. C.; Lee, E.; Ariafard, A.; Sanford, M. S.; Yates, B. F.; Canty, A. J.; Ritter, T. *J. Am. Chem. Soc.* **2012**, *134*, 12002–12009. (b) Powers, D. C.; Geibel, M. A. L.; Klein, J. E. M. N.; Ritter, T.

J. Am. Chem. Soc. **2009**, *131*, 17050–17051. (c) Deprez, N. R.; Sanford, M. S. *J. Am. Chem. Soc.* **2009**, *131*, 11234–11241. (d) Powers, D. C.; Ritter, T. *Nat. Chem.* **2009**, *1*, 302–309.

(255) Williams, D. H.; Bhacca, N. S. *Tetrahedron* **1965**, *21*, 2021–2028.

(256) Simmons, E. M.; Hartwig, J. F. *Angew. Chem. Int. Ed.* **2012**, *51*, 3066–3072.

(257) (a) Burés, J. *Angew. Chem. Int. Ed.* **2016**, *55*, 16084–16087. (b) Burés, J. *Angew. Chem. Int. Ed.* **2016**, *55*, 2028–2031.

(258) For a recent review, see: Nielsen, C. D.-T.; Burés, J. *Chem. Sci.* **2019**, *10*, 348–353.

(259) For a study on the effect of low concentration of catalyst on the order determination in the presence of irreversible deactivation, see: Burés, J. *Top. Catal.* **2017**, *60*, 631–633.

(260) Hammett, L. P. *J. Am. Chem. Soc.* **1937**, *59*, 96–103.

(261) For an extensive collection of tabulated experimental σ constants, see: Hansch, C.; Leo, A.; Taft, R. W. *Chem. Rev.* **1991**, *91*, 165–195.

(262) Brown, H. C.; Okamoto, Y. *J. Am. Chem. Soc.* **1958**, *80*, 4979–4987.

(263) Gaussian 09, Revision D.01; Frisch, M. J.; Trucks, G. W.; Schlegel, H. B.; Scuseria, G. E.; Robb, M. A.; Cheeseman, J. R.; Scalmani, G.; Barone, V.; Mennucci, B.; Petersson, G. A.; *et al.* Gaussian, Inc., Wallingford CT, 2013.

(264) For selected examples, see: (a) St John-Campbell, S.; Ou, A. K.; Bull, J. A. *Chem. Eur. J.* **2018**, *24*, 17838–17843. (b) Baxter, R. D.; Sale, D.; Engle, K. M.; Yu, J.-Q.; Blackmond, D. G. *J. Am. Chem. Soc.* **2012**, *134*, 4600–4606.

(265) Wisniewski, S. R.; Savage, S. A.; Romero, E. O.; Eastgate, M. D.; Tan, Y.; Simmons, E. M.; Plata, R. E.; Sowa, J. R.; Blackmond, D. G. *J. Org. Chem.* **2019**, *84*, 7961–7970.

(266) (a) Naveen; Rajkumar, V.; Babu, S. A.; Gopalakrishnan, B. *J. Org. Chem.* **2016**, *81*, 12197–12211. (b) Wang, C.; Chen, C.; Zhang, J.; Han, J.; Wang, Q.; Guo, K.; Liu, P.; Guan, M.; Yao, Y.; Zhao, Y. *Angew. Chem. Int. Ed.* **2014**, *53*, 9884–9888. c) Pearson, R.; Zhang, S.; He, G.; Edwards, N.; Chen, G. *Beilstein J. Org. Chem.* **2013,** *9,* 891–899.

(267) Blackmond, D. G. *Angew. Chem. Int. Ed.* **2005**, *44*, 4302–4320.

(268) Martínez-Carrión, A.; Howlett, M. G.; Alamillo-Ferrer, C.; Clayton, A. D.; Bourne, R. A.; Codina, A.; Vidal-Ferran, A.; Adams, R. W.; Burés, J. *Angew. Chem. Int. Ed.* **2019**, *58*, 10189–10193.

(269) Hartman, M.; Svoboda, K.; Čech, B.; Pohořelý, M.; Šyc, M. *Ind. Eng. Chem. Res.* **2019**, *58*, 2868–2881.

(270) Wang, X.-C.; Hu, Y.; Bonacorsi, S.; Hong, Y.; Burrell, R.; Yu, J.-Q. *J. Am. Chem. Soc.* **2013**, *135*, 10326–10329.

(271) Arroniz, C.; Denis, J. G.; Ironmonger, A.; Rassias, G.; Larrosa, I. *Chem. Sci.* **2014**, *5*, 3509–3514.

(272) Shao, Q.; Wu, K.; Zhuang, Z.; Qian, S.; Yu, J.-Q. *Acc. Chem. Res.* **2020**, *53*, 833–851.

(273) Hill, D. E.; Yu, J.-Q.; Blackmond, D. G. *J. Org. Chem.* **2020**, *85*, 13674–13679.

(274) Wu, C.-Z.; He, C.-Y.; Huang, Y.; Zhang, X. *Org. Lett.* **2013**, *15*, 5266–5269.

(275) For a study on the effect of different monodentate pyridine-based DGs on the C(sp^2)–H acetoxylation of aromatic rings, see: Desai, L. V; Stowers, K. J.; Sanford, M. S. *J. Am. Chem. Soc*. **2008**, *130*, 13285–13293.

(276) Motati, D. R.; Uredi, D.; Watkins, E. B. *Chem. Sci.* **2018**, *9*, 1782–1788.
(277) Taylor, R. A.; Bonanno, N. M.; Mirza, D.; Lough, A. J.; Lemaire, M. T. *Polyhedron* **2017**, *131*, 34–39.
(278) Kuninobu, Y.; Nishi, M.; Kanai, M. *Org. Biomol. Chem.* **2016**, *14*, 8092–8100.
(279) For original conditions, see: Yang, C.; Zhang, F.; Deng, G.-J.; Gong, H. *J. Org. Chem.* **2019**, *84*, 181–190.
(280) Yang, X.; Sun, Y.; Sun, T.; Rao, Y. *Chem. Commun.* **2016**, *52*, 6423–6426.
(281) Coe, B. J.; Glenwright, S. J. *Coord. Chem. Rev.* **2000**, *203*, 5–80.
(282) Lee, Y. H.; Morandi, B. *Nat. Chem.* **2018**, *10*, 1016–1022.
(283) Mason, R. M. *Ann. Rheum. Dis.* **1954**, *13*, 120–130.
(284) Irby, C. E.; Yentzer, B. A.; Feldman, S. R. *J. Adolesc. Heal.* **2008**, *43*, 421–424.
(285) Welch, E. M.; Barton, E. R.; Zhuo, J.; Tomizawa, Y.; Friesen, W. J.; Trifillis, P.; Paushkin, S.; Patel, M.; Trotta, C. R.; Hwang, S.; *et al. Nature* **2007**, *447*, 87–91.
(286) (a) Carter, A. *Palladium-catalysed C(sp^3)-H Functionalisation of Piperidine Derivatives with the use of Amine Linked Auxiliaries*. MSci Thesis. Imperial College London, London, **2019**. (b) Larribeau, T. *C(sp^3)-H functionalisation of pyrrolidines with the aid of removable directing groups*. Visiting Msci student report. Imperial College London, London, **2019**.
(287) Gou, Q.; Liu, G.; Liu, Z.-N.; Qin, J. *Chem. Eur. J.* **2015**, *21*, 15491–15495.
(288) Bull, J. A.; Mousseau, J. J.; Charette, A. B. *Org. Lett.* **2008**, *10*, 5485–5488.
(289) Martin, A. R.; Gharat, L. A. *Heterocycles* **1996**, *43*, 185–189.
(290) Zhang, Y.-F.; Zhao, H.-W.; Wang, H.; Wei, J.-B.; Shi, Z.-J. *Angew. Chem. Int. Ed.* **2015**, *54*, 13686–13690.
(291) Konermann, L.; Pan, J.; Liu, Y.-H. *Chem. Soc. Rev.* **2011**, *40*, 1224–1234.

10. Appendices

10.1 Appendix I: LLAMA Default set of Reactants and Reactions

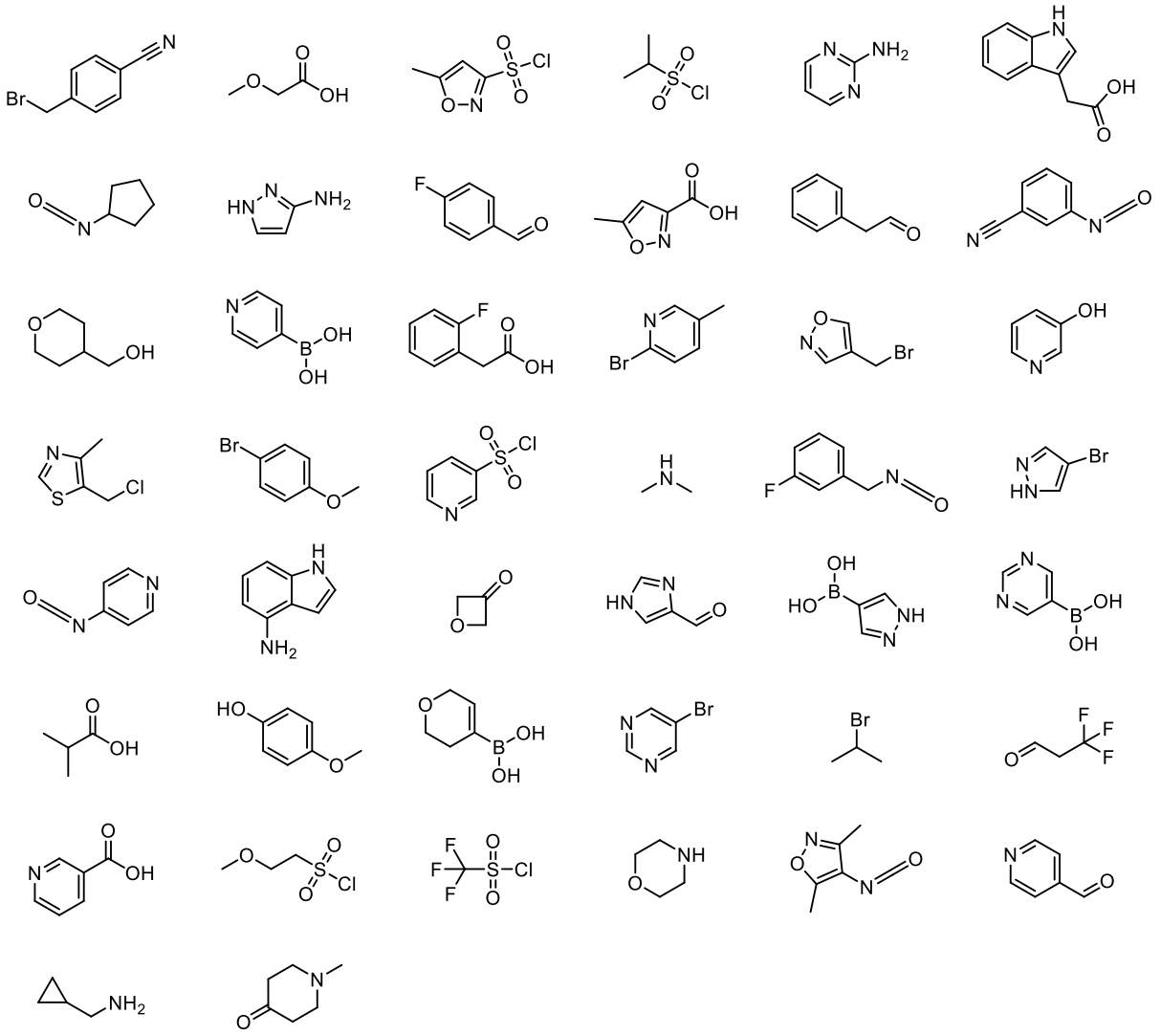


Figure 10.1 LLAMA Default set of reactants.

Reactions used for Virtual Scaffolds Elaboration: Reductive amination; Suzuki coupling; Buchwald-Hartwig amination; Sulfonamide formation; Urea formation; Alcohol alkylation; Carbamate formation; Secondary amide formation; Secondary amide alkylation; Amide formation; Alcohol arylation; Urea alkylation; Urea arylation.

10.2 Appendix II: Raw Kinetic Data for Deuteration Experiments

Table 10.1 Raw kinetic data for the deuteration of pyrrolidine **9.**

time (h)	int. *cis*-C(4)H[a]	integral *trans*-C(4)H[b]	integral *cis*-C(2)H[c]	%D *cis*-C(4)	%D *trans*-C(4)	%D *cis*-C(2)
0.033	0.93584	0.97697	1.00812	6.416	2.303	-0.812
0.116	0.91364	0.93759	0.95631	8.636	6.241	4.369
0.199	0.78703	0.94194	1.00234	21.297	5.806	-0.234
0.282	0.79888	0.90445	0.99515	20.112	9.555	0.485
0.365	0.74745	0.87091	0.99467	25.255	12.909	0.533
0.448	0.69643	0.88293	1.01162	30.357	11.707	-1.162
0.531	0.67486	0.85922	1.00833	32.514	14.078	-0.833
0.614	0.68995	0.83932	1.01164	31.005	16.068	-1.164
0.697	0.68217	0.81982	0.97237	31.783	18.018	2.763
0.78	0.66828	0.82162	0.99455	33.172	17.838	0.545
0.863	0.66254	0.80641	0.97227	33.746	19.359	2.773
0.946	0.61051	0.81868	1.04052	38.949	18.132	-4.052
1.029	0.69018	0.75056	0.93058	30.982	24.944	6.942
1.279	0.59871	0.79336	1.02058	40.129	20.664	-2.058
1.529	0.594	0.75997	0.99826	40.6	24.003	0.174
1.779	0.5836	0.70674	0.97408	41.64	29.326	2.592
2.029	0.59353	0.67758	0.92557	40.647	32.242	7.443
2.279	0.56091	0.67644	0.92918	43.909	32.356	7.082
2.529	0.51231	0.68317	0.98168	48.769	31.683	1.832
2.779	0.51221	0.65252	0.95741	48.779	34.748	4.259
3.029	0.53834	0.63769	0.91616	46.166	36.231	8.384
3.279	0.50159	0.63368	0.89876	49.841	36.632	10.124
3.529	0.50515	0.6237	0.93944	49.485	37.63	6.056
3.779	0.51747	0.59514	0.88861	48.253	40.486	11.139
4.029	0.50606	0.57039	0.88416	49.394	42.961	11.584
4.279	0.49929	0.56622	0.89849	50.071	43.378	10.151
4.529	0.49962	0.55415	0.87616	50.038	44.585	12.384
4.779	0.47268	0.55421	0.8926	52.732	44.579	10.74
5.029	0.47028	0.55302	0.91021	52.972	44.698	8.979
5.279	0.48543	0.53158	0.85806	51.457	46.842	14.194
5.529	0.46766	0.53537	0.87377	53.234	46.463	12.623
5.779	0.45503	0.53181	0.88487	54.497	46.819	11.513
6.029	0.44375	0.51525	0.83037	55.625	48.475	16.963
6.279	0.42626	0.53386	0.92227	57.374	46.614	7.773
6.529	0.44881	0.51482	0.86697	55.119	48.518	13.303
6.779	0.45322	0.50541	0.85039	54.678	49.459	14.961
7.029	0.437	0.50849	0.86972	56.3	49.151	13.028
7.279	0.44727	0.49701	0.84681	55.273	50.299	15.319
7.529	0.43244	0.49541	0.84768	56.756	50.459	15.232
7.779	0.41204	0.49997	0.87319	58.796	50.003	12.681
8.029	0.41822	0.49218	0.85335	58.178	50.782	14.665
8.279	0.39071	0.50072	0.88892	60.929	49.928	11.108

8.529	0.41068	0.48546	0.85045	58.932	51.454	14.955
8.779	0.40453	0.48498	0.86078	59.547	51.502	13.922
9.029	0.41482	0.47646	0.8334	58.518	52.354	16.66
9.279	0.40696	0.47323	0.83907	59.304	52.677	16.093
9.529	0.40958	0.47212	0.83512	59.042	52.788	16.488
9.779	0.39196	0.47485	0.85249	60.804	52.515	14.751
10.029	0.40108	0.46287	0.81901	59.892	53.713	18.099
10.279	0.3757	0.47324	0.8585	62.43	52.676	14.15
10.529	0.39132	0.46091	0.83496	60.868	53.909	16.504
10.779	0.38167	0.46386	0.84534	61.833	53.614	15.466
11.029	0.39639	0.45477	0.82604	60.361	54.523	17.396
11.279	0.39503	0.45118	0.81975	60.497	54.882	18.025
11.529	0.3741	0.45559	0.84232	62.59	54.441	15.768
11.779	0.37282	0.45491	0.84084	62.718	54.509	15.916
12.029	0.37459	0.44868	0.82592	62.541	55.132	17.408
12.279	0.37105	0.44767	0.82603	62.895	55.233	17.397
12.529	0.37034	0.44496	0.83289	62.966	55.504	16.711
12.779	0.38099	0.43862	0.81984	61.901	56.138	18.016
13.029	0.3603	0.4429	0.8316	63.97	55.71	16.84
13.279	0.35739	0.44132	0.83535	64.261	55.868	16.465
13.529	0.36388	0.43485	0.80982	63.612	56.515	19.018
13.779	0.37209	0.42995	0.80159	62.791	57.005	19.841
14.029	0.34744	0.43697	0.82762	65.256	56.303	17.238
14.279	0.36831	0.42715	0.80189	63.169	57.285	19.811
14.529	0.33844	0.43581	0.83529	66.156	56.419	16.471
14.779	0.35617	0.42438	0.80473	64.383	57.562	19.527
15.029	0.36172	0.41964	0.79965	63.828	58.036	20.035
15.279	0.33121	0.43555	0.84777	66.879	56.445	15.223
15.529	0.32484	0.43345	0.83892	67.516	56.655	16.108
15.779	0.34733	0.41994	0.81338	65.267	58.006	18.662
16.029	0.35163	0.41715	0.8055	64.837	58.285	19.45
16.279	0.34771	0.41725	0.80642	65.229	58.275	19.358
16.529	0.3368	0.41741	0.80774	66.32	58.259	19.226
16.779	0.34305	0.41435	0.80746	65.695	58.565	19.254
17.029	0.34257	0.41506	0.80723	65.743	58.494	19.277
17.279	0.33927	0.41521	0.80957	66.073	58.479	19.043
17.529	0.35132	0.4062	0.79792	64.868	59.38	20.208
17.779	0.35234	0.40657	0.78878	64.766	59.343	21.122
18.029	0.33322	0.40926	0.8065	66.678	59.074	19.35
18.279	0.33684	0.40406	0.79467	66.316	59.594	20.533
18.529	0.3405	0.40171	0.78467	65.95	59.829	21.533
18.779	0.34173	0.40201	0.79415	65.827	59.799	20.585
19.029	0.3236	0.40639	0.80869	67.64	59.361	19.131
19.279	0.32405	0.40366	0.8008	67.595	59.634	19.92
19.529	0.31079	0.41262	0.79118	68.921	58.738	20.882
19.779	0.33449	0.39883	0.79452	66.551	60.117	20.548
20.029	0.30607	0.40658	0.81799	69.393	59.342	18.201

20.279	0.32227	0.39616	0.79618	67.773	60.384	20.382
20.529	0.33727	0.39203	0.78258	66.273	60.797	21.742
20.779	0.32756	0.39555	0.79402	67.244	60.445	20.598
21.029	0.32995	0.38928	0.758	67.005	61.072	24.2

Data from ^{1}H NMR experiments (400 MHz, toluene-d_8, 100 °C, 6 scans, d_1 = 1 s). [a] δ 2.05–1.93 ppm. [b] δ 1.81–1.70 ppm. [c] δ 3.70–3.62 ppm

Table 10.2 Raw kinetic data for the deuteration of 4-tolyl-pyrrolidine **13b**.

time (h)	int. CH_{Ar}[a]	int. tol[b]	% D CH_{Ar}[c]	integral *trans*-C(4)H[d]	integral *cis*-C(2)H[e]	% D *trans*-C(4)	% D *cis*-C(2)
0.08	4.734	1.724	20.77	1.004	-0.404	1.0602	0
0.16	5.1453	1.822	3.472	0.9791	2.089	1.1118	-5.16
0.24	5.1398	1.803	3.098	0.9621	3.788	1.0986	-3.85
0.32	4.9418	1.774	12.03	0.9762	2.384	1.0602	-0
0.4	4.9532	1.734	10.14	0.8938	10.62	1.0483	1.19
0.48	4.9147	1.726	11.79	0.8749	12.51	1.0383	2.19
0.56	4.8776	1.714	13.26	0.8543	14.57	1.0336	2.656
0.64	4.8391	1.705	14.89	0.8557	14.43	1.0288	3.138
0.72	4.7866	1.686	16.87	0.8321	16.79	1.0037	5.647
0.8	4.7524	1.675	18.22	0.8221	17.79	1.0021	5.812
0.88	4.7647	1.679	17.73	0.8188	18.12	0.9991	6.111
0.96	4.7401	1.665	18.51	0.808	19.2	0.9898	7.041
1.04	4.716	1.661	19.56	0.8006	19.94	0.9825	7.769
1.12	4.69	1.655	20.65	0.7878	21.22	0.974	8.621
1.2	4.7003	1.658	20.27	0.7947	20.53	0.9736	8.66
1.28	4.694	1.641	20.01	0.7786	22.14	0.9694	9.081
1.36	4.6651	1.646	21.62	0.7715	22.85	0.9609	9.923
1.44	4.6563	1.637	21.75	0.7644	23.56	0.9553	10.49
1.52	4.6261	1.63	23.03	0.765	23.5	0.9512	10.9
1.6	4.6461	1.631	22.07	0.7527	24.73	0.9445	11.56
1.68	4.6375	1.624	22.26	0.7604	23.96	0.9423	11.79
1.76	4.6238	1.625	22.96	0.7511	24.89	0.936	12.41
1.84	4.6098	1.619	23.48	0.7482	25.18	0.9306	12.96
1.92	4.6323	1.629	22.69	0.7488	25.12	0.9382	12.2
2	4.6154	1.635	23.74	0.7592	24.08	0.9367	12.35
2.08	4.5943	1.62	24.28	0.7417	25.83	0.9261	13.41
2.16	4.6111	1.631	23.83	0.7449	25.51	0.9327	12.75
2.24	4.6248	1.636	23.28	0.754	24.6	0.9377	12.25
2.32	4.5799	1.616	24.88	0.7394	26.06	0.9212	13.9
2.4	4.5957	1.632	24.6	0.738	26.2	0.9282	13.2
2.48	4.5637	1.609	25.46	0.7368	26.32	0.9172	14.3
2.56	4.5674	1.628	25.89	0.7309	26.91	0.9139	14.62
2.64	4.5741	1.631	25.68	0.7305	26.95	0.9213	13.89
2.72	4.5655	1.623	25.84	0.7217	27.83	0.9134	14.68
2.8	4.5496	1.628	26.77	0.7226	27.74	0.9104	14.98

2.88	4.5577	1.624	26.25	0.7267	27.33	0.9091	15.1
2.96	4.5635	1.629	26.11	0.7286	27.14	0.9097	15.05
3.04	4.5543	1.623	26.38	0.7182	28.18	0.9048	15.54
3.12	4.5505	1.628	26.74	0.7232	27.68	0.9104	14.98
3.2	4.5555	1.625	26.4	0.732	26.8	0.9102	15
3.28	4.5407	1.619	26.92	0.7241	27.59	0.904	15.61
3.36	4.5604	1.621	26.01	0.7194	28.06	0.9024	15.78
3.44	4.5492	1.624	26.69	0.7165	28.35	0.9077	15.25
3.52	4.5566	1.634	26.64	0.723	27.7	0.9111	14.91
3.6	4.5225	1.622	27.95	0.7118	28.82	0.8941	16.61
3.68	4.568	1.635	26.11	0.7148	28.52	0.9029	15.73
3.76	4.5498	1.634	26.98	0.7168	28.32	0.9048	15.54
3.84	4.5331	1.629	27.64	0.7117	28.83	0.9001	16.01
3.92	4.5337	1.631	27.68	0.7132	28.68	0.8936	16.66
4	4.5411	1.634	27.41	0.7199	28.01	0.901	15.92
4.08	4.5544	1.636	26.82	0.7073	29.27	0.8943	16.59
4.16	4.5305	1.637	28.04	0.7077	29.23	0.8917	16.85
4.24	4.534	1.622	27.38	0.7012	29.88	0.8891	17.11
4.32	4.5492	1.636	27.08	0.7113	28.87	0.8997	16.04
4.4	4.5395	1.633	27.47	0.7115	28.85	0.8956	16.46
4.48	4.5229	1.629	28.17	0.7038	29.62	0.8956	16.46
4.56	4.5277	1.638	28.2	0.7064	29.36	0.892	16.81
4.64	4.5556	1.64	26.88	0.7173	28.27	0.8966	16.35
4.72	4.5304	1.635	27.97	0.7079	29.21	0.8909	16.93
4.8	4.5306	1.639	28.09	0.7018	29.82	0.8935	16.67
4.88	4.5337	1.638	27.91	0.7046	29.54	0.8926	16.76
4.96	4.5524	1.656	27.59	0.7048	29.52	0.9	16.02
5.04	4.5204	1.645	28.81	0.705	29.5	0.8901	17.01
5.12	4.5029	1.633	29.3	0.6933	30.67	0.8812	17.9
5.2	4.5379	1.646	27.98	0.7015	29.85	0.8893	17.09
5.28	4.5176	1.642	28.87	0.7039	29.61	0.8865	17.37
5.36	4.526	1.649	28.67	0.6985	30.15	0.8885	17.17
5.44	4.5159	1.642	28.92	0.7002	29.98	0.889	17.12
5.52	4.5248	1.641	28.46	0.696	30.4	0.8887	17.15
5.6	4.5273	1.64	28.31	0.6953	30.47	0.8822	17.8
5.68	4.5378	1.65	28.11	0.7024	29.76	0.891	16.92
5.76	4.5336	1.652	28.37	0.6992	30.08	0.8889	17.13
5.84	4.5161	1.651	29.21	0.697	30.3	0.8845	17.56
5.92	4.5098	1.643	29.27	0.6916	30.84	0.881	17.92
6	4.5454	1.657	27.96	0.6992	30.08	0.8837	17.64
6.08	4.4983	1.646	29.95	0.6981	30.19	0.879	18.11
6.16	4.4839	1.648	30.74	0.7	30	0.879	18.11
6.24	4.4985	1.655	30.26	0.6905	30.95	0.8841	17.6
6.32	4.5171	1.658	29.42	0.7044	29.56	0.8891	17.11
6.4	4.5241	1.654	28.94	0.6907	30.93	0.8832	17.7
6.48	4.5091	1.654	29.69	0.6935	30.65	0.8848	17.54
6.56	4.5195	1.652	29.09	0.6921	30.79	0.8805	17.96

6.64	4.4988	1.649	30.03	0.6866	31.34	0.8795	18.07
6.72	4.5126	1.661	29.72	0.6911	30.89	0.8812	17.9
6.8	4.5138	1.652	29.37	0.6843	31.57	0.8803	17.98
6.88	4.5378	1.661	28.49	0.6955	30.45	0.8842	17.6
6.96	4.5212	1.653	29.04	0.6913	30.87	0.8833	17.69
7.04	4.526	1.664	29.16	0.6934	30.66	0.8856	17.46
7.12	4.5254	1.657	28.97	0.682	31.8	0.8822	17.8
7.2	4.5183	1.658	29.34	0.6907	30.93	0.8801	18.01
7.28	4.5157	1.662	29.61	0.6911	30.89	0.8868	17.33
7.36	4.5288	1.665	29.07	0.6904	30.96	0.8872	17.3
7.44	4.5083	1.659	29.89	0.6863	31.37	0.8741	18.6
7.52	4.5052	1.657	29.97	0.6832	31.68	0.8751	18.5
7.6	4.5489	1.663	28	0.6852	31.48	0.8805	17.97
7.68	4.4993	1.645	29.88	0.6789	32.11	0.8733	18.69
7.76	4.4812	1.644	30.74	0.6778	32.22	0.8698	19.04
7.84	4.5031	1.658	30.11	0.6931	30.69	0.8751	18.51
7.92	4.5035	1.661	30.19	0.6851	31.49	0.8766	18.36
8	4.4993	1.656	30.24	0.6867	31.33	0.8775	18.26
8.08	4.515	1.666	29.8	0.6829	31.71	0.8783	18.18
8.16	4.5046	1.654	29.89	0.6828	31.72	0.8708	18.94
8.24	4.5054	1.661	30.1	0.6775	32.25	0.8719	18.83
8.32	4.527	1.67	29.32	0.6796	32.04	0.8745	18.57
8.4	4.5067	1.662	30.07	0.6849	31.51	0.8752	18.49
8.48	4.506	1.666	30.22	0.6815	31.85	0.8768	18.34
8.56	4.4926	1.66	30.71	0.6759	32.41	0.873	18.72
8.64	4.517	1.669	29.78	0.6862	31.38	0.8775	18.26
8.72	4.5083	1.662	29.99	0.6781	32.19	0.8736	18.66
8.8	4.5206	1.675	29.82	0.6799	32.01	0.877	18.32
8.88	4.5017	1.663	30.35	0.672	32.8	0.866	19.41
8.96	4.4973	1.666	30.66	0.6757	32.43	0.8736	18.66
9.04	4.479	1.655	31.21	0.6687	33.13	0.8624	19.78
9.12	4.5123	1.662	29.78	0.6742	32.58	0.8724	18.77
9.2	4.491	1.665	30.95	0.6772	32.28	0.873	18.71
9.28	4.5272	1.67	29.3	0.6775	32.25	0.8764	18.37
9.36	4.5155	1.671	29.94	0.6787	32.13	0.8716	18.86
9.44	4.5122	1.673	30.15	0.6788	32.12	0.8718	18.83
9.52	4.4956	1.662	30.61	0.6626	33.74	0.8624	19.78
9.6	4.5183	1.676	29.94	0.6733	32.67	0.8733	18.69
9.68	4.5157	1.674	30	0.6701	32.99	0.8713	18.89
9.76	4.5168	1.673	29.94	0.6765	32.35	0.8765	18.37
9.84	4.5016	1.675	30.75	0.6737	32.63	0.8765	18.37
9.92	4.5106	1.68	30.48	0.6741	32.59	0.874	18.61
10	4.5042	1.677	30.69	0.6728	32.72	0.8708	18.94
10.08	4.5038	1.68	30.82	0.679	32.1	0.877	18.32
10.16	4.5221	1.68	29.89	0.6732	32.68	0.8761	18.4
10.24	4.5118	1.677	30.32	0.6716	32.84	0.8681	19.21
10.32	4.4963	1.676	31.05	0.6687	33.13	0.8662	19.39

10.4	4.5046	1.668	30.36	0.667	33.3	0.8626	19.76
10.48	4.5261	1.686	29.9	0.6732	32.68	0.8767	18.35
10.56	4.5107	1.681	30.49	0.6689	33.11	0.8721	18.8
10.64	4.513	1.678	30.29	0.6743	32.57	0.8716	18.86
10.72	4.5244	1.676	29.66	0.6689	33.11	0.8718	18.83
10.8	4.4983	1.671	30.77	0.6599	34.01	0.8649	19.53
10.88	4.5151	1.68	30.24	0.6653	33.47	0.8698	19.04
10.96	4.5138	1.677	30.21	0.662	33.8	0.869	19.12
11.04	4.5153	1.681	30.27	0.6651	33.49	0.8721	18.81
11.12	4.5016	1.675	30.77	0.6631	33.69	0.8719	18.83
11.2	4.5227	1.69	30.18	0.67	33	0.8795	18.07
11.28	4.5143	1.687	30.51	0.6659	33.41	0.8723	18.79
11.36	4.5094	1.684	30.67	0.6651	33.49	0.874	18.62
11.44	4.4936	1.687	31.57	0.6686	33.14	0.872	18.82
11.52	4.4804	1.666	31.52	0.6577	34.23	0.8632	19.7

Data from ^{1}H NMR experiments (400 MHz, toluene-d_8, 100 °C, 1 scan, d_1 = 70 s). [a] δ 7.00–6.94 ppm, overlaps with toluene signal and 2 × H_{Cbz}. [b] Toluene reference at δ 2.08 ppm. [c] Calculated after correction of the integral value for contribution from toluene and Cbz protons. [d] δ 3.33–3.24 ppm. [e] δ 4.17–4.09 ppm.

Table 10.3 Raw kinetic data for the deuteration of a mixture of **9** and **13b**. Integration for pyrrolidine **9**.

time (h)	int. *cis*-C(2)H[a]	% D *cis*-C(2)	int. *cis*-C(4)H[b]	% D *cis*-C(4)	int. *trans*-C(4)H[c]	int. CH_{Ar} (13b)[d]	% D *trans*-C(4)[e]
0.083	1.219	0.077	1.058	-5.818	4.83	1.199	-0.22
0.166	1.239	-1.93	1.014	-1.41	4.906	1.213	-3.61
0.249	1.274	-5.37	0.843	15.67	4.825	1.223	7.401
0.332	1.247	-2.73	0.932	6.794	4.89	1.222	0.745
0.415	1.241	-2.1	0.898	10.21	4.888	1.225	1.724
0.498	1.226	-0.62	0.879	12.14	4.841	1.217	3.955
0.581	1.21	0.97	0.833	16.68	4.778	1.206	7.063
0.664	1.192	2.761	0.878	12.2	4.798	1.201	3.43
0.747	1.193	2.686	0.816	18.37	4.783	1.216	9.479
0.83	1.17	5.029	0.815	18.53	4.797	1.218	8.533
0.913	1.171	4.86	0.78	22	4.781	1.214	9.161
0.996	1.157	6.265	0.844	15.65	4.776	1.205	7.032
1.079	1.142	7.803	0.765	23.51	4.703	1.192	10.39
1.162	1.133	8.703	0.895	10.48	4.817	1.206	2.971
1.245	1.125	9.472	0.765	23.52	4.656	1.192	15.04
1.328	1.129	9.101	0.734	26.6	4.697	1.202	13.82
1.411	1.138	8.198	0.752	24.83	4.744	1.204	9.607
1.494	1.11	11.01	0.772	22.82	4.684	1.191	11.98
1.577	1.116	10.42	0.719	28.06	4.668	1.196	14.96
1.66	1.106	11.41	0.72	27.98	4.649	1.2	17.99

1.743	1.09	13.05	0.724	27.57	4.634	1.185	14.93
1.826	1.112	10.8	0.65	35	4.599	1.199	22.7
1.909	1.091	12.86	0.718	28.16	4.646	1.184	13.58
1.992	1.07	14.97	0.713	28.7	4.629	1.193	17.94
2.075	1.076	14.36	0.682	31.79	4.555	1.183	22.3
2.158	1.085	13.46	0.624	37.62	4.556	1.198	26.74
2.241	1.089	13.08	0.651	34.86	4.591	1.184	18.98
2.324	1.072	14.77	0.649	35.15	4.594	1.185	19.01
2.407	1.087	13.31	0.623	37.74	4.511	1.185	27.56
2.49	1.061	15.9	0.707	29.31	4.578	1.187	21.39
2.573	1.076	14.4	0.63	36.99	4.527	1.181	24.72
2.656	1.075	14.54	0.587	41.35	4.518	1.192	28.86
2.739	1.08	14.05	0.599	40.12	4.531	1.199	29.67
2.822	1.065	15.54	0.642	35.78	4.505	1.183	27.54
2.905	1.059	16.06	0.597	40.25	4.48	1.181	29.27
2.988	1.062	15.85	0.61	39.03	4.471	1.177	28.96
3.071	1.049	17.09	0.592	40.85	4.513	1.187	27.9
3.154	1.059	16.06	0.527	47.33	4.447	1.181	32.57
3.237	1.041	17.86	0.583	41.71	4.516	1.186	27.18
3.32	1.036	18.35	0.605	39.52	4.45	1.175	30.44
3.403	1.047	17.31	0.594	40.57	4.487	1.189	30.87
3.486	1.034	18.65	0.578	42.17	4.431	1.185	35.55
3.569	1.039	18.13	0.576	42.37	4.495	1.186	29.41
3.652	1.019	20.09	0.63	37.02	4.48	1.184	30.05
3.735	1.027	19.26	0.548	45.22	4.412	1.178	35.1
3.818	1.005	21.54	0.677	32.27	4.48	1.162	23.45
3.901	1.012	20.82	0.61	38.96	4.411	1.176	34.66
3.984	1.028	19.25	0.592	40.77	4.417	1.173	33.15
4.067	1.016	20.38	0.551	44.88	4.425	1.182	35.01
4.15	1.015	20.51	0.576	42.35	4.447	1.178	31.76
4.233	1.011	20.92	0.576	42.39	4.447	1.186	34.04
4.316	1.006	21.37	0.604	39.62	4.464	1.182	31.35
4.399	1.006	21.45	0.568	43.19	4.381	1.168	35.36
4.482	1.033	18.66	0.481	51.94	4.387	1.19	41.23
4.565	1.018	20.21	0.504	49.59	4.388	1.184	39.21
4.648	0.999	22.07	0.568	43.23	4.355	1.166	37.35
4.731	1	22.01	0.579	42.11	4.387	1.169	35.12
4.814	0.996	22.41	0.581	41.95	4.383	1.164	33.75
4.897	1	22.02	0.53	46.96	4.357	1.171	38.49
4.98	0.995	22.53	0.601	39.94	4.394	1.169	34.45
5.063	1.019	20.06	0.522	47.78	4.365	1.171	37.67
5.146	1.011	20.9	0.491	50.87	4.324	1.172	42.06
5.229	1.014	20.56	0.522	47.83	4.354	1.174	39.73
5.312	0.988	23.25	0.564	43.56	4.359	1.164	36.23
5.395	0.993	22.65	0.517	48.29	4.349	1.174	40.25
5.478	0.988	23.16	0.546	45.36	4.366	1.171	37.83
5.561	0.993	22.73	0.53	46.99	4.325	1.156	37.43

5.644	0.987	23.29	0.547	45.32	4.314	1.157	38.8
5.727	0.975	24.48	0.576	42.44	4.347	1.156	35
5.81	0.983	23.7	0.532	46.77	4.329	1.169	40.8
5.893	0.996	22.39	0.539	46.06	4.322	1.158	38.2
5.976	0.995	22.47	0.509	49.09	4.302	1.166	42.62
6.059	0.975	24.53	0.546	45.35	4.329	1.159	37.76
6.142	0.997	22.33	0.498	50.17	4.35	1.181	42.15
6.225	0.977	24.32	0.547	45.3	4.347	1.166	37.96
6.308	0.971	24.87	0.546	45.39	4.337	1.159	36.9
6.391	0.968	25.25	0.545	45.53	4.336	1.158	36.9
6.474	0.97	25.04	0.496	50.35	4.274	1.16	43.68
6.557	0.984	23.64	0.524	47.56	4.29	1.157	41.14
6.64	0.99	22.97	0.483	51.66	4.303	1.179	46.57
6.723	0.959	26.12	0.56	43.97	4.347	1.169	39.11
6.806	0.984	23.6	0.471	52.89	4.265	1.17	47.43
6.889	0.959	26.09	0.583	41.75	4.32	1.151	36.48
6.972	0.977	24.27	0.543	45.72	4.306	1.164	41.59
7.055	0.972	24.76	0.531	46.87	4.333	1.167	39.85
7.138	0.988	23.18	0.496	50.42	4.345	1.177	41.4
7.221	0.979	24.1	0.459	54.08	4.253	1.159	45.39
7.304	0.986	23.35	0.459	54.09	4.25	1.161	46.24
7.387	0.974	24.62	0.487	51.33	4.25	1.153	43.84
7.47	0.953	26.72	0.54	45.99	4.278	1.154	41.41
7.553	0.971	24.92	0.464	53.65	4.282	1.175	47.19
7.636	0.962	25.79	0.52	48.01	4.296	1.164	42.56
7.719	0.948	27.17	0.57	42.99	4.275	1.148	39.92
7.802	0.958	26.17	0.511	48.92	4.241	1.147	43.17
7.885	0.954	26.59	0.575	42.5	4.34	1.161	37.39
7.968	0.963	25.73	0.471	52.85	4.238	1.172	50.91
8.051	0.959	26.11	0.54	46.02	4.304	1.167	42.58
8.134	0.96	26.04	0.539	46.15	4.285	1.164	43.7
8.217	0.959	26.15	0.518	48.2	4.257	1.16	45.29
8.3	0.955	26.49	0.461	53.89	4.276	1.167	45.63
8.383	0.946	27.36	0.5	49.98	4.229	1.149	44.82
8.466	0.954	26.57	0.524	47.56	4.321	1.174	43.14
8.549	0.952	26.83	0.482	51.78	4.248	1.151	43.5
8.632	0.941	27.94	0.532	46.78	4.277	1.149	40.1
8.715	0.958	26.18	0.499	50.13	4.268	1.16	44.11
8.798	0.954	26.62	0.494	50.58	4.236	1.157	46.42
8.881	0.936	28.36	0.541	45.87	4.254	1.15	42.74
8.964	0.955	26.47	0.522	47.81	4.284	1.161	42.85
9.047	0.935	28.5	0.507	49.28	4.216	1.14	43.55
9.13	0.933	28.7	0.571	42.9	4.283	1.148	39.19
9.213	0.923	29.71	0.562	43.77	4.266	1.145	39.81
9.296	0.956	26.44	0.503	49.7	4.29	1.172	45.51
9.379	0.932	28.81	0.533	46.68	4.251	1.156	44.7
9.462	0.947	27.35	0.503	49.75	4.246	1.165	47.94

9.545	0.945	27.53	0.483	51.75	4.232	1.163	48.62
9.628	0.935	28.52	0.537	46.28	4.315	1.154	37.84
9.711	0.935	28.48	0.49	51	4.188	1.143	47.01
9.794	0.935	28.5	0.566	43.38	4.289	1.154	40.31
9.877	0.939	28.11	0.529	47.14	4.275	1.16	43.61
9.96	0.926	29.38	0.534	46.6	4.263	1.147	40.72
10.04	0.94	27.98	0.493	50.68	4.24	1.152	44.61
10.13	0.933	28.75	0.493	50.66	4.249	1.171	49.35
10.21	0.934	28.6	0.574	42.62	4.287	1.151	39.54
10.29	0.965	25.47	0.454	54.64	4.224	1.169	51.44
10.38	0.959	26.15	0.463	53.72	4.244	1.163	47.33
10.46	0.942	27.79	0.482	51.82	4.202	1.15	47.63
10.54	0.941	27.88	0.513	48.7	4.246	1.159	46.21
10.62	0.947	27.28	0.448	55.23	4.18	1.154	51.24
10.71	0.93	29.04	0.505	49.55	4.196	1.143	46.44
10.79	0.922	29.76	0.497	50.3	4.17	1.141	48.31
10.87	0.914	30.61	0.557	44.28	4.227	1.153	46.19
10.96	0.936	28.36	0.45	55.04	4.192	1.163	52.84
11.04	0.938	28.19	0.507	49.34	4.246	1.166	48.14
11.12	0.918	30.22	0.507	49.35	4.162	1.141	49.01
11.21	0.923	29.75	0.523	47.73	4.19	1.144	47.15
11.29	0.915	30.48	0.534	46.57	4.212	1.149	46.46
11.37	0.929	29.1	0.481	51.87	4.167	1.151	51.72
11.45	0.929	29.13	0.467	53.28	4.164	1.14	48.69
11.54	0.92	30	0.507	49.28	4.228	1.148	44.47
11.62	0.923	29.66	0.511	48.87	4.235	1.157	46.49
11.7	0.937	28.35	0.498	50.24	4.225	1.154	46.7
11.79	0.931	28.91	0.462	53.75	4.175	1.154	51.51
11.87	0.931	28.86	0.495	50.52	4.211	1.149	46.69

Data from ^{1}H NMR experiments (500 MHz, toluene-d_8, 100 °C, 8 scans, d_1 = 1 s). [a] δ 3.70–3.63 ppm. [b] δ 2.05–1.94 ppm. [c] δ 1.82–1.71 ppm, overlaps with CH_3 signal from **13b**. [d] Integral reference for **13b** at δ 8.63 ppm. [e] Calculated after correction of the integral value for contribution from **13b**.

Table 10.4 Raw kinetic data for the deuteration of a mixture of **9** and **13b**. Integration for pyrrolidine **13b**.

time (h)	int. *cis*-C(2)H[a]	% D *cis*-C(2)	int. *trans*-C(4)H[b]	% D *trans*-C(4)	int. CH_{Ar}[c]	int. tol[d]	int. CHCO (9)[e]	% D CH_{Ar}[f]
0.083	0.9842	1.58	1.105	0.49	6.507	2.386	0.7451	6.104
0.166	0.9687	3.13	1.105	0.47	6.594	2.391	0.7336	1.37
0.249	1.004	-0.4	1.128	-1.8	6.657	2.494	0.7705	3.482
0.332	0.9695	3.05	1.12	-1	6.671	2.422	0.7433	-0.99
0.415	0.9529	4.71	1.109	0.07	6.656	2.417	0.7428	-0.41

0.498	0.9473	5.27	1.112	-0.2	6.6	2.404	0.7395	1.779
0.581	0.9411	5.89	1.105	0.52	6.596	2.4	0.7338	1.527
0.664	0.9062	9.38	1.099	1.14	6.579	2.354	0.7284	0.617
0.747	0.9225	7.75	1.099	1.13	6.626	2.388	0.7361	-0.23
0.83	0.9129	8.71	1.092	1.84	6.57	2.354	0.7289	1.101
0.913	0.8981	10.2	1.097	1.32	6.563	2.367	0.7293	1.871
0.996	0.8919	10.8	1.089	2.07	6.536	2.34	0.7217	1.946
1.079	0.8865	11.3	1.083	2.66	6.546	2.344	0.7272	1.893
1.162	0.8653	13.5	1.078	3.23	6.536	2.279	0.7219	-0.09
1.245	0.897	10.3	1.091	1.87	6.583	2.345	0.738	0.568
1.328	0.8655	13.4	1.07	4.03	6.48	2.328	0.7177	4.149
1.411	0.865	13.5	1.07	4.05	6.47	2.319	0.7124	4.076
1.494	0.8674	13.3	1.068	4.24	6.51	2.316	0.7195	2.346
1.577	0.8743	12.6	1.07	3.96	6.504	2.334	0.7248	3.531
1.66	0.877	12.3	1.069	4.08	6.505	2.339	0.7184	3.282
1.743	0.861	13.9	1.062	4.85	6.463	2.307	0.7102	3.916
1.826	0.8728	12.7	1.066	4.39	6.481	2.352	0.7281	5.41
1.909	0.8467	15.3	1.058	5.21	6.427	2.297	0.7179	5.752
1.992	0.8575	14.2	1.056	5.38	6.438	2.286	0.7058	4.242
2.075	0.8476	15.2	1.044	6.65	6.38	2.3	0.7079	7.755
2.158	0.8607	13.9	1.05	5.97	6.418	2.347	0.7096	7.482
2.241	0.8509	14.9	1.061	4.86	6.408	2.33	0.7113	7.503
2.324	0.8307	16.9	1.047	6.28	6.411	2.307	0.6989	5.972
2.407	0.8821	11.8	1.062	4.78	6.43	2.356	0.7312	8.255
2.49	0.8423	15.8	1.052	5.76	6.425	2.286	0.7191	5.589
2.573	0.8416	15.8	1.04	6.96	6.343	2.297	0.7019	9.185
2.656	0.8748	12.5	1.065	4.52	6.497	2.379	0.7268	5.453
2.739	0.8546	14.5	1.048	6.24	6.374	2.331	0.7129	9.322
2.822	0.8517	14.8	1.046	6.43	6.386	2.319	0.7151	8.408
2.905	0.8595	14	1.045	6.47	6.359	2.319	0.7168	9.831
2.988	0.8341	16.6	1.033	7.69	6.347	2.317	0.7044	9.782
3.071	0.8671	13.3	1.051	5.92	6.465	2.35	0.722	5.828
3.154	0.8636	13.6	1.043	6.68	6.416	2.369	0.7257	9.094
3.237	0.8375	16.3	1.04	7	6.4	2.329	0.7076	7.69
3.32	0.8203	18	1.023	8.73	6.332	2.305	0.7004	9.895
3.403	0.8324	16.8	1.028	8.18	6.32	2.303	0.7005	10.43
3.486	0.8523	14.8	1.039	7.08	6.393	2.332	0.7152	8.503
3.569	0.8329	16.7	1.026	8.37	6.365	2.323	0.702	8.923
3.652	0.8277	17.2	1.024	8.57	6.35	2.285	0.703	8.468

3.735	0.85	15	1.032	7.77	6.362	2.326	0.7116	9.685
3.818	0.8193	18.1	1.027	8.34	6.317	2.258	0.6939	8.782
3.901	0.8382	16.2	1.034	7.55	6.364	2.312	0.7117	9.106
3.984	0.8215	17.8	1.012	9.78	6.251	2.289	0.7007	13.47
4.067	0.8406	15.9	1.031	7.89	6.372	2.328	0.7052	8.924
4.15	0.8336	16.6	1.023	8.66	6.378	2.317	0.7044	8.202
4.233	0.8415	15.8	1.025	8.49	6.35	2.308	0.711	9.648
4.316	0.8204	18	1.014	9.58	6.307	2.277	0.6927	9.858
4.399	0.8182	18.2	1.009	10.1	6.254	2.286	0.6933	12.81
4.482	0.856	14.4	1.023	8.71	6.327	2.362	0.7113	12.62
4.565	0.8342	16.6	1.018	9.19	6.301	2.322	0.7007	12.05
4.648	0.8199	18	1.018	9.2	6.306	2.31	0.6993	11.36
4.731	0.8152	18.5	1.004	10.6	6.287	2.29	0.6942	11.36
4.814	0.8174	18.3	1.009	10.1	6.28	2.307	0.6879	11.97
4.897	0.8257	17.4	1.012	9.8	6.289	2.316	0.705	12.65
4.98	0.8201	18	1.01	10	6.283	2.291	0.6935	11.56
5.063	0.827	17.3	1.011	9.85	6.264	2.324	0.697	13.79
5.146	0.8363	16.4	1.013	9.66	6.3	2.344	0.7019	12.91
5.229	0.8153	18.5	1.008	10.2	6.253	2.312	0.6919	13.69
5.312	0.8111	18.9	1.003	10.7	6.279	2.293	0.6921	11.75
5.395	0.8353	16.5	1.01	9.97	6.297	2.33	0.7055	12.75
5.478	0.83	17	1.013	9.71	6.317	2.322	0.6965	11.04
5.561	0.8073	19.3	1	11	6.209	2.296	0.6874	15.12
5.644	0.8195	18	1.007	10.3	6.27	2.321	0.695	13.28
5.727	0.793	20.7	0.994	11.6	6.205	2.282	0.6784	14.42
5.81	0.8198	18	1.001	10.9	6.269	2.305	0.6988	13
5.893	0.8189	18.1	1.002	10.8	6.238	2.311	0.6981	14.73
5.976	0.828	17.2	1.001	10.9	6.21	2.324	0.6881	16.04
6.059	0.7951	20.5	0.989	12.1	6.191	2.273	0.6805	14.92
6.142	0.8386	16.1	1.012	9.78	6.276	2.344	0.7022	14.15
6.225	0.817	18.3	1.006	10.4	6.275	2.314	0.6949	12.77
6.308	0.8044	19.6	1.003	10.7	6.275	2.304	0.6941	12.44
6.391	0.8017	19.8	0.992	11.8	6.225	2.29	0.6807	13.76
6.474	0.8196	18	1.001	10.9	6.265	2.334	0.6887	13.64
6.557	0.8246	17.5	1.004	10.6	6.294	2.334	0.7012	12.84
6.64	0.8253	17.5	1.005	10.5	6.27	2.339	0.7039	14.32
6.723	0.8092	19.1	1	11	6.301	2.3	0.6903	10.78
6.806	0.8326	16.7	0.999	11.1	6.292	2.36	0.7004	13.74
6.889	0.792	20.8	0.99	12	6.235	2.282	0.6828	13.13

6.972	0.8098	19	0.994	11.6	6.265	2.316	0.6861	12.92
7.055	0.8216	17.8	0.993	11.7	6.267	2.318	0.6923	13.19
7.138	0.8136	18.6	0.993	11.7	6.266	2.328	0.6888	13.38
7.221	0.8037	19.6	0.984	12.6	6.209	2.32	0.6802	15.55
7.304	0.8225	17.7	0.993	11.7	6.233	2.345	0.6973	16.04
7.387	0.8101	19	0.991	11.9	6.209	2.324	0.6846	15.92
7.47	0.7971	20.3	0.987	12.3	6.218	2.298	0.6848	14.63
7.553	0.8379	16.2	0.998	11.2	6.305	2.354	0.705	13.15
7.636	0.8036	19.6	0.992	11.8	6.258	2.324	0.6885	13.63
7.719	0.7961	20.4	0.985	12.5	6.181	2.273	0.6753	15.14
7.802	0.802	19.8	0.99	12	6.212	2.306	0.684	15.16
7.885	0.8071	19.3	0.99	12	6.272	2.302	0.687	12.12
7.968	0.8208	17.9	0.998	11.2	6.28	2.362	0.6971	14.22
8.051	0.8089	19.1	0.989	12.1	6.247	2.32	0.6842	13.84
8.134	0.8153	18.5	0.996	11.4	6.271	2.336	0.6906	13.51
8.217	0.8043	19.6	0.987	12.3	6.207	2.32	0.6808	15.67
8.3	0.8313	16.9	1	11	6.357	2.365	0.7024	10.75
8.383	0.7884	21.2	0.976	13.4	6.159	2.283	0.6694	16.27
8.466	0.8039	19.6	0.986	12.4	6.25	2.316	0.6812	13.43
8.549	0.8023	19.8	0.99	12	6.251	2.337	0.6808	14.05
8.632	0.7852	21.5	0.984	12.6	6.213	2.289	0.6742	14.03
8.715	0.811	18.9	0.994	11.6	6.271	2.339	0.6863	13.39
8.798	0.8152	18.5	0.99	12	6.296	2.364	0.6891	13.15
8.881	0.7877	21.2	0.975	13.5	6.153	2.281	0.6787	16.97
8.964	0.8025	19.7	0.991	11.9	6.248	2.335	0.6917	14.7
9.047	0.7891	21.1	0.98	13	6.196	2.309	0.6699	15.34
9.13	0.77	23	0.969	14.1	6.163	2.267	0.6636	15.27
9.213	0.7881	21.2	0.976	13.4	6.184	2.274	0.6676	14.66
9.296	0.7998	20	0.985	12.5	6.227	2.328	0.6826	15.01
9.379	0.7884	21.2	0.989	12.1	6.276	2.32	0.6841	12.42
9.462	0.7969	20.3	0.981	12.9	6.219	2.316	0.6738	14.57
9.545	0.801	19.9	0.977	13.3	6.177	2.318	0.6739	16.76
9.628	0.7795	22.1	0.982	12.8	6.223	2.29	0.6728	13.52
9.711	0.7904	21	0.975	13.5	6.206	2.323	0.6752	15.58
9.794	0.7862	21.4	0.98	13	6.21	2.301	0.672	14.48
9.877	0.774	22.6	0.972	13.8	6.152	2.28	0.6656	16.34
9.96	0.7896	21	0.988	12.2	6.25	2.316	0.675	13.14
10.04	0.7984	20.2	0.98	13	6.196	2.322	0.6738	15.98
10.13	0.7954	20.5	0.973	13.7	6.228	2.304	0.6766	13.88

10.21	0.7844	21.6	0.984	12.6	6.226	2.296	0.6749	13.62
10.29	0.8021	19.8	0.982	12.8	6.172	2.337	0.6836	18.15
10.38	0.8077	19.2	0.981	12.9	6.17	2.346	0.6805	18.4
10.46	0.8088	19.1	0.984	12.6	6.249	2.348	0.684	14.69
10.54	0.7912	20.9	0.973	13.7	6.172	2.319	0.6742	17.07
10.62	0.8028	19.7	0.977	13.3	6.203	2.349	0.6794	16.79
10.71	0.7863	21.4	0.969	14.1	6.18	2.317	0.6716	16.51
10.79	0.7966	20.3	0.974	13.6	6.177	2.328	0.6793	17.36
10.87	0.8002	20	0.98	13	6.196	2.314	0.678	15.9
10.96	0.8236	17.6	0.989	12.1	6.295	2.378	0.6859	13.5
11.04	0.7951	20.5	0.972	13.8	6.187	2.319	0.6776	16.5
11.12	0.7859	21.4	0.969	14.1	6.124	2.303	0.6681	18.64
11.21	0.791	20.9	0.973	13.7	6.162	2.306	0.672	17.06
11.29	0.7838	21.6	0.977	13.3	6.22	2.307	0.6706	14.06
11.37	0.7935	20.7	0.979	13.1	6.211	2.32	0.6766	15.29
11.45	0.7961	20.4	0.978	13.2	6.198	2.333	0.6805	16.56
11.54	0.7841	21.6	0.972	13.8	6.191	2.311	0.6675	15.5
11.62	0.7975	20.2	0.976	13.4	6.209	2.326	0.6791	15.71
11.7	0.7904	21	0.973	13.7	6.156	2.314	0.6756	17.76
11.79	0.8079	19.2	0.978	13.2	6.223	2.35	0.6805	15.87
11.87	0.786	21.4	0.968	14.2	6.159	2.306	0.6668	16.95
11.95	0.8391	16.1	0.959	15.1	6.085	2.348	0.6825	22.83

Data from ^{1}H NMR experiments (500 MHz, toluene-d_8, 100 °C, 8 scans, d_1 = 1 s). [a] δ 4.16–4.03 ppm. [b] δ 3.41–3.30 ppm. [c] δ 7.00–6.90 ppm, overlaps with toluene signal, 2 × H_{Cbz} (from **13b**) and 1 × H_{Cbz} (from 9). [d] Toluene reference at δ 2.08 ppm. [e] Integral reference for **9** at δ 2.73–2.62 ppm. [f] Calculated after correction of the integral value for contribution from toluene and Cbz protons **13b** and **9.**

10.3 Appendix III: Crystallographic Data for Palladacycle 100-PCy_3

Single crystals for X-ray diffraction were grown by slow diffusion of hexane vapours in a solution of palladacycle **100-PCy_3** in THF at 25 °C.

Crystal data and structure refinement

Formula	$C_{40}H_{52}N_3O_3PPd$	
Formula weight	760.21	
Temperature	173(2) K	
Diffractometer, wavelength	Agilent Xcalibur PX Ultra A, 1.54184 Å	
Crystal system, space group	Orthorhombic, $Pna2_1$	
Unit cell dimensions	a = 18.1493(4) Å	α = 90°
	b = 20.4764(6) Å	β = 90°
	c = 9.48078(20) Å	γ = 90°
Volume, Z	3523.36(14) $Å^3$, 4	
Density (calculated)	1.433 Mg/m^3	
Absorption coefficient	5.011 mm^{-1}	
F(000)	1592	
Crystal colour / morphology	Yellow tablets	
Crystal size	0.285 x 0.183 x 0.058 mm^3	
θ range for data collection	3.254 to 73.534°	
Index ranges	-20<=h<=21, -16<=k<=24, -11<=l<=7	
Reflns collected / unique	7275 / 4549 [R(int) = 0.0401]	
Reflns observed [F>4σ(F)]	3946	
Absorption correction	Analytical	
Max. and min. transmission	0.761 and 0.501	
Refinement method	Full-matrix least-squares on F^2	
Data / restraints / parameters	4549 / 1 / 433	
Goodness-of-fit on F^2	1.039	
Final R indices [F>4σ(F)]	R1 = 0.0394, wR2 = 0.0911	
R indices (all data)	R1 = 0.0509, wR2 = 0.1008	
Absolute structure parameter	-0.030(13)	
Largest diff. peak, hole	0.578, -0.552 $eÅ^{-3}$	
Mean and maximum shift/error	0.000 and 0.001	

Bond Lengths [Å]

Pd(1)-N(11)	2.049(6)	C(18)-O(18)	1.223(10)
Pd(1)-C(14)	2.051(7)	C(18)-O(19)	1.351(10)
Pd(1)-N(1)	2.184(6)	O(19)-C(20)	1.439(10)
Pd(1)-P(1)	2.2964(15)	C(20)-C(21)	1.505(11)
P(1)-C(39)	1.850(7)	C(21)-C(22)	1.381(12)
P(1)-C(33)	1.857(7)	C(21)-C(26)	1.381(12)
P(1)-C(27)	1.864(7)	C(22)-C(23)	1.390(13)
N(1)-C(2)	1.328(10)	C(23)-C(24)	1.358(14)
N(1)-C(10)	1.369(9)	C(24)-C(25)	1.353(15)
C(2)-C(3)	1.420(12)	C(25)-C(26)	1.370(13)
C(3)-C(4)	1.353(13)	C(27)-C(32)	1.530(9)
C(4)-C(5)	1.410(13)	C(27)-C(28)	1.538(11)
C(5)-C(6)	1.404(12)	C(28)-C(29)	1.531(11)
C(5)-C(10)	1.422(11)	C(29)-C(30)	1.521(11)
C(6)-C(7)	1.365(15)	C(30)-C(31)	1.511(12)
C(7)-C(8)	1.391(13)	C(31)-C(32)	1.532(10)
C(8)-C(9)	1.377(10)	C(33)-C(38)	1.508(11)
C(9)-N(11)	1.380(10)	C(33)-C(34)	1.527(10)
C(9)-C(10)	1.432(11)	C(34)-C(35)	1.539(13)
N(11)-C(12)	1.344(10)	C(35)-C(36)	1.488(15)
C(12)-O(12)	1.230(9)	C(36)-C(37)	1.504(14)
C(12)-C(13)	1.517(12)	C(37)-C(38)	1.531(11)
C(13)-C(14)	1.525(11)	C(39)-C(40)	1.520(9)
C(13)-C(17)	1.531(11)	C(39)-C(44)	1.532(9)
C(14)-C(15)	1.525(10)	C(40)-C(41)	1.530(10)
C(15)-N(16)	1.475(9)	C(41)-C(42)	1.512(12)
N(16)-C(18)	1.342(10)	C(42)-C(43)	1.525(11)
N(16)-C(17)	1.439(10)	C(43)-C(44)	1.537(10)

Bond Angles [°]

N(11)-Pd(1)-C(14)	81.6(3)	C(6)-C(7)-C(8)	122.1(8)
N(11)-Pd(1)-N(1)	78.4(2)	C(9)-C(8)-C(7)	121.4(8)
C(14)-Pd(1)-N(1)	159.9(3)	C(8)-C(9)-N(11)	127.4(8)
N(11)-Pd(1)-P(1)	175.98(18)	C(8)-C(9)-C(10)	117.7(7)
C(14)-Pd(1)-P(1)	94.5(2)	N(11)-C(9)-C(10)	114.9(6)
N(1)-Pd(1)-P(1)	105.50(16)	N(1)-C(10)-C(5)	120.8(7)
C(39)-P(1)-C(33)	108.8(3)	N(1)-C(10)-C(9)	119.0(6)
C(39)-P(1)-C(27)	103.2(3)	C(5)-C(10)-C(9)	120.2(7)
C(33)-P(1)-C(27)	105.5(3)	C(12)-N(11)-C(9)	125.2(6)
C(39)-P(1)-Pd(1)	112.6(2)	C(12)-N(11)-Pd(1)	117.9(5)
C(33)-P(1)-Pd(1)	114.8(2)	C(9)-N(11)-Pd(1)	116.8(5)
C(27)-P(1)-Pd(1)	111.0(2)	O(12)-C(12)-N(11)	125.4(8)
C(2)-N(1)-C(10)	118.6(7)	O(12)-C(12)-C(13)	123.1(7)
C(2)-N(1)-Pd(1)	130.8(5)	N(11)-C(12)-C(13)	111.2(6)
C(10)-N(1)-Pd(1)	110.5(5)	C(12)-C(13)-C(14)	112.0(6)
N(1)-C(2)-C(3)	123.2(7)	C(12)-C(13)-C(17)	113.4(6)
C(4)-C(3)-C(2)	118.9(8)	C(14)-C(13)-C(17)	105.0(6)
C(3)-C(4)-C(5)	119.6(8)	C(15)-C(14)-C(13)	103.3(6)
C(6)-C(5)-C(4)	121.6(8)	C(15)-C(14)-Pd(1)	115.0(5)
C(6)-C(5)-C(10)	119.5(8)	C(13)-C(14)-Pd(1)	107.8(5)
C(4)-C(5)-C(10)	118.8(7)	N(16)-C(15)-C(14)	102.9(6)
C(7)-C(6)-C(5)	119.1(9)	C(18)-N(16)-C(17)	121.3(6)

C(18)-N(16)-C(15)	125.4(7)	C(30)-C(29)-C(28)	111.5(7)
C(17)-N(16)-C(15)	113.2(6)	C(31)-C(30)-C(29)	110.5(6)
N(16)-C(17)-C(13)	103.8(6)	C(30)-C(31)-C(32)	112.2(7)
O(18)-C(18)-N(16)	124.5(7)	C(27)-C(32)-C(31)	111.7(6)
O(18)-C(18)-O(19)	123.4(7)	C(38)-C(33)-C(34)	110.1(6)
N(16)-C(18)-O(19)	112.1(6)	C(38)-C(33)-P(1)	111.0(5)
C(18)-O(19)-C(20)	116.8(6)	C(34)-C(33)-P(1)	118.6(6)
O(19)-C(20)-C(21)	112.3(7)	C(33)-C(34)-C(35)	108.9(7)
C(22)-C(21)-C(26)	119.3(8)	C(36)-C(35)-C(34)	113.8(7)
C(22)-C(21)-C(20)	120.4(7)	C(35)-C(36)-C(37)	112.2(7)
C(26)-C(21)-C(20)	120.3(7)	C(36)-C(37)-C(38)	111.5(8)
C(21)-C(22)-C(23)	119.2(8)	C(33)-C(38)-C(37)	110.5(7)
C(24)-C(23)-C(22)	120.6(9)	C(40)-C(39)-C(44)	110.8(5)
C(25)-C(24)-C(23)	119.8(8)	C(40)-C(39)-P(1)	118.9(5)
C(24)-C(25)-C(26)	121.1(9)	C(44)-C(39)-P(1)	113.7(5)
C(25)-C(26)-C(21)	119.9(8)	C(39)-C(40)-C(41)	109.2(6)
C(32)-C(27)-C(28)	109.6(6)	C(42)-C(41)-C(40)	111.3(6)
C(32)-C(27)-P(1)	110.2(5)	C(41)-C(42)-C(43)	111.4(6)
C(28)-C(27)-P(1)	111.3(5)	C(42)-C(43)-C(44)	111.8(6)
C(29)-C(28)-C(27)	111.5(7)	C(39)-C(44)-C(43)	110.9(6)

10.4 Appendix IV: Effect of Stirring Rate

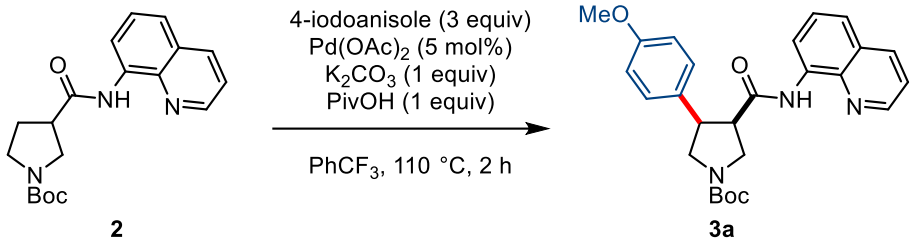


Table 10.1 Effect of stirring rate on the C(4)–H arylation of pyrrolidine **2**.

entry	stirring rate (rpm)	yield (%)[a]		
		2	**3a**	**tot**
1	0	82	20	92
2	150	63	35	98
3	500	59	37	96
4	750	54	38	92
5	1000	52	41	93
6	1500	54	39	93

Reaction scale: 0.2 mmol. [a] Calculated by ^{1}H NMR using 1,3,5-TMB as internal standard.

10.5 Appendix V: Computational Modelling of C(4) *vs* C(2) Selectivity

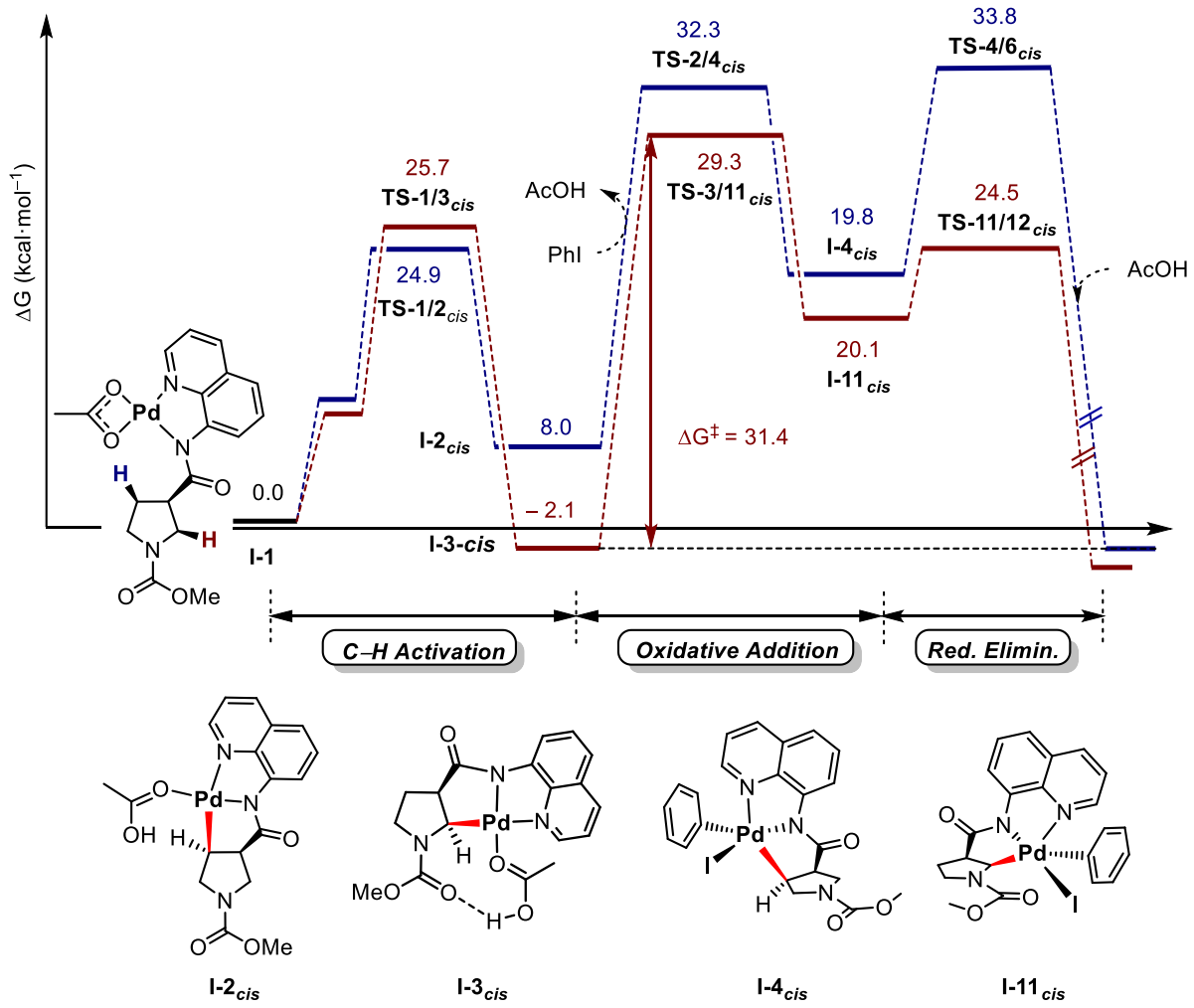


Figure 10.2 Computational modelling of C–H arylation at *cis*-C(4)- and *cis*-C(2)-positions. Calculated at DFT/m062x/Def2tzvpp.

10.6 Appendix VI: Computational Comparison of AQ and DMAQ Directing Groups

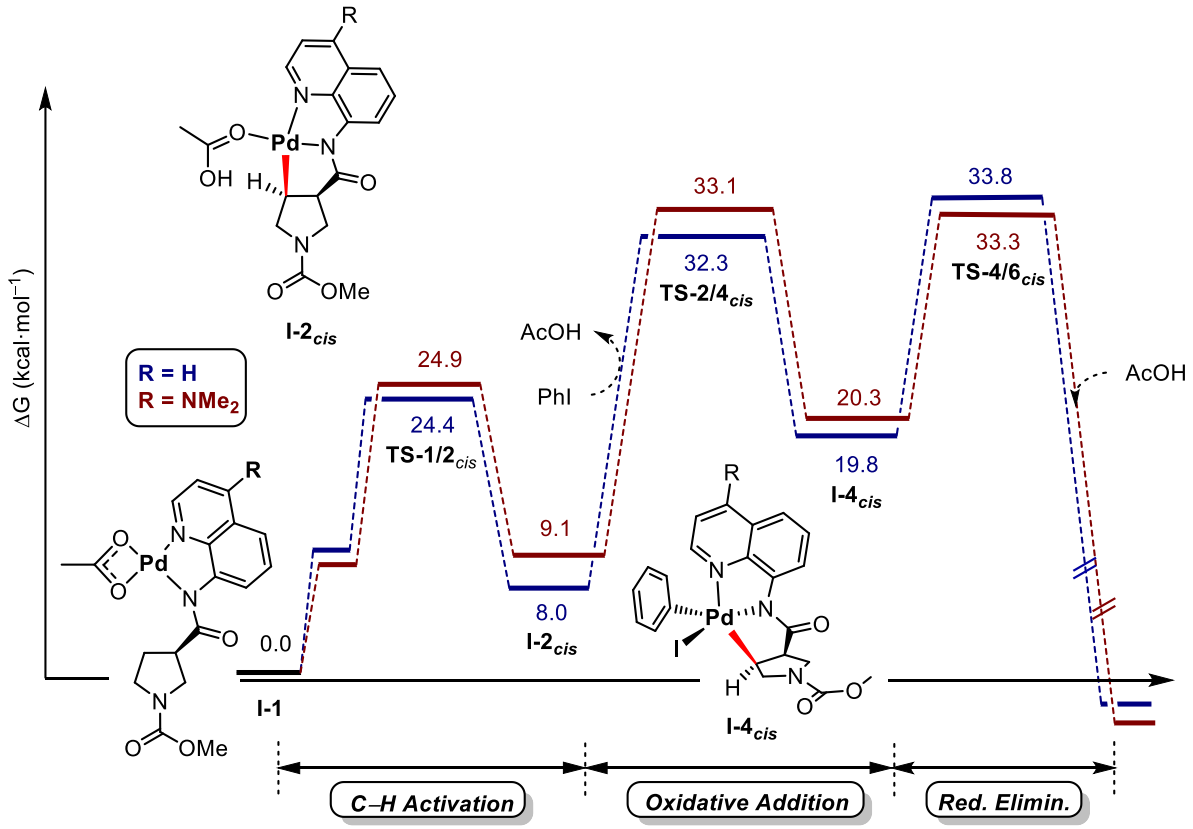


Figure 10.3 Computational modelling of *cis*-C(4)–H arylation using AQ and DMAQ directing groups. Calculated at DFT/m062x/Def2tzvpp.